

# The EIC

Charlotte Van Hulse  
University of Alcalá

AdT



**Comunidad  
de Madrid**

22nd STFC Nuclear Physics Summer School  
University of Durham  
11–24 August 2024

# On the menu

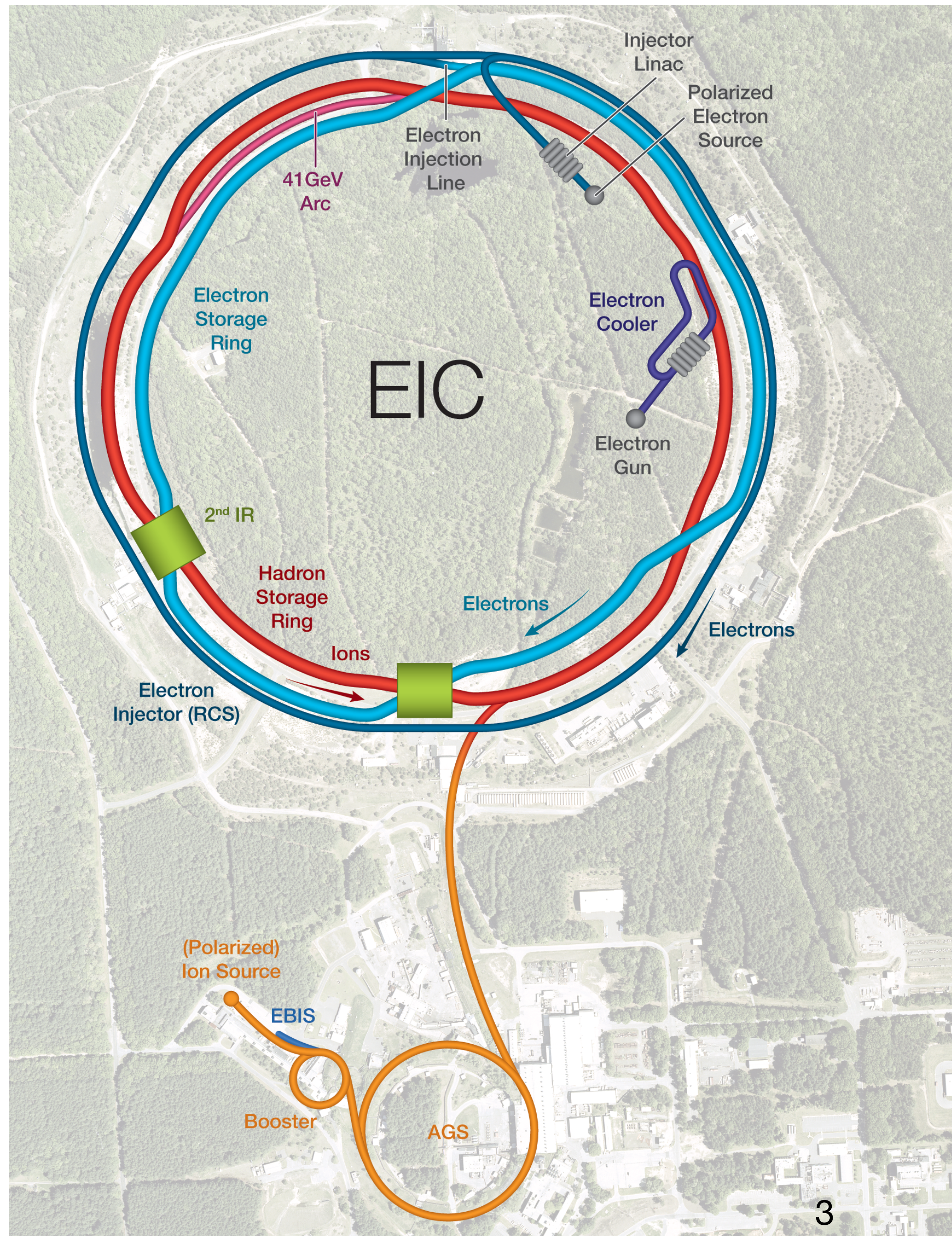


- EIC machine: overview
- ePIC: the first EIC detector
- Why an EIC?
  - Nucleon spin
  - Multi-dimensional nucleon structure
  - Saturation
  - Hadronisation

# The electron-ion collider (EIC)

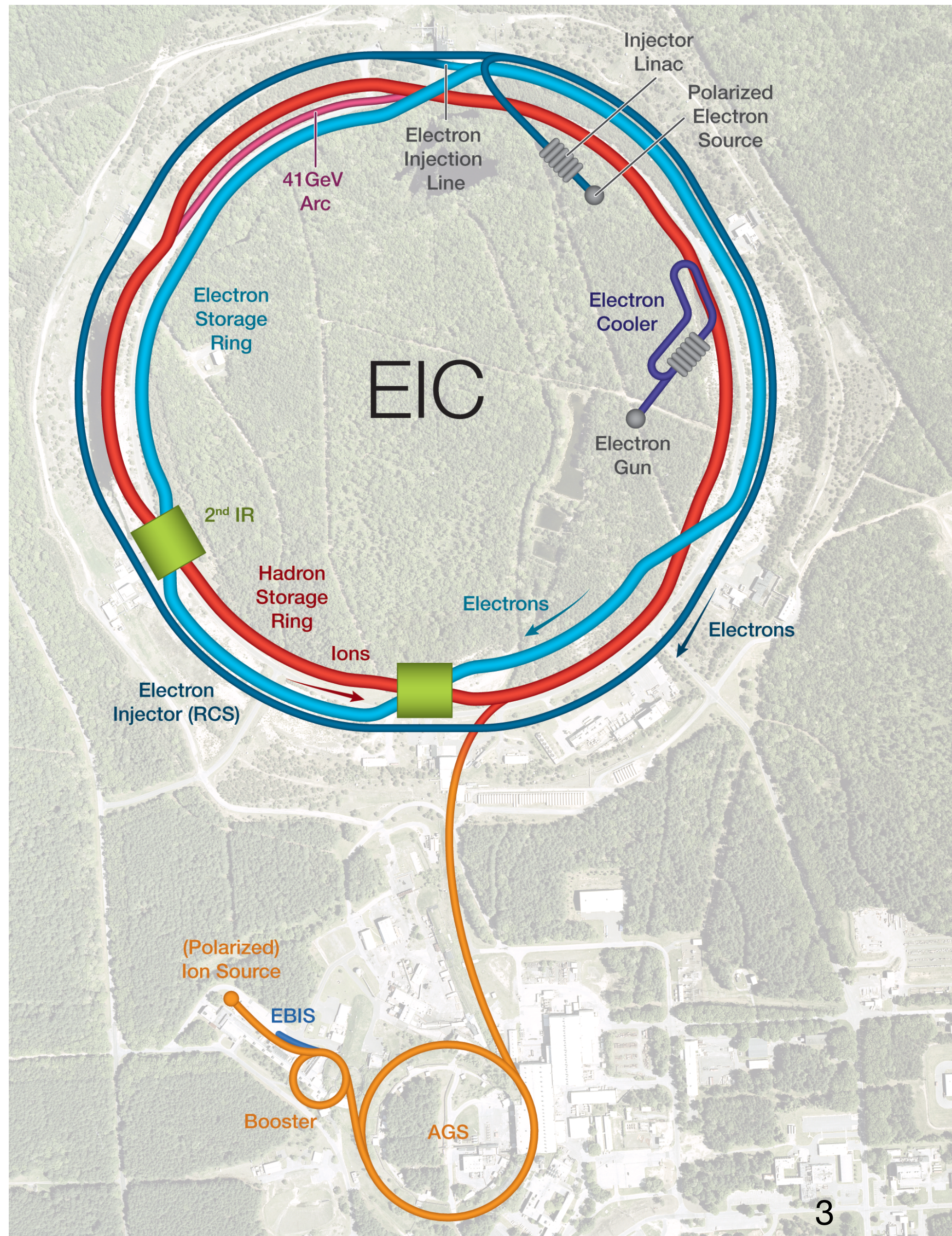


# The electron-ion collider (EIC)



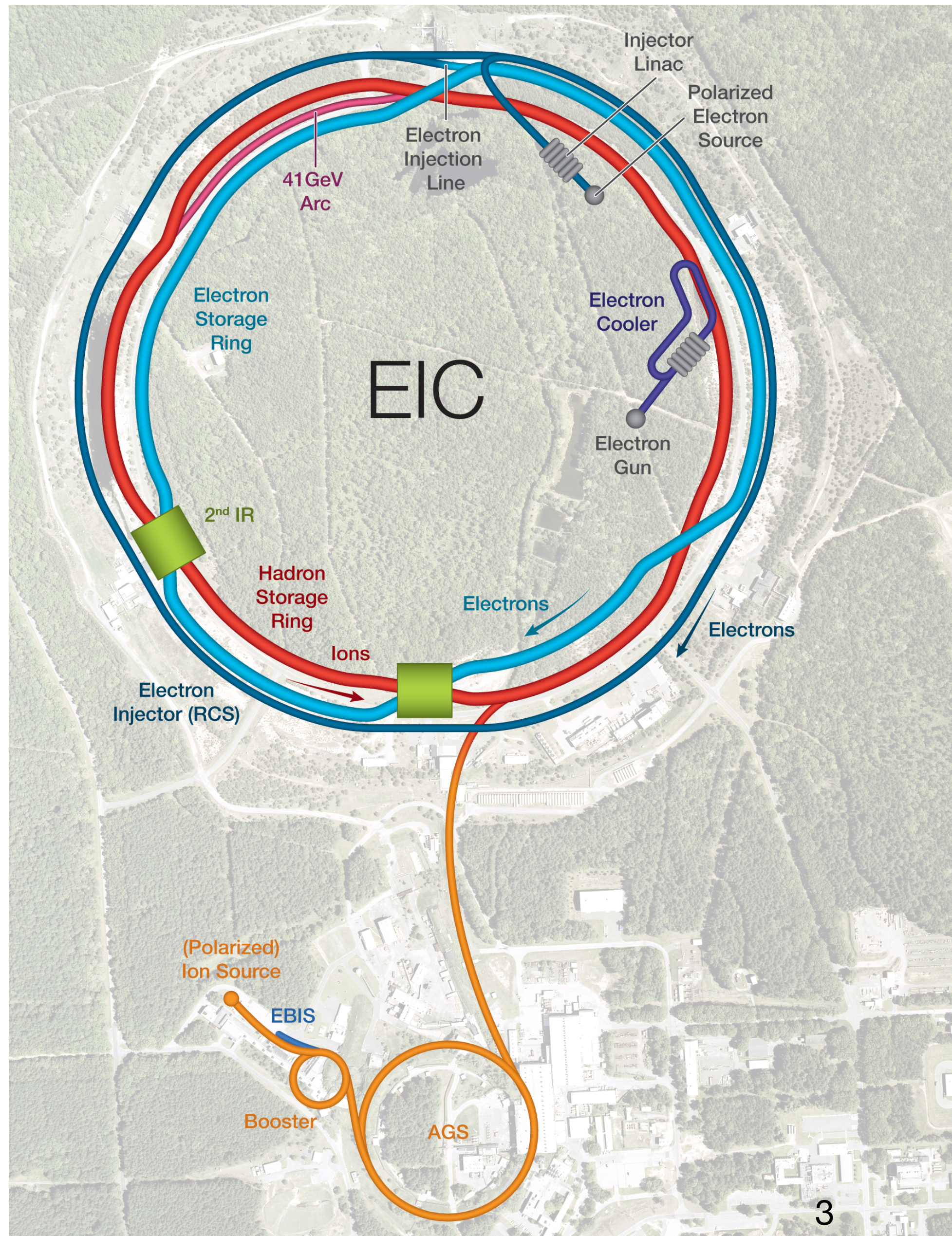
- Based on RHIC:
    - use existing hadron storage ring energy: 41–275 GeV
    - add electron storage ring in RHIC tunnel energy: 5–18 GeV
- $\sqrt{s} = 29 - 141$  GeV

# The electron-ion collider (EIC)



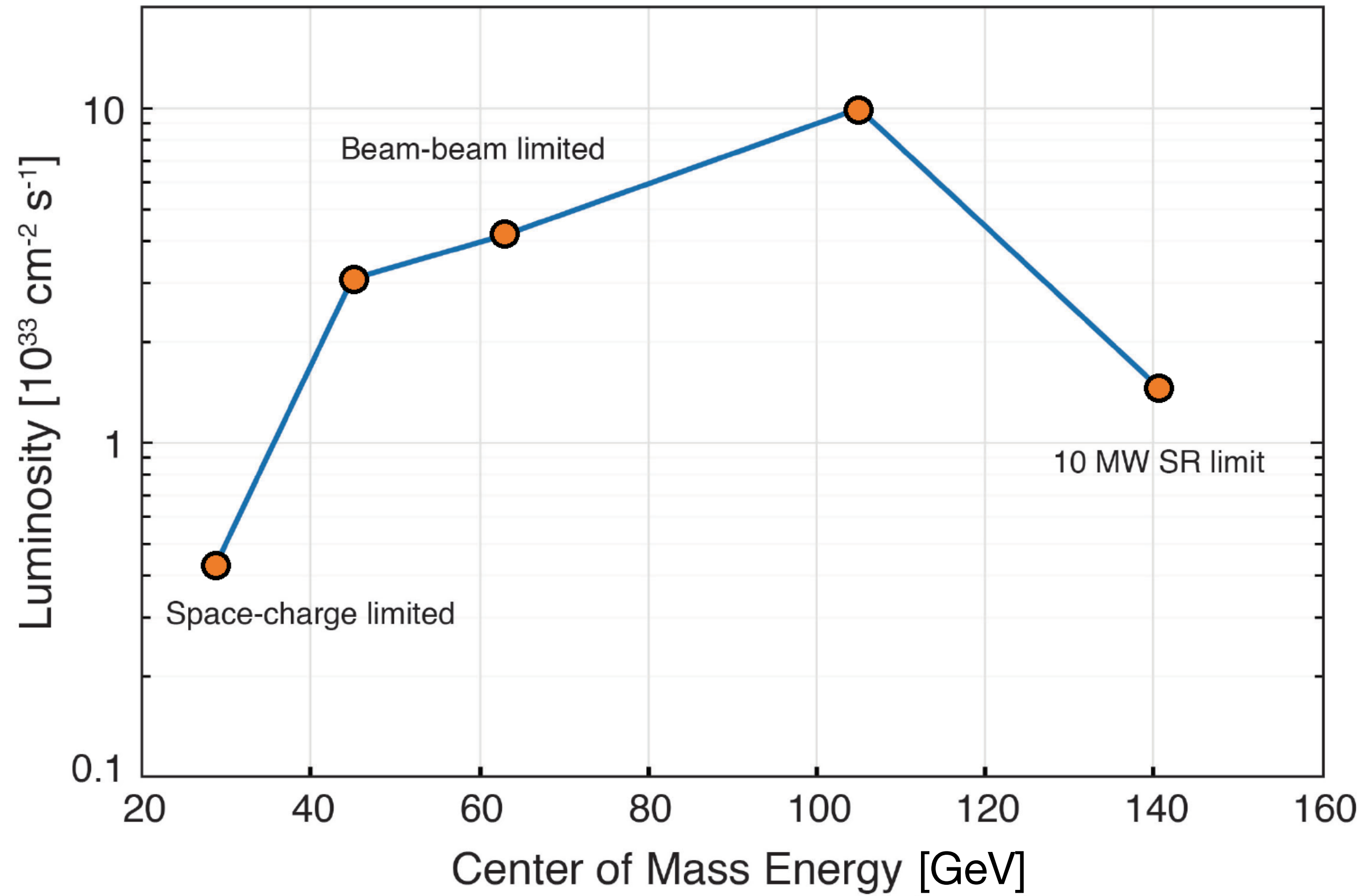
- Based on RHIC:
  - use existing hadron storage ring energy: 41–275 GeV
  - add electron storage ring in RHIC tunnel energy: 5–18 GeV
$$\rightarrow \sqrt{s} = 29 - 141 \text{ GeV}$$
- $\vec{e} + \vec{p}^\uparrow, \vec{d}^\uparrow, \vec{He}^\uparrow$ , unpolarised ions up to U  
~ 70% polarisation

# The electron-ion collider (EIC)



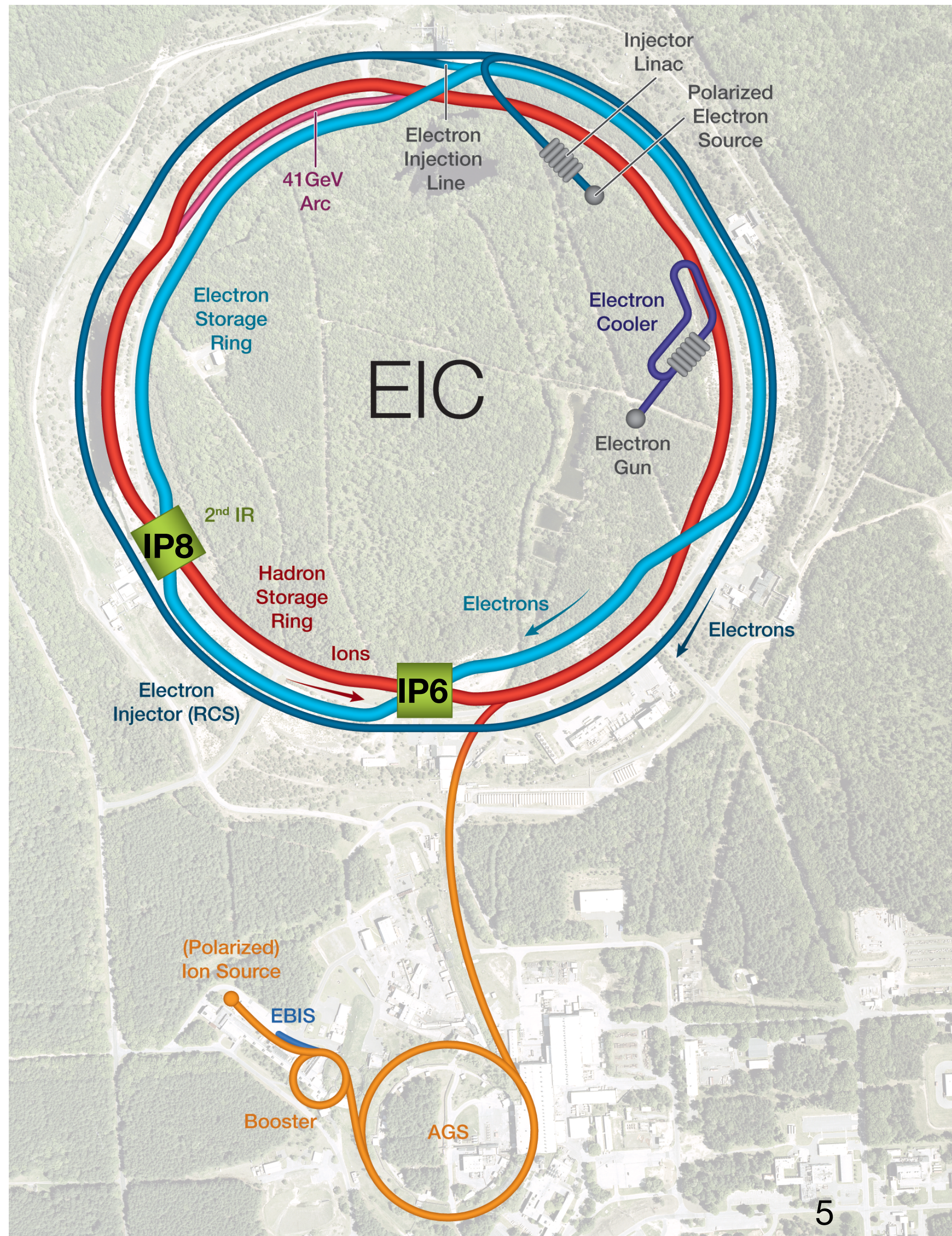
- Based on RHIC:
  - use existing hadron storage ring energy: 41–275 GeV
  - add electron storage ring in RHIC tunnel energy: 5–18 GeV
$$\rightarrow \sqrt{s} = 29 - 141 \text{ GeV}$$
- $\vec{e} + \vec{p}^\uparrow, \vec{d}^\uparrow, \vec{He}^\uparrow$ , unpolarised ions up to U  
 ~ 70% polarisation
- $\mathcal{L} = 10^{33-34} \text{ cm}^{-2} \text{ s}^{-1}$   
 $\leftrightarrow \mathcal{L}_{\text{int}} = 10 - 100 \text{ fb}^{-1}/\text{year}$

# Luminosity and centre-of-mass energy: ep collisions



Luminosity for eA similar within factor 2–3

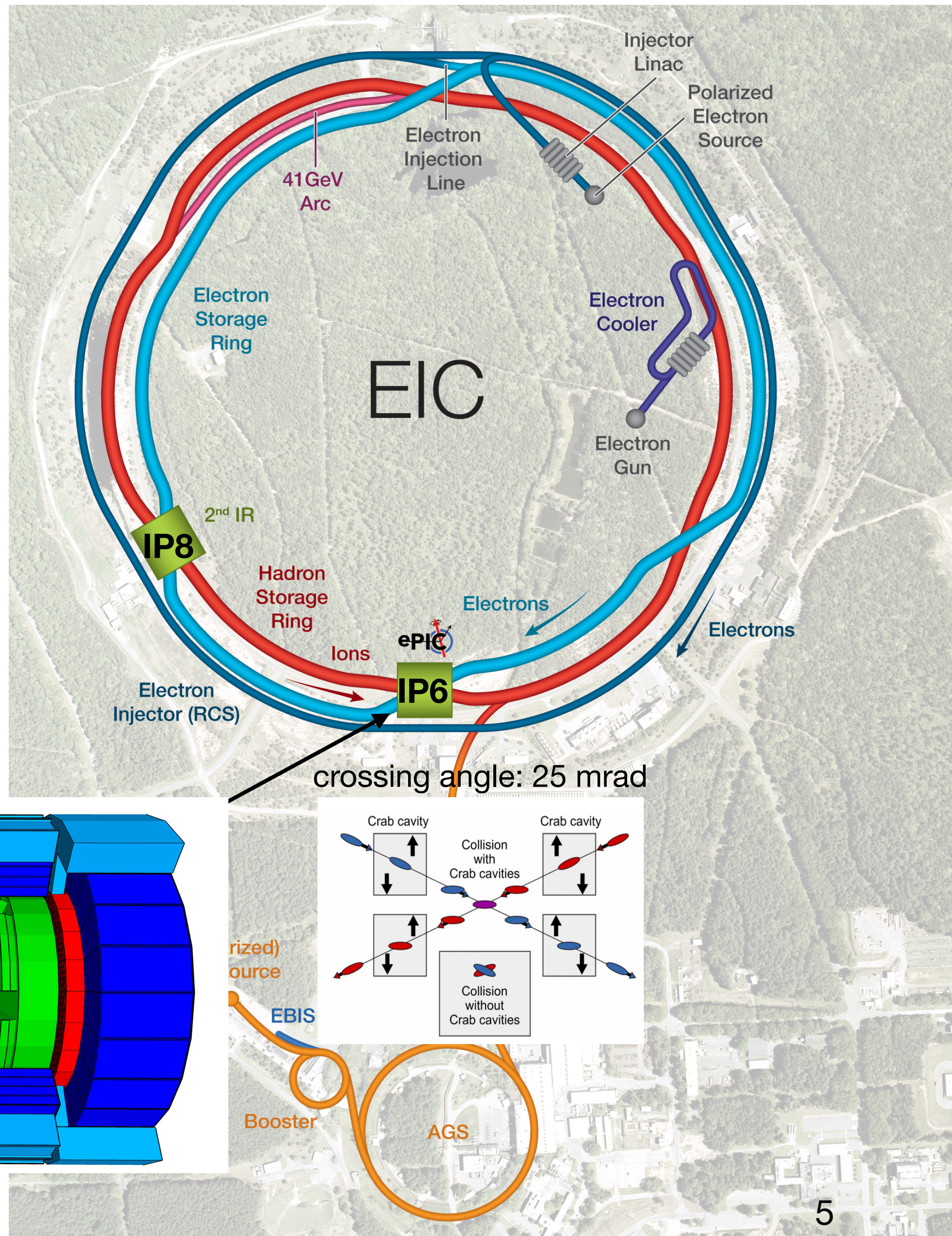
# The electron-ion collider (EIC)



- Based on RHIC:
  - use existing hadron storage ring energy: 41–275 GeV
  - add electron storage ring in RHIC tunnel energy: 5–18 GeV
    - $\sqrt{s} = 29 - 141$  GeV (per nucleon)
- ion beam: proton to Uranium
- $\vec{e} + \vec{p}^\uparrow, \vec{d}^\uparrow, \vec{He}^\uparrow$
- ~ 70% polarisation
- $\mathcal{L} = 10^{33-34} \text{ cm}^{-2} \text{ s}^{-1}$ 
  - ↔  $\mathcal{L}_{\text{int}} = 10 - 100 \text{ fb}^{-1}/\text{year}$

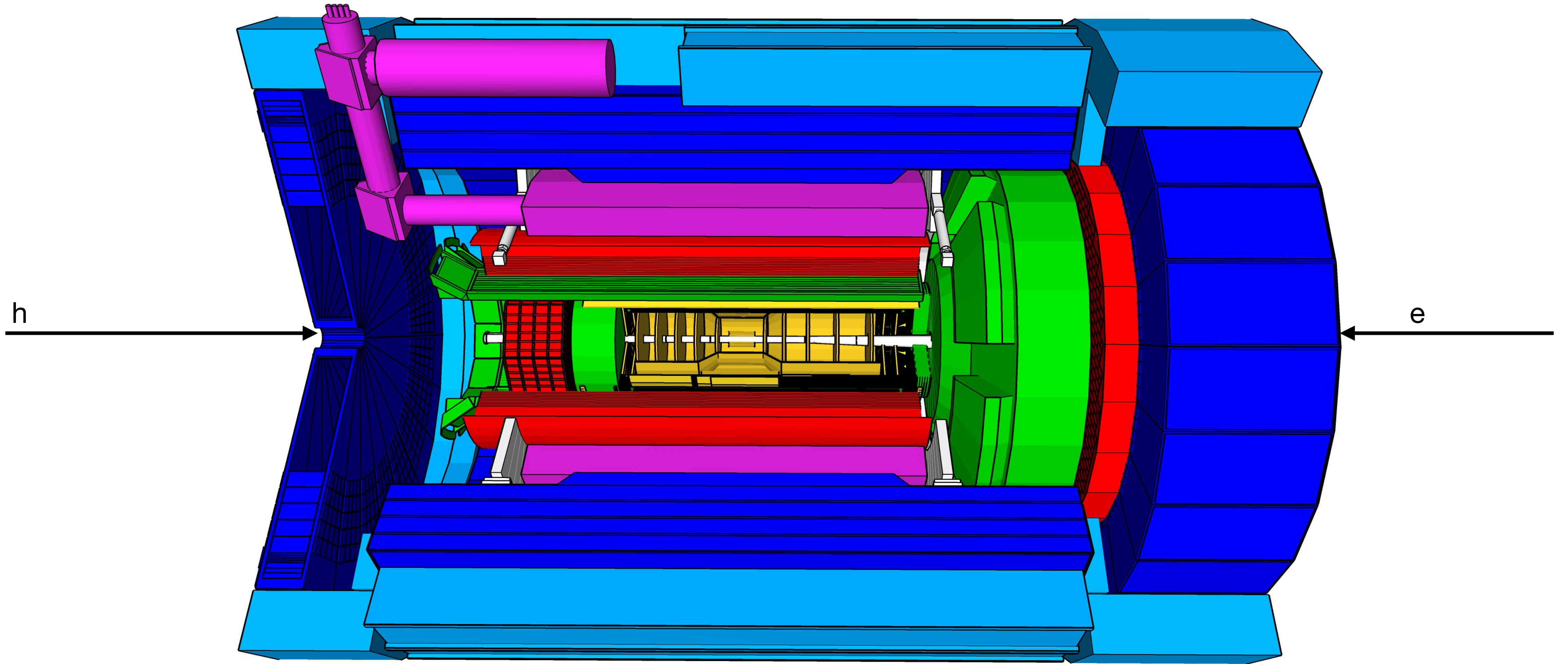


# The electron-ion collider (EIC)

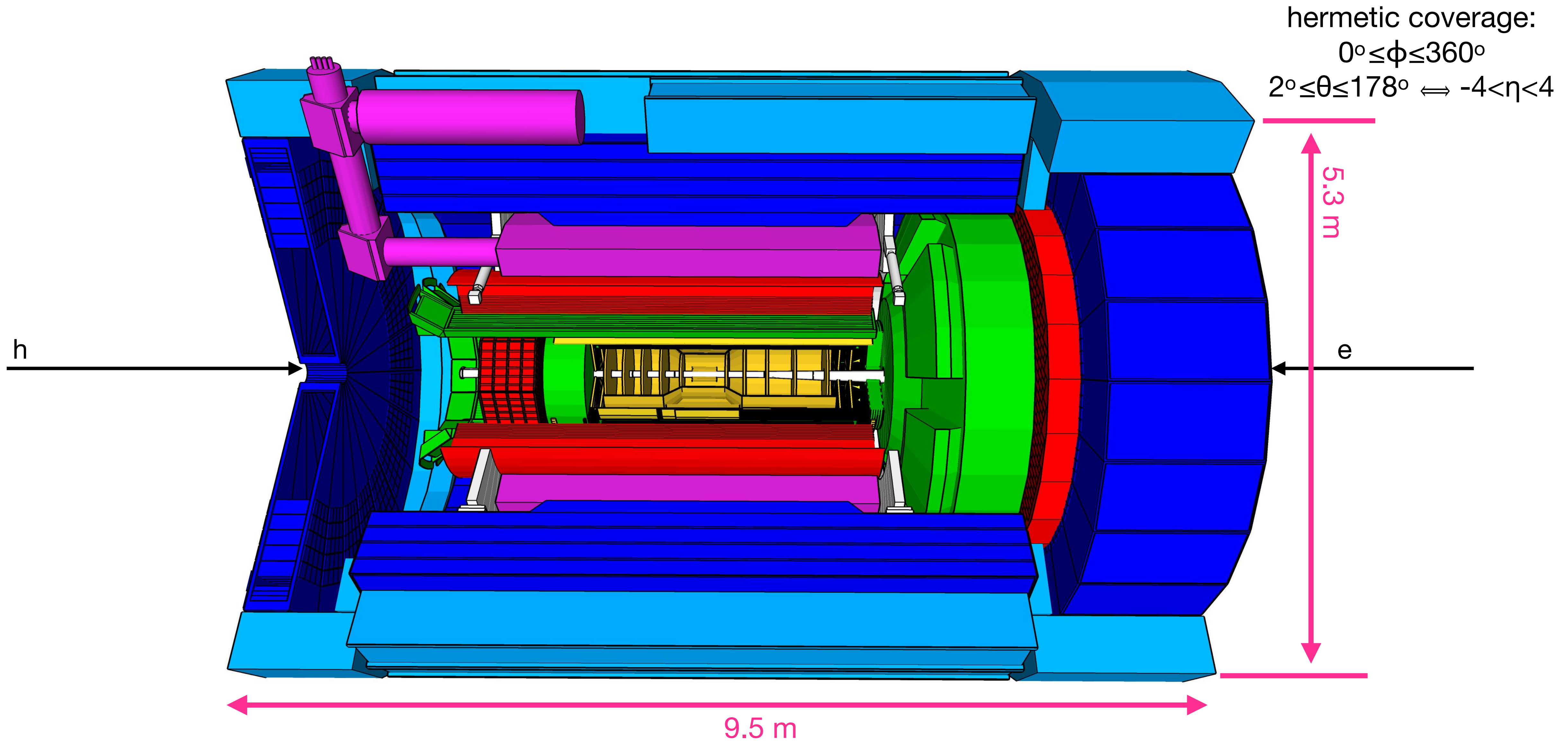


- Based on RHIC:
  - use existing hadron storage ring energy: 41–275 GeV
  - add electron storage ring in RHIC tunnel energy: 5–18 GeV
- $\sqrt{s} = 29 - 141 \text{ GeV}$  (per nucleon)
- ion beam: proton to Uranium
- $\vec{e} + \vec{p}^\uparrow, \vec{d}^\uparrow, \vec{He}^\uparrow$
- ~ 70% polarisation
- $\mathcal{L} = 10^{33-34} \text{ cm}^{-2} \text{ s}^{-1}$
- ↔  $\mathcal{L}_{\text{int}} = 10 - 100 \text{ fb}^{-1}/\text{year}$

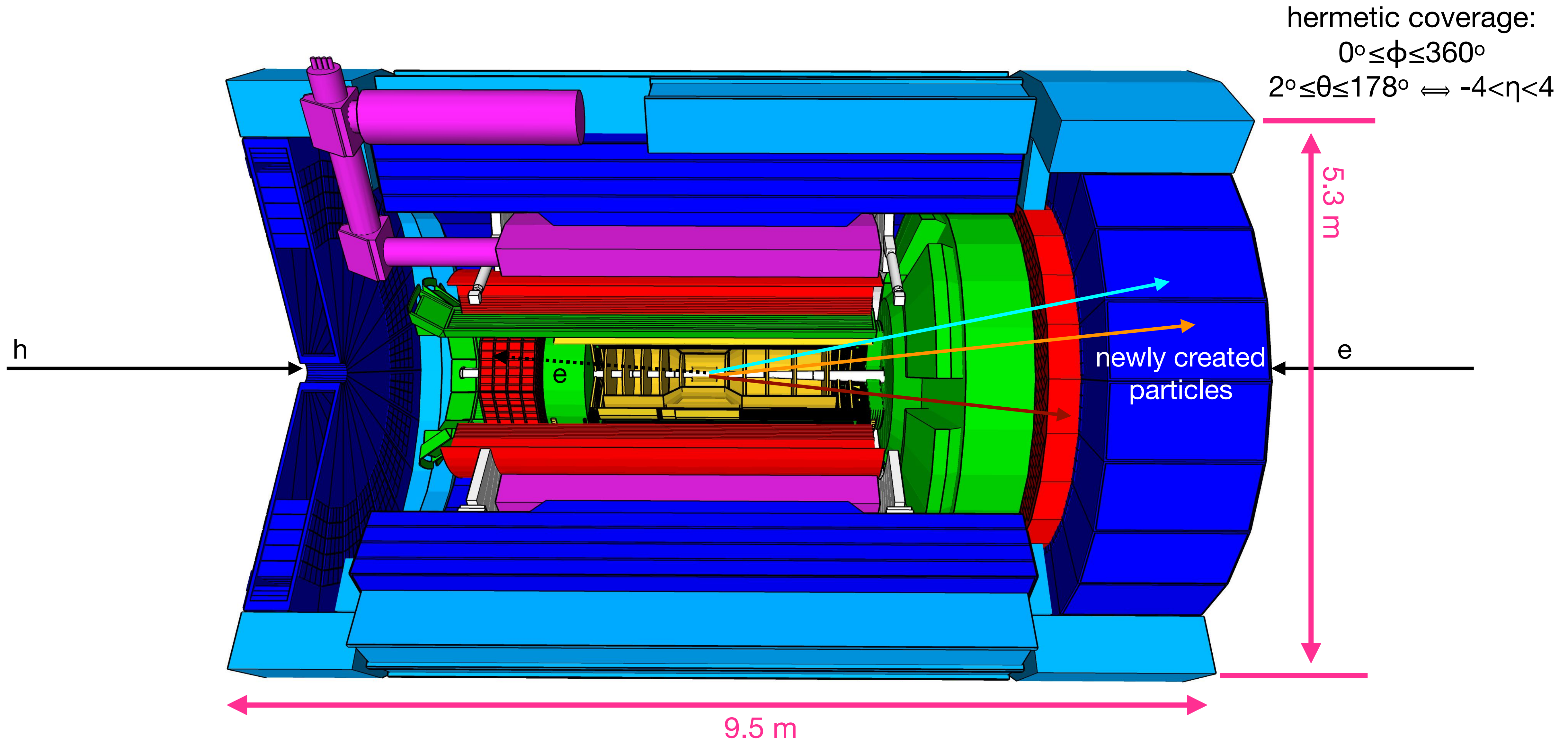
# The electron-proton/ion collider (ePIC) detector



# The electron-proton/ion collider (ePIC) detector

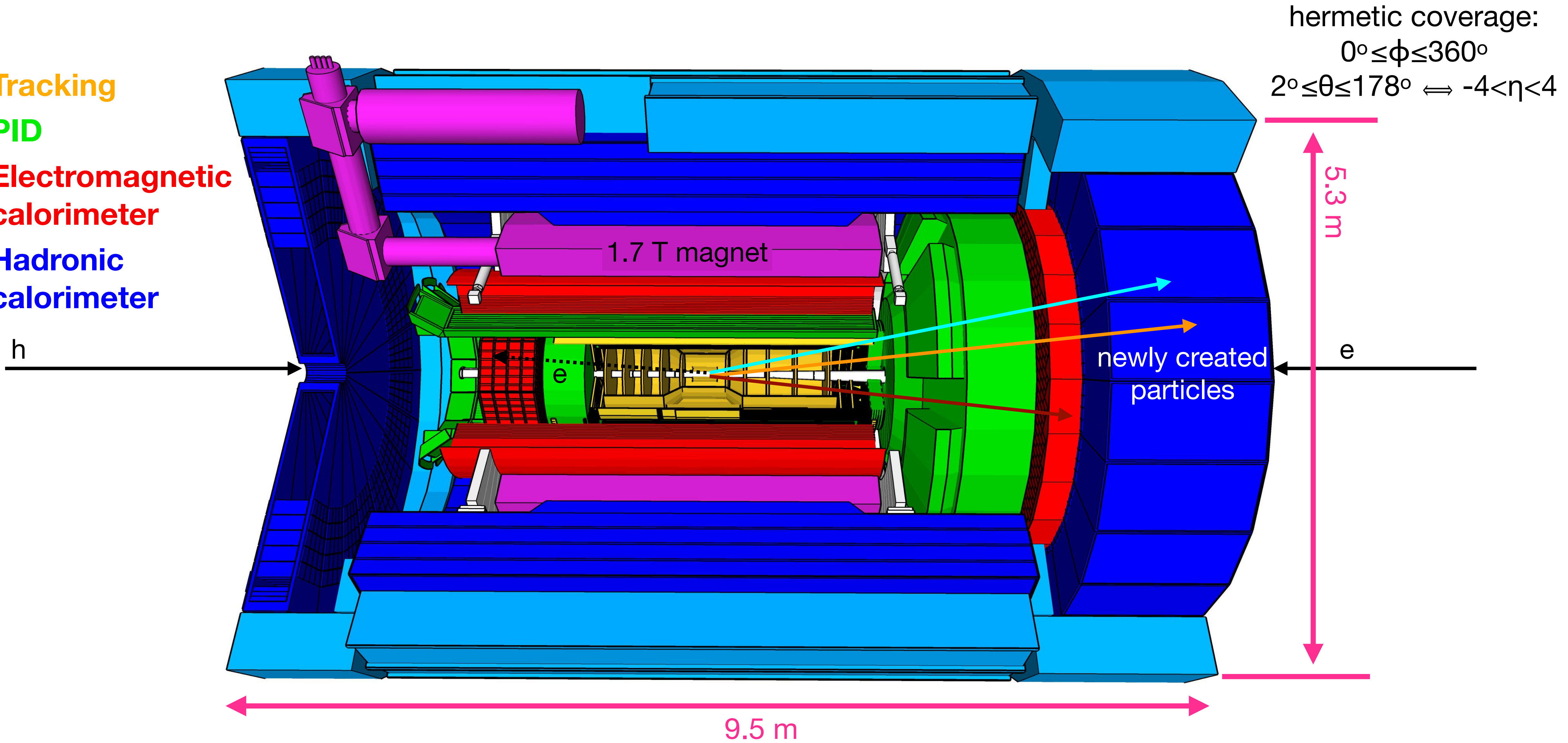


# The electron-proton/ion collider (ePIC) detector

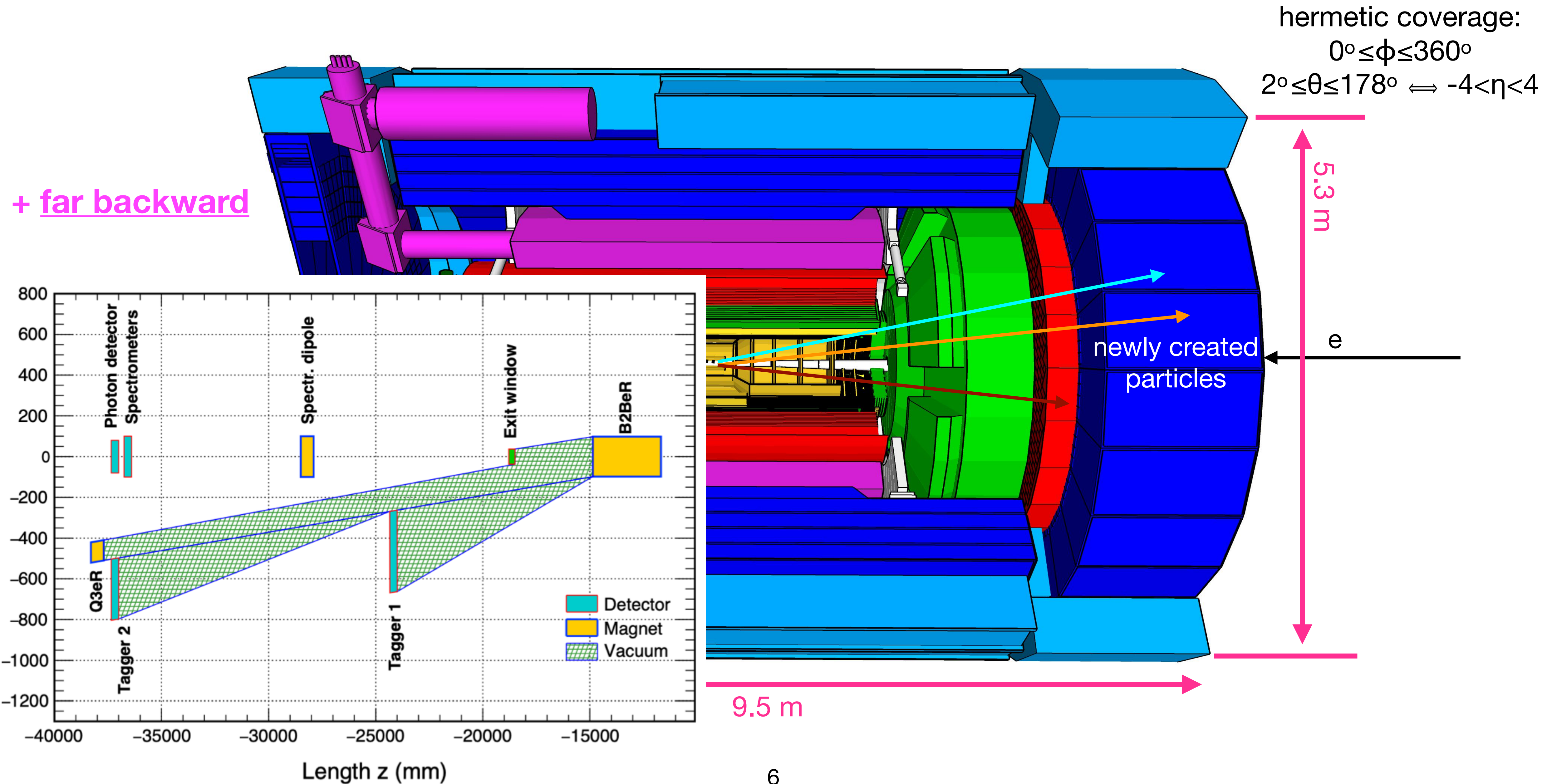


# The electron-proton/ion collider (ePIC) detector

- Tracking
- PID
- Electromagnetic calorimeter
- Hadronic calorimeter

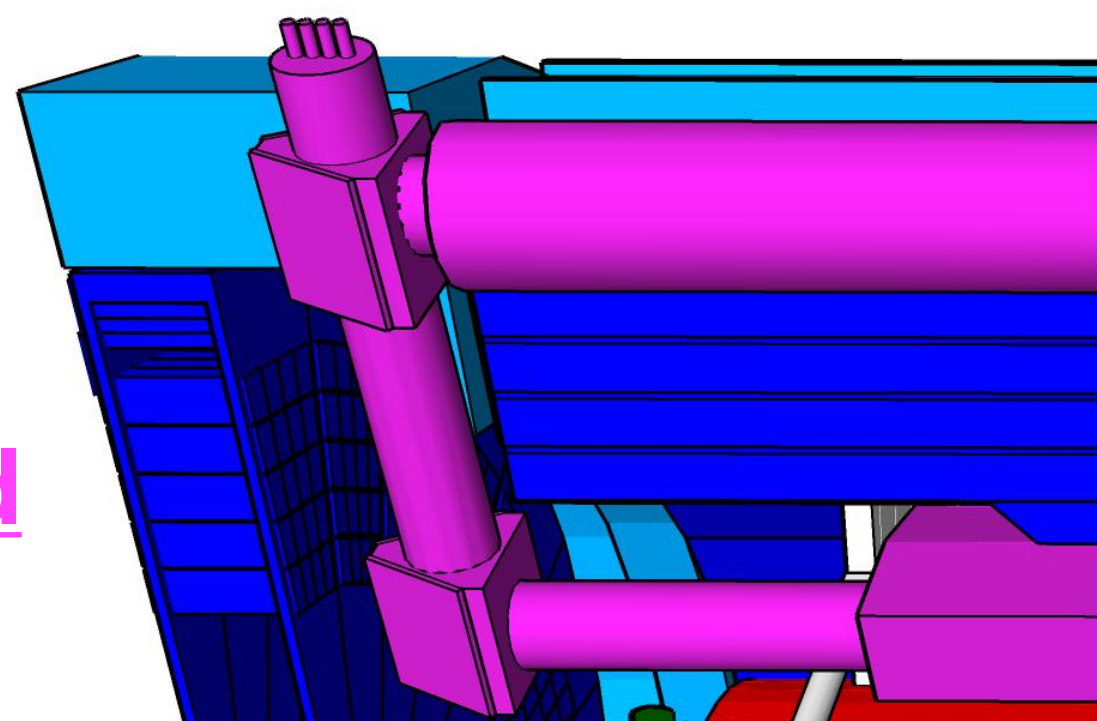


# The electron-proton/ion collider (ePIC) detector

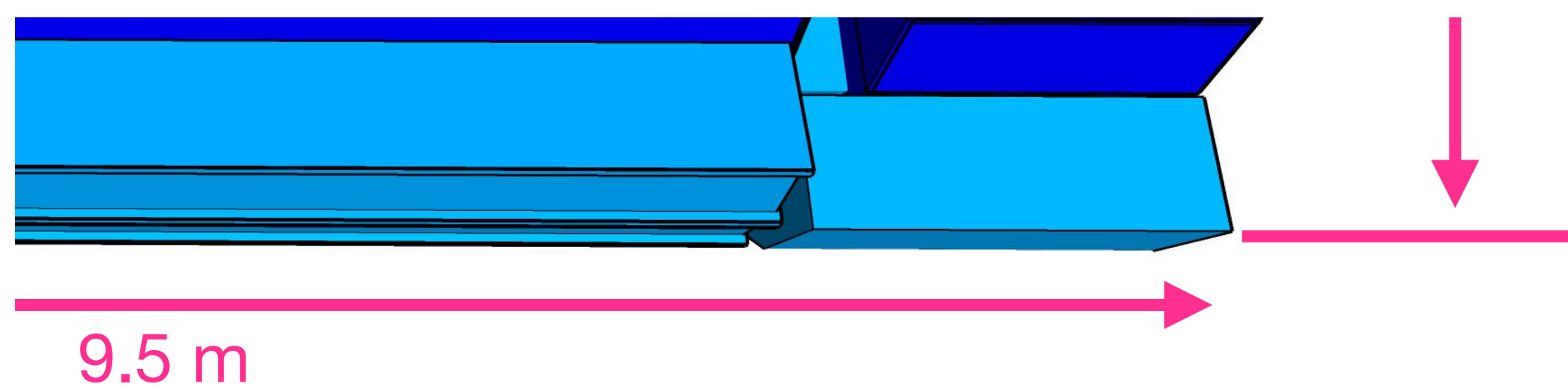
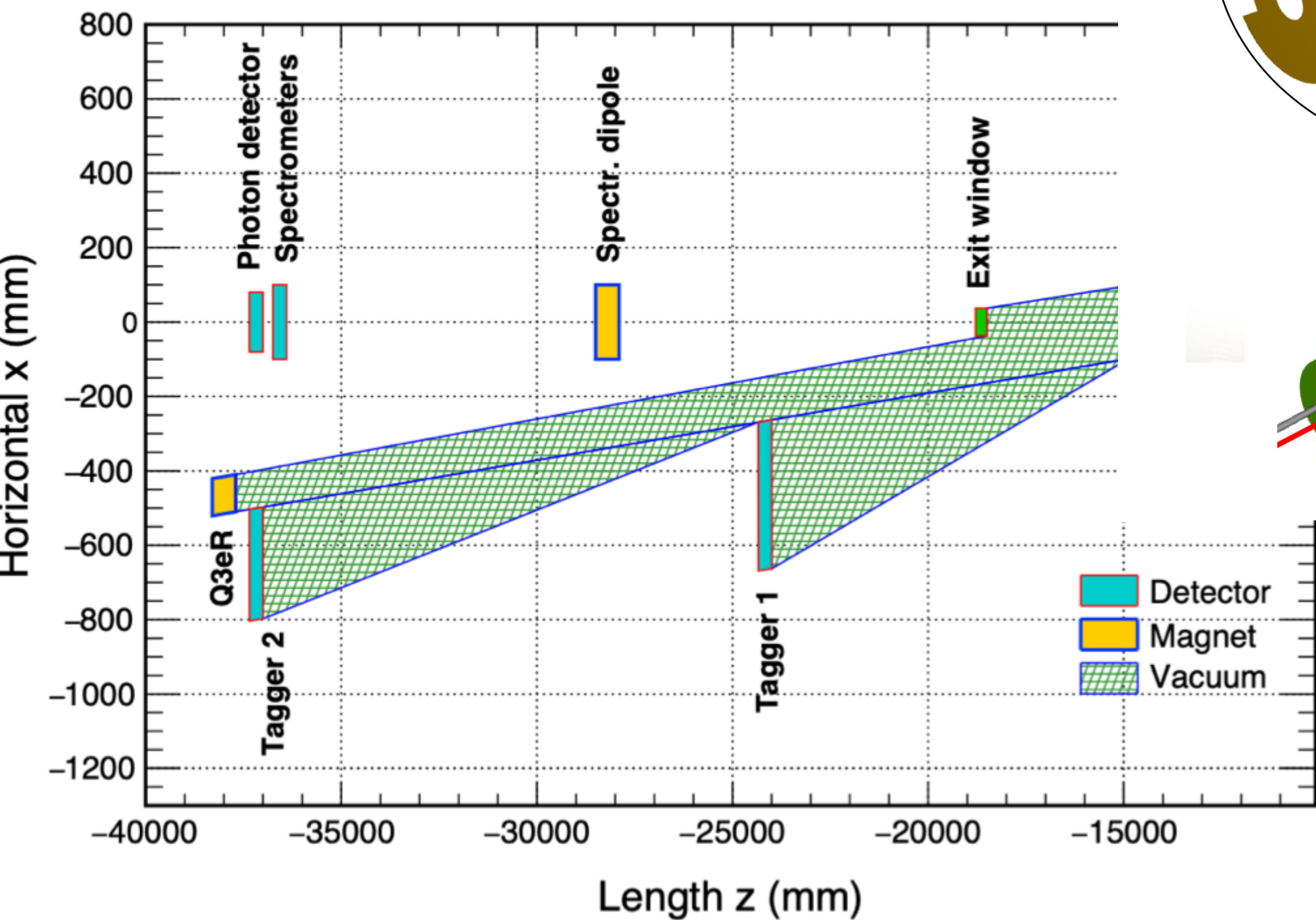
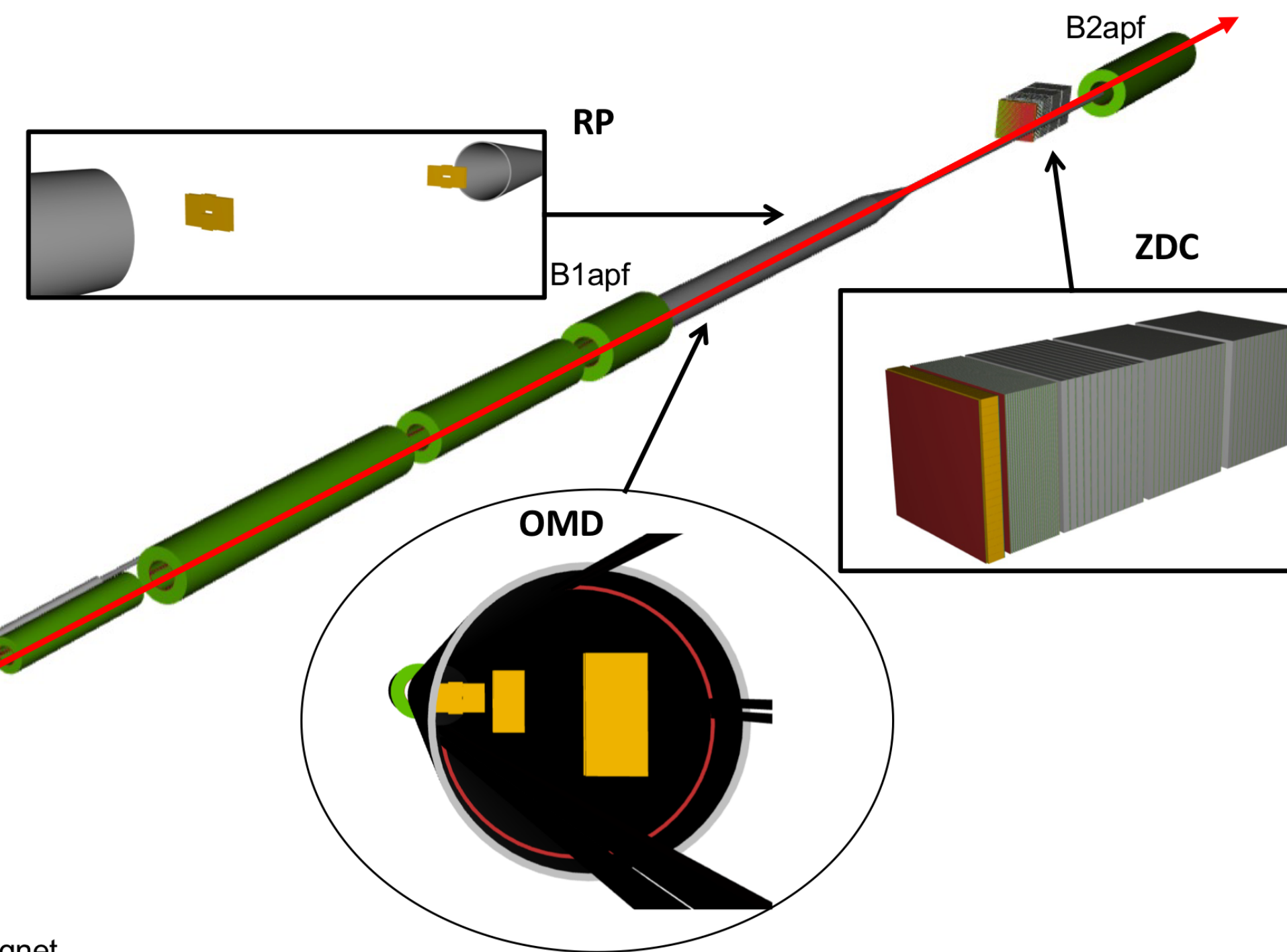
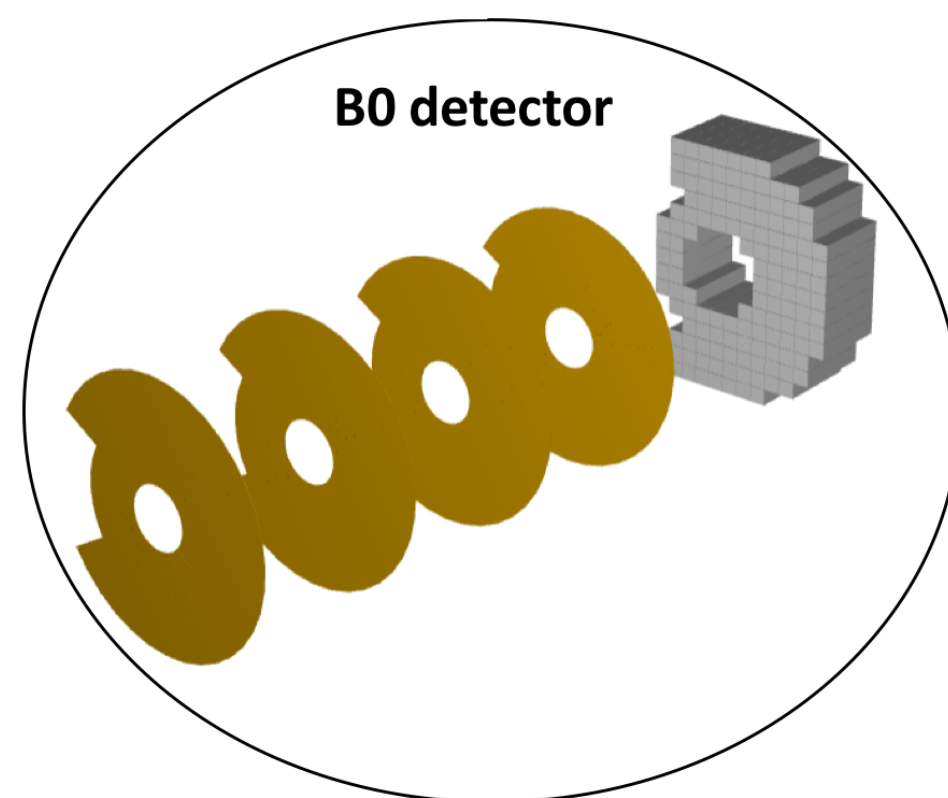


# The electron-proton/ion collider (ePIC) detector

+ far backward

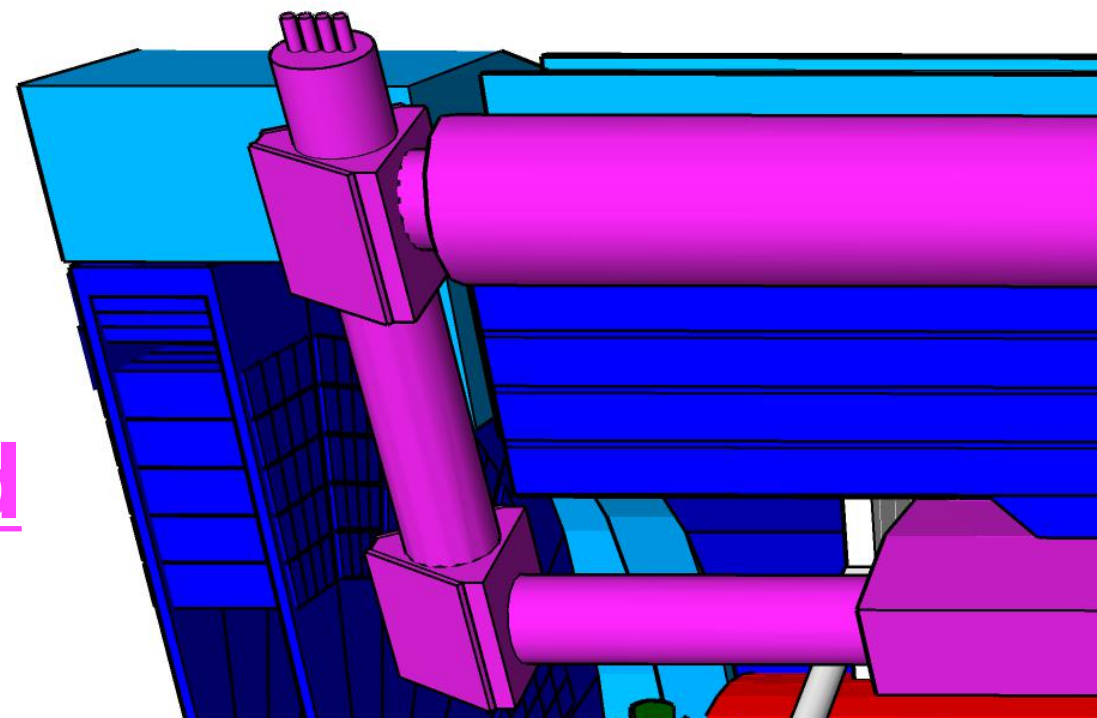


+ far forward

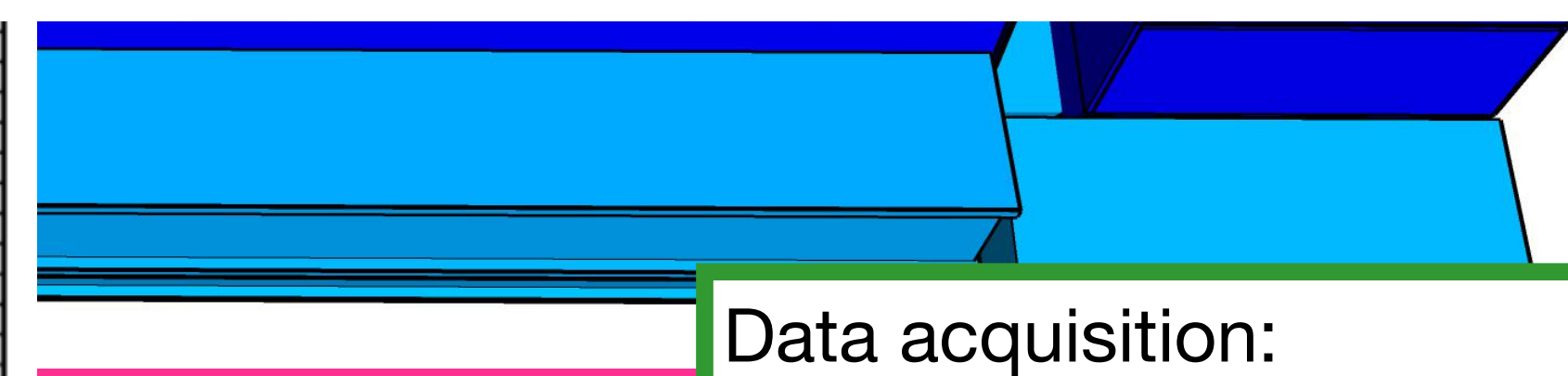
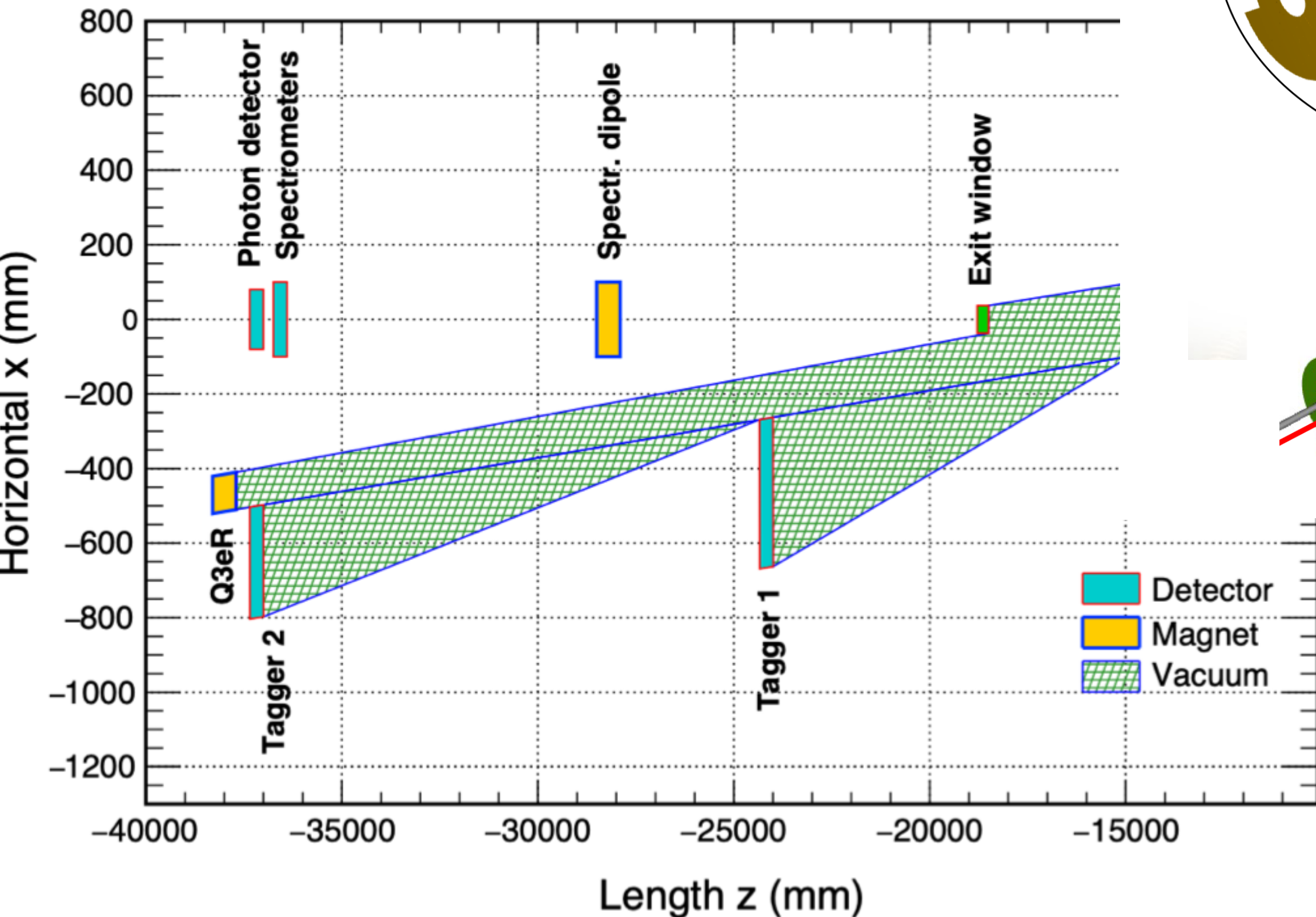
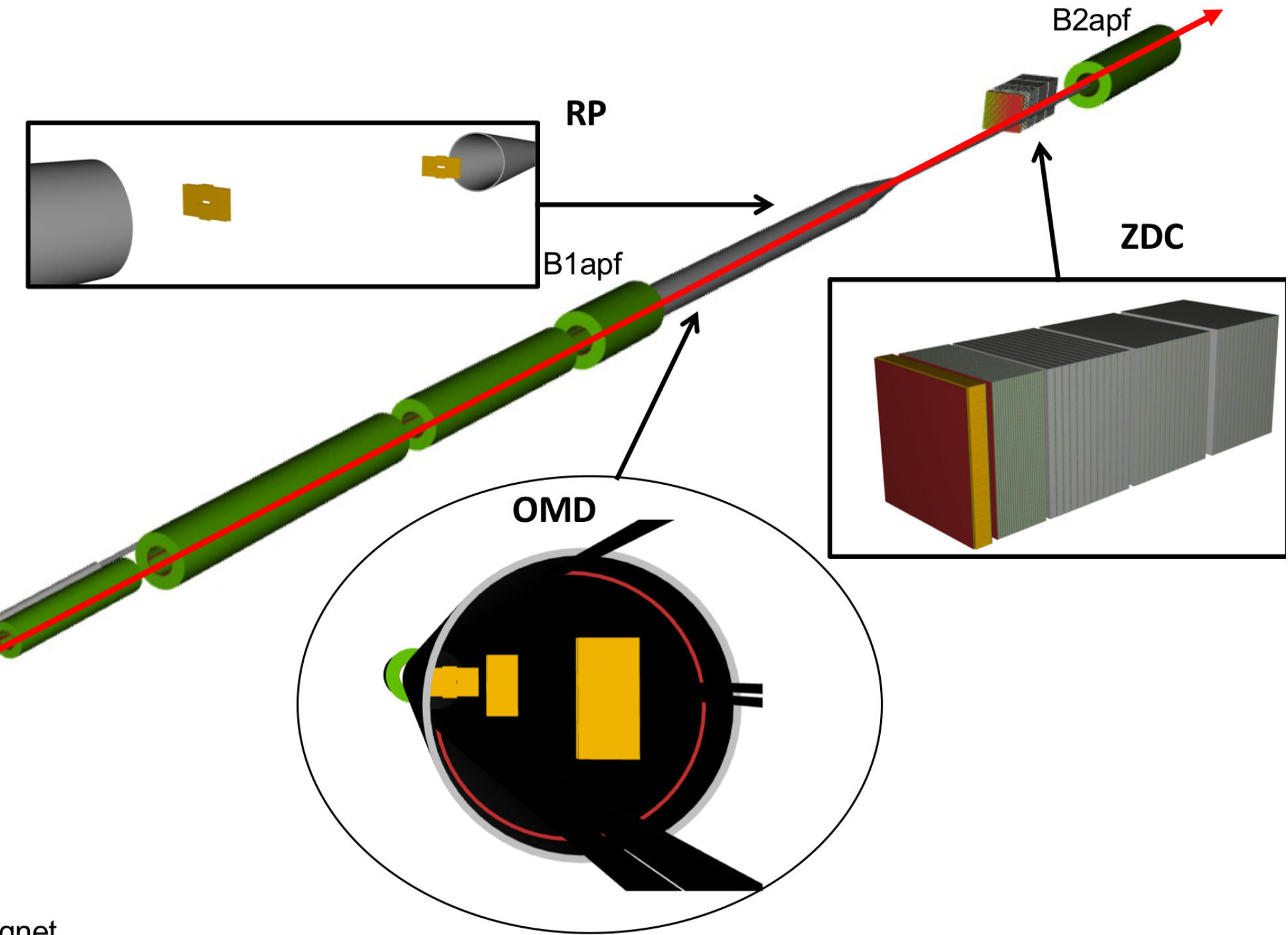
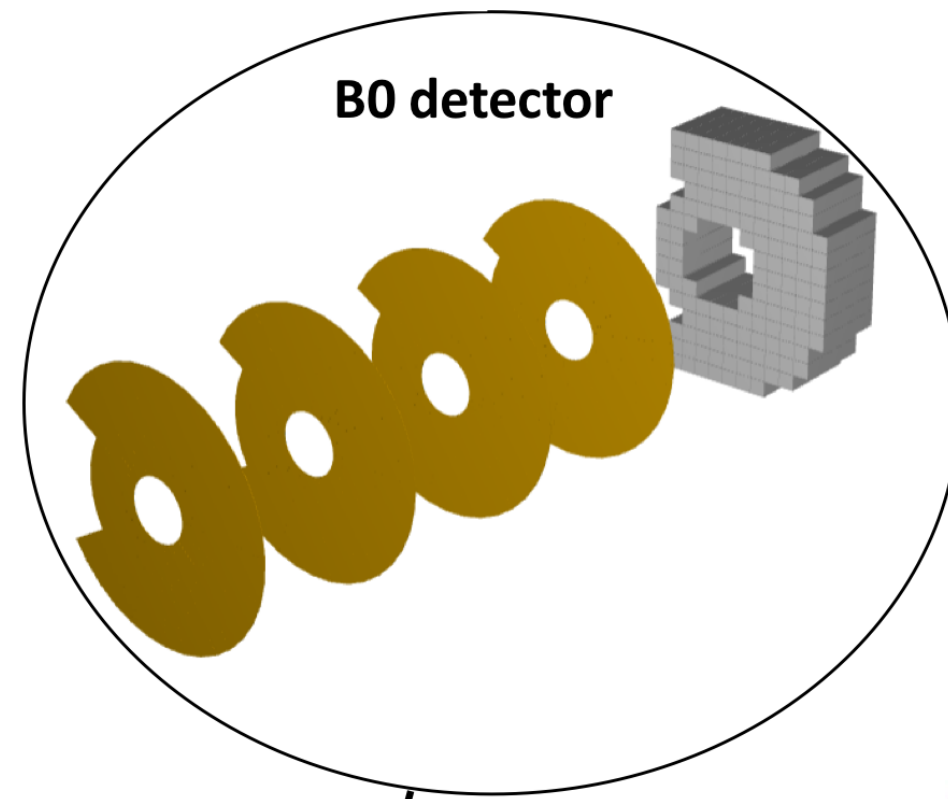


# The electron-proton/ion collider (ePIC) detector

+ far backward



+ far forward



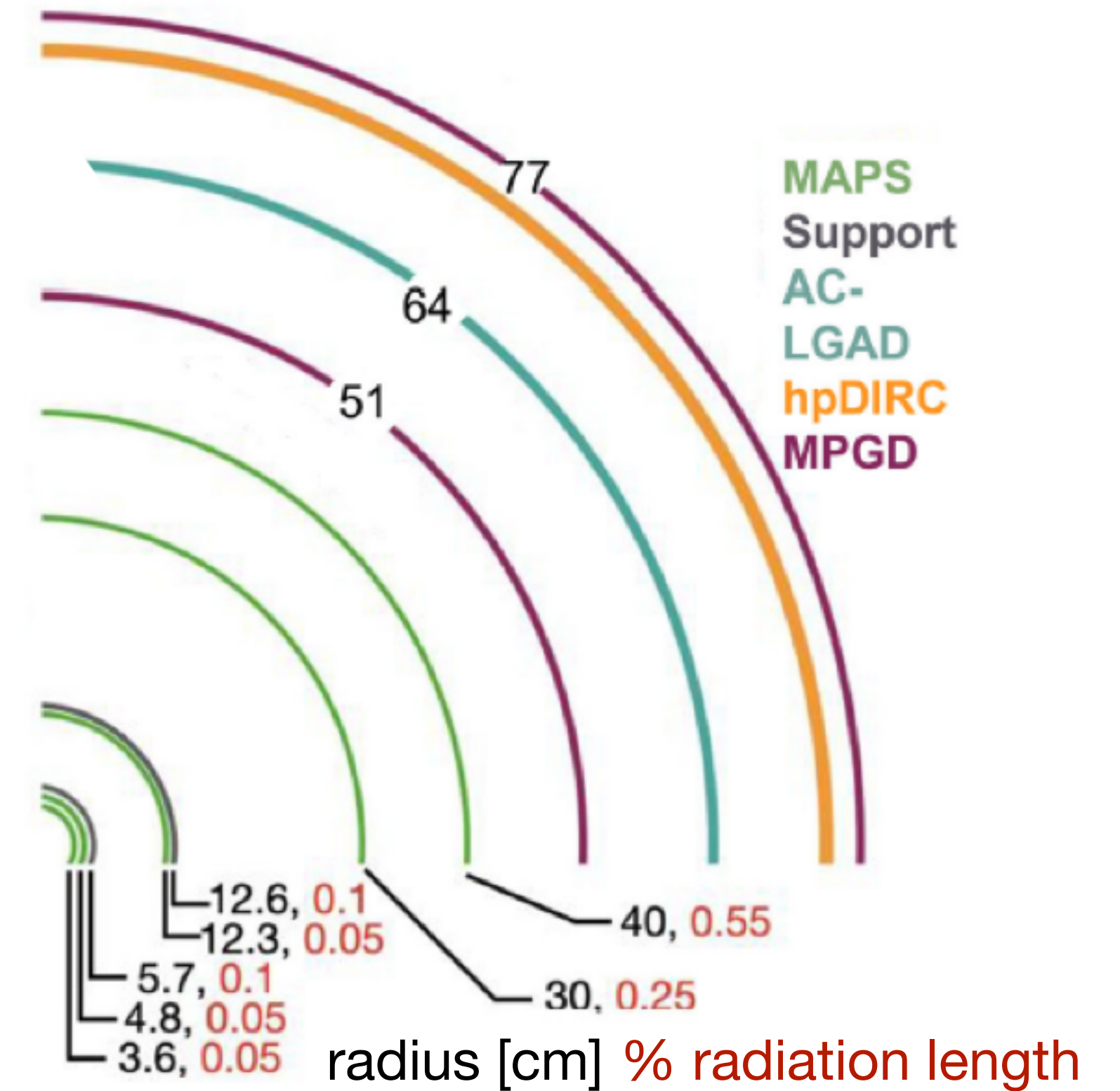
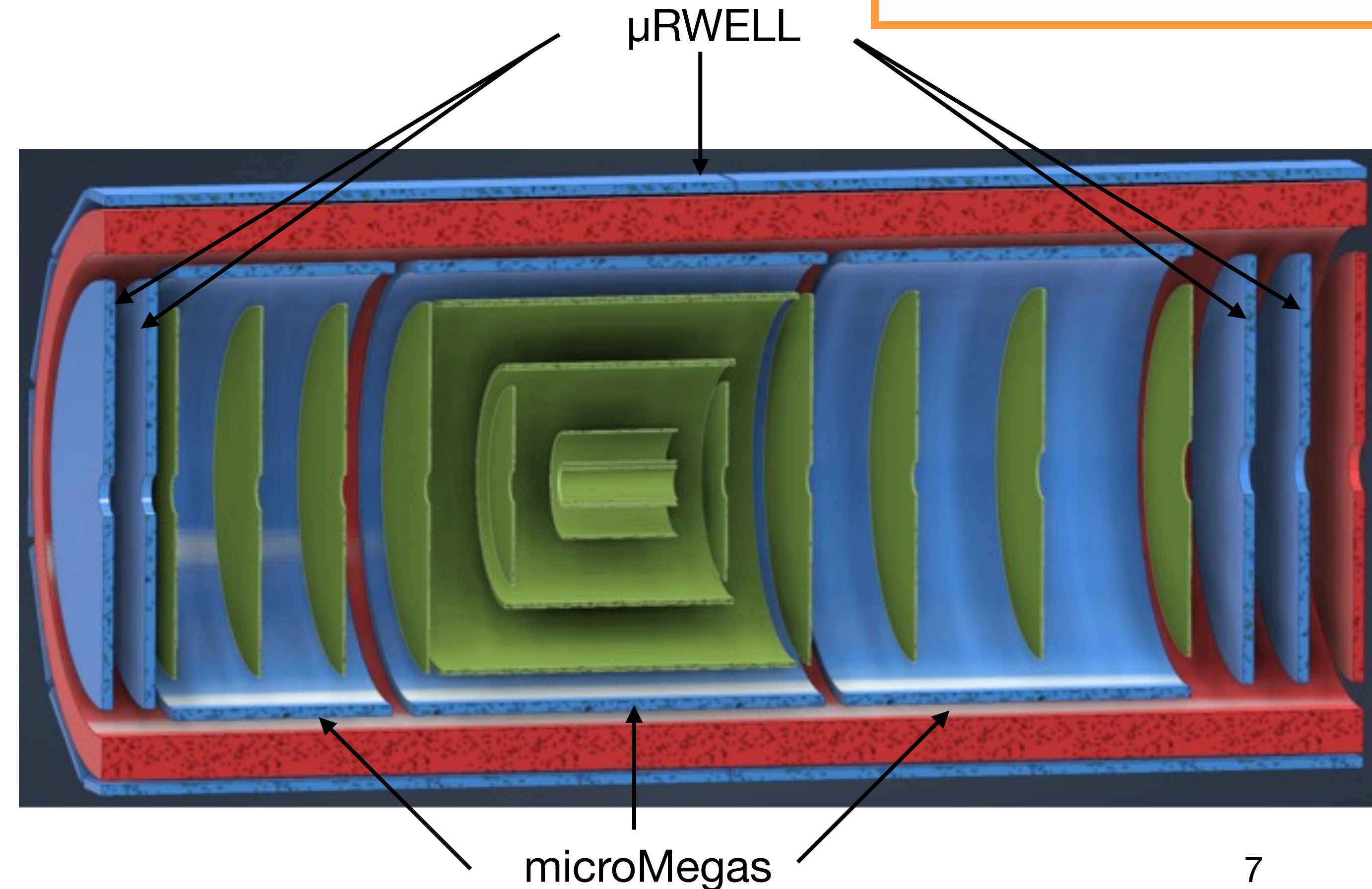
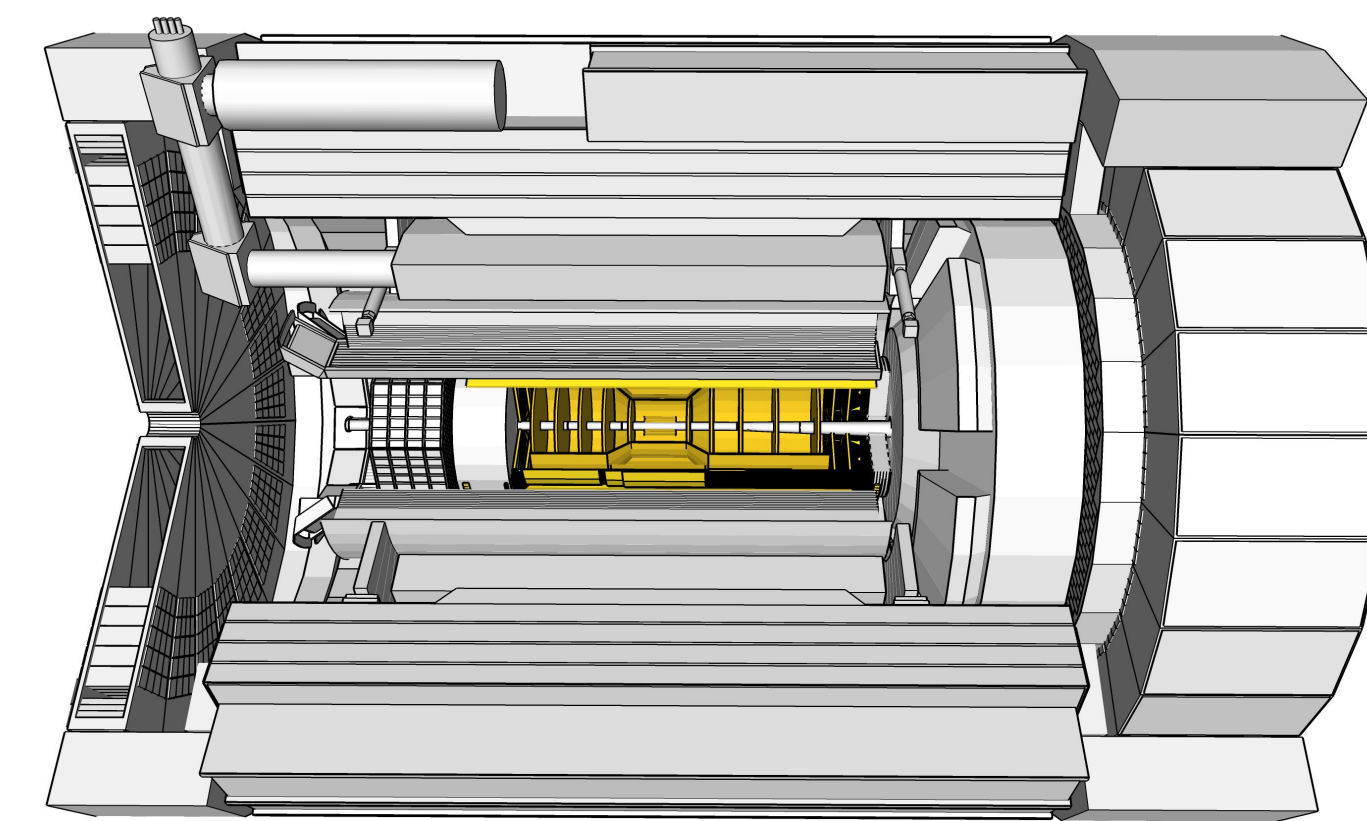
9.5 m

Data acquisition:  
no trigger  
all collision data is digitised  
with strong zero-suppression at front-end electronics



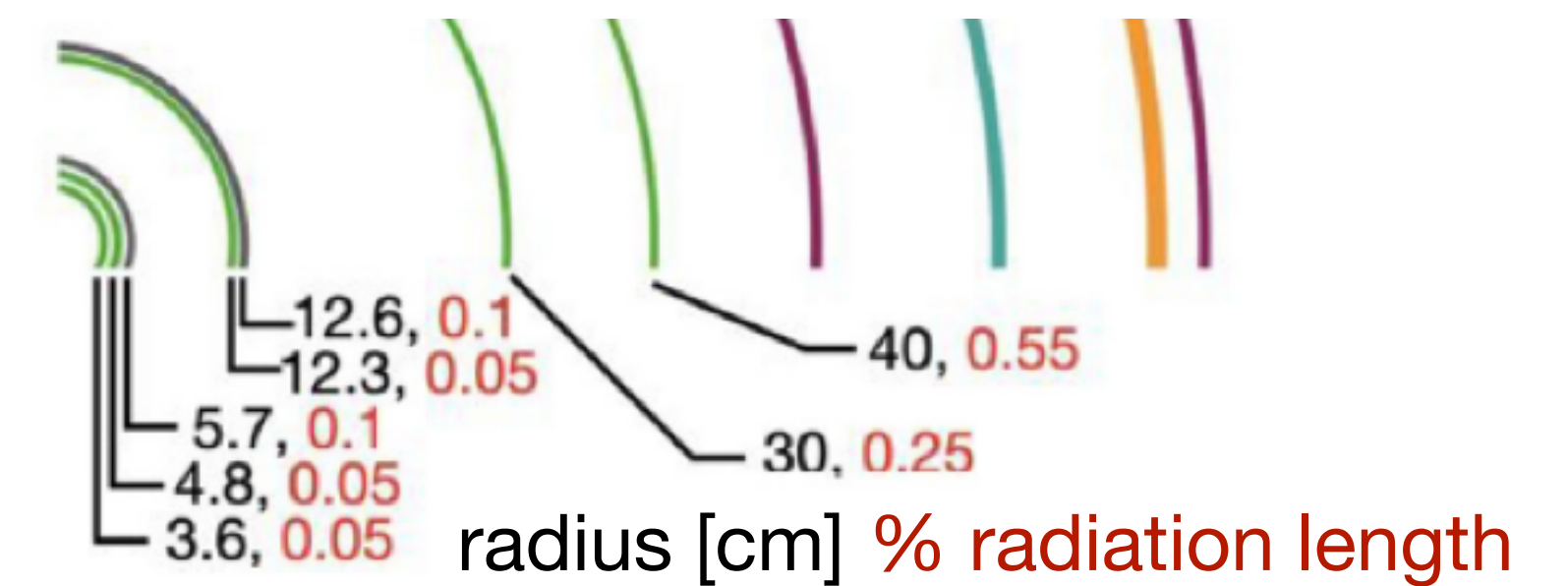
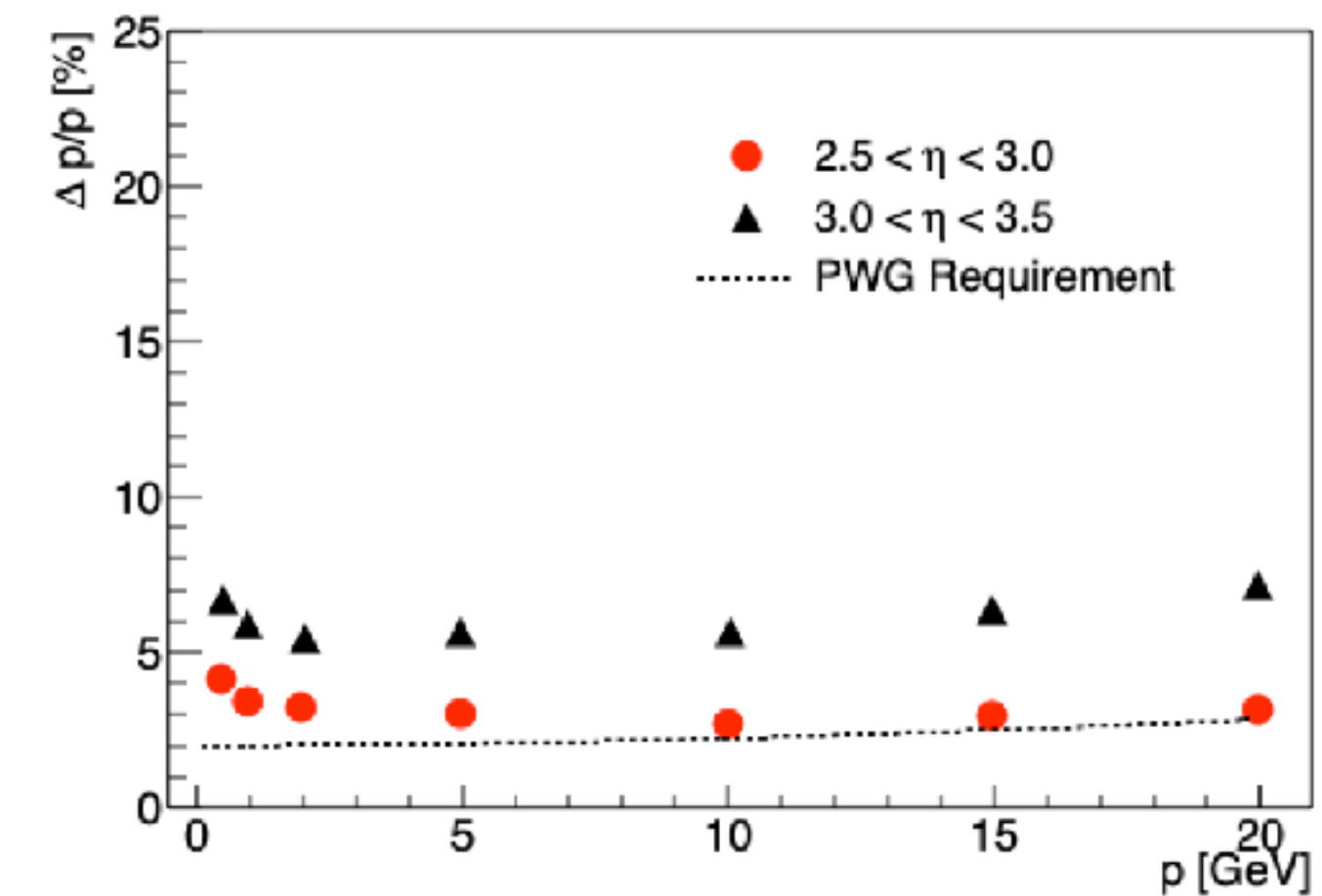
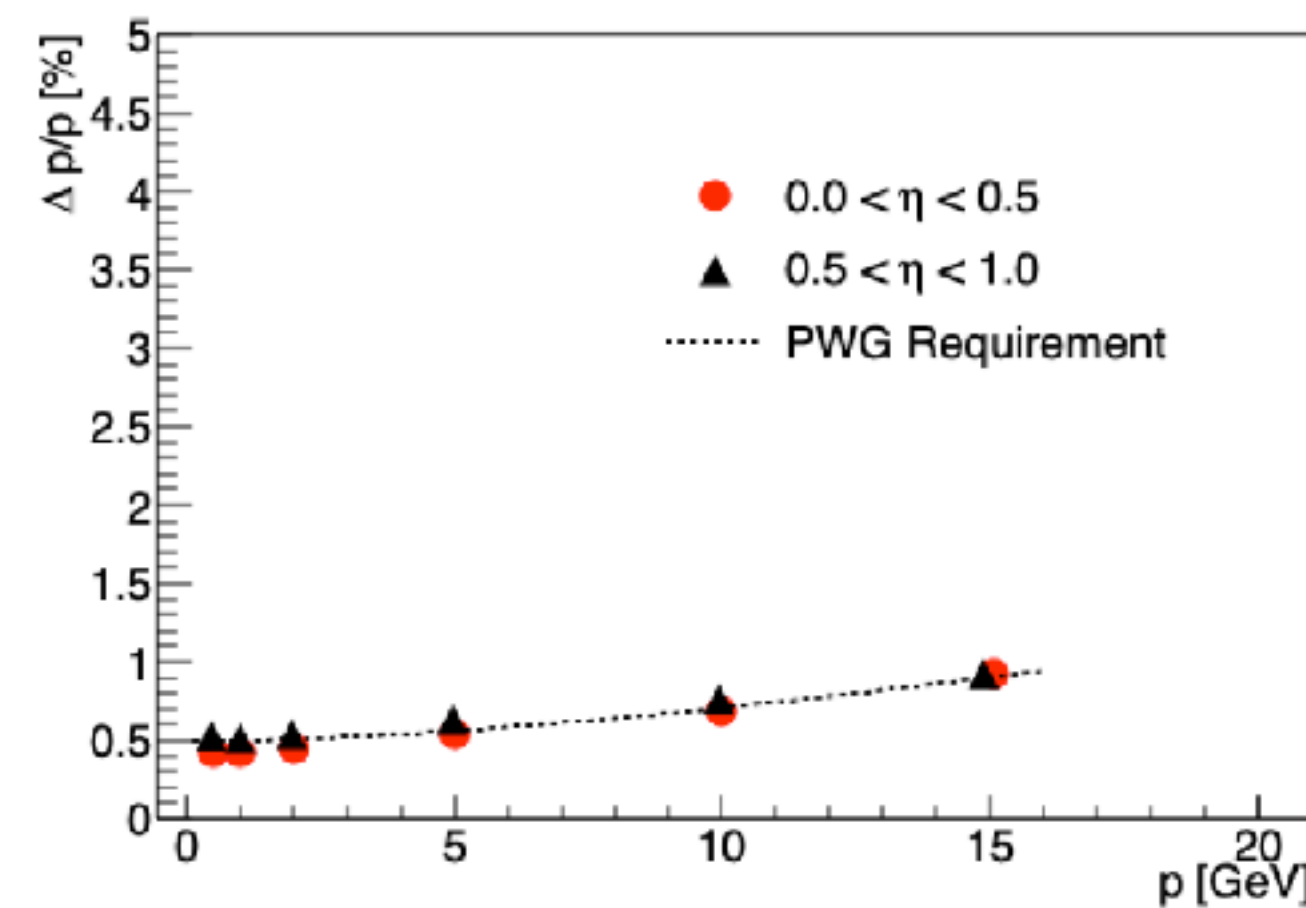
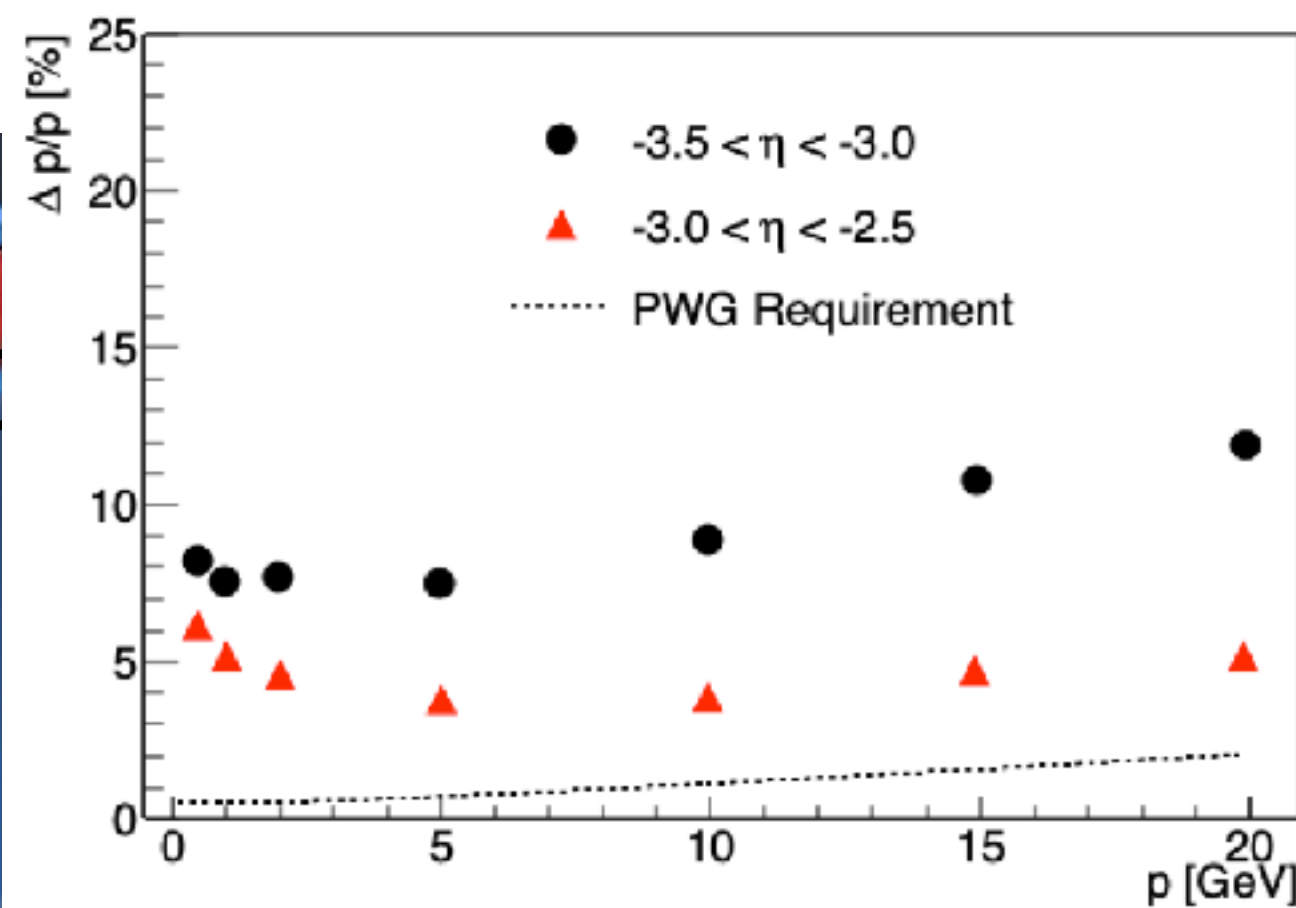
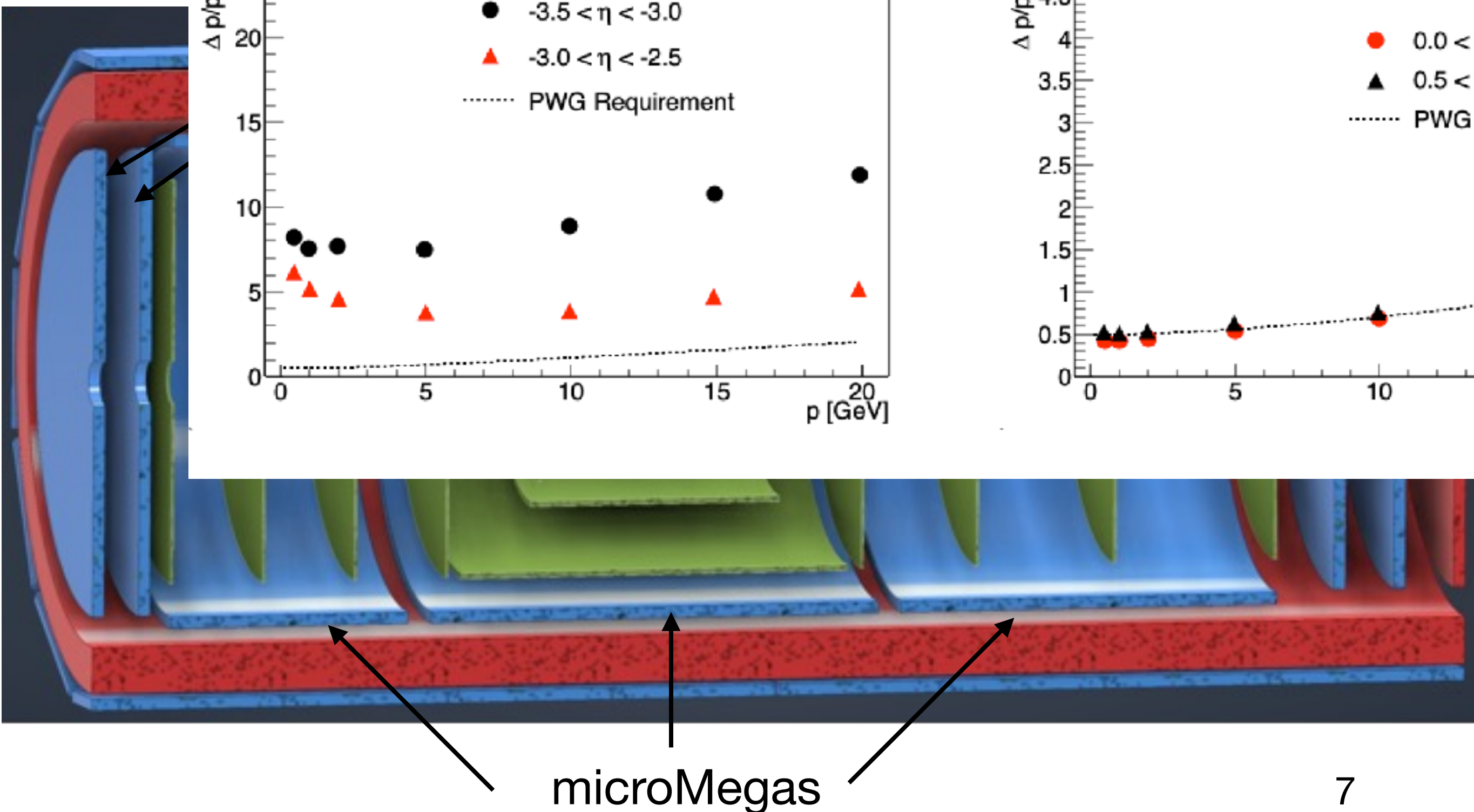
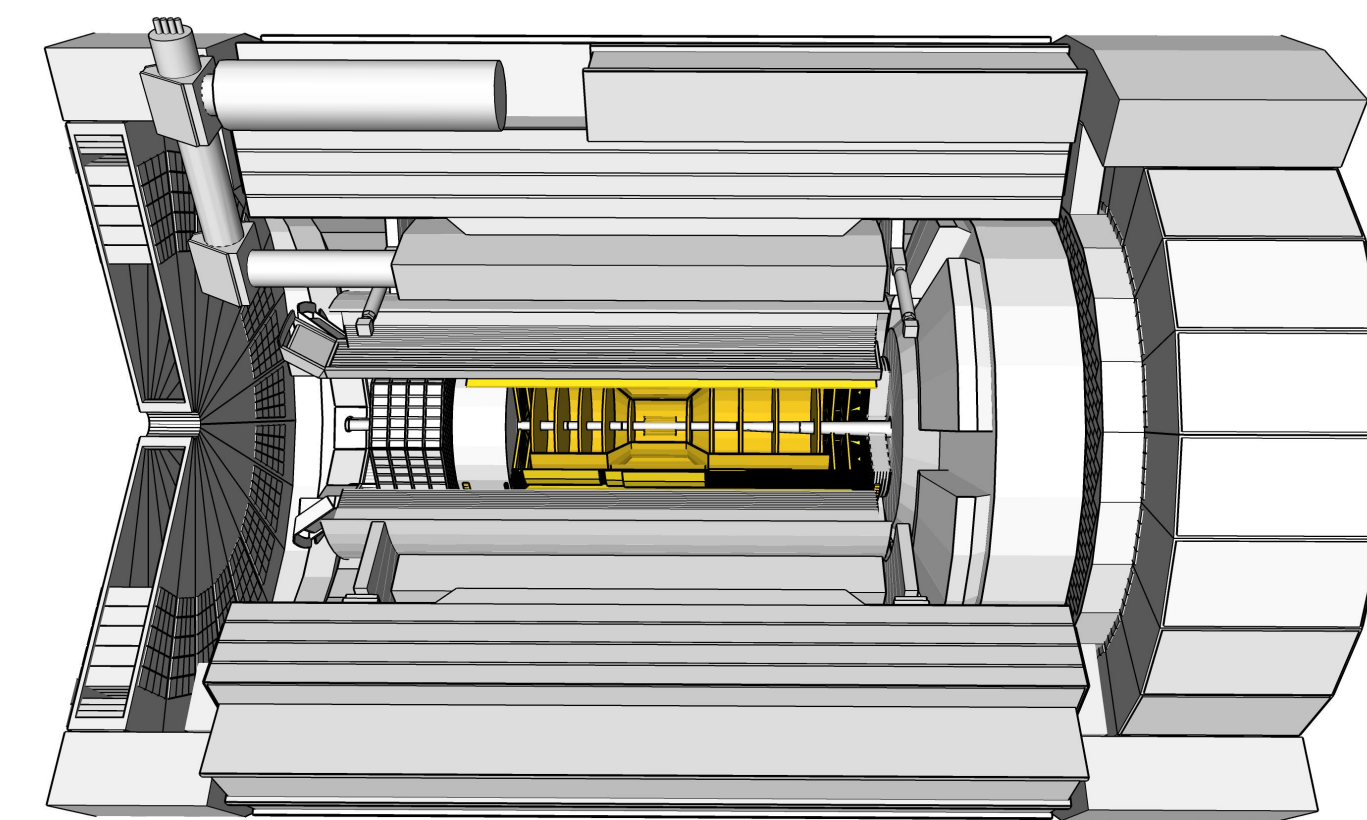
# Tracking system

- 1.7 T magnet
- Monolithic Active Pixel Sensor (MAPS)  
Silicon vertexing/inner tracker
- Micro-pattern gaseous detectors  
 $\mu$ RWELL/microMegas:  
timing & pattern recognition
- AC-LGAD based TOF:  
PID & additional tracking point



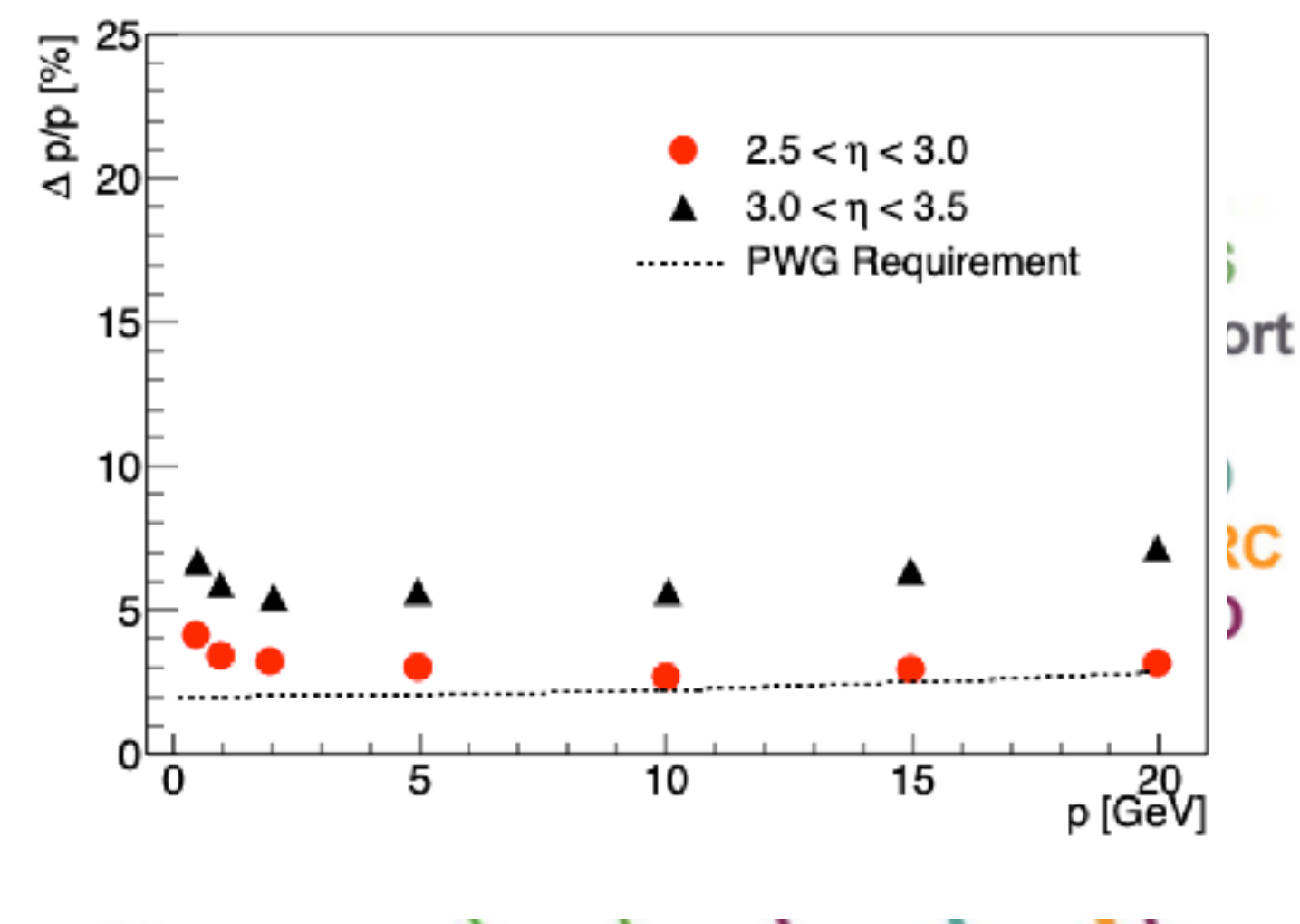
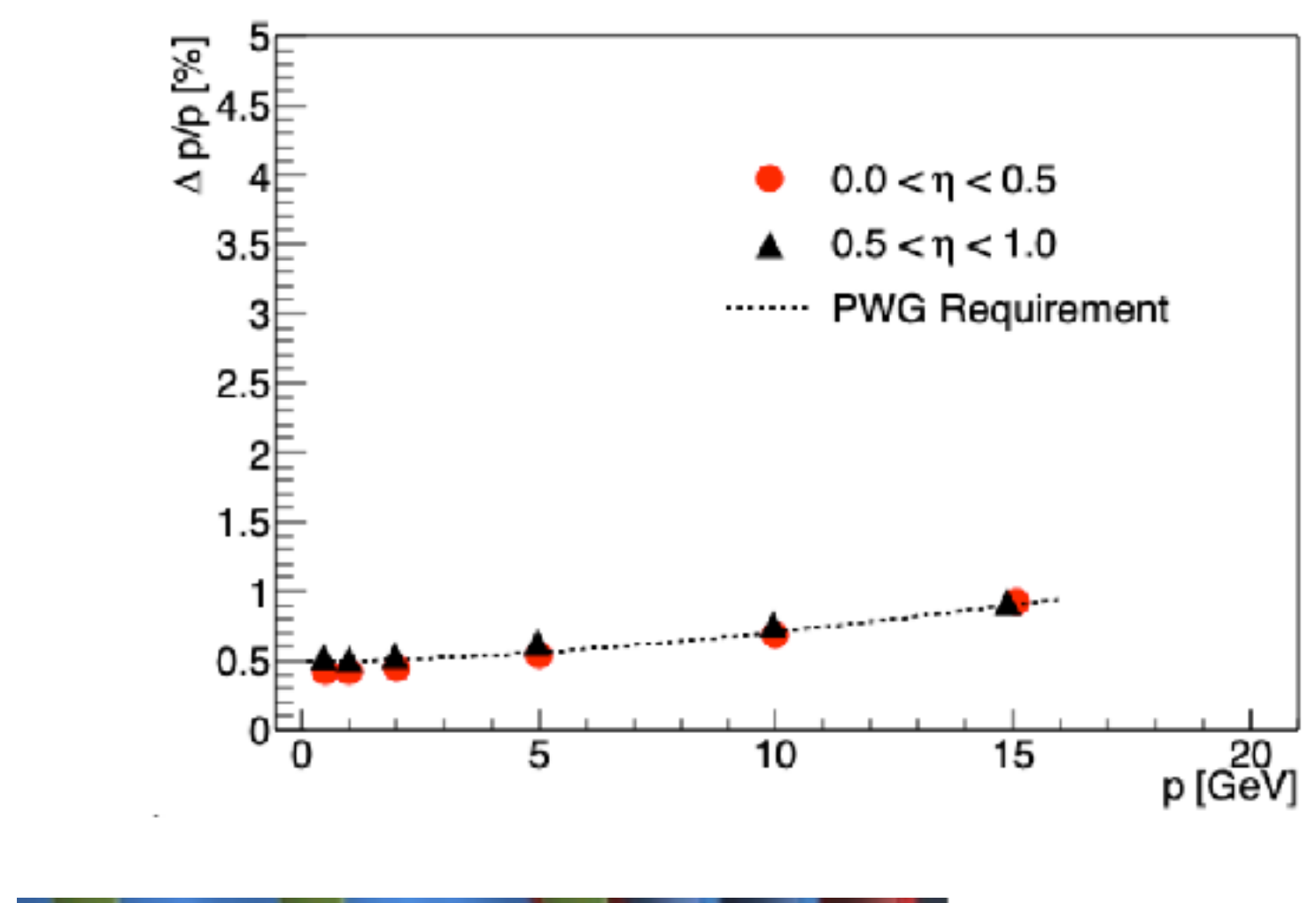
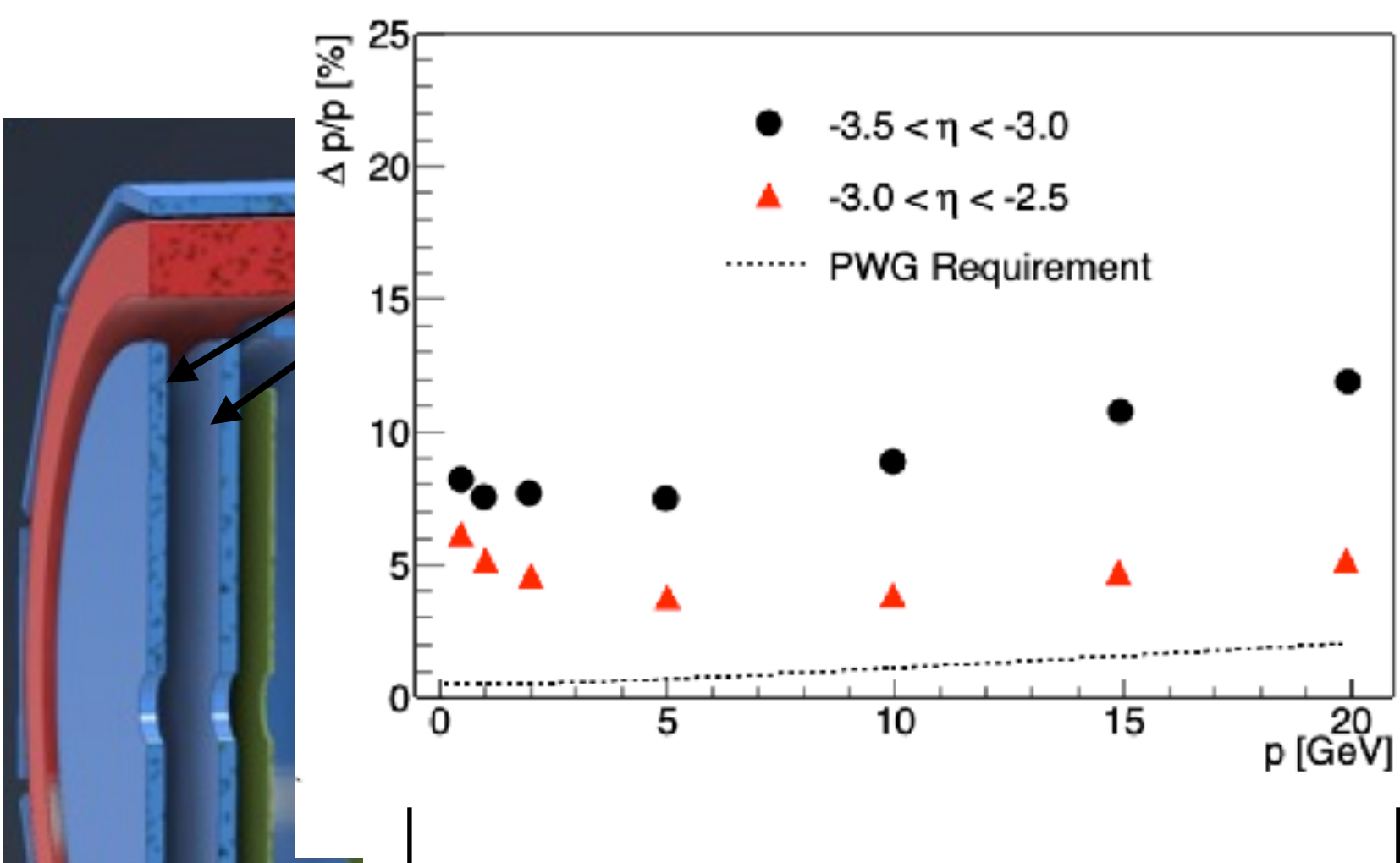
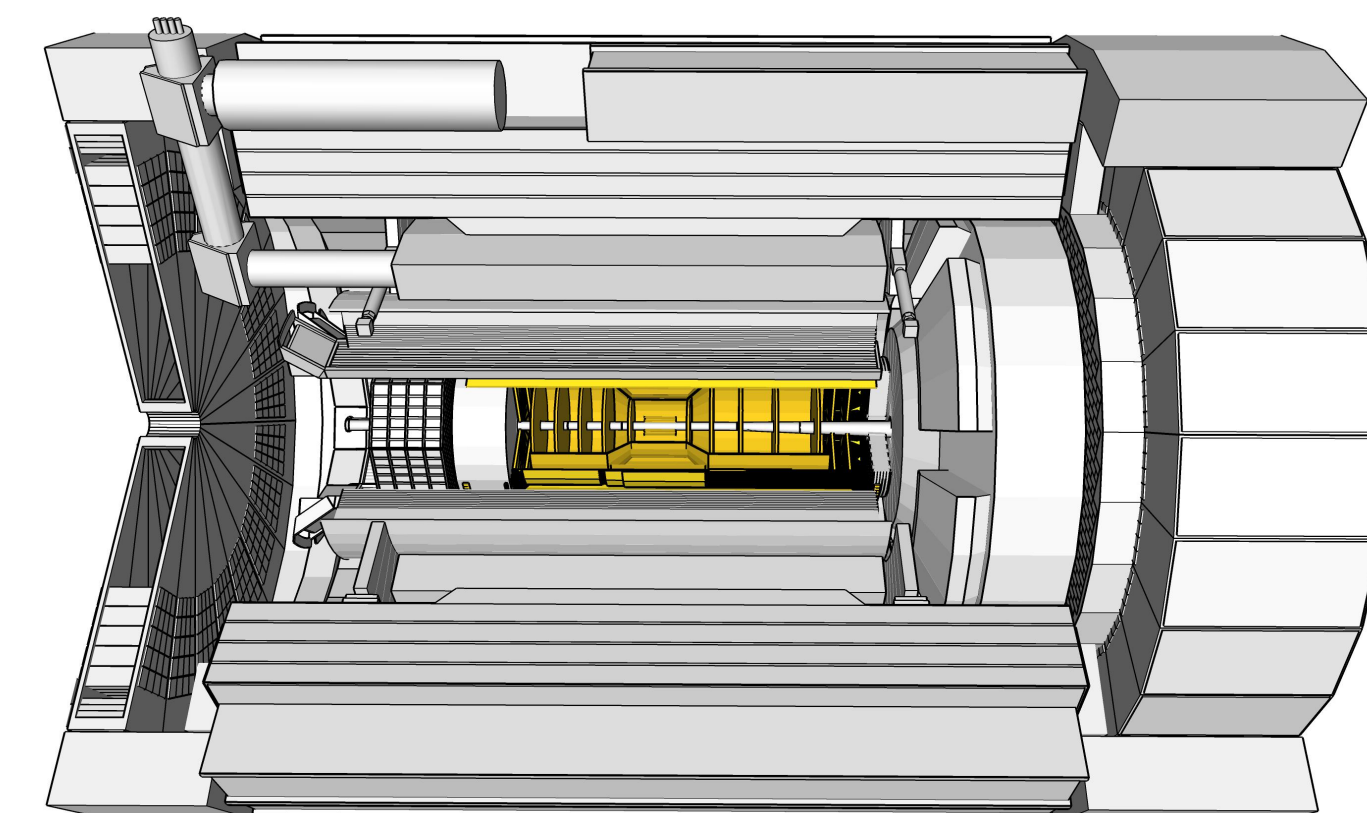
# Tracking system

- 1.7 T magnet
- Monolithic Active Pixel Sensor (MAPS)  
Silicon vertexing/inner tracker
- Micro-pattern gaseous detectors  
 $\mu$ RWELL/microMegas:  
timing & pattern recognition
- AC-LGAD based TOF:  
PID & additional tracking point  
momentum resolution



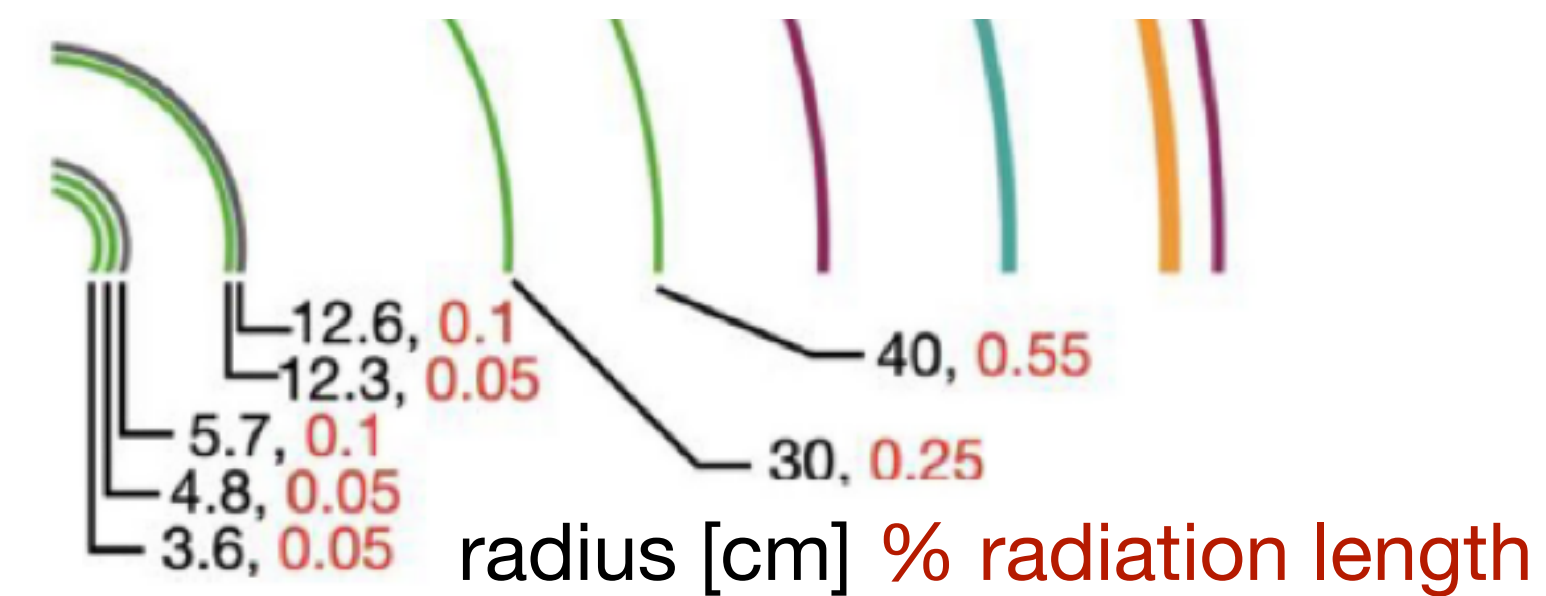
# Tracking system

- 1.7 T magnet
- Monolithic Active Pixel Sensor (MAPS)  
Silicon vertexing/inner tracker
- Micro-pattern gaseous detectors  
 $\mu$ RWELL/microMegas:  
timing & pattern recognition
- AC-LGAD based TOF:  
PID & additional tracking point  
momentum resolution

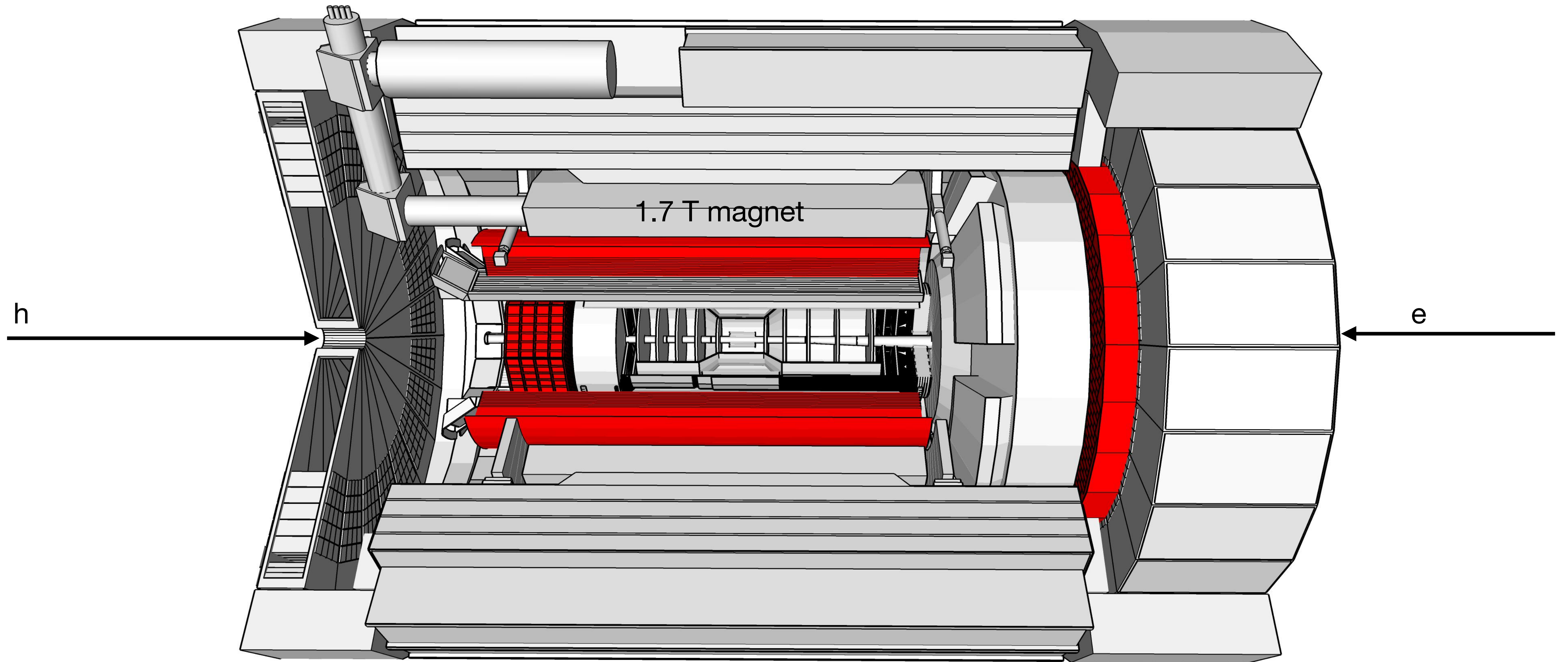


complemented with electromagnetic calorimeter

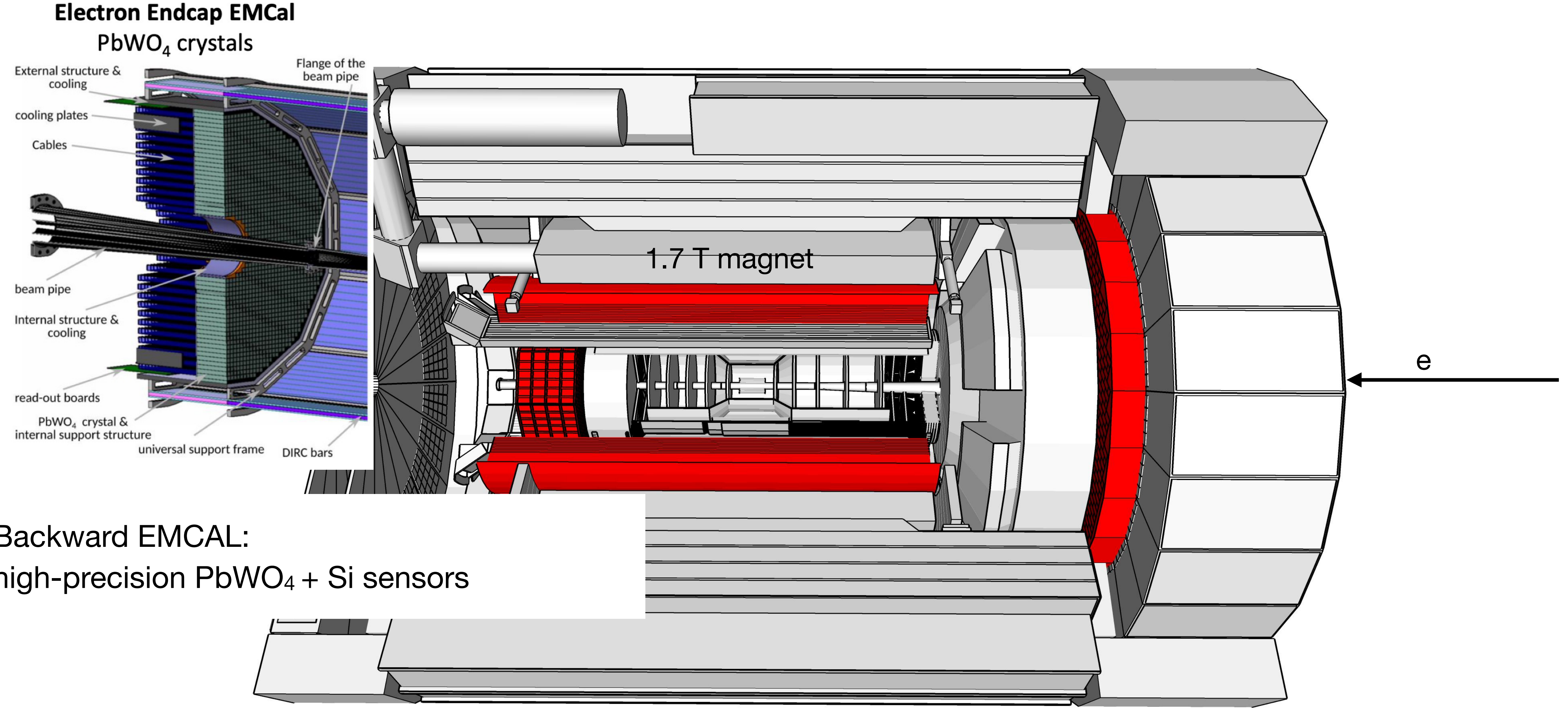
microMegas



# Electromagnetic calorimeter

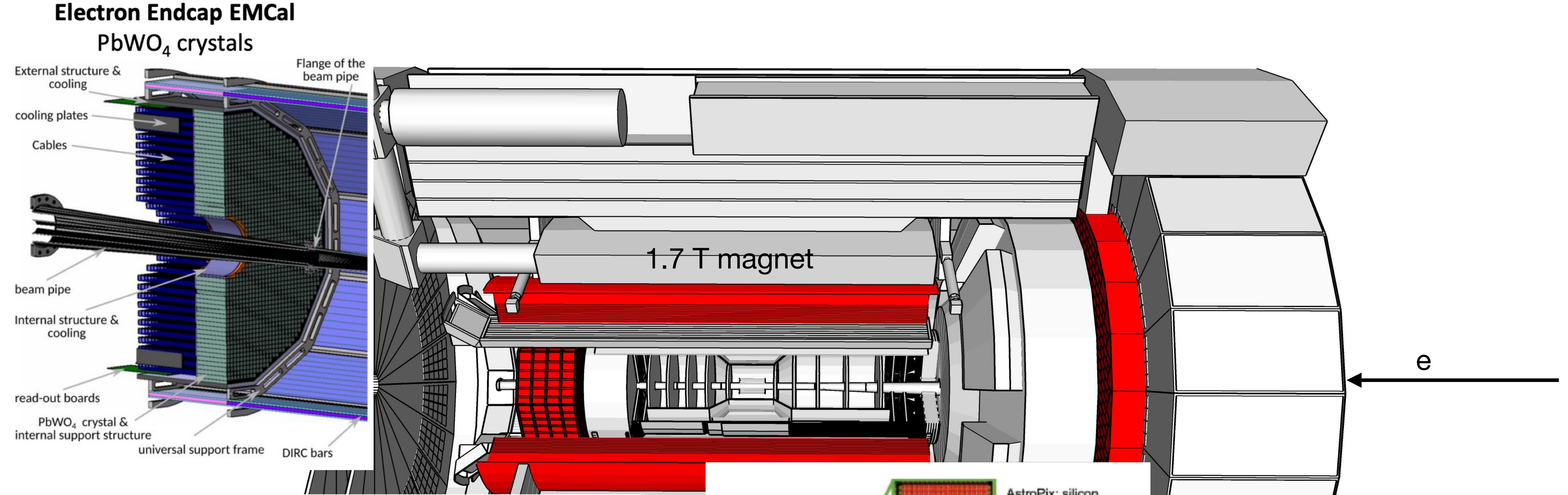


# Electromagnetic calorimeter

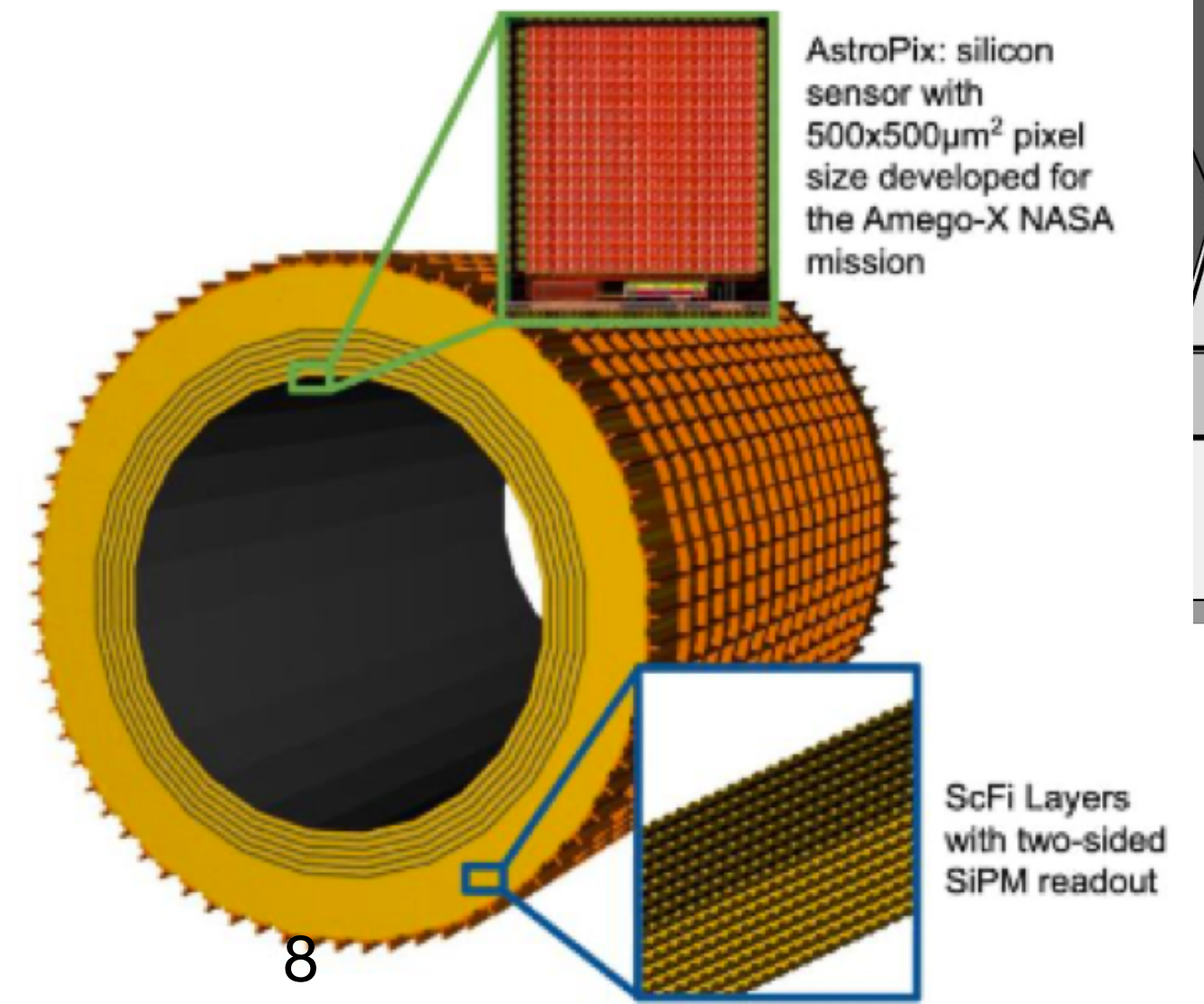


- Backward EMCAL:  
high-precision PbWO<sub>4</sub> + Si sensors

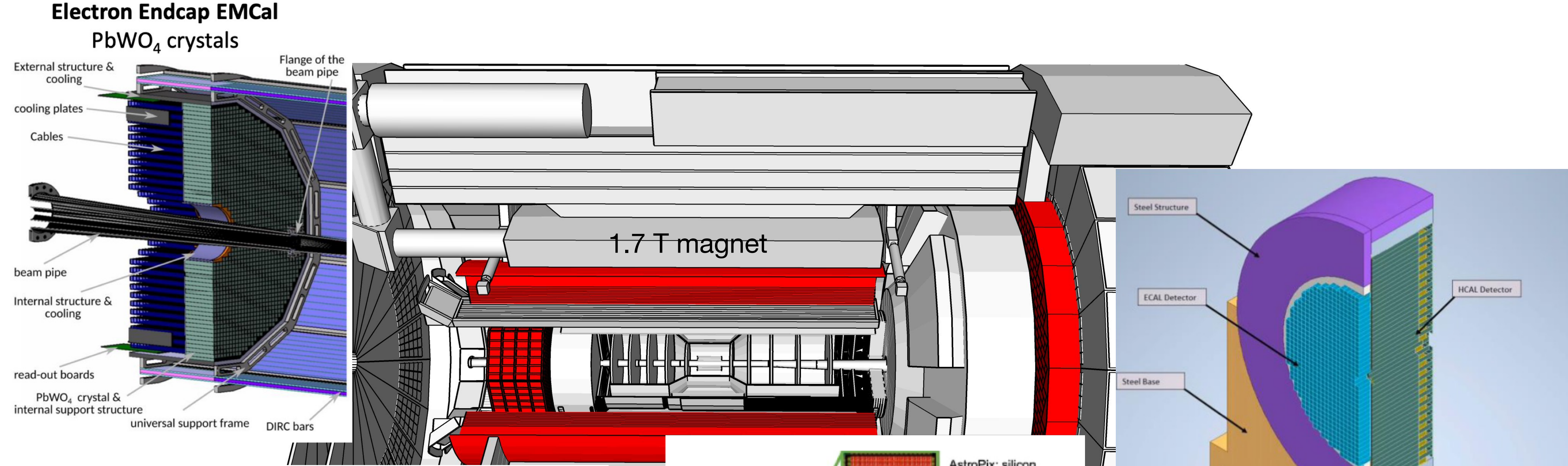
# Electromagnetic calorimeter



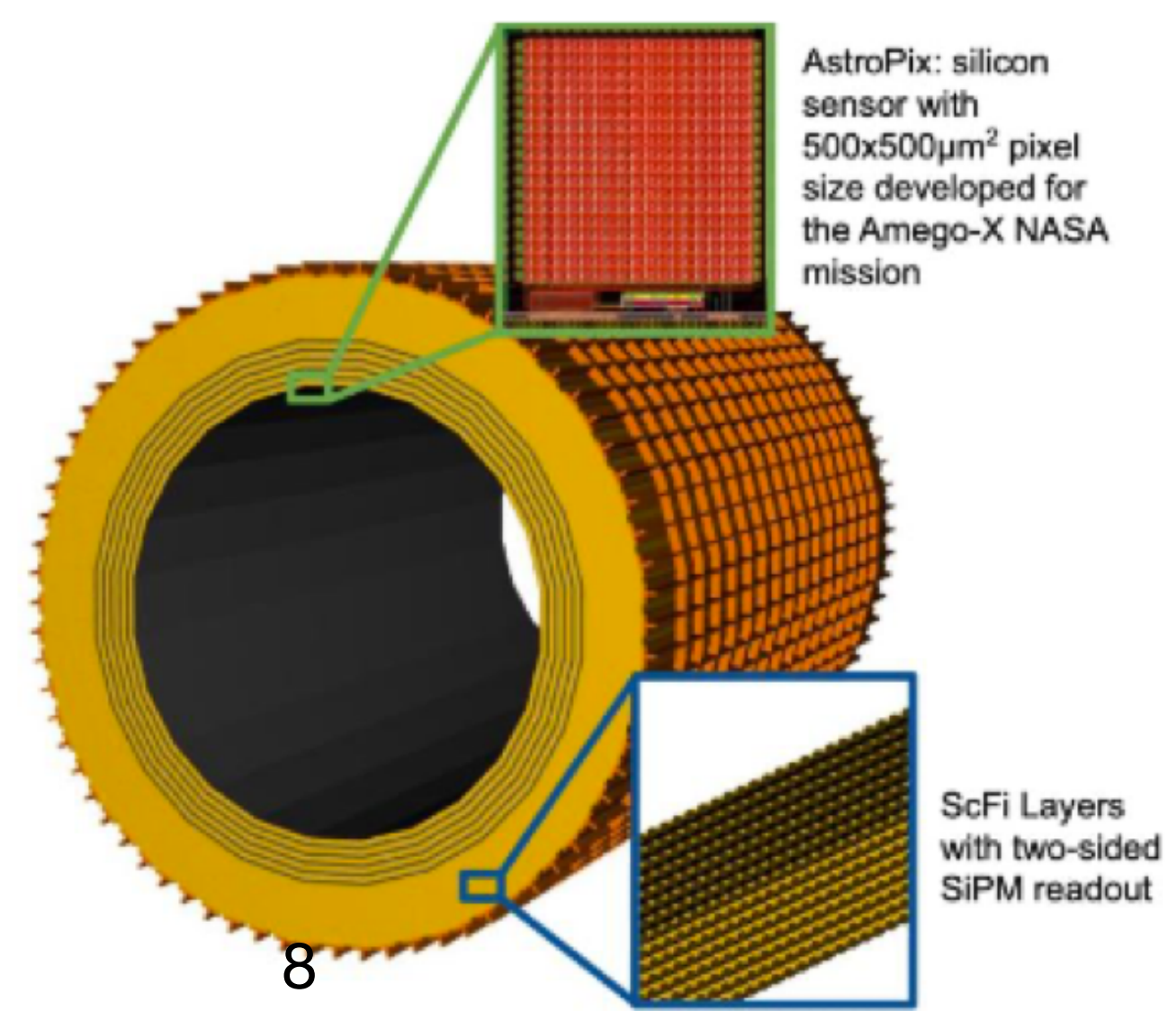
- Backward EMCAL:  
high-precision PbWO<sub>4</sub> + Si sensors
- Barrel EMCAL:  
3D imaging with MAPS and sampling Pb/  
scintillating fibres with Si sensors



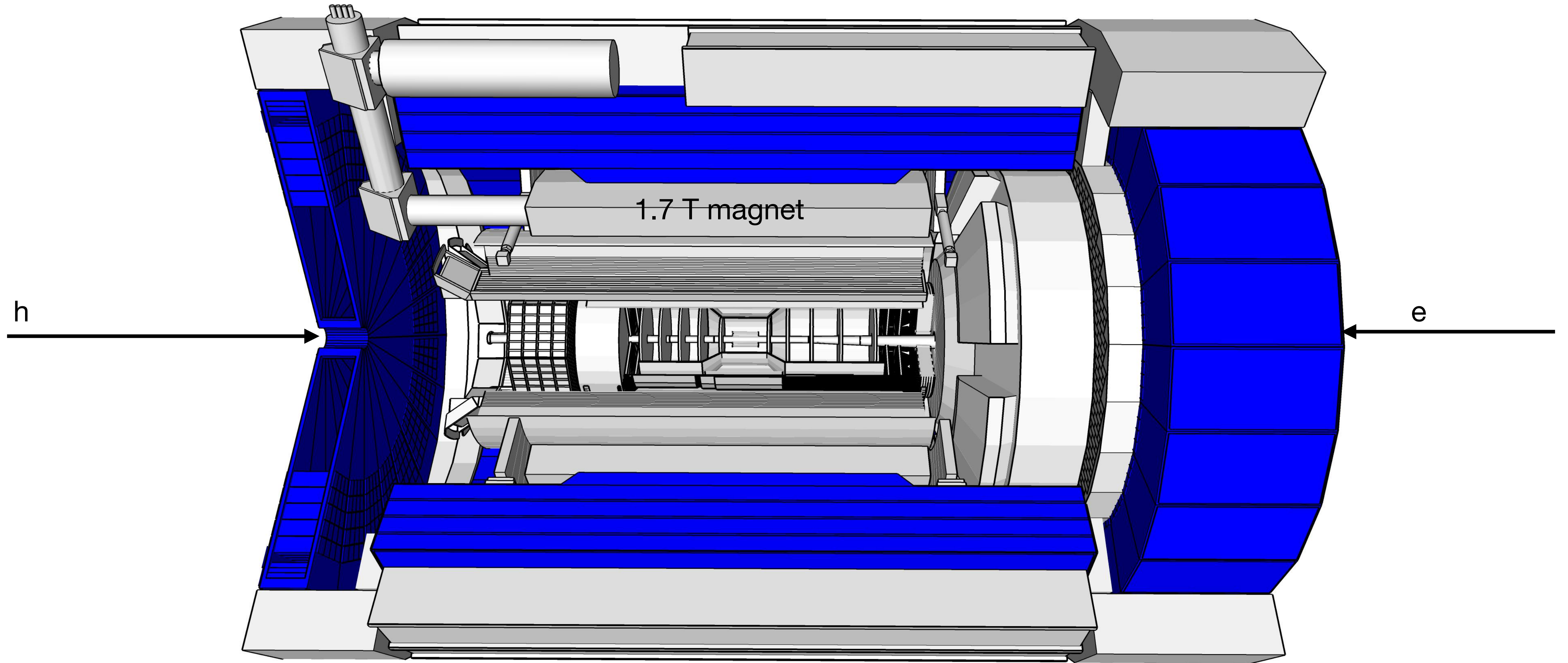
# Electromagnetic calorimeter



- Backward EMCAL: high-precision  $\text{PbWO}_4$  + Si sensors
- Barrel EMCAL: 3D imaging with MAPS and sampling Pb/scintillating fibres with Si sensors
- Forward EMCAL: finely segmented W powder/scintillating fibres

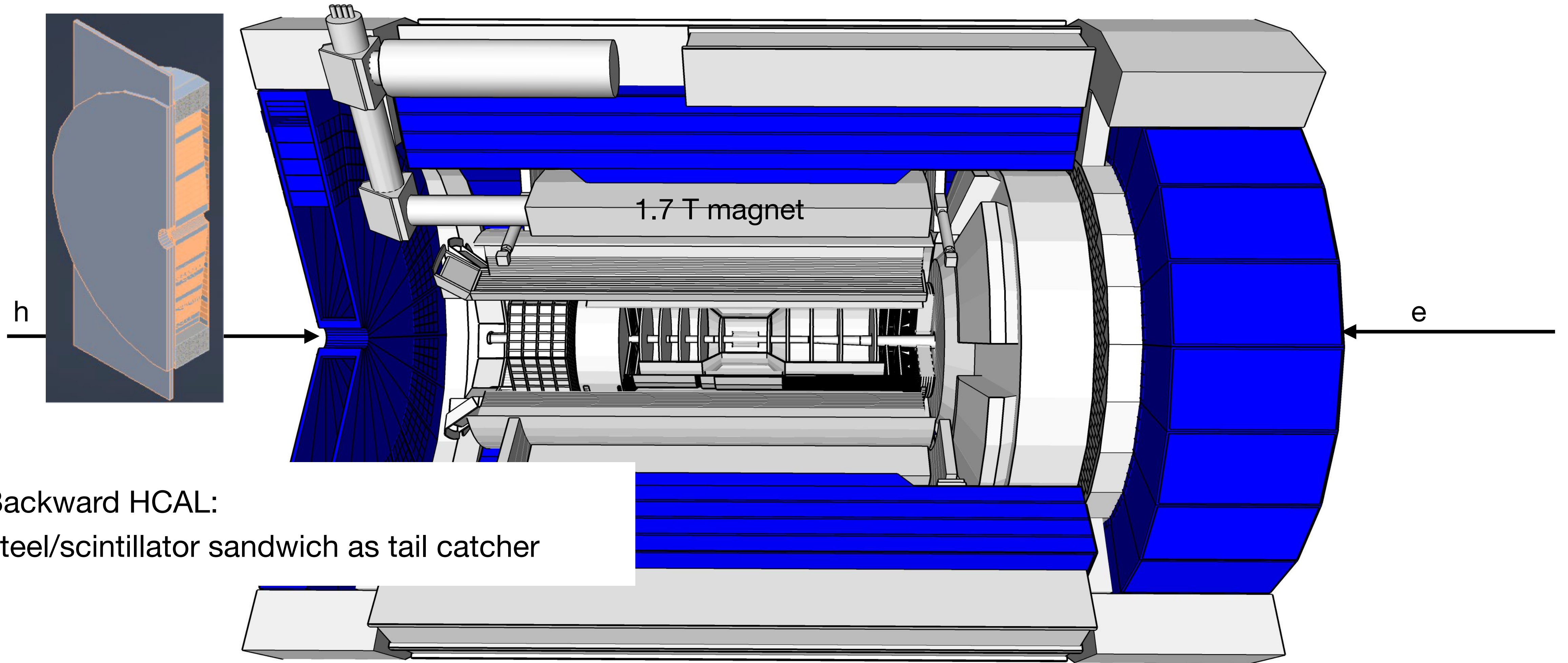


# Hadronic calorimeter



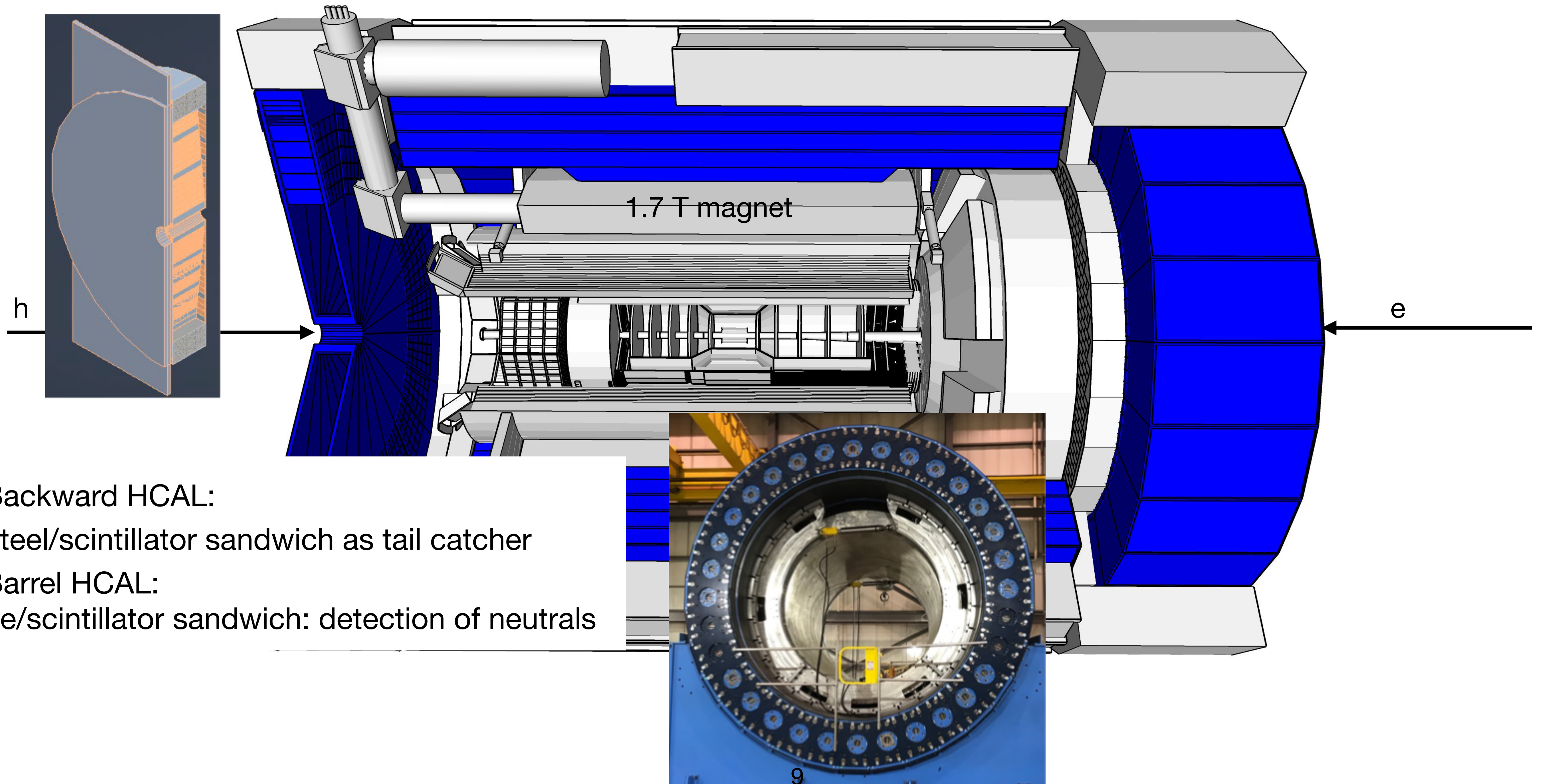


# Hadronic calorimeter



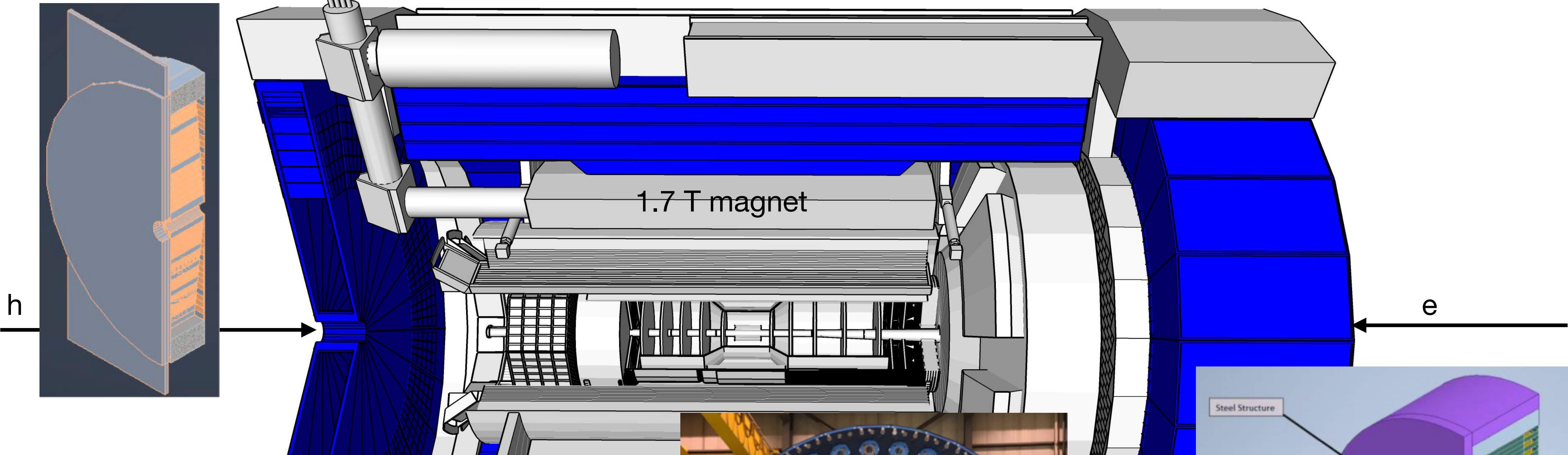
- Backward HCAL:  
steel/scintillator sandwich as tail catcher

# Hadronic calorimeter

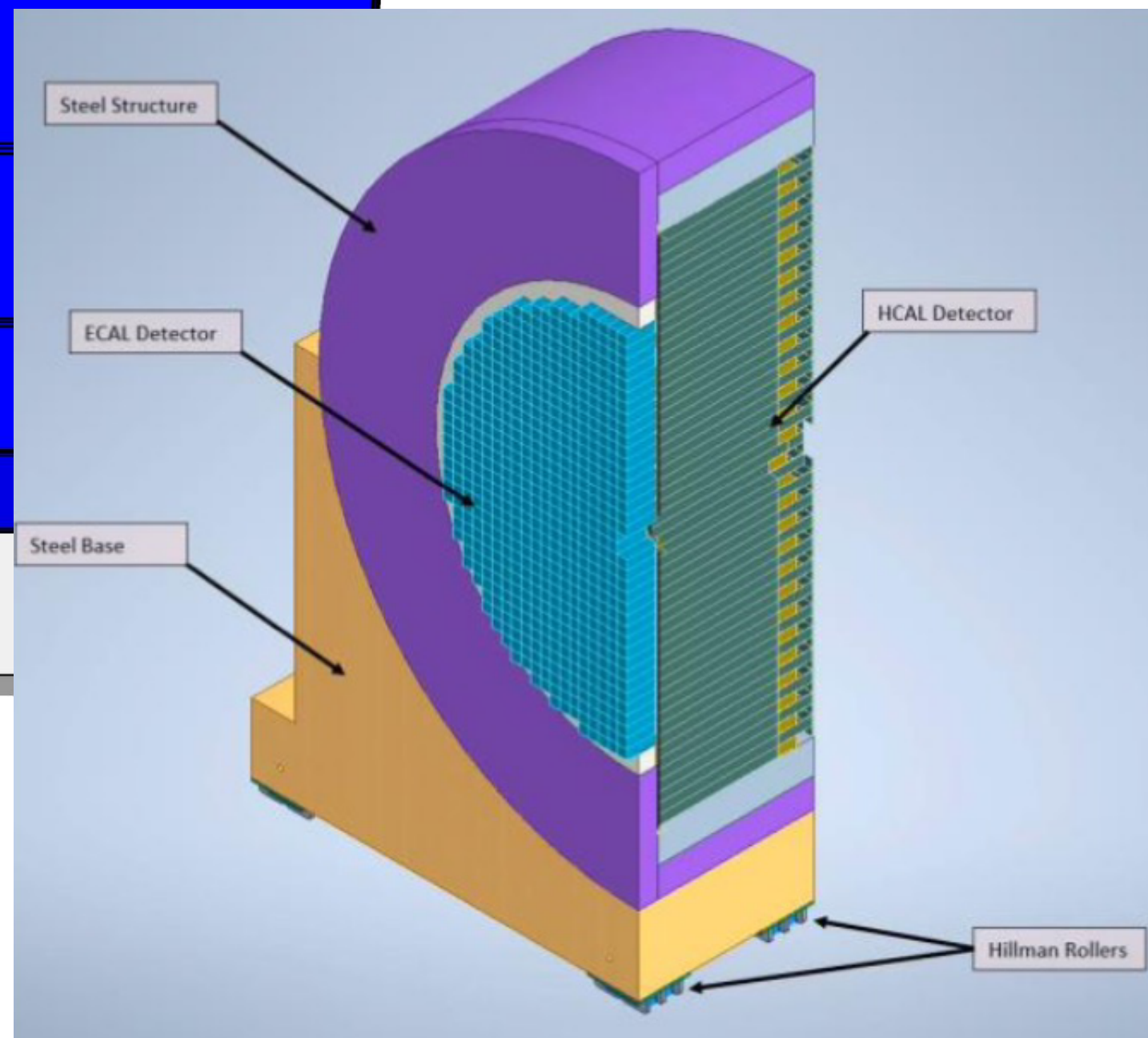


- Backward HCAL:  
steel/scintillator sandwich as tail catcher
- Barrel HCAL:  
Fe/scintillator sandwich: detection of neutrals

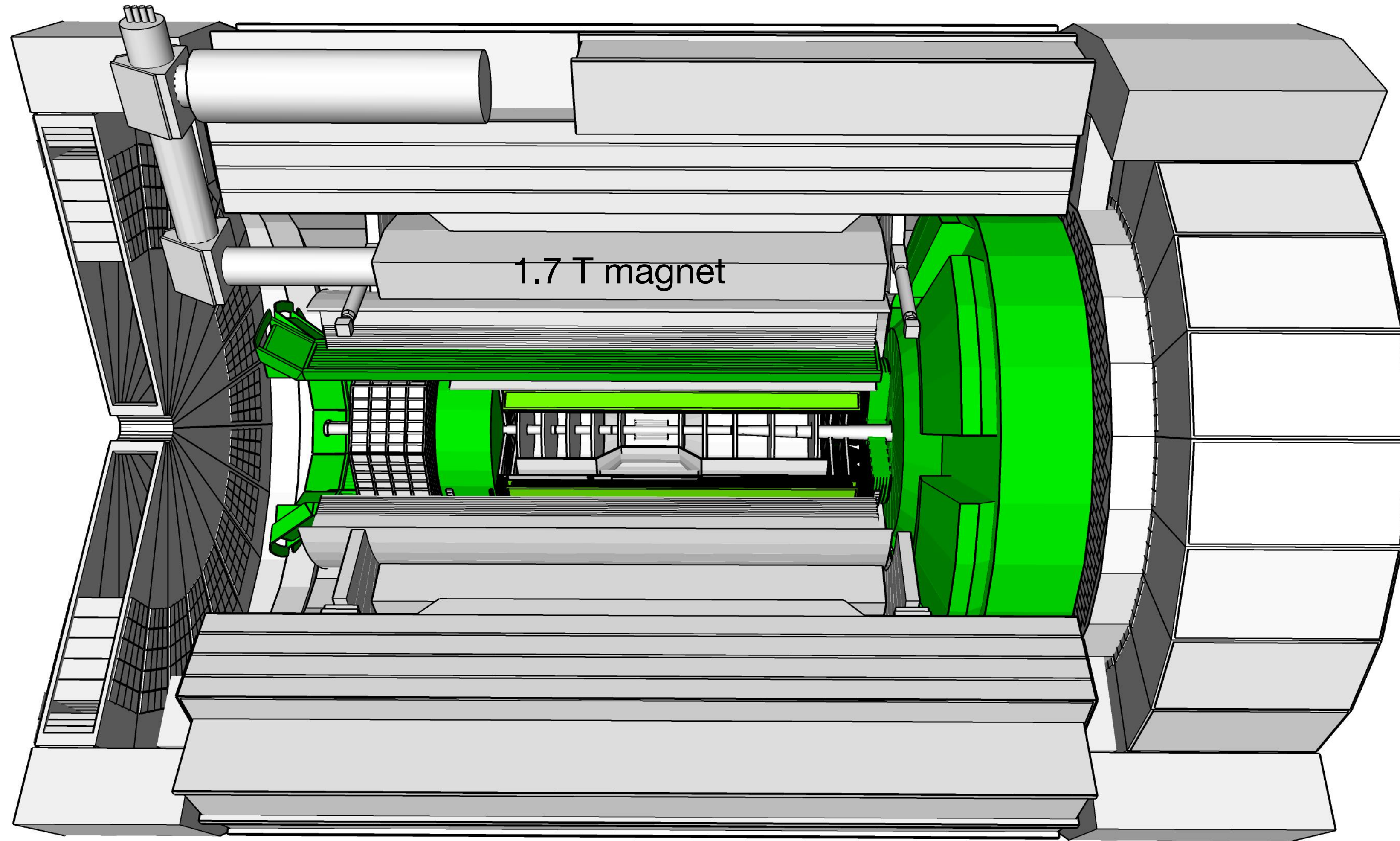
# Hadronic calorimeter



- Backward HCAL: steel/scintillator sandwich as tail catcher
- Barrel HCAL: Fe/scintillator sandwich: detection of neutrals
- Forward HCAL: W/scintillator sandwich longitudinally segmented, high granularity: good E resolution

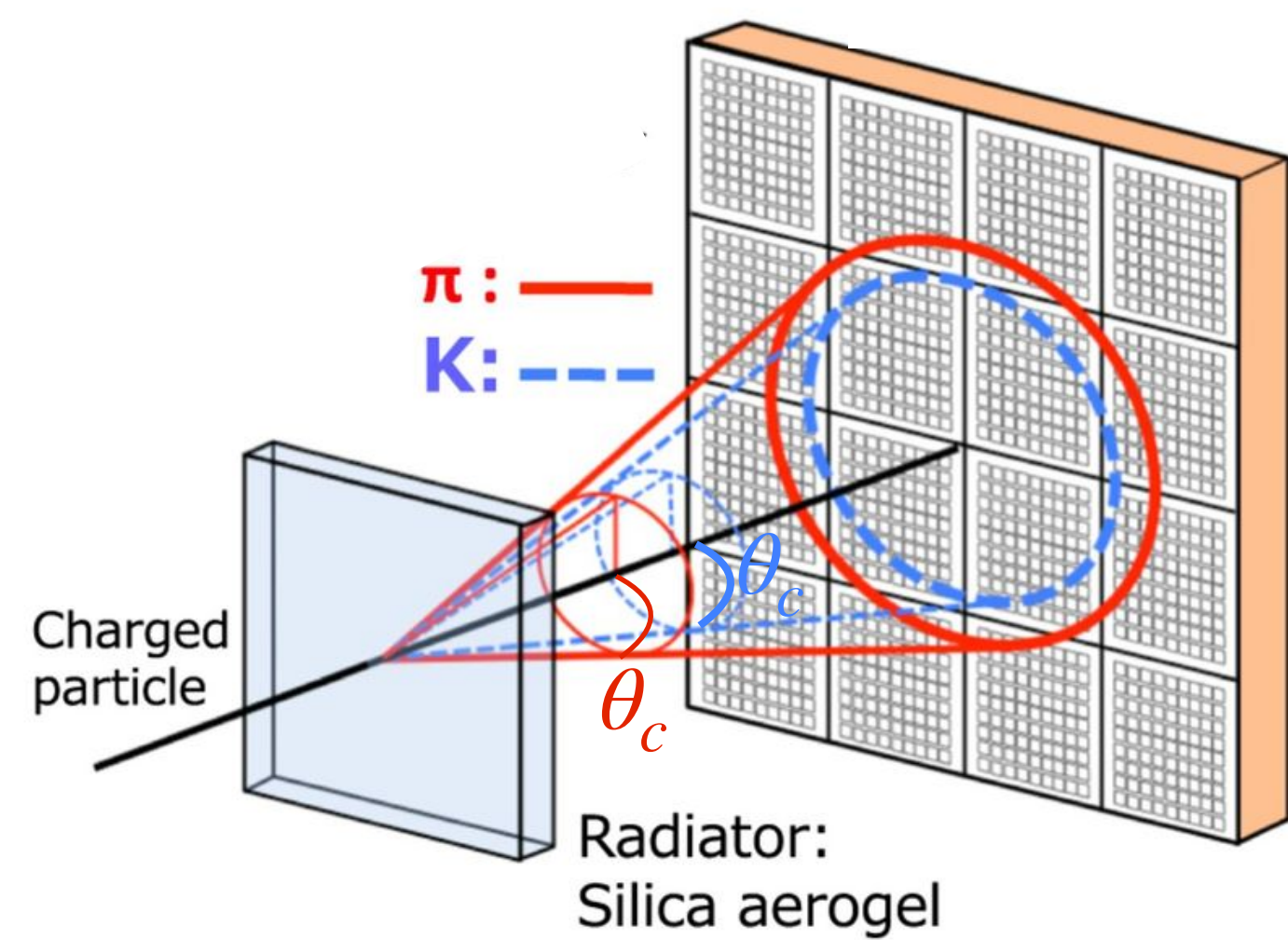
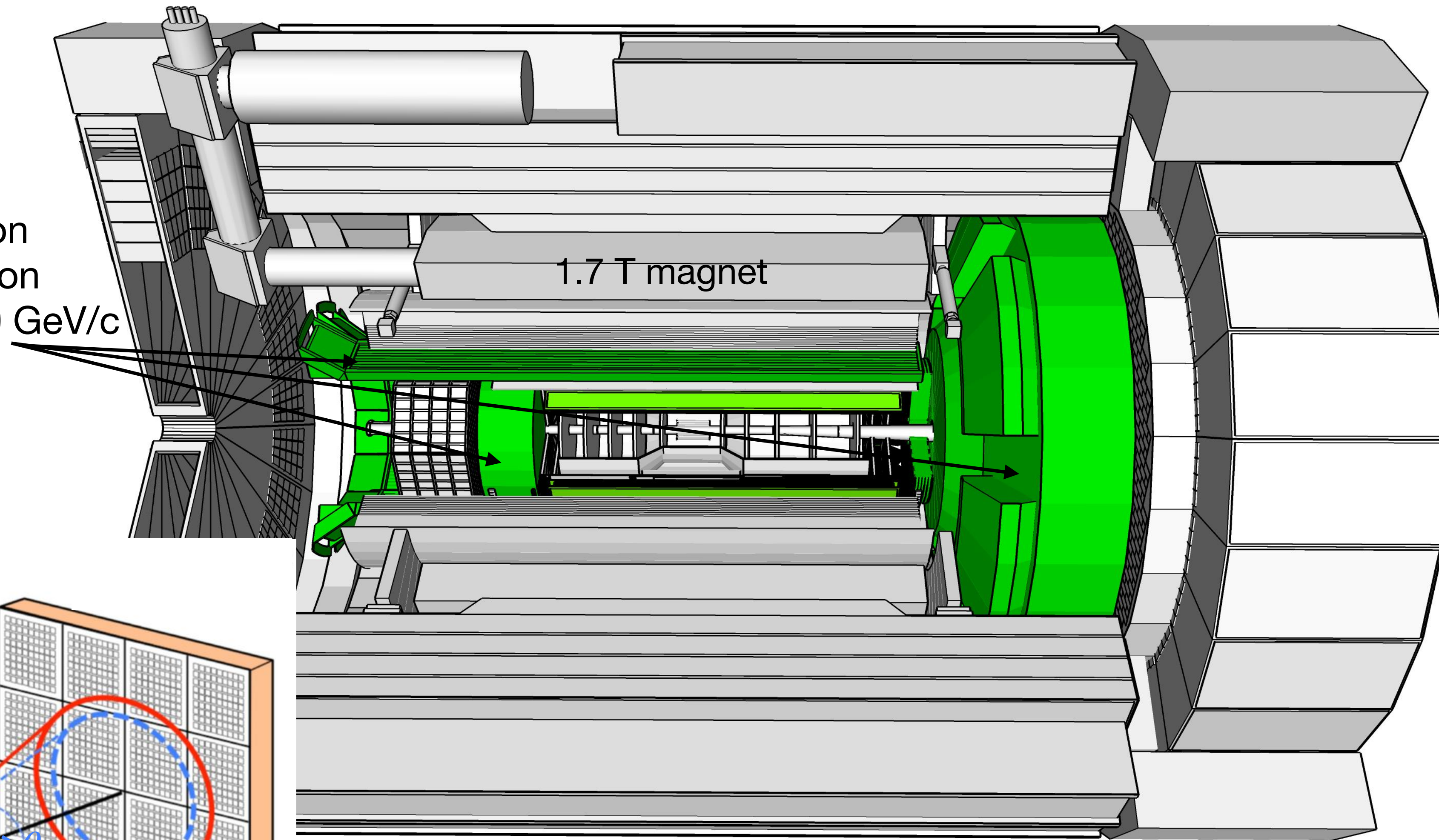


# Particle identification



# Particle identification

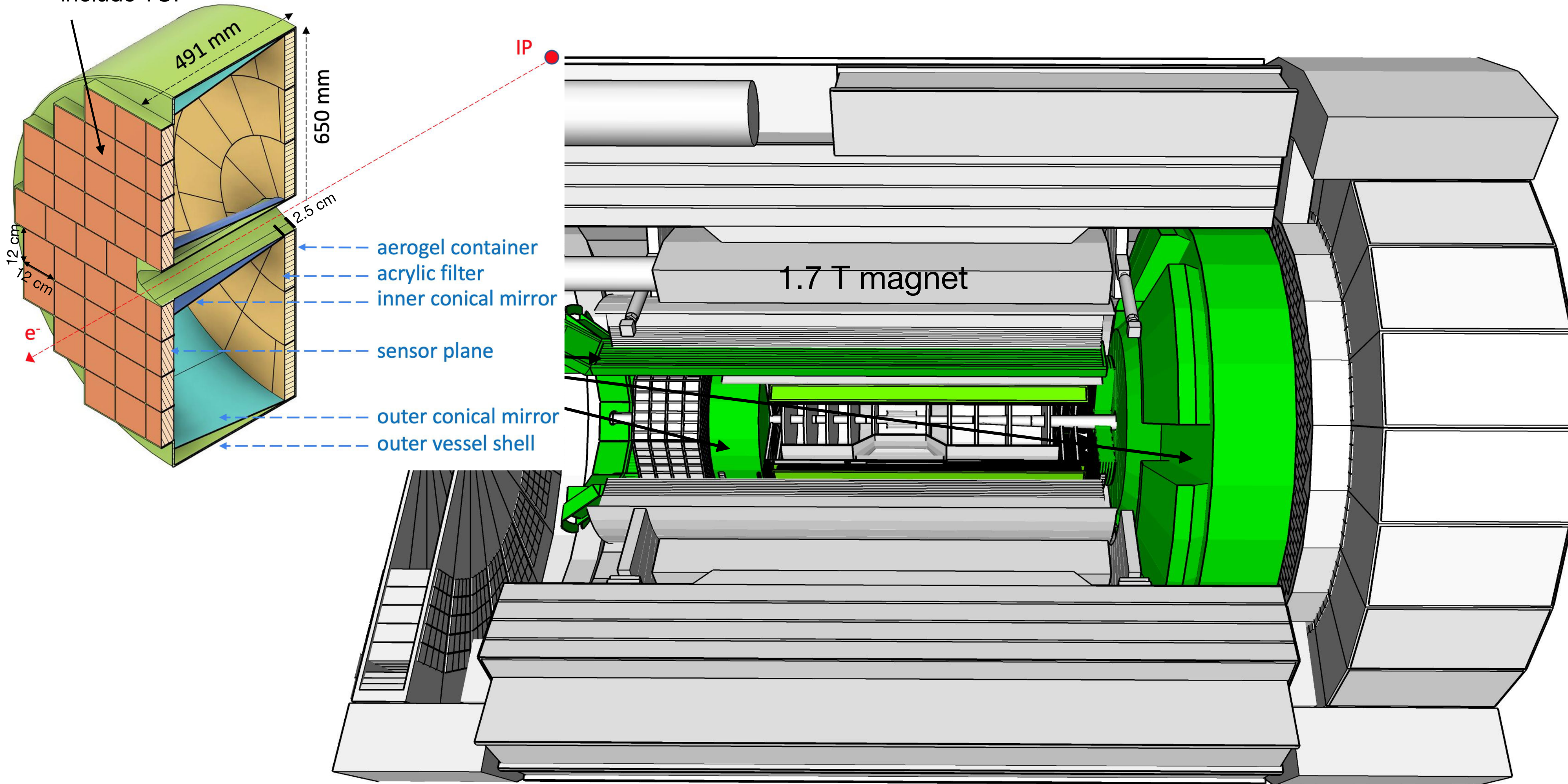
detectors based on Cherenkov radiation for  $1 \text{ GeV}/c < p < 50 \text{ GeV}/c$



$$\cos \theta_c \propto \frac{1}{v}$$

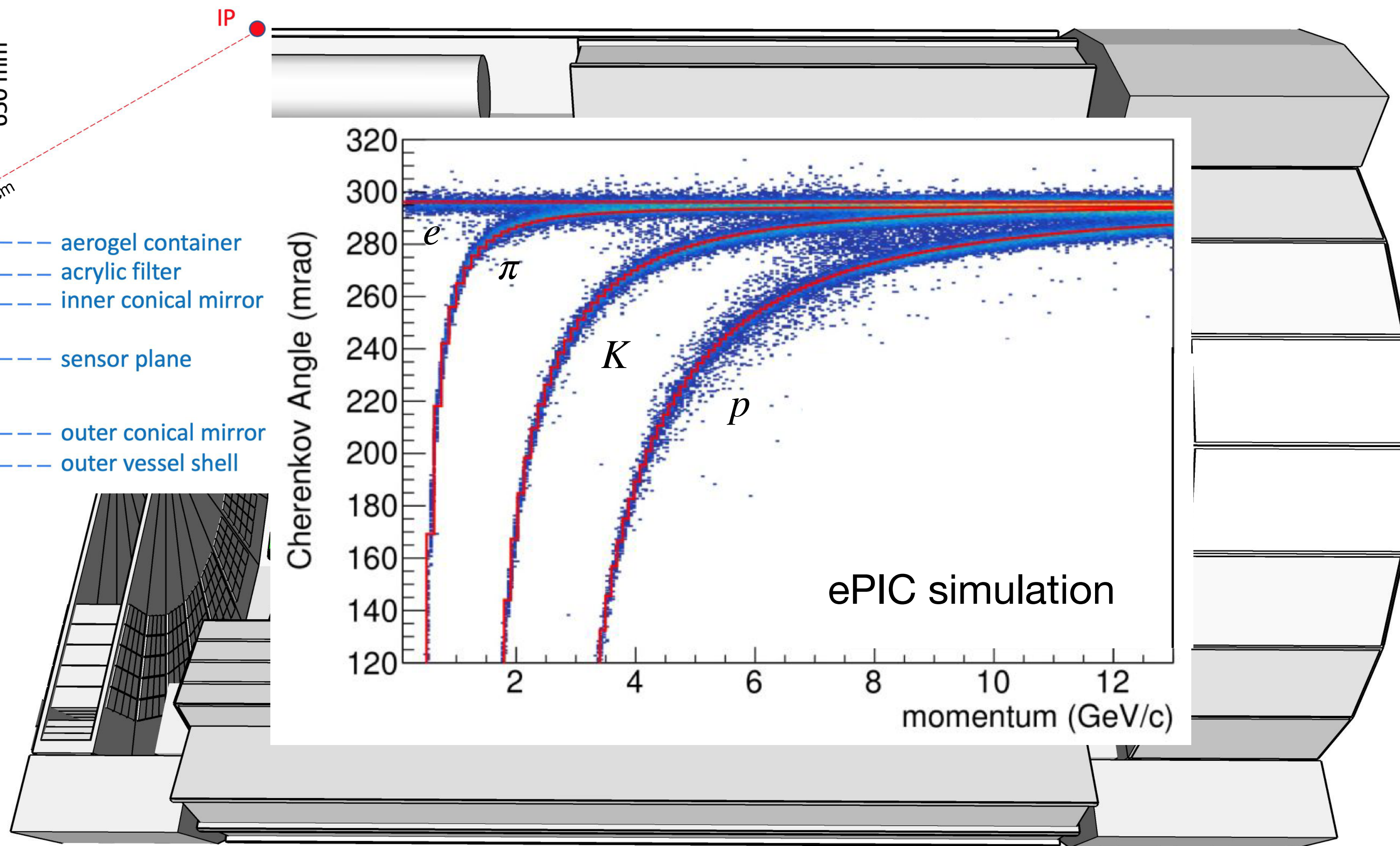
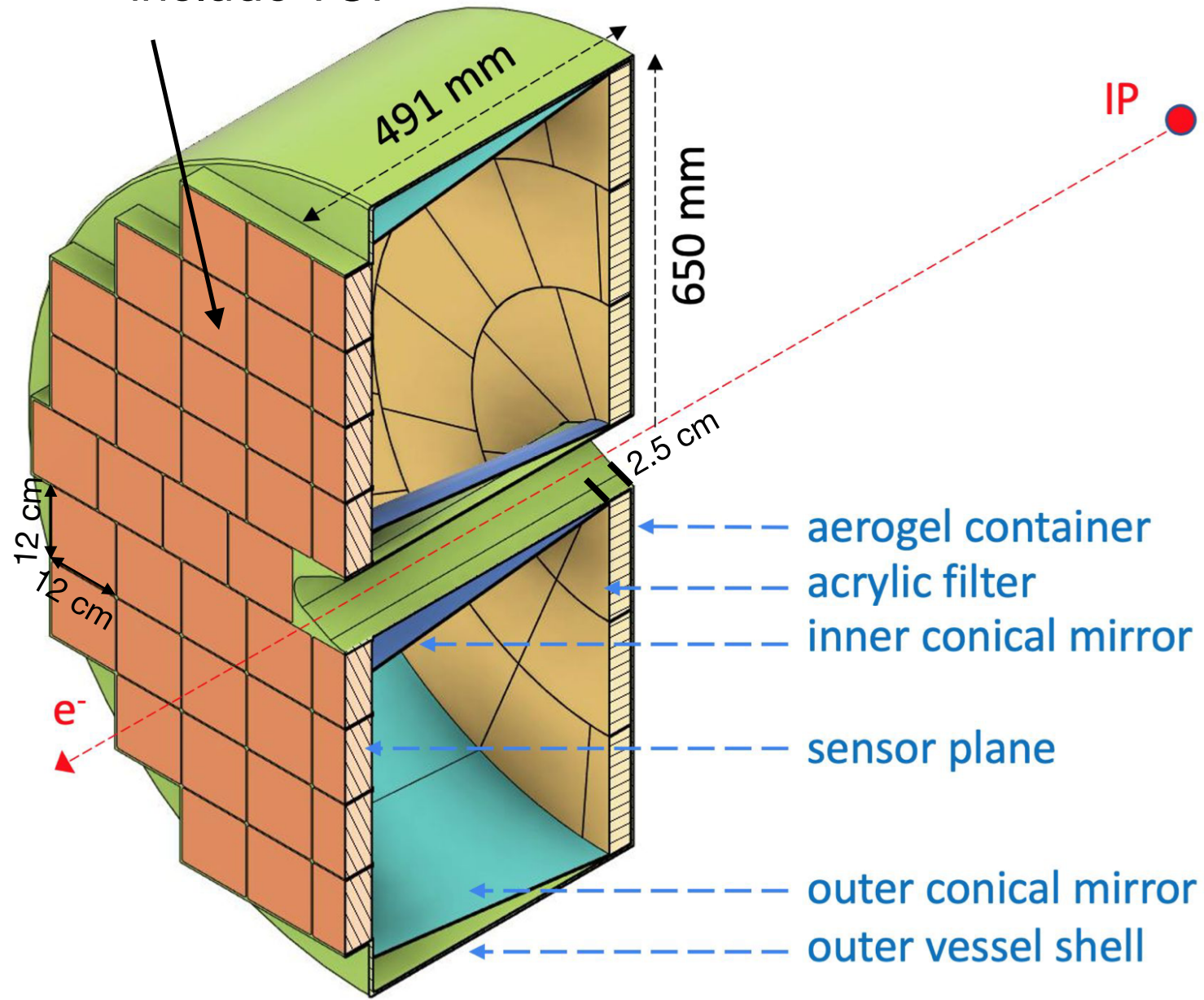
# Particle identification

HRPPD photosensors,  
include TOF



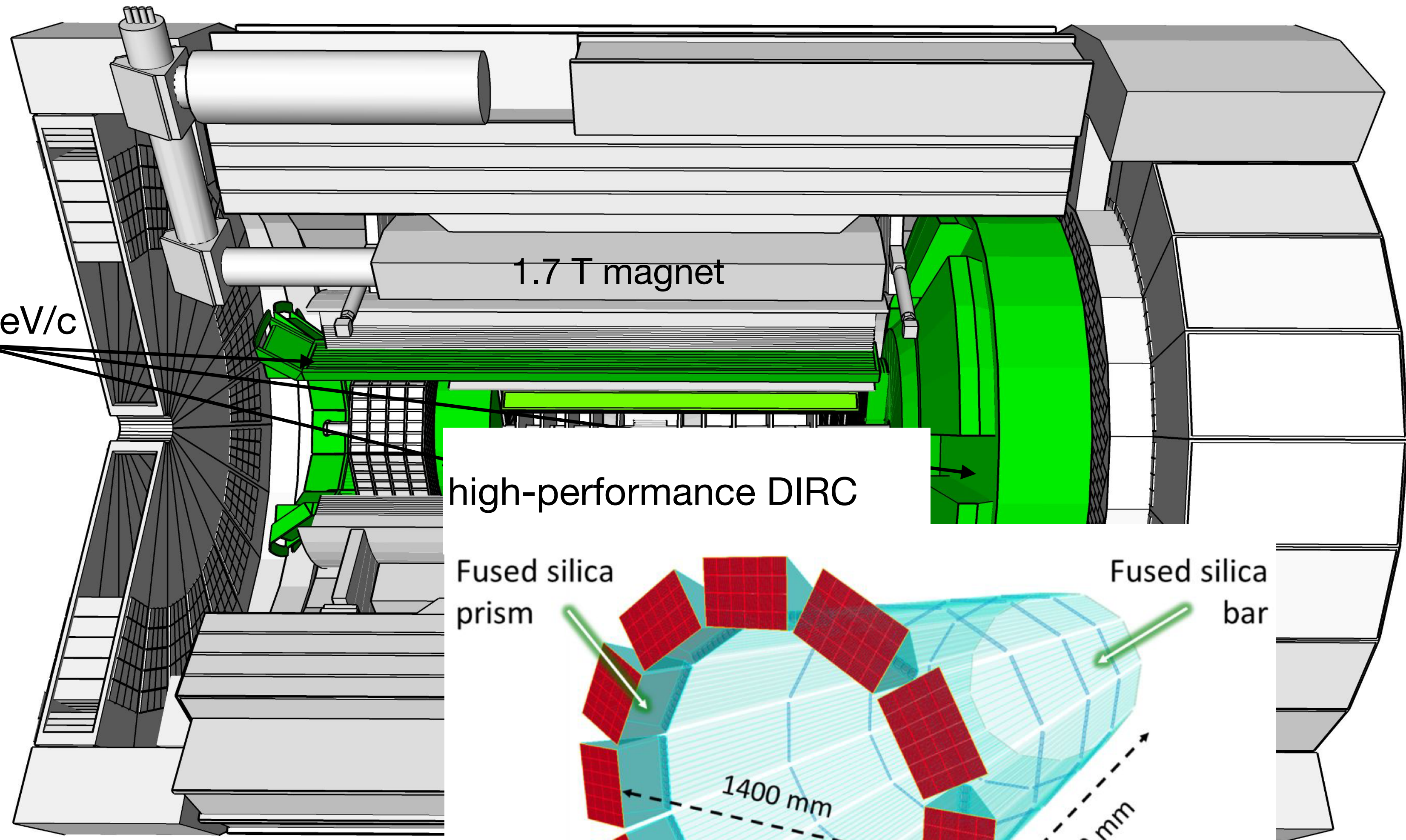
# Particle identification

HRPPD photosensors,  
include TOF

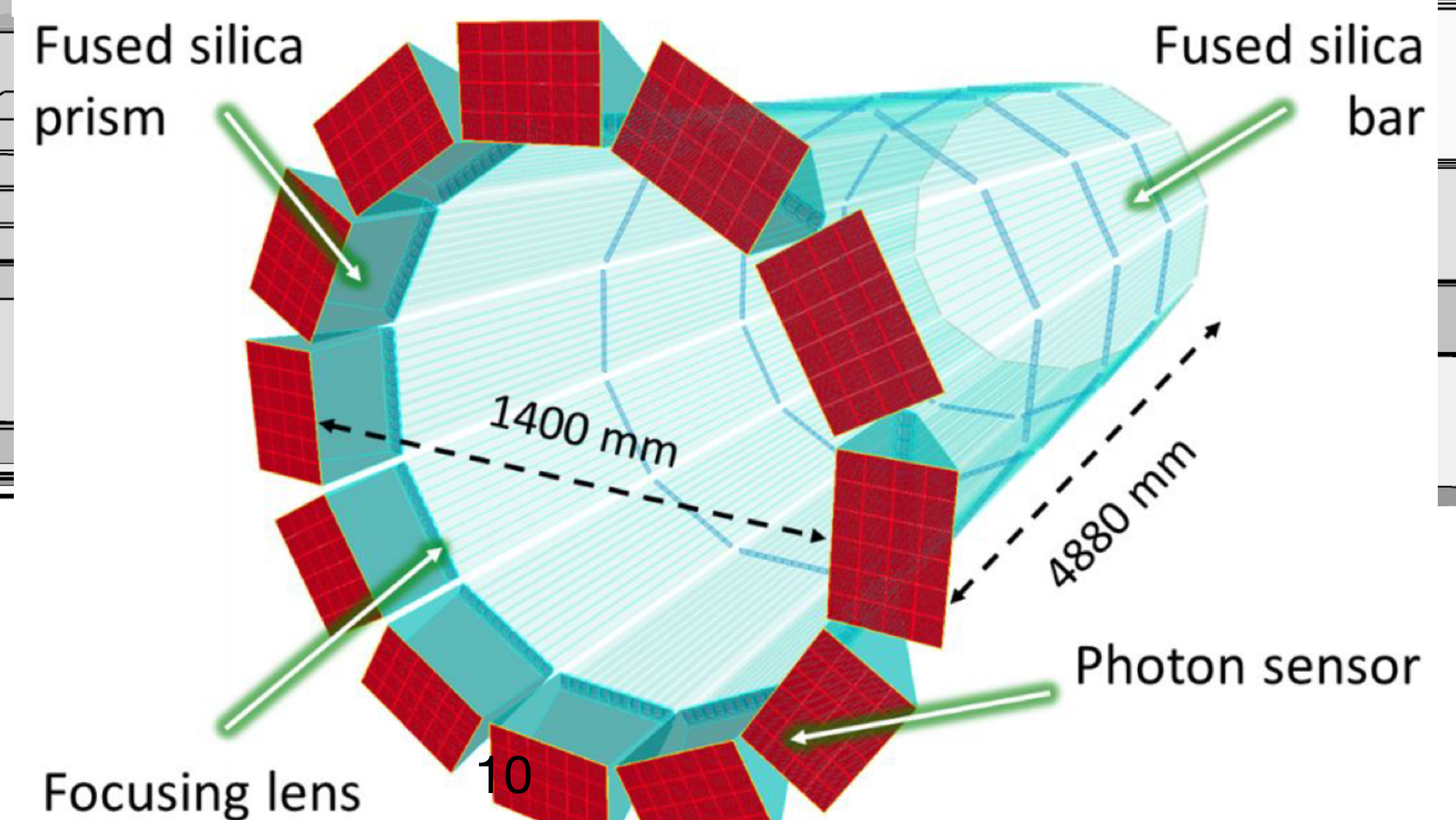


# Particle identification

detectors based on Cherenkov radiation for  $1 \text{ GeV}/c < p < 50 \text{ GeV}/c$



high-performance DIRC

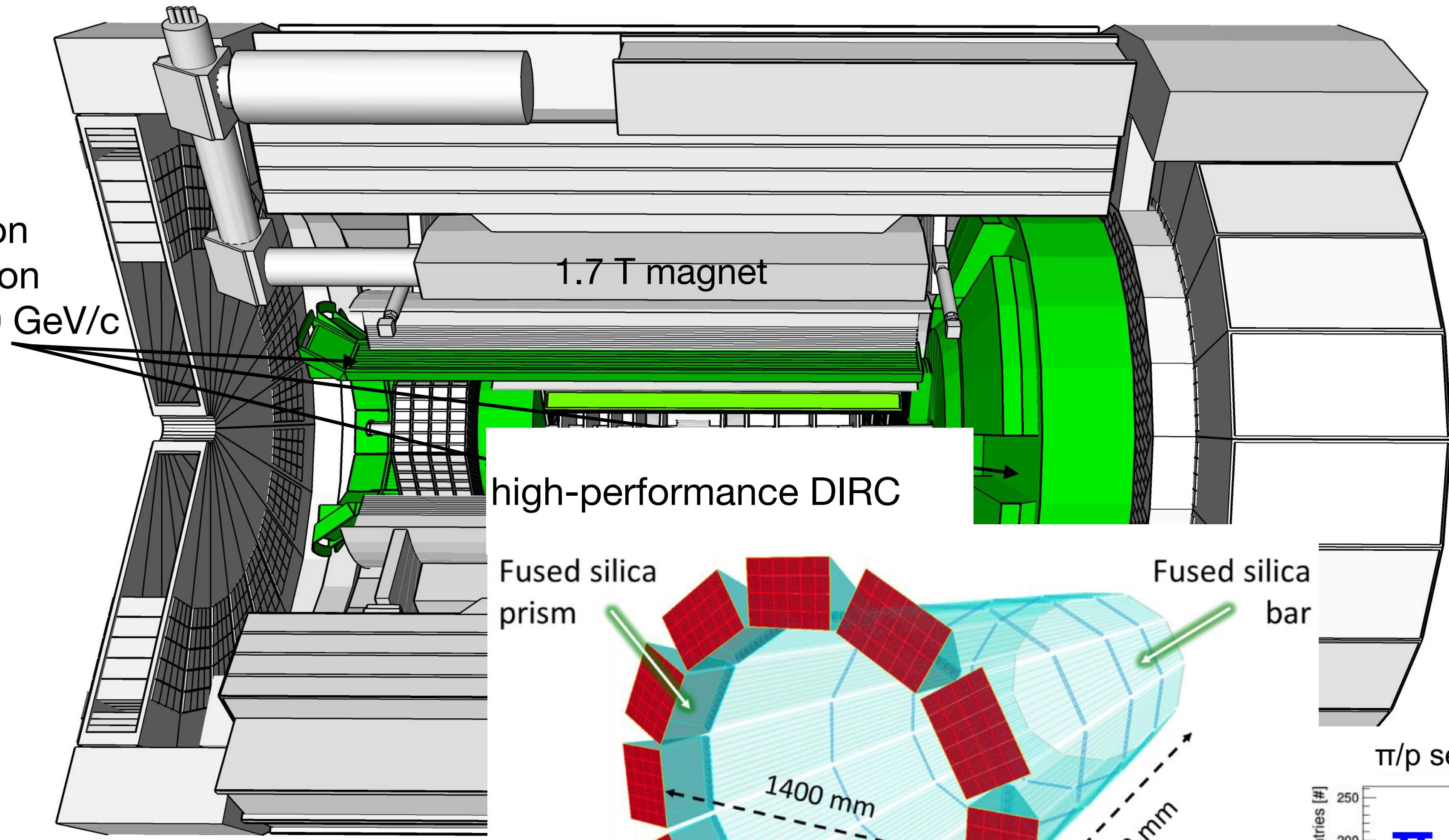


10

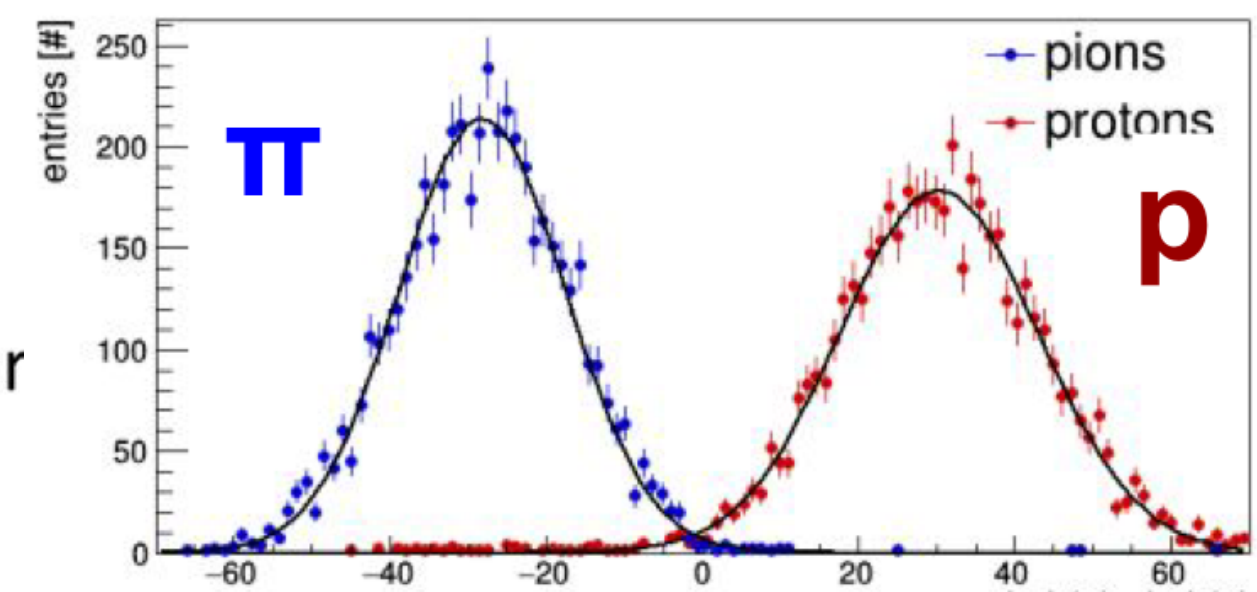


# Particle identification

detectors based on Cherenkov radiation for  $1 \text{ GeV}/c < p < 50 \text{ GeV}/c$

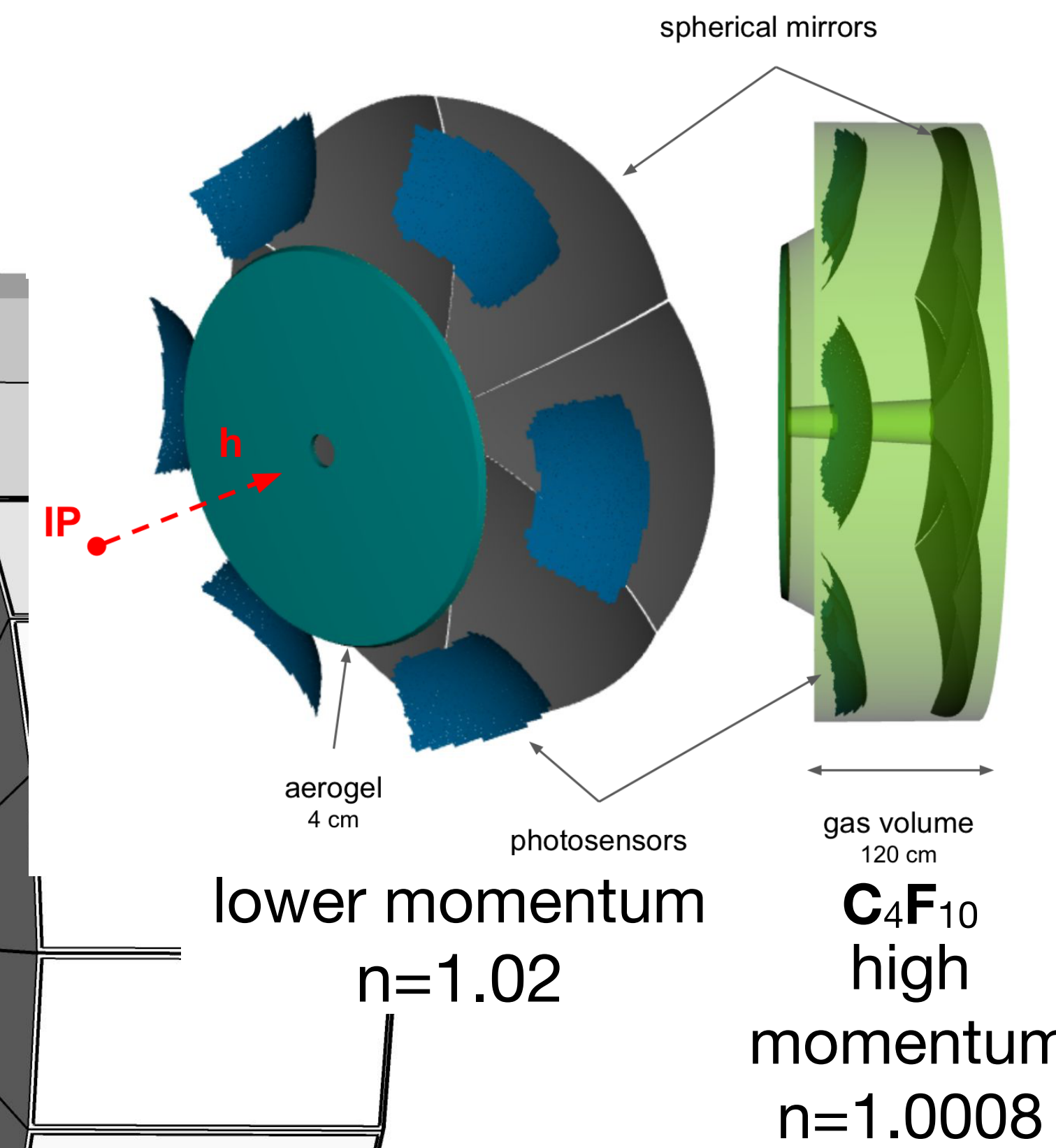
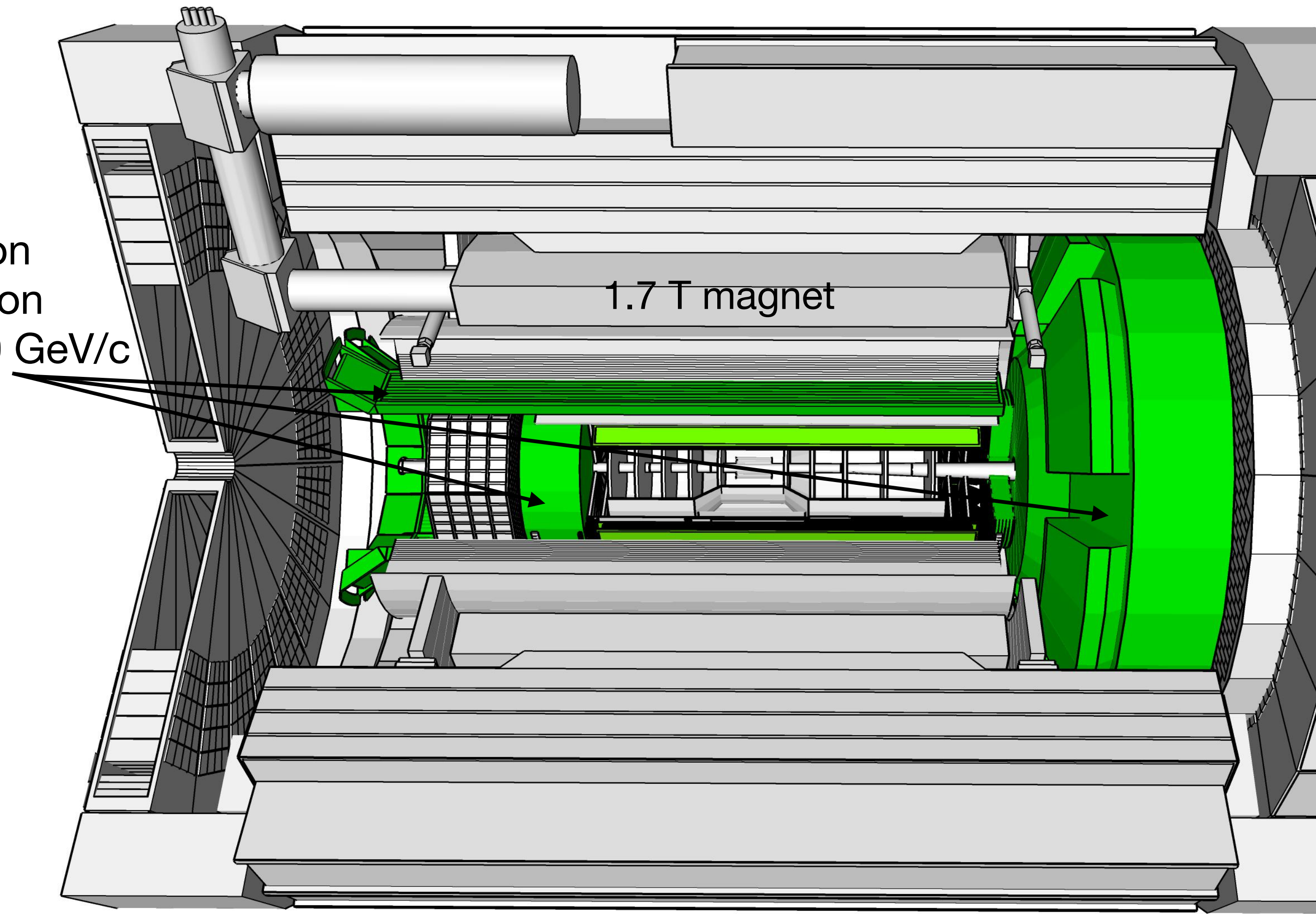


$\pi/p$  separation power at 7 GeV/c



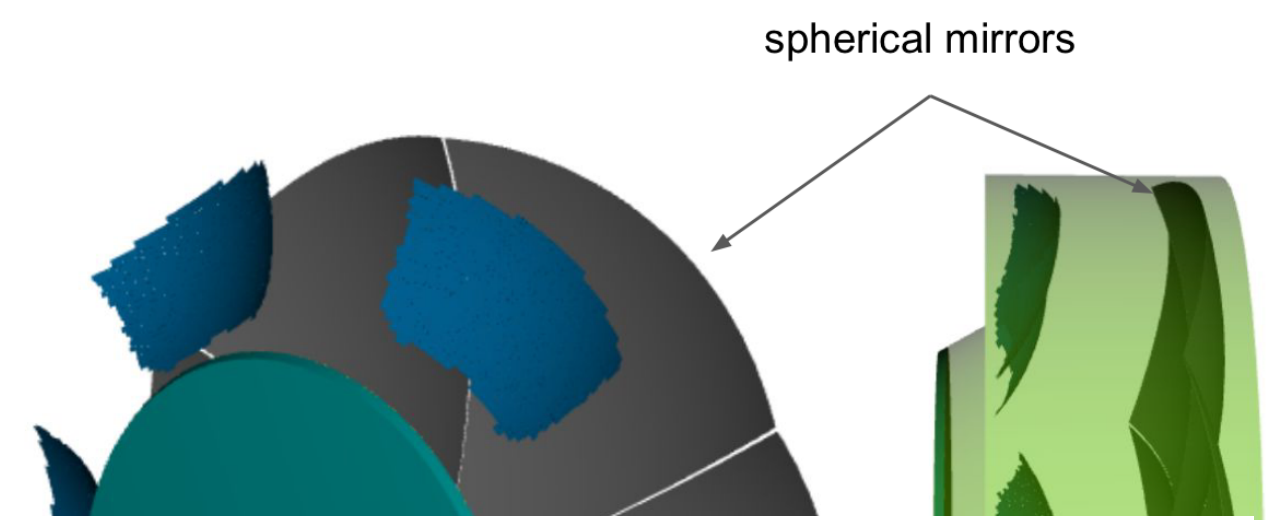
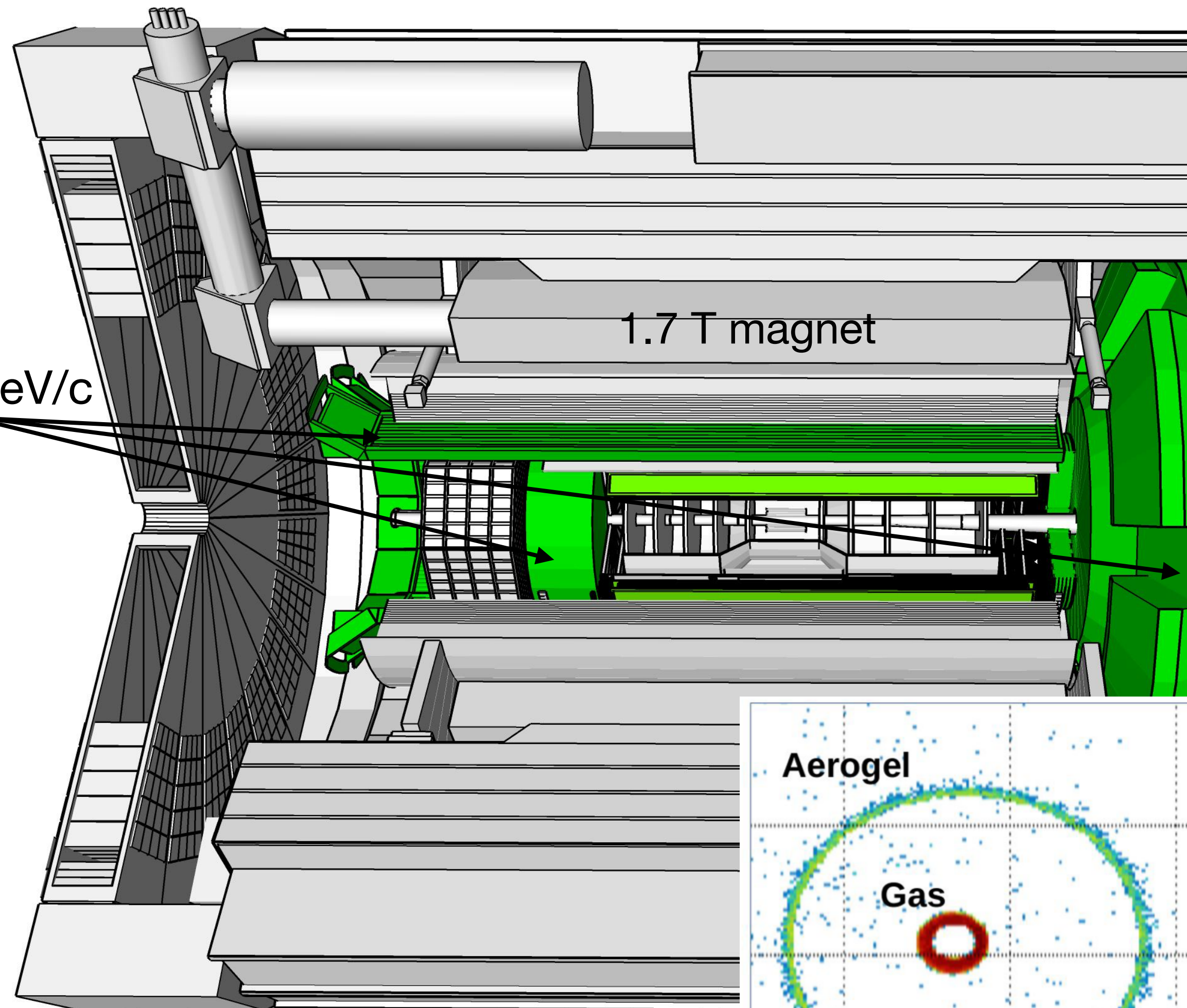
# Particle identification

detectors based on Cherenkov radiation for  $1 \text{ GeV}/c < p < 50 \text{ GeV}/c$

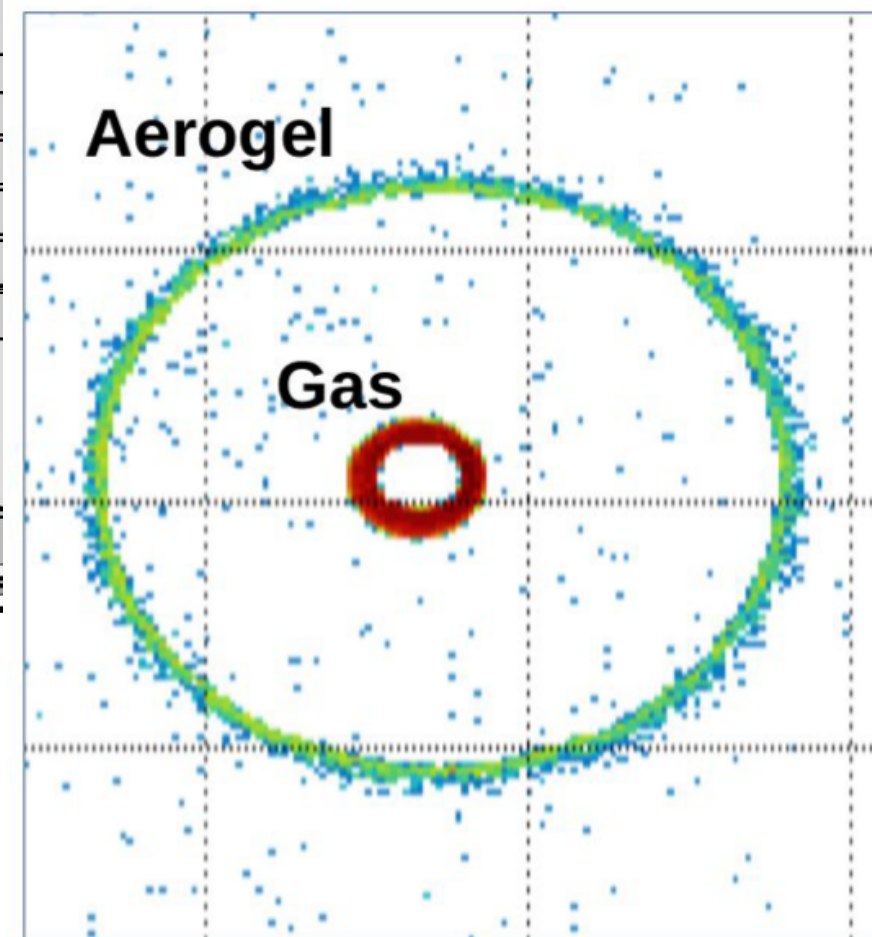
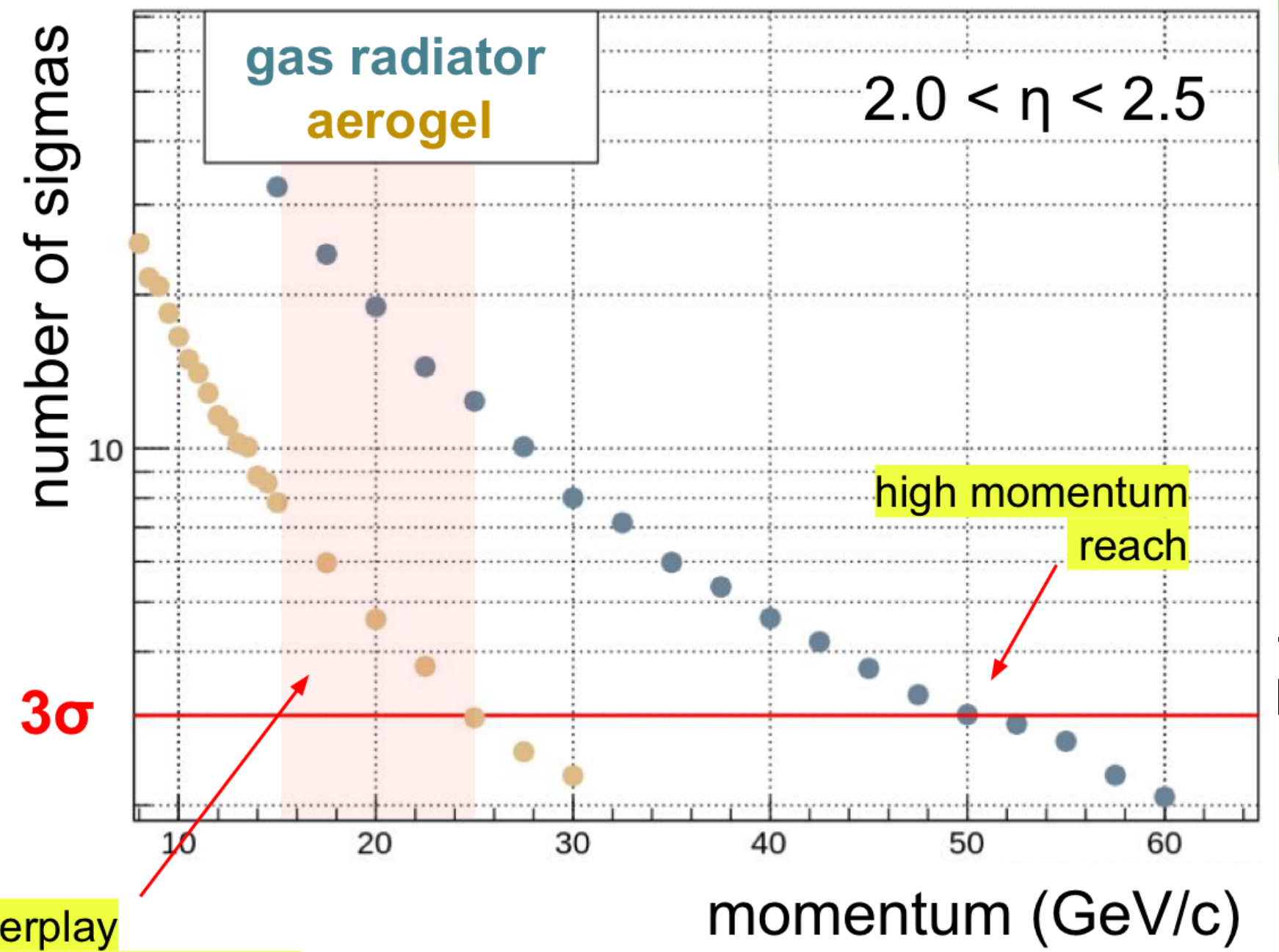


# Particle identification

detectors based on Cherenkov radiation for  $1 \text{ GeV}/c < p < 50 \text{ GeV}/c$



$\pi/K$  separation power

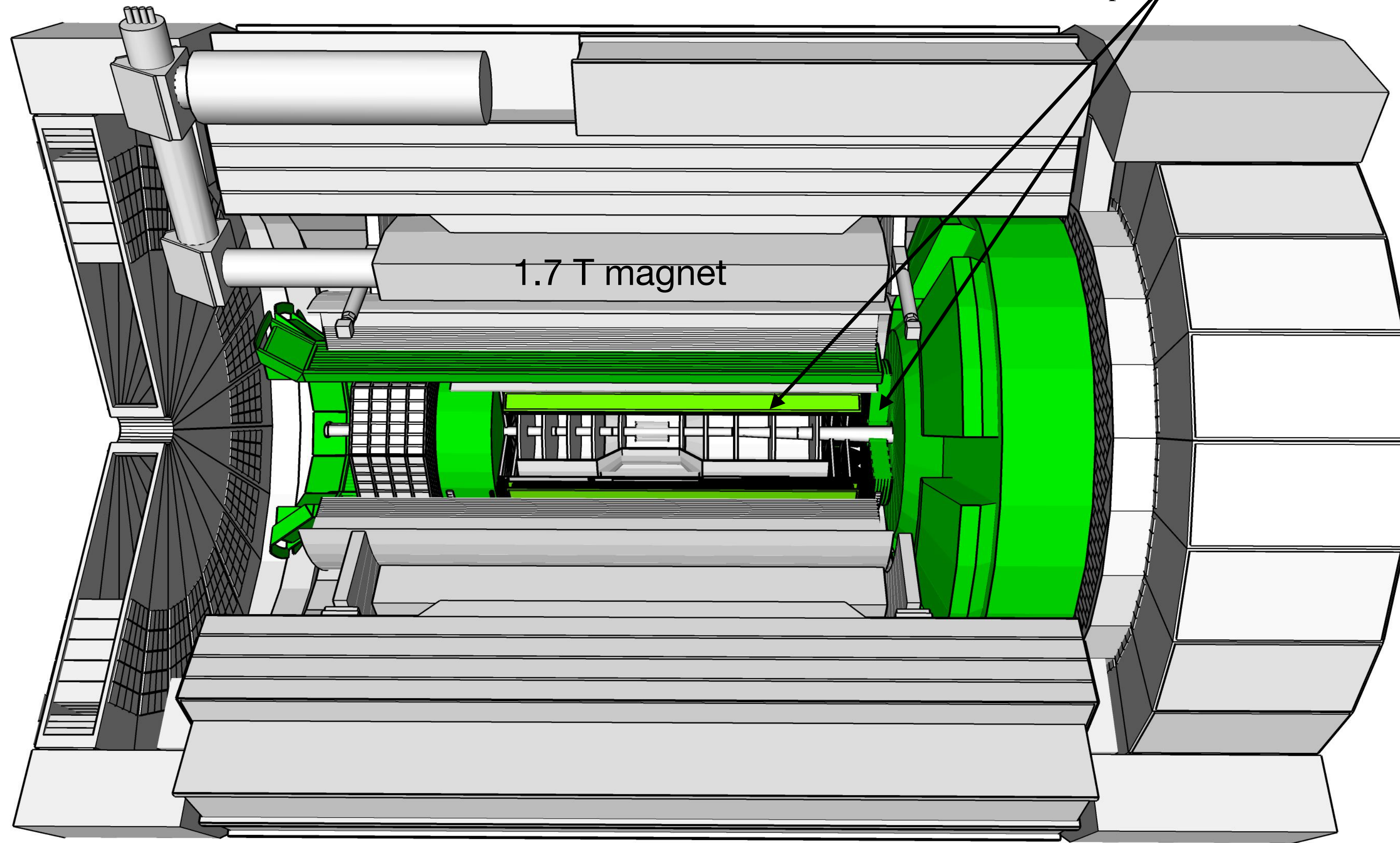


within ePIC simulation framework

# Particle identification

AC-LGAD based TOF, for  $p < 0.5 - 3 \text{ GeV}/c$

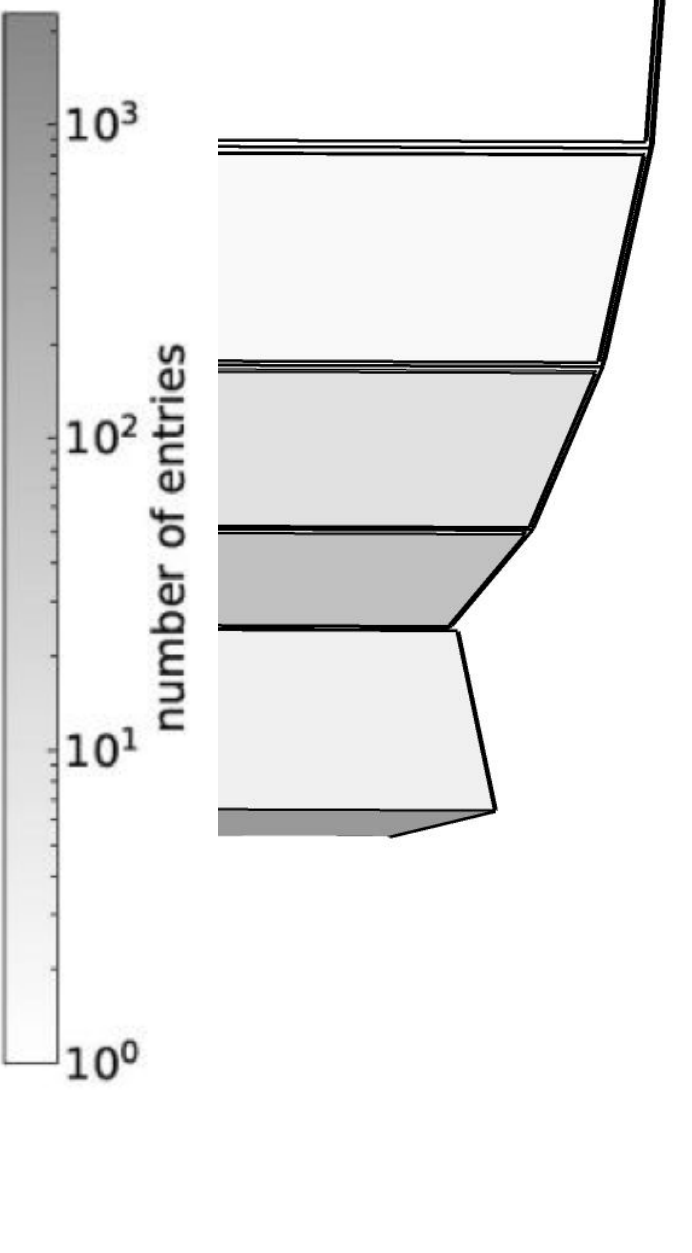
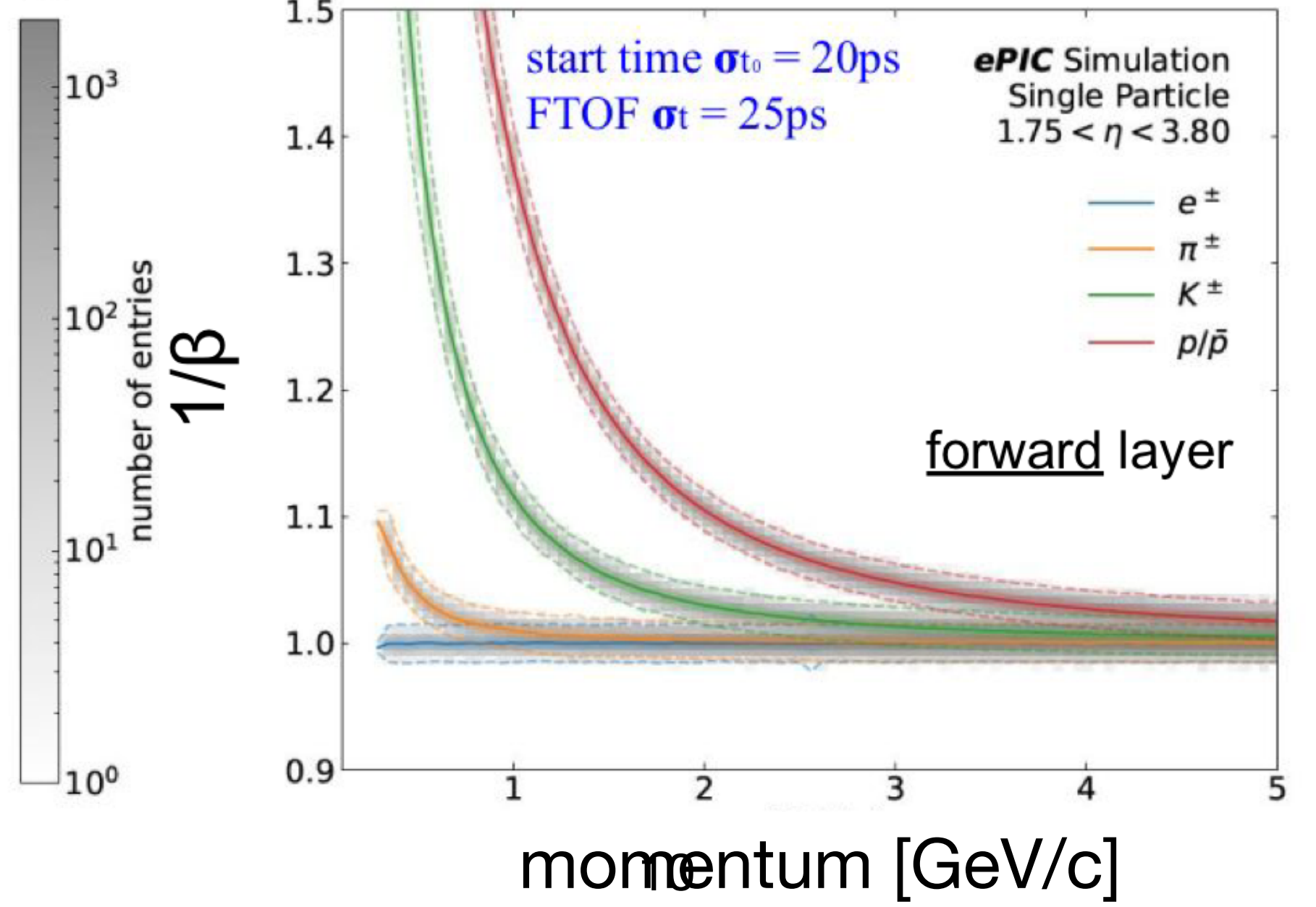
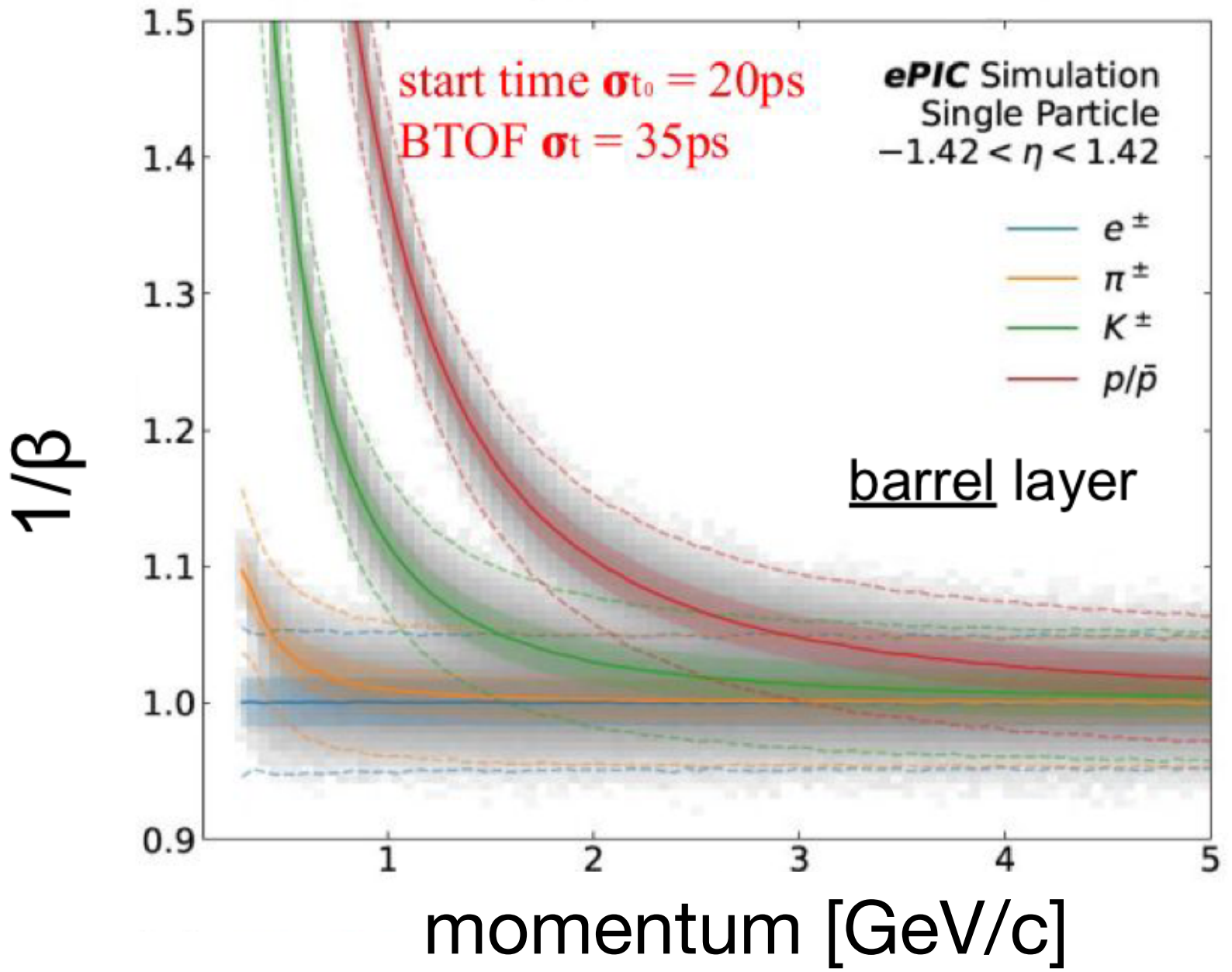
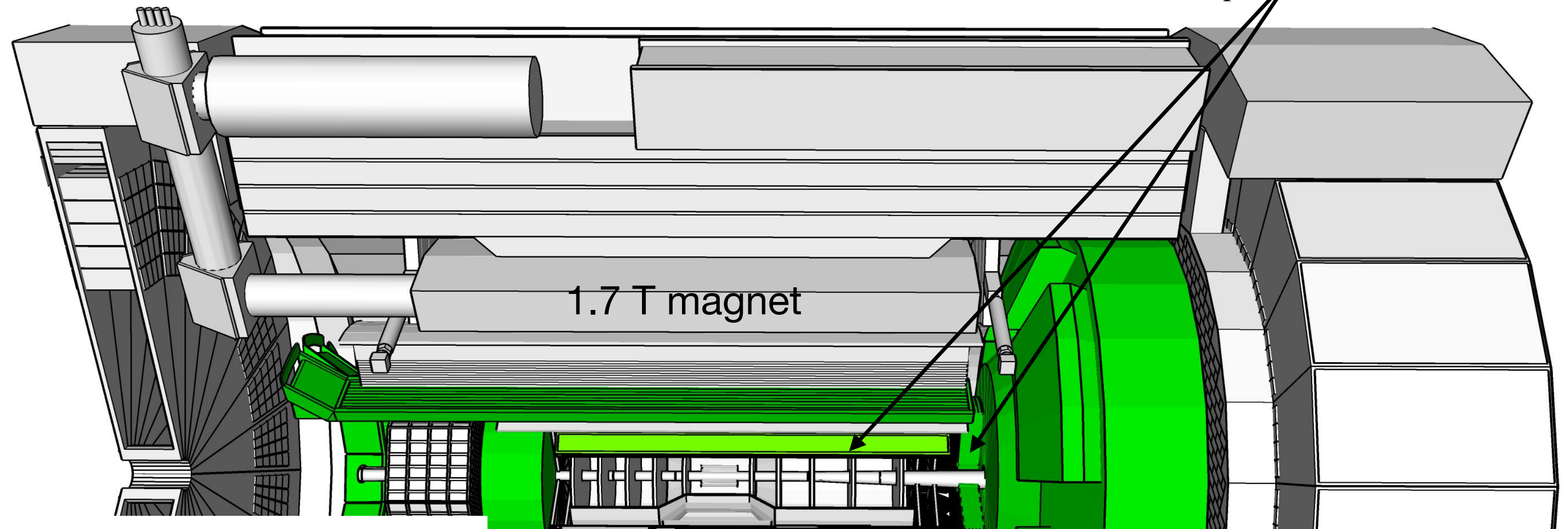
$$v = \frac{L}{t_{stop} - t_{start}}$$



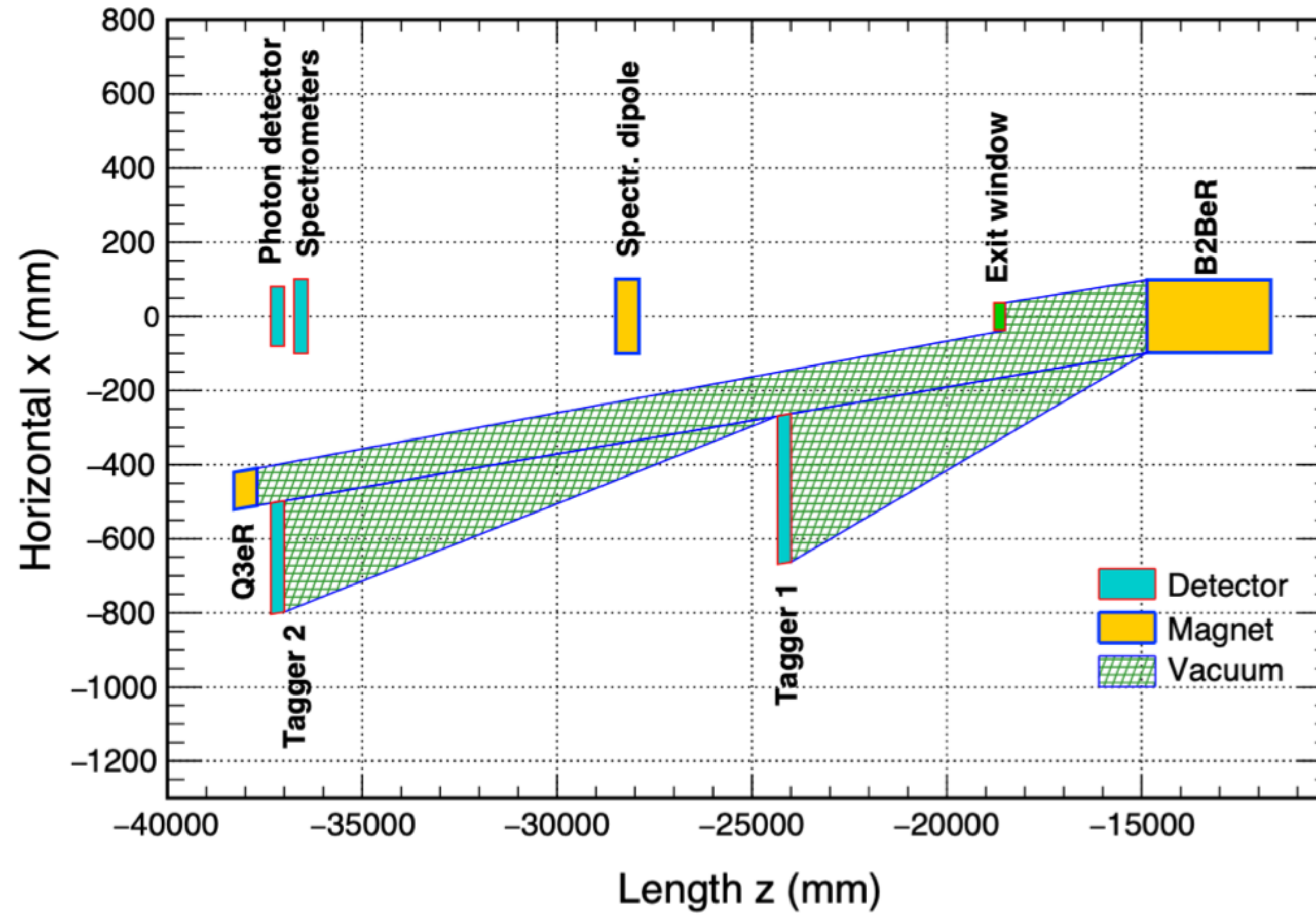
# Particle identification

AC-LGAD based TOF, for  $p < 0.5 - 3 \text{ GeV}/c$

$$v = \frac{L}{t_{stop} - t_{start}}$$

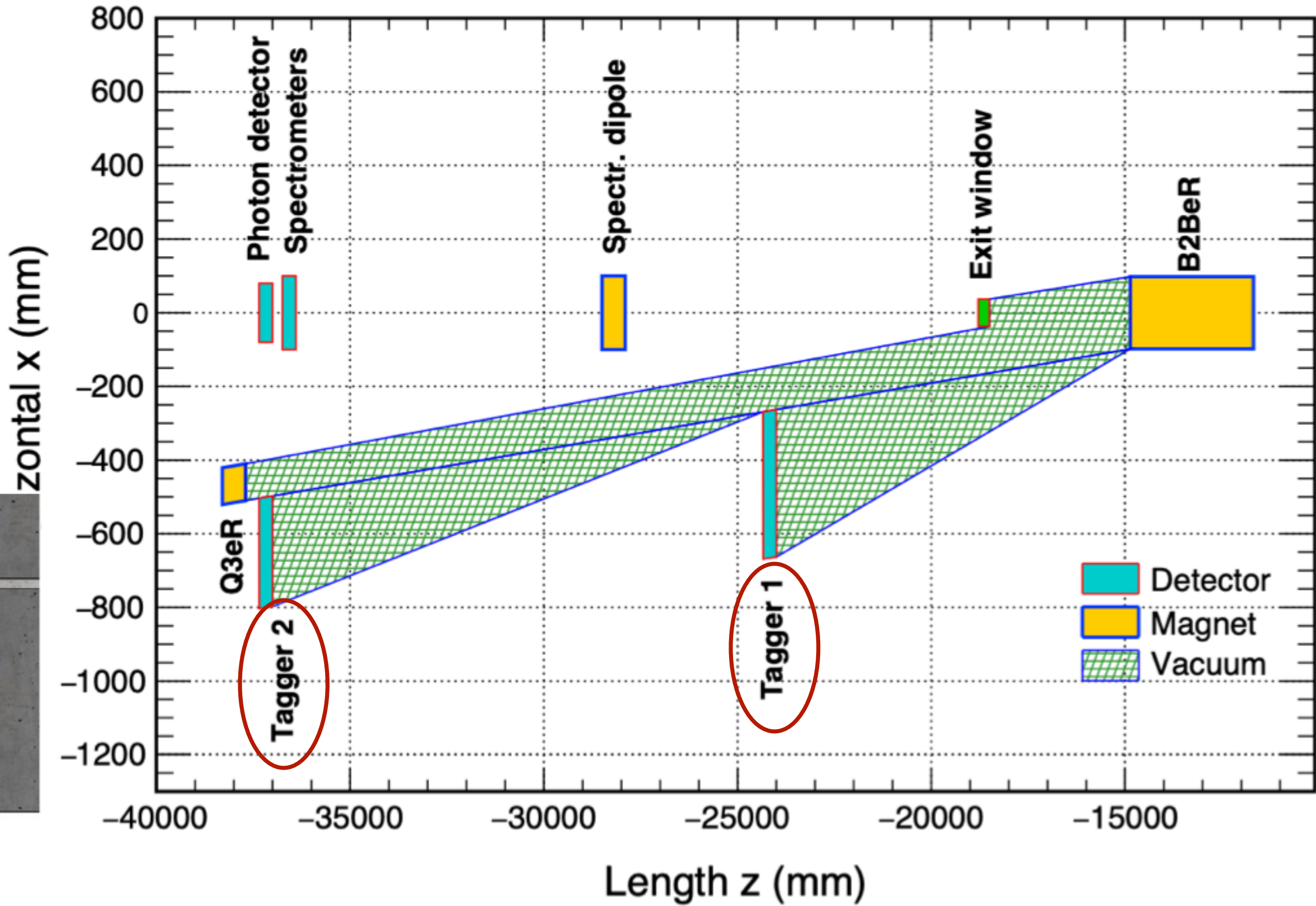
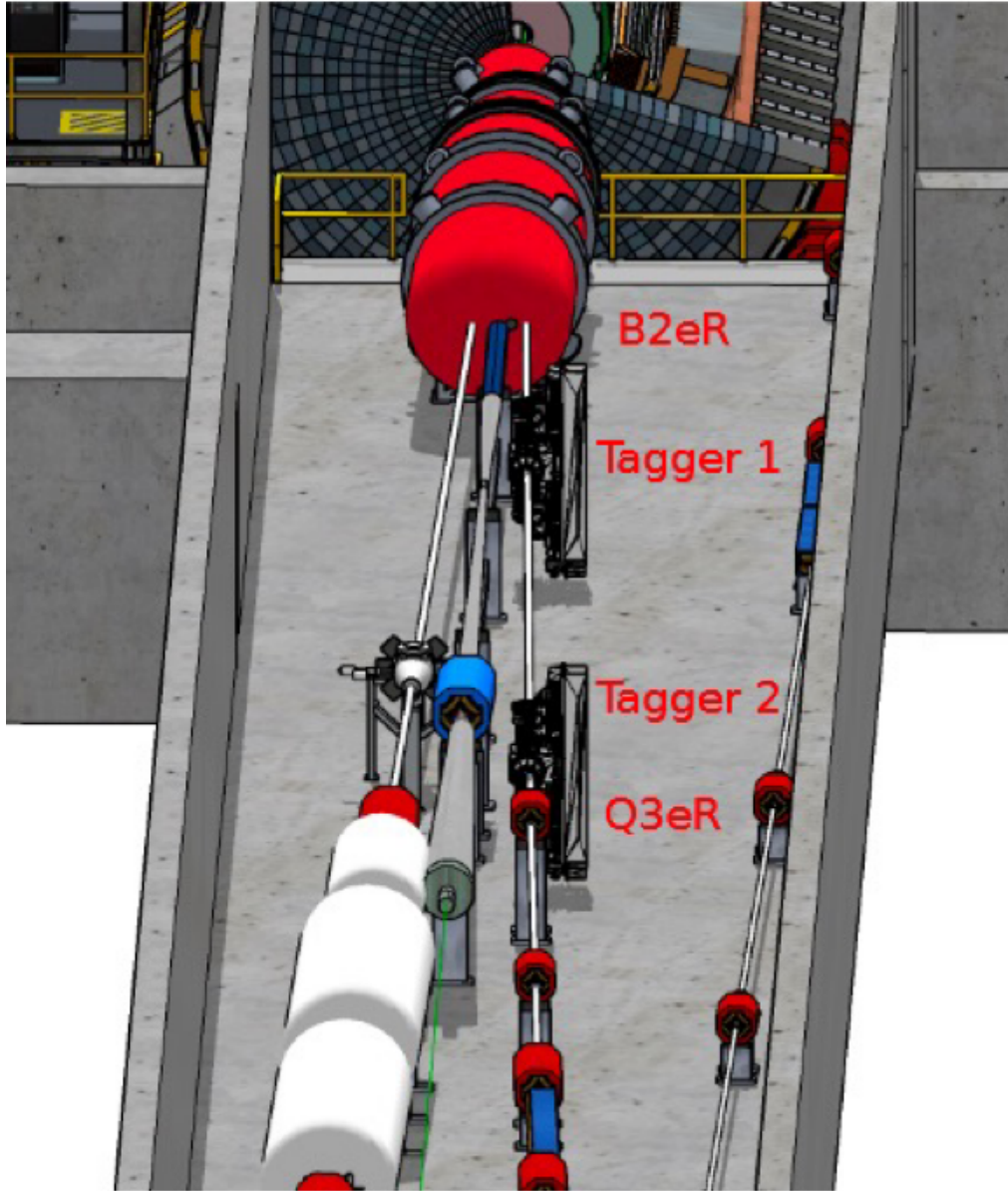


# Far-backward region

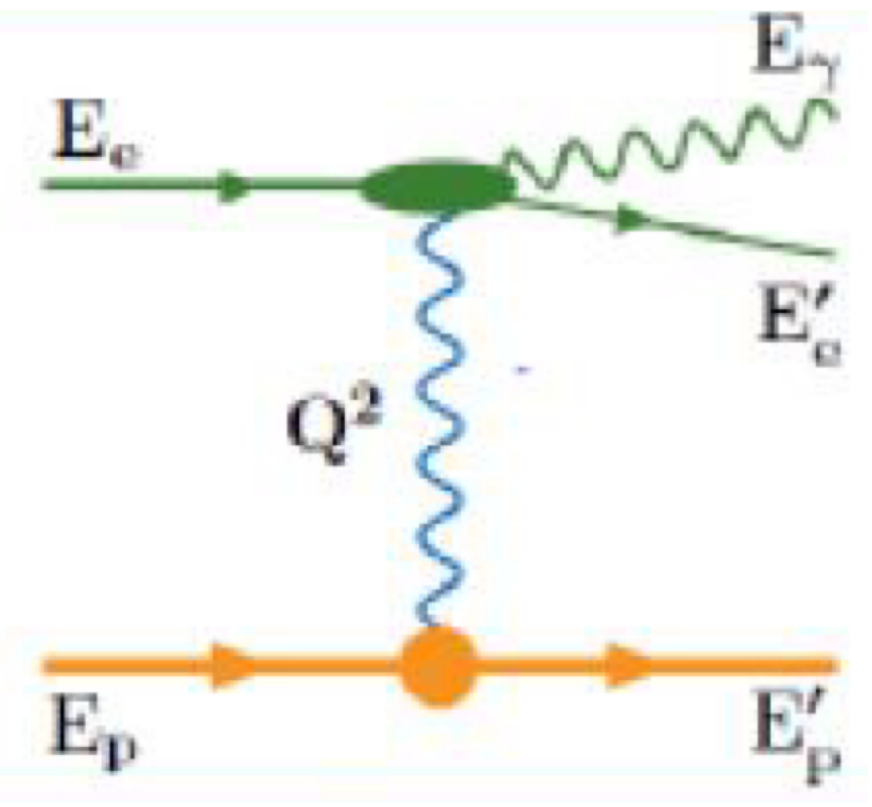


# Far-backward region

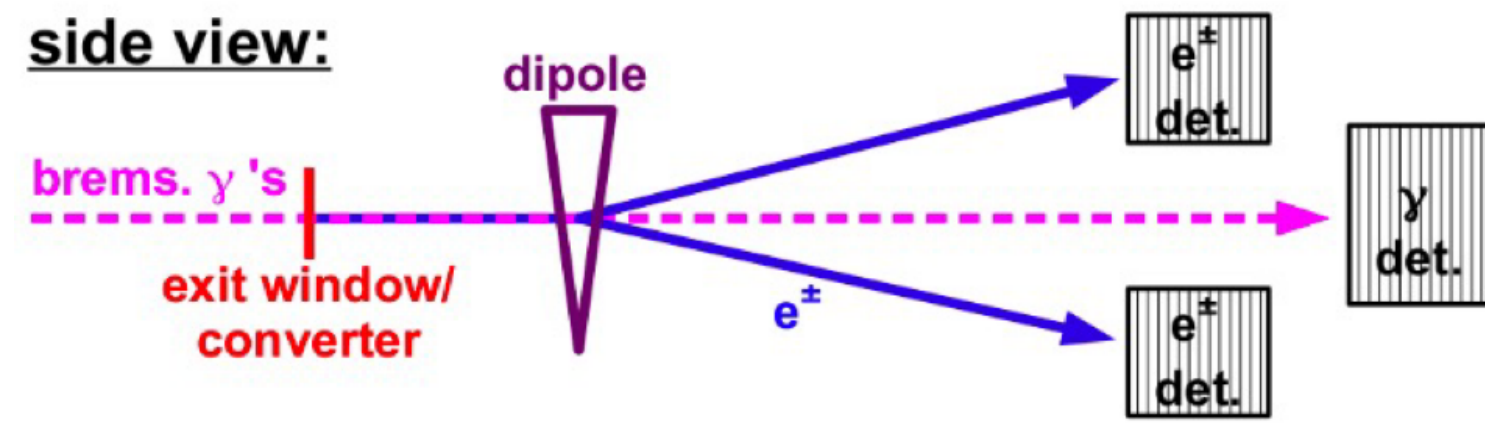
low- $Q^2$  taggers



# Far-backward region

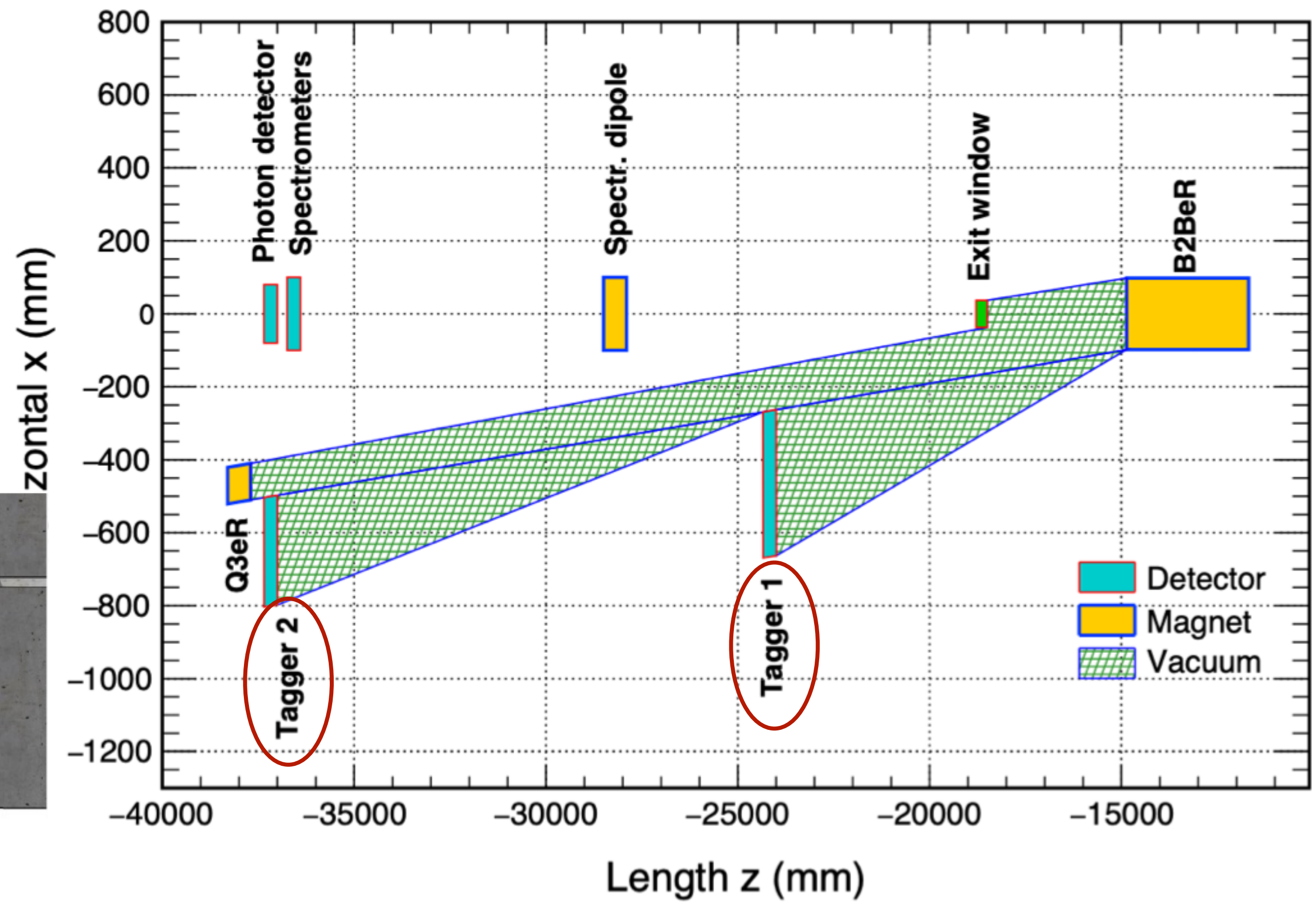
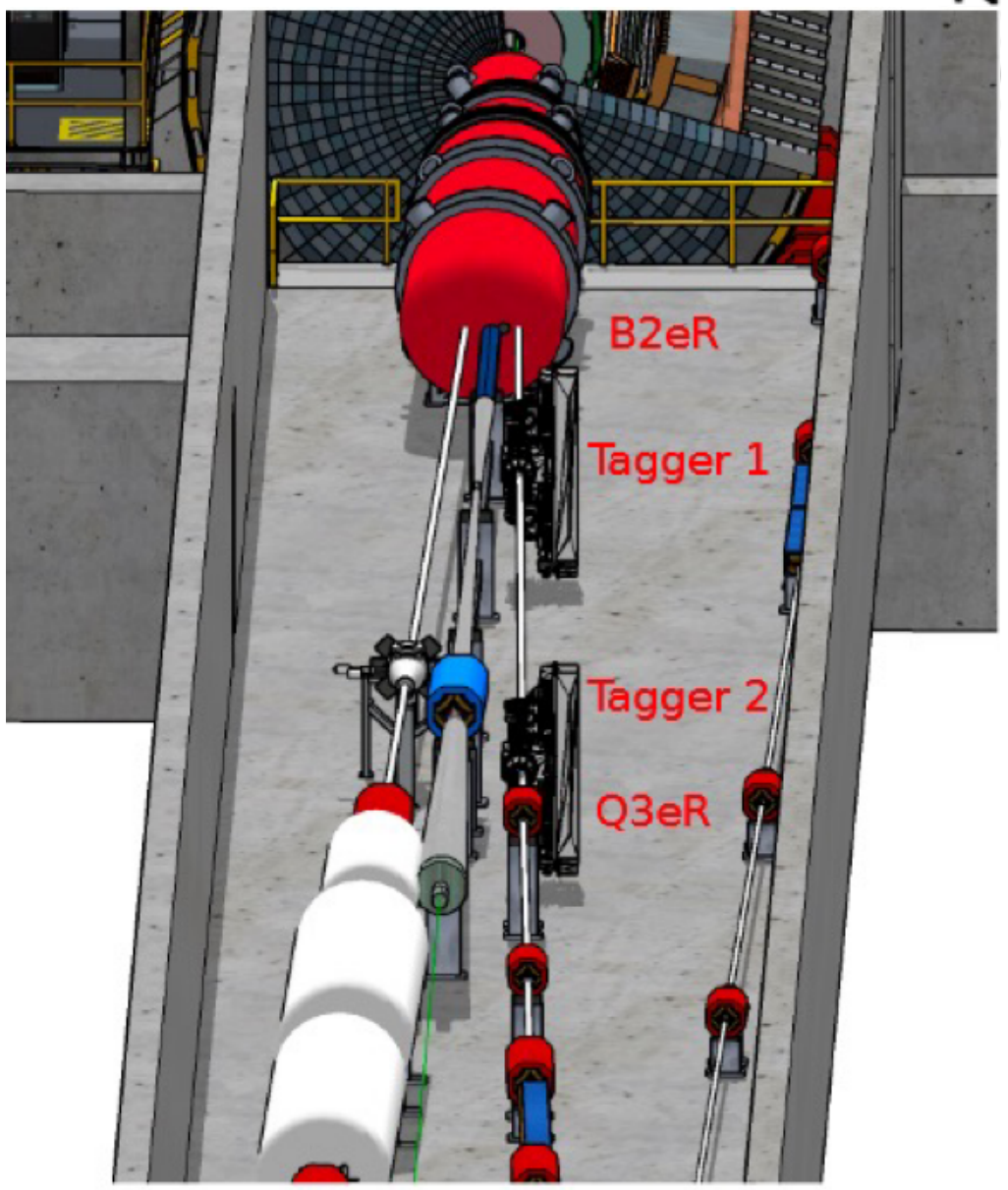


luminosity monitor



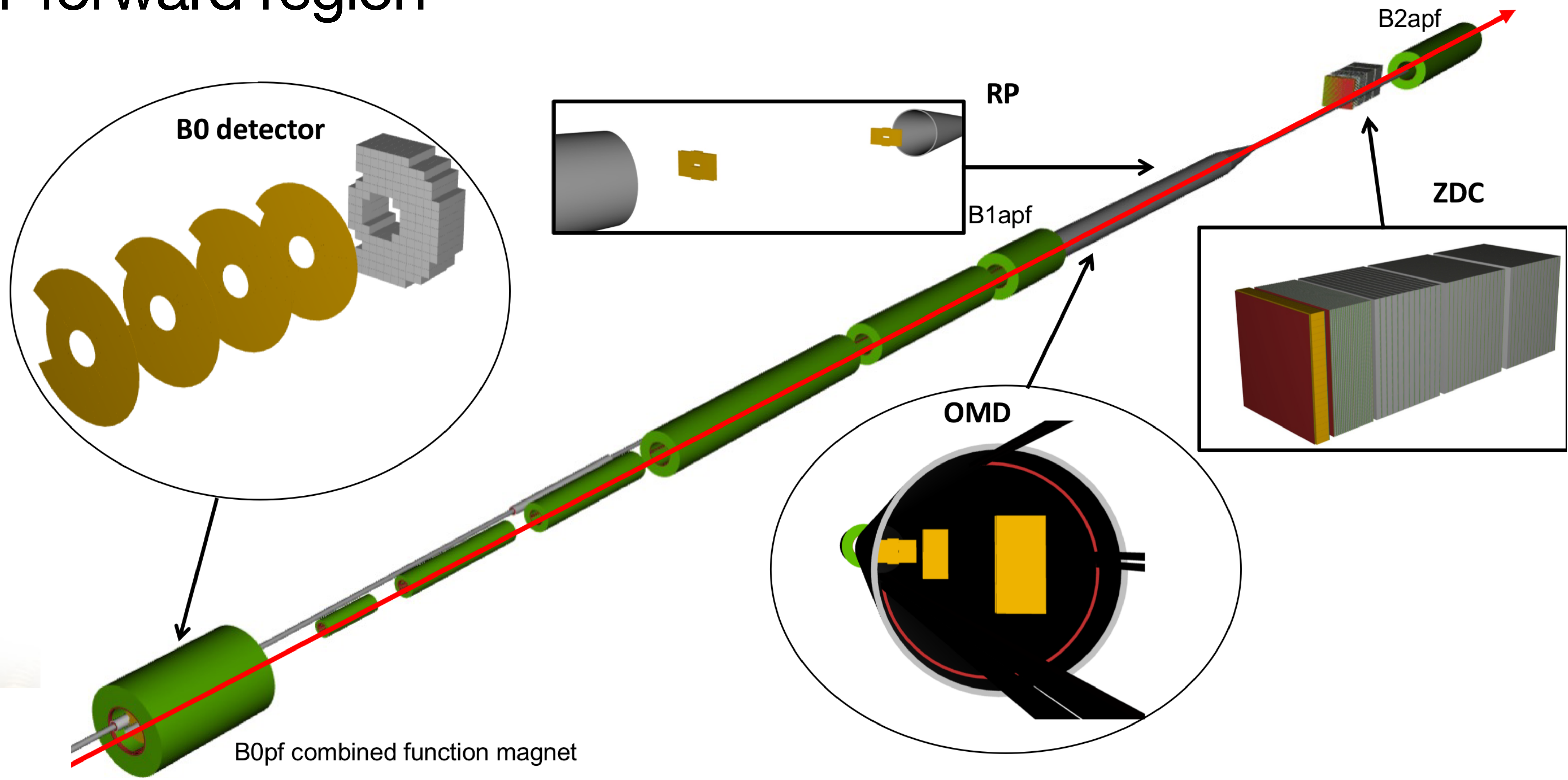
required absolute precision: 1%  
 required relative precision: 0.01%

low- $Q^2$  taggers

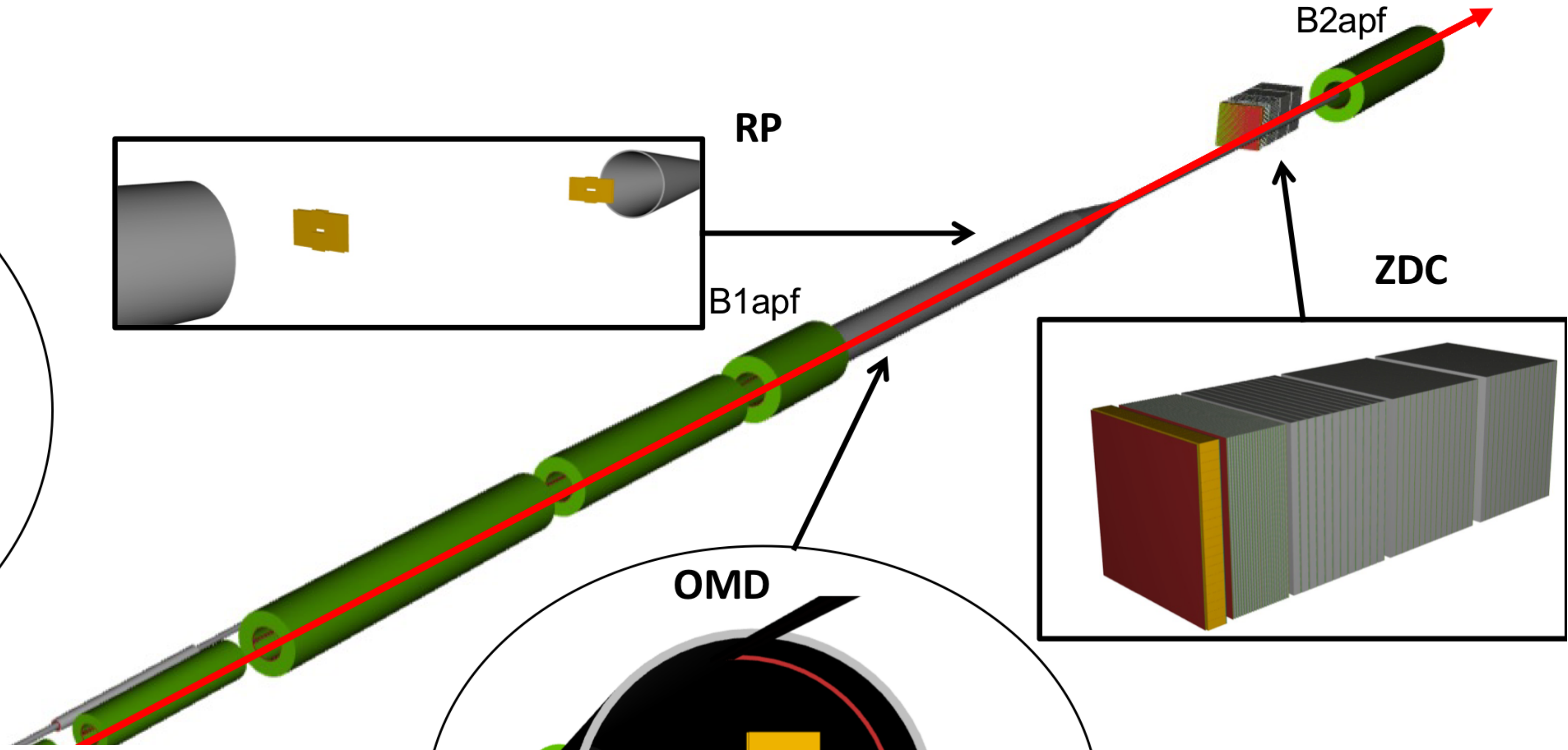
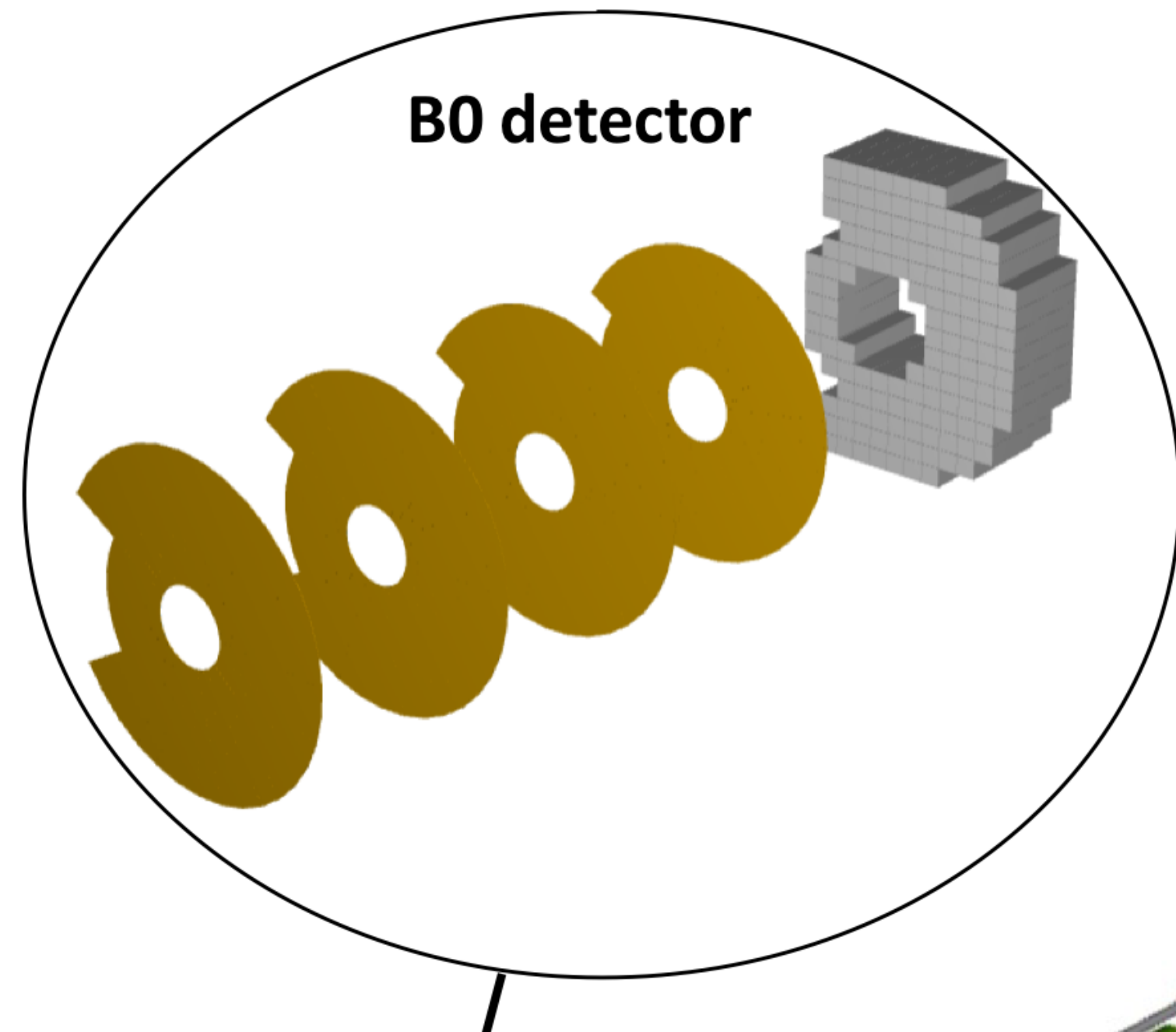




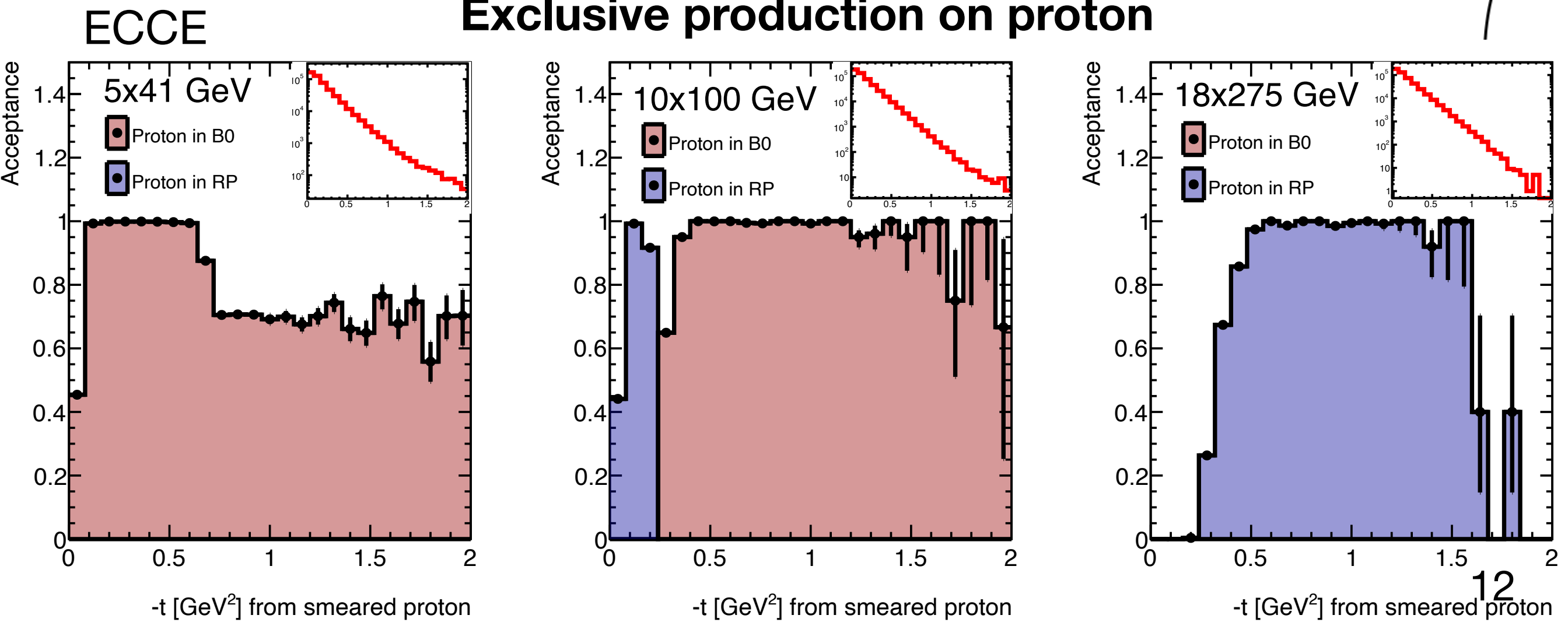
# Far-forward region



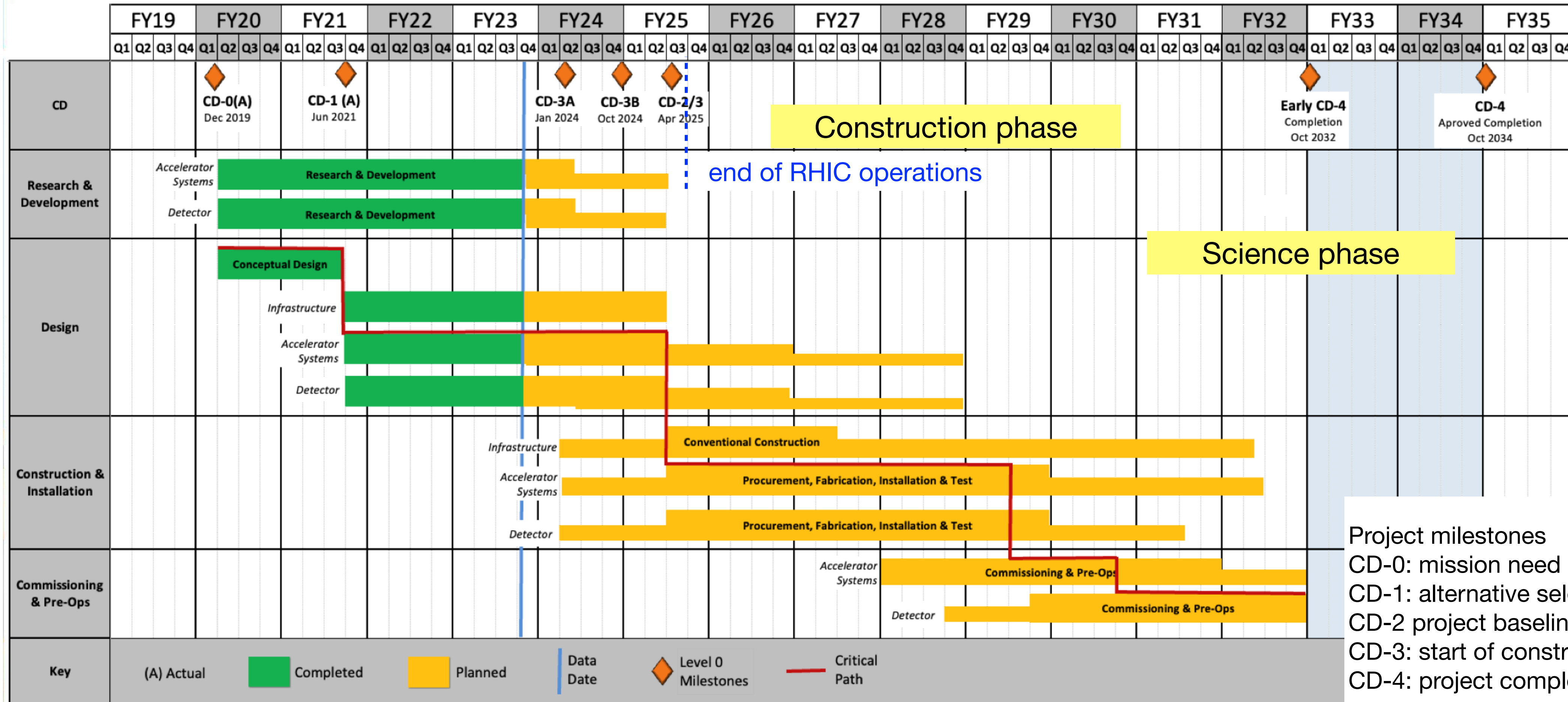
# Far-forward region



**Exclusive production on proton**



# Timeline

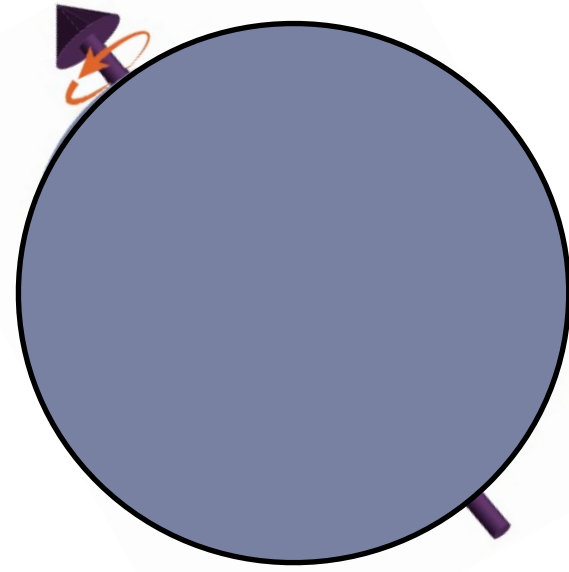


Project milestones  
 CD-0: mission need  
 CD-1: alternative selection, cost range  
 CD-2 project baseline  
 CD-3: start of construction  
 CD-4: project completion, start of operation

# Why an EIC?

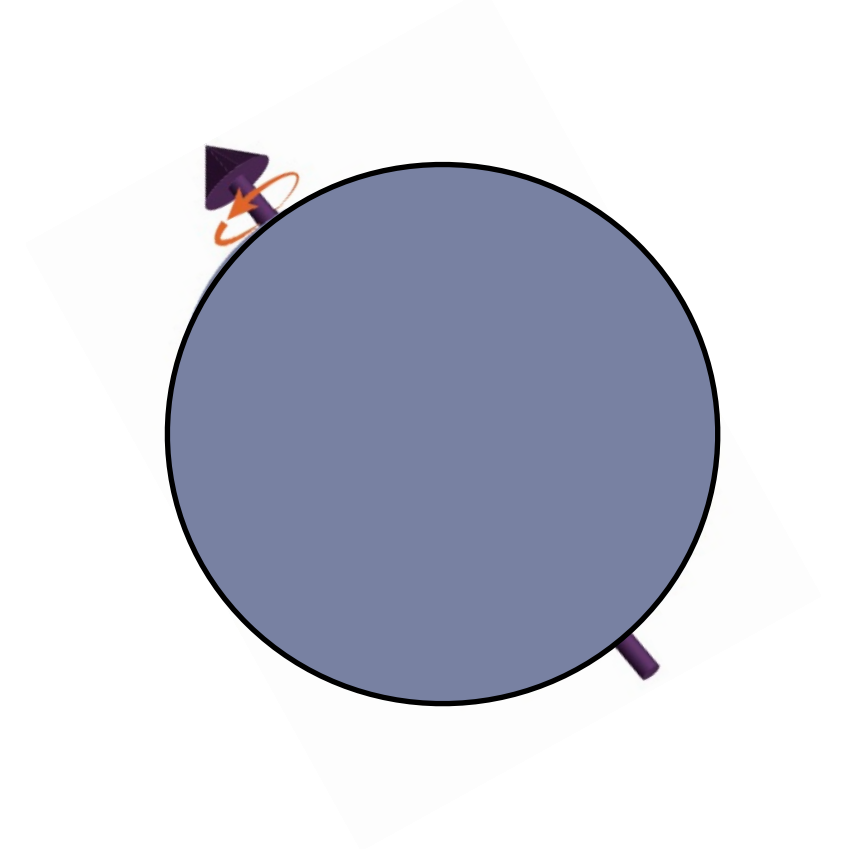
# Why an EIC?

Nucleon spin structure

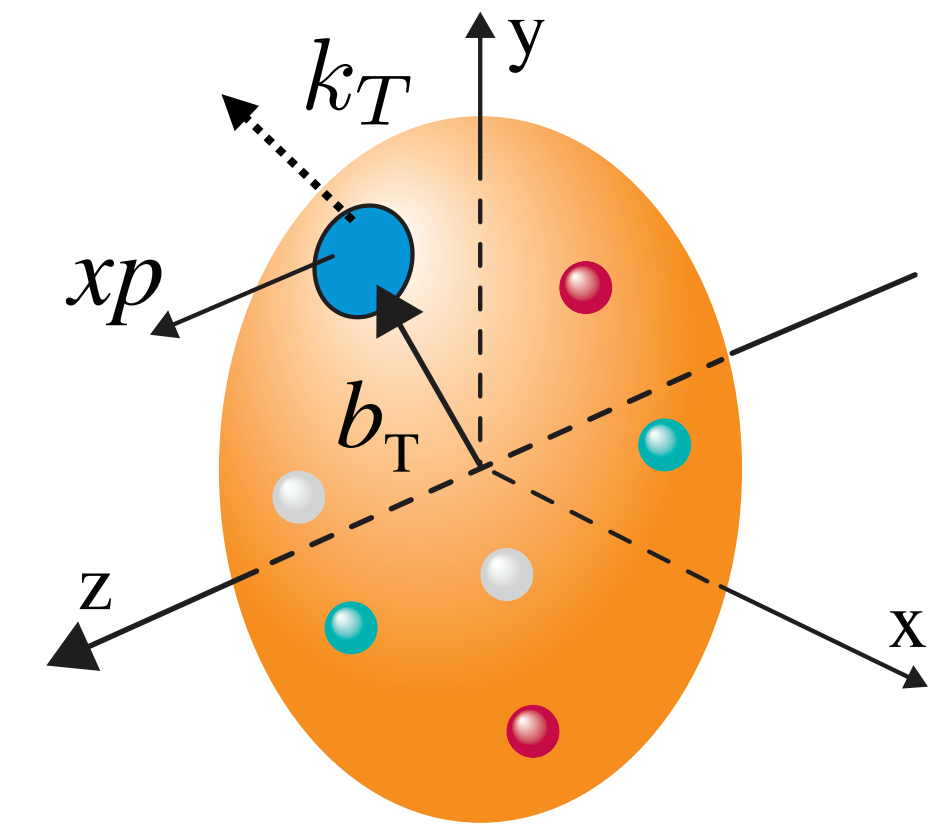


# Why an EIC?

Nucleon spin structure

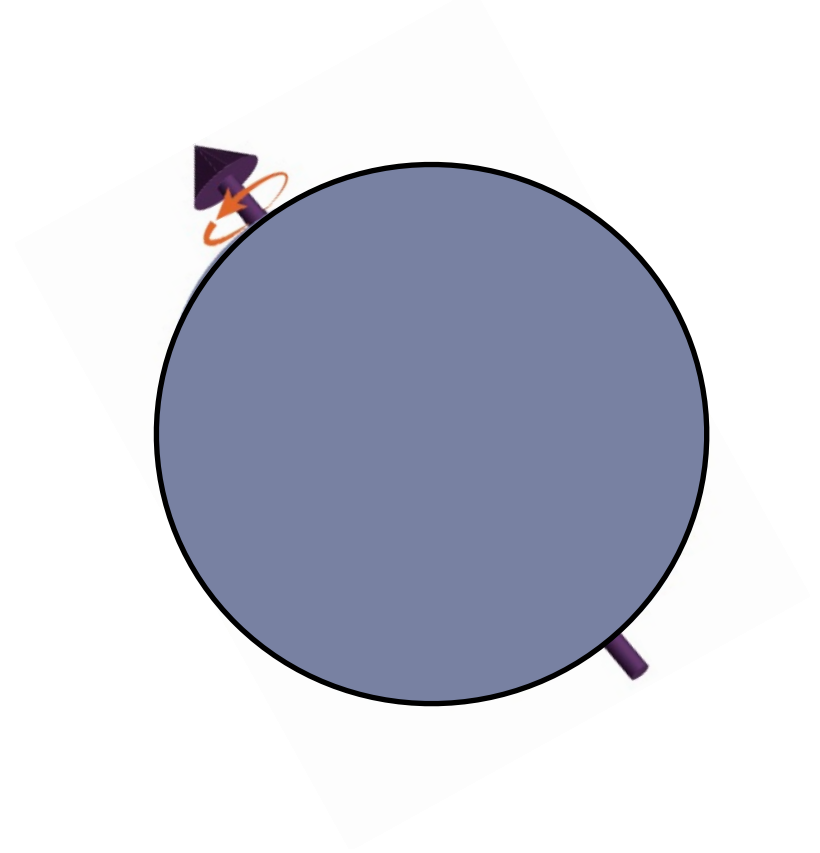


Nucleon multi-dimensional structure

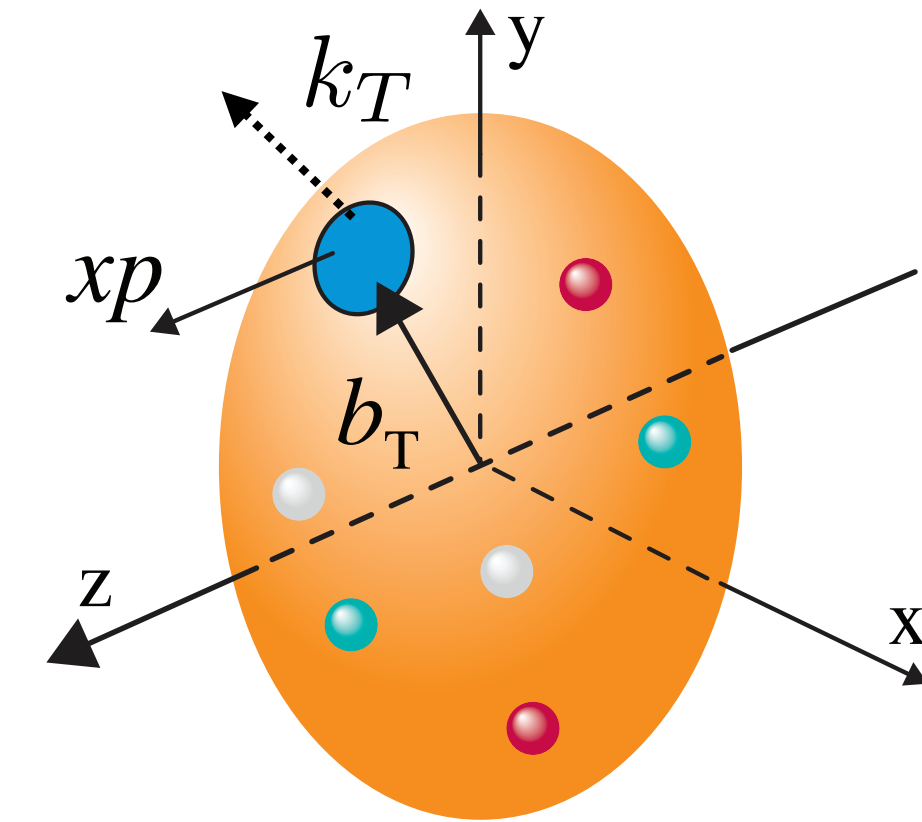


# Why an EIC?

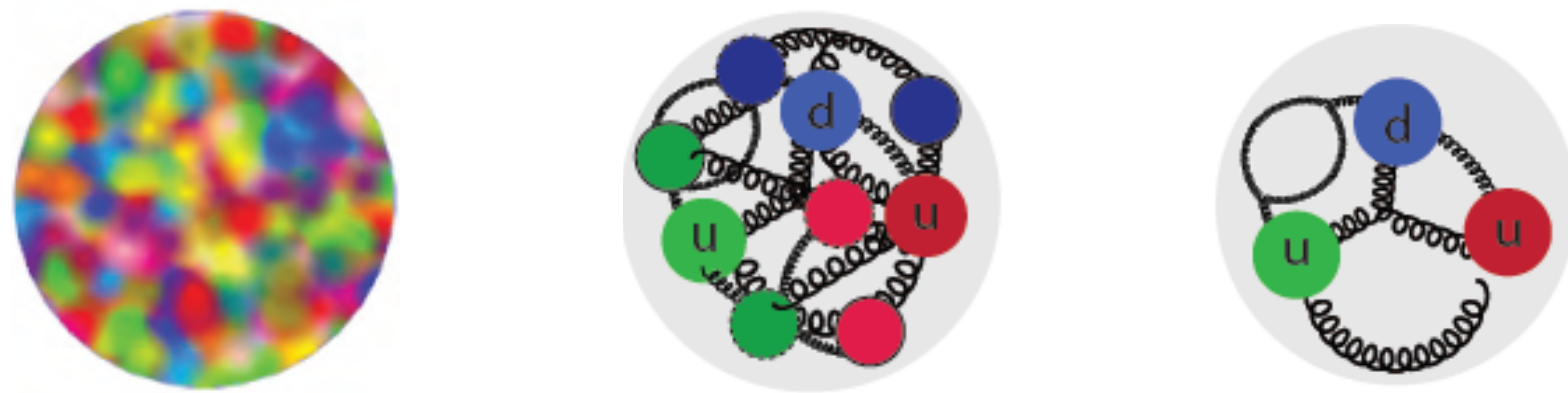
Nucleon spin structure



Nucleon multi-dimensional structure

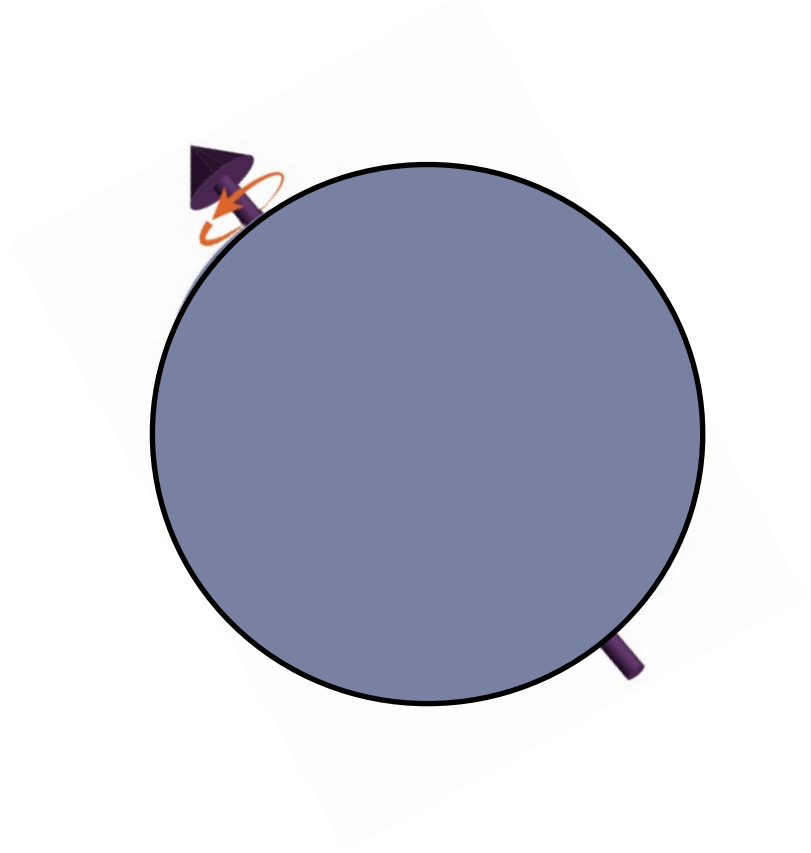


Gluon saturation

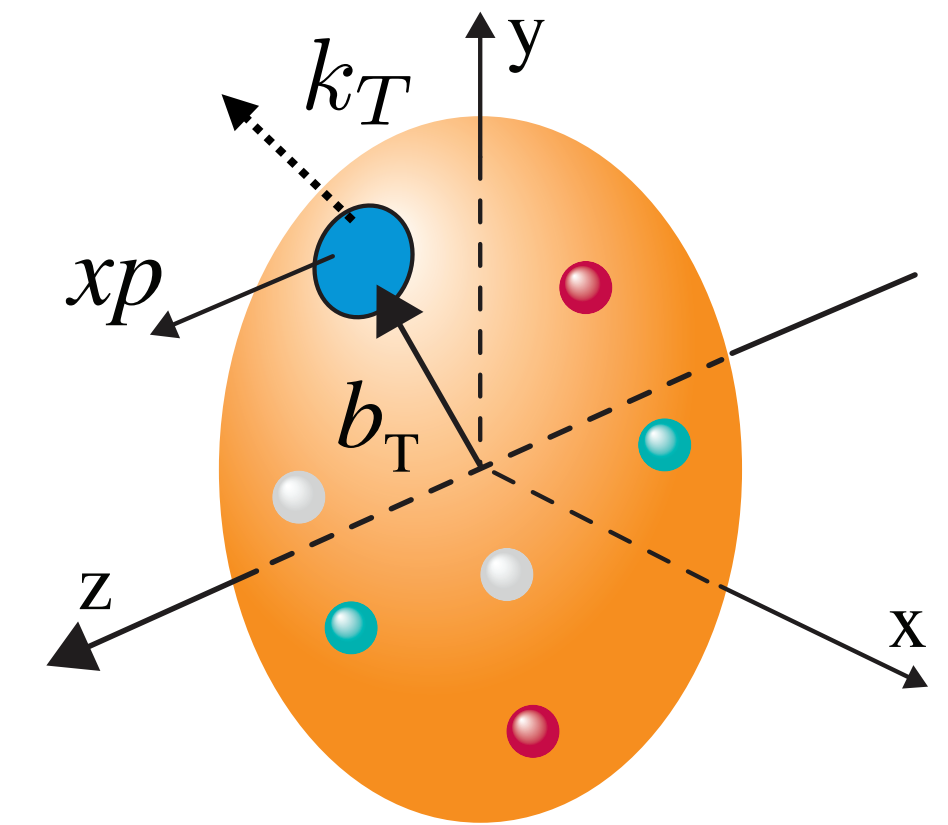


# Why an EIC?

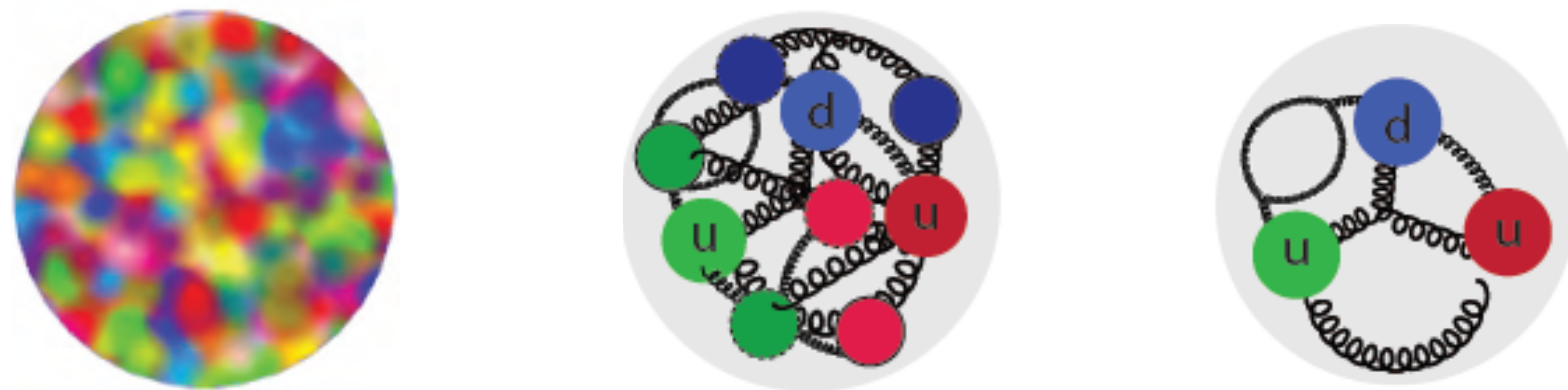
Nucleon spin structure



Nucleon multi-dimensional structure



Gluon saturation

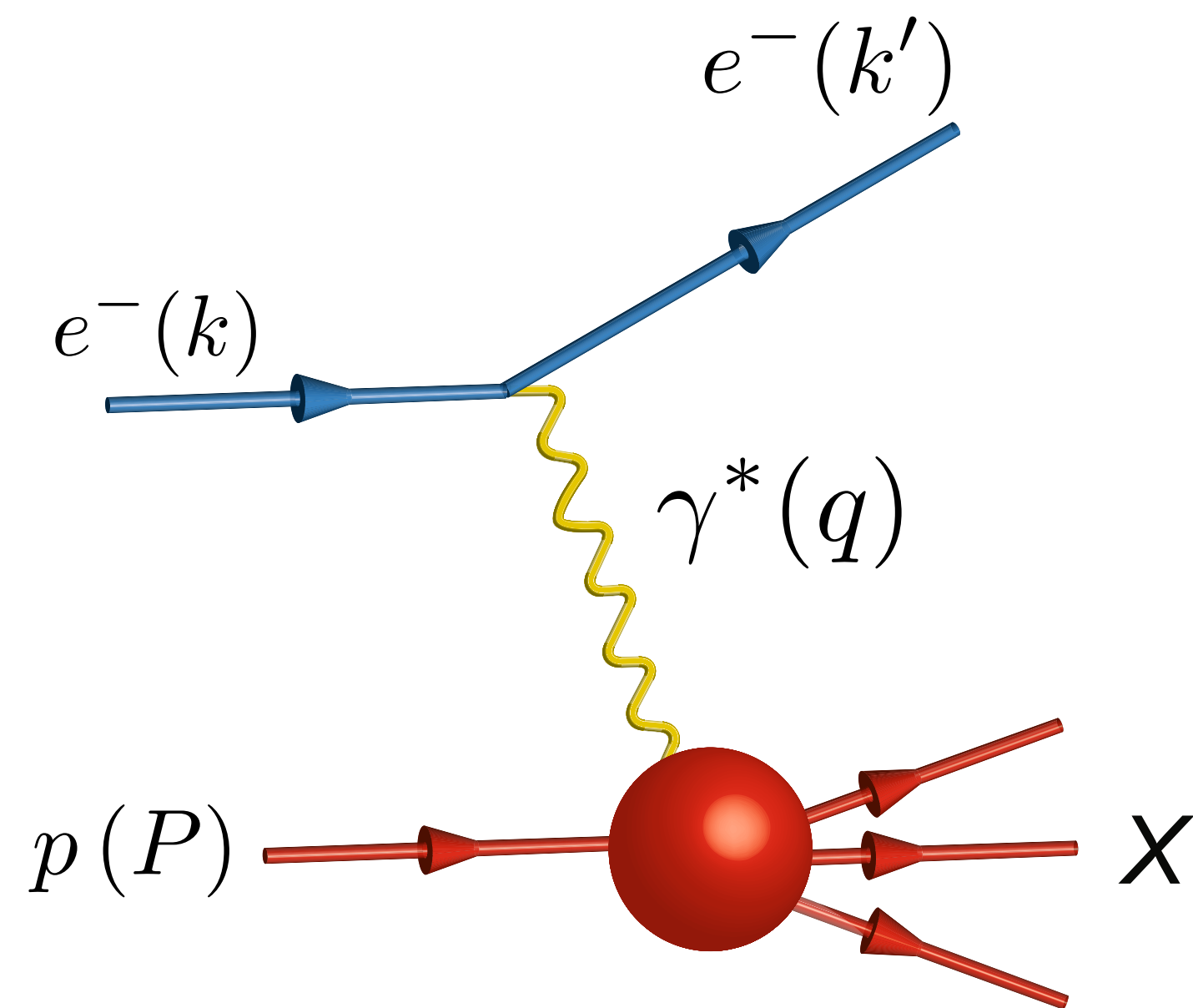


Hadronisation

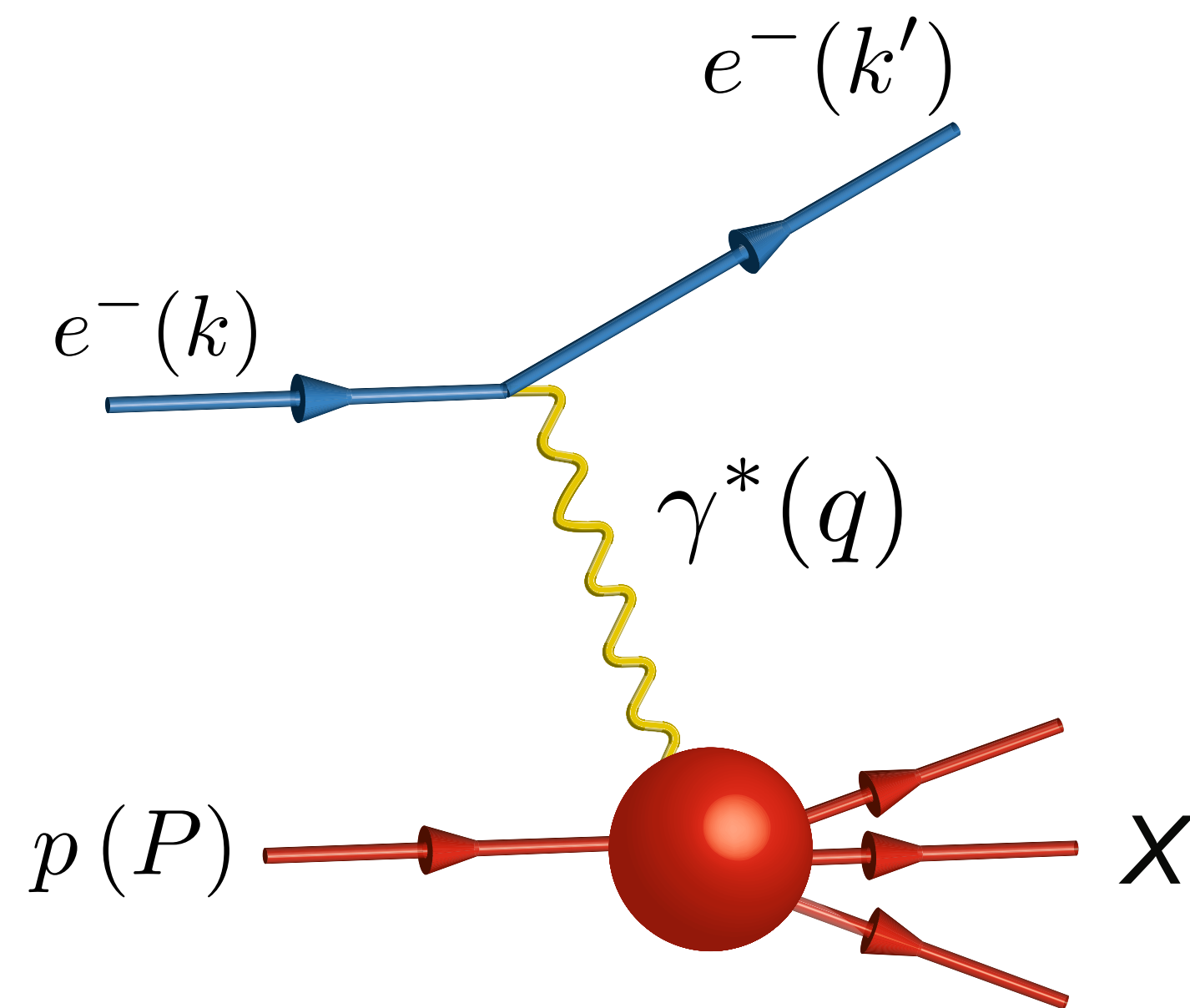




# Deep-inelastic scattering (DIS) of electrons and nucleons/nuclei

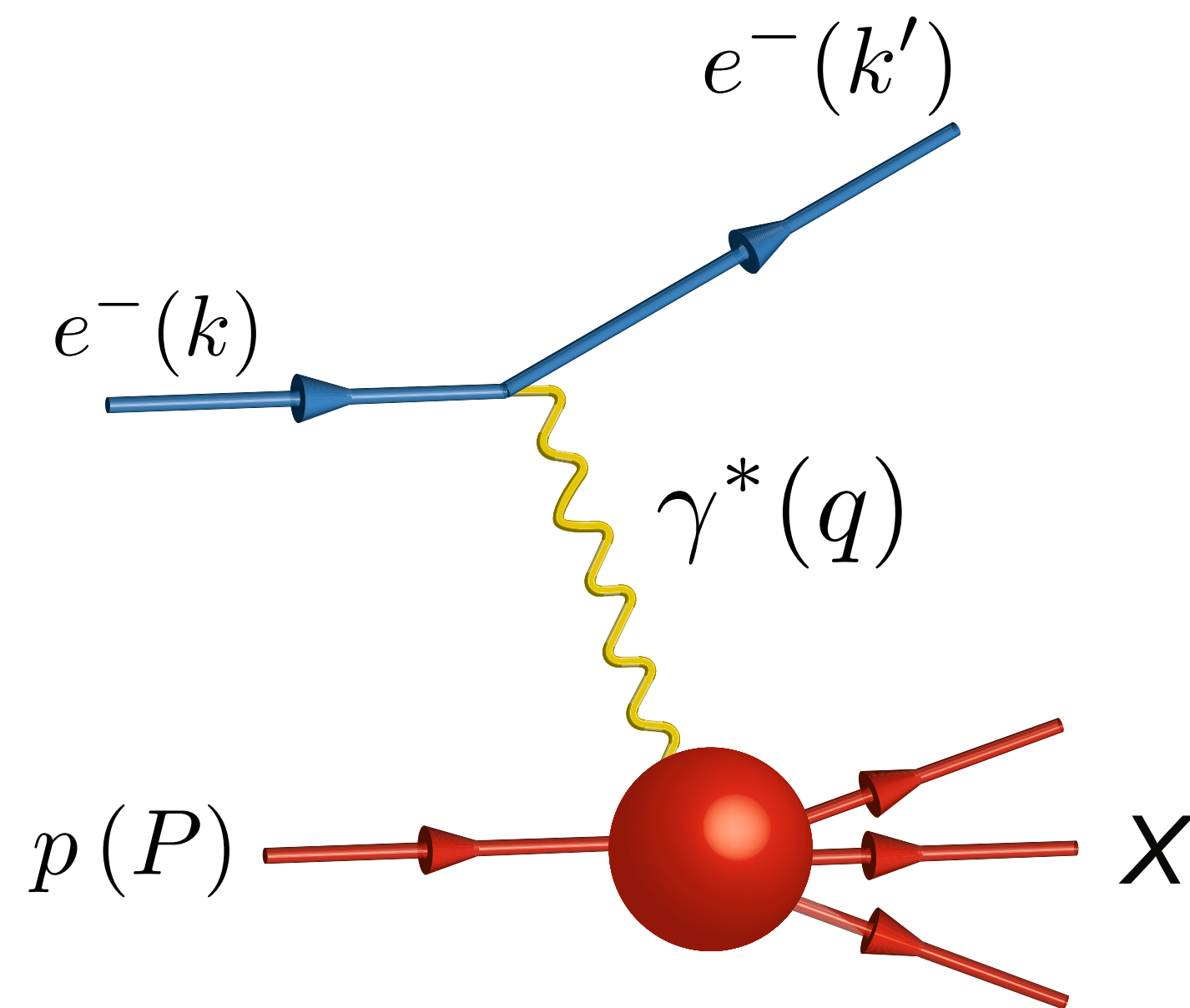


# Deep-inelastic scattering (DIS) of electrons and nucleons/nuclei



$$Q^2 = -q^2$$

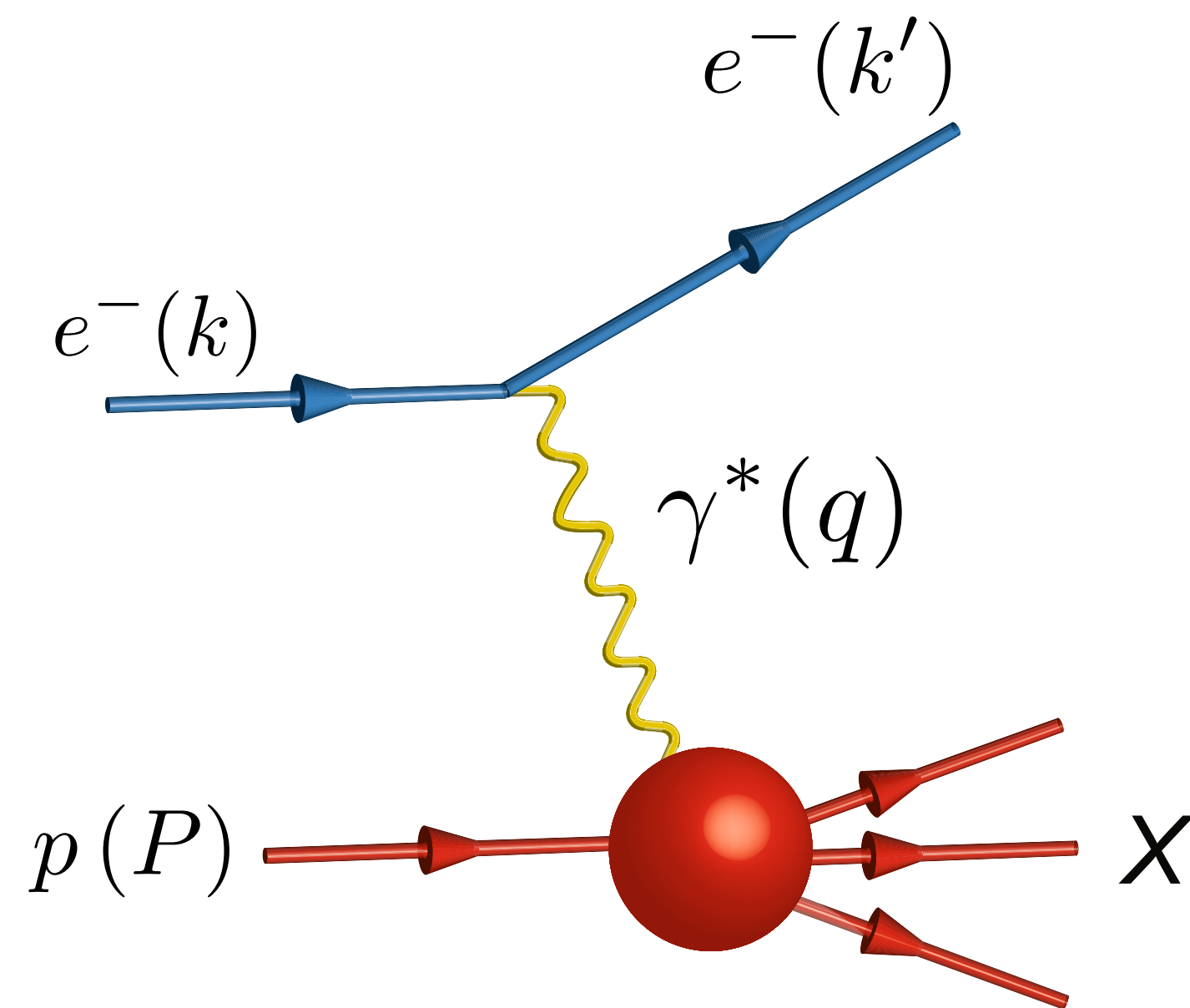
# Deep-inelastic scattering (DIS) of electrons and nucleons/nuclei



$$Q^2 = -q^2$$

Highly virtual photon:  
 $Q^2 \gg 1 \text{ GeV}^2$   
provides hard  
scale of process

# Deep-inelastic scattering (DIS) of electrons and nucleons/nuclei

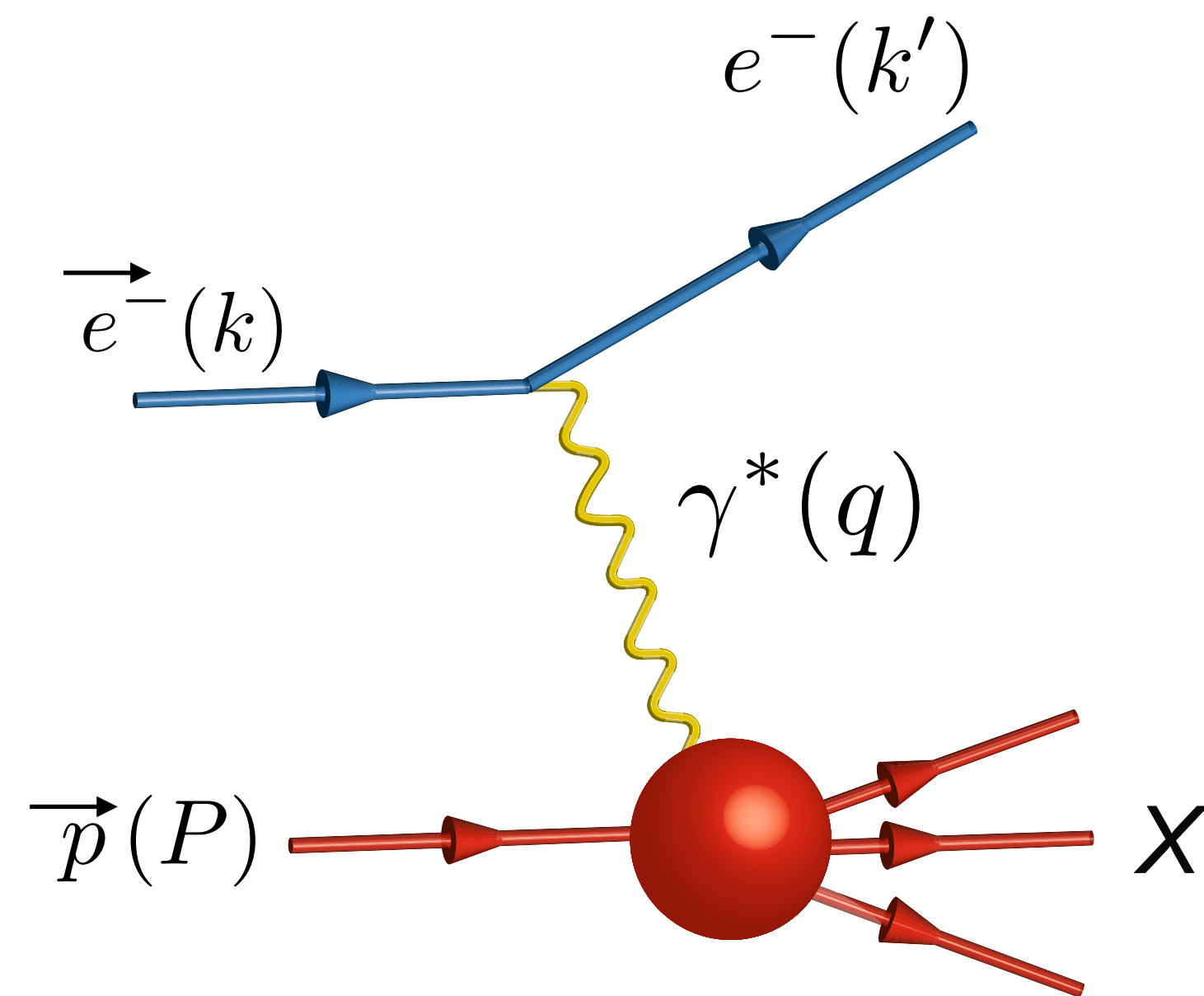


$$Q^2 = -q^2$$

Highly virtual photon:  
 $Q^2 \gg 1 \text{ GeV}^2$   
provides hard  
scale of process

$$x_B = \frac{Q^2}{2P \cdot q}$$

# Deep-inelastic scattering (DIS) of electrons and nucleons/nuclei

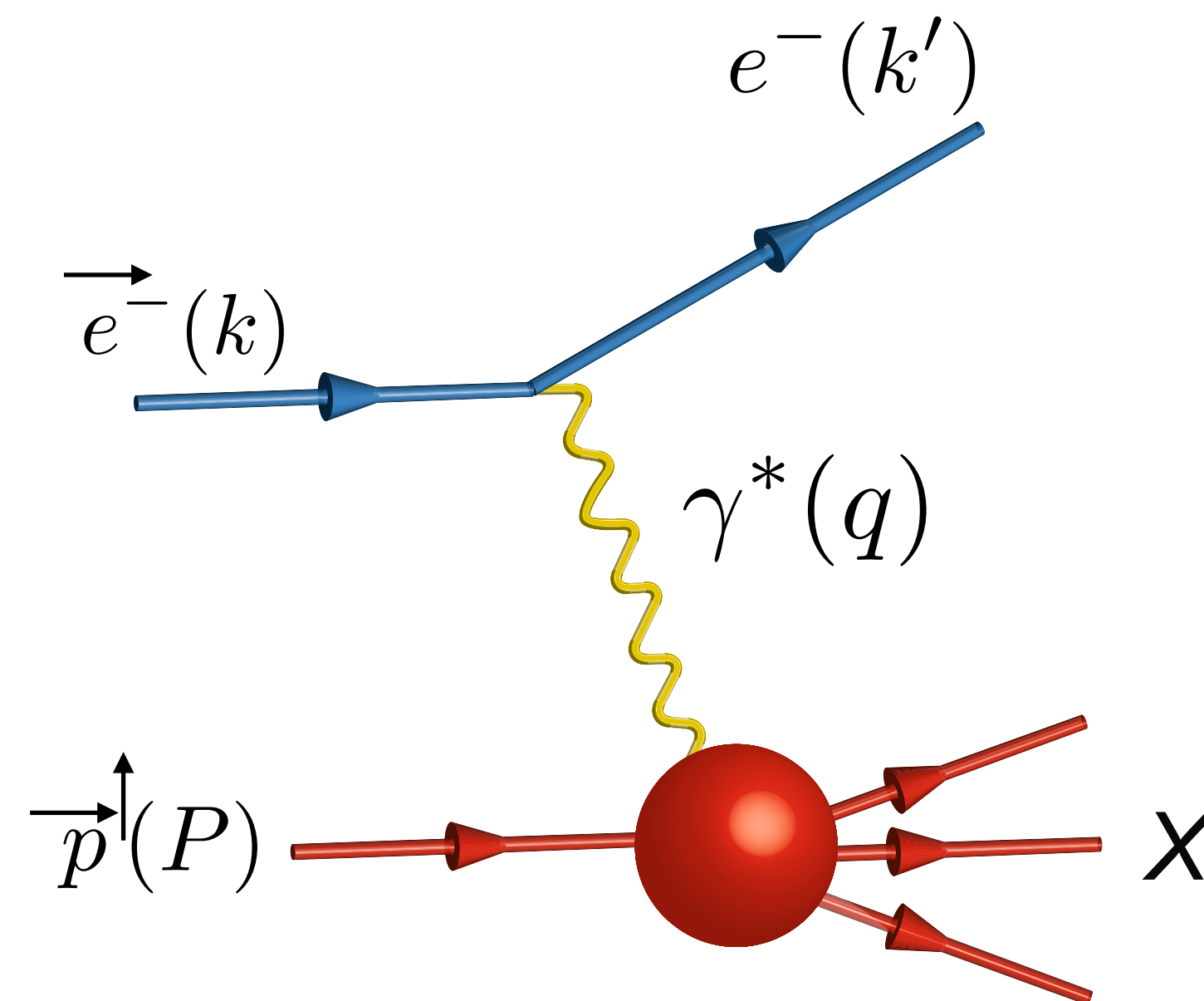


$$Q^2 = -q^2$$

Highly virtual photon:  
 $Q^2 \gg 1 \text{ GeV}^2$   
provides hard  
scale of process

$$x_B = \frac{Q^2}{2P \cdot q}$$

# Deep-inelastic scattering (DIS) of electrons and nucleons/nuclei

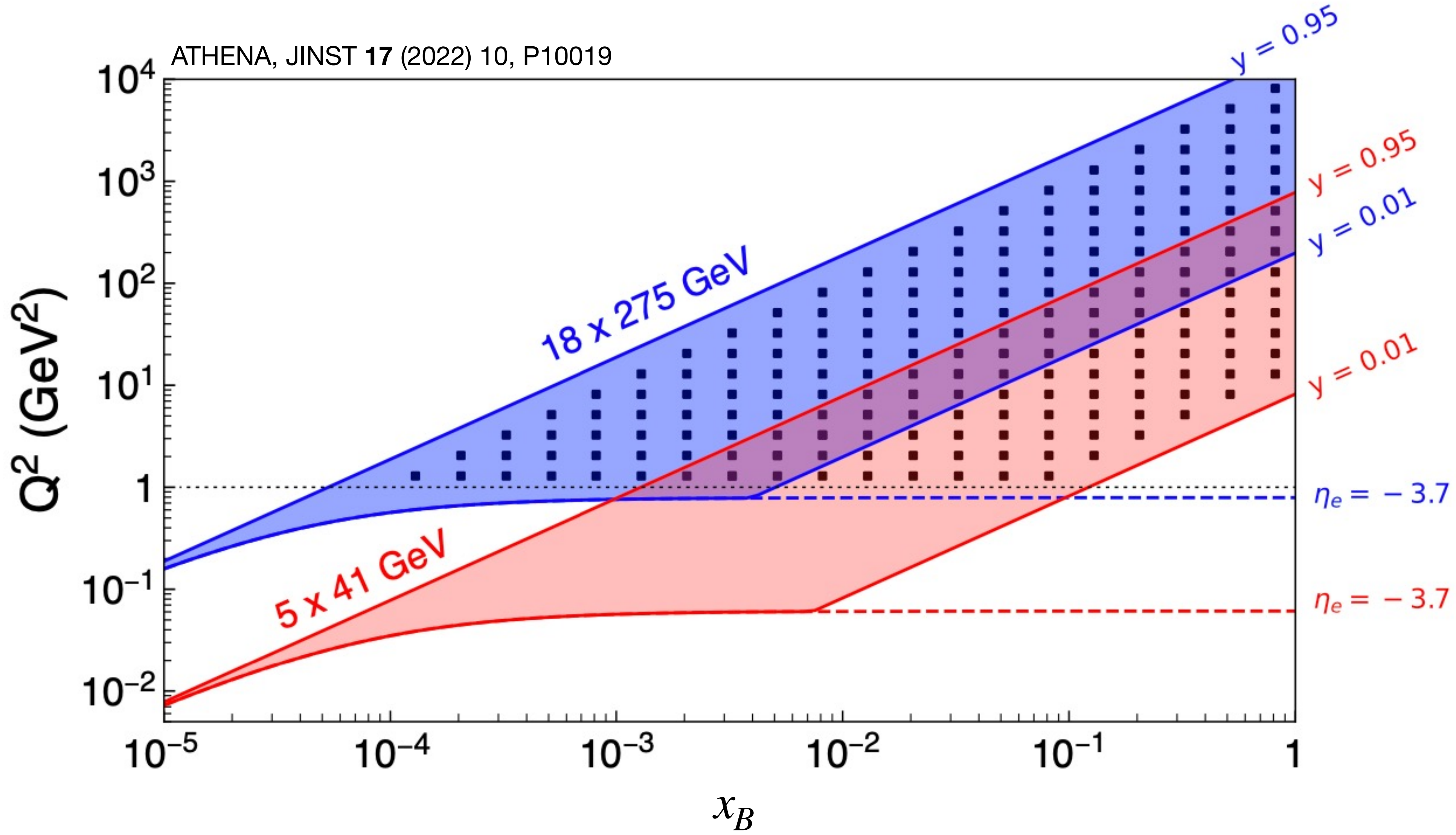


$$Q^2 = -q^2$$

Highly virtual photon:  
 $Q^2 \gg 1 \text{ GeV}^2$   
provides hard  
scale of process

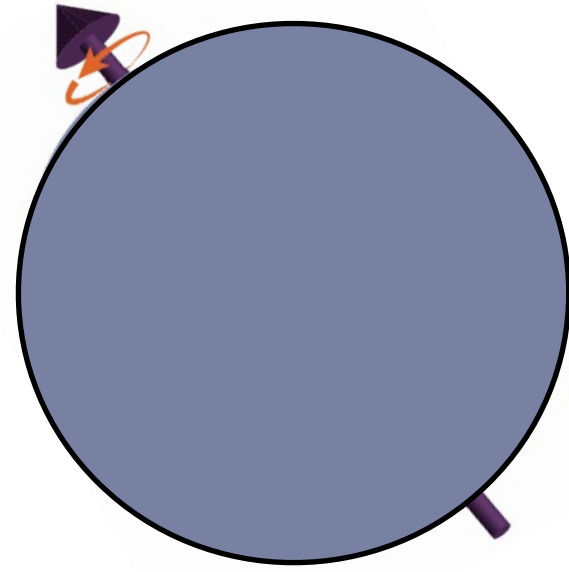
$$x_B = \frac{Q^2}{2P \cdot q}$$

# Kinematic coverage at the EIC



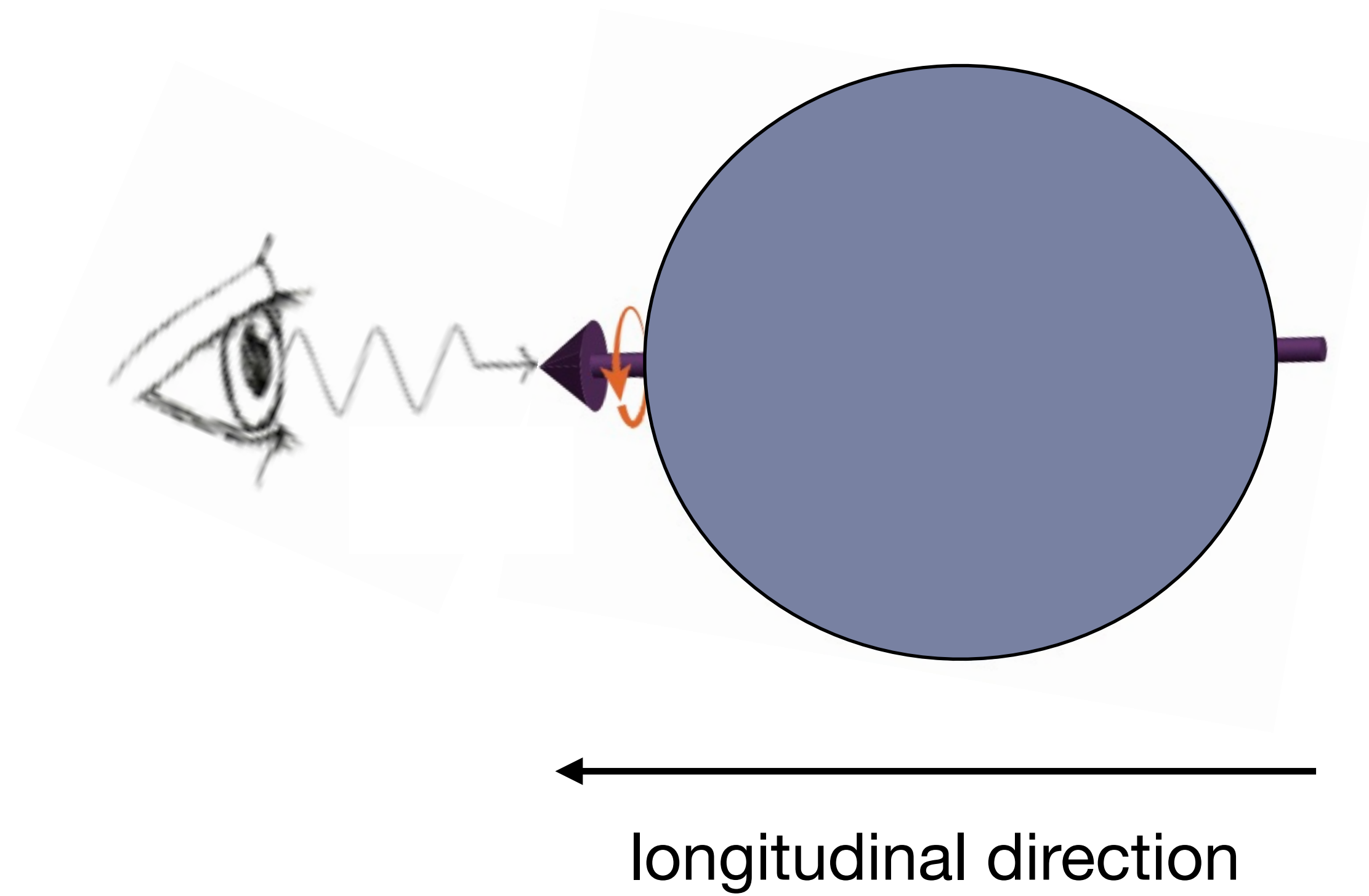
# Why an EIC?

Nucleon spin structure

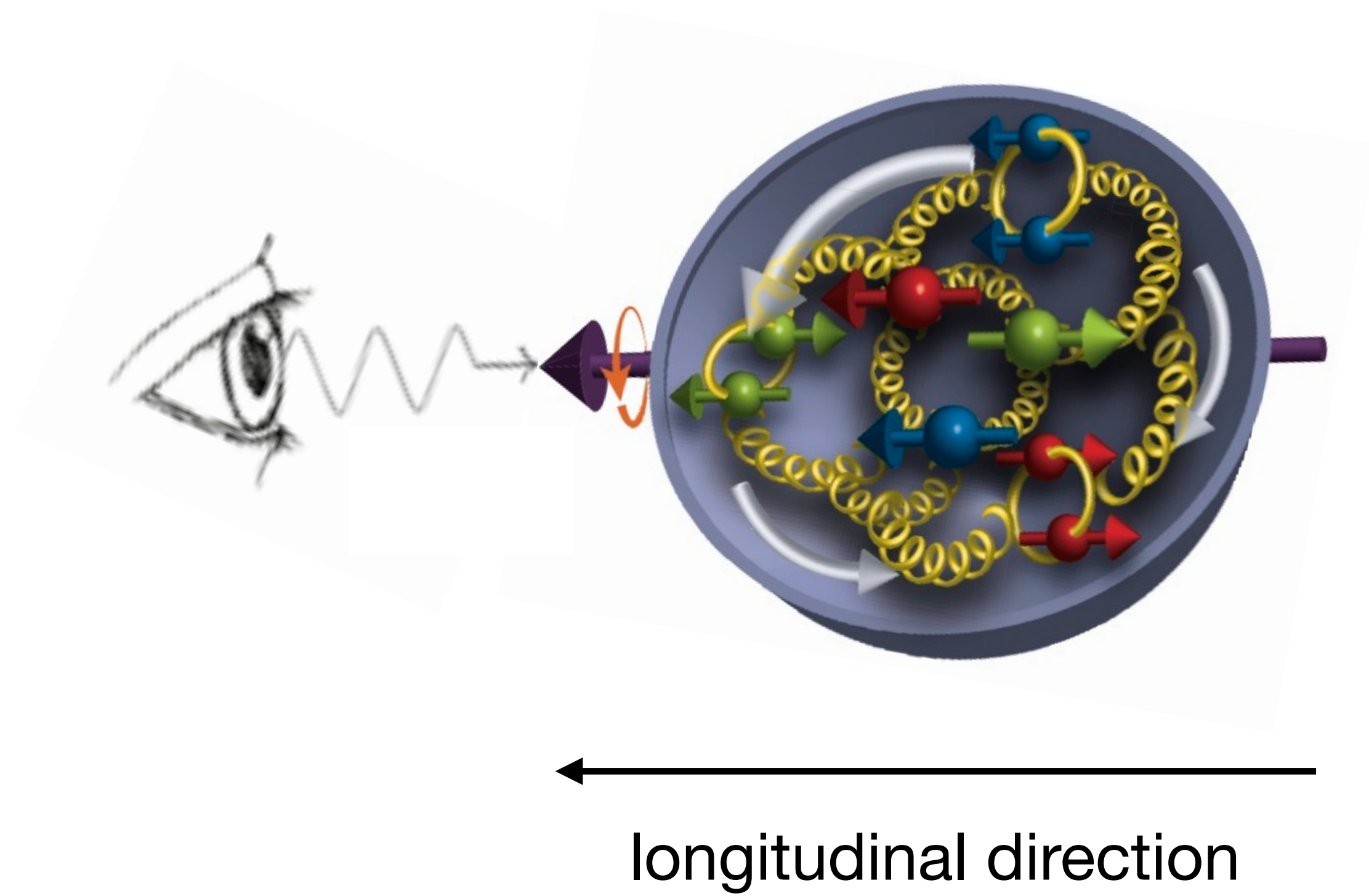




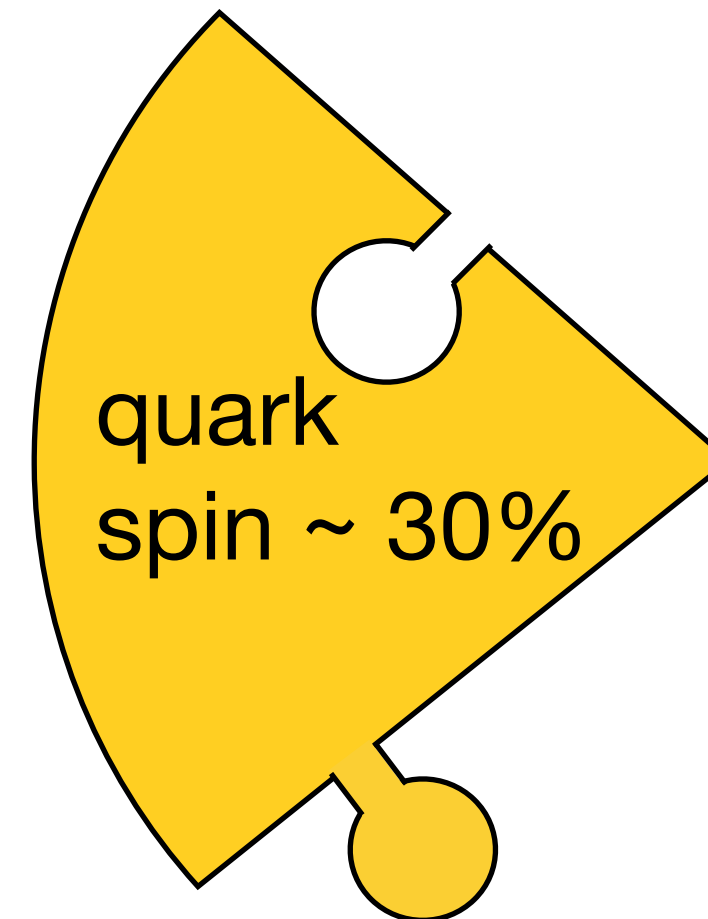
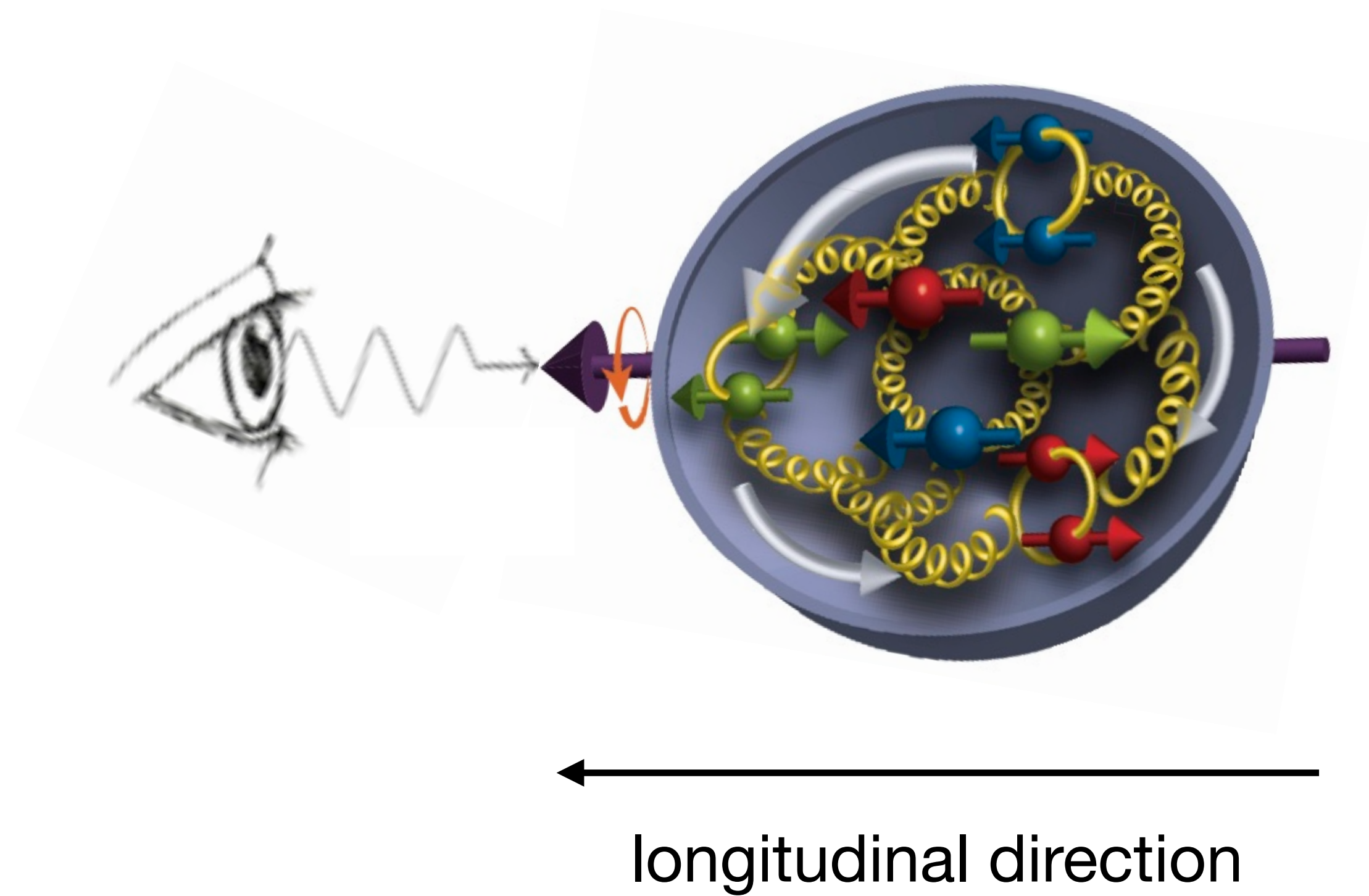
# The nucleon spin



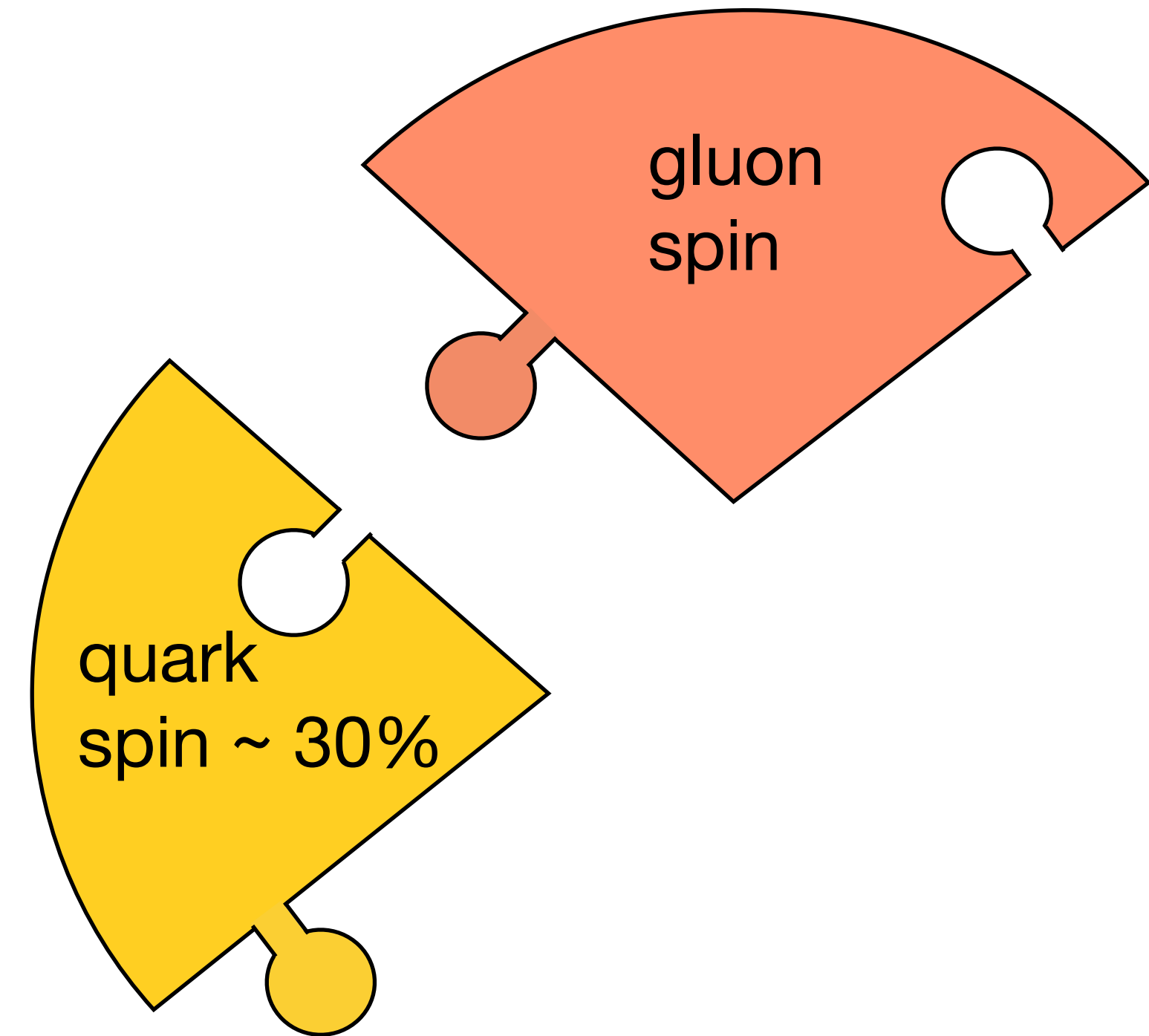
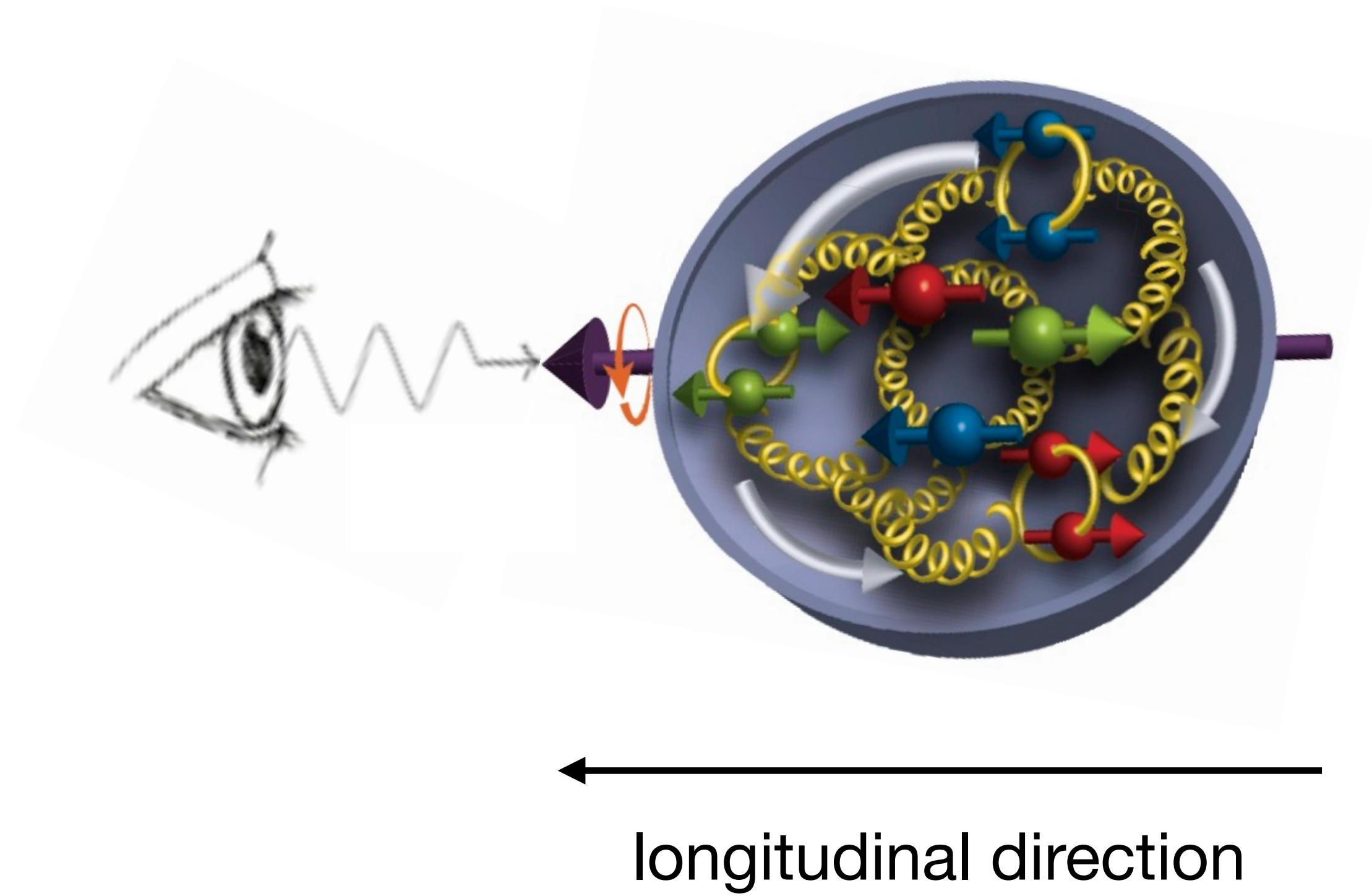
# The nucleon spin



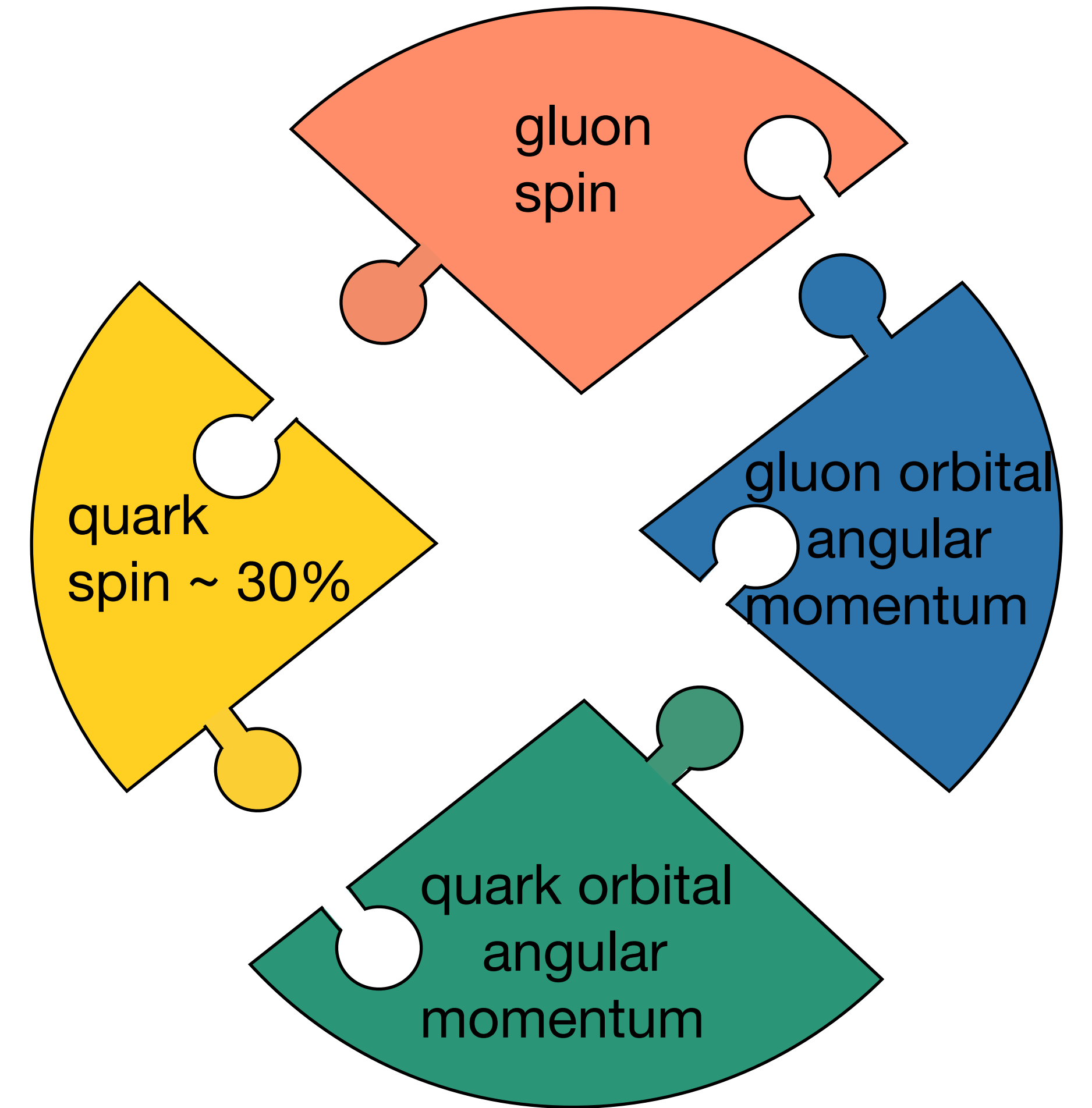
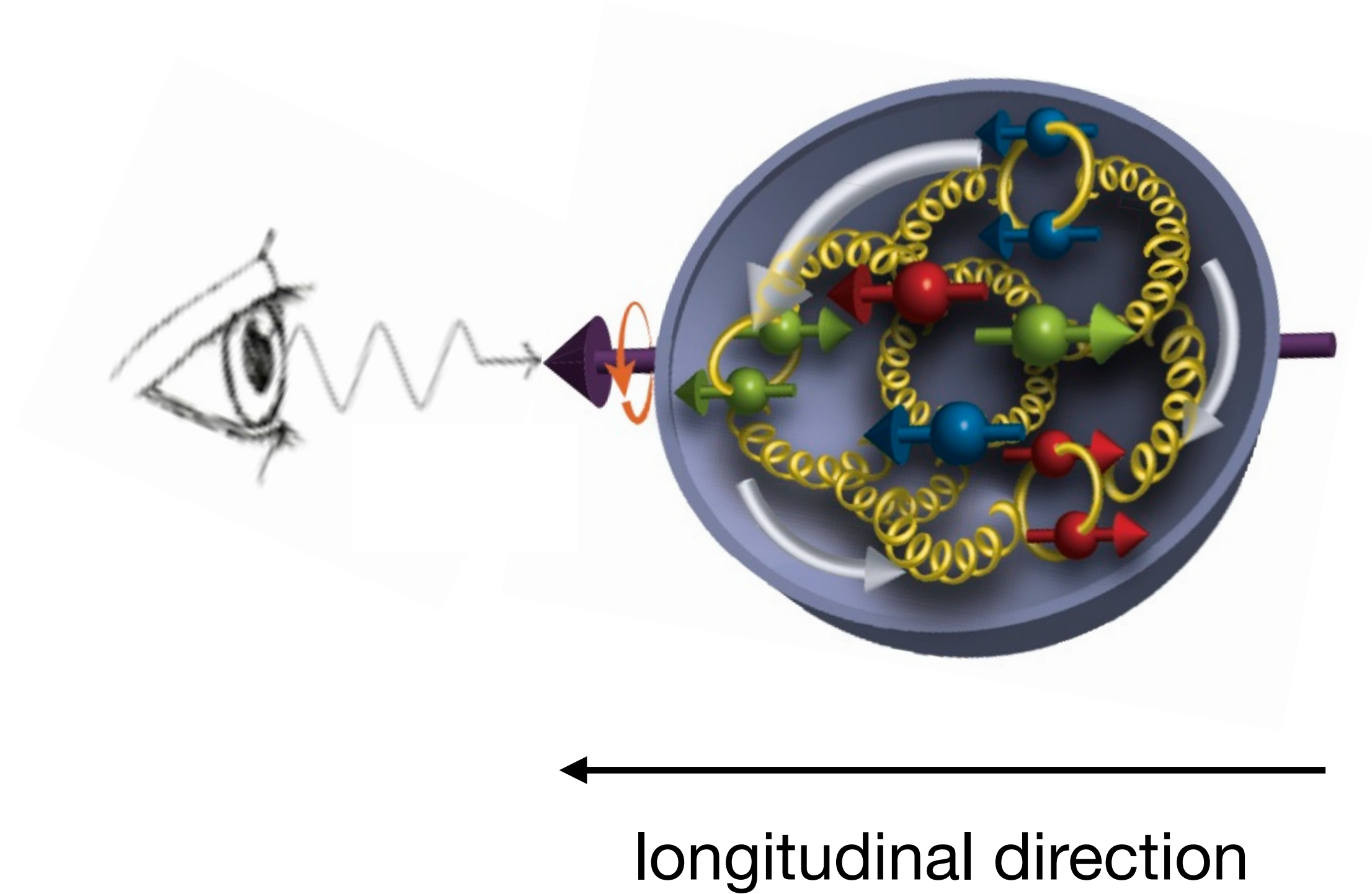
# The nucleon spin



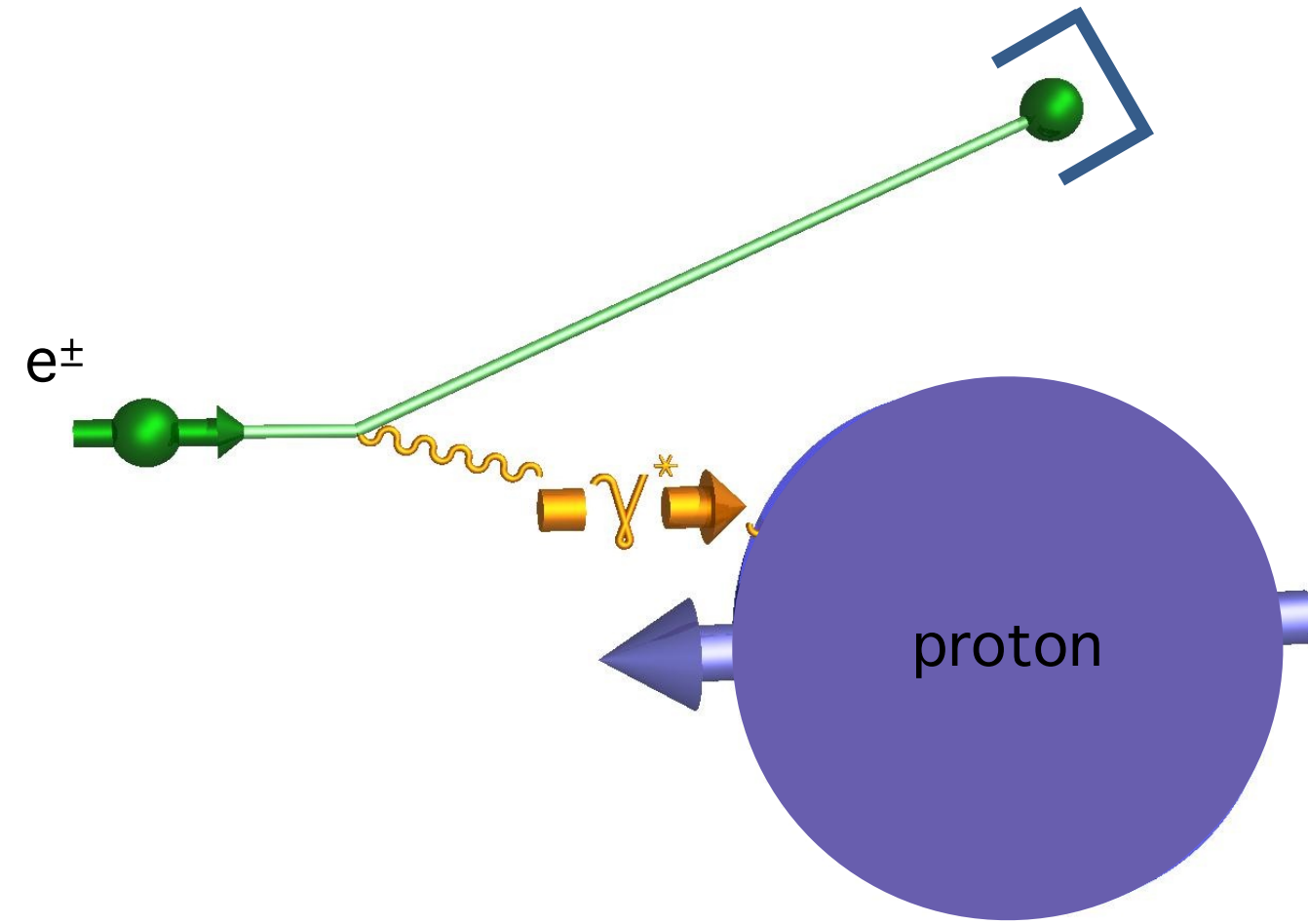
# The nucleon spin



# The nucleon spin

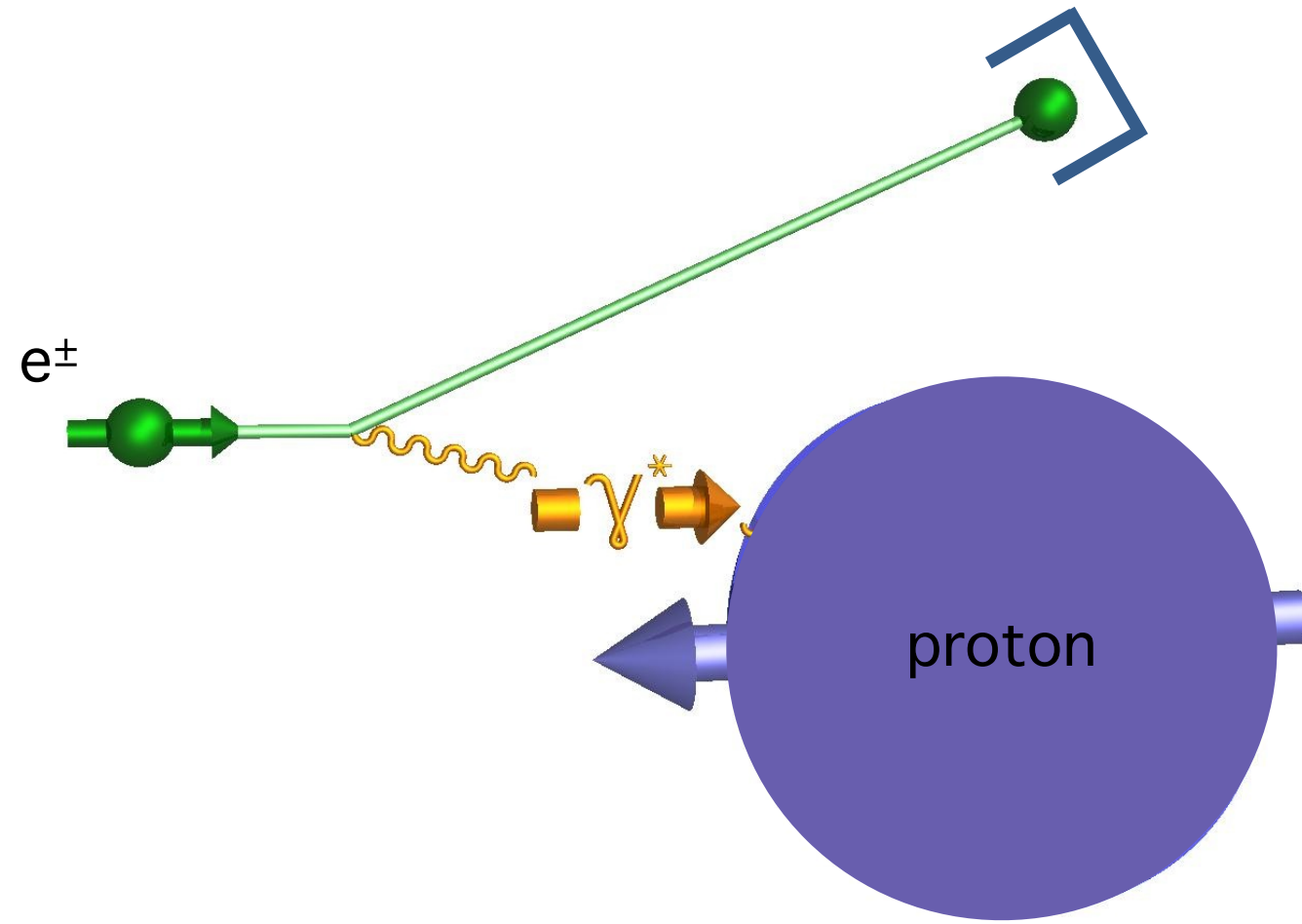


# Helicity structure of the nucleon

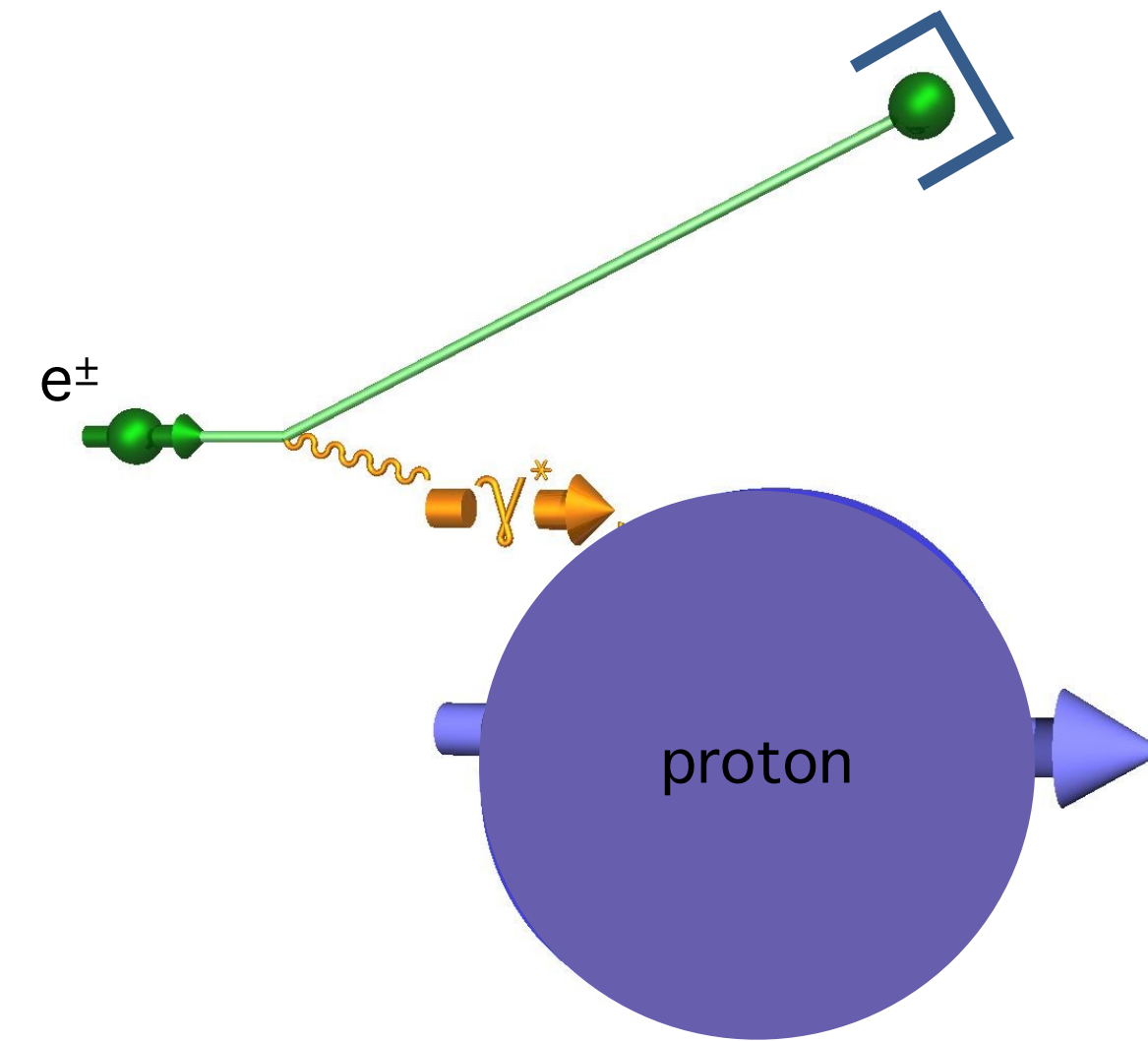


- longitudinally polarised proton
- longitudinally polarised  $e^\pm$  beam
- count... **024000**

# Helicity structure of the nucleon

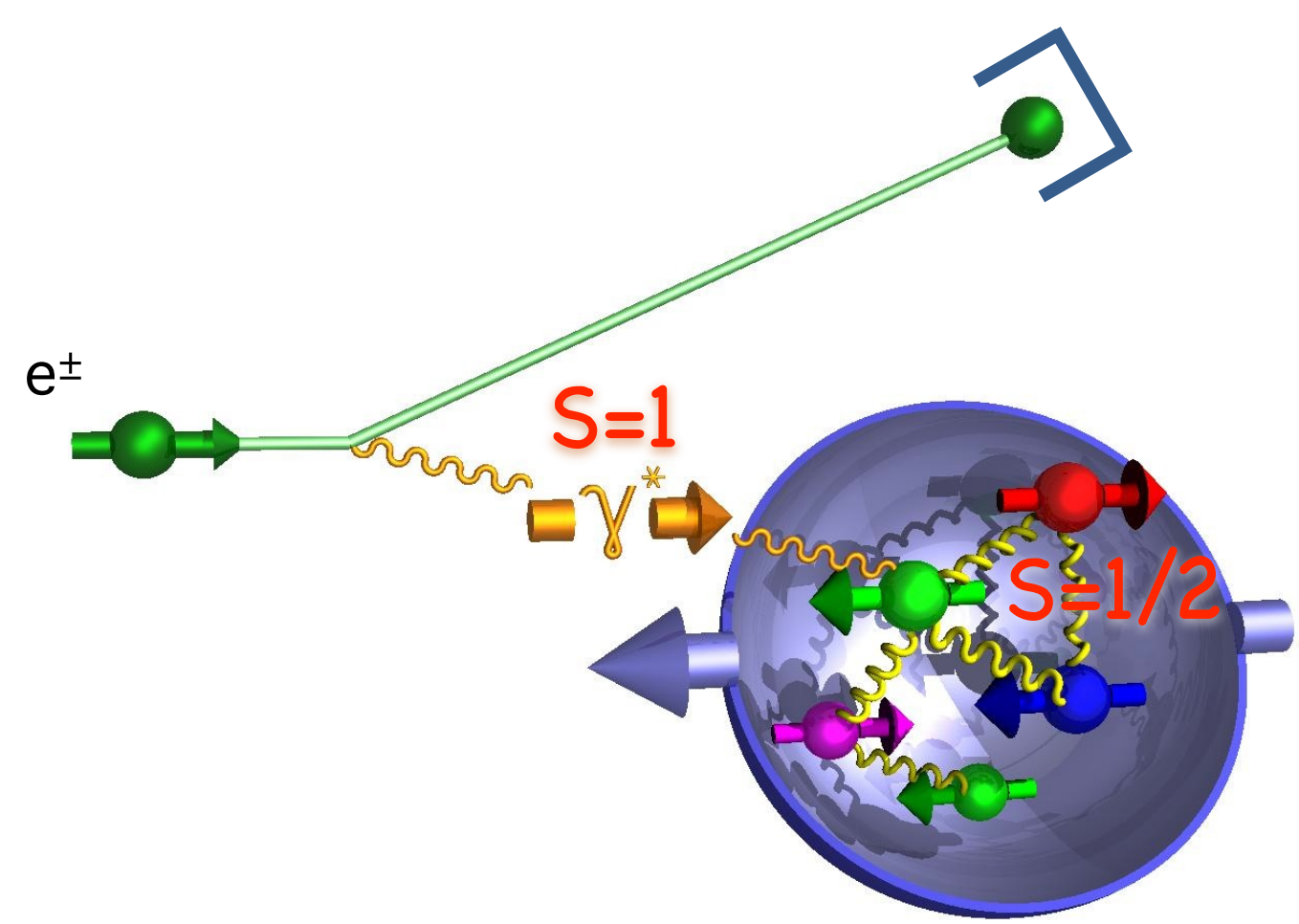


- longitudinally polarised proton
- longitudinally polarised  $e^\pm$  beam
- count... **024000**

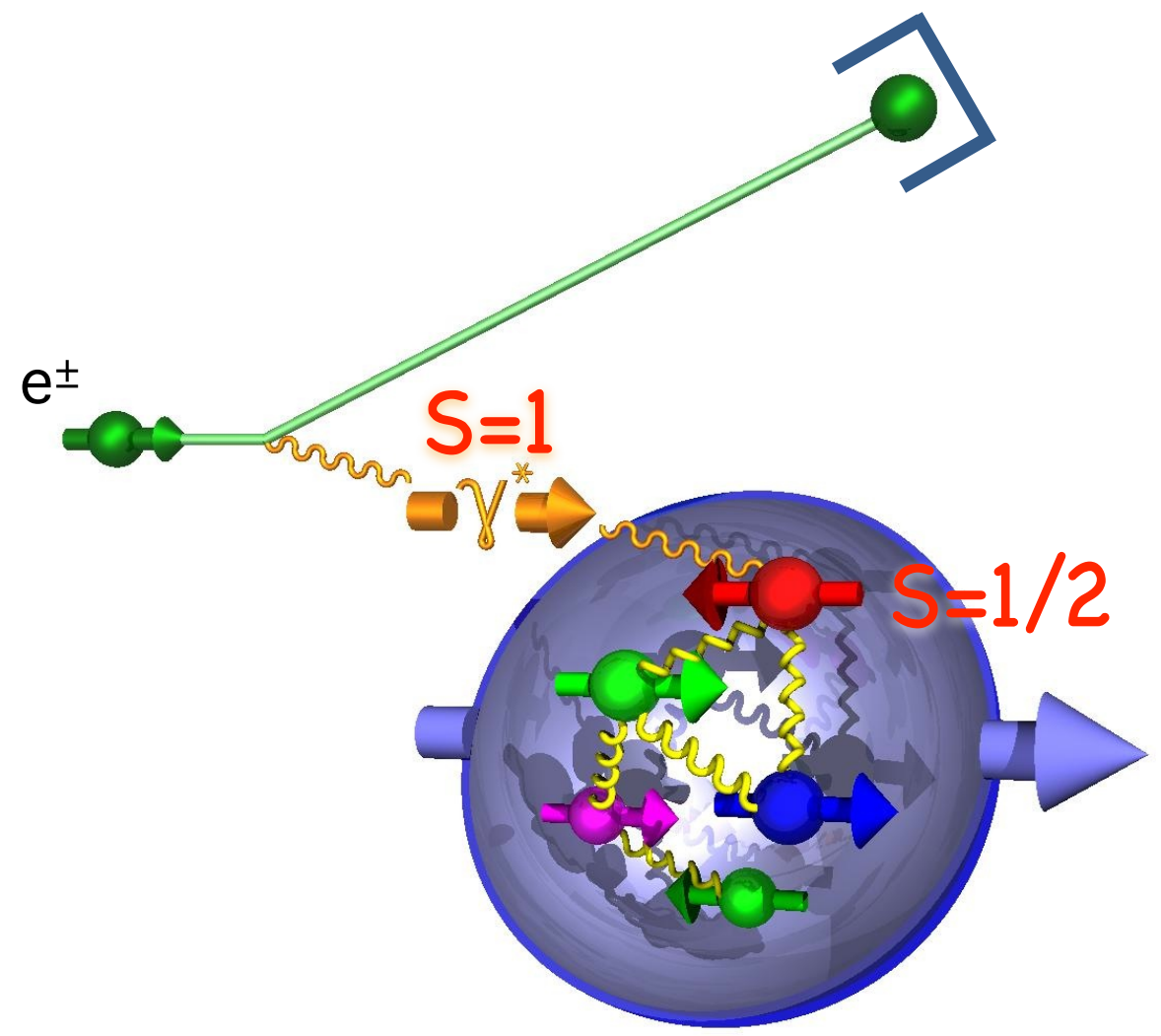


- flip proton spin and count... **024000**

# Helicity structure of the nucleon



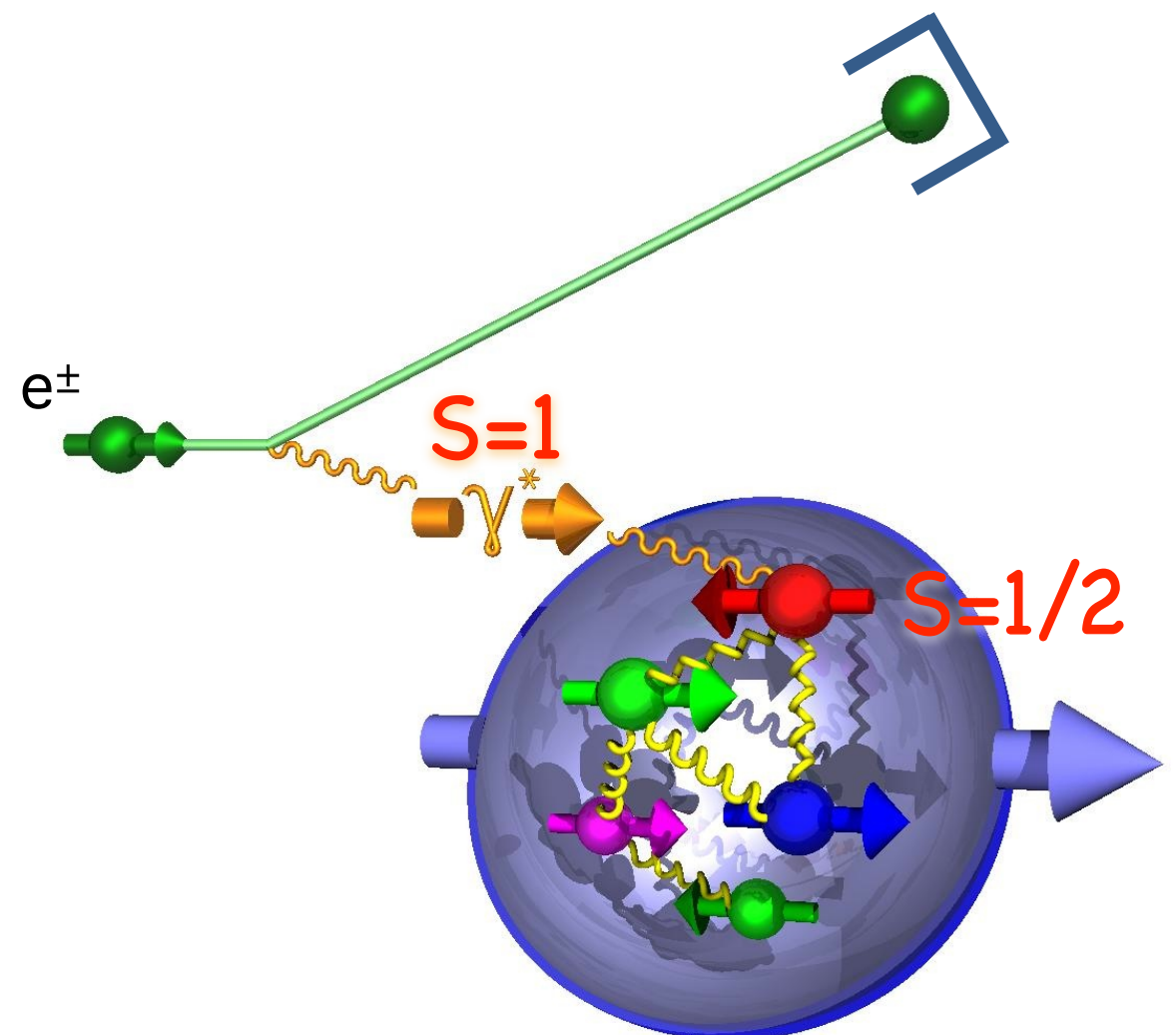
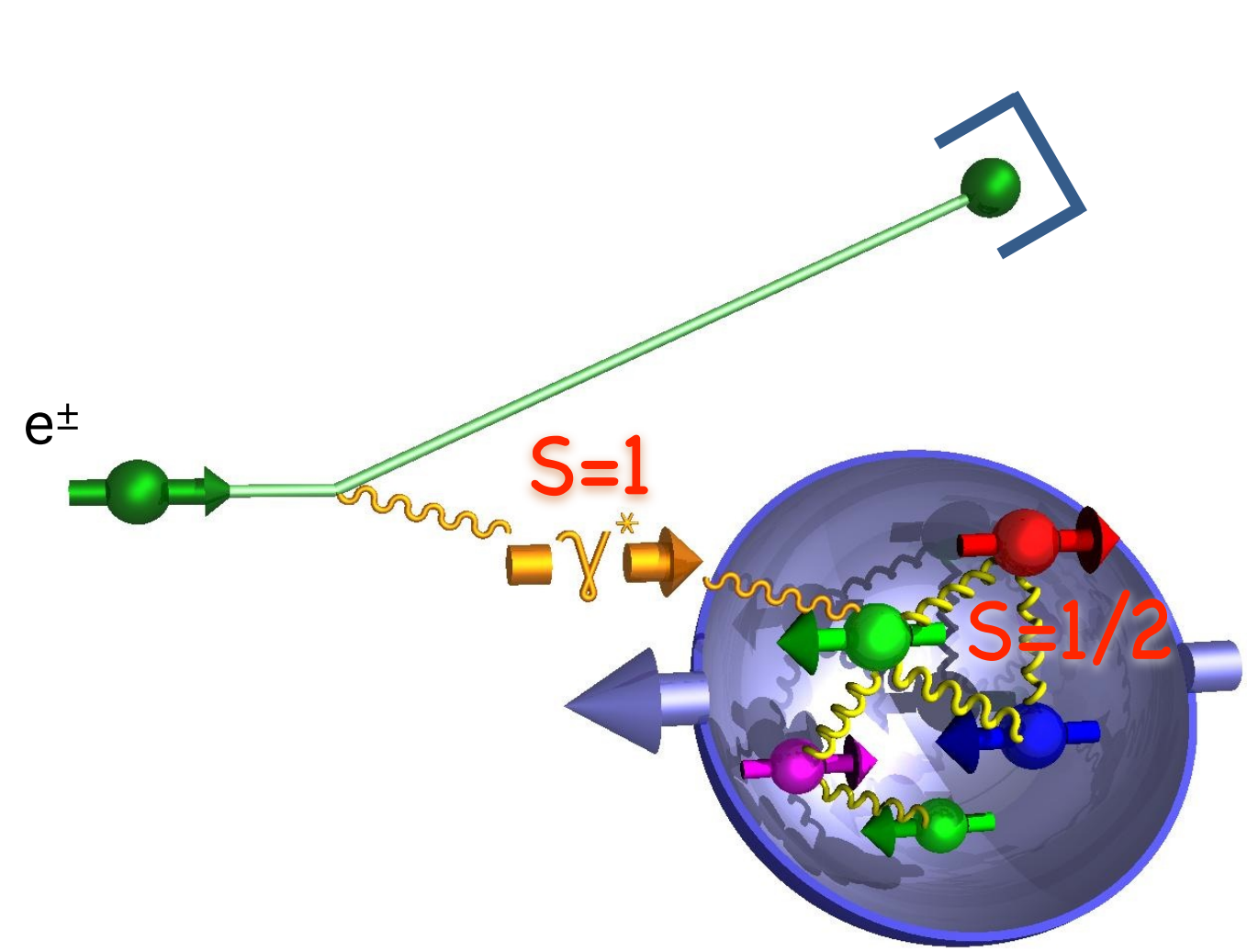
- longitudinally polarised proton
- longitudinally polarised  $e^\pm$  beam
- count... 



- flip proton spin and count... 



# Helicity structure of the nucleon



- longitudinally polarised proton
- longitudinally polarised e± beam
- count... 

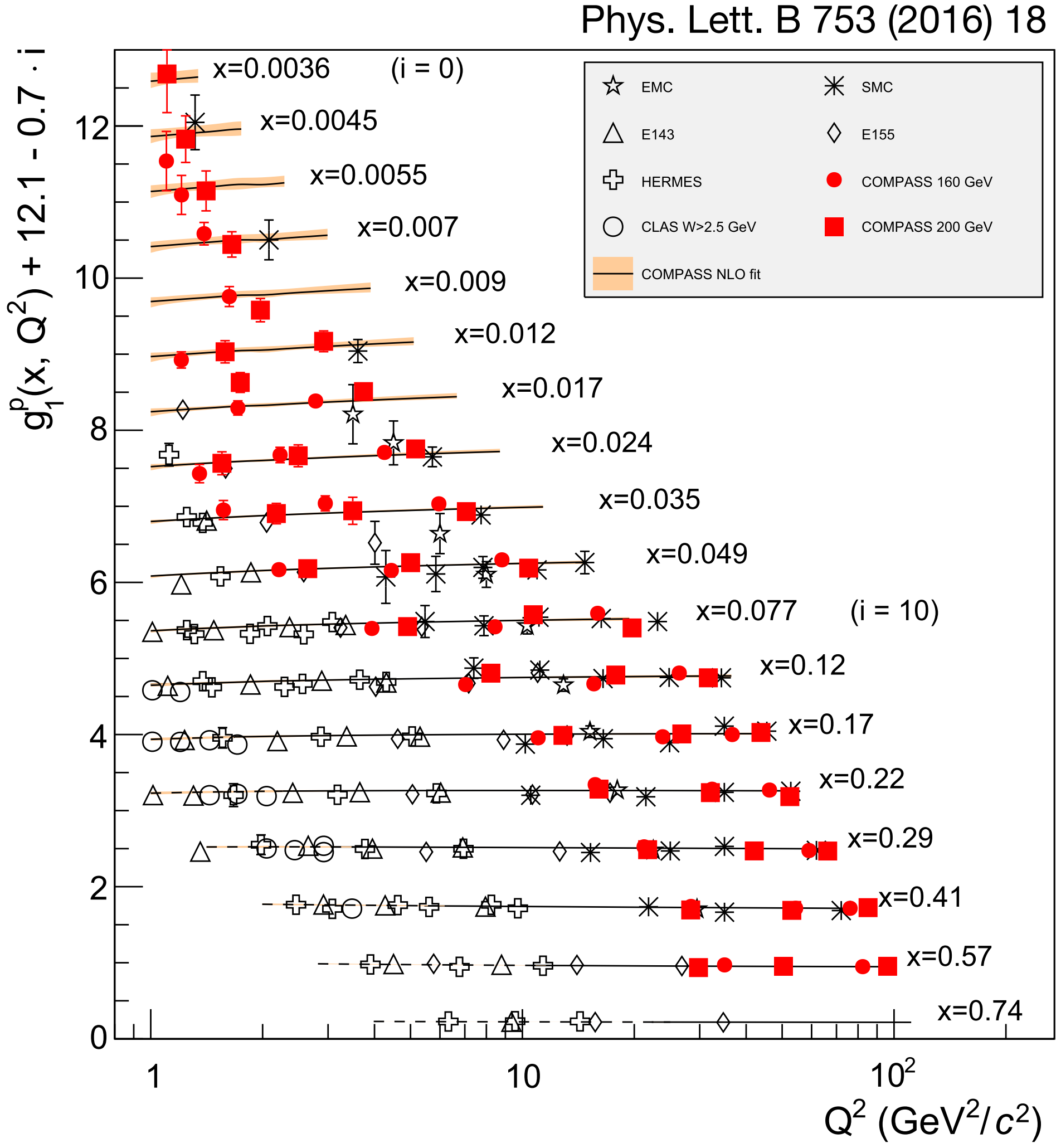
- flip proton spin and count... 

$$\frac{\begin{matrix} \leftarrow\leftarrow & \rightarrow\rightarrow \\ \sigma & - & \sigma \\ \leftarrow\leftarrow & \rightarrow\rightarrow \\ \sigma & + & \sigma \end{matrix}}{\sigma + \sigma} \propto g_1(x) = \frac{1}{2} \sum_q e_q^2 \Delta q(x) = \frac{1}{2} \sum_q e_q^2 \left( \overleftarrow{q}(x) - \overrightarrow{q}(x) \right)$$

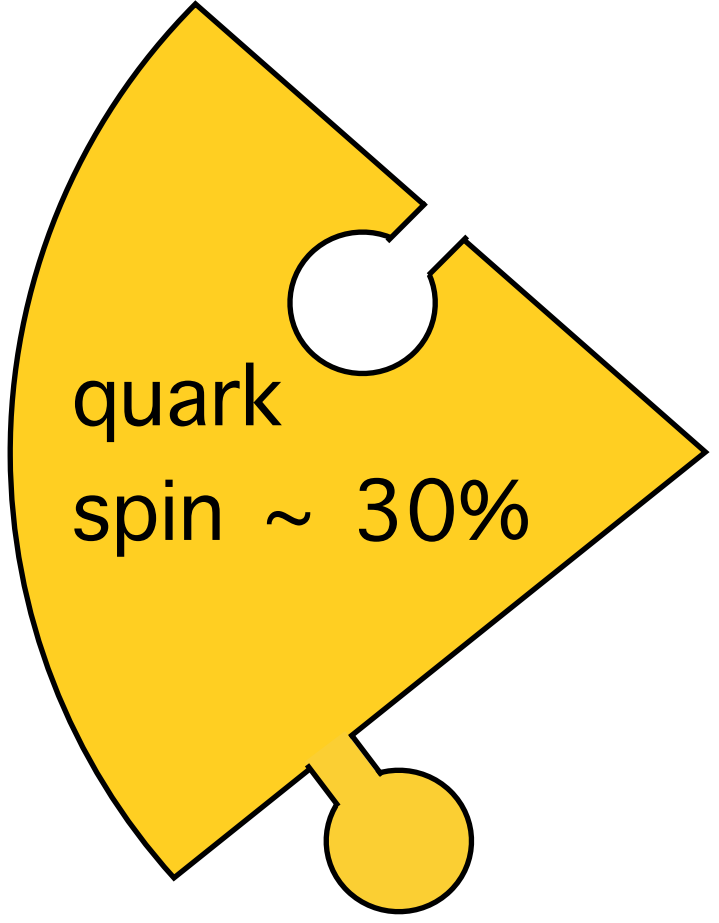
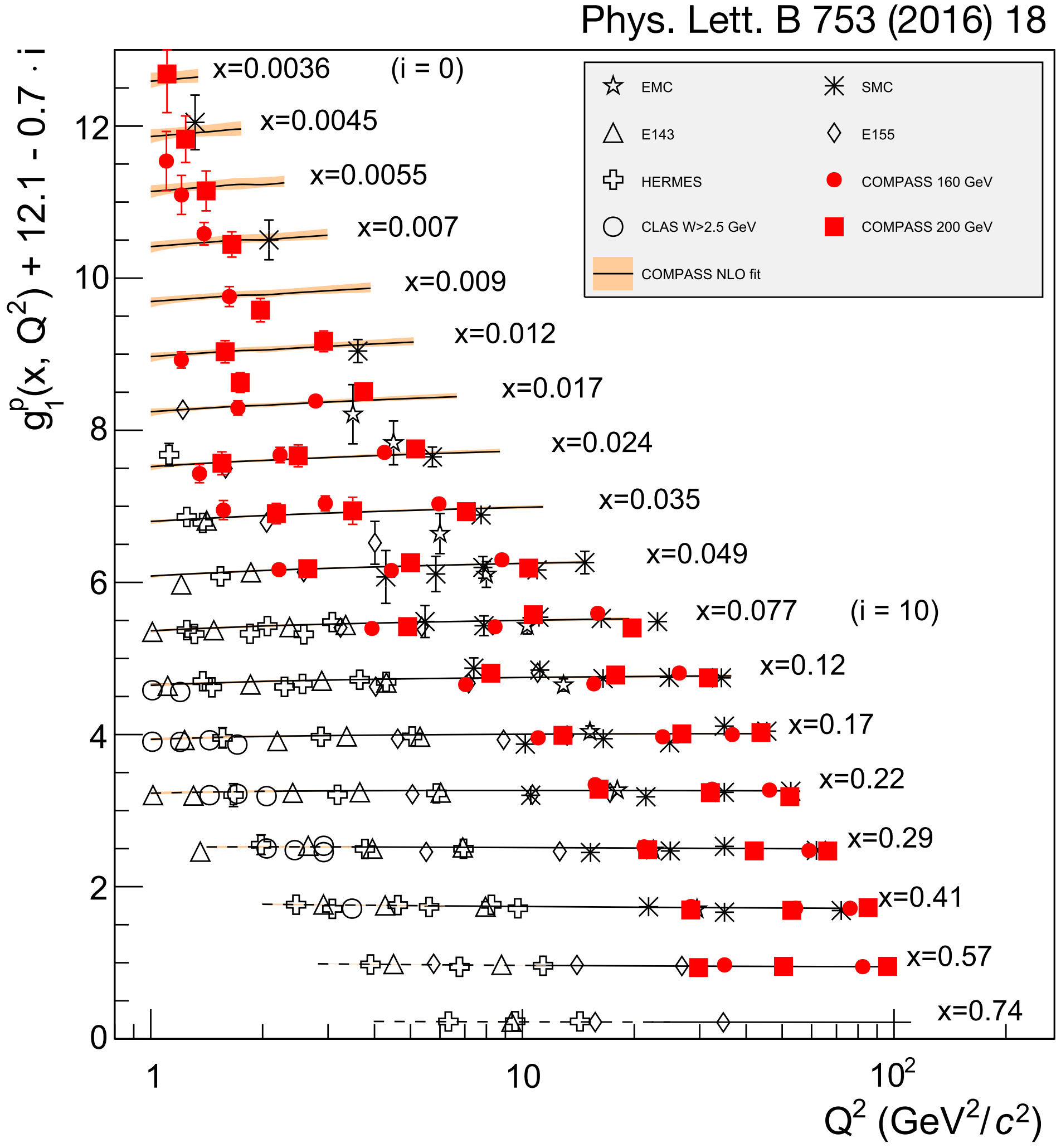
helicity parton distribution function (PDF)

parton fractional longitudinal momentum:  $x_B$

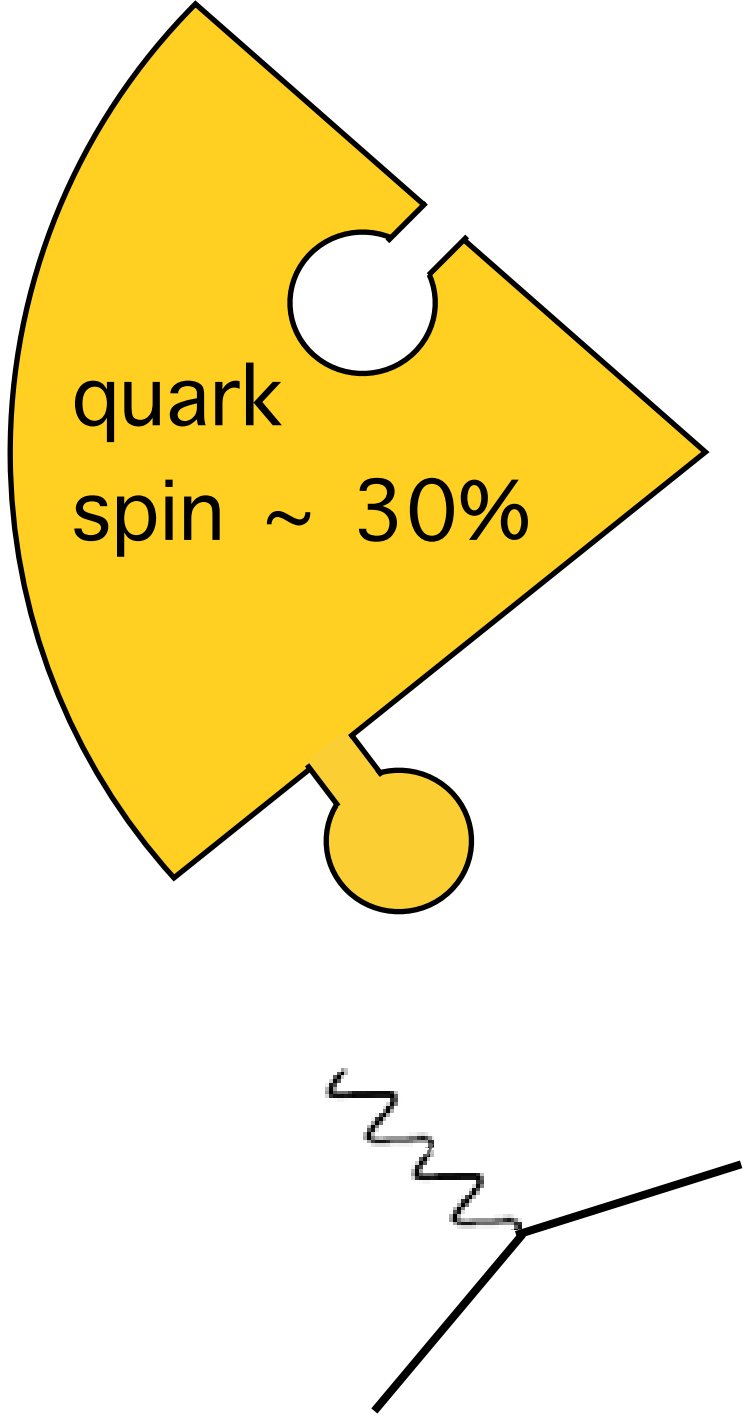
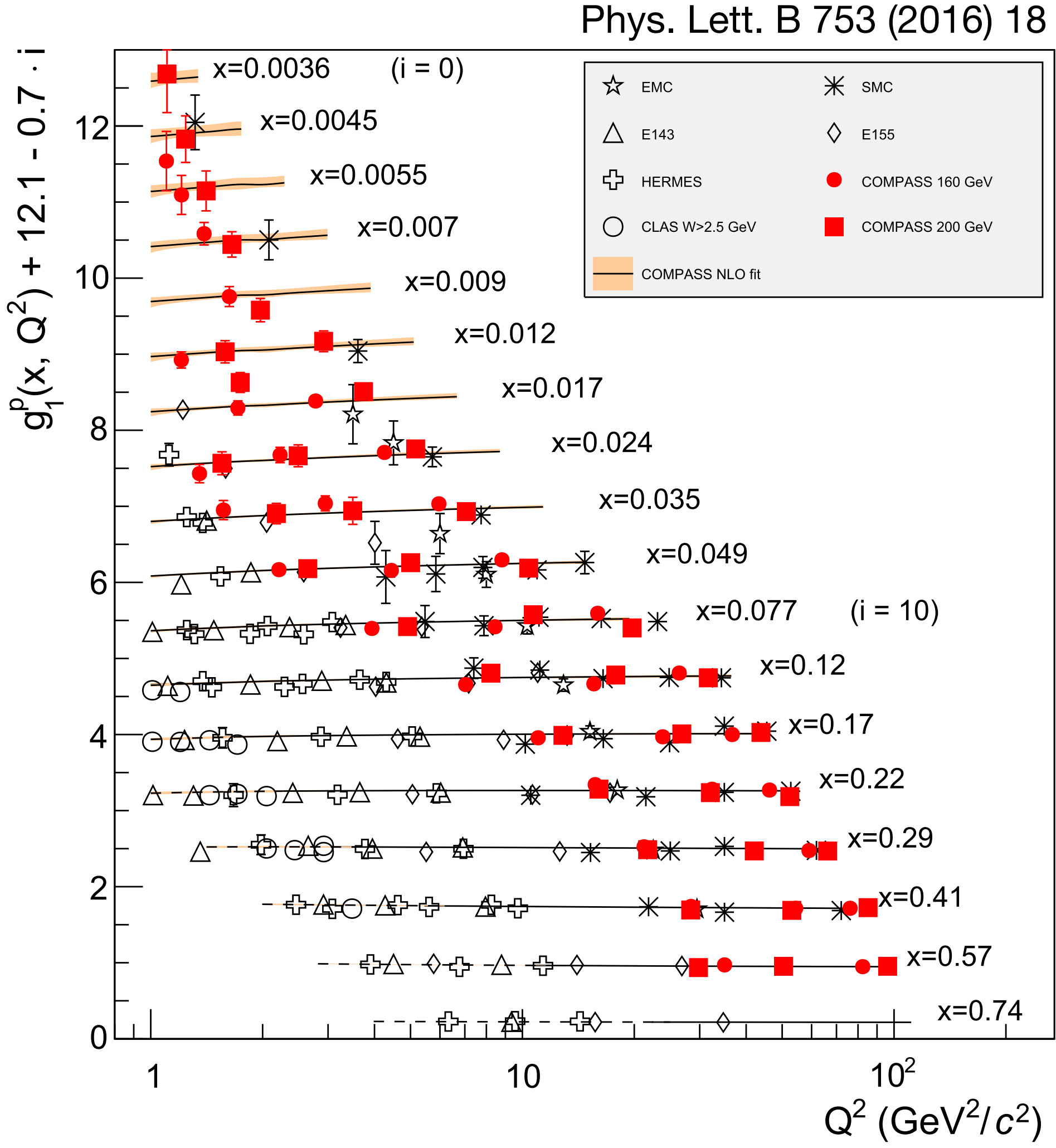
# Helicity structure of the nucleon: existing measurements



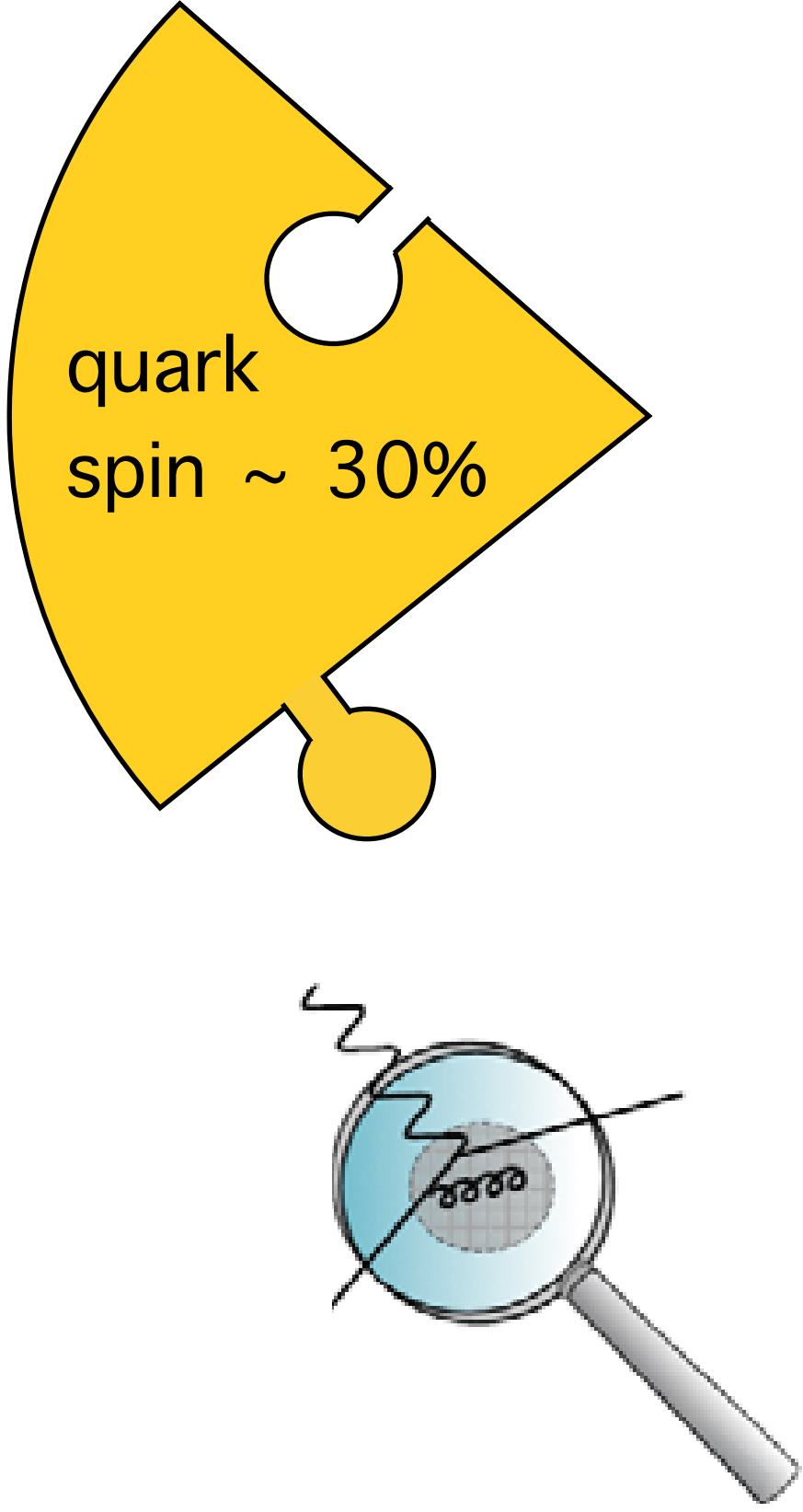
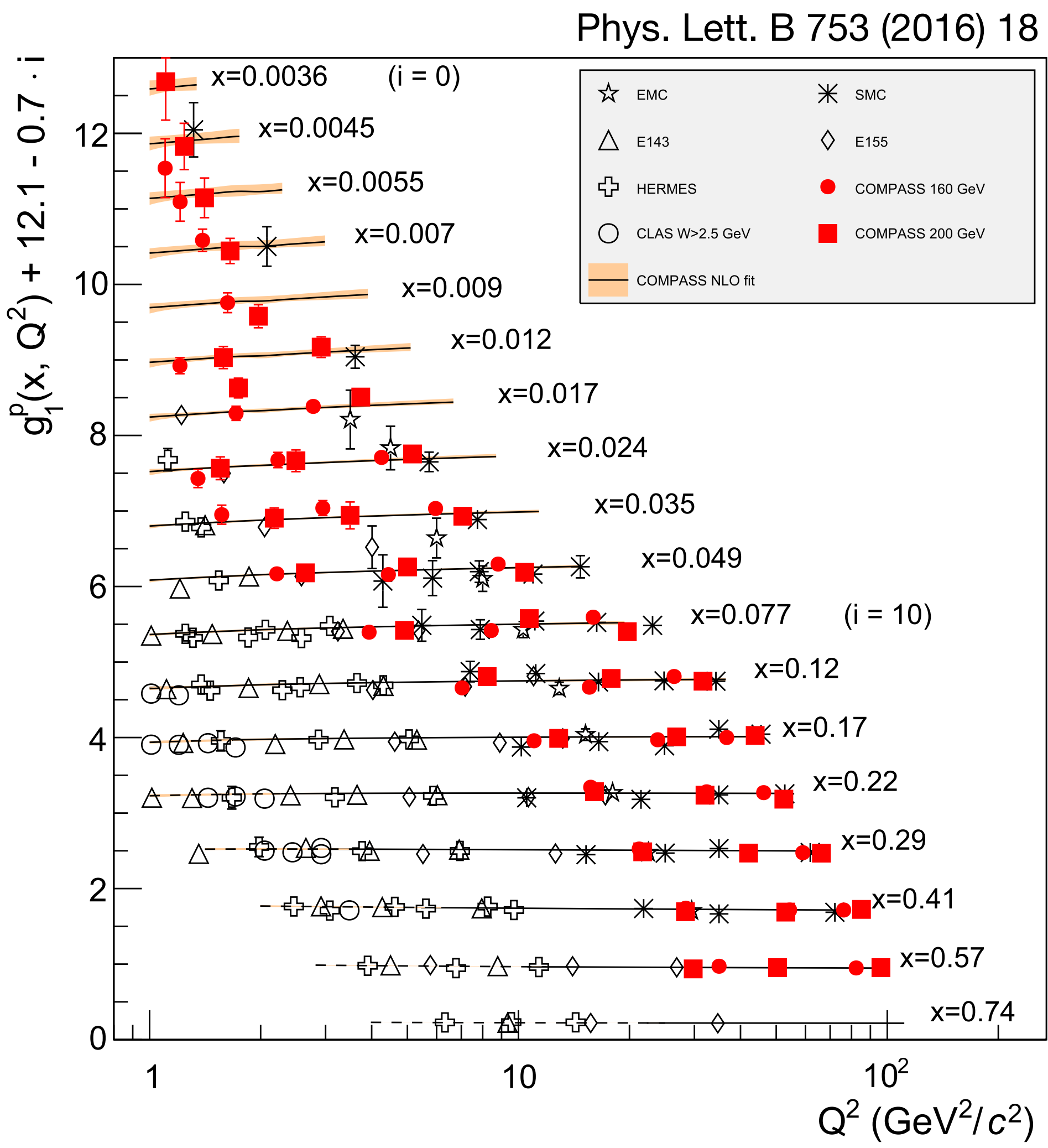
# Helicity structure of the nucleon: existing measurements



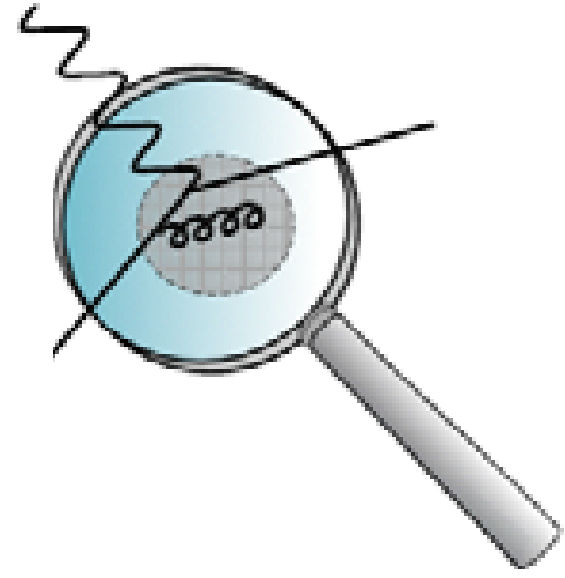
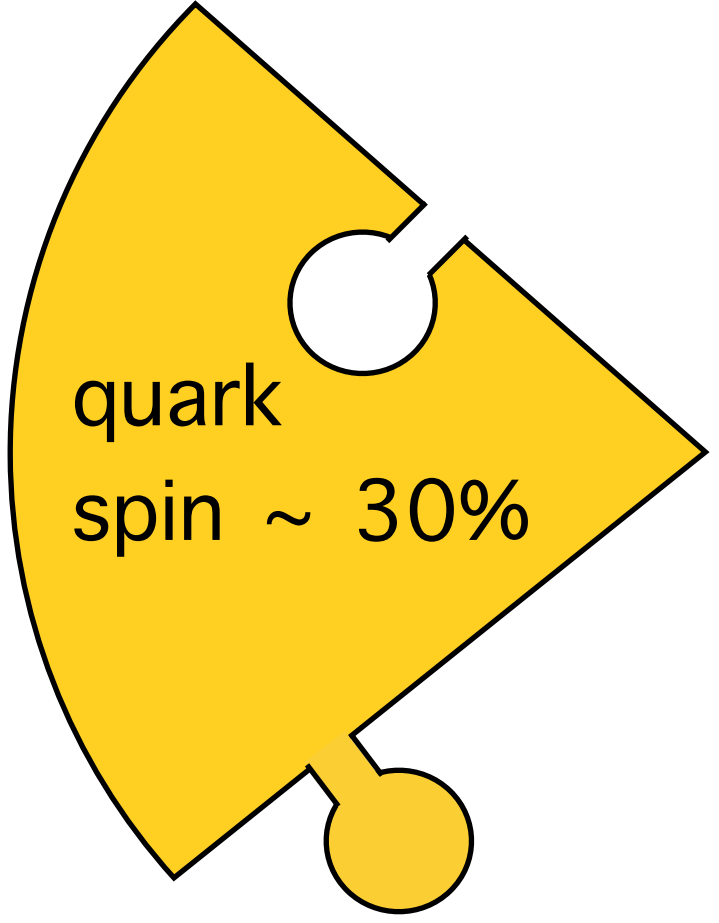
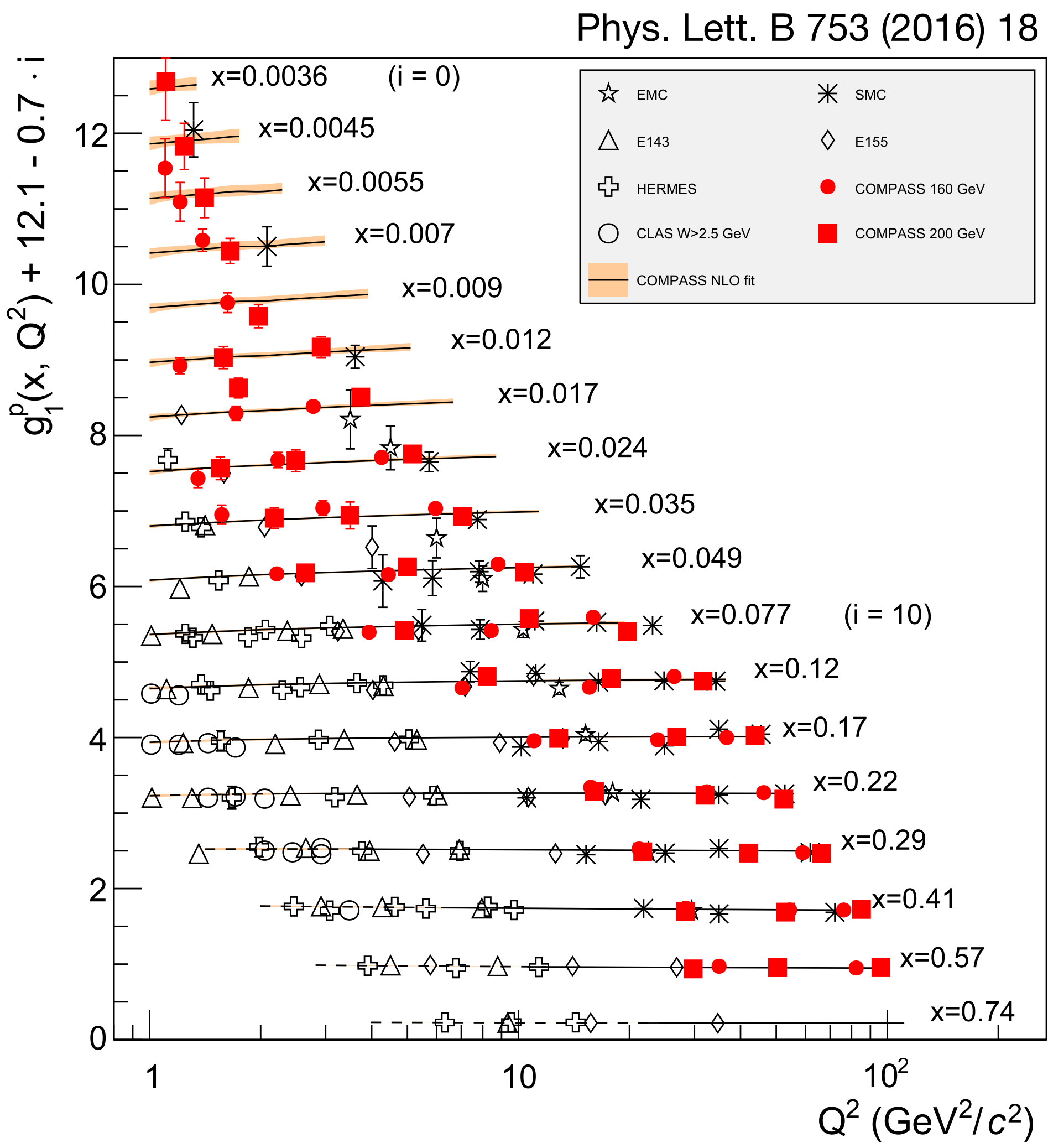
# Helicity structure of the nucleon: existing measurements



# Helicity structure of the nucleon: existing measurements

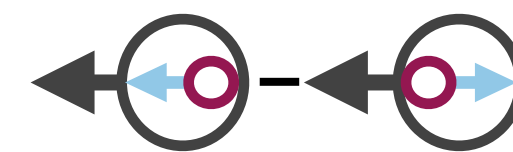


# Helicity structure of the nucleon: existing measurements

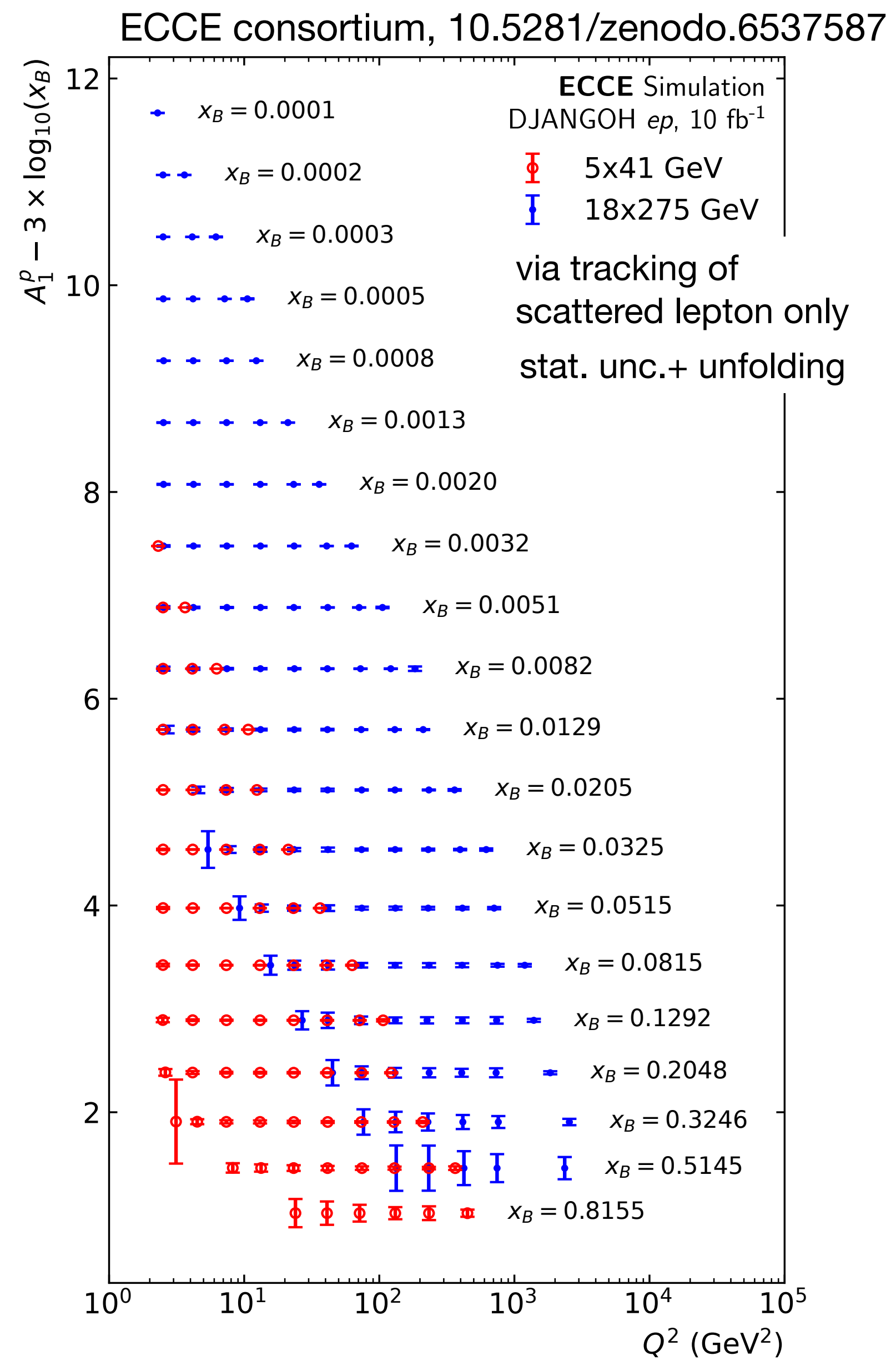


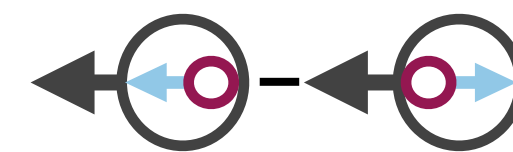
$$\frac{dg_1(x, Q^2)}{d \ln Q^2} \propto -\Delta g(x, Q^2)$$

→ gluon spin



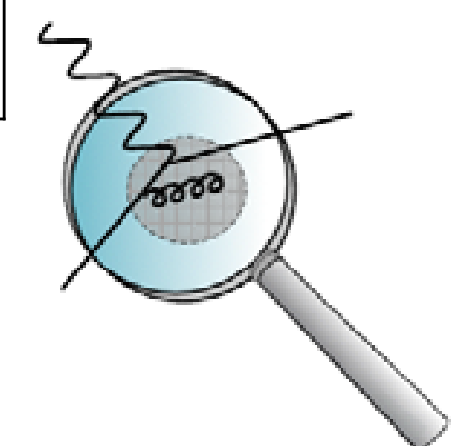
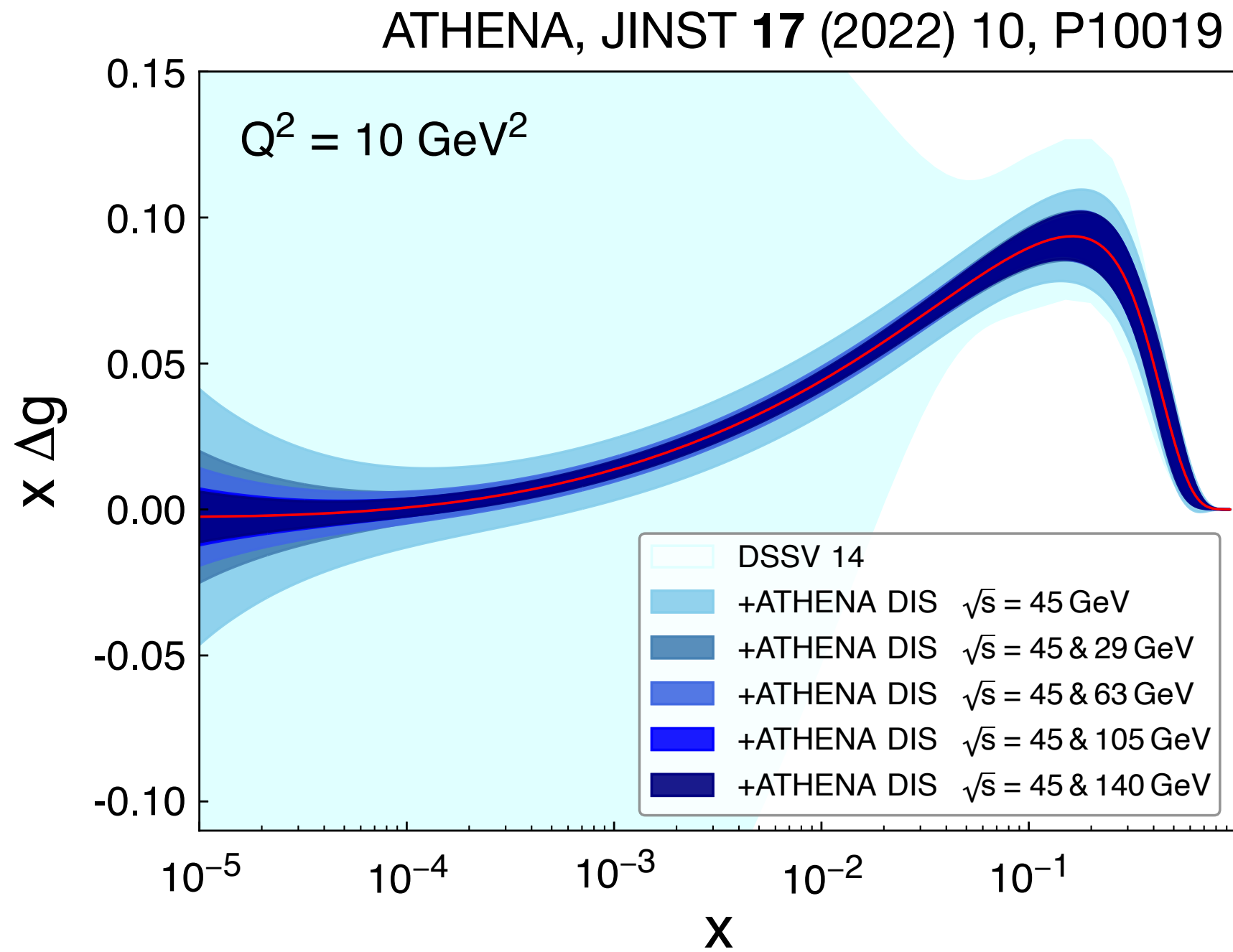
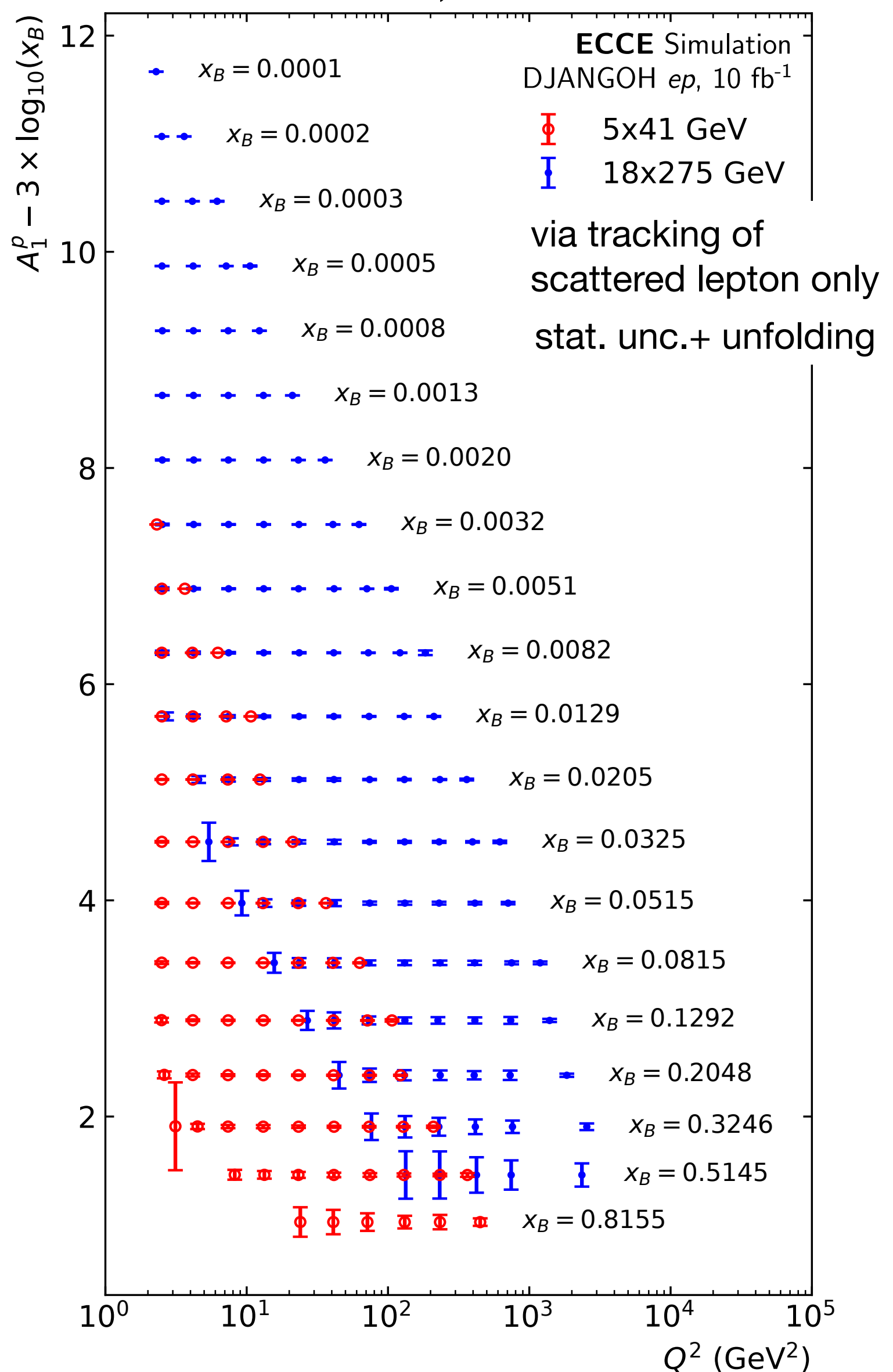
# Gluon helicity distribution at the EIC





# Gluon helicity distribution at the EIC

ECCE consortium, 10.5281/zenodo.6537587



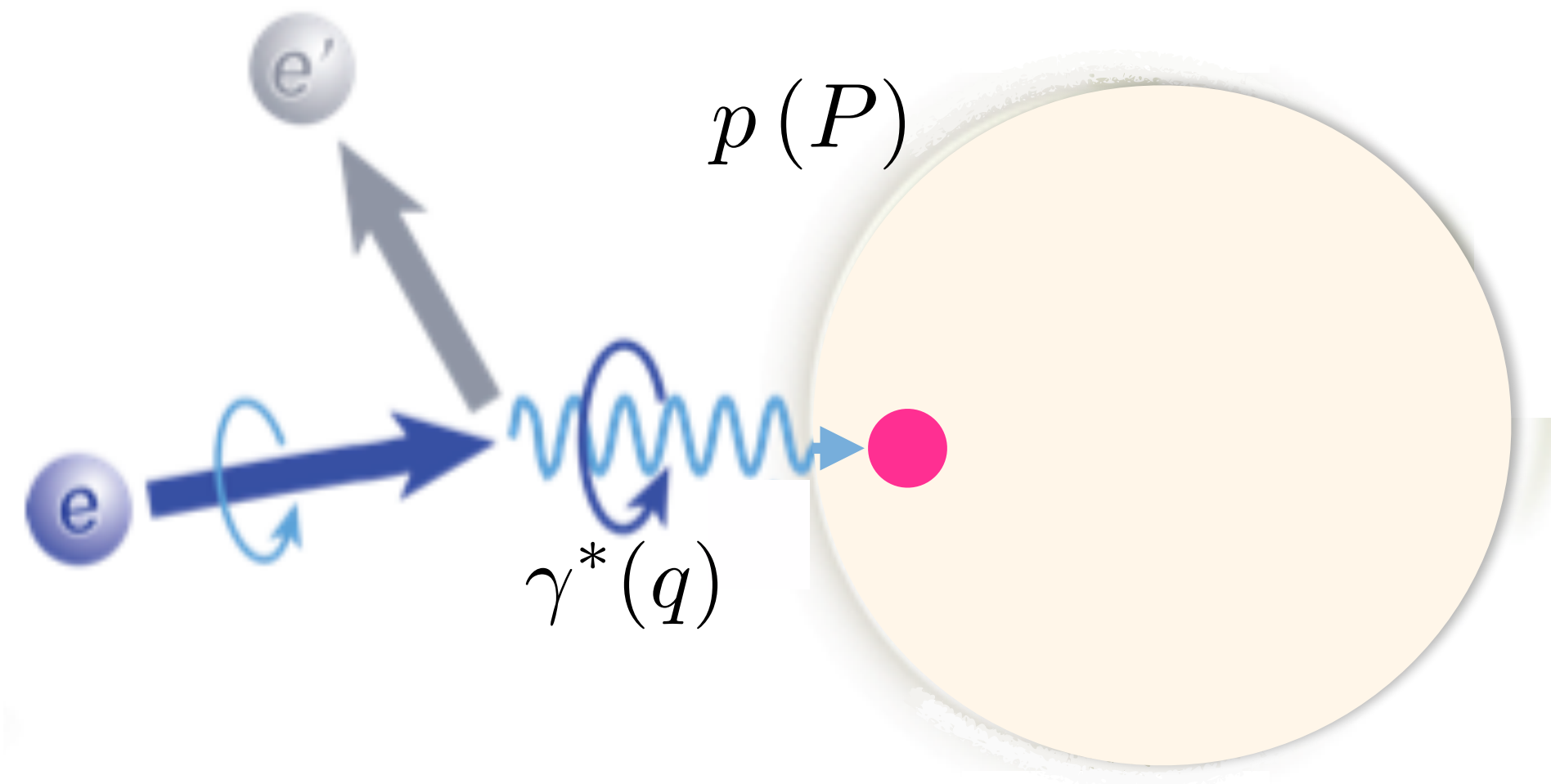
scaling violation from  $g_1(x, Q^2)$



# Single-hadron production in semi-inclusive DIS

$$Q^2 = -q^2$$

$$x_B = \frac{Q^2}{2P \cdot q}$$



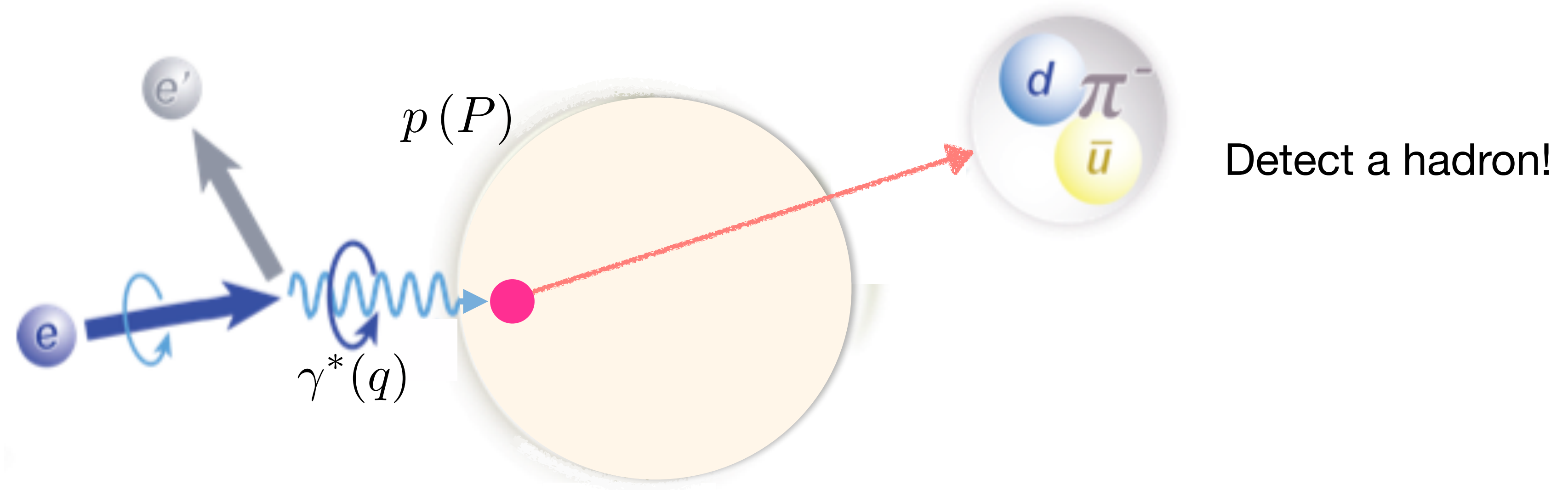
Highly virtual photon:

$$Q^2 \gg 1 \text{ GeV}^2$$

provides hard  
scale of process

# Single-hadron production in semi-inclusive DIS

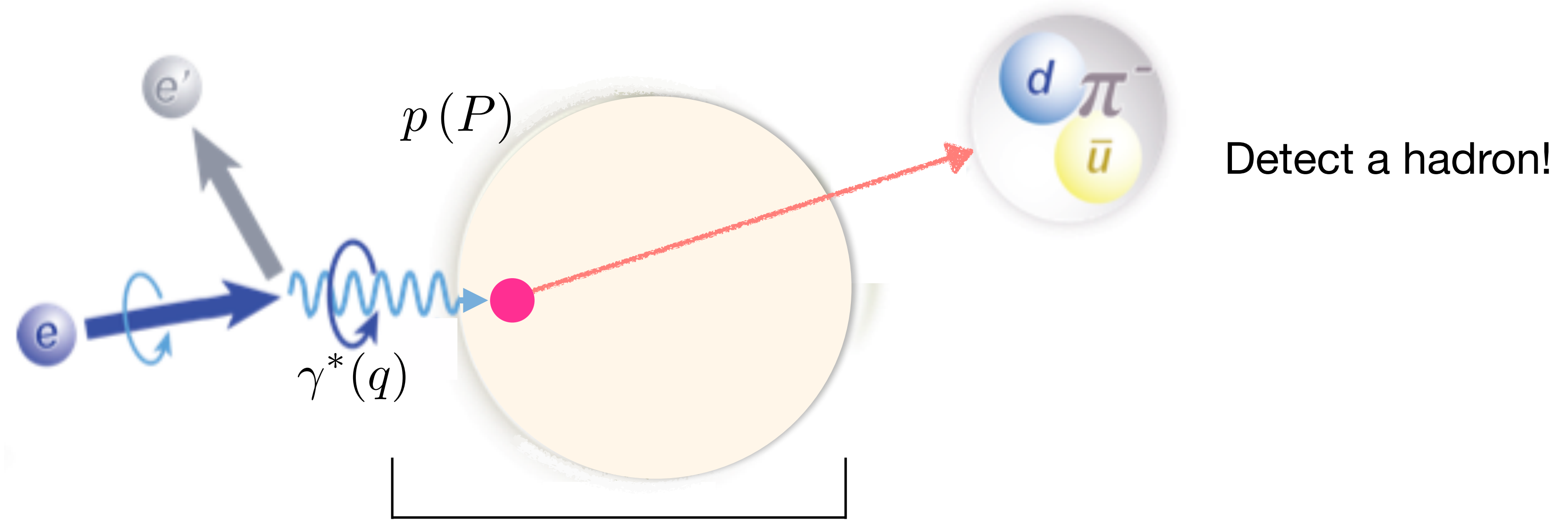
$$Q^2 = -q^2$$
$$x_B = \frac{Q^2}{2P \cdot q}$$



Highly virtual photon:  
 $Q^2 \gg 1 \text{ GeV}^2$   
provides hard  
scale of process

# Single-hadron production in semi-inclusive DIS

$$Q^2 = -q^2$$
$$x_B = \frac{Q^2}{2P \cdot q}$$



Highly virtual photon:  
 $Q^2 \gg 1 \text{ GeV}^2$   
provides hard  
scale of process

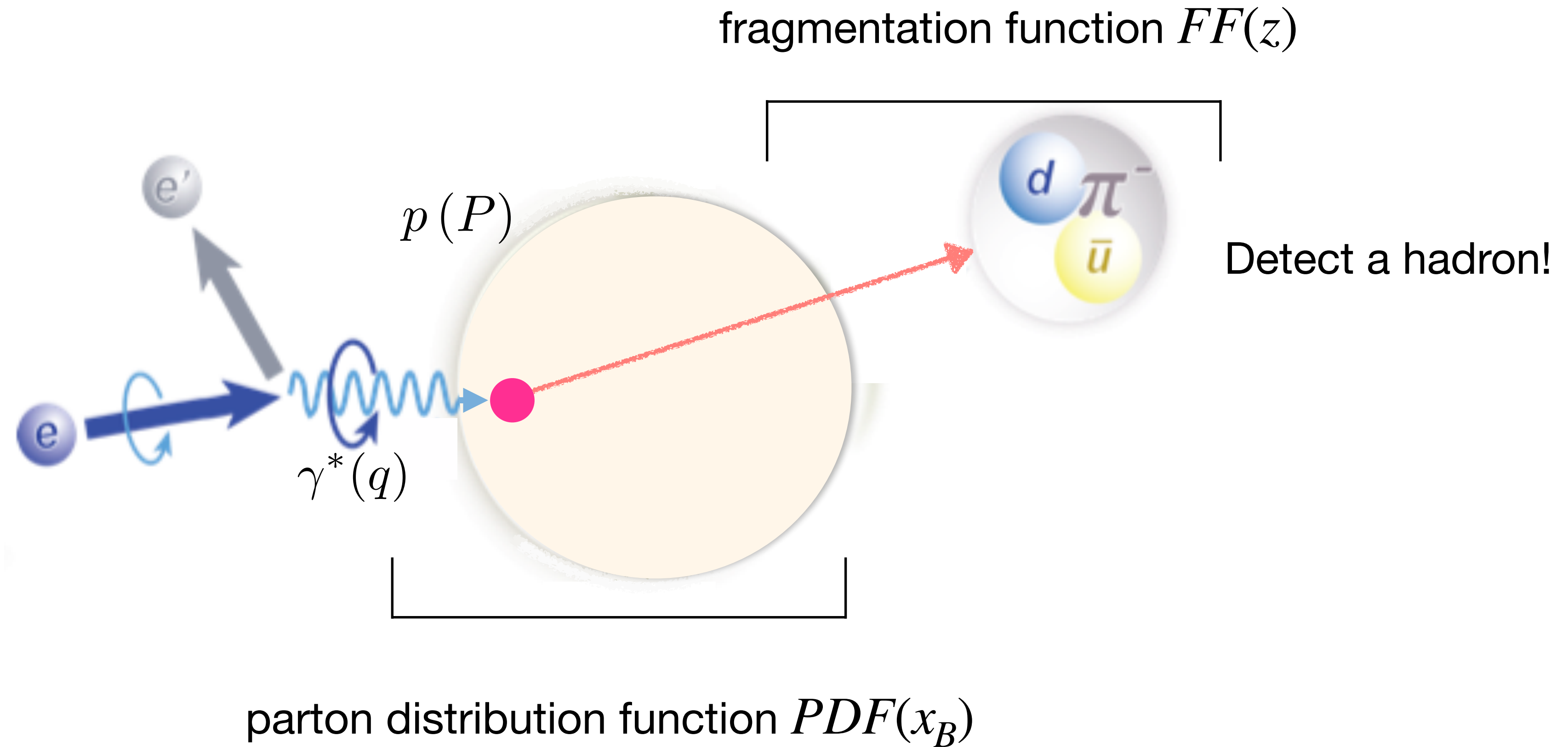
parton distribution function  $PDF(x_B)$

# Single-hadron production in semi-inclusive DIS

$$Q^2 = -q^2$$

$$x_B = \frac{Q^2}{2P \cdot q}$$

$$z \stackrel{\text{lab}}{=} \frac{E_h}{E_{\gamma^*}}$$



Highly virtual photon:

$$Q^2 \gg 1 \text{ GeV}^2$$

provides hard  
scale of process

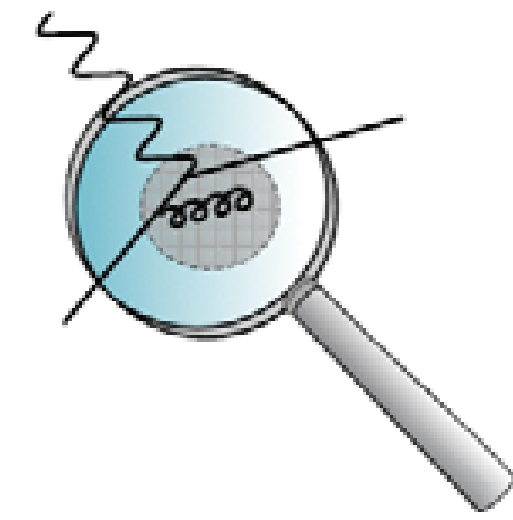
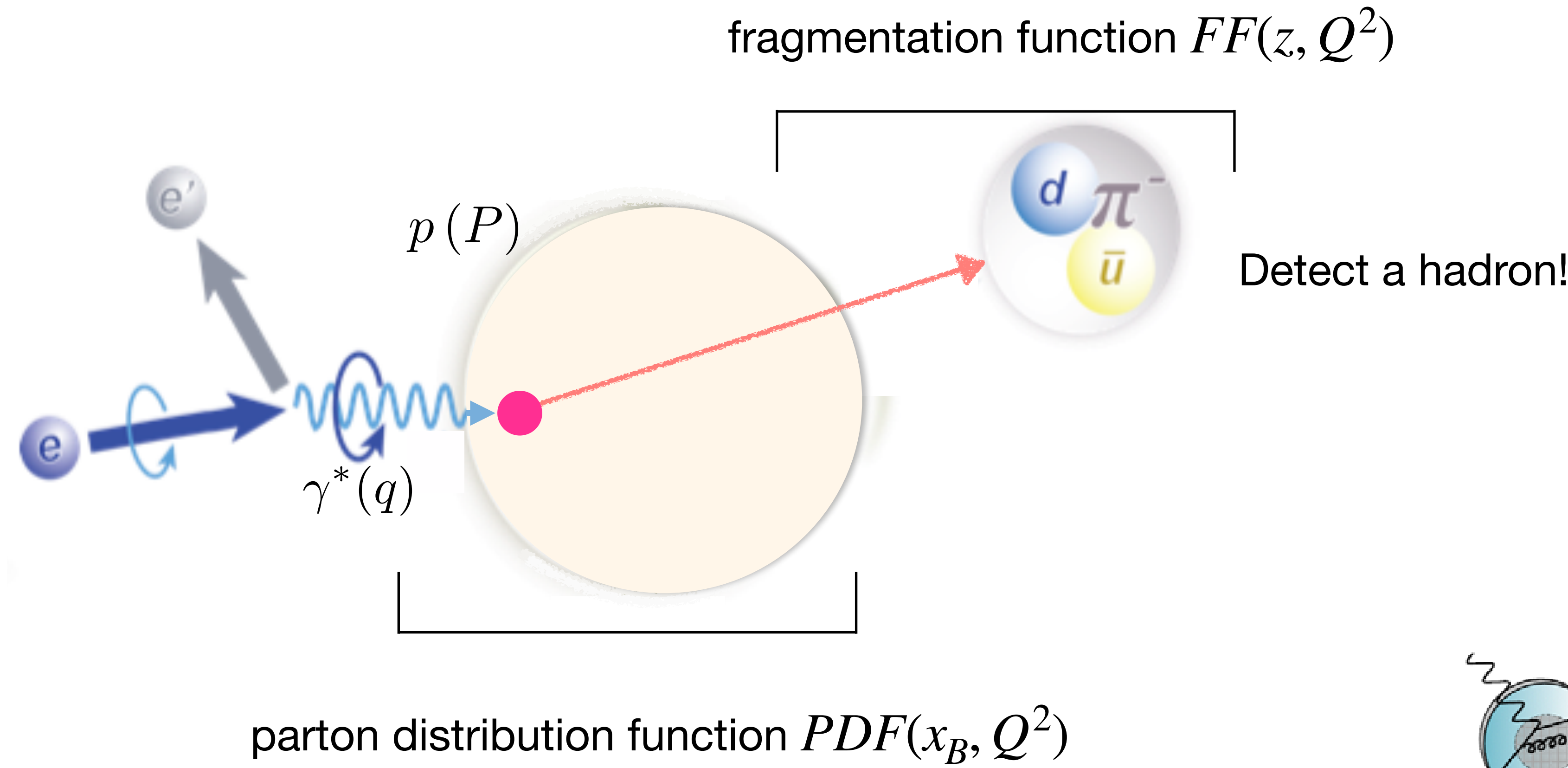
# Single-hadron production in semi-inclusive DIS

$$Q^2 = -q^2$$

$$x_B = \frac{Q^2}{2P \cdot q}$$

$$z \stackrel{\text{lab}}{=} \frac{E_h}{E_{\gamma^*}}$$

Highly virtual photon:  
 $Q^2 \gg 1 \text{ GeV}^2$   
 provides hard  
 scale of process



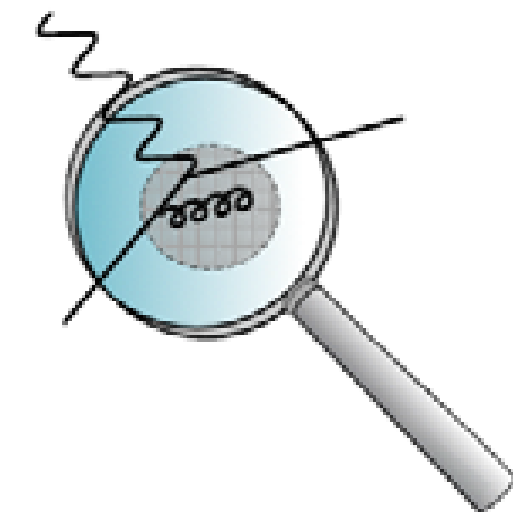
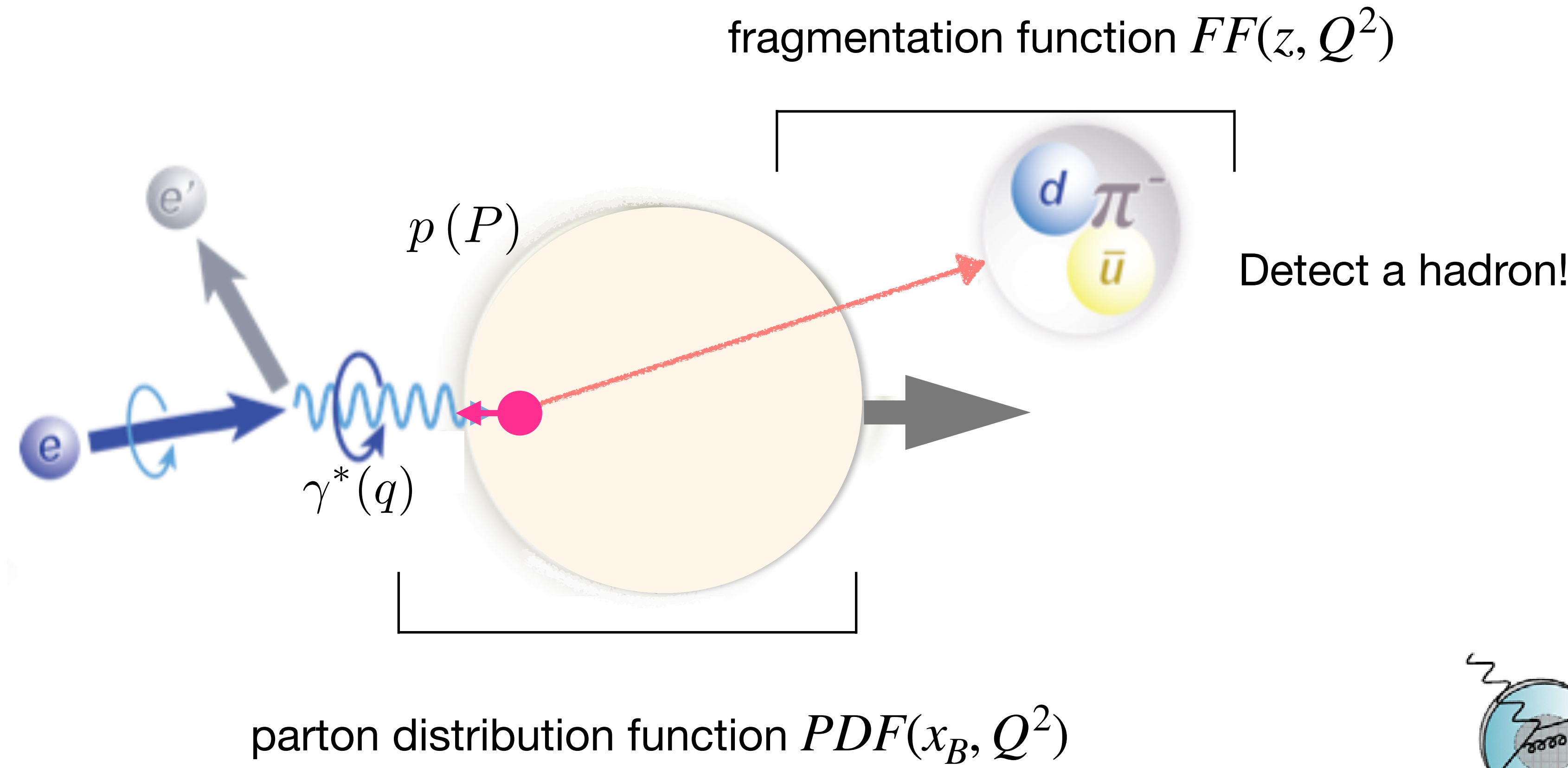
# Single-hadron production in semi-inclusive DIS

$$Q^2 = -q^2$$

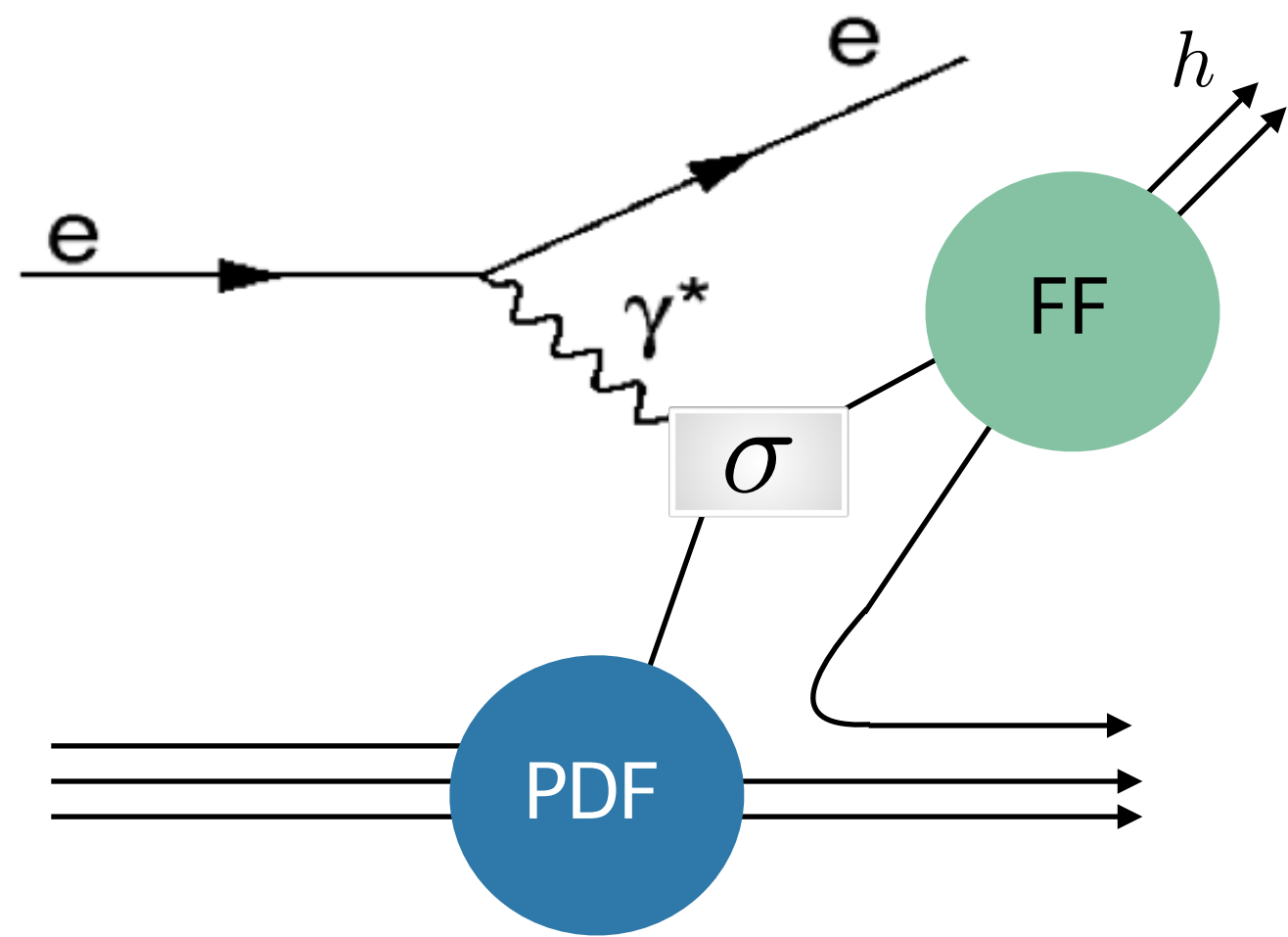
$$x_B = \frac{Q^2}{2P \cdot q}$$

$$z \stackrel{\text{lab}}{=} \frac{E_h}{E_{\gamma^*}}$$

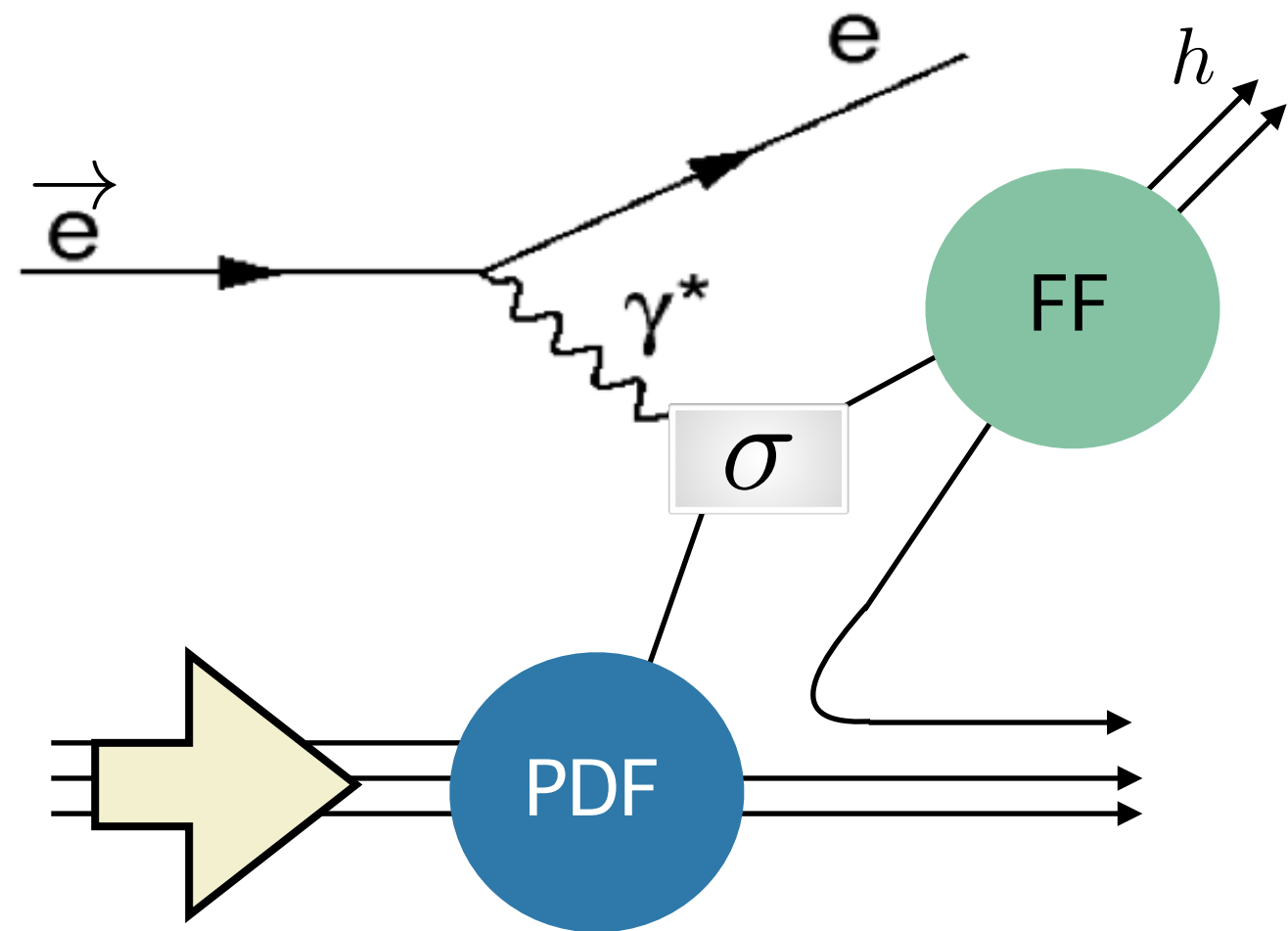
Highly virtual photon:  
 $Q^2 \gg 1 \text{ GeV}^2$   
 provides hard  
 scale of process



# Sea-quark helicity distributions



# Sea-quark helicity distributions

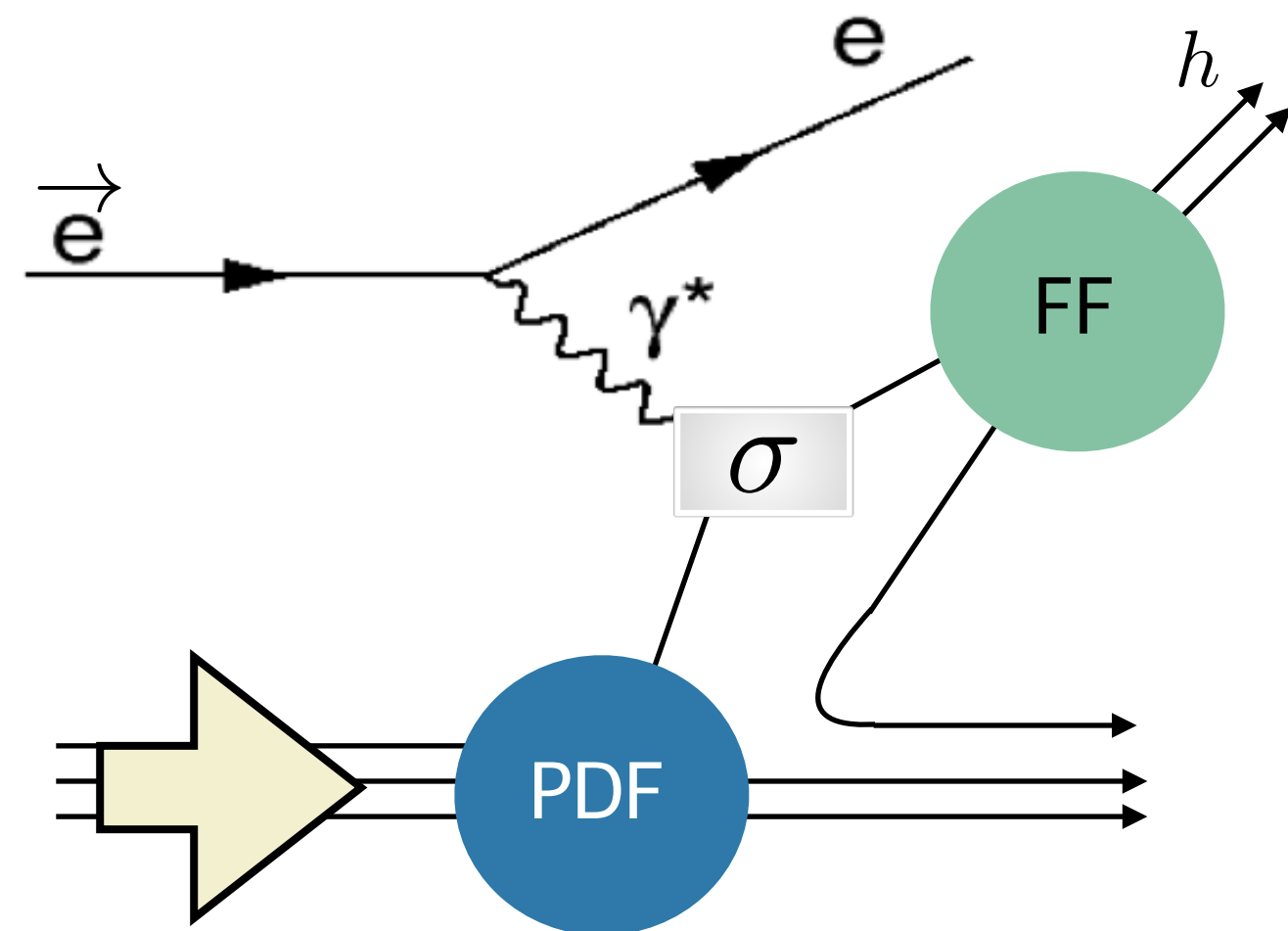


$$A_{\parallel}^h(x_B, Q^2, z) = \frac{1}{P_e P_p} \frac{\frac{\overrightarrow{N}^h}{L} - \frac{\overleftarrow{N}^h}{L}}{\frac{\overrightarrow{N}^h}{L} + \frac{\overleftarrow{N}^h}{L}}(x_B, Q^2, z)$$

$$= D(y) A_1^h(x_B, Q^2, z)$$

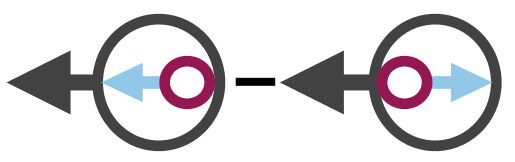


# Sea-quark helicity distributions

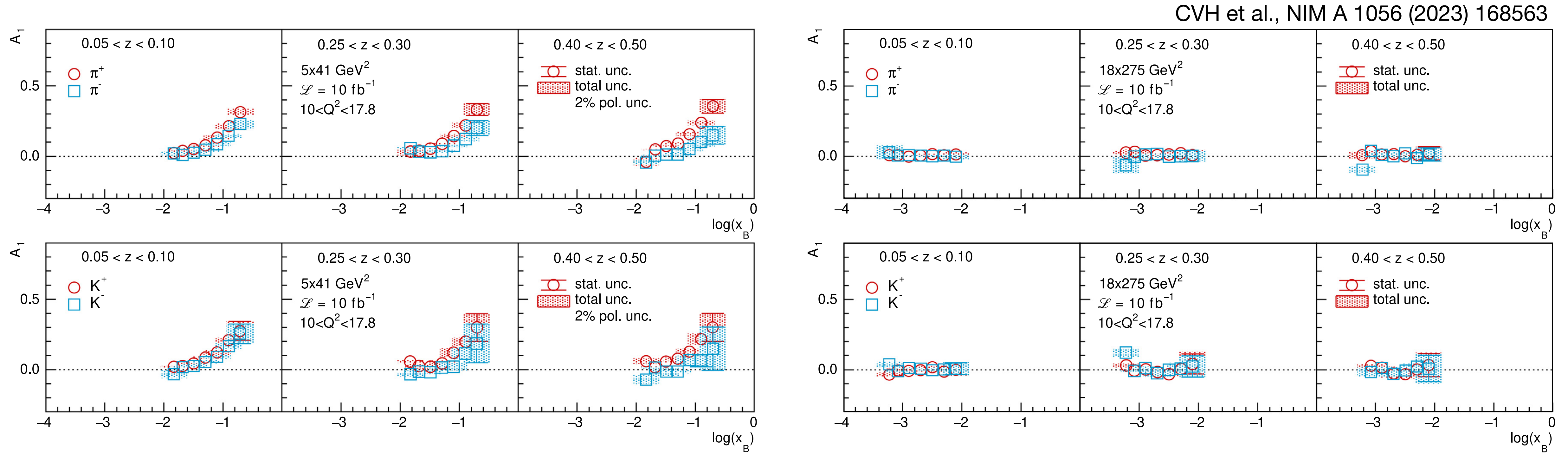


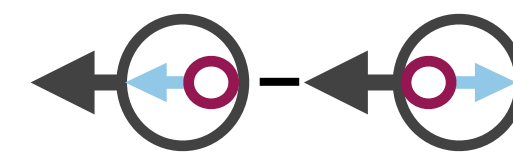
Semi-inclusive measurements  
 → access to sea-quark spin

$$\begin{aligned}
 A_{\parallel}^h(x_B, Q^2, z) &= \frac{1}{P_e P_p} \frac{\frac{\overrightarrow{N}^h}{L} - \frac{\overleftarrow{N}^h}{L}}{\frac{\overrightarrow{N}^h}{L} + \frac{\overleftarrow{N}^h}{L}}(x_B, Q^2, z) \\
 &= D(y) A_1^h(x_B, Q^2, z) \\
 &\propto \sum_q e_q^2 \left[ \Delta q \otimes w_1 D_1^{q \rightarrow h} \right]
 \end{aligned}$$

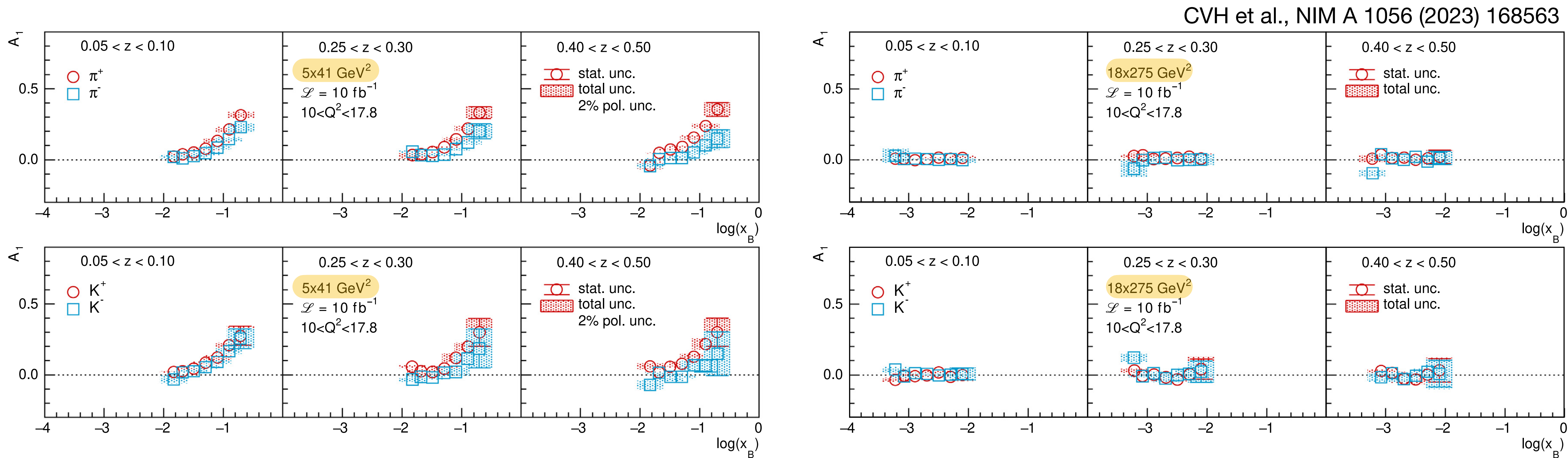


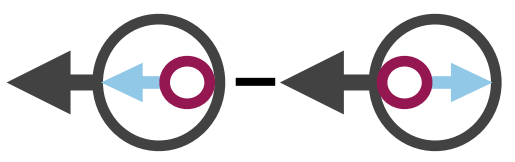
# Sea-quark helicity distributions at the EIC





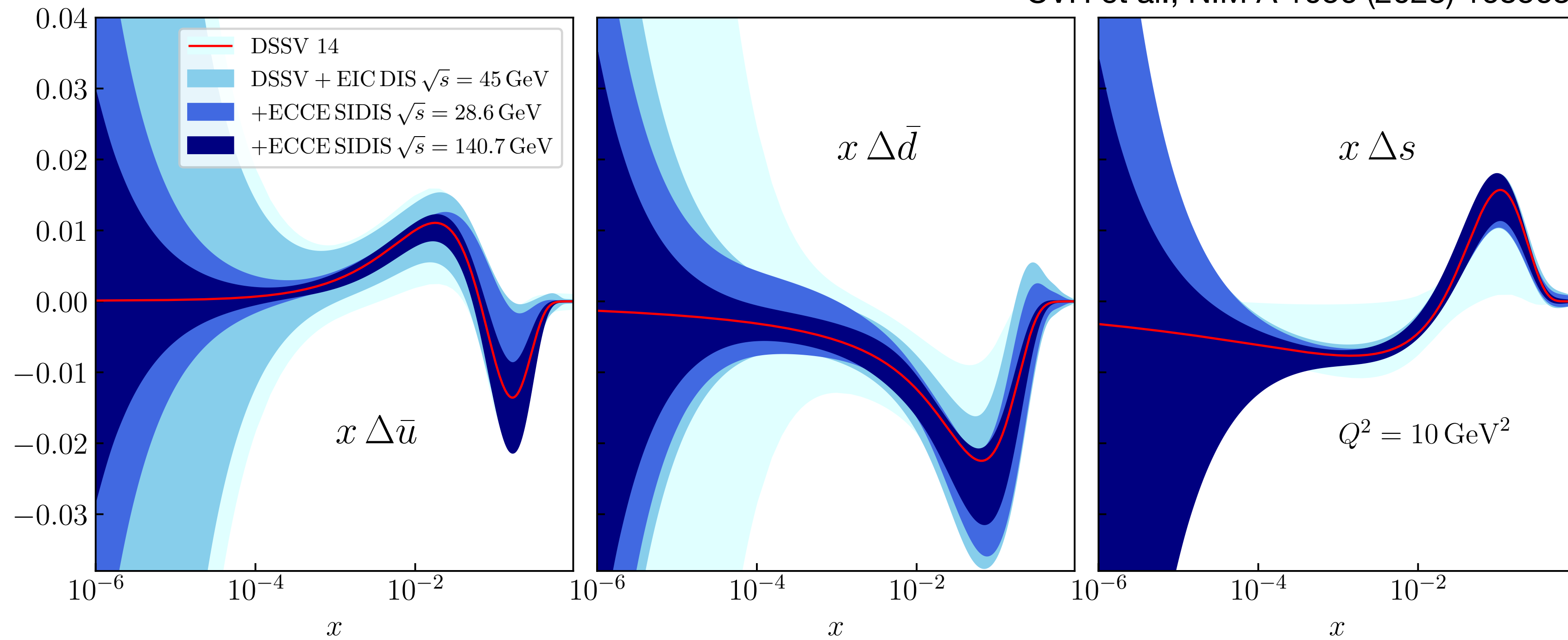
# Sea-quark helicity distributions at the EIC





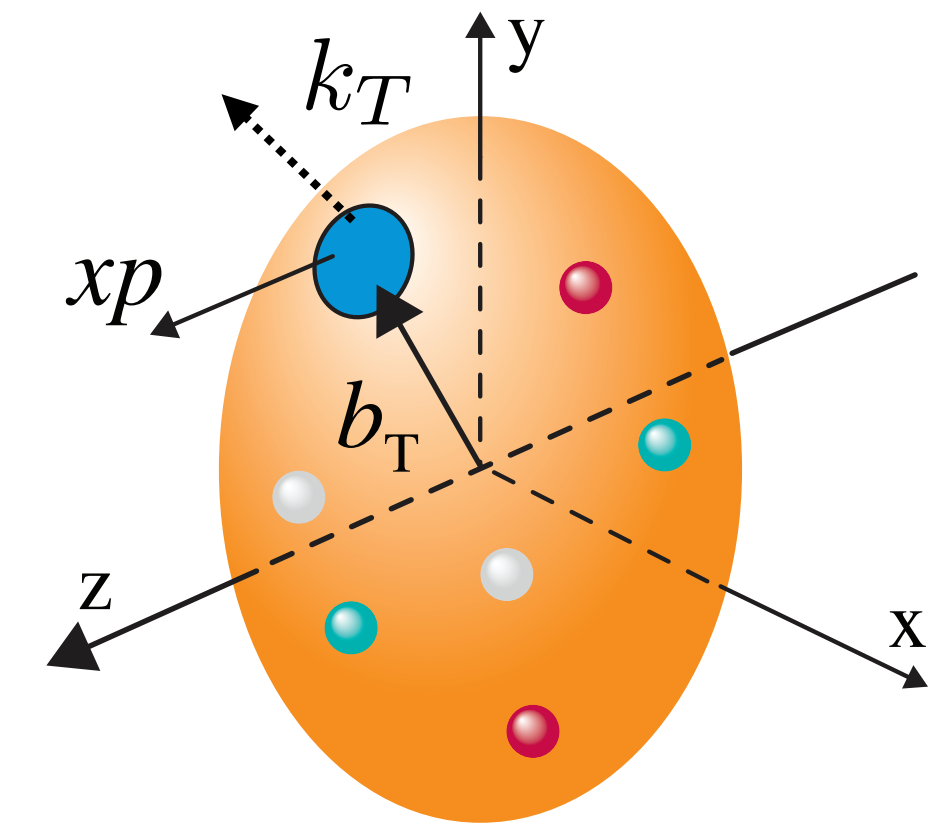
# Sea-quark helicity distributions at the EIC

CVH et al., NIM A 1056 (2023) 168563



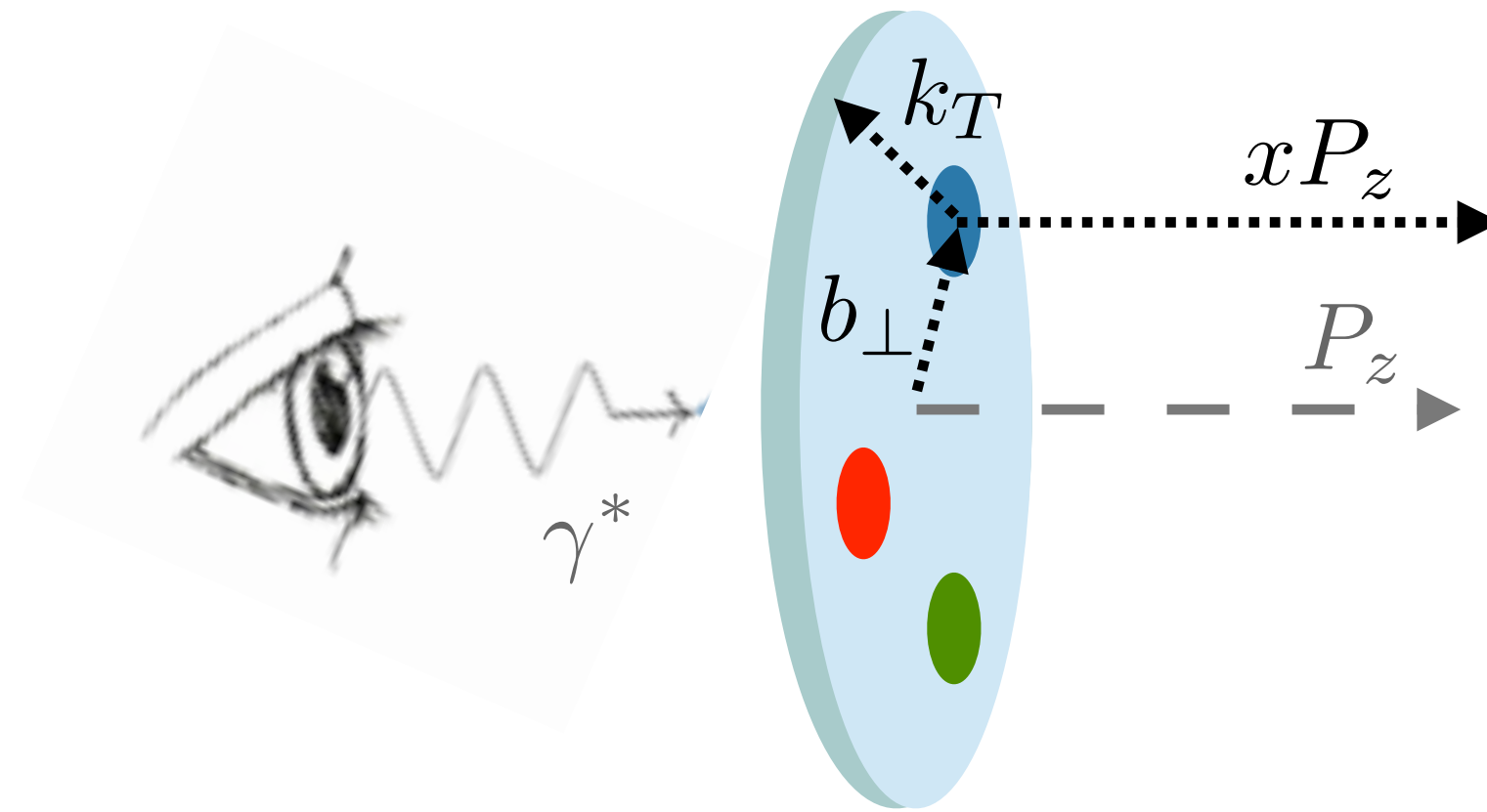
# Why an EIC?

Nucleon multi-dimensional structure

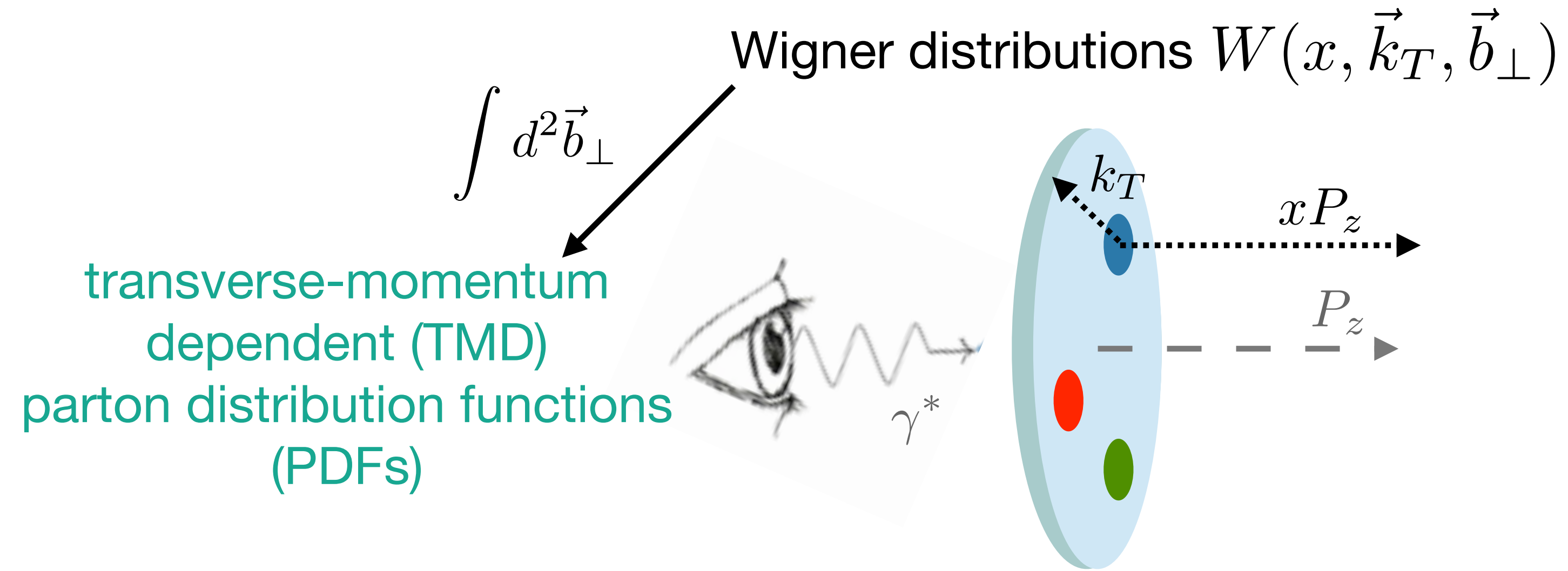


# The nucleon multi-dimensional structure

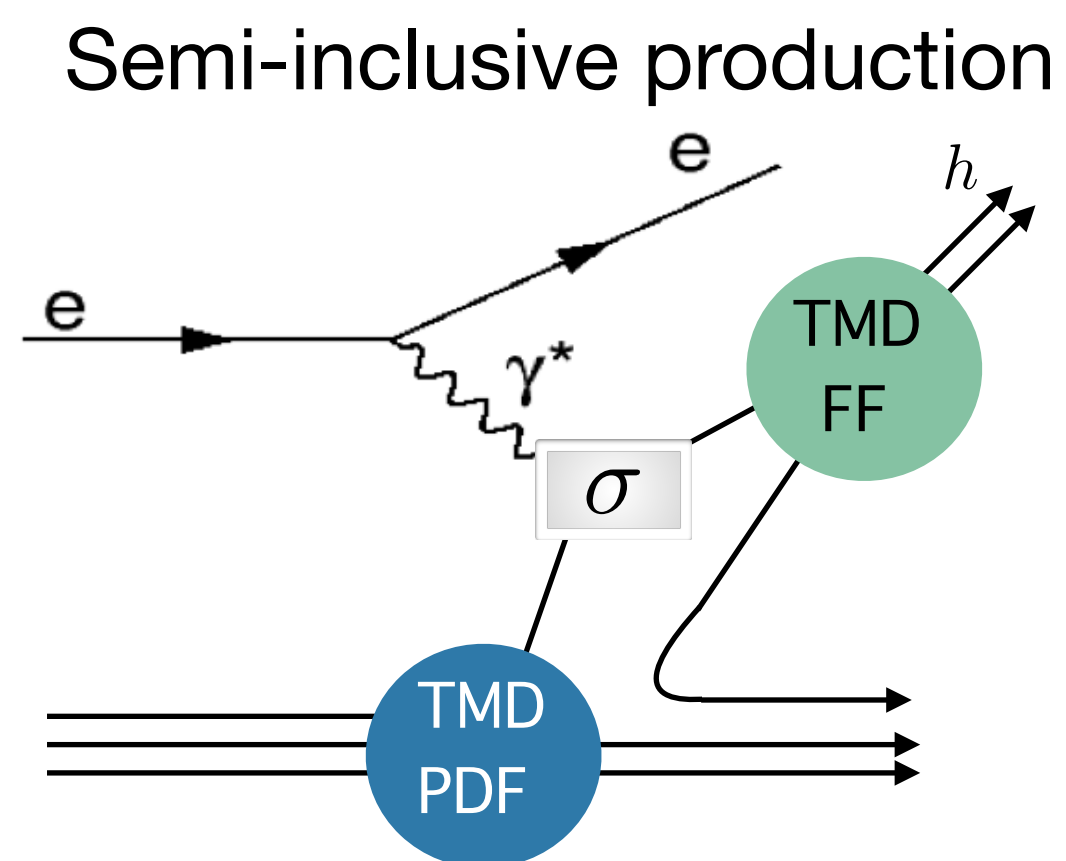
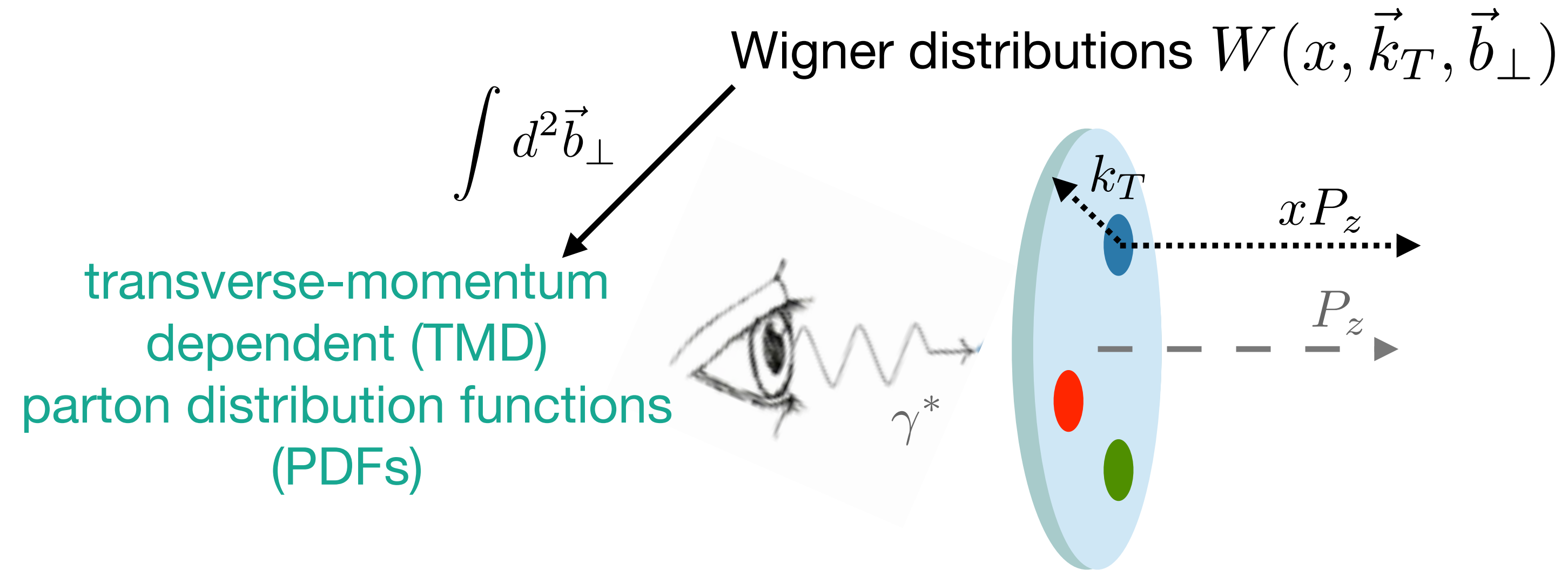
Wigner distributions  $W(x, \vec{k}_T, \vec{b}_\perp)$



# The nucleon multi-dimensional structure

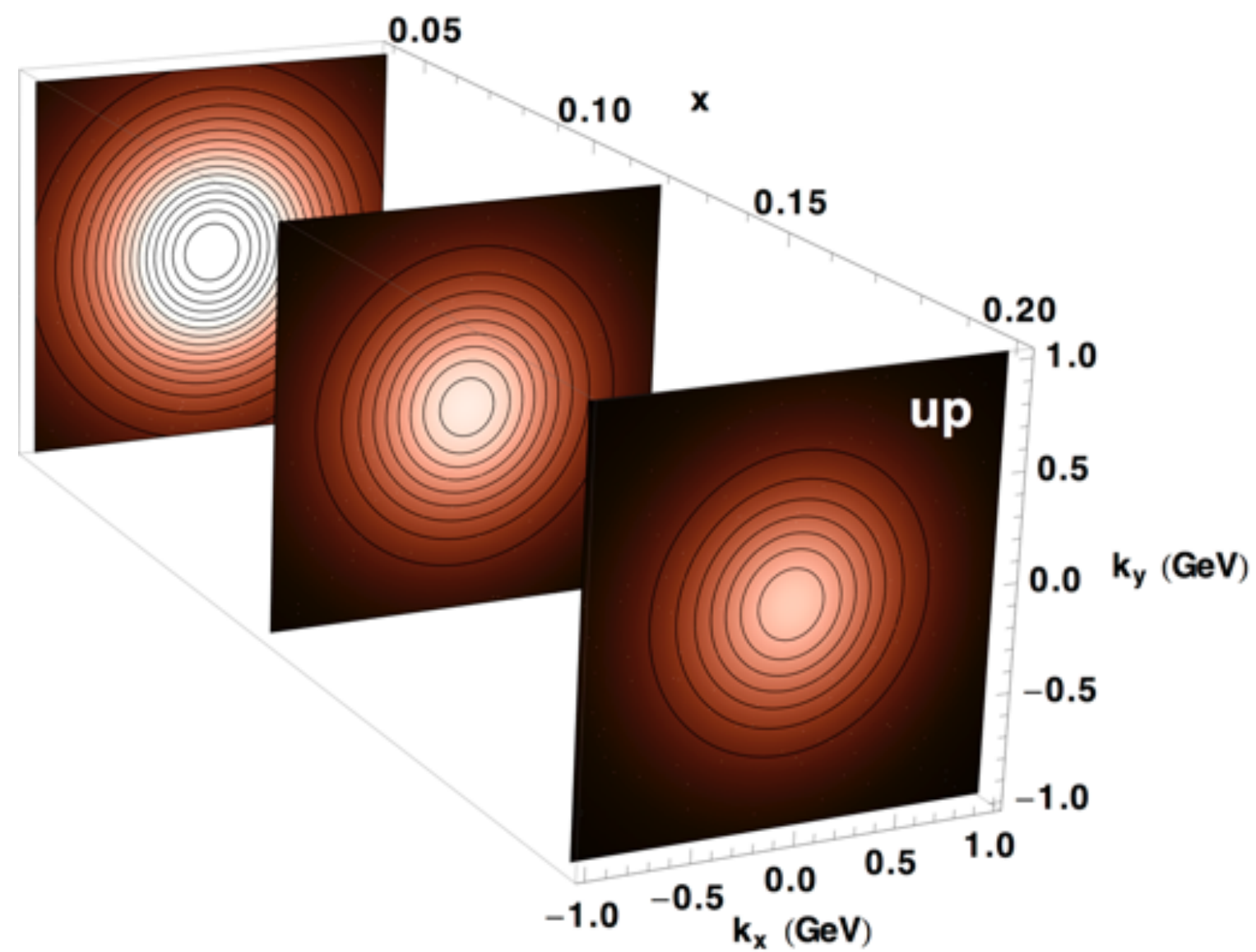
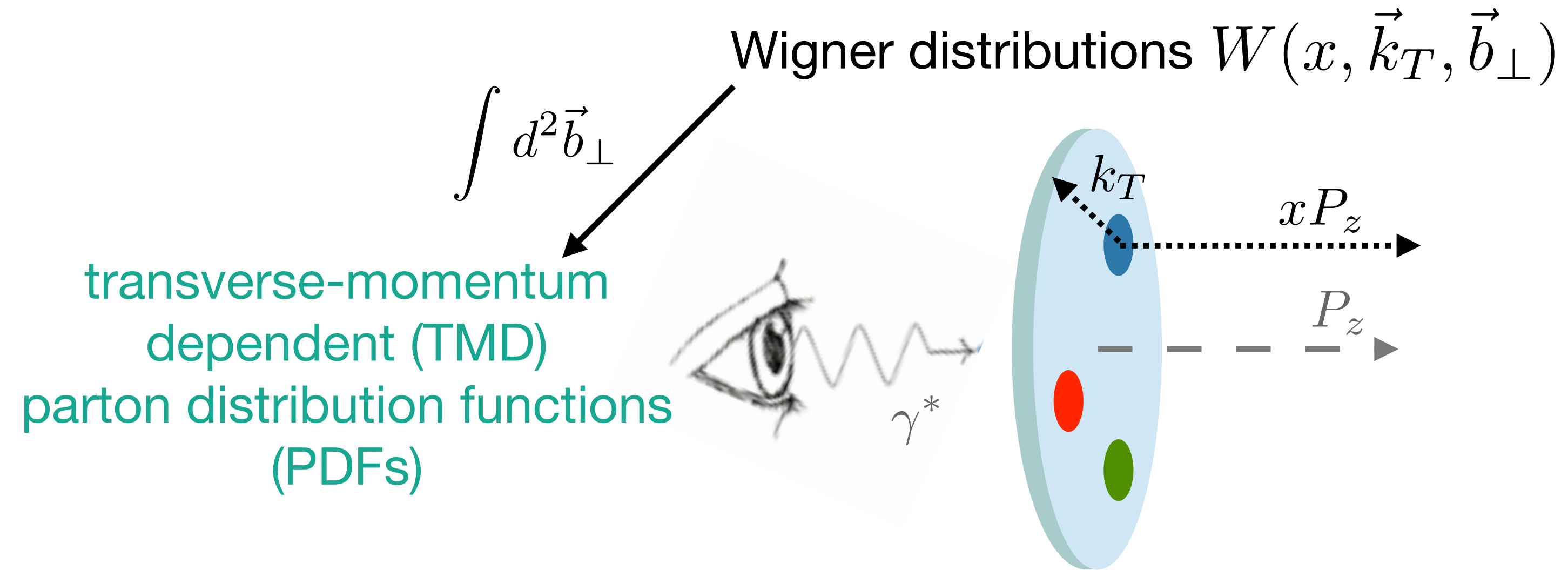


# The nucleon multi-dimensional structure

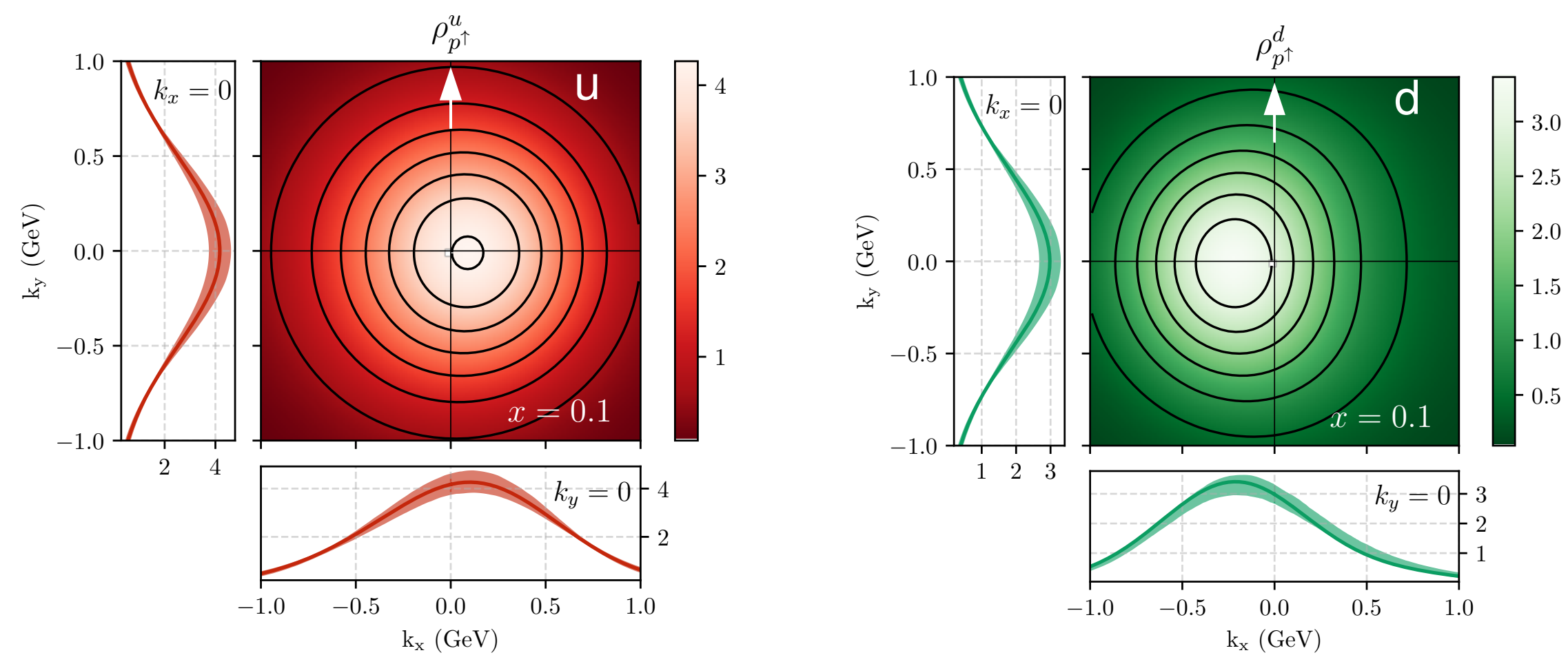
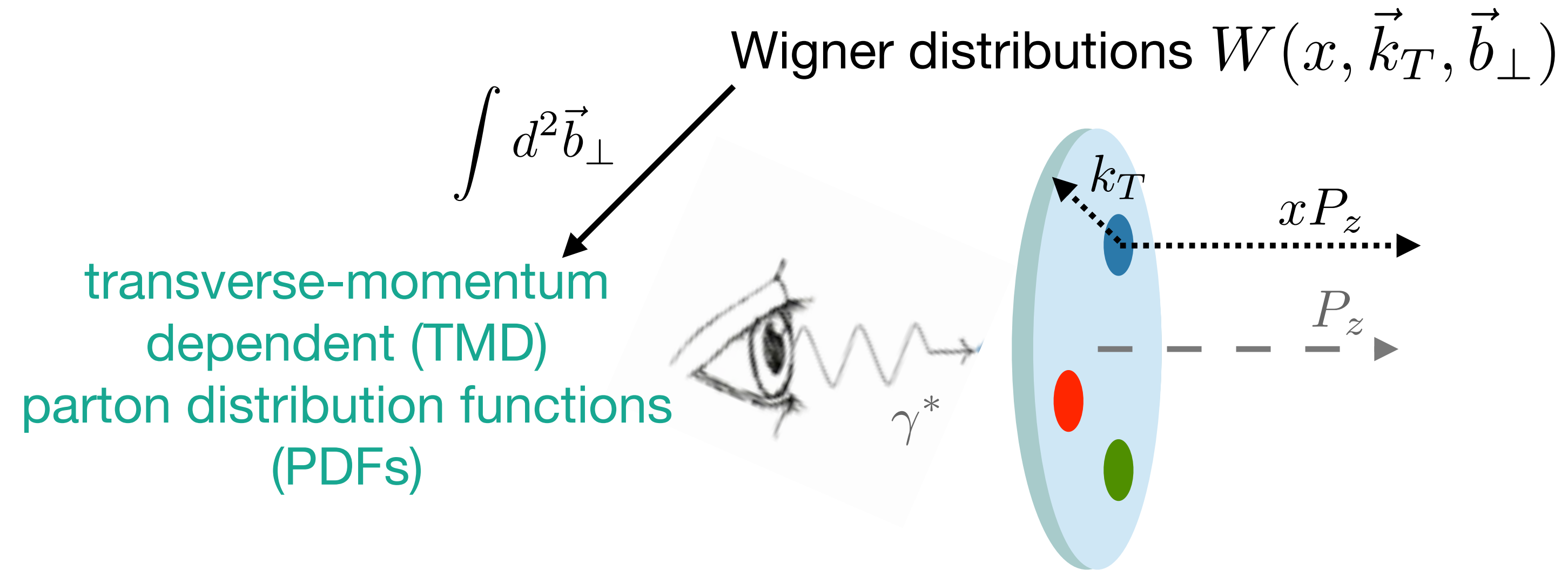




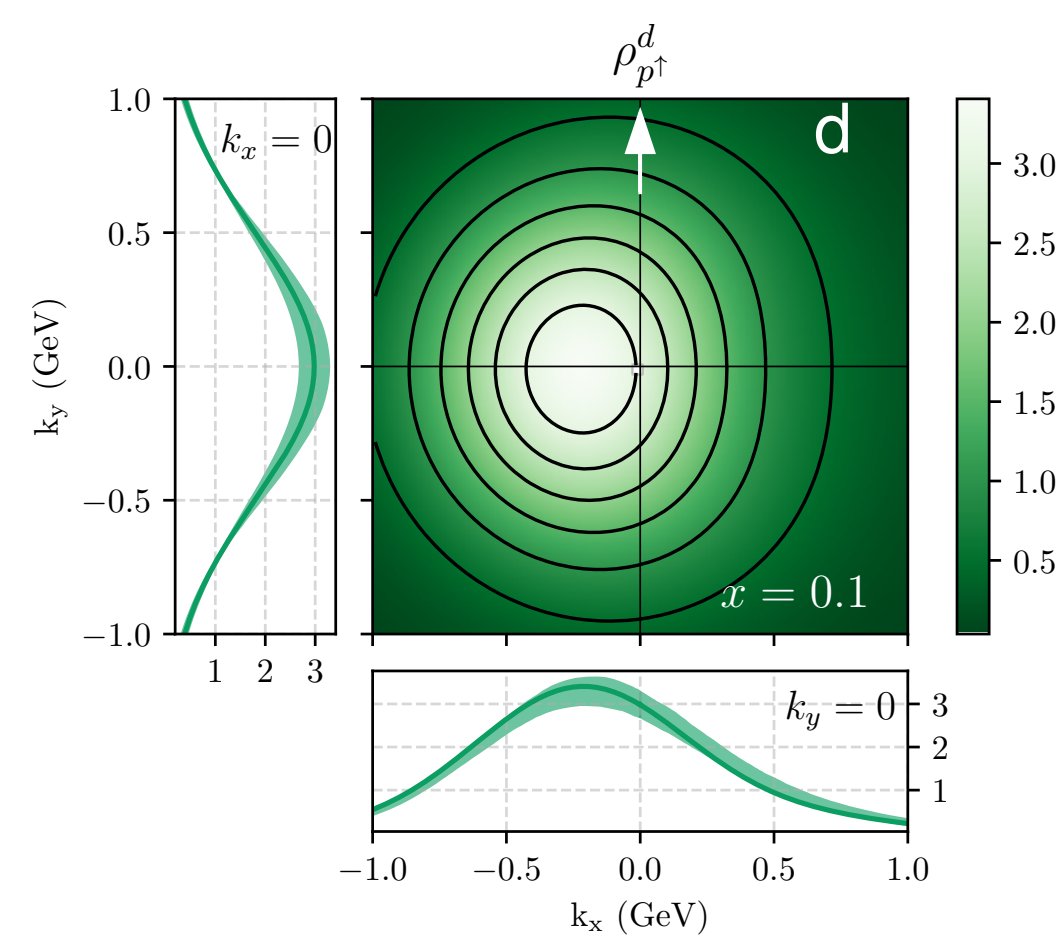
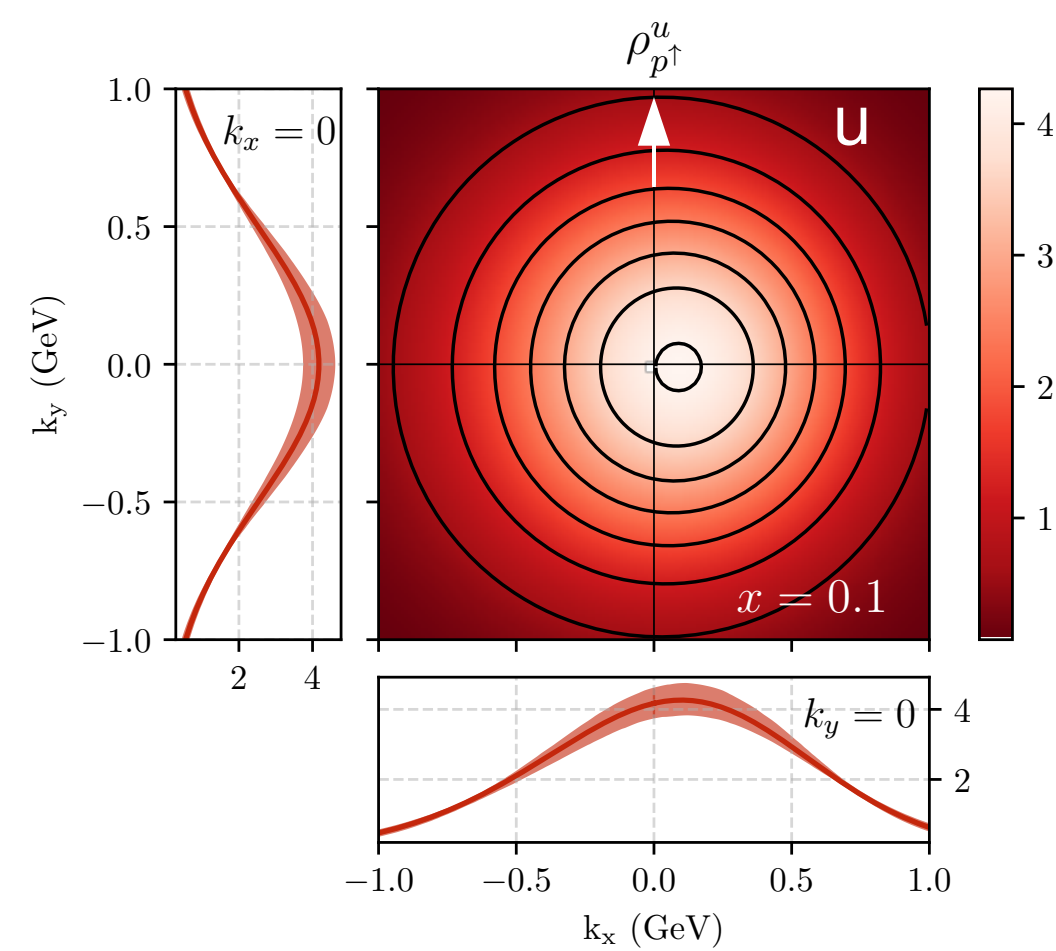
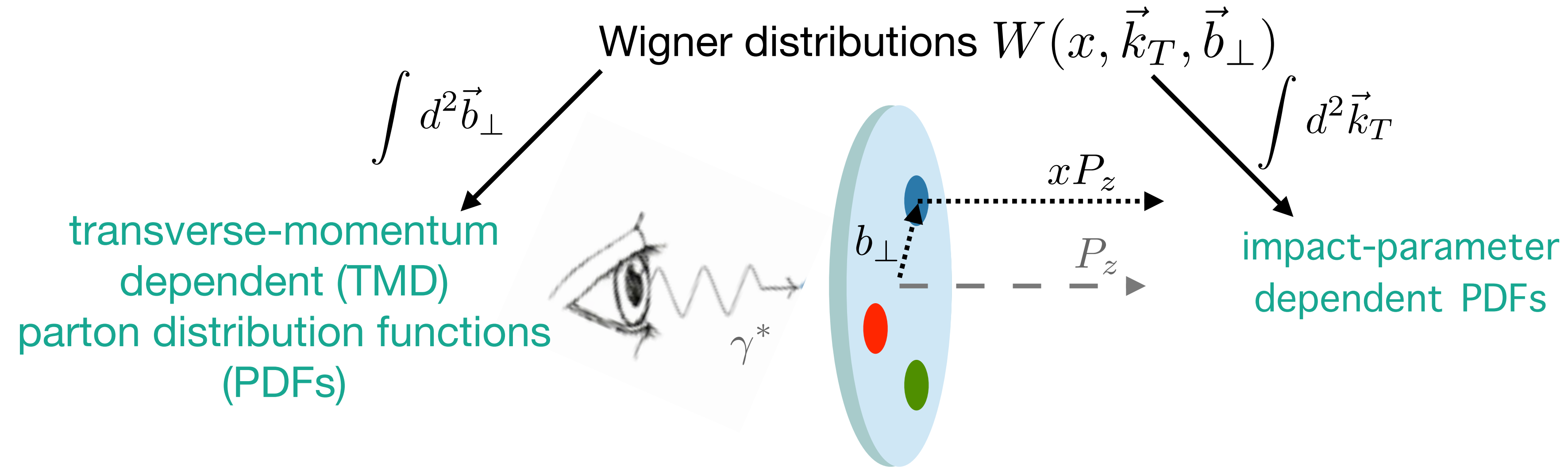
# The nucleon multi-dimensional structure



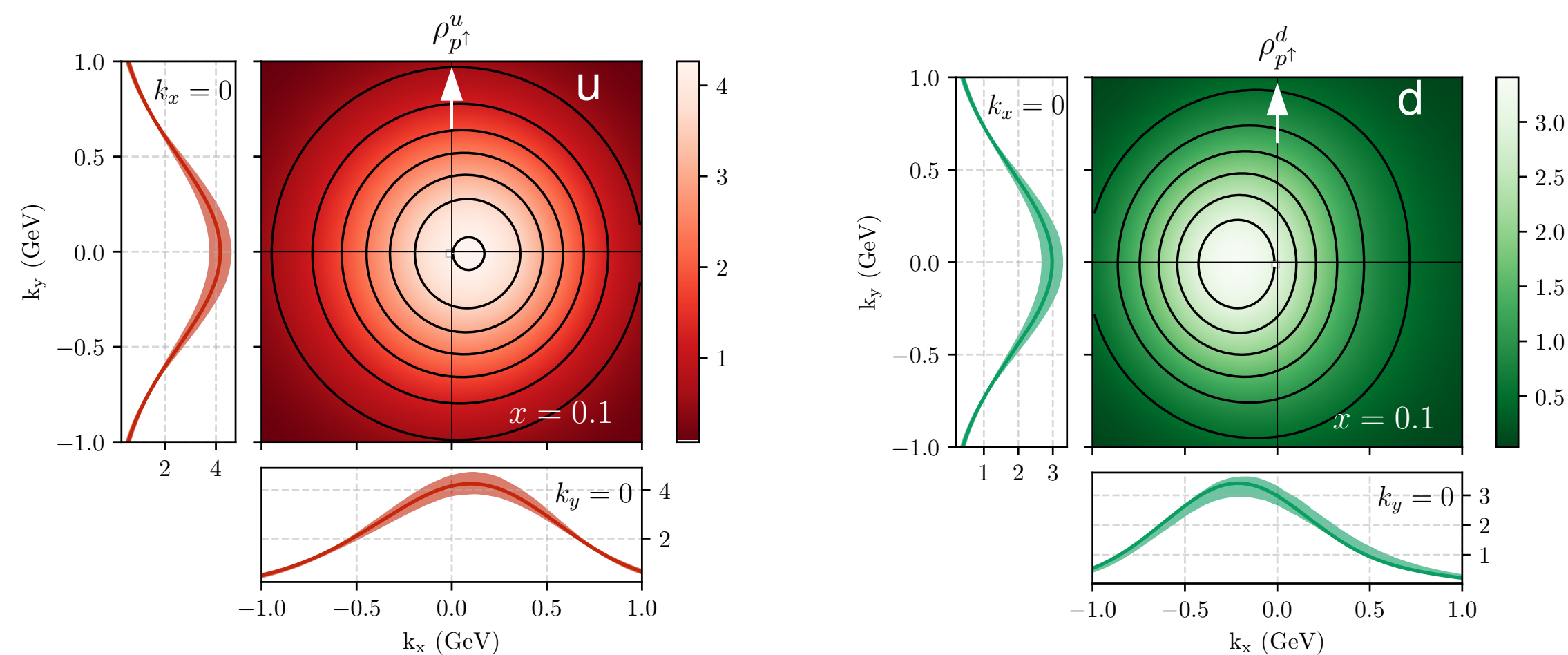
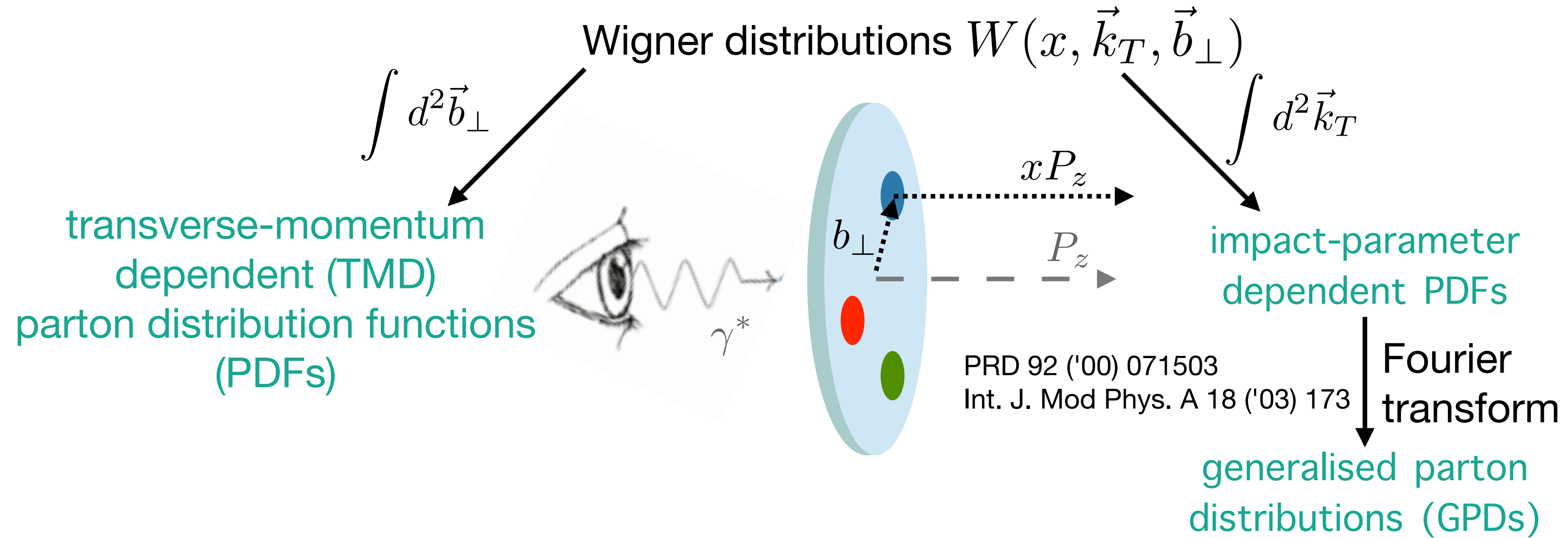
# The nucleon multi-dimensional structure



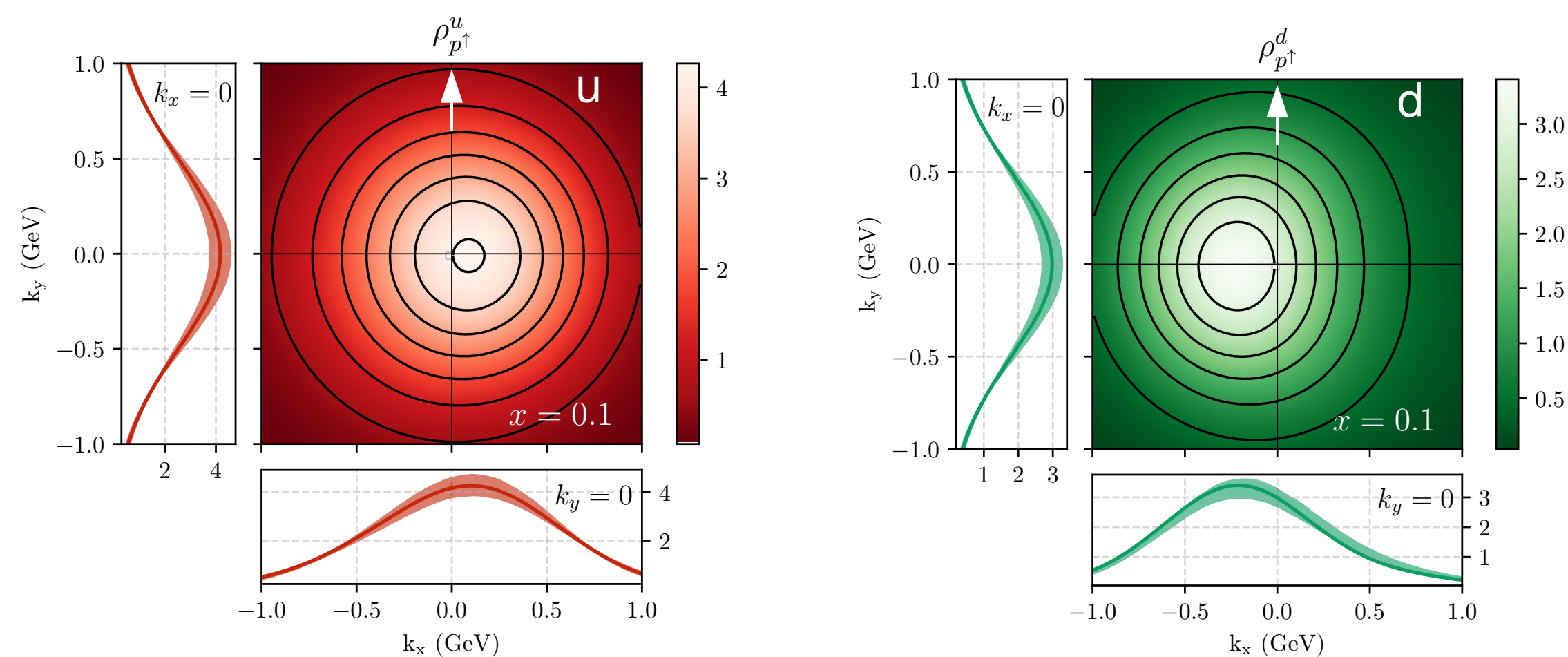
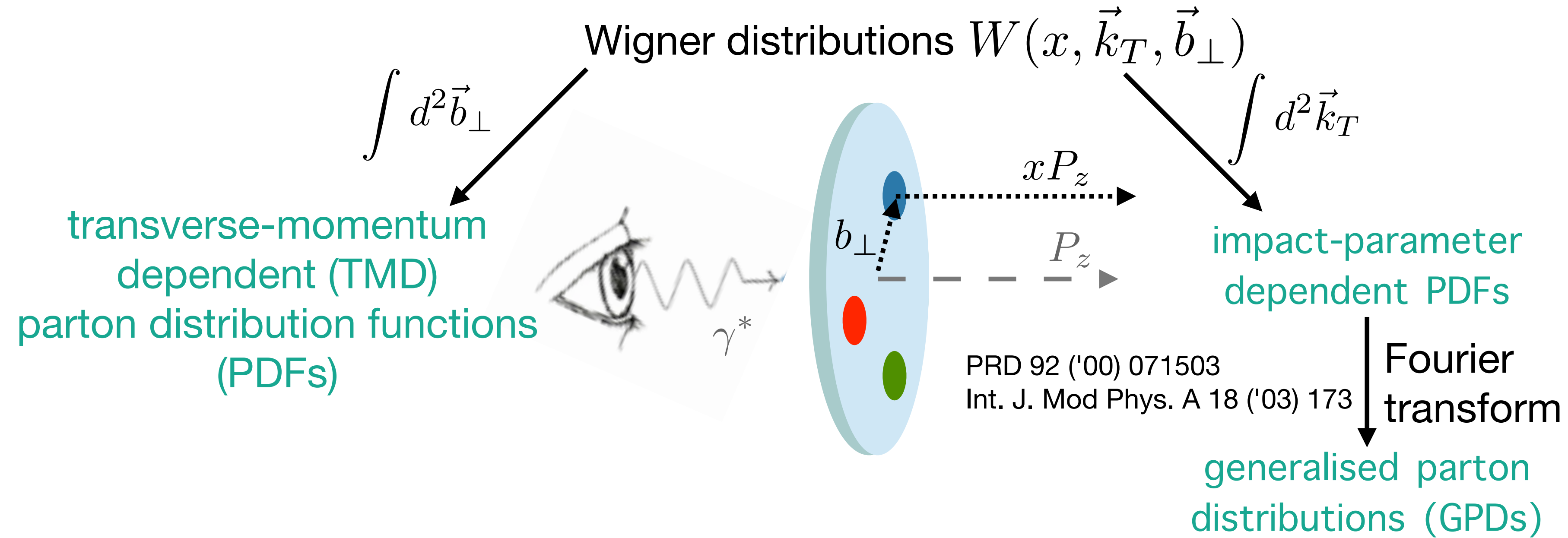
# The nucleon multi-dimensional structure



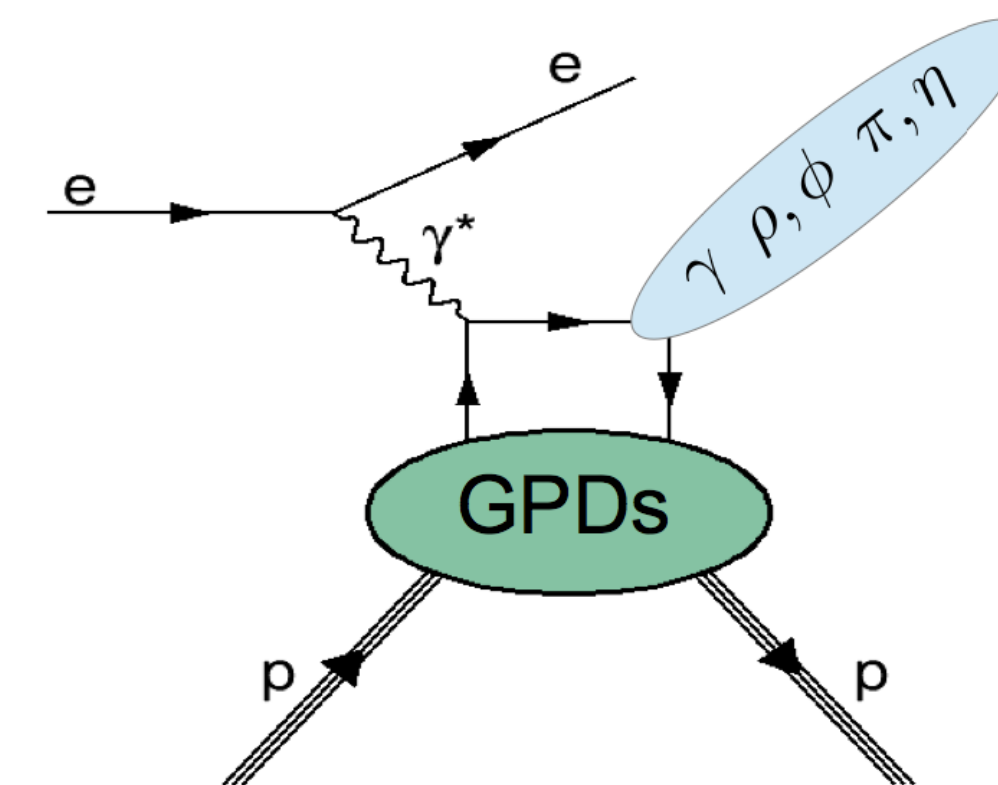
# The nucleon multi-dimensional structure



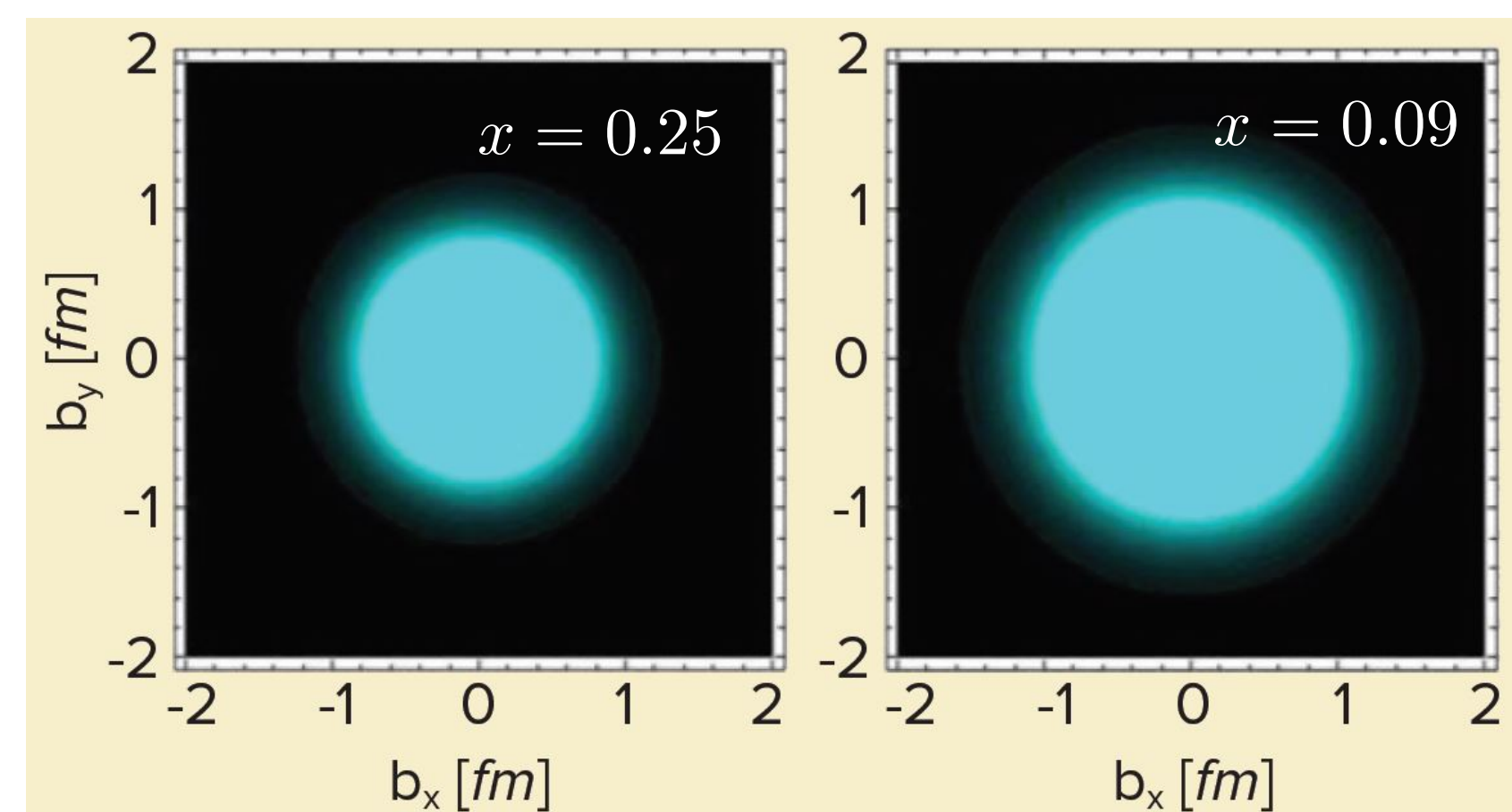
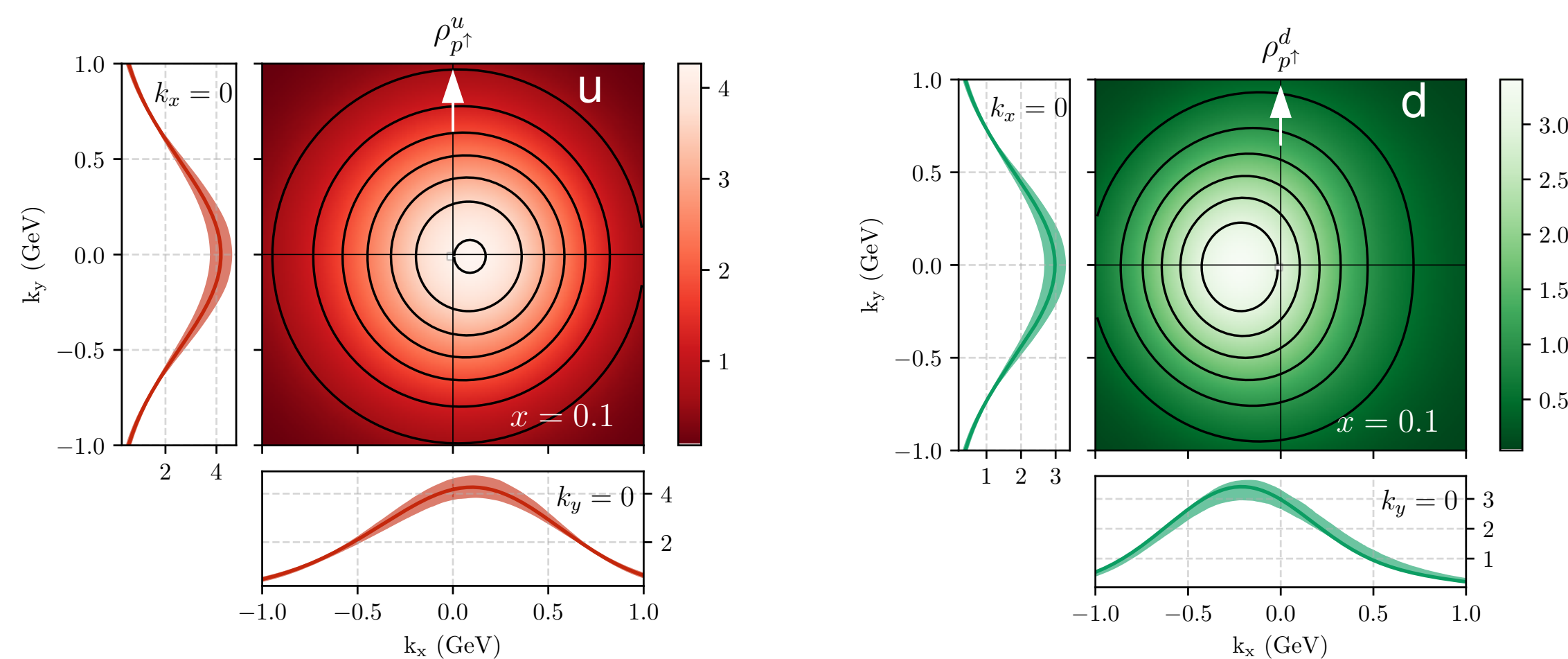
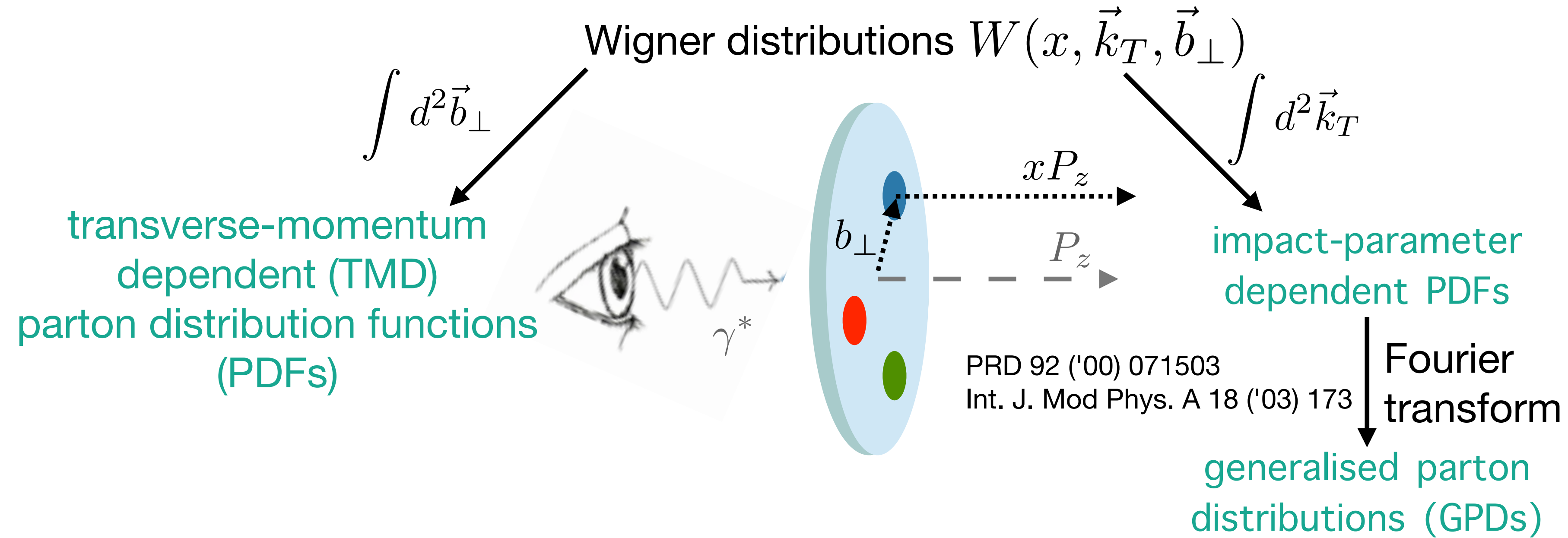
# The nucleon multi-dimensional structure



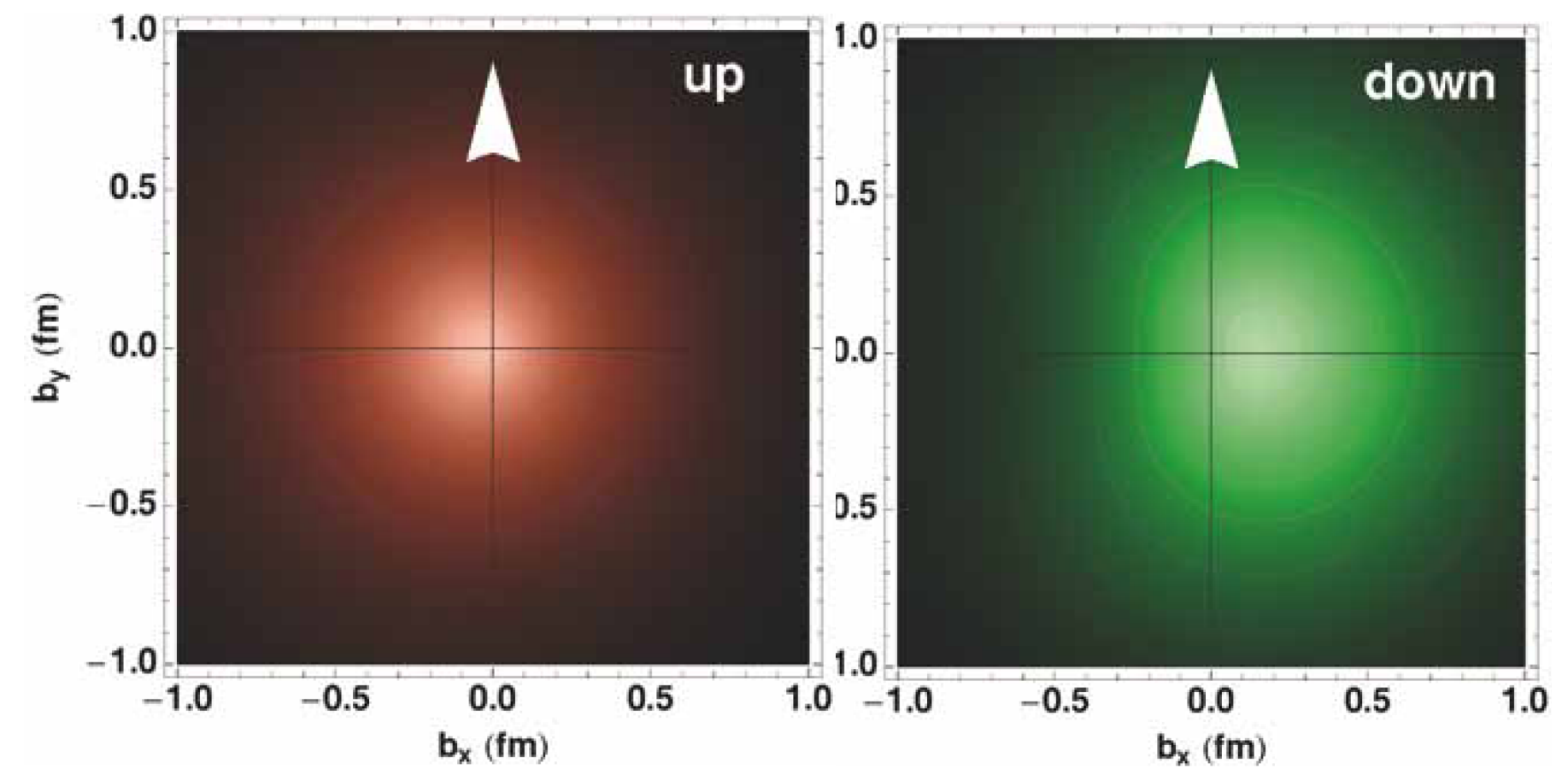
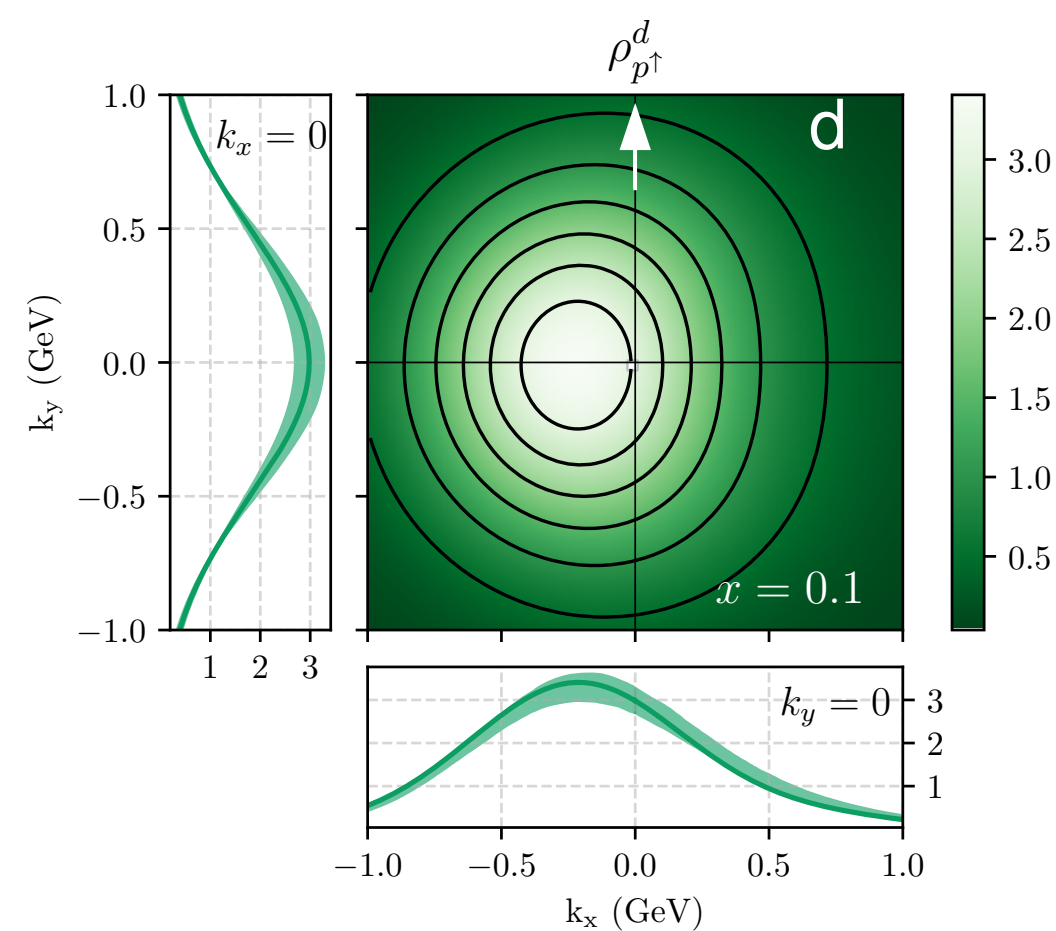
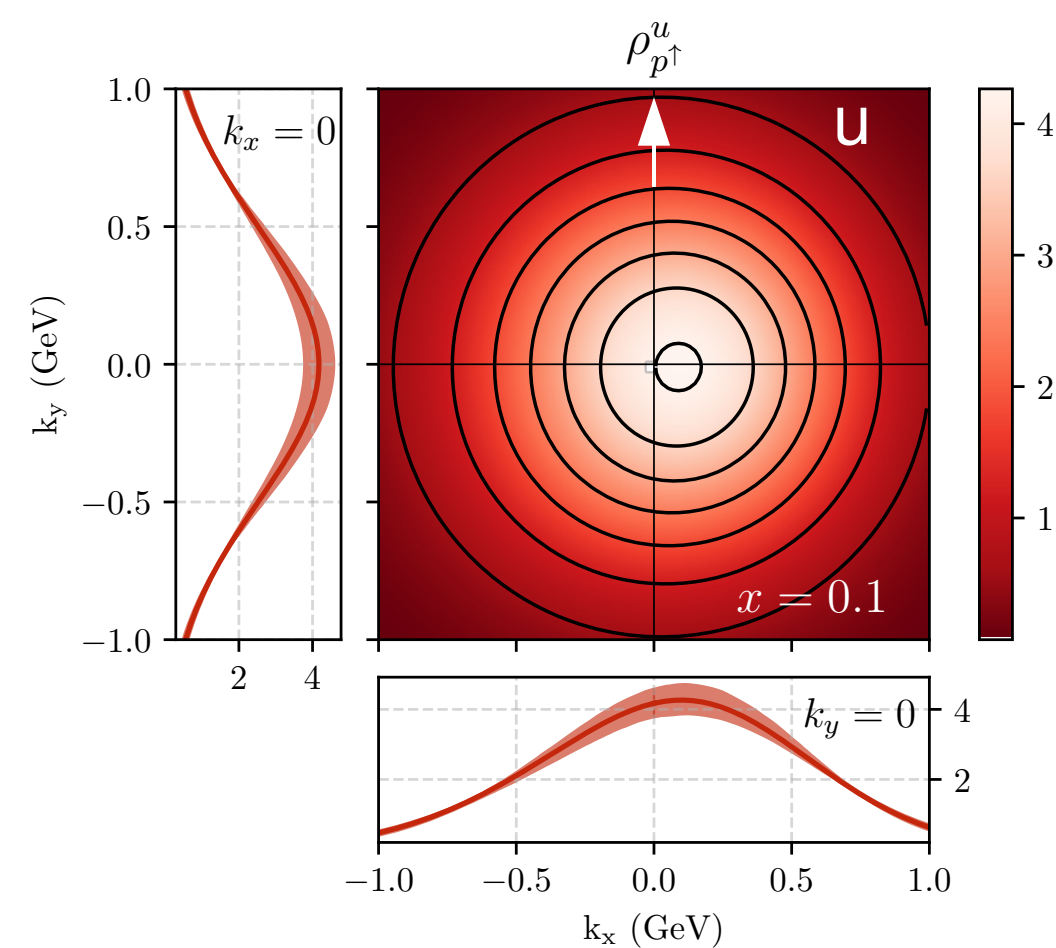
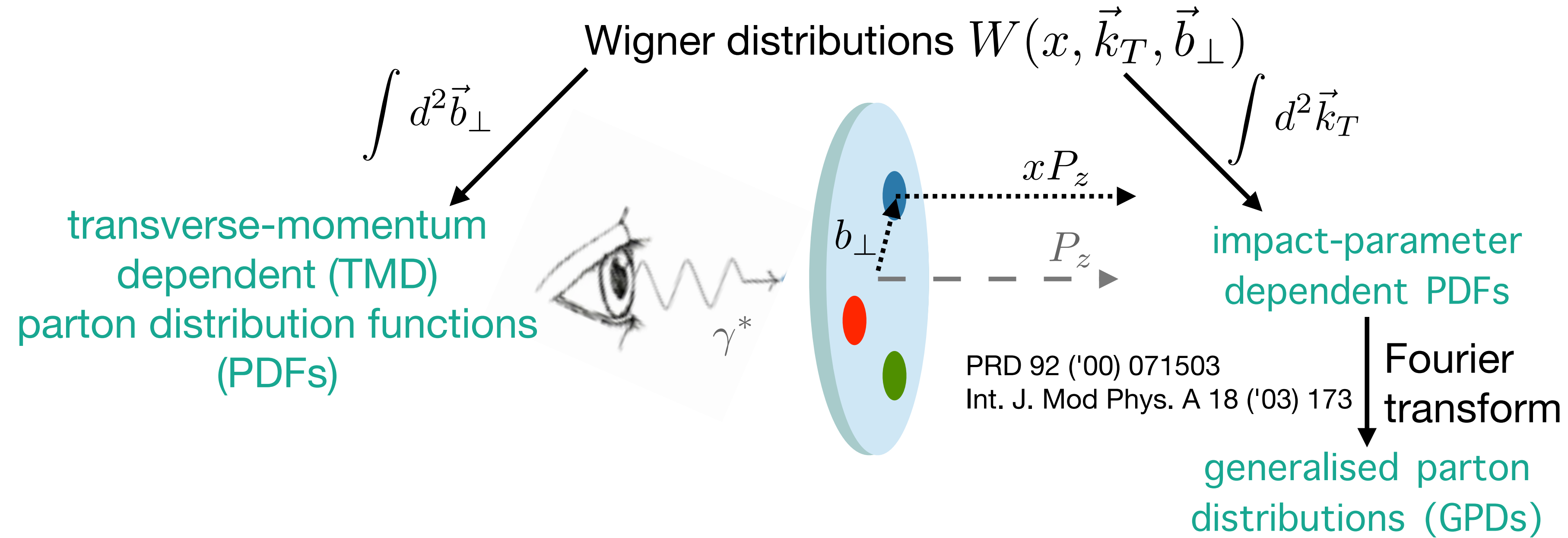
Exclusive production



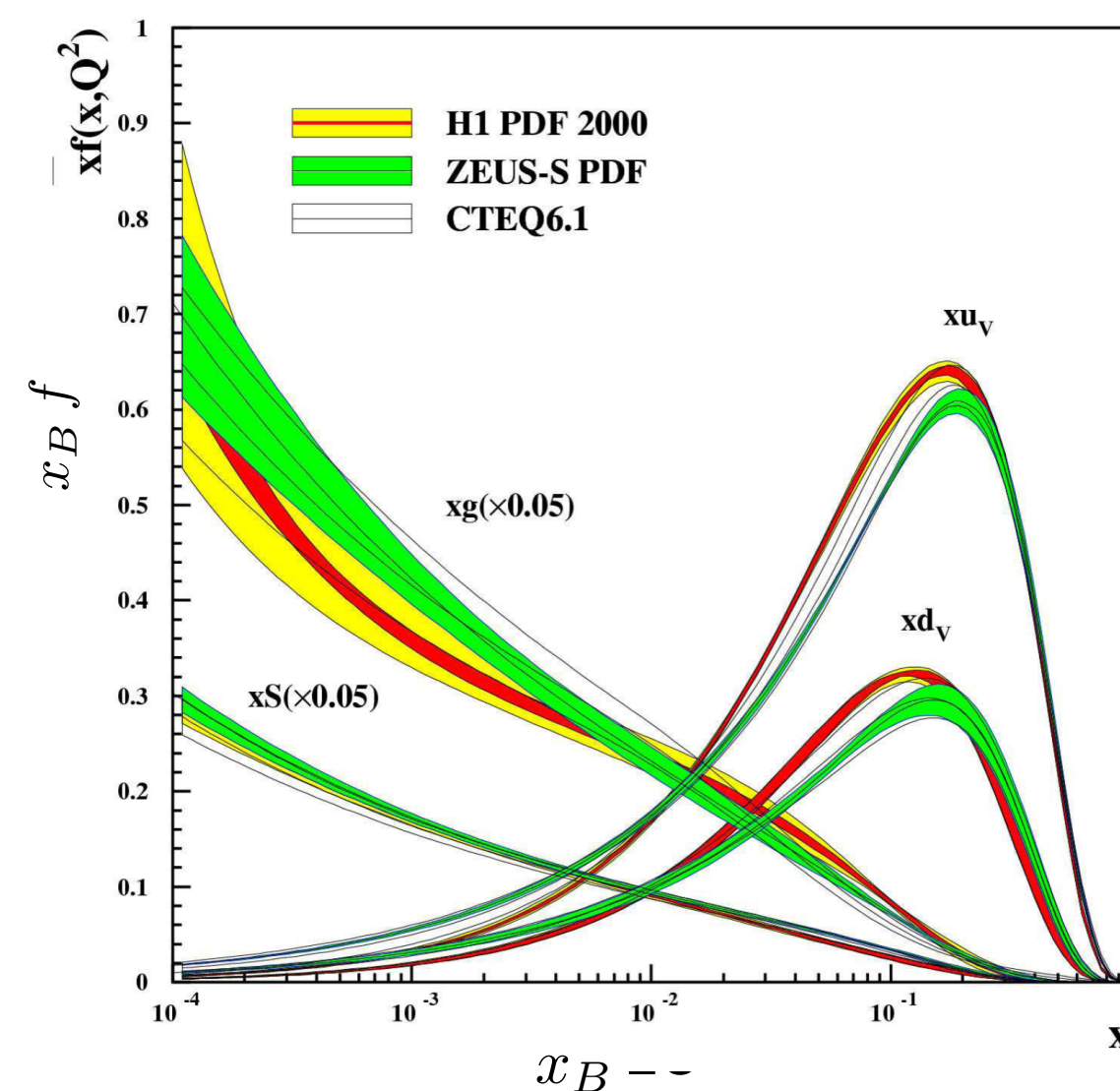
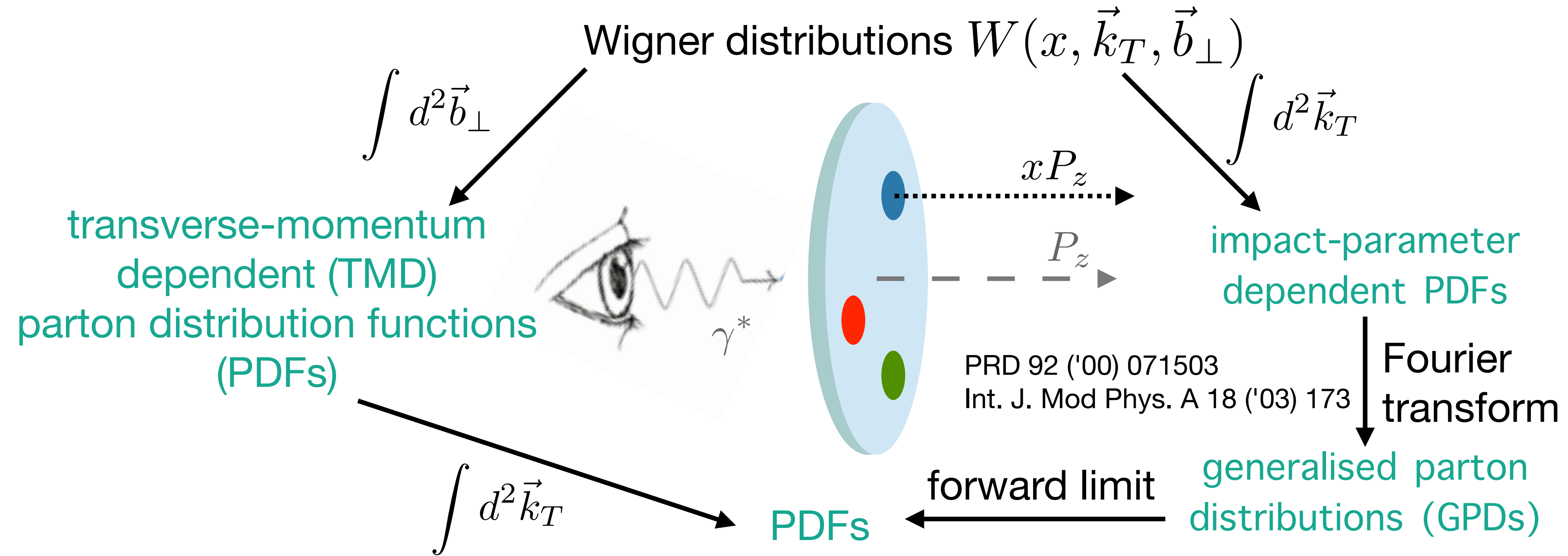
# The nucleon multi-dimensional structure



# The nucleon multi-dimensional structure



# The nucleon multi-dimensional structure

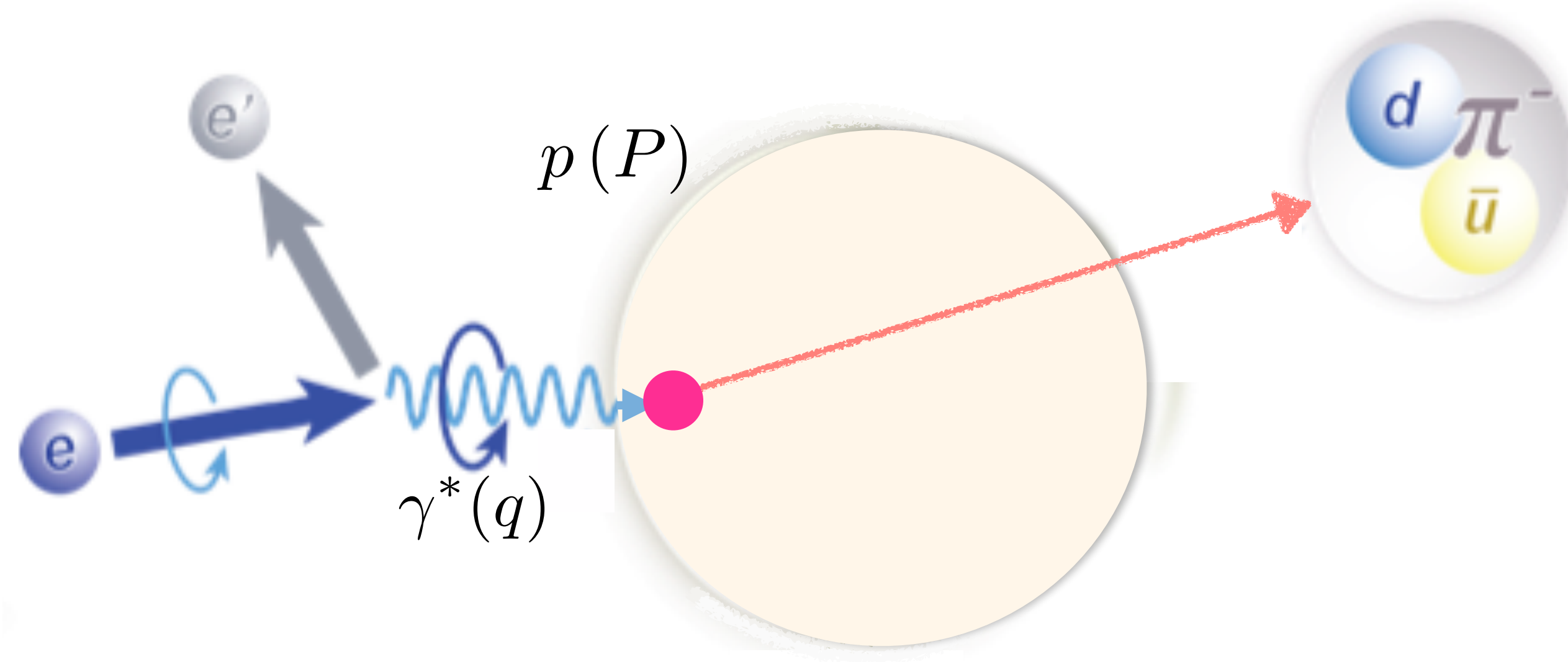




# Single-hadron production in semi-inclusive DIS

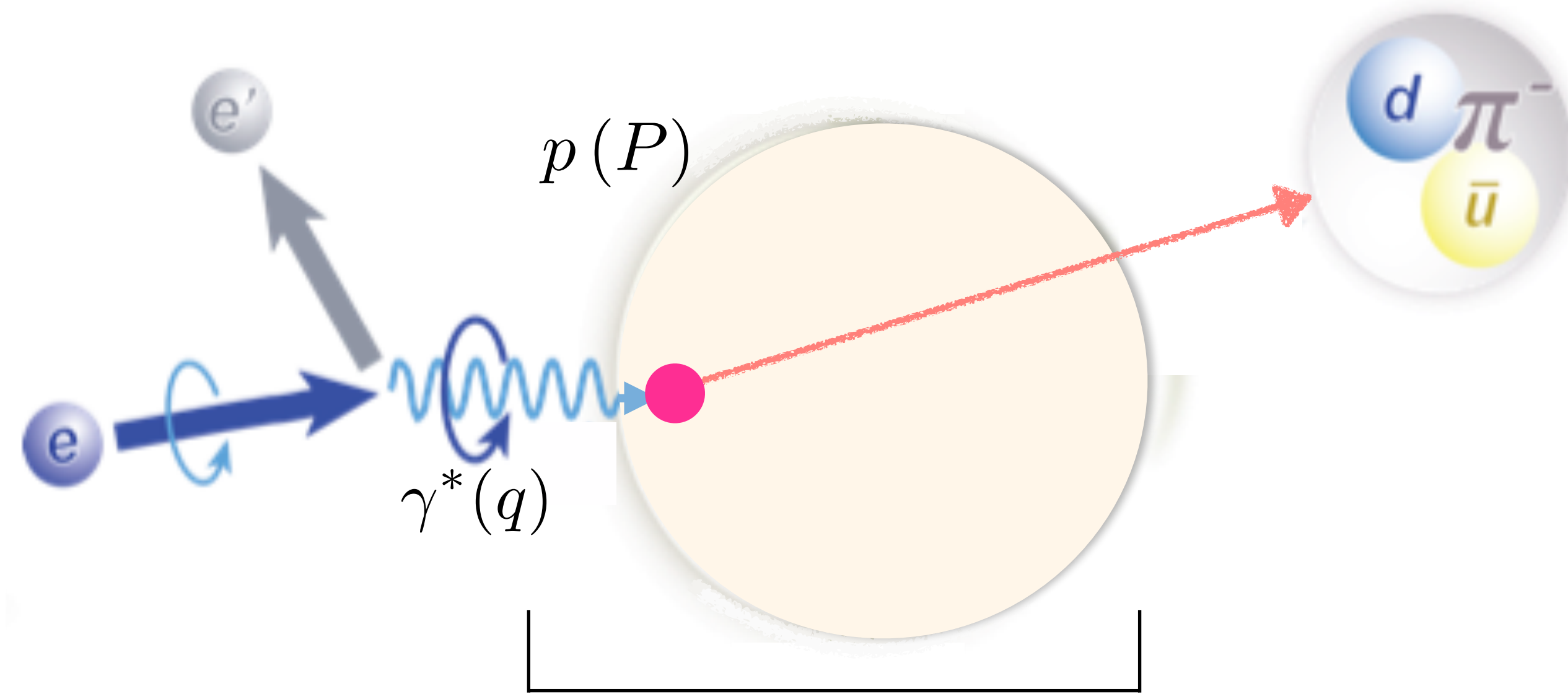
$$Q^2 = -q^2$$

$$x_B = \frac{Q^2}{2P \cdot q}$$



# Single-hadron production in semi-inclusive DIS

$$Q^2 = -q^2$$
$$x_B = \frac{Q^2}{2P \cdot q}$$



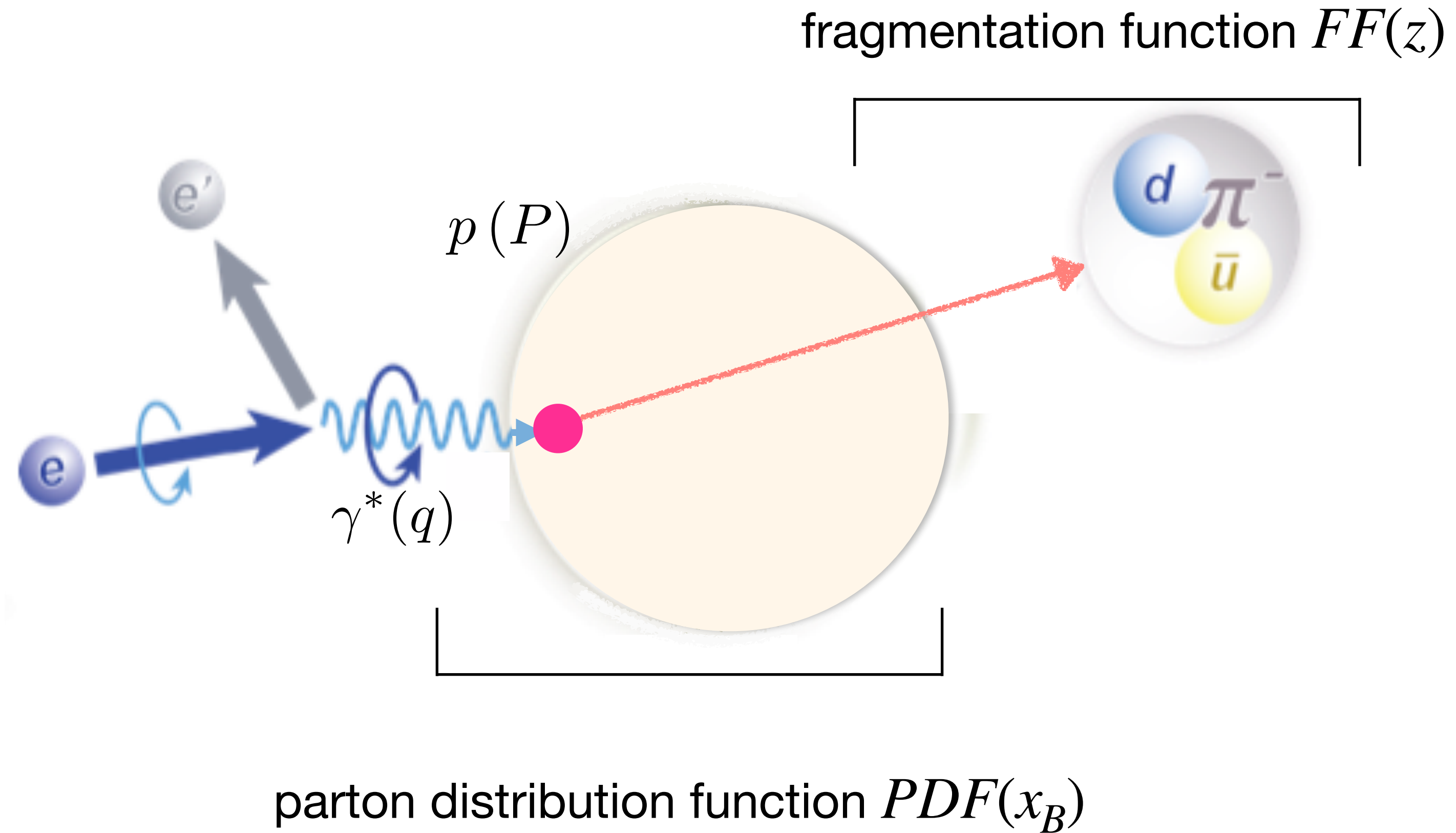
parton distribution function  $PDF(x_B)$

# Single-hadron production in semi-inclusive DIS

$$Q^2 = -q^2$$

$$x_B = \frac{Q^2}{2P \cdot q}$$

$$z \stackrel{\text{lab}}{=} \frac{E_h}{E_{\gamma^*}}$$

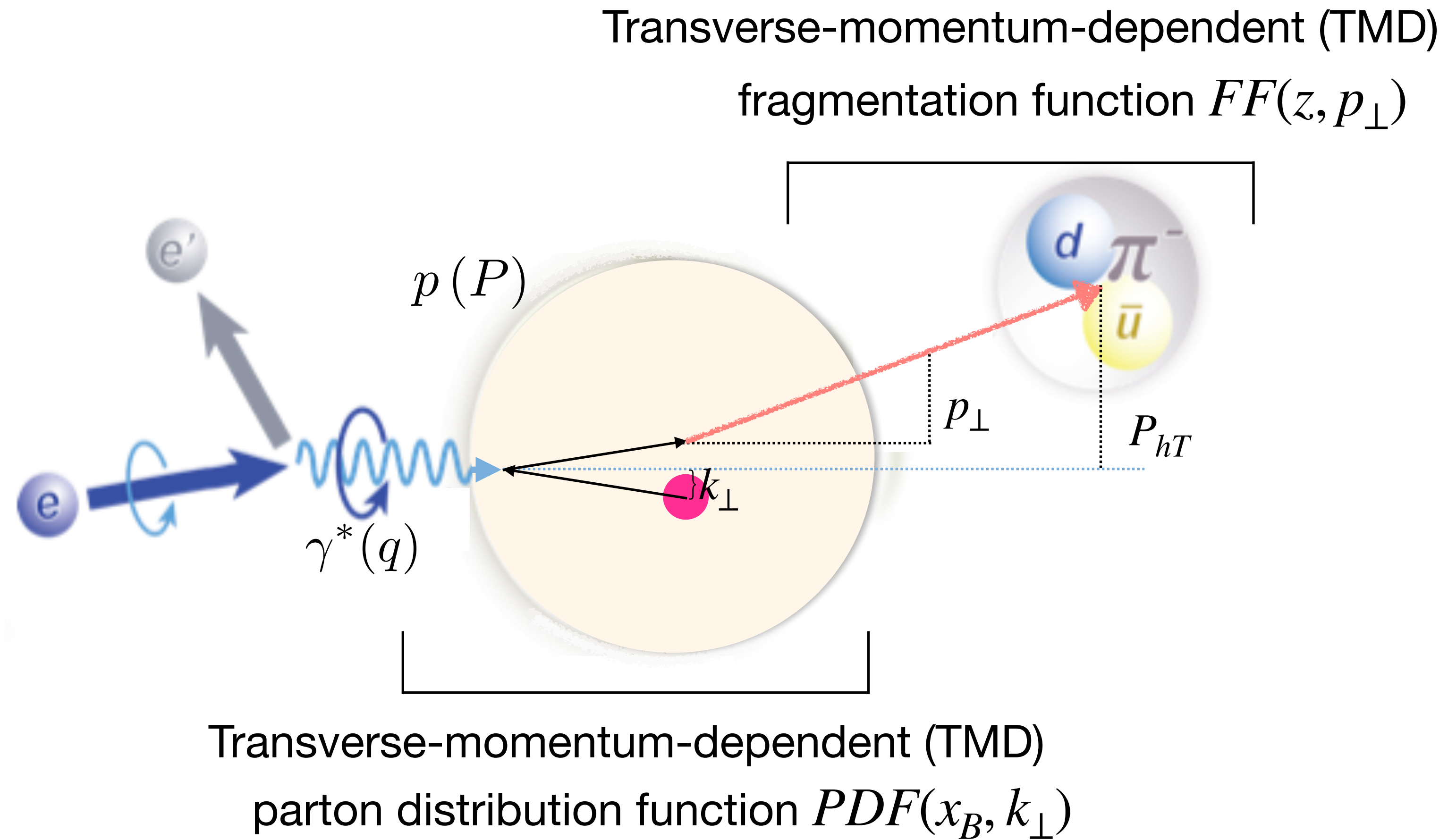


# Single-hadron production in semi-inclusive DIS

$$Q^2 = -q^2$$

$$x_B = \frac{Q^2}{2P \cdot q}$$

$$z \stackrel{\text{lab}}{=} \frac{E_h}{E_{\gamma^*}}$$

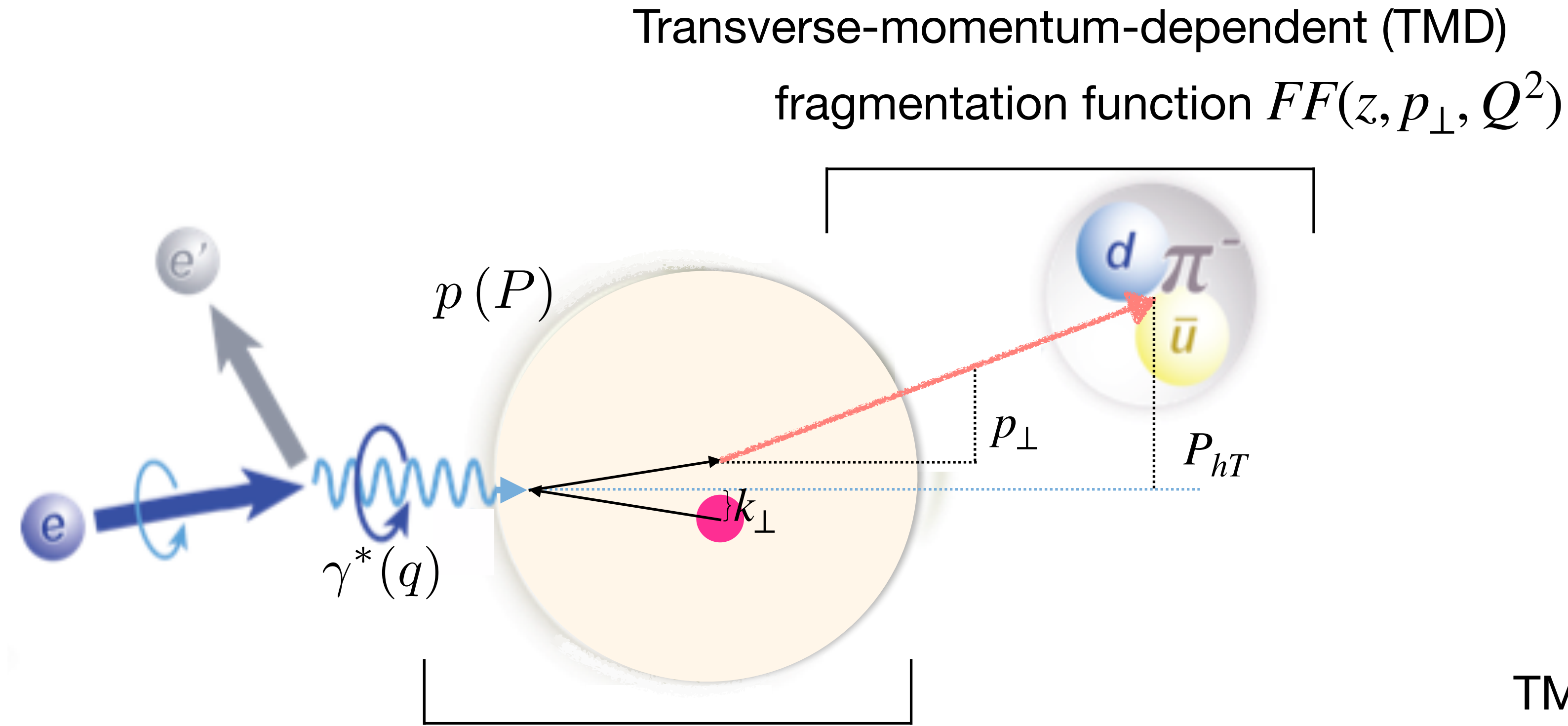


# Single-hadron production in semi-inclusive DIS

$$Q^2 = -q^2$$

$$x_B = \frac{Q^2}{2P \cdot q}$$

$$z \stackrel{\text{lab}}{=} \frac{E_h}{E_{\gamma^*}}$$



Transverse-momentum-dependent (TMD)  
parton distribution function  $PDF(x_B, k_\perp, Q^2)$

TMD evolution

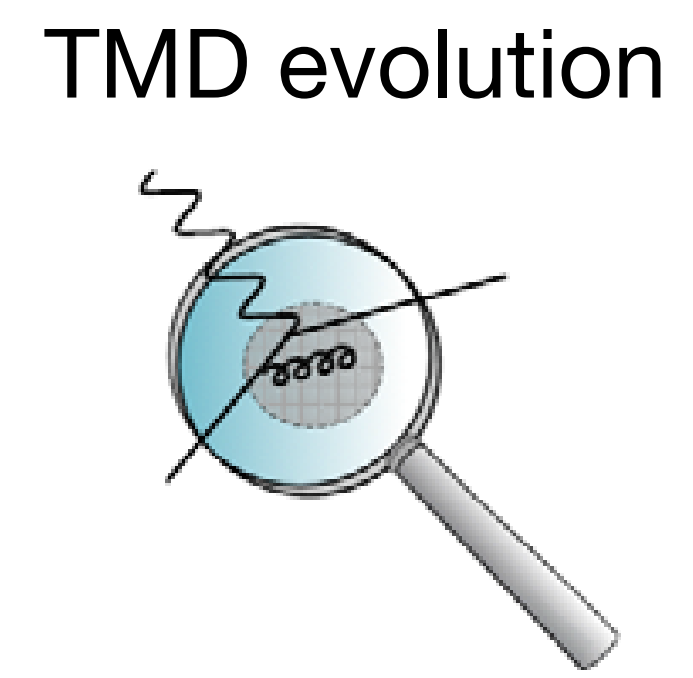
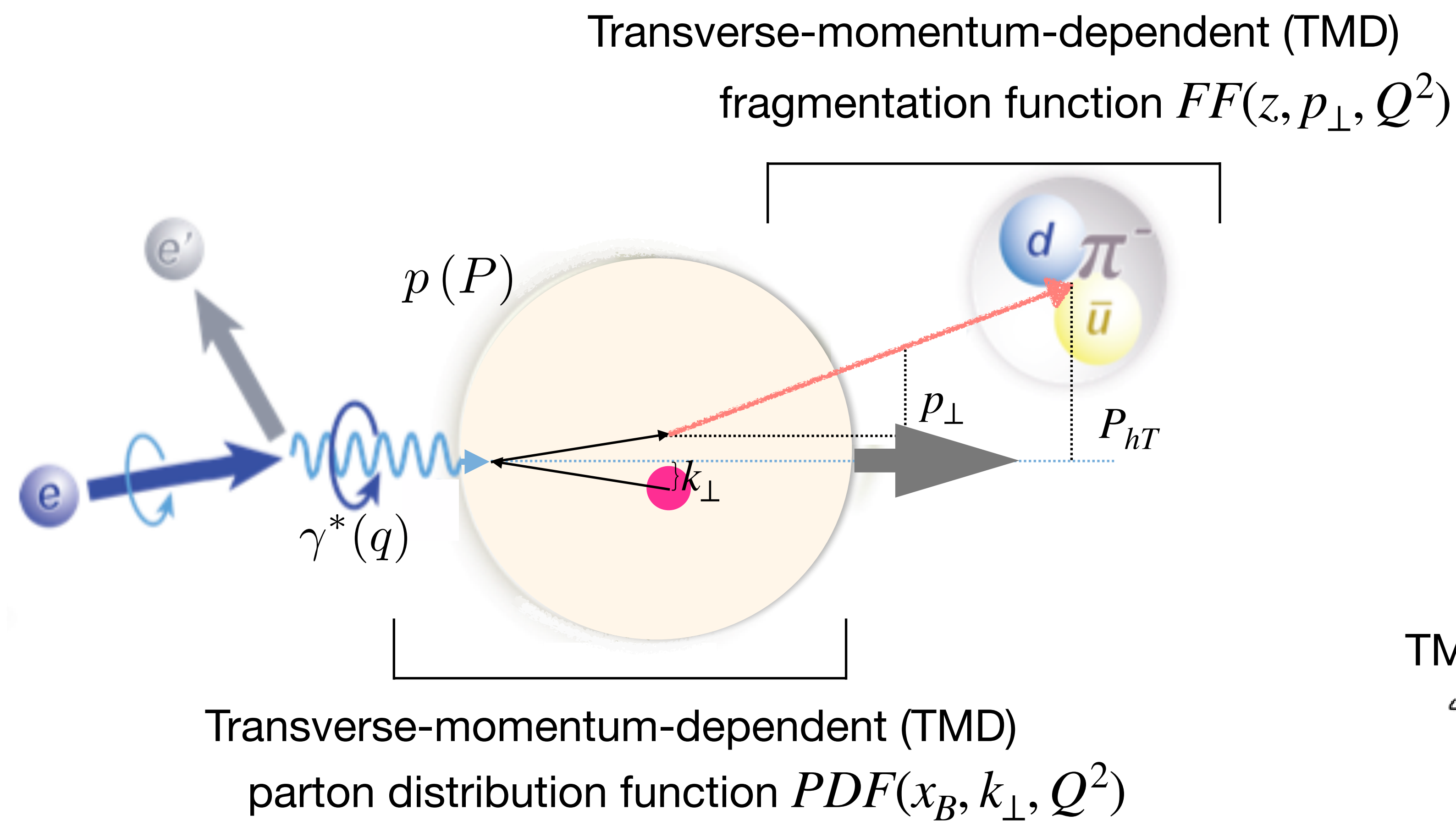


# Single-hadron production in semi-inclusive DIS

$$Q^2 = -q^2$$

$$x_B = \frac{Q^2}{2P \cdot q}$$

$$z \stackrel{\text{lab}}{=} \frac{E_h}{E_{\gamma^*}}$$

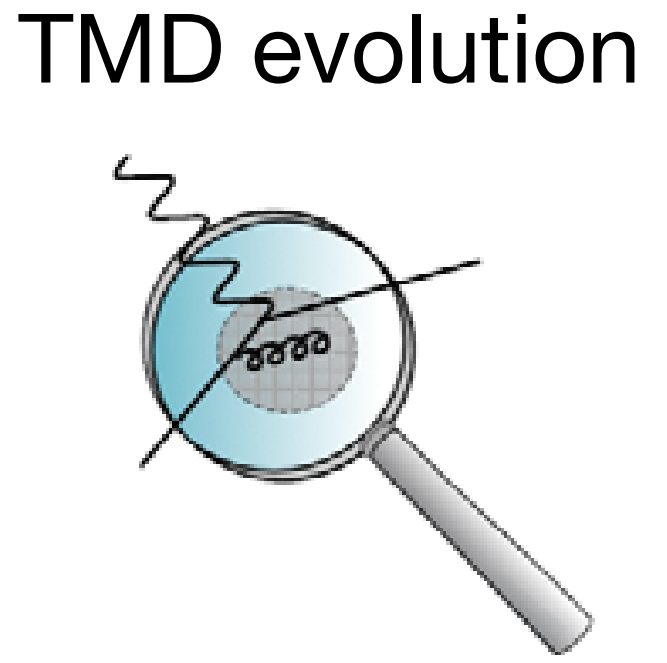
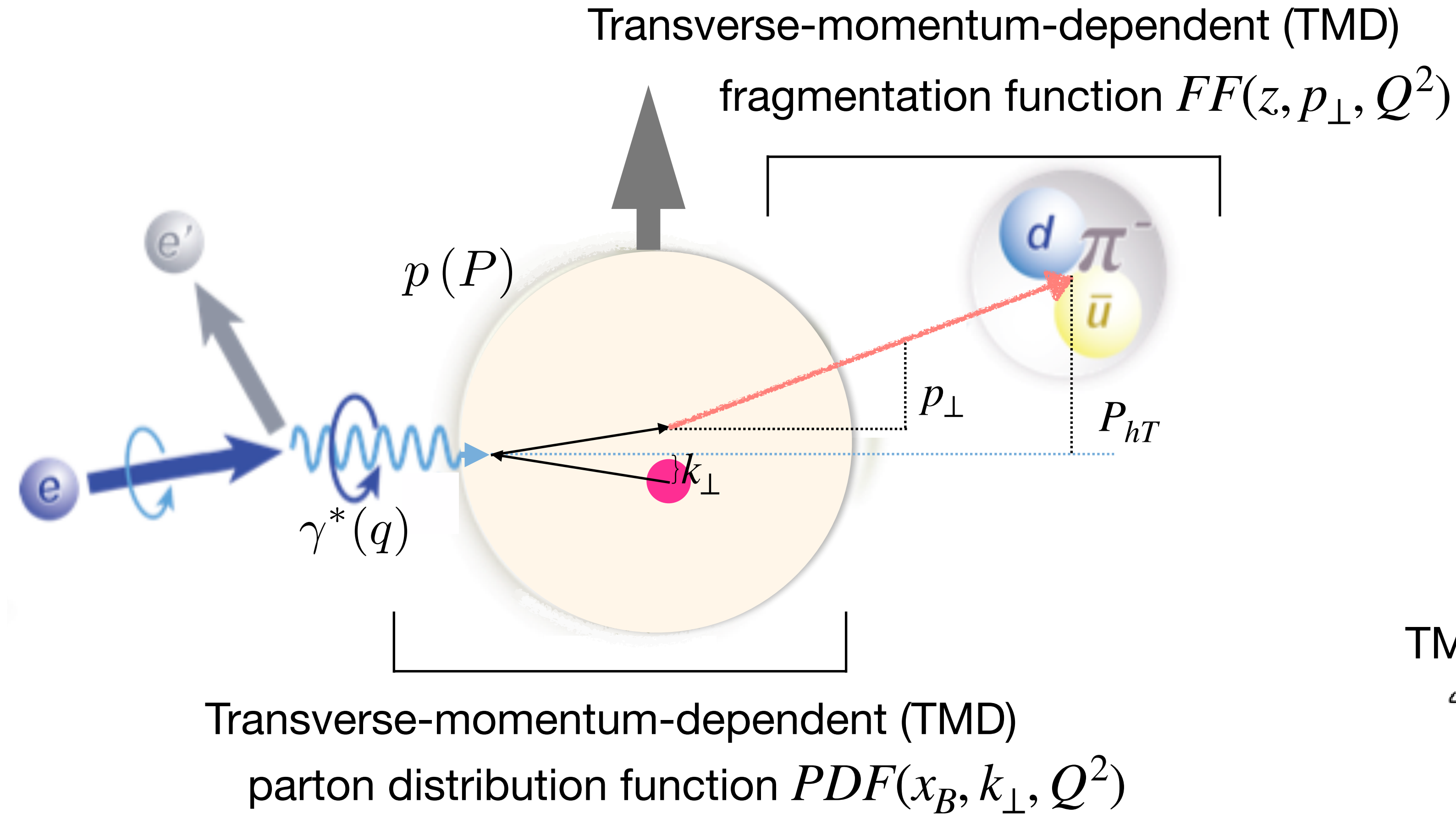


# Single-hadron production in semi-inclusive DIS

$$Q^2 = -q^2$$

$$x_B = \frac{Q^2}{2P \cdot q}$$

$$z \stackrel{\text{lab}}{=} \frac{E_h}{E_{\gamma^*}}$$

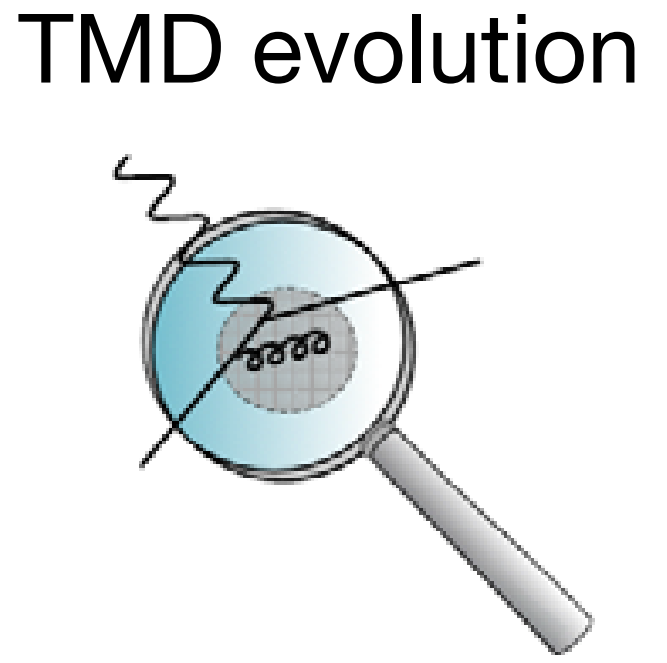
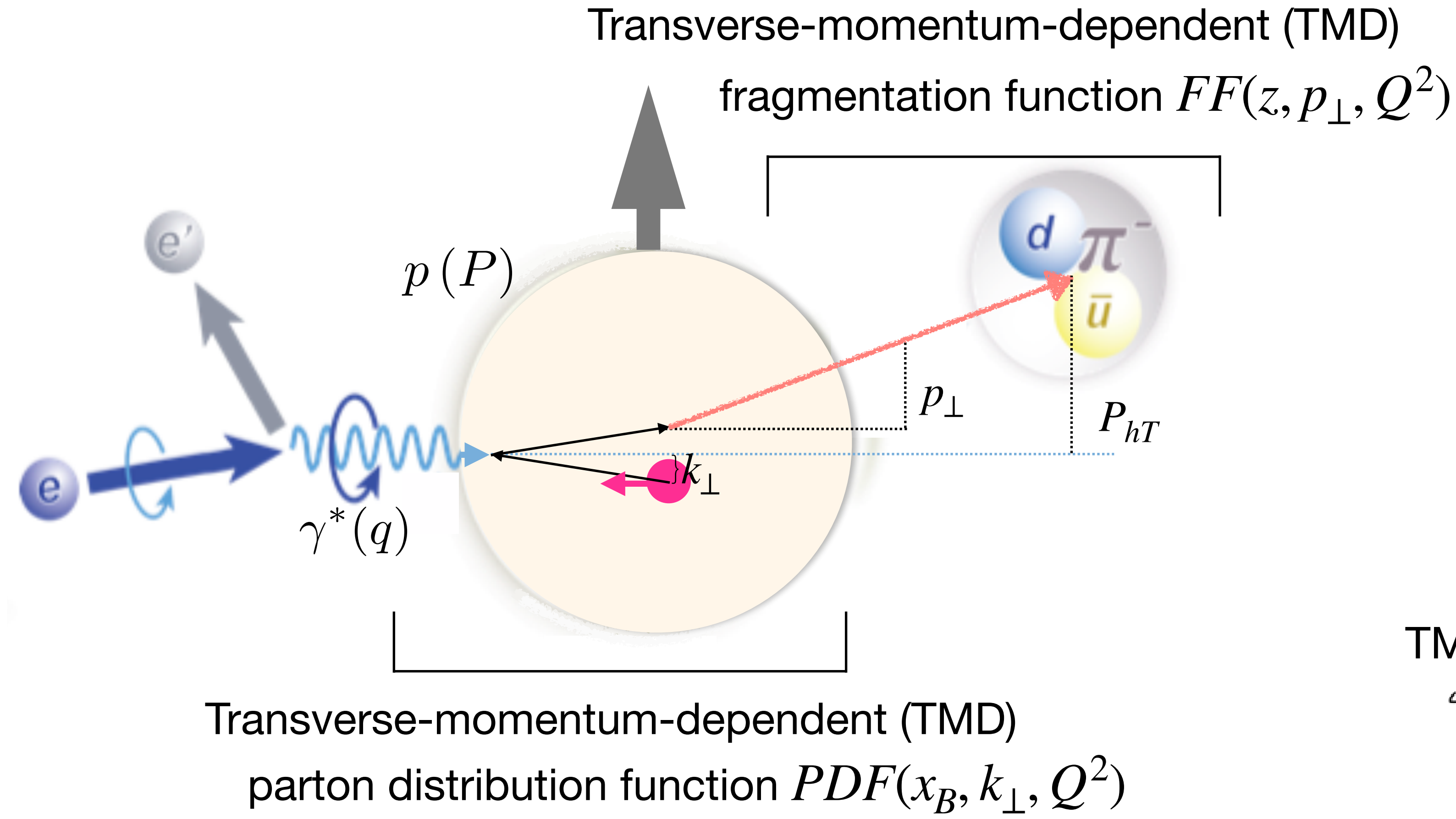


# Single-hadron production in semi-inclusive DIS

$$Q^2 = -q^2$$

$$x_B = \frac{Q^2}{2P \cdot q}$$

$$z \stackrel{\text{lab}}{=} \frac{E_h}{E_{\gamma^*}}$$



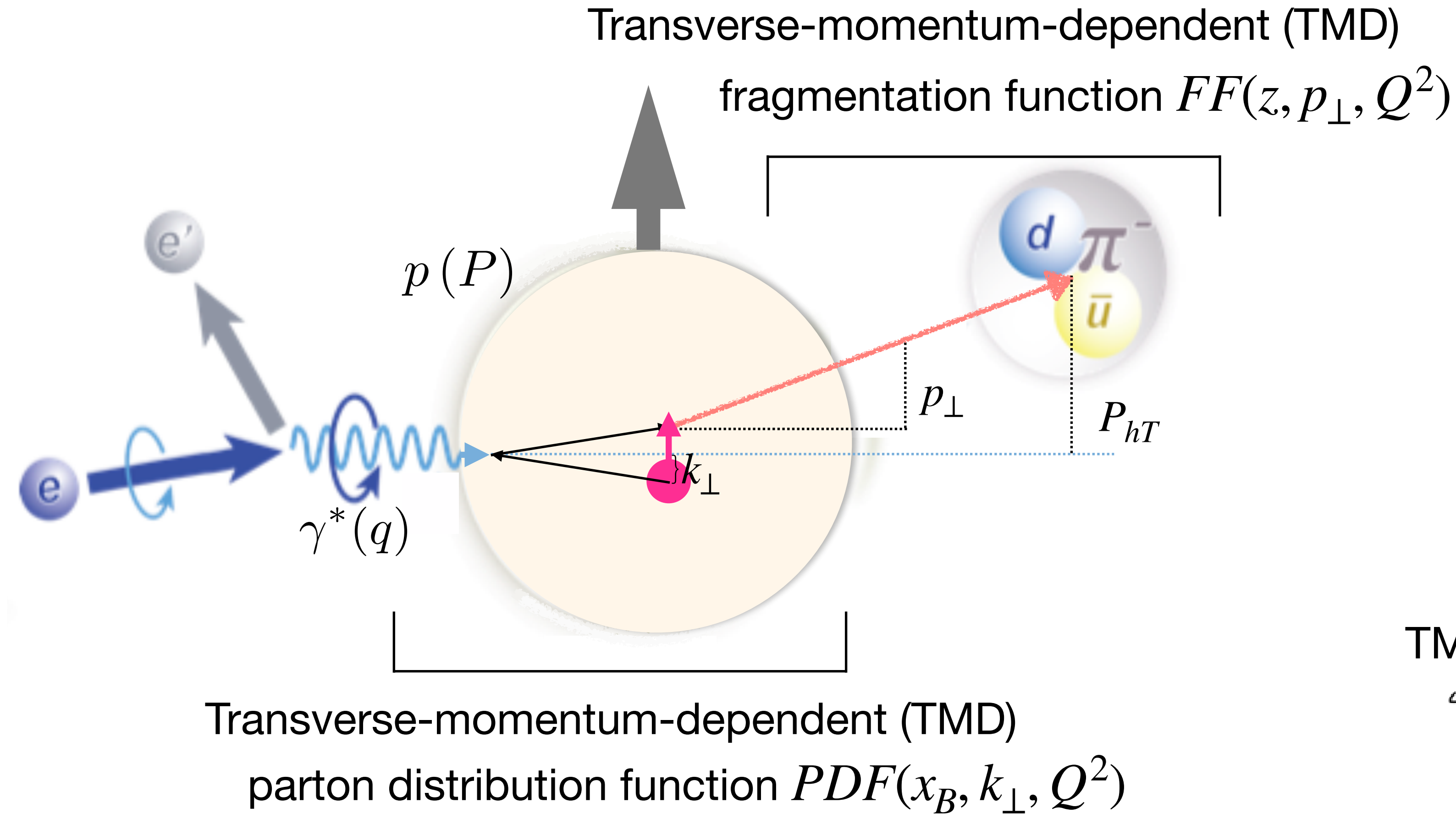


# Single-hadron production in semi-inclusive DIS

$$Q^2 = -q^2$$

$$x_B = \frac{Q^2}{2P \cdot q}$$

$$z \stackrel{\text{lab}}{=} \frac{E_h}{E_{\gamma^*}}$$



TMD evolution



# Transverse momentum dependent parton distribution functions

quark polarisation

	U	L	T
U	$f_1$		
L		$g_{1L}$	
T			$h_{1T}$

nucleon polarisation

survive integration over parton  
transverse momentum

# Transverse momentum dependent parton distribution functions

quark polarisation

	U	L	T
U	$f_1$		$h_1^\perp$
L		$g_{1L}$	$h_{1L}^\perp$
T	$f_{1T}^\perp$	$g_{1T}^\perp$	$h_{1T} h_{1T}^\perp$

nucleon polarisation

# Transverse momentum dependent parton distribution functions

spin-independent

$$f_1 = \text{yellow circle with blue center}$$

spin-spin  
correlations

$$g_1 = \text{yellow circle with blue center and right-pointing arrow} - \text{yellow circle with blue center and left-pointing arrow}$$

$$h_1 = \text{yellow circle with blue center and up-pointing arrow} - \text{yellow circle with blue center and down-pointing arrow}$$

$$g_{1T} = \text{yellow circle with blue center, right-pointing arrow, and up-pointing arrow} - \text{yellow circle with blue center, left-pointing arrow, and up-pointing arrow}$$

spin-momentum  
correlations

$$f_{1T}^\perp = \text{yellow circle with blue center and up-pointing arrow} - \text{yellow circle with blue center and down-pointing arrow}$$

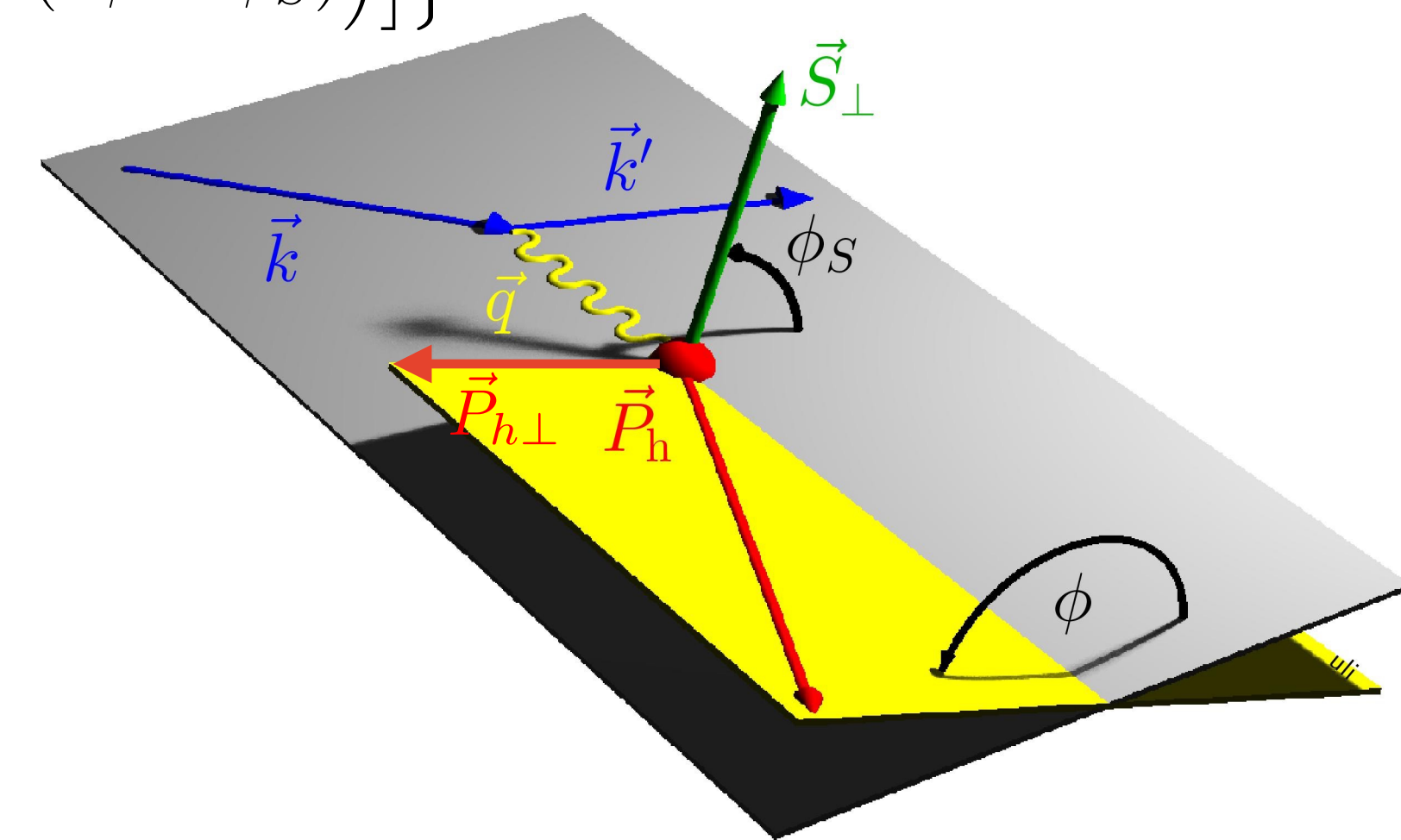
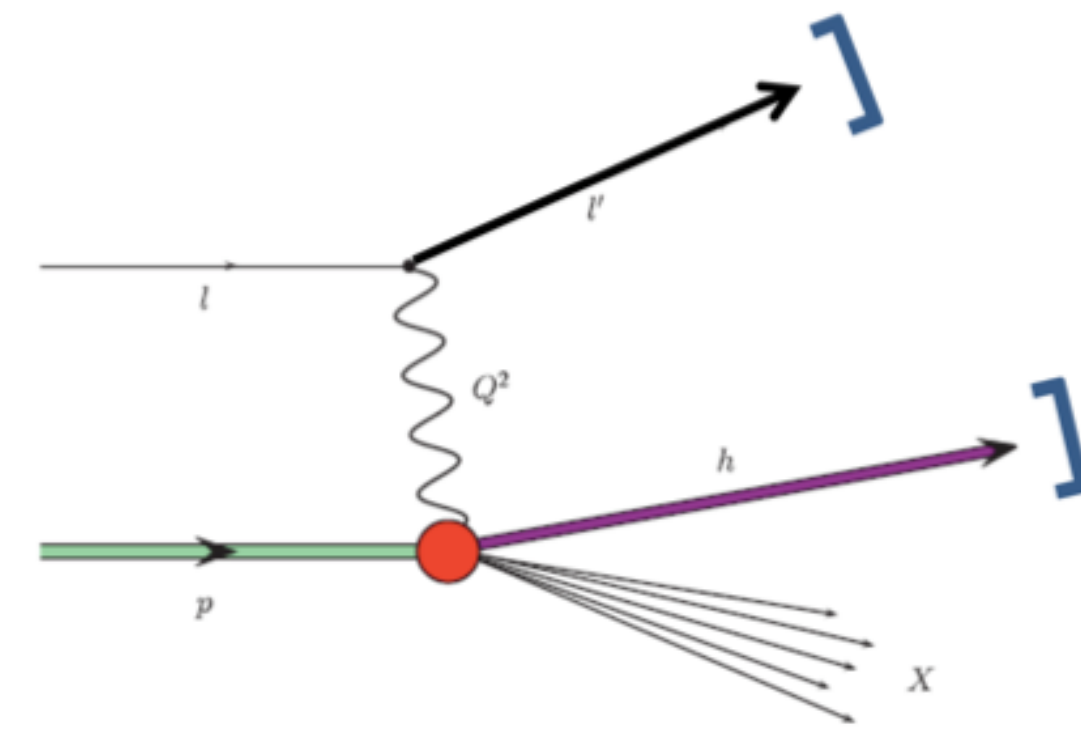
$$h_1^\perp = \text{yellow circle with blue center and down-pointing arrow} - \text{yellow circle with blue center and up-pointing arrow}$$

$$h_{1L}^\perp = \text{yellow circle with blue center, right-pointing arrow, and diagonal arrow} - \text{yellow circle with blue center, right-pointing arrow, and diagonal arrow}$$

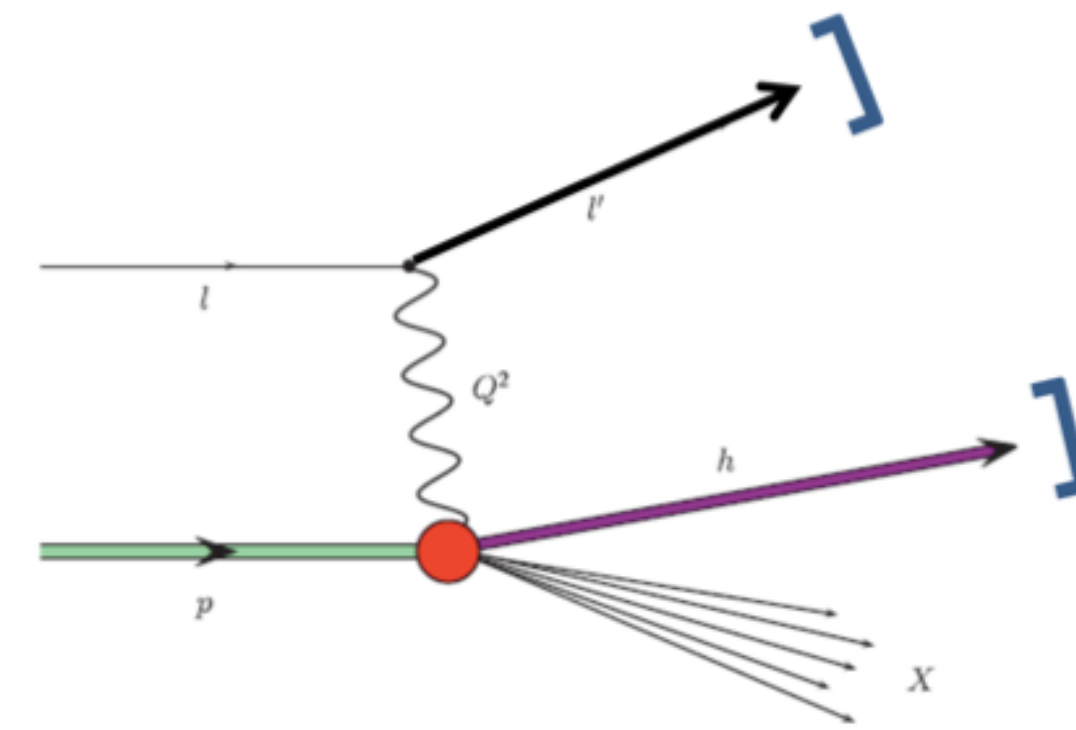
$$h_{1T}^\perp = \text{yellow circle with blue center, up-pointing arrow, and diagonal arrow} - \text{yellow circle with blue center, up-pointing arrow, and diagonal arrow}$$

# Semi-inclusive DIS cross section

$$\begin{aligned}
 \sigma^h(\phi, \phi_S) = & \sigma_{UU}^h \left\{ 1 + 2\langle \cos(\phi) \rangle_{UU}^h \cos(\phi) + 2\langle \cos(2\phi) \rangle_{UU}^h \cos(2\phi) \right. \\
 & + \lambda_l 2\langle \sin(\phi) \rangle_{LU}^h \sin(\phi) \\
 & + S_L \left[ 2\langle \sin(\phi) \rangle_{UL}^h \sin(\phi) + 2\langle \sin(2\phi) \rangle_{UL}^h \sin(2\phi) \right. \\
 & + \lambda_l \left( 2\langle \cos(0\phi) \rangle_{LL}^h \cos(0\phi) + 2\langle \cos(\phi) \rangle_{LL}^h \cos(\phi) \right) \left. \right] \\
 & + S_T \left[ 2\langle \sin(\phi - \phi_S) \rangle_{UT}^h \sin(\phi - \phi_S) + 2\langle \sin(\phi + \phi_S) \rangle_{UT}^h \sin(\phi + \phi_S) \right. \\
 & + 2\langle \sin(3\phi - \phi_S) \rangle_{UT}^h \sin(3\phi - \phi_S) + 2\langle \sin(\phi_S) \rangle_{UT}^h \sin(\phi_S) \\
 & + 2\langle \sin(2\phi - \phi_S) \rangle_{UT}^h \sin(2\phi - \phi_S) \\
 & + \lambda_l \left( 2\langle \cos(\phi - \phi_S) \rangle_{LT}^h \cos(\phi - \phi_S) \right. \\
 & \left. \left. + 2\langle \cos(\phi_S) \rangle_{LT}^h \cos(\phi_S) + 2\langle \cos(2\phi - \phi_S) \rangle_{LT}^h \cos(2\phi - \phi_S) \right) \right] \left. \right\}
 \end{aligned}$$

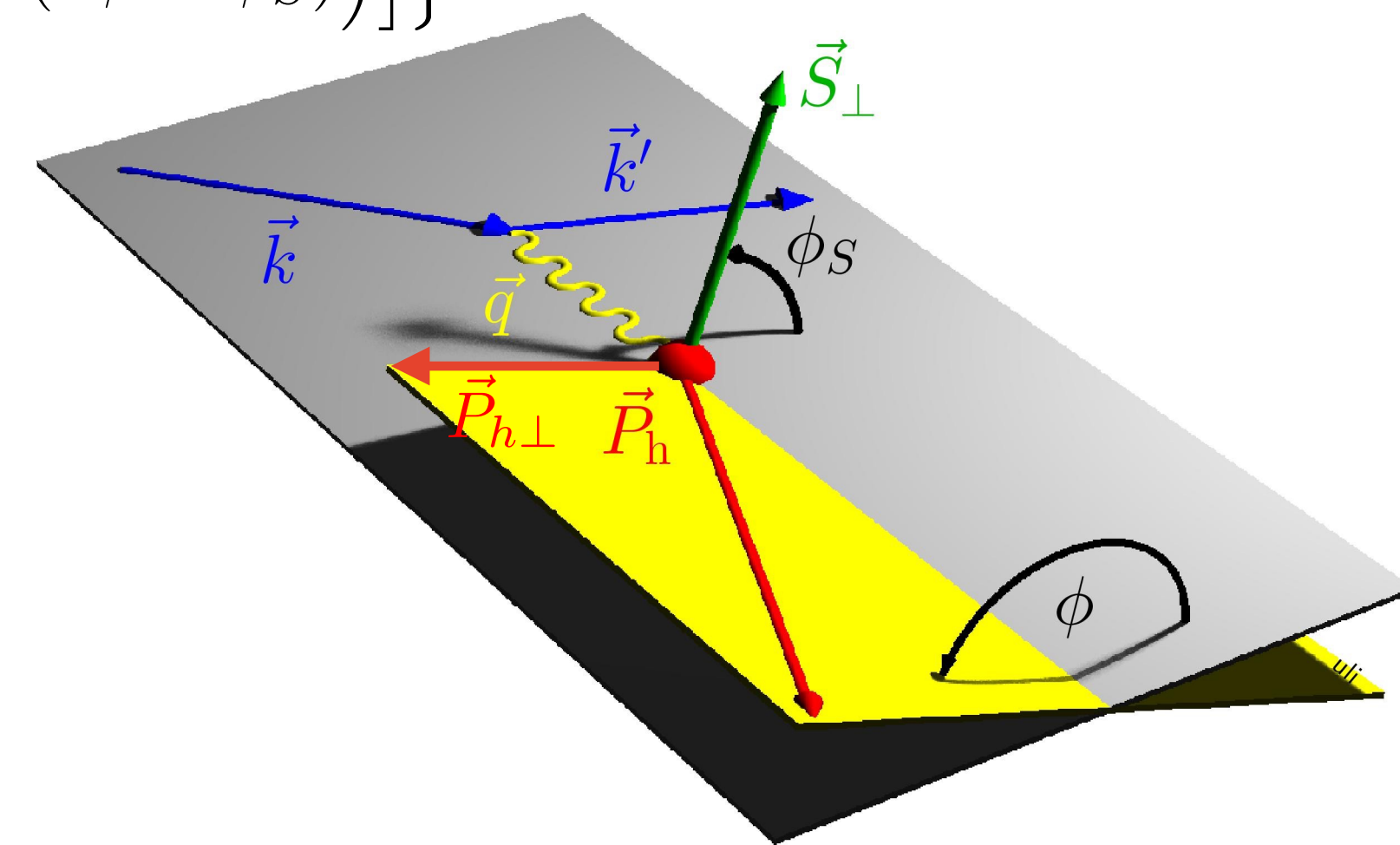


# Semi-inclusive DIS cross section



$$\begin{aligned}
 \sigma^h(\phi, \phi_S) = & \sigma_{UU}^h \left\{ 1 + 2\langle \cos(\phi) \rangle_{UU}^h \cos(\phi) + 2\langle \cos(2\phi) \rangle_{UU}^h \cos(2\phi) \right. \\
 & + \lambda_l 2\langle \sin(\phi) \rangle_{LU}^h \sin(\phi) \\
 \text{longitudinal target} & \leftarrow + S_L \left[ 2\langle \sin(\phi) \rangle_{UL}^h \sin(\phi) + 2\langle \sin(2\phi) \rangle_{UL}^h \sin(2\phi) \right. \\
 \text{polarisation} & \left. + \lambda_l \left( 2\langle \cos(0\phi) \rangle_{LL}^h \cos(0\phi) + 2\langle \cos(\phi) \rangle_{LL}^h \cos(\phi) \right) \right] \\
 \text{transverse target} & \leftarrow + S_T \left[ 2\langle \sin(\phi - \phi_S) \rangle_{UT}^h \sin(\phi - \phi_S) + 2\langle \sin(\phi + \phi_S) \rangle_{UT}^h \sin(\phi + \phi_S) \right. \\
 & + 2\langle \sin(3\phi - \phi_S) \rangle_{UT}^h \sin(3\phi - \phi_S) + 2\langle \sin(\phi_S) \rangle_{UT}^h \sin(\phi_S) \\
 & + 2\langle \sin(2\phi - \phi_S) \rangle_{UT}^h \sin(2\phi - \phi_S) \\
 \text{beam} & \leftarrow + \lambda_l \left( 2\langle \cos(\phi - \phi_S) \rangle_{LT}^h \cos(\phi - \phi_S) \right. \\
 \text{polarisation} & \left. + 2\langle \cos(\phi_S) \rangle_{LT}^h \cos(\phi_S) + 2\langle \cos(2\phi - \phi_S) \rangle_{LT}^h \cos(2\phi - \phi_S) \right) \left. \right\}
 \end{aligned}$$

beam polarisation
target polarisation



# TMD PDFs and fragmentation functions (FFs)

Azimuthal amplitudes related to structure functions  $F_{XY}$  :

$$2\langle \sin(\phi + \phi_S) \rangle_{UT}^h = \epsilon F_{UT}^{\sin(\phi + \phi_S)}$$

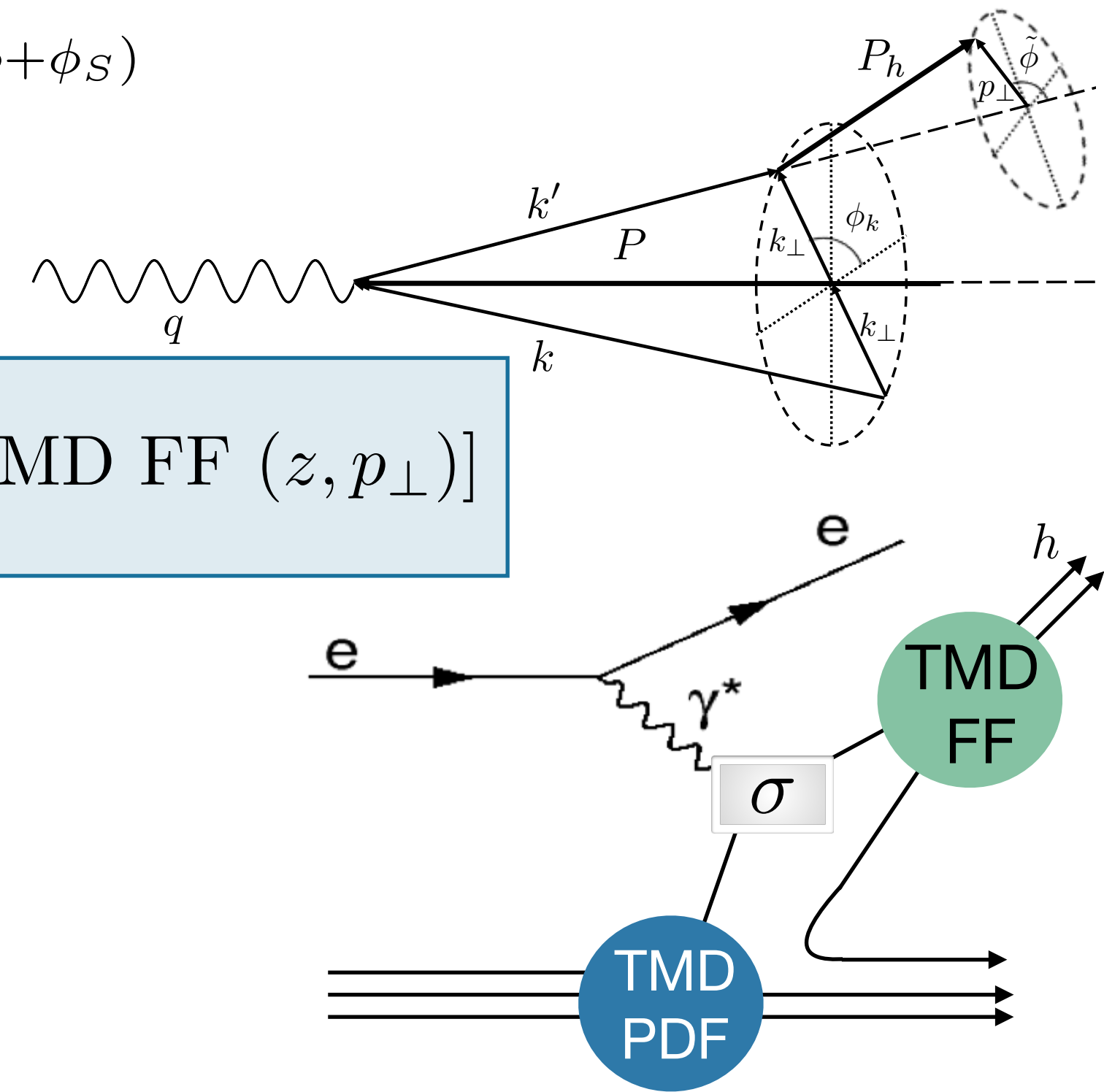
# TMD PDFs and fragmentation functions (FFs)

Azimuthal amplitudes related to structure functions  $F_{XY}$  :

$$2\langle \sin(\phi + \phi_S) \rangle_{UT}^h = \epsilon F_{UT}^{\sin(\phi + \phi_S)}$$

$$F_{XY} \propto \mathcal{C} [\text{TMD PDF}(x, k_{\perp}) \times \text{TMD FF}(z, p_{\perp})]$$

$$z \stackrel{\text{lab}}{=} \frac{E_h}{E_{\gamma^*}}$$



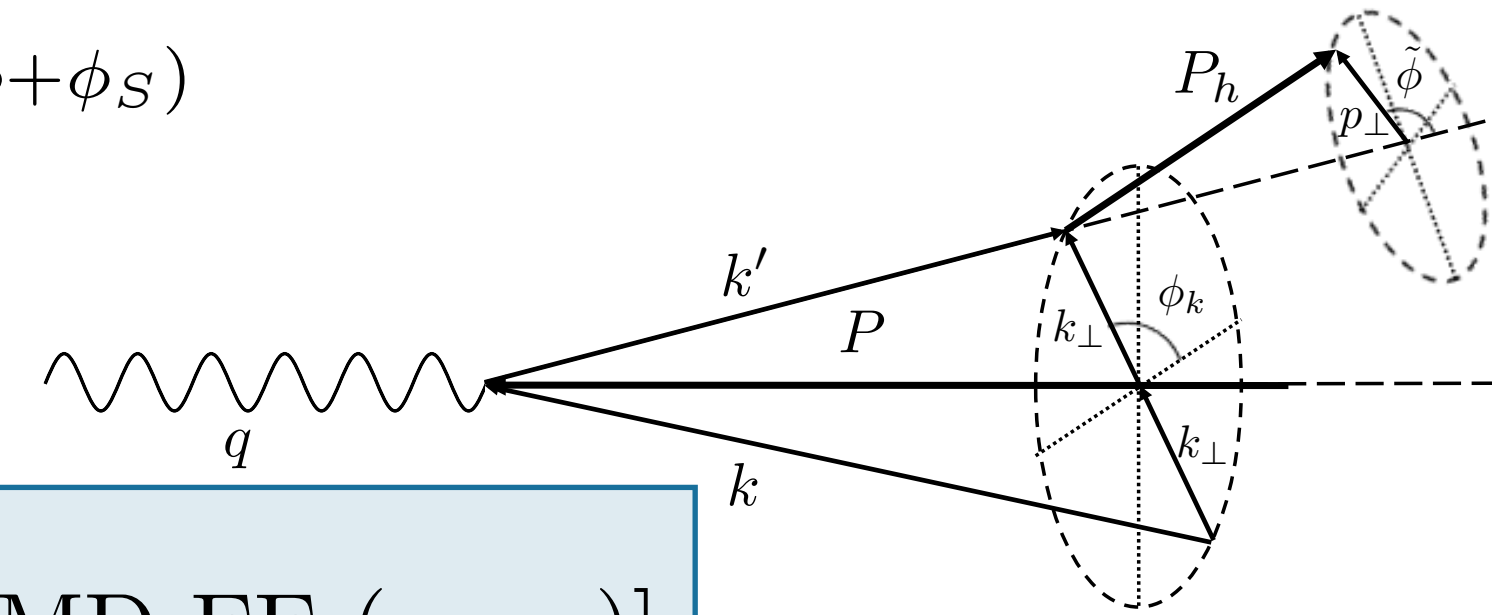


# TMD PDFs and fragmentation functions (FFs)

Azimuthal amplitudes related to structure functions  $F_{XY}$  :

$$2\langle \sin(\phi + \phi_S) \rangle_{UT}^h = \epsilon F_{UT}^{\sin(\phi + \phi_S)}$$

$$F_{XY} \propto \mathcal{C} [\text{TMD PDF}(x, k_{\perp}) \times \text{TMD FF}(z, p_{\perp})]$$

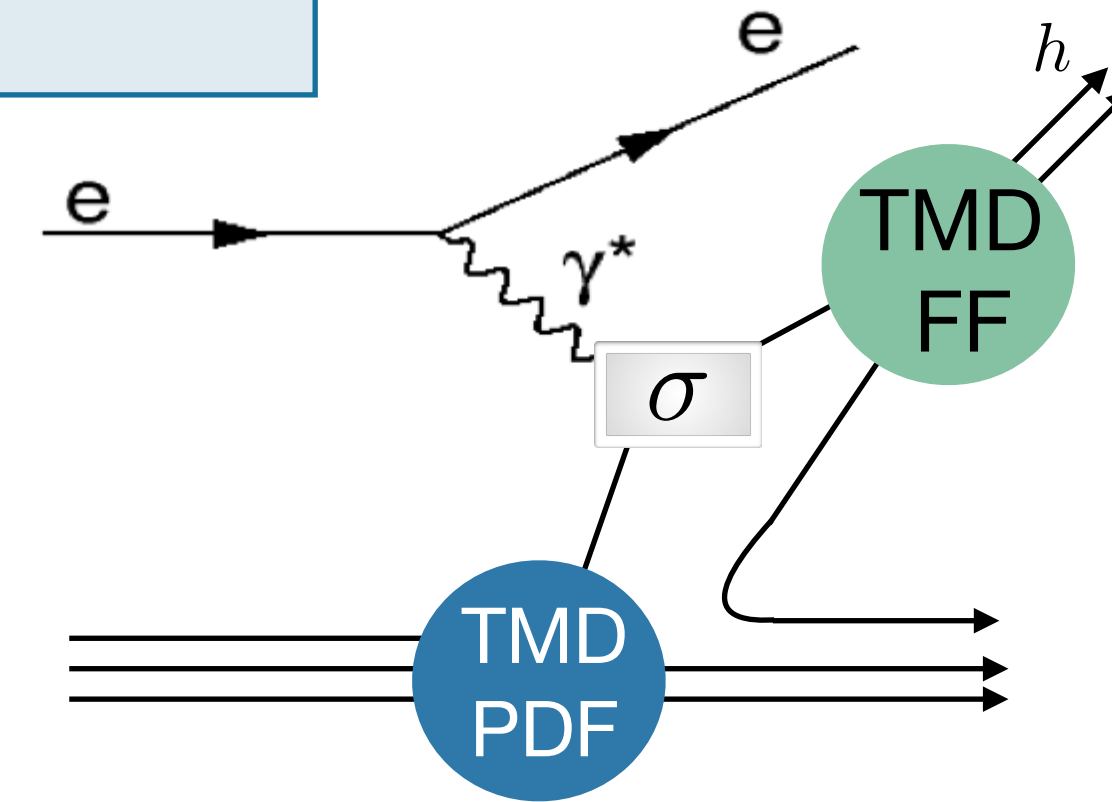


nucleon polarisation

quark polarisation

	U	L	T
U	$f_1$		$h_1^{\perp}$
L		$g_{1L}$	$h_{1L}^{\perp}$
T	$f_{1T}^{\perp}$	$g_{1T}^{\perp}$	$h_{1T} h_{1T}^{\perp}$

$$z \stackrel{\text{lab}}{=} \frac{E_h}{E_{\gamma^*}}$$

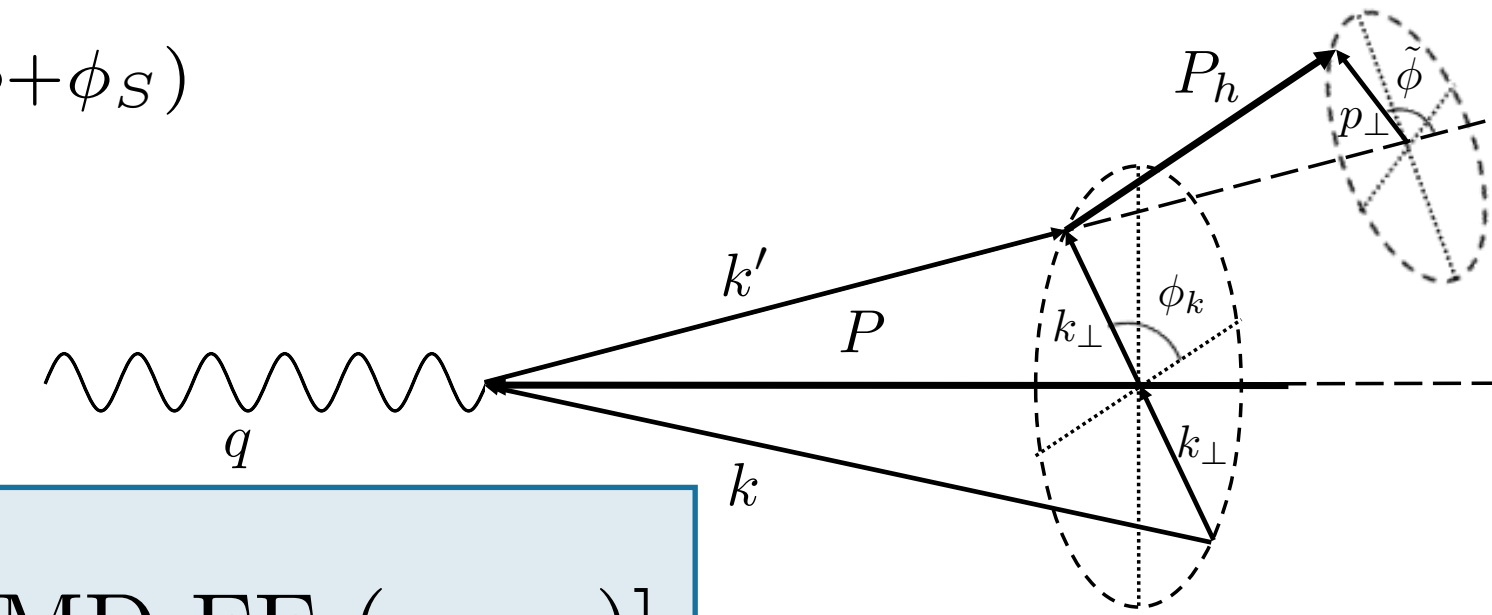


# TMD PDFs and fragmentation functions (FFs)

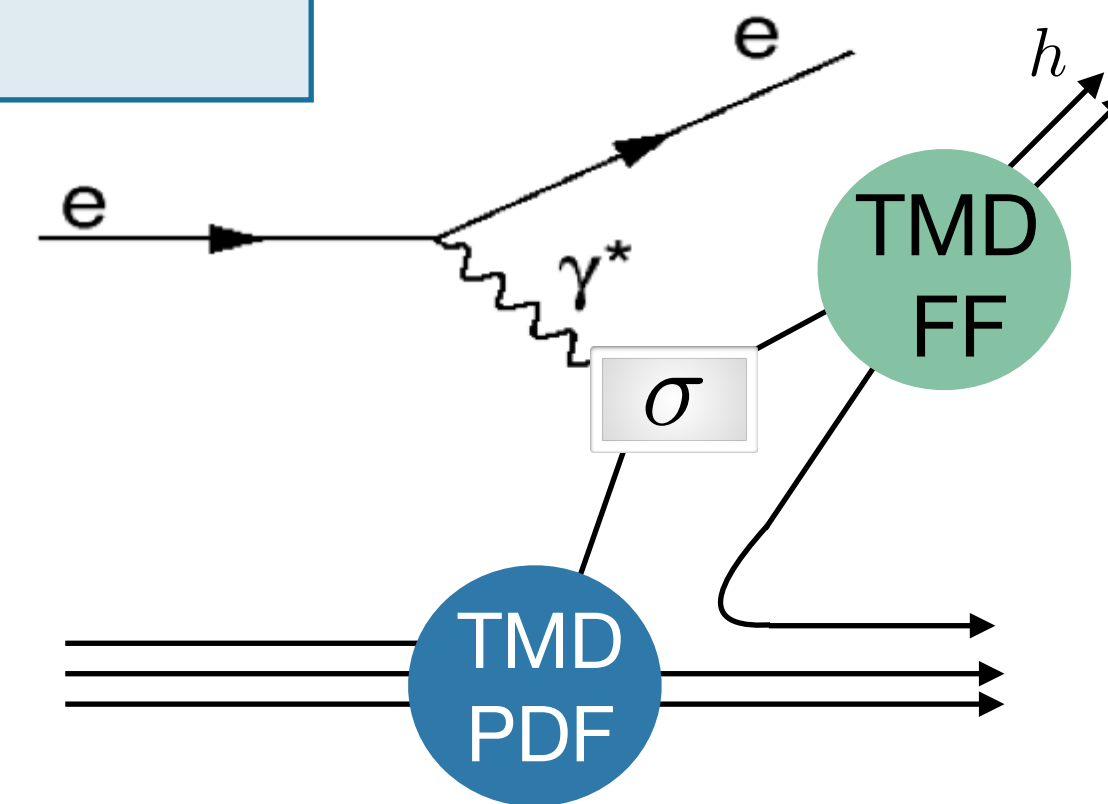
Azimuthal amplitudes related to structure functions  $F_{XY}$  :

$$2\langle \sin(\phi + \phi_S) \rangle_{UT}^h = \epsilon F_{UT}^{\sin(\phi + \phi_S)}$$

$$F_{XY} \propto \mathcal{C} [\text{TMD PDF}(x, k_{\perp}) \times \text{TMD FF}(z, p_{\perp})]$$



$$z \stackrel{\text{lab}}{=} \frac{E_h}{E_{\gamma^*}}$$



quark polarisation

	U	L	T
U	$f_1$		$h_1^{\perp}$
L		$g_{1L}$	$h_{1L}^{\perp}$
T	$f_{1T}^{\perp}$	$g_{1T}^{\perp}$	$h_{1T} h_{1T}^{\perp}$

nucleon polarisation

quark polarisation

	U	L	T
U	$D_1$		$H_1^{\perp}$

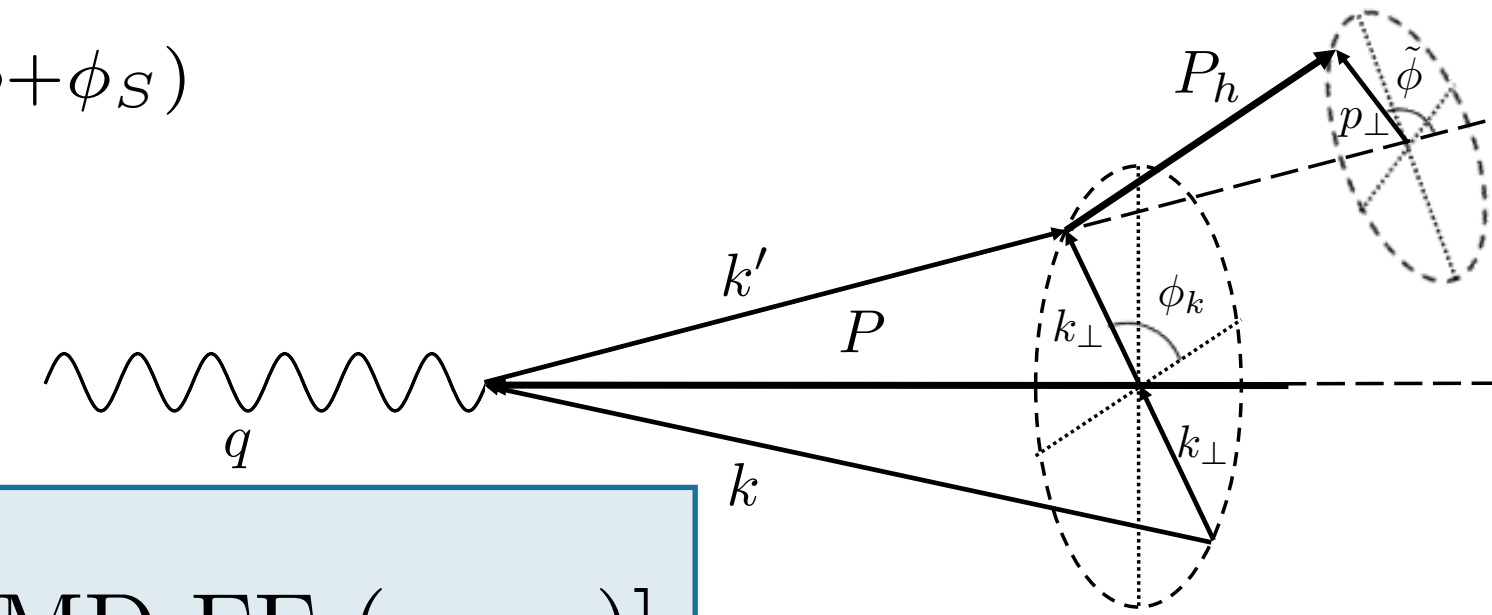
hadron polarisation

# TMD PDFs and fragmentation functions (FFs)

Azimuthal amplitudes related to structure functions  $F_{XY}$  :

$$2\langle \sin(\phi + \phi_S) \rangle_{UT}^h = \epsilon F_{UT}^{\sin(\phi + \phi_S)}$$

$$F_{XY} \propto \mathcal{C} [\text{TMD PDF}(x, k_{\perp}) \times \text{TMD FF}(z, p_{\perp})]$$

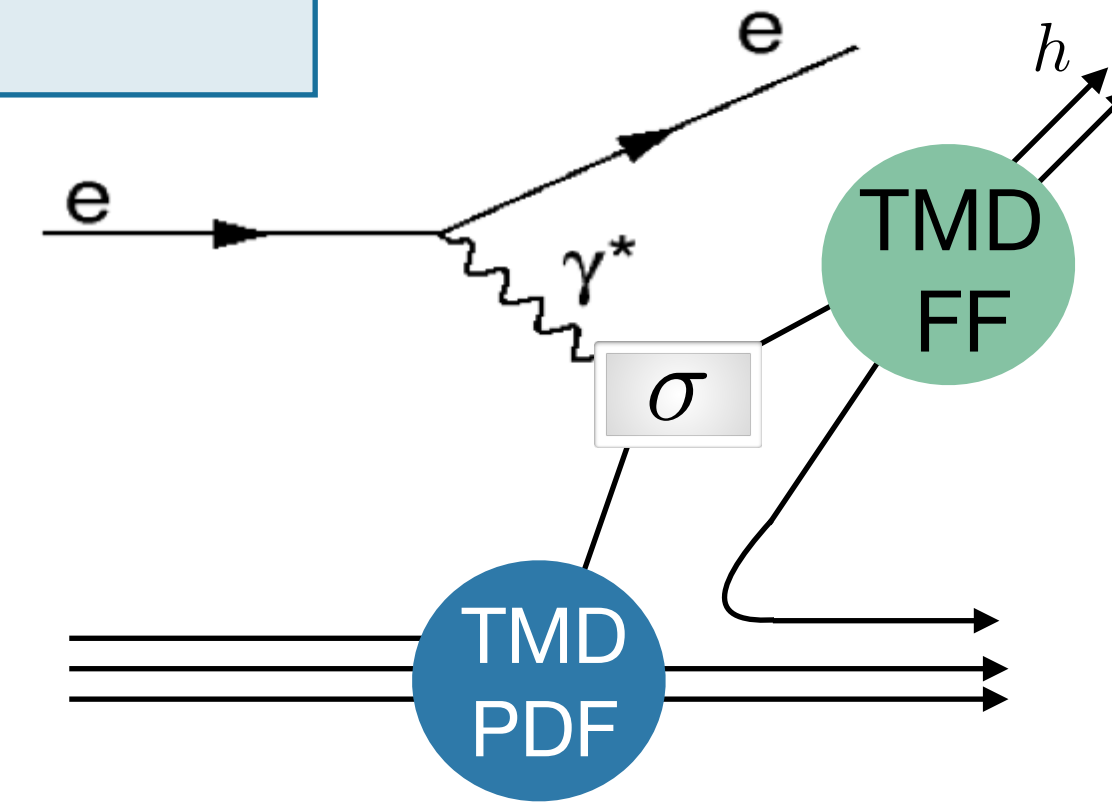


quark polarisation

	U	L	T
U	$f_1$		$h_1^{\perp}$
L		$g_{1L}$	$h_{1L}^{\perp}$
T	$f_{1T}^{\perp}$	$g_{1T}^{\perp}$	$h_{1T} h_{1T}^{\perp}$

nucleon polarisation

$$z \stackrel{\text{lab}}{=} \frac{E_h}{E_{\gamma^*}}$$



quark polarisation

	U	L	T
U	$D_1$		$H_1^{\perp}$

hadron polarisation

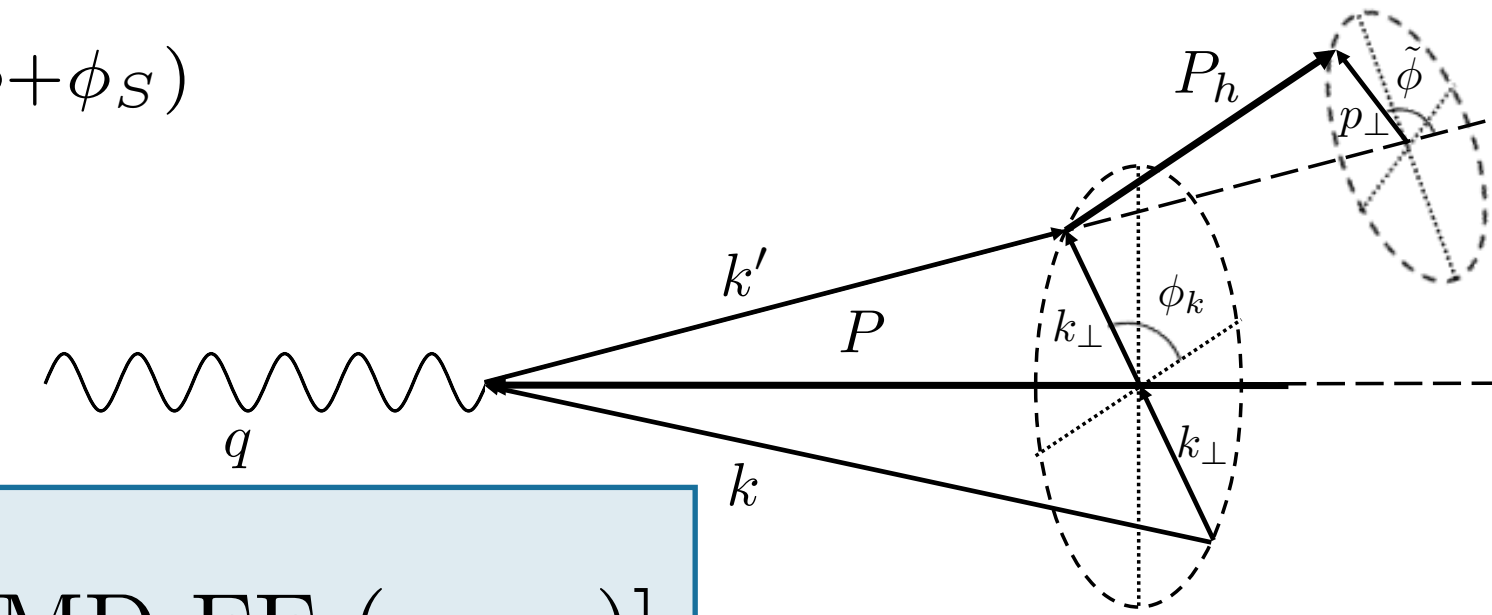
Chiral odd

# TMD PDFs and fragmentation functions (FFs)

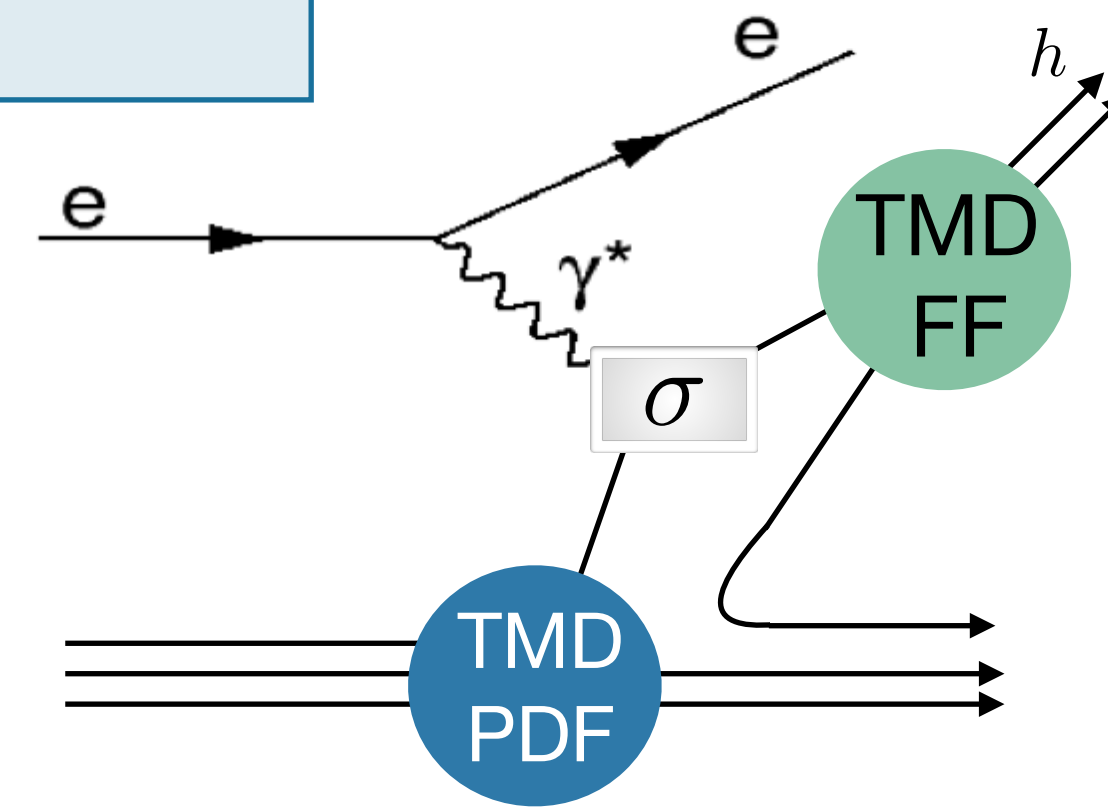
Azimuthal amplitudes related to structure functions  $F_{XY}$  :

$$2\langle \sin(\phi + \phi_S) \rangle_{UT}^h = \epsilon F_{UT}^{\sin(\phi + \phi_S)}$$

$$F_{XY} \propto \mathcal{C} [\text{TMD PDF}(x, k_{\perp}) \times \text{TMD FF}(z, p_{\perp})]$$



$$z \stackrel{\text{lab}}{=} \frac{E_h}{E_{\gamma^*}}$$



quark polarisation

	U	L	T
U	$f_1$		$h_1^{\perp}$
L		$g_{1L}$	$h_{1L}^{\perp}$
T	$f_{1T}^{\perp}$	$g_{1T}^{\perp}$	$h_{1T} h_{1T}^{\perp}$

nucleon polarisation

quark polarisation

	U	L	T
U	$D_1$		$H_1^{\perp}$

hadron polarisation

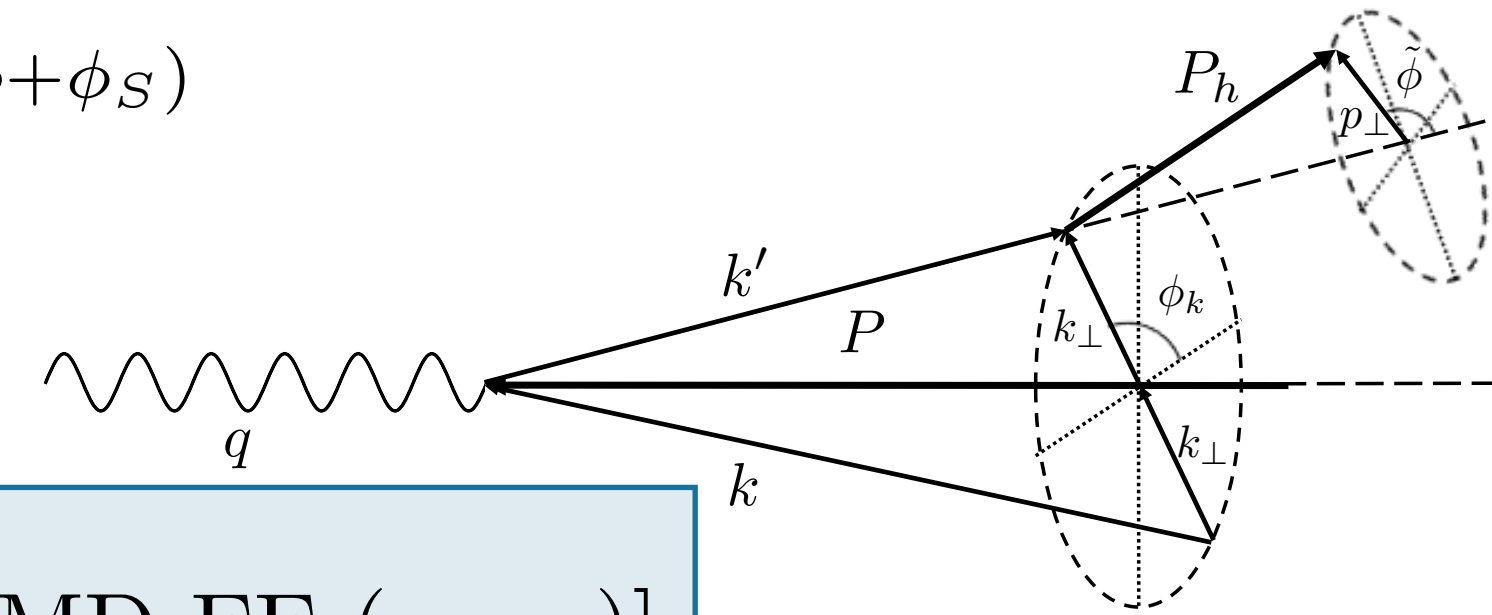
Chiral odd

# TMD PDFs and fragmentation functions (FFs)

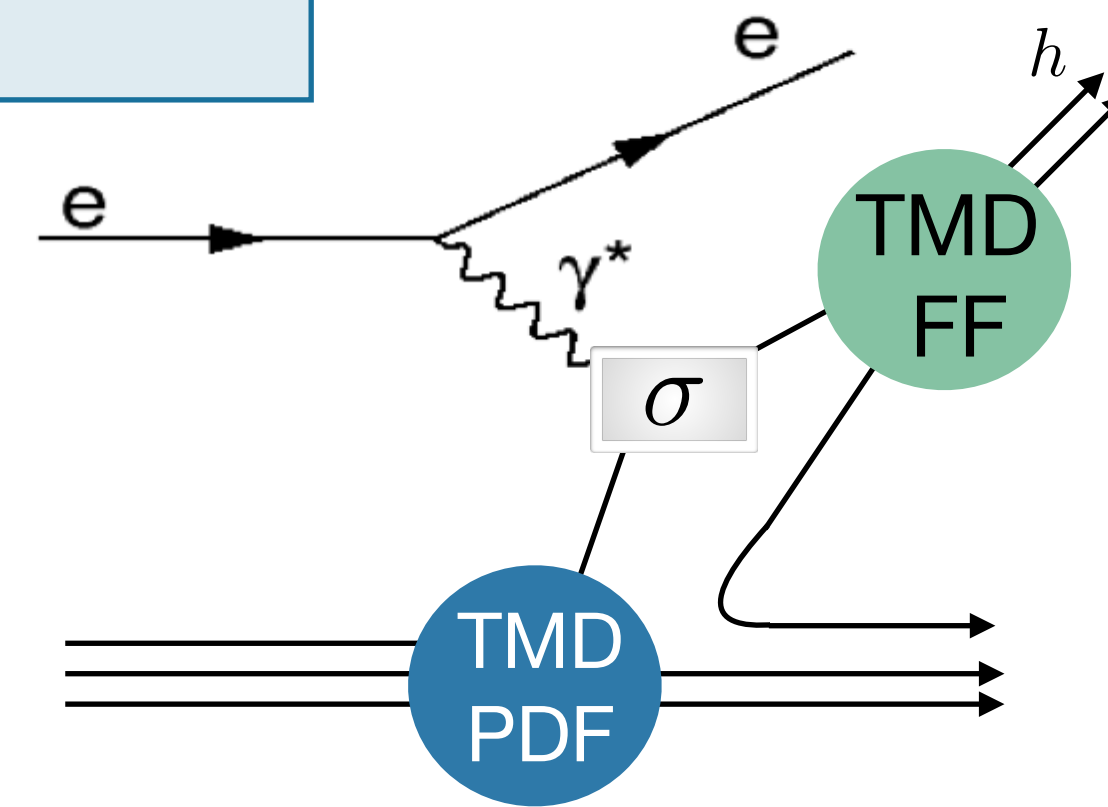
Azimuthal amplitudes related to structure functions  $F_{XY}$  :

$$2\langle \sin(\phi + \phi_S) \rangle_{UT}^h = \epsilon F_{UT}^{\sin(\phi + \phi_S)}$$

$$F_{XY} \propto \mathcal{C} [\text{TMD PDF}(x, k_{\perp}) \times \text{TMD FF}(z, p_{\perp})]$$



$$z \stackrel{\text{lab}}{=} \frac{E_h}{E_{\gamma^*}}$$



quark polarisation

	U	L	T
U	$f_1$		$h_1^{\perp}$
L		$g_{1L}$	$h_{1L}^{\perp}$
T	$f_{1T}^{\perp}$	$g_{1T}^{\perp}$	$h_{1T} h_{1T}^{\perp}$

nucleon polarisation

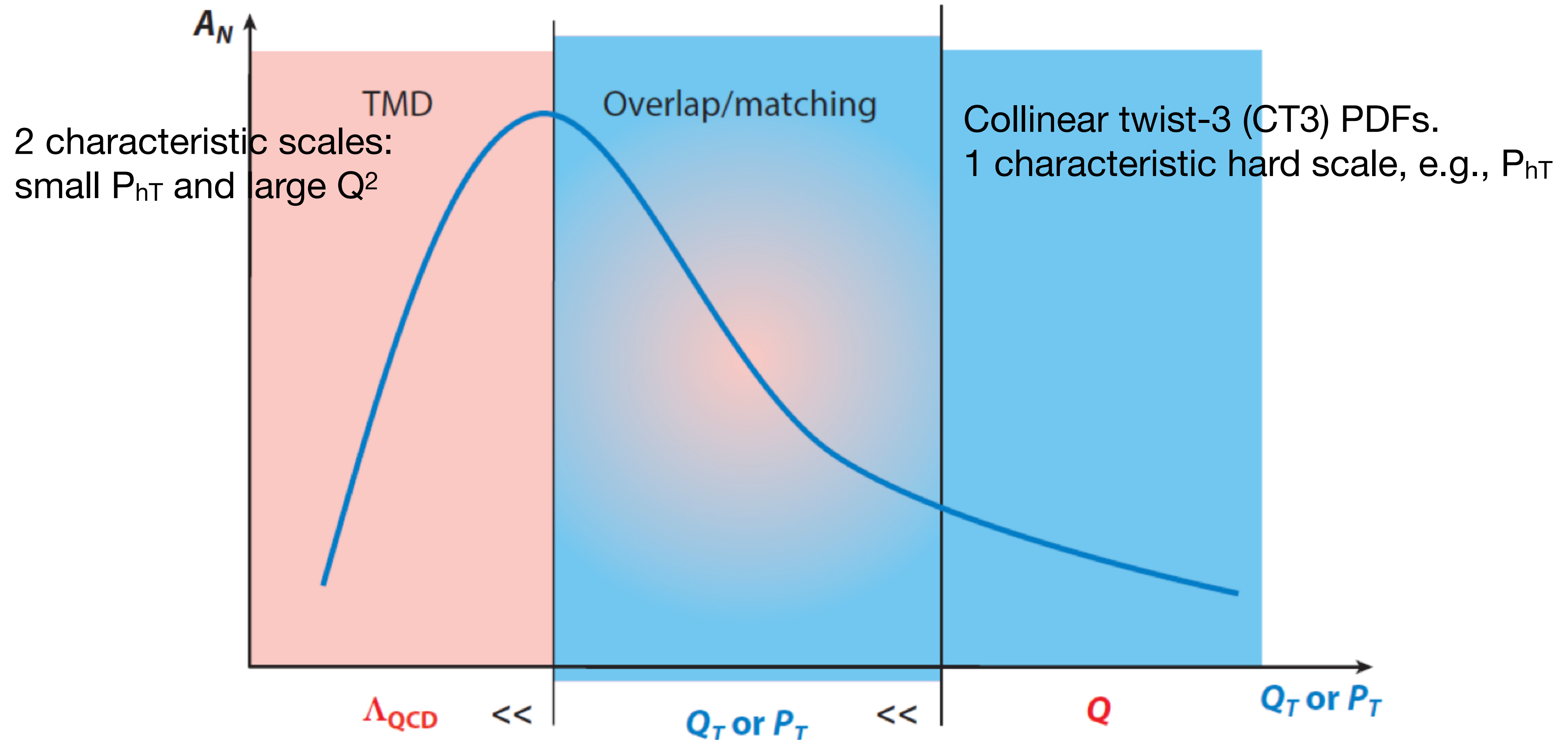
quark polarisation

	U	L	T
U	$D_1$		$H_1^{\perp}$

hadron polarisation

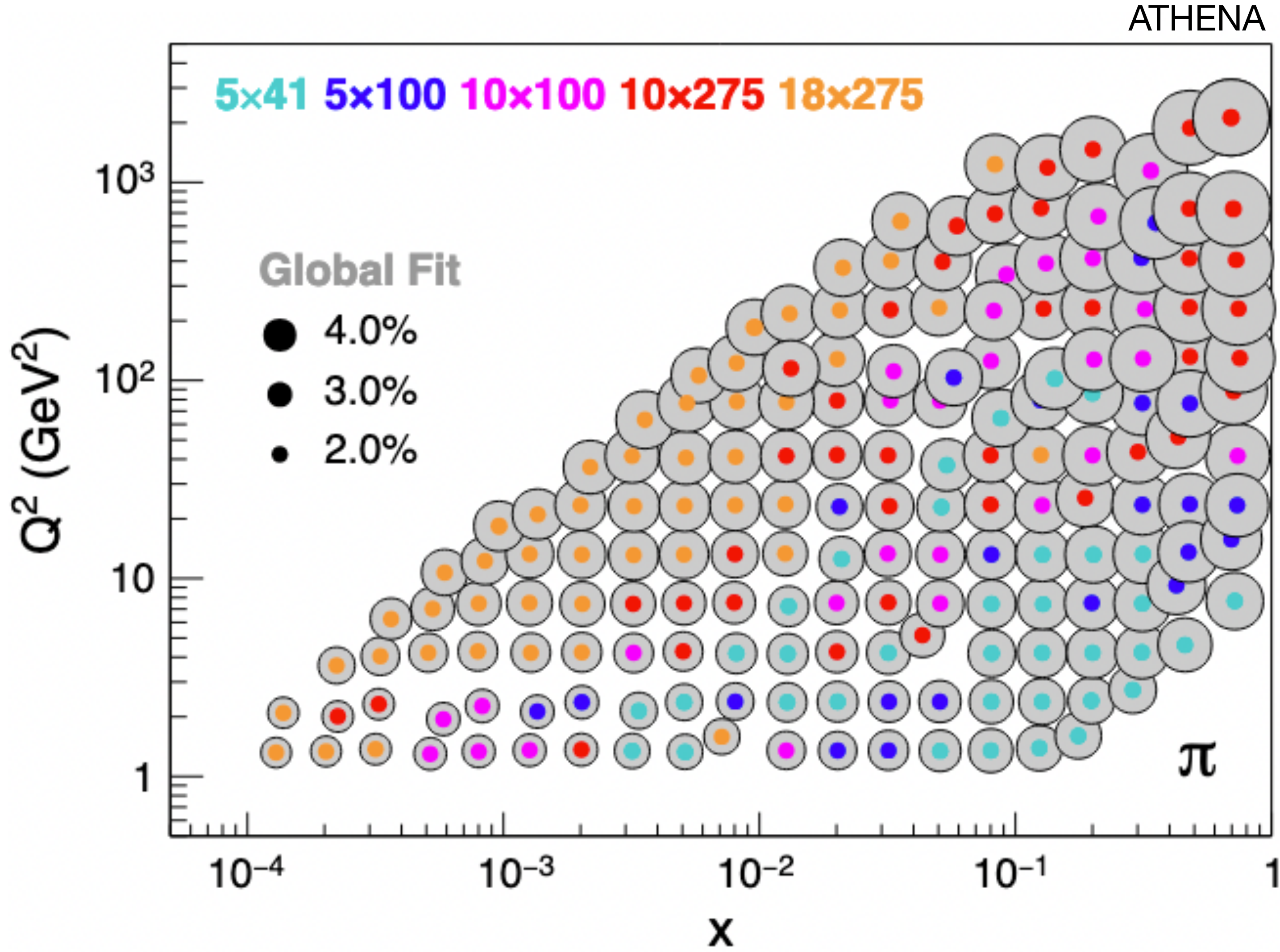
Chiral odd

# Validity of TMD description



Consistent results for TMD  
and CT3 in overlap region

# Spin-independent TMD PDFs at EIC



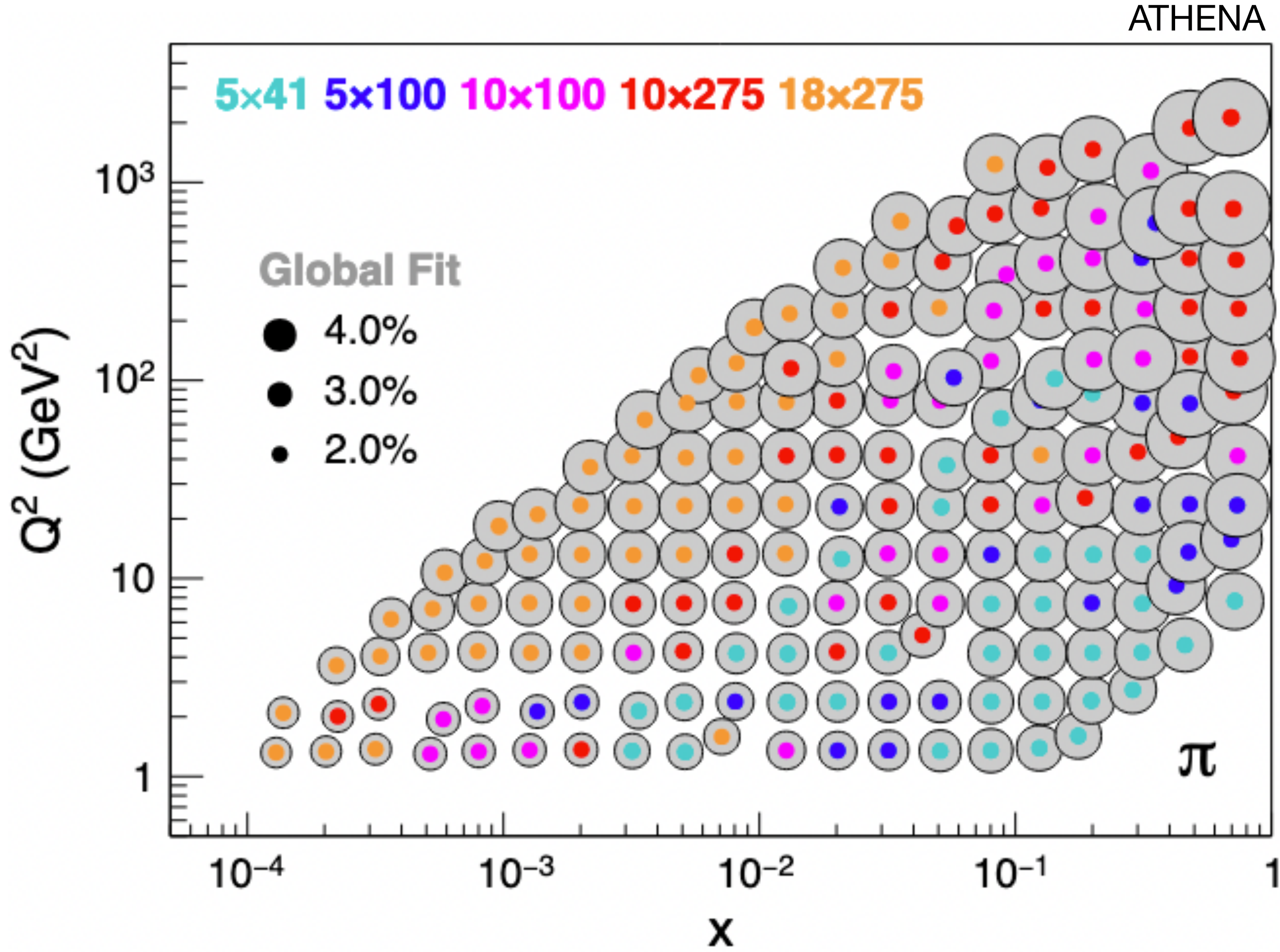
Fit:  
 A. Bacchetta et al.,  
 JHEP 06 (2017) 081,  
 JHEP 06 (2019) 051 (erratum)

EIC uncertainties dominated  
 by assumed  
 3% point-to-point uncorrelated uncertainty  
 3% scale uncertainty

Theory uncertainties dominated by  
 TMD evolution.

# Spin-independent TMD PDFs at EIC

Large lever-arm in  $Q^2$  over large  $x$  range  
 →  $Q^2$  evolution of TMD PDF



Fit:  
 A. Bacchetta et al.,  
 JHEP 06 (2017) 081,  
 JHEP 06 (2019) 051 (erratum)

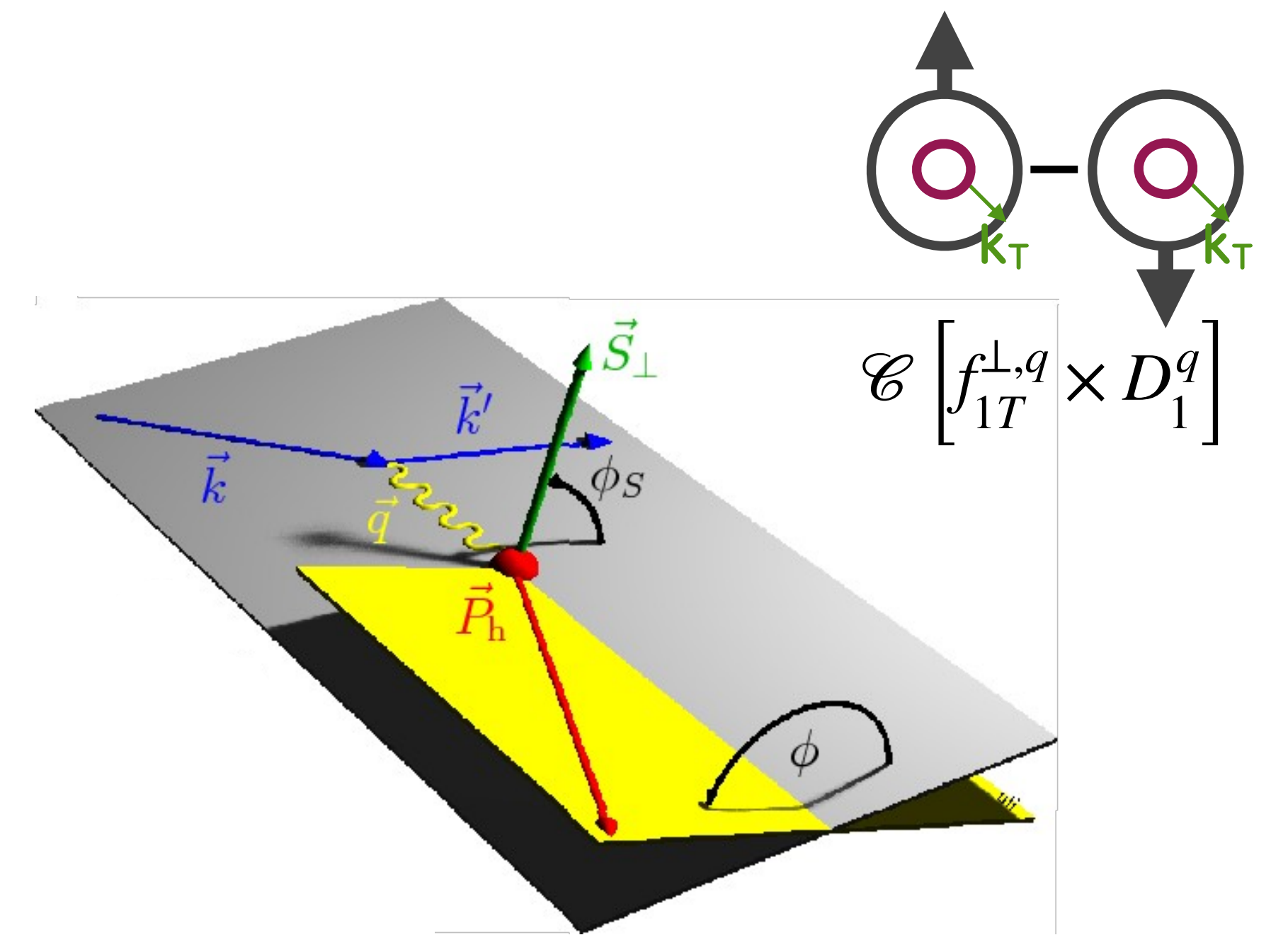
EIC uncertainties dominated  
 by assumed  
 3% point-to-point uncorrelated uncertainty  
 3% scale uncertainty

Theory uncertainties dominated by  
 TMD evolution.



# Sivers amplitudes: measurement

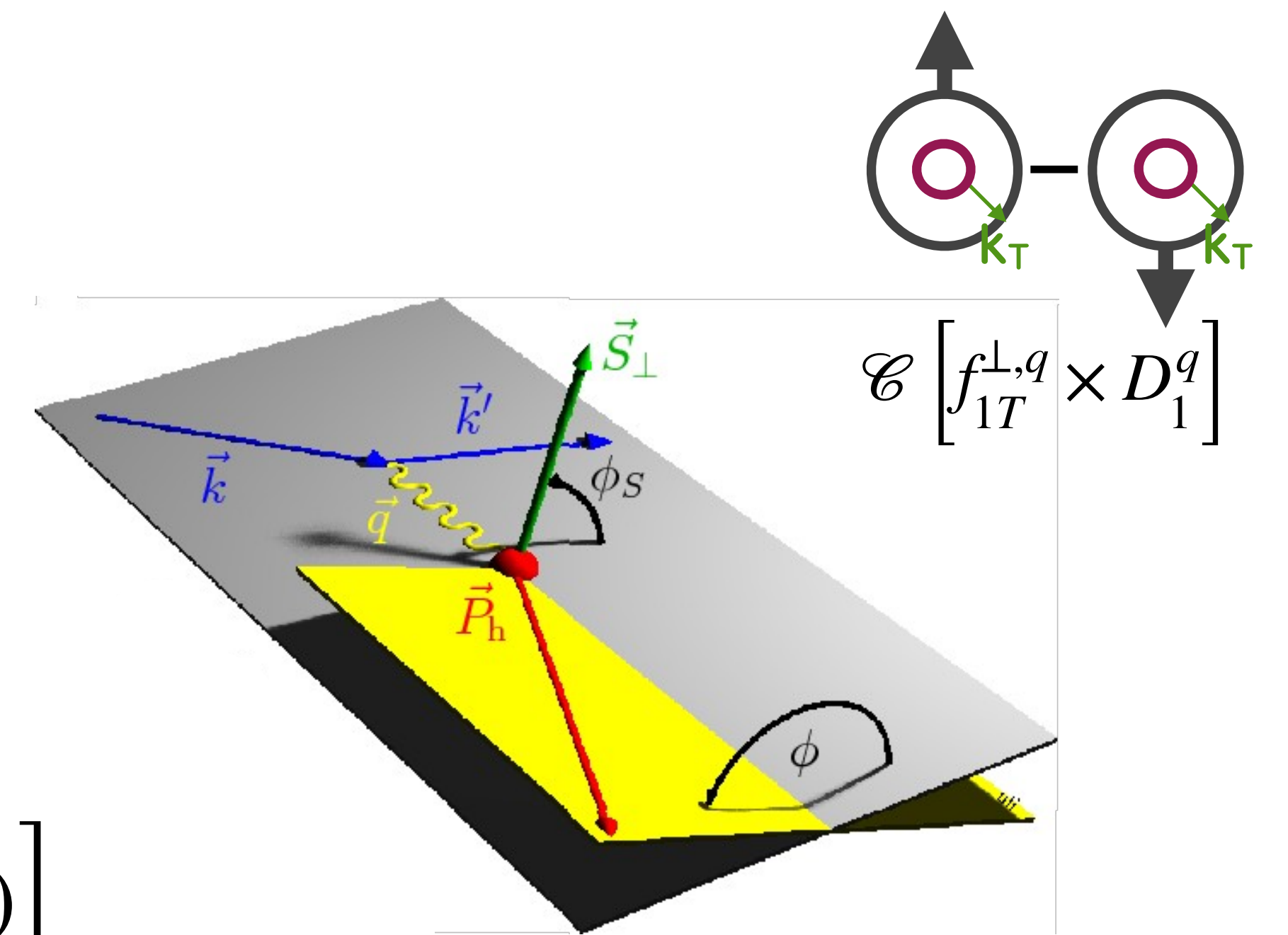
$$A_{UT} = \frac{1}{\langle |S_T| \rangle} \frac{N^\uparrow(\phi, \phi_S) - N^\downarrow(\phi, \phi_S)}{N^\uparrow(\phi, \phi_S) + N^\downarrow(\phi, \phi_S)}$$



# Sivers amplitudes: measurement

$$A_{UT} = \frac{1}{\langle |S_T| \rangle} \frac{N^\uparrow(\phi, \phi_S) - N^\downarrow(\phi, \phi_S)}{N^\uparrow(\phi, \phi_S) + N^\downarrow(\phi, \phi_S)}$$

$$\sim \sin(\phi - \phi_S) \sum_q e_q^2 \mathcal{C} \left[ f_{1T}^{\perp,q}(x, k_\perp) \times D_1^q(z, p_\perp) \right]$$

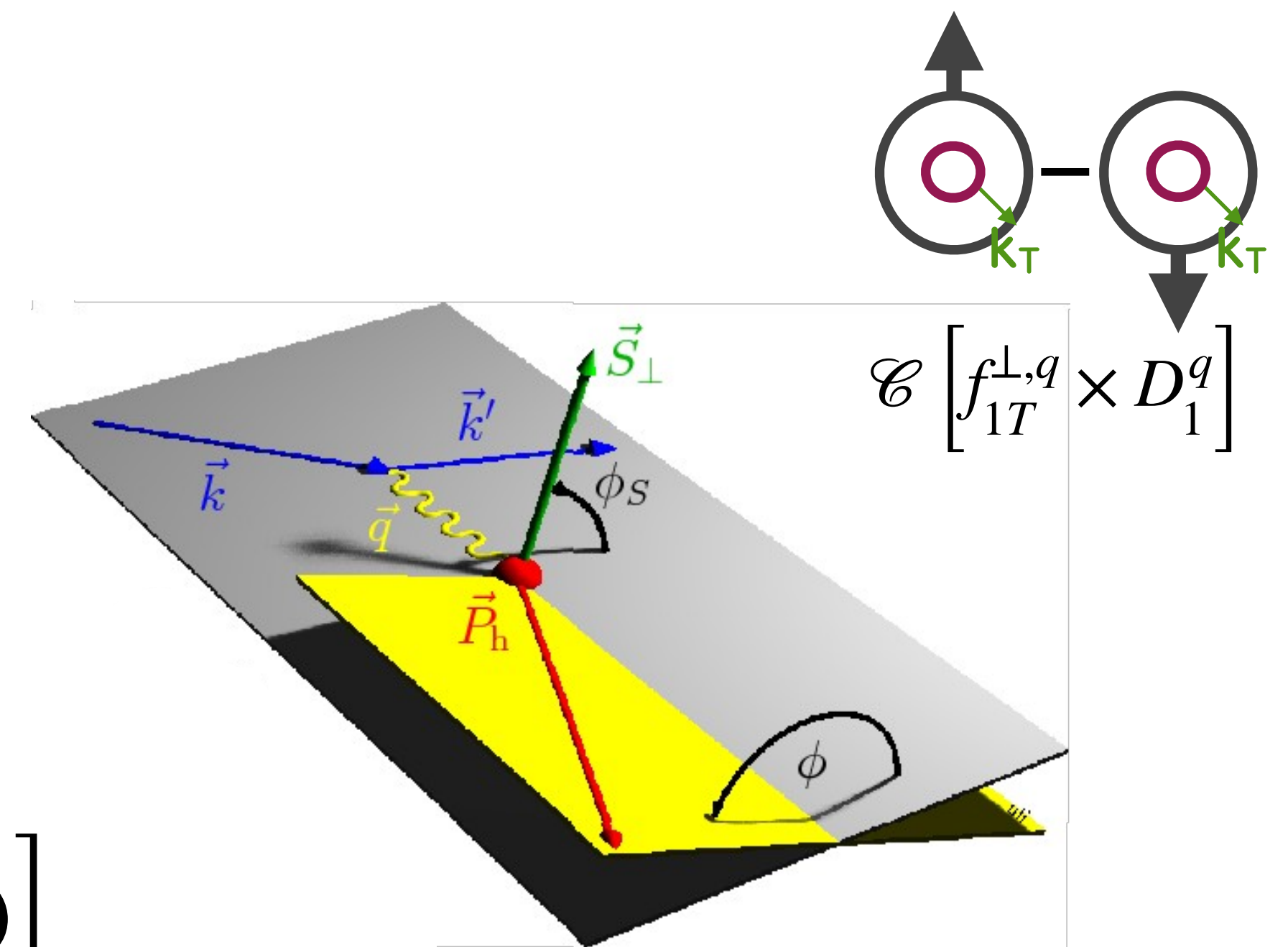
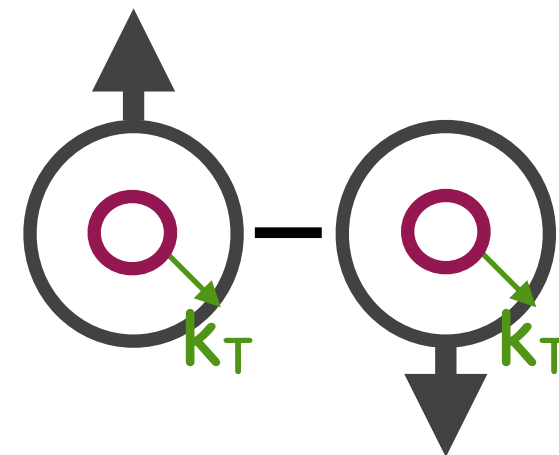


# Sivers amplitudes: measurement

$$A_{UT} = \frac{1}{\langle |S_T| \rangle} \frac{N^\uparrow(\phi, \phi_S) - N^\downarrow(\phi, \phi_S)}{N^\uparrow(\phi, \phi_S) + N^\downarrow(\phi, \phi_S)}$$

$$\sim \sin(\phi - \phi_S) \sum_q e_q^2 \mathcal{C} \left[ f_{1T}^{\perp,q}(x, k_\perp) \times D_1^q(z, p_\perp) \right]$$

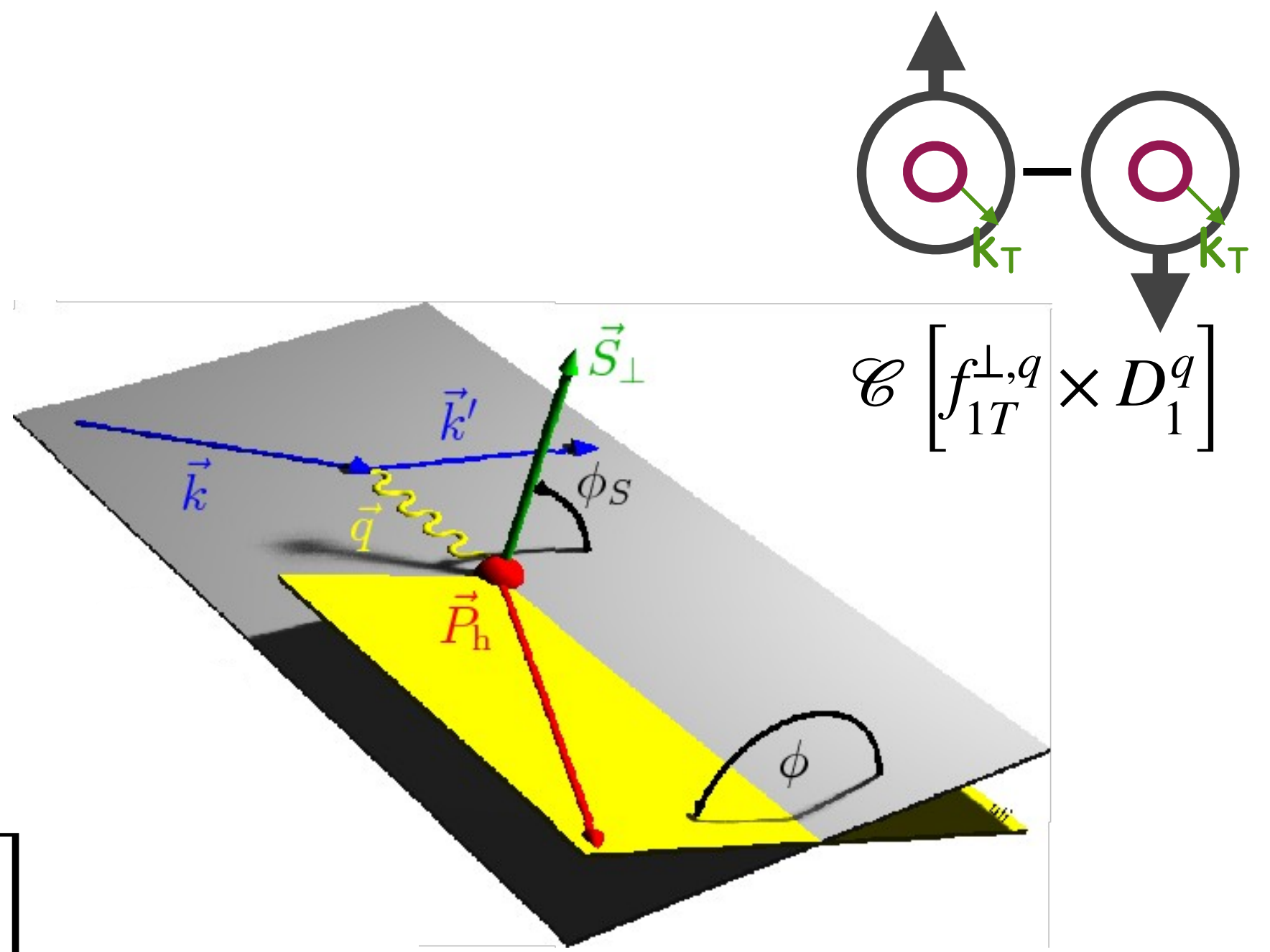
$f_{1T}^{\perp,q}(x, k_\perp)$  : Sivers function



# Sivers amplitudes: measurement

$$A_{UT} = \frac{1}{\langle |S_T| \rangle} \frac{N^\uparrow(\phi, \phi_S) - N^\downarrow(\phi, \phi_S)}{N^\uparrow(\phi, \phi_S) + N^\downarrow(\phi, \phi_S)}$$

$$\sim \sin(\phi - \phi_S) \sum_q e_q^2 \mathcal{C} \left[ f_{1T}^{\perp,q}(x, k_\perp) \times D_1^q(z, p_\perp) \right]$$



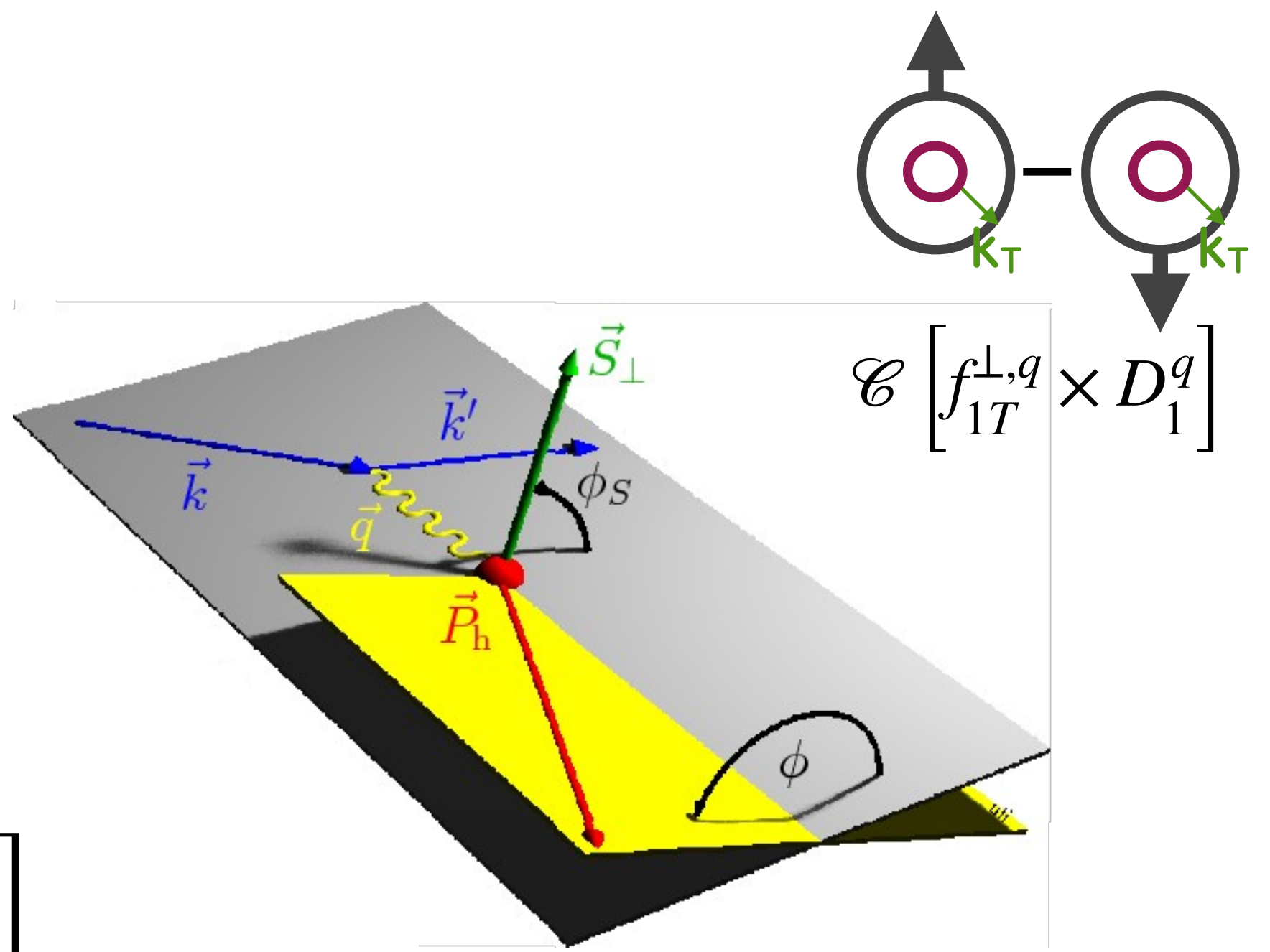
$f_{1T}^{\perp,q}(x, k_\perp)$  : Sivers function 

$D_1^q(z, p_\perp)$  : spin-independent fragmentation function

# Sivers amplitudes: measurement

$$A_{UT} = \frac{1}{\langle |S_T| \rangle} \frac{N^\uparrow(\phi, \phi_S) - N^\downarrow(\phi, \phi_S)}{N^\uparrow(\phi, \phi_S) + N^\downarrow(\phi, \phi_S)}$$

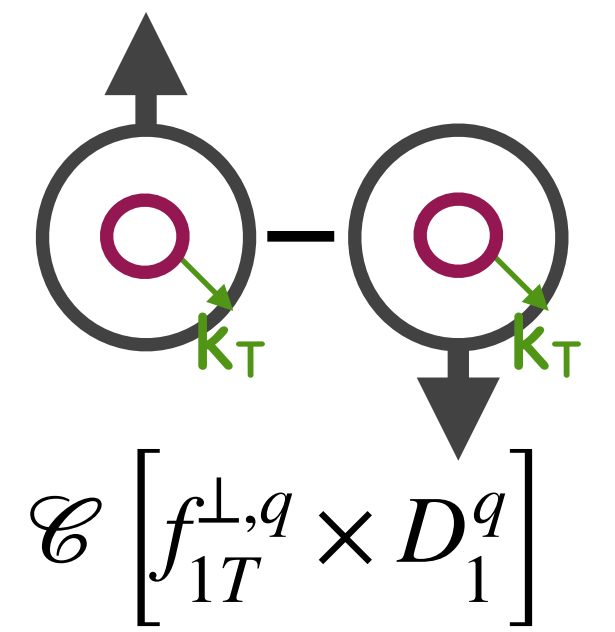
$$\sim \sin(\phi - \phi_S) \sum_q e_q^2 \mathcal{C} \left[ f_{1T}^{\perp,q}(x, k_\perp) \times D_1^q(z, p_\perp) \right]$$



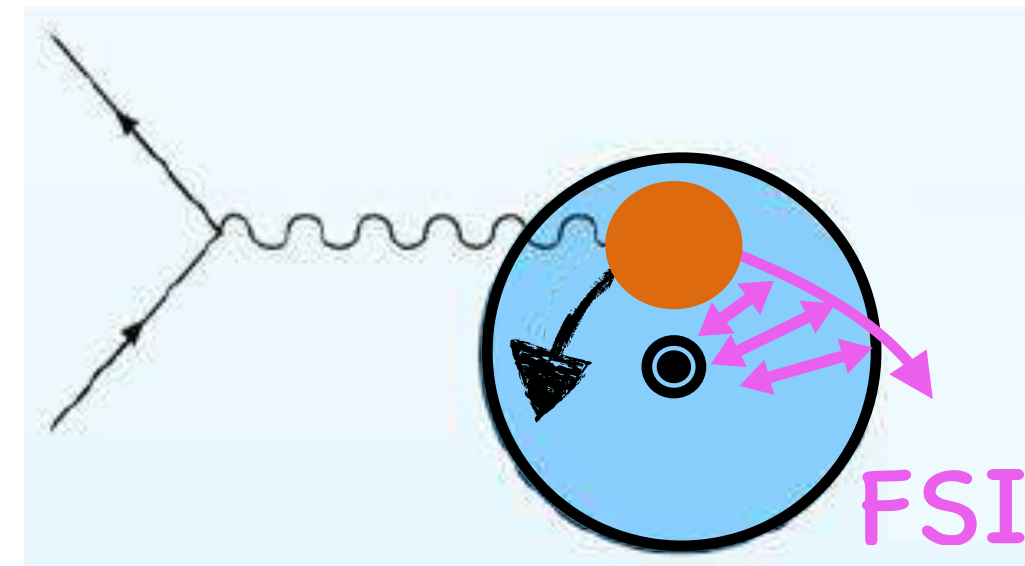
$f_{1T}^{\perp,q}(x, k_\perp)$  : Sivers function

$D_1^q(z, p_\perp)$  : spin-independent fragmentation function

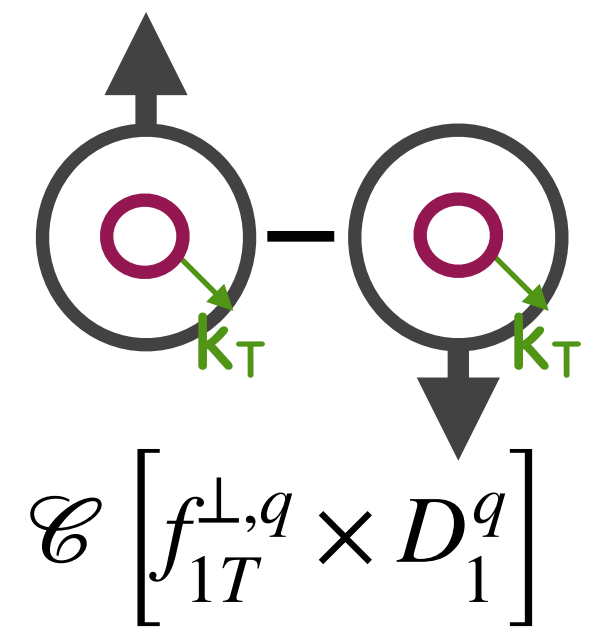
# Sivers amplitudes



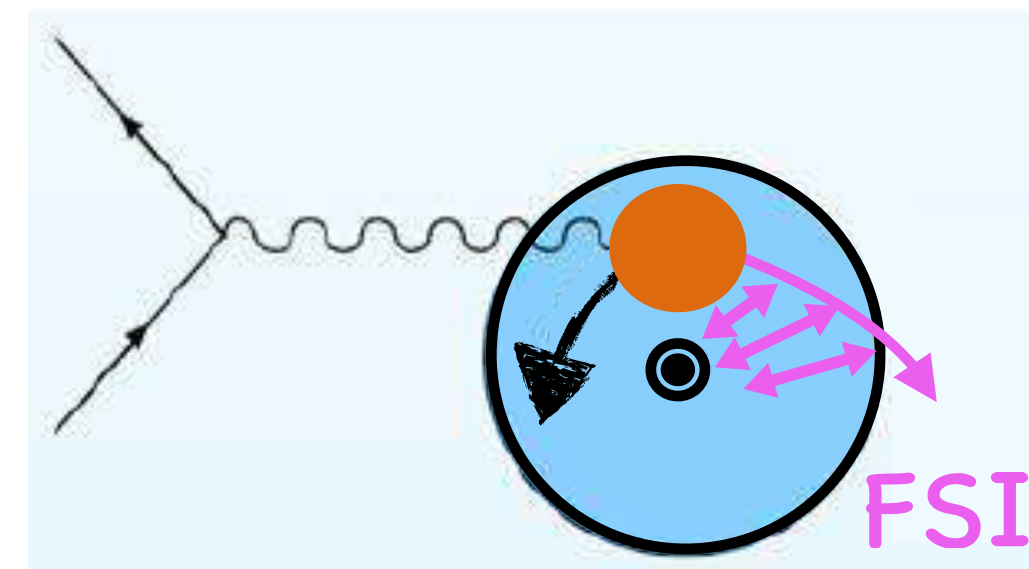
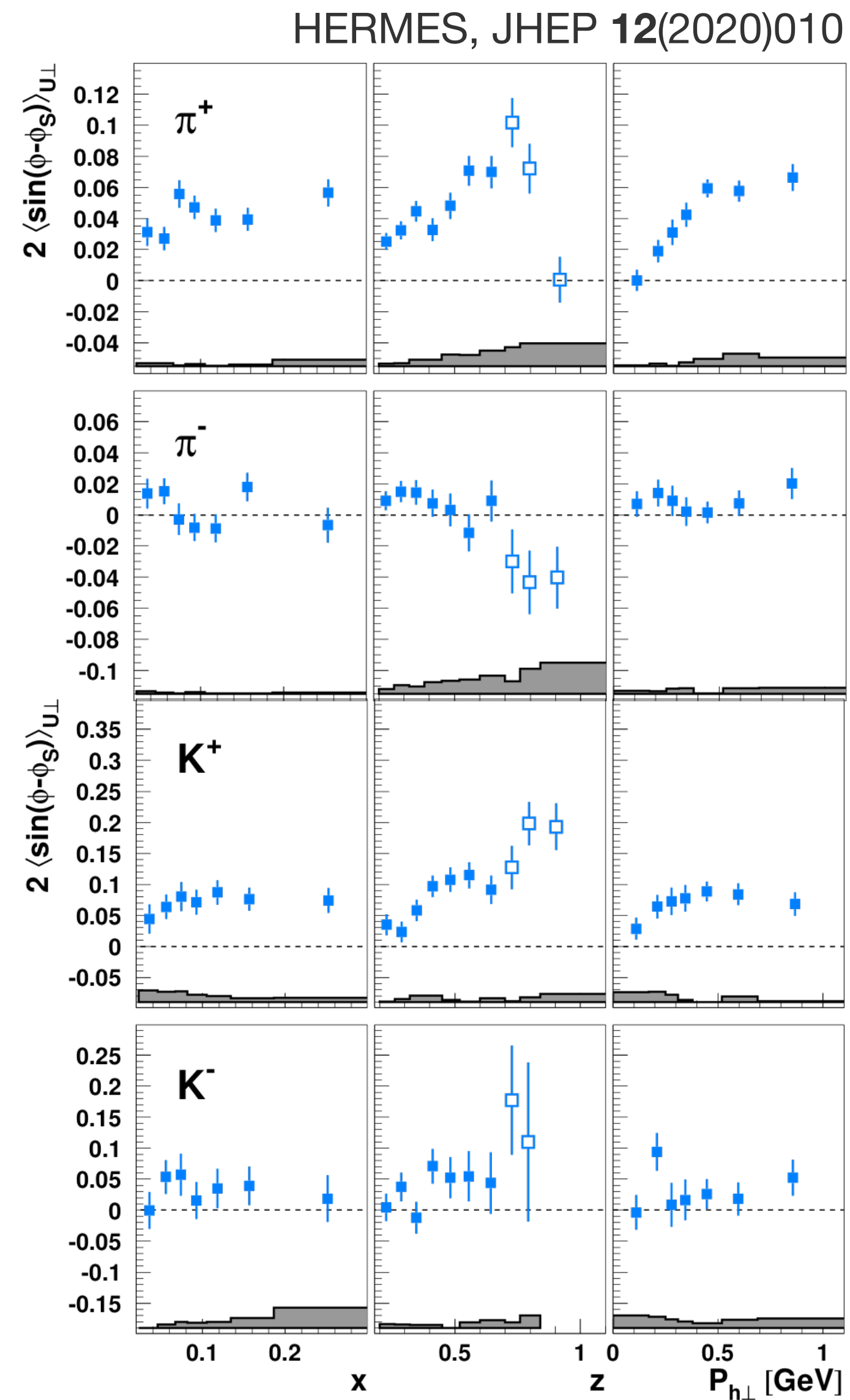
- Sivers function:
  - requires non-zero orbital angular momentum
  - final-state interactions  $\rightarrow$  azimuthal asymmetries



# Sivers amplitudes

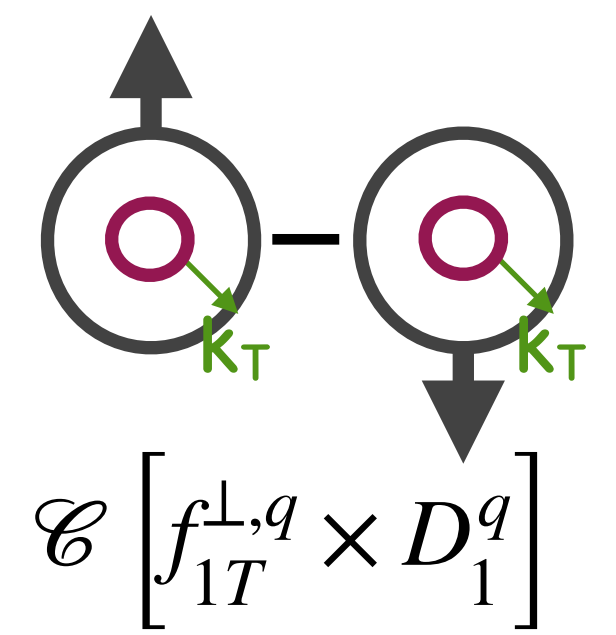
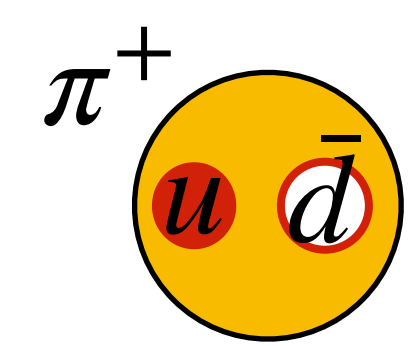
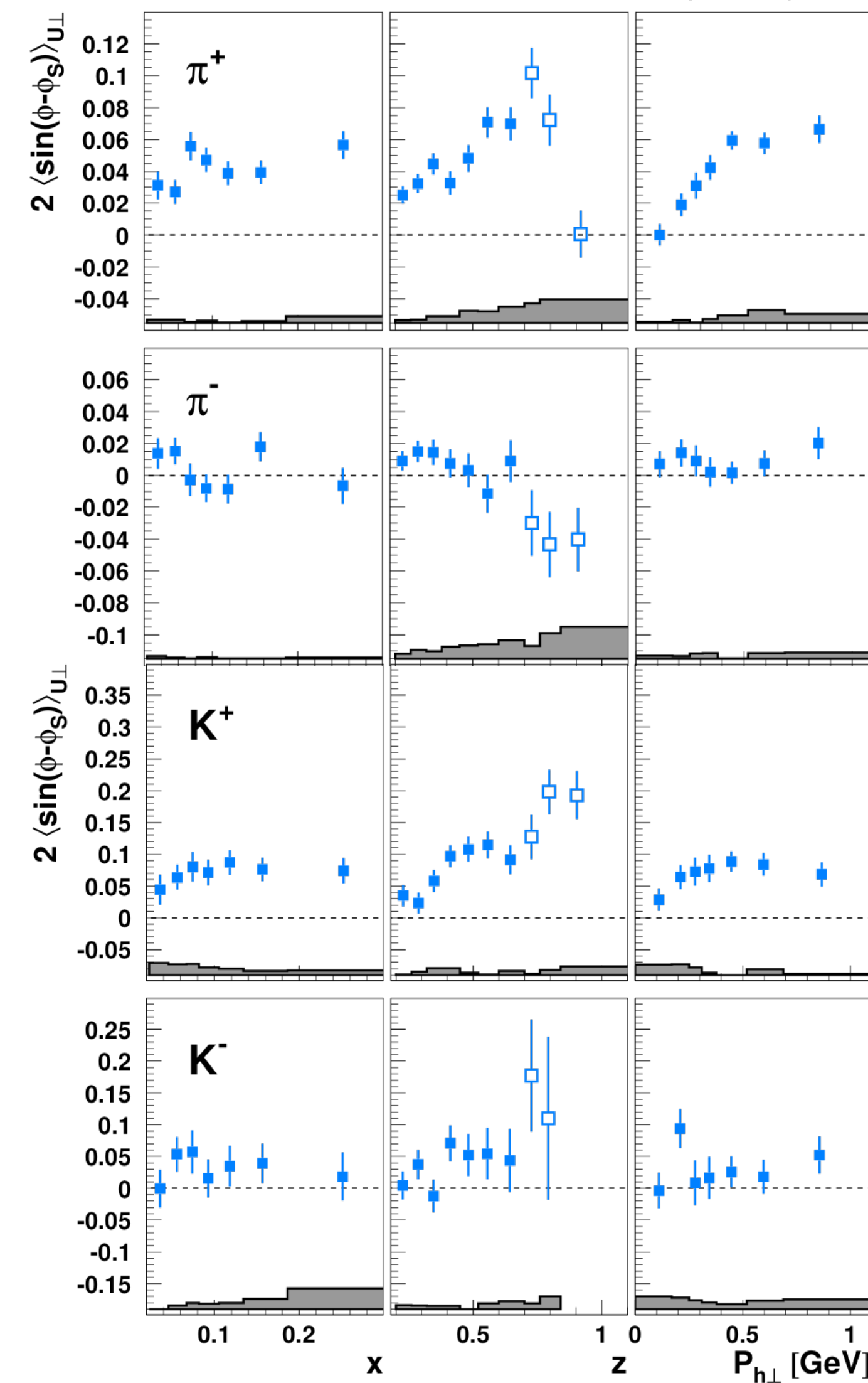


- Sivers function:
  - requires non-zero orbital angular momentum
  - final-state interactions  $\rightarrow$  azimuthal asymmetries

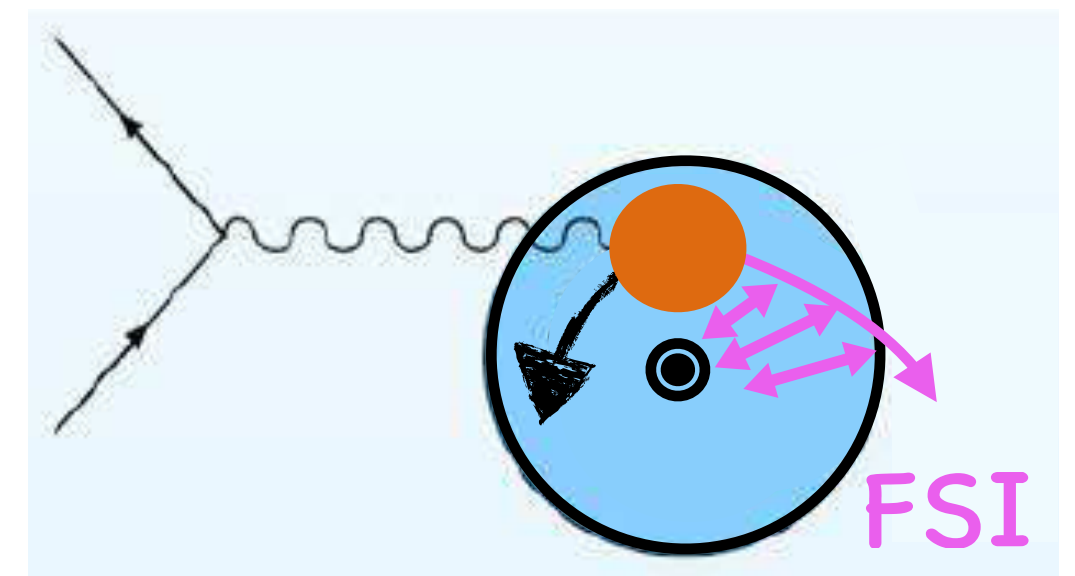


# Sivers amplitudes

HERMES, JHEP 12(2020)010



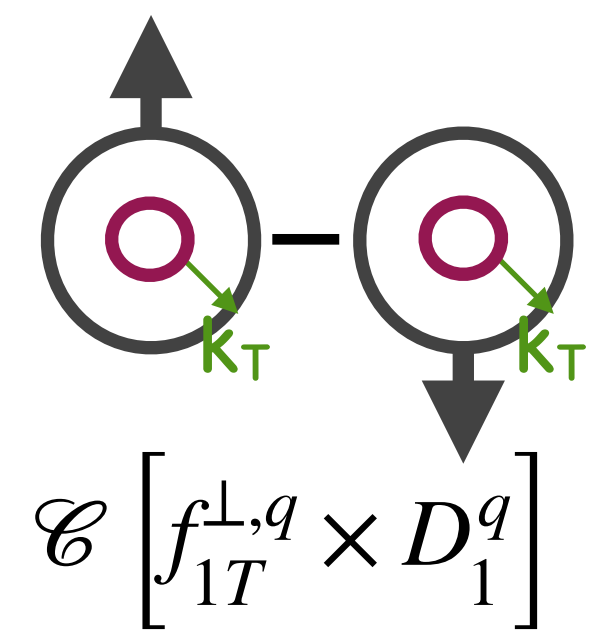
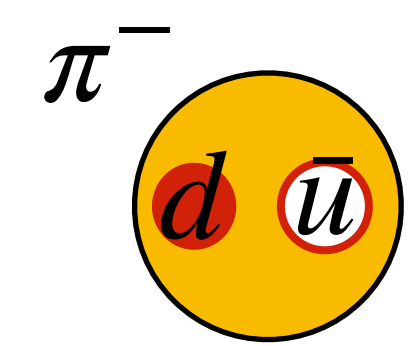
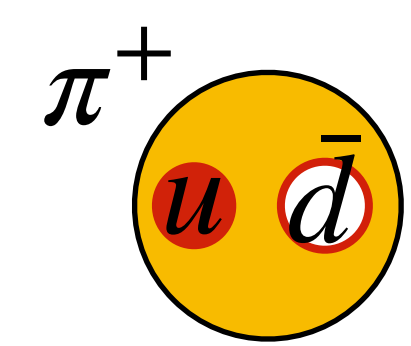
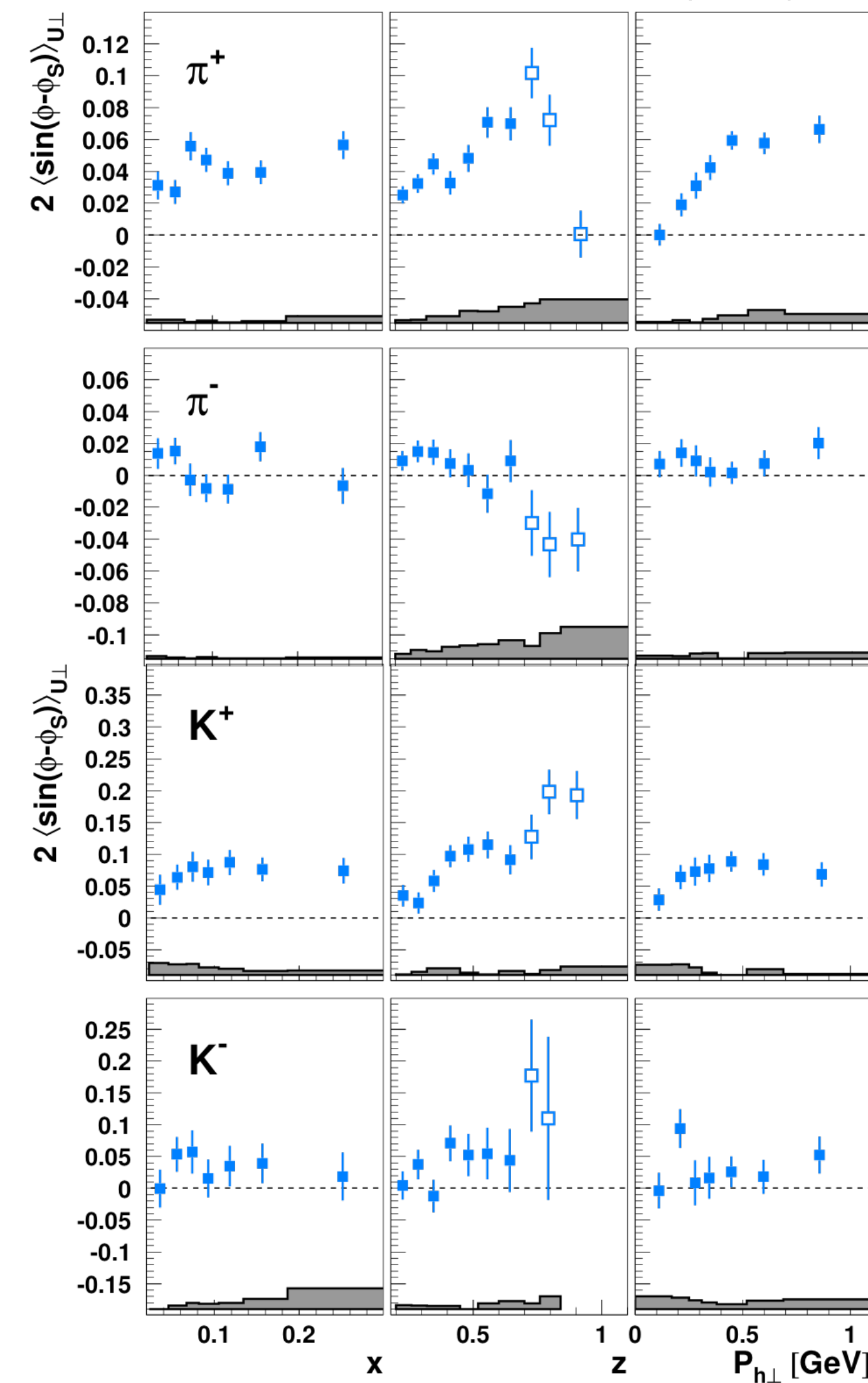
- Sivers function:
  - requires non-zero orbital angular momentum
  - final-state interactions  $\rightarrow$  azimuthal asymmetries



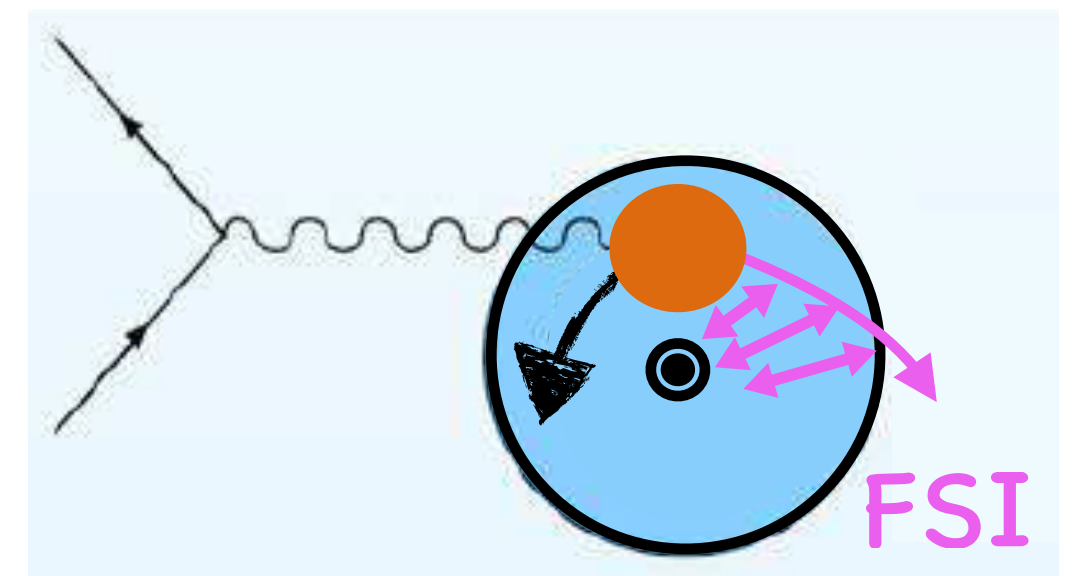


# Sivers amplitudes

HERMES, JHEP 12(2020)010

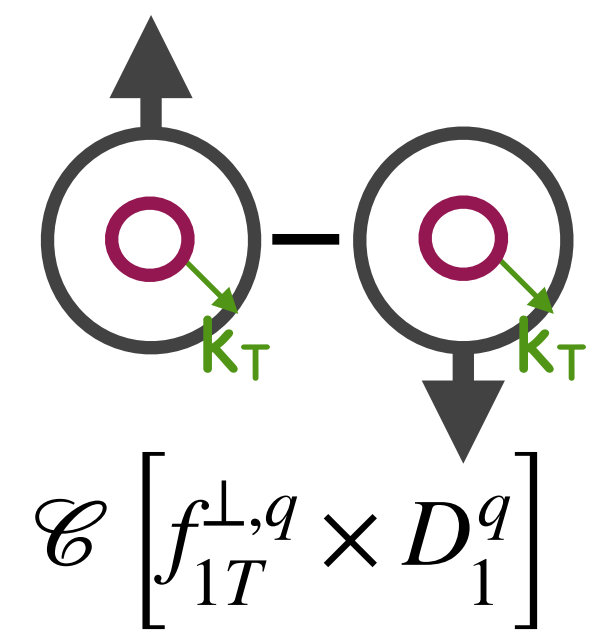
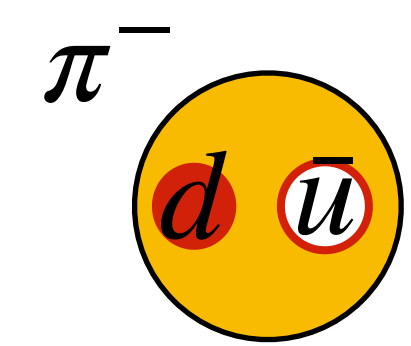
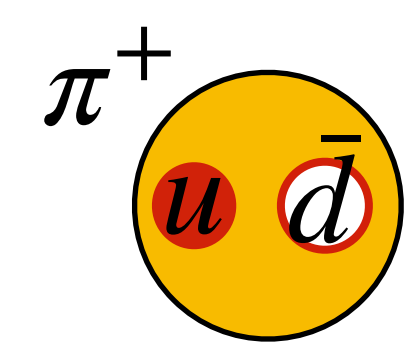
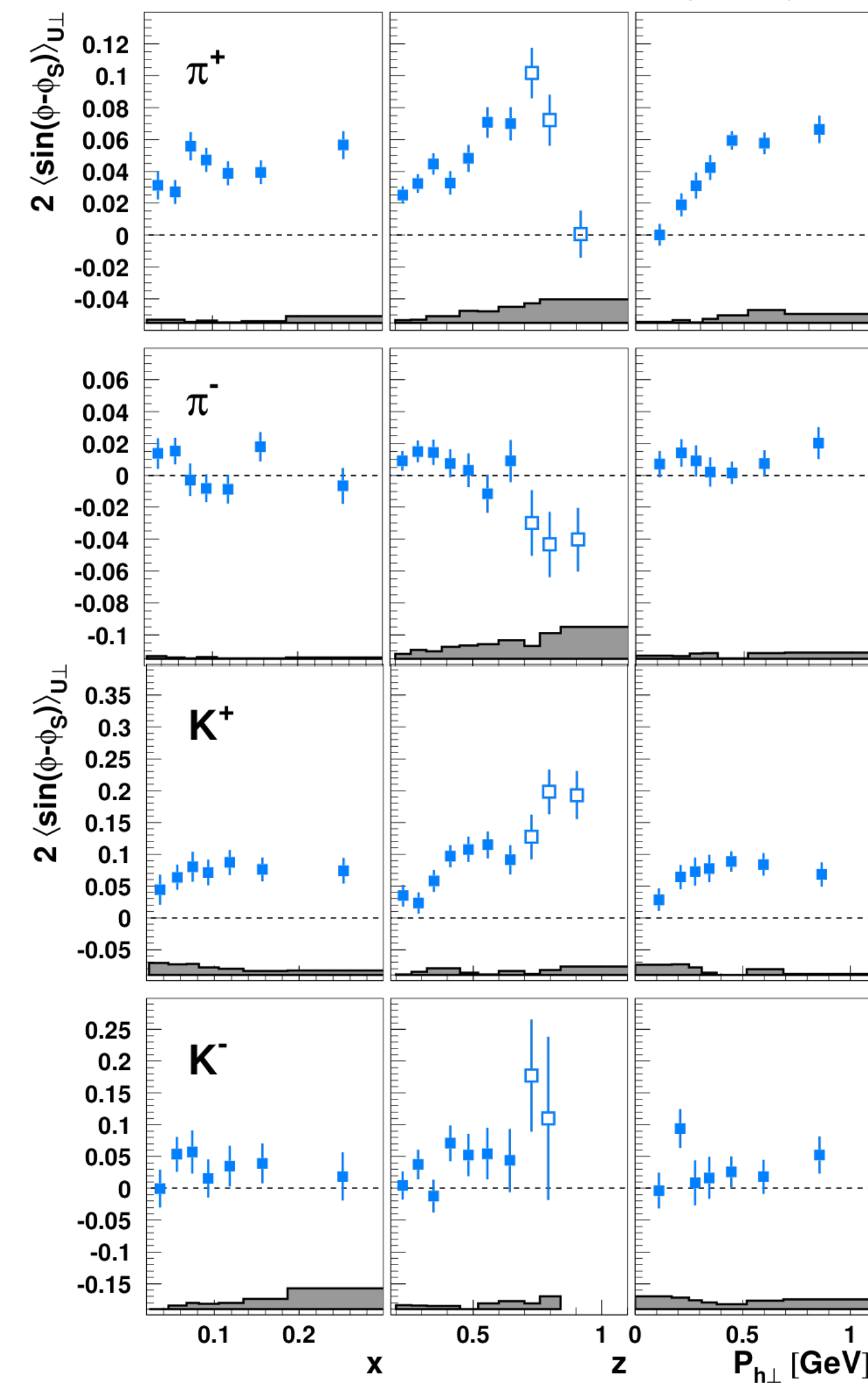


- Sivers function:
  - requires non-zero orbital angular momentum
  - final-state interactions  $\rightarrow$  azimuthal asymmetries

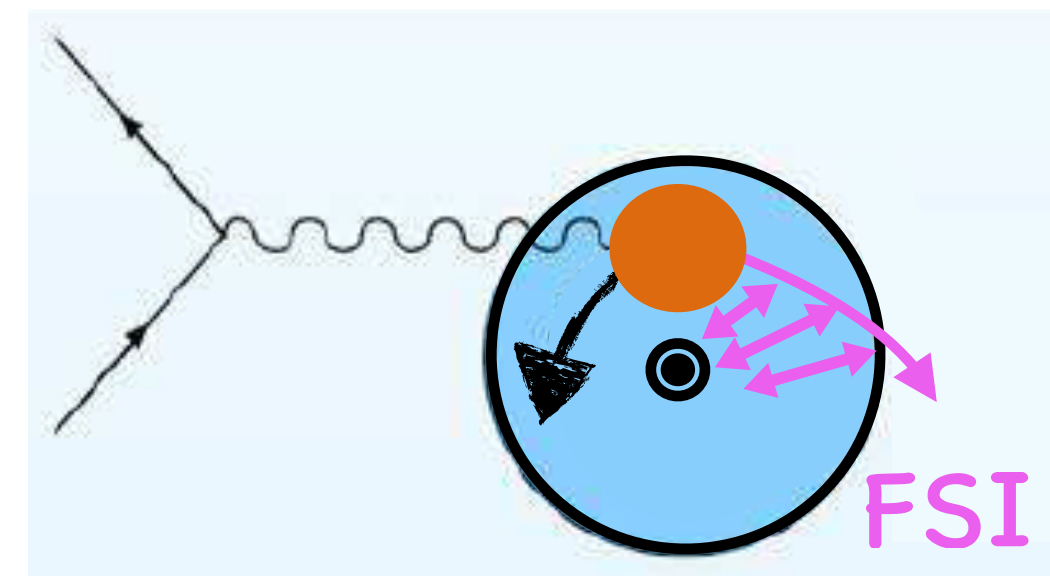


# Sivers amplitudes

HERMES, JHEP 12(2020)010



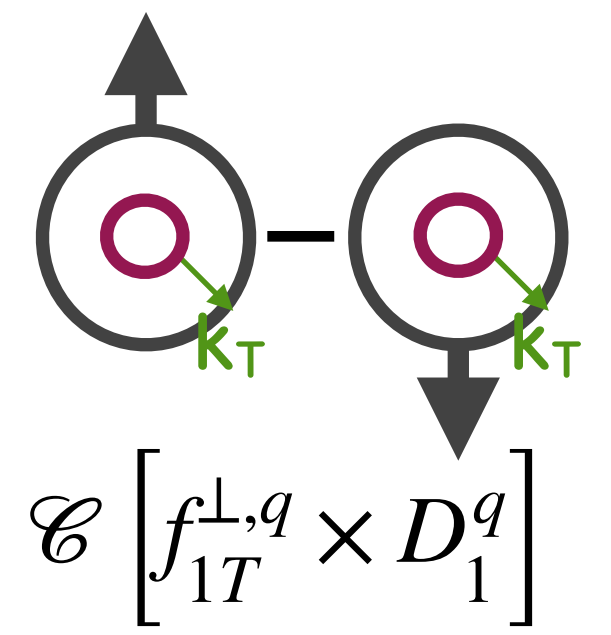
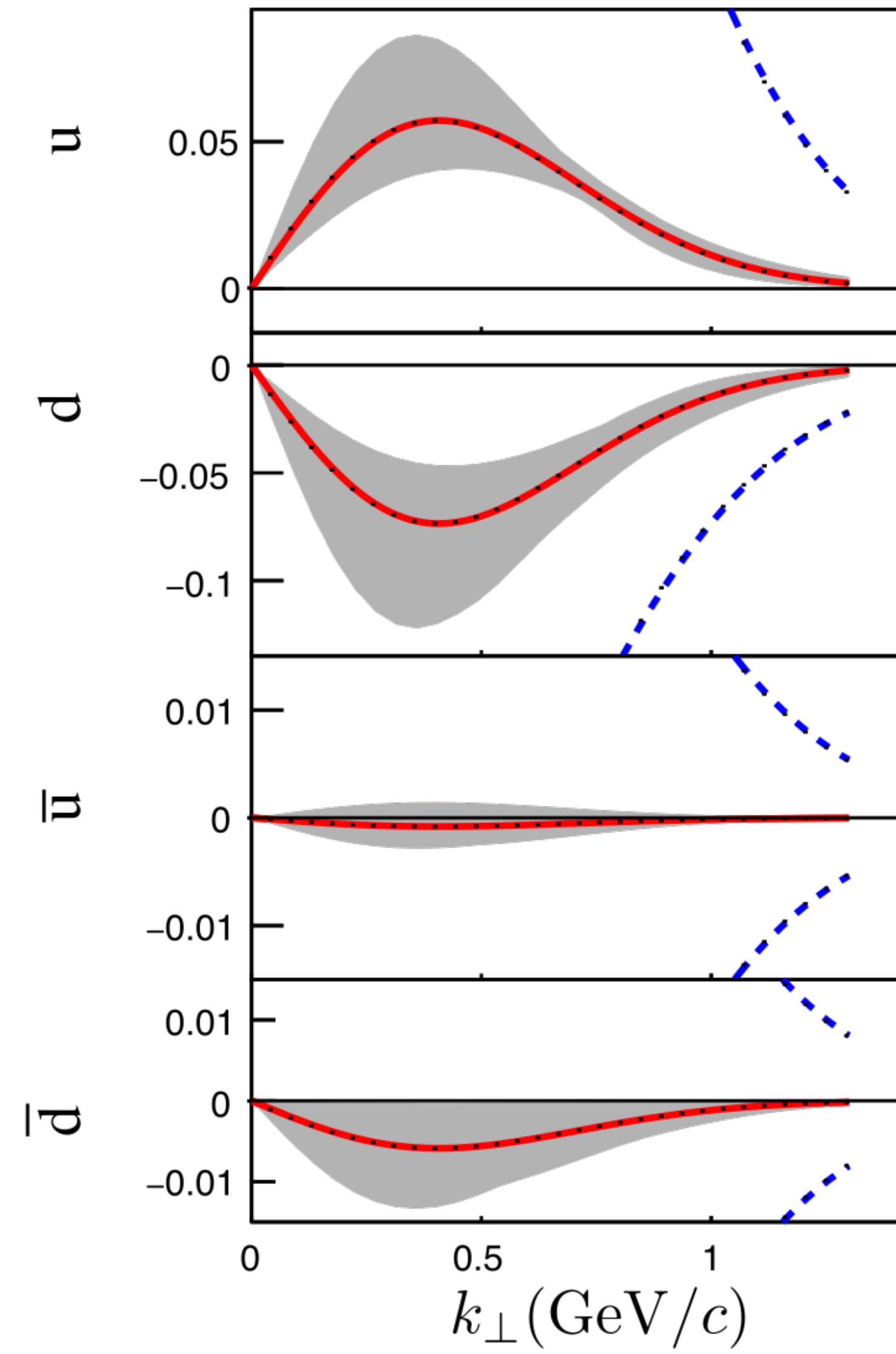
- Sivers function:
  - requires non-zero orbital angular momentum
  - final-state interactions  $\rightarrow$  azimuthal asymmetries



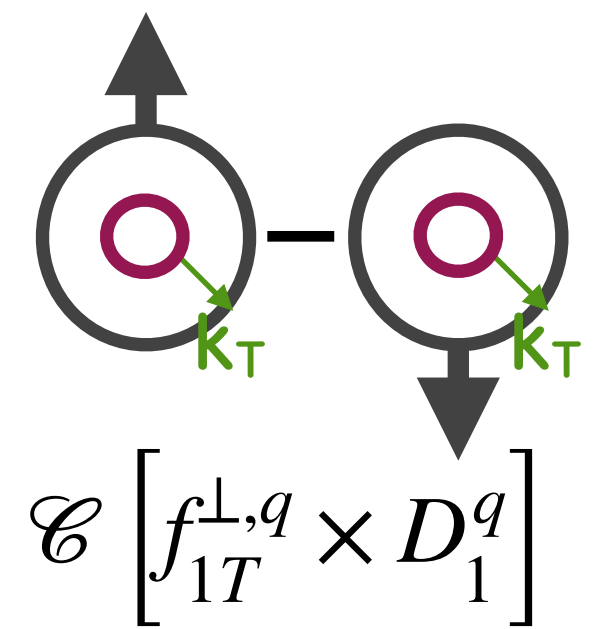
- $\pi^+$ :
  - positive  $\rightarrow$  non-zero orbital angular momentum
- $\pi^-$ :
  - consistent with zero  $\rightarrow$   $u$  and  $d$  quark cancelation

# Sivers function

M. Anselmino et al., JHEP **04** (2017) 046

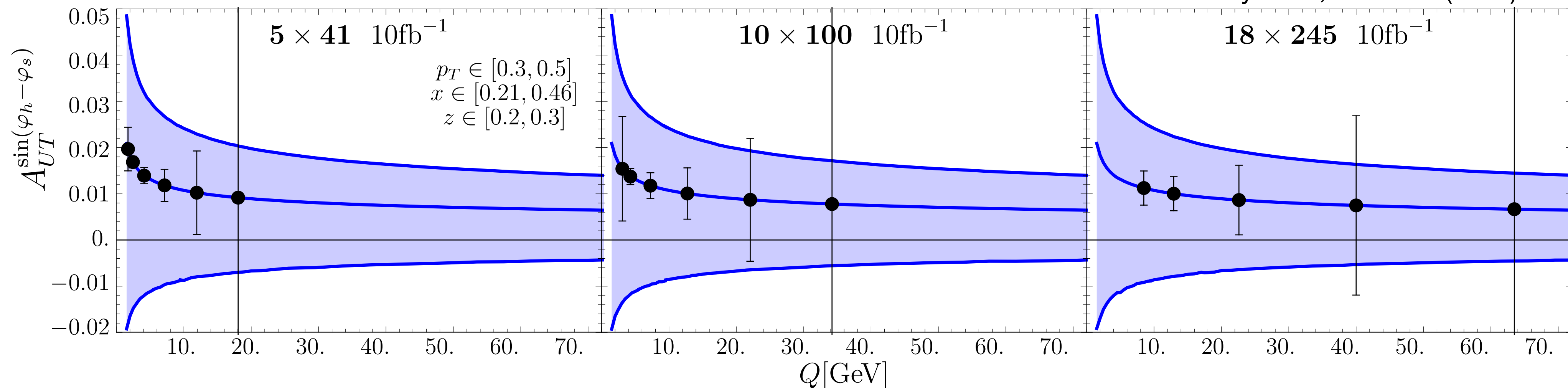


# Sivers amplitude and $Q^2$



R. Seidl, A. Vladimirov et al., NIM A **1055** (2023) 168458

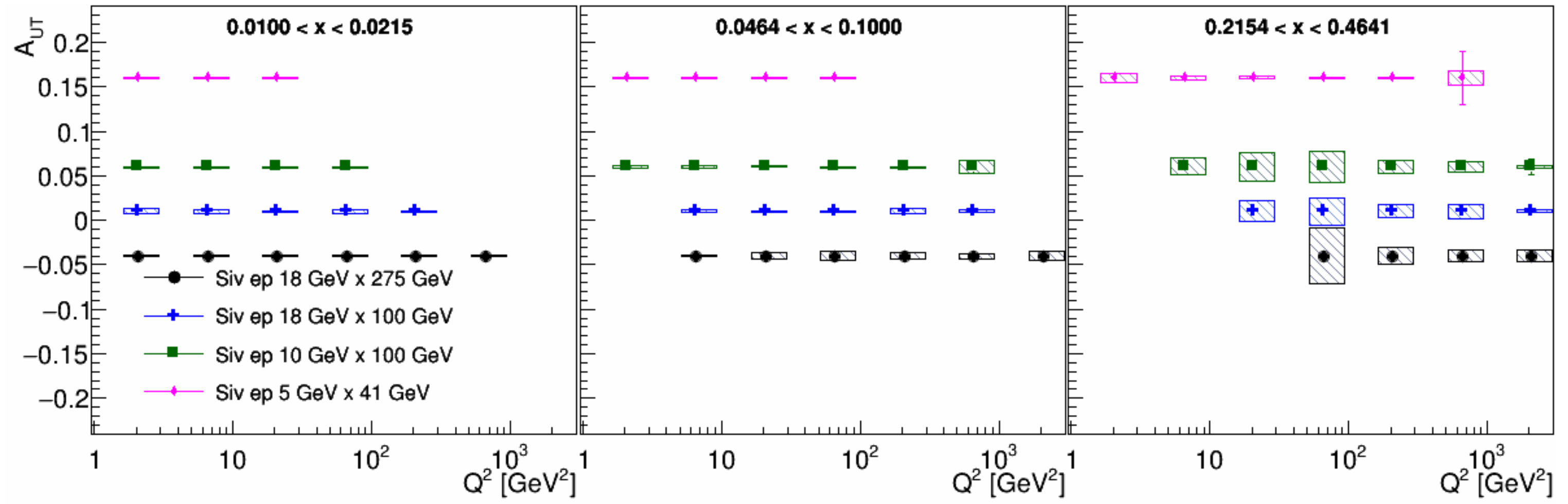
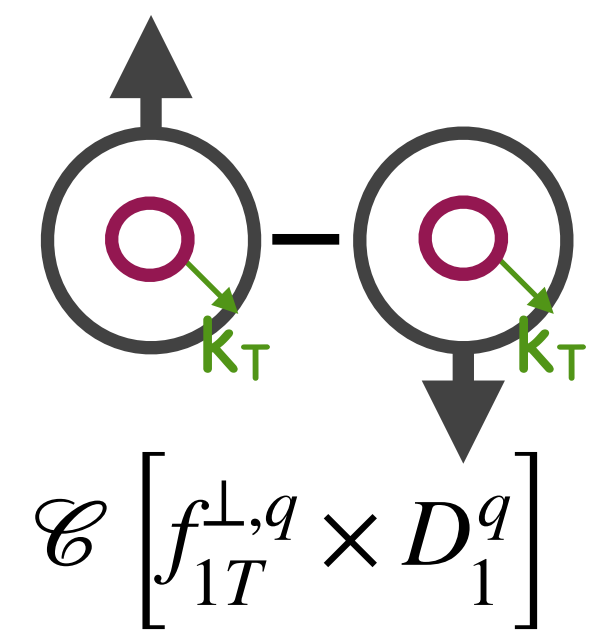
Parametrisation: M. Bury et al., JHEP **05** (2021)151



Decrease of asymmetry with increasing  $Q^2 \rightarrow$  need high precision ( $<1\%$ ) to measure asymmetry at high  $Q^2$

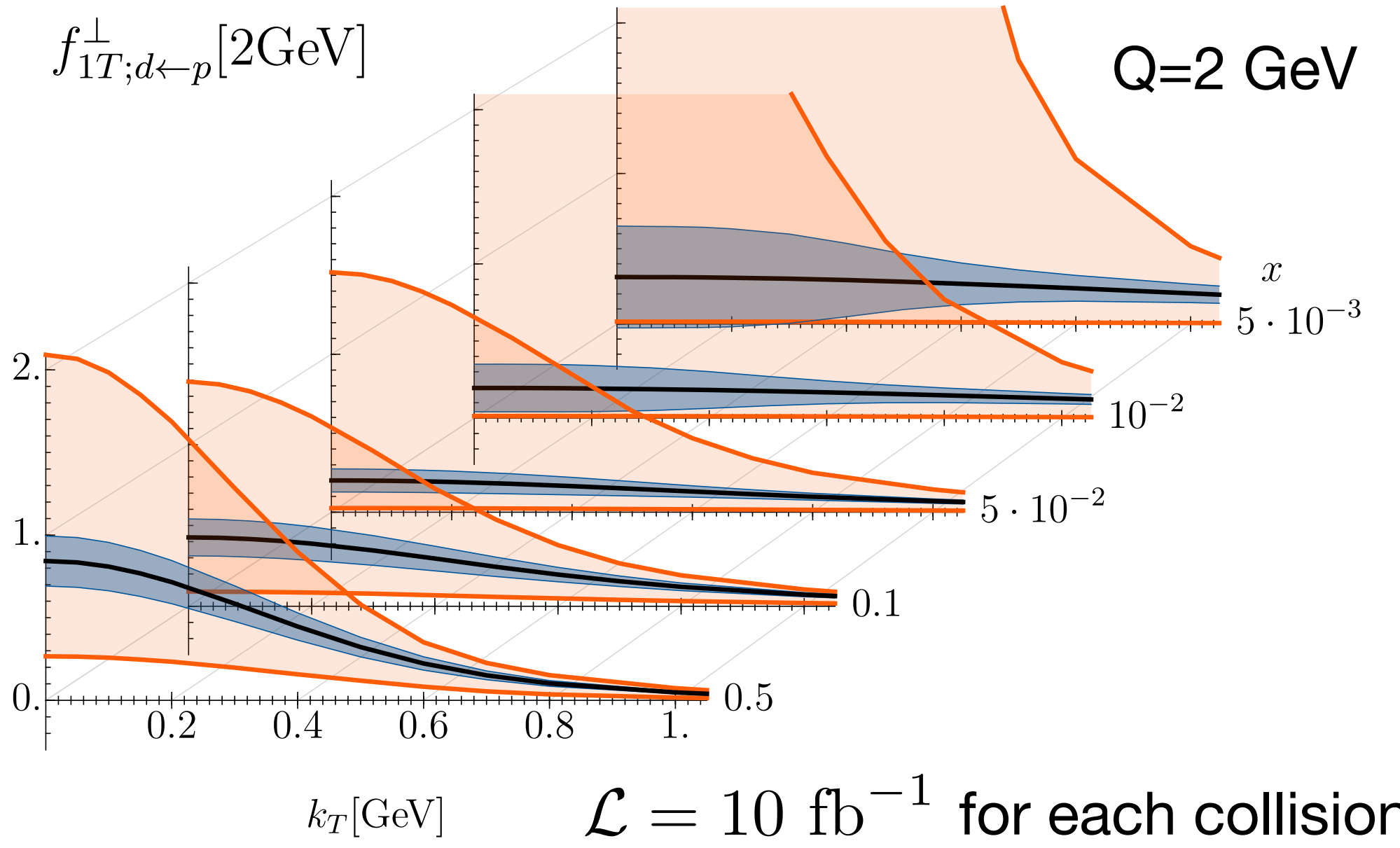
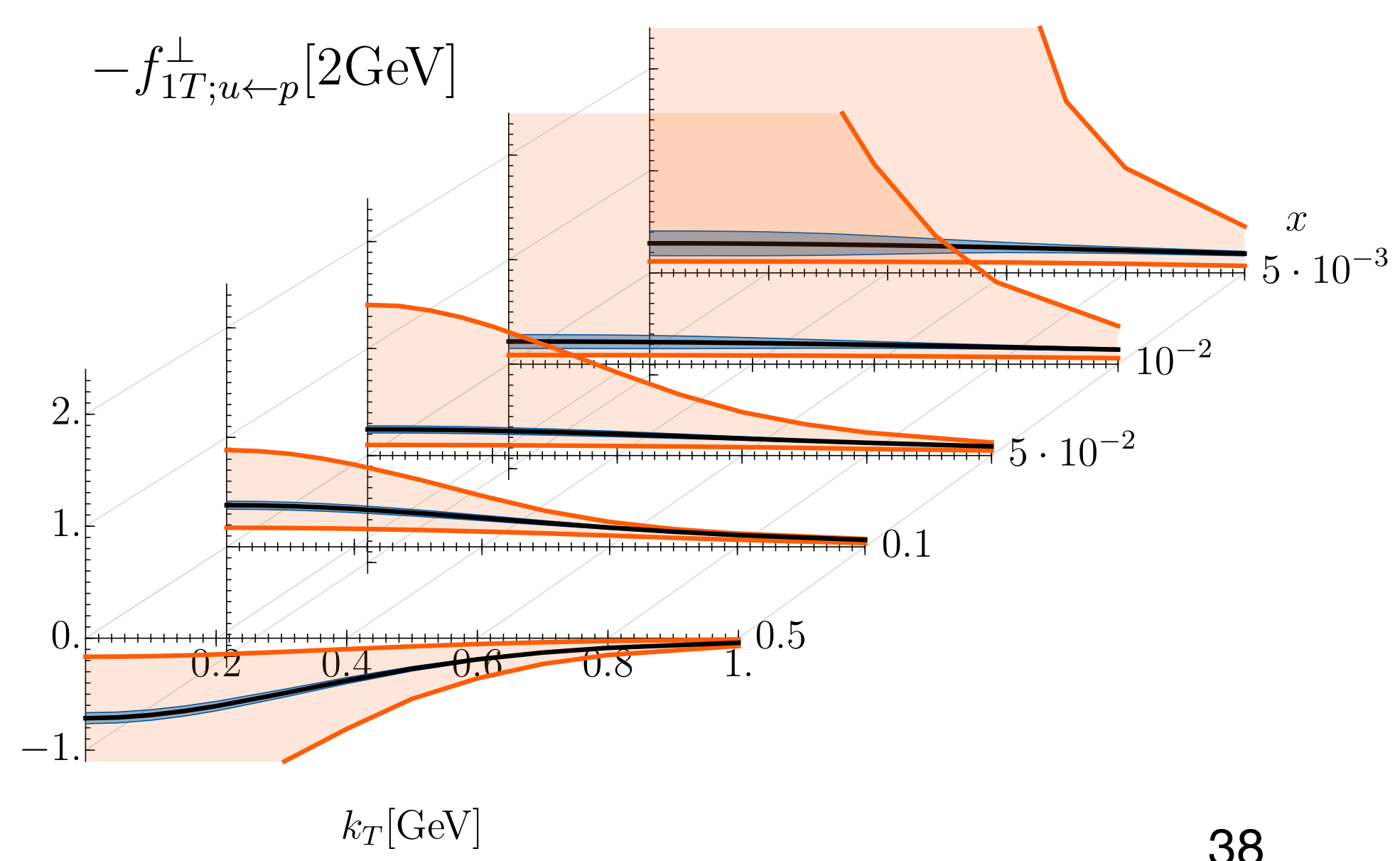
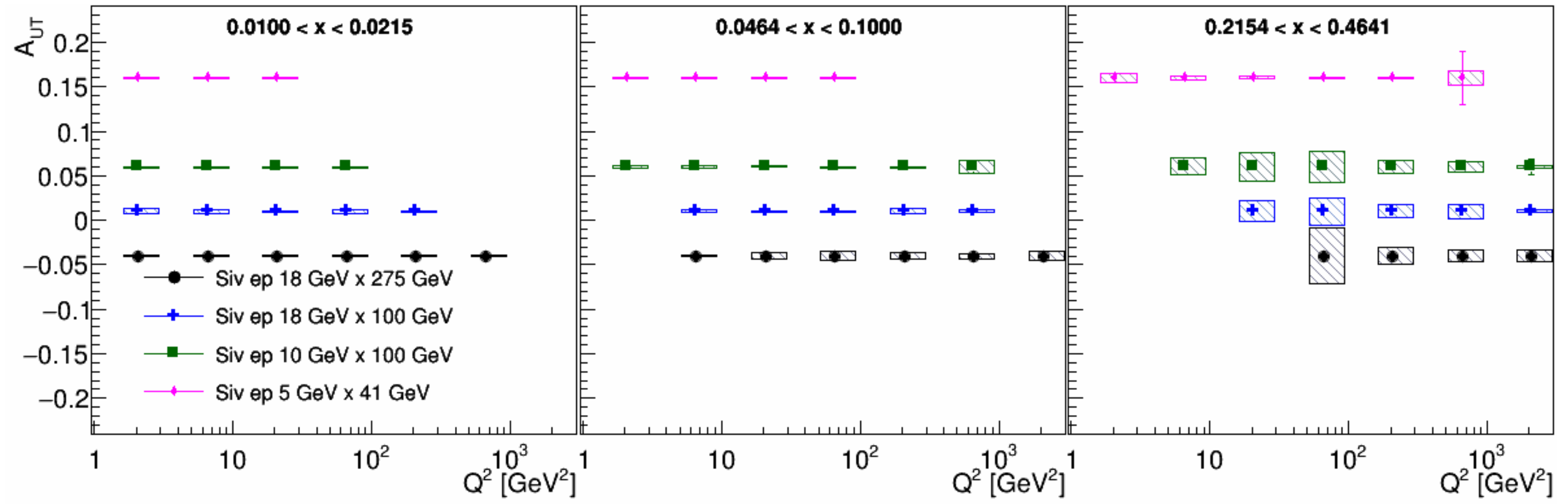
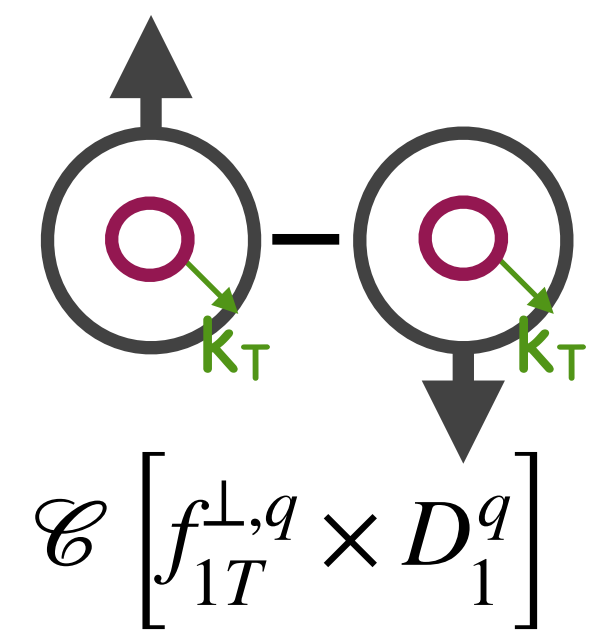
# Impact of EIC on Sivers TMD PDFs

R. Seidl, A. Vladimirov et al., NIM A **1055** (2023) 168458



# Impact of EIC on Sivers TMD PDFs

R. Seidl, A. Vladimirov et al., NIM A **1055** (2023) 168458



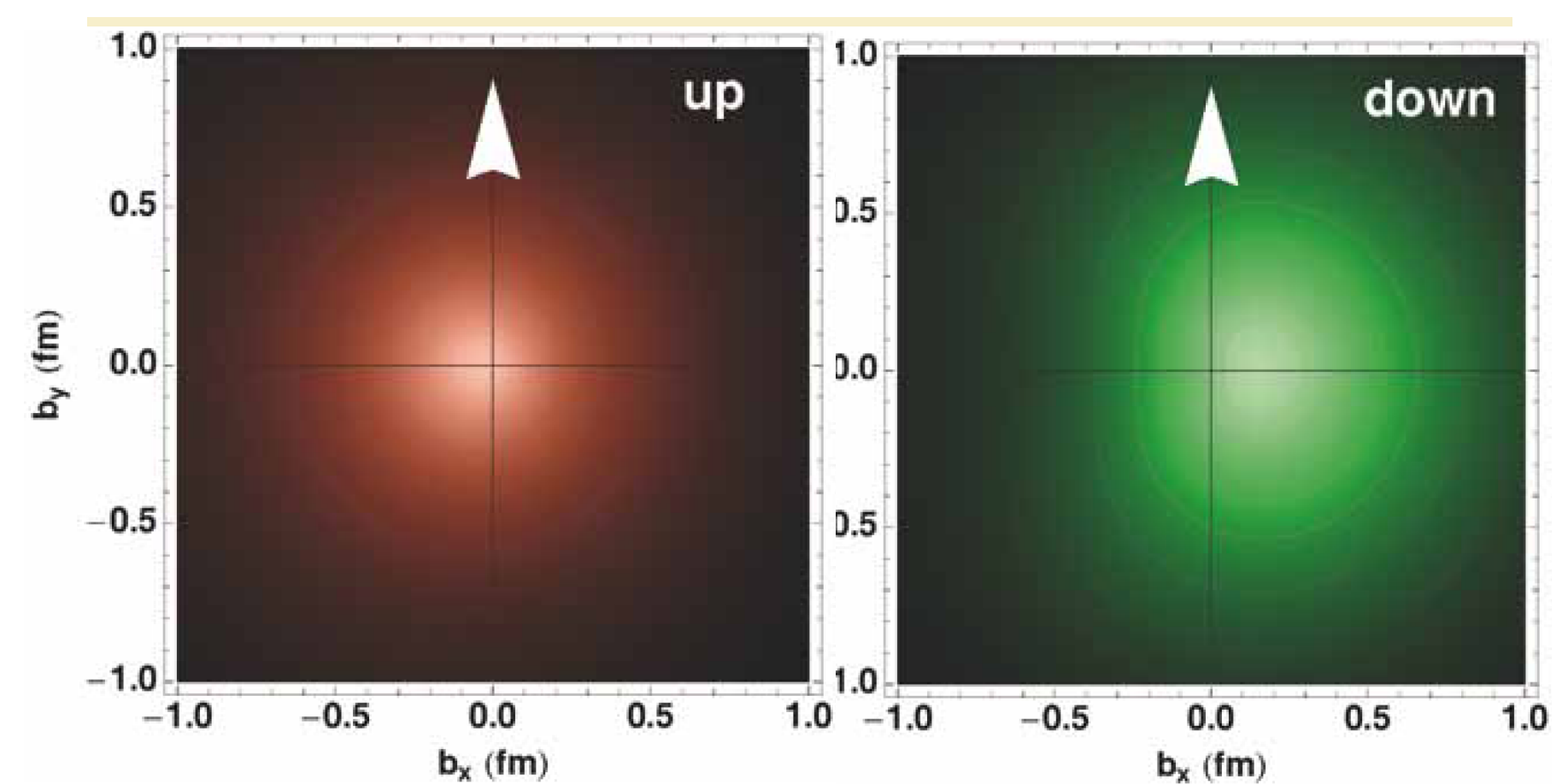
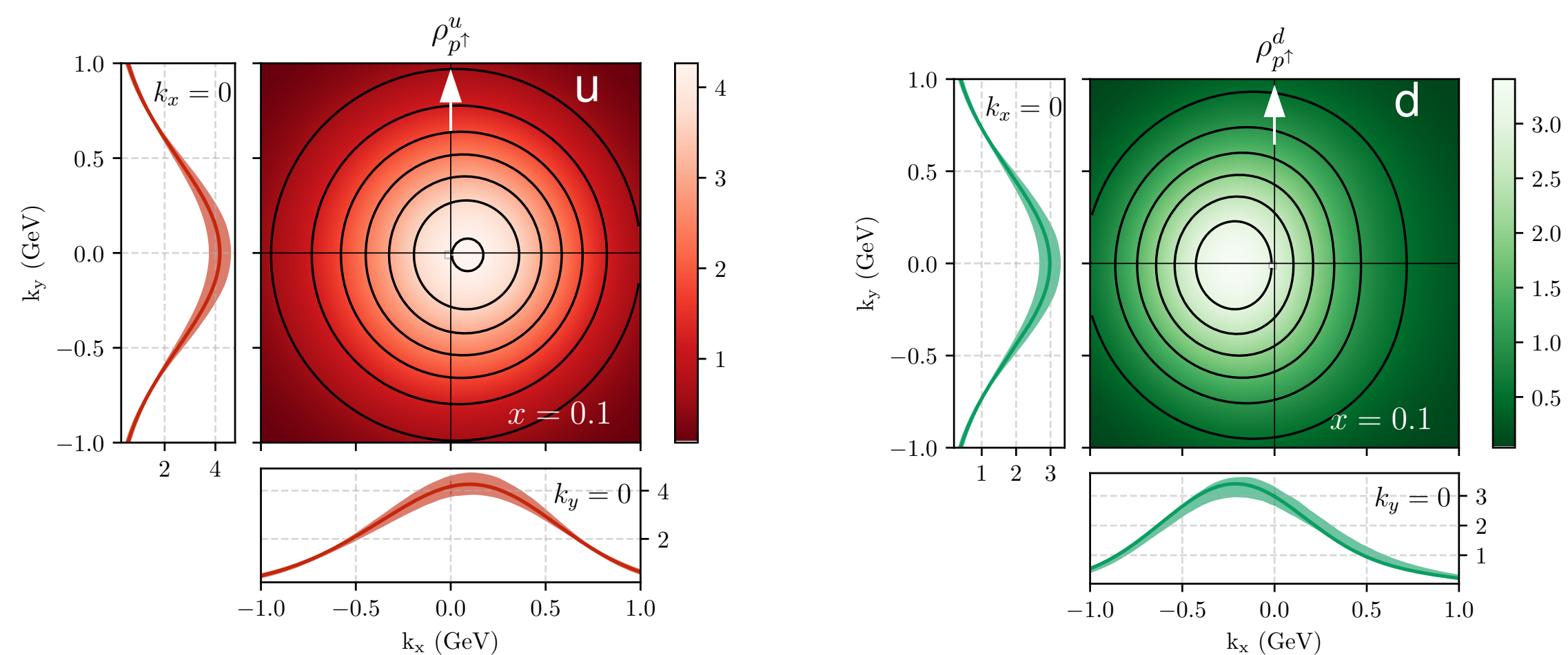
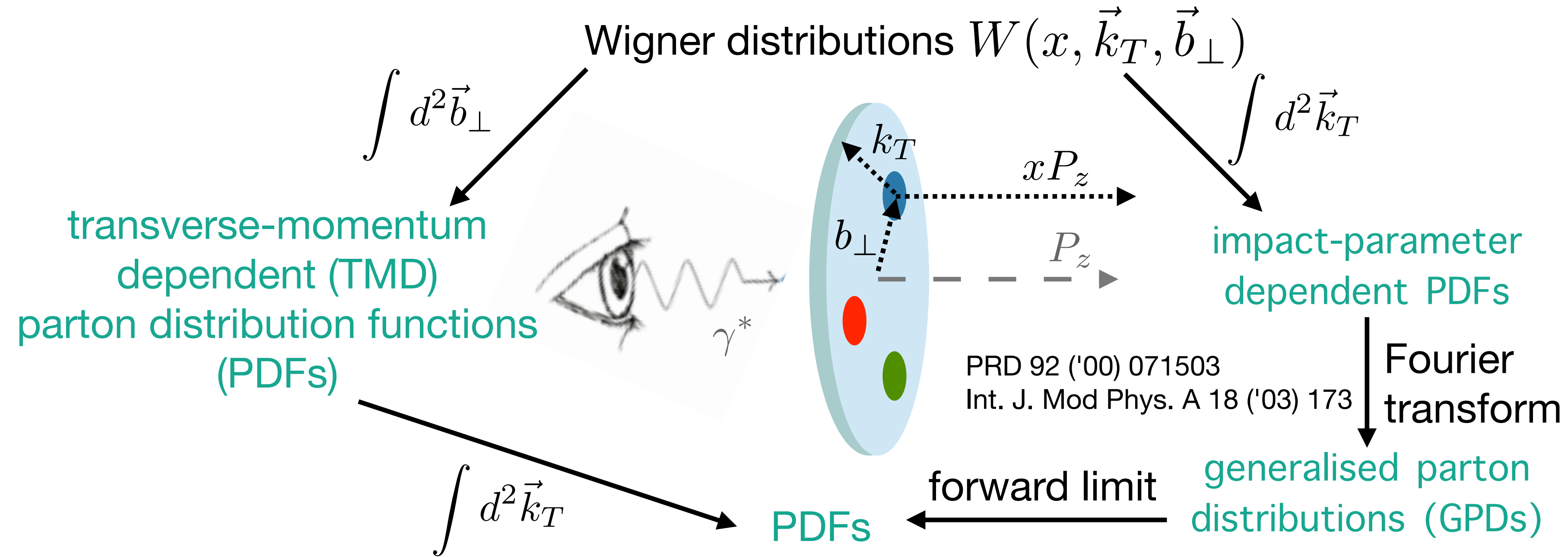
$\mathcal{L} = 10 \text{ fb}^{-1}$  for each collision energy

# Gluon TMDs

<b>GLUONS</b>	<i>unpolarized</i>	<i>circular</i>	<i>linear</i>
<b>U</b>	$f_1^g$		$h_1^{\perp g}$
<b>L</b>		$g_{1L}^g$	$h_{1L}^{\perp g}$
<b>T</b>	$f_{1T}^{\perp g}$	$g_{1T}^g$	$h_{1T}^g, h_{1T}^{\perp g}$

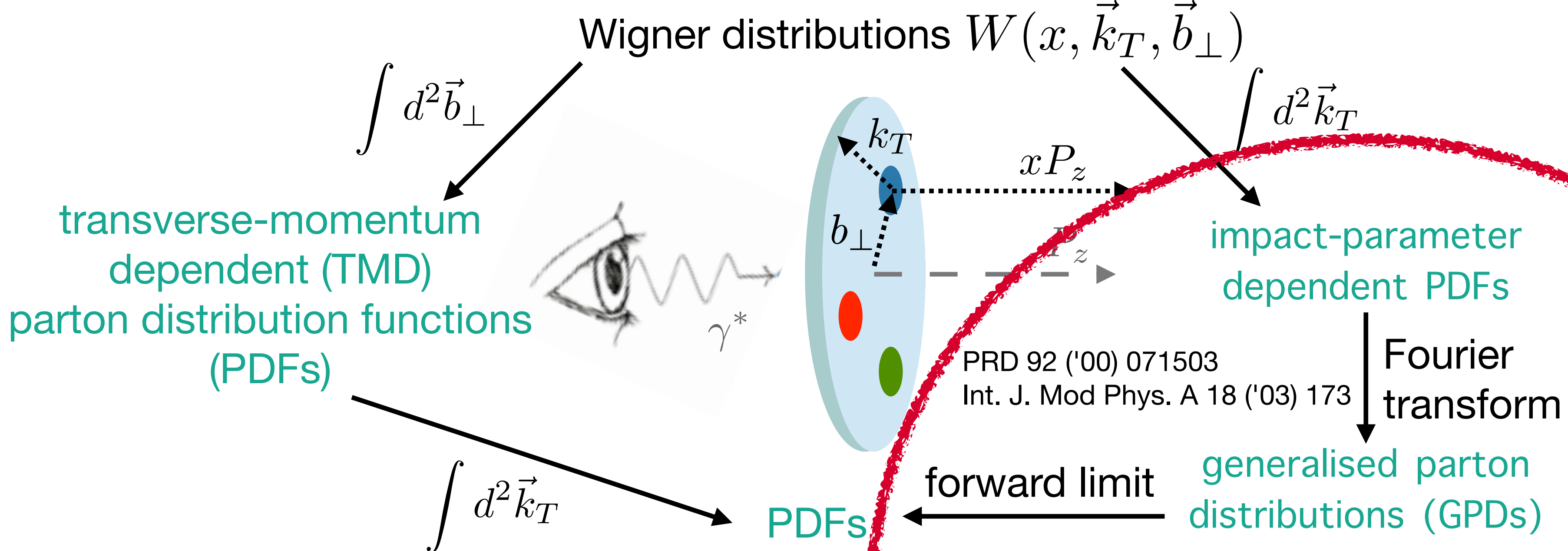
- In contrast to quark TMDs, gluon TMDs are almost unknown
- Accessible through production of dijets, high- $P_T$  hadron pairs, quarkonia

# The various dimensions of the nucleon structure

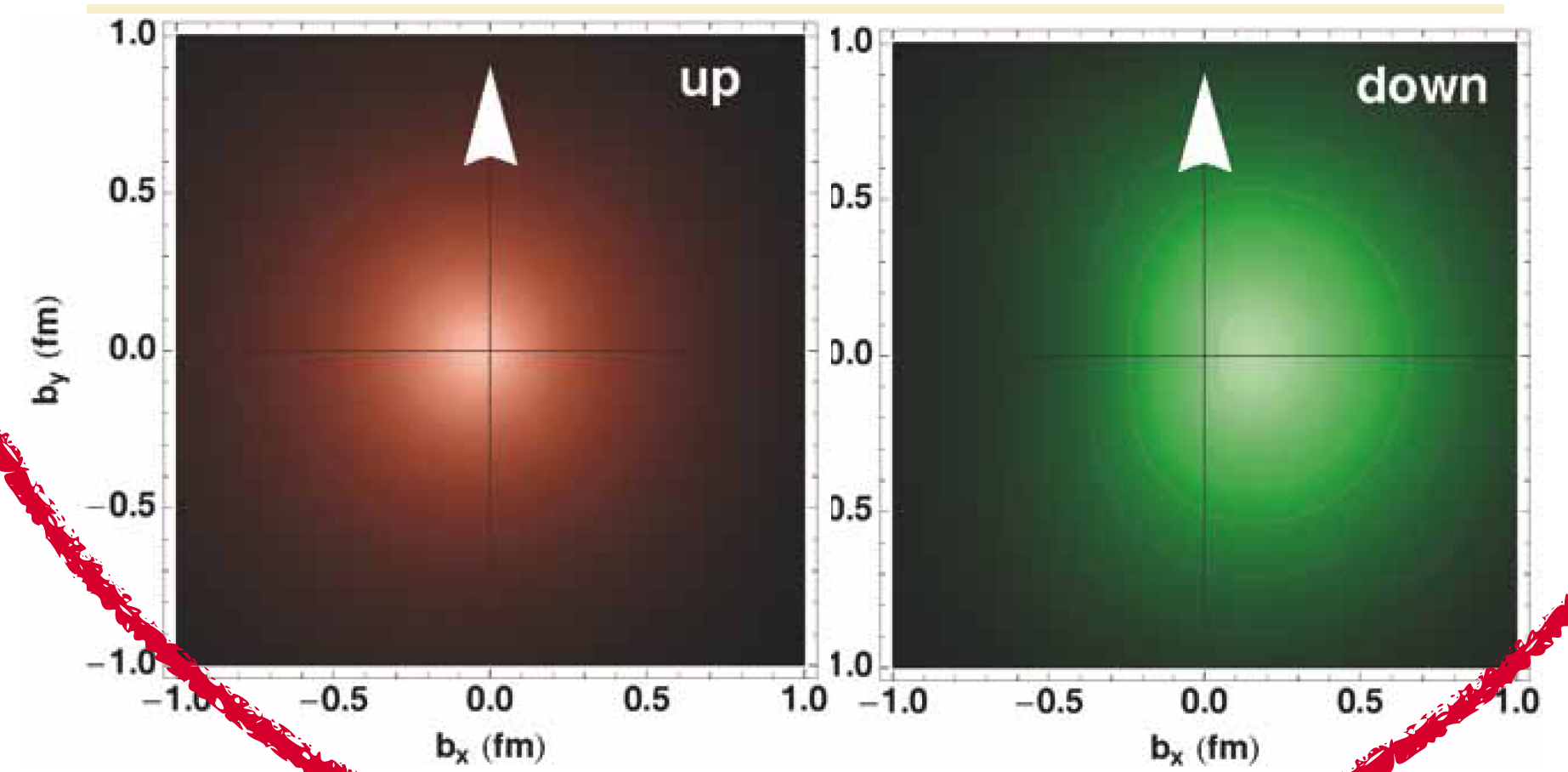
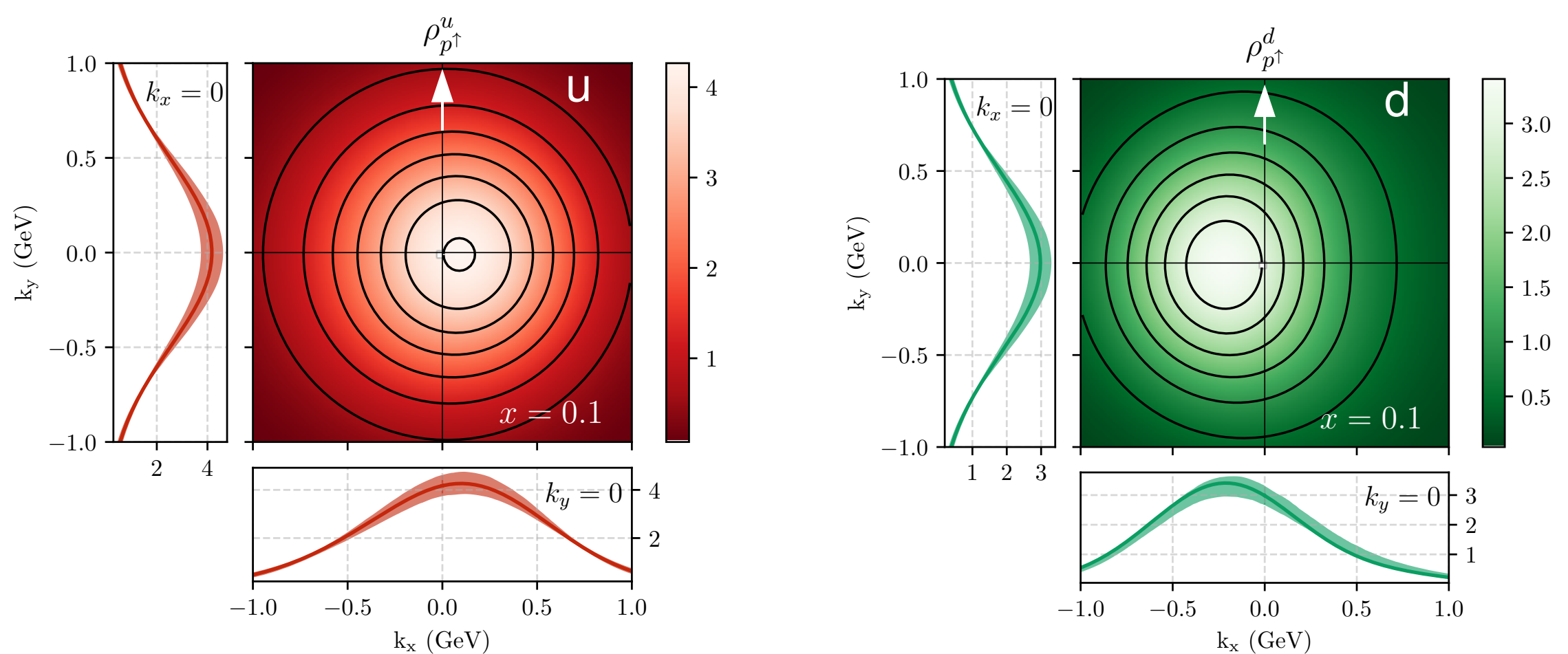




# The various dimensions of the nucleon structure

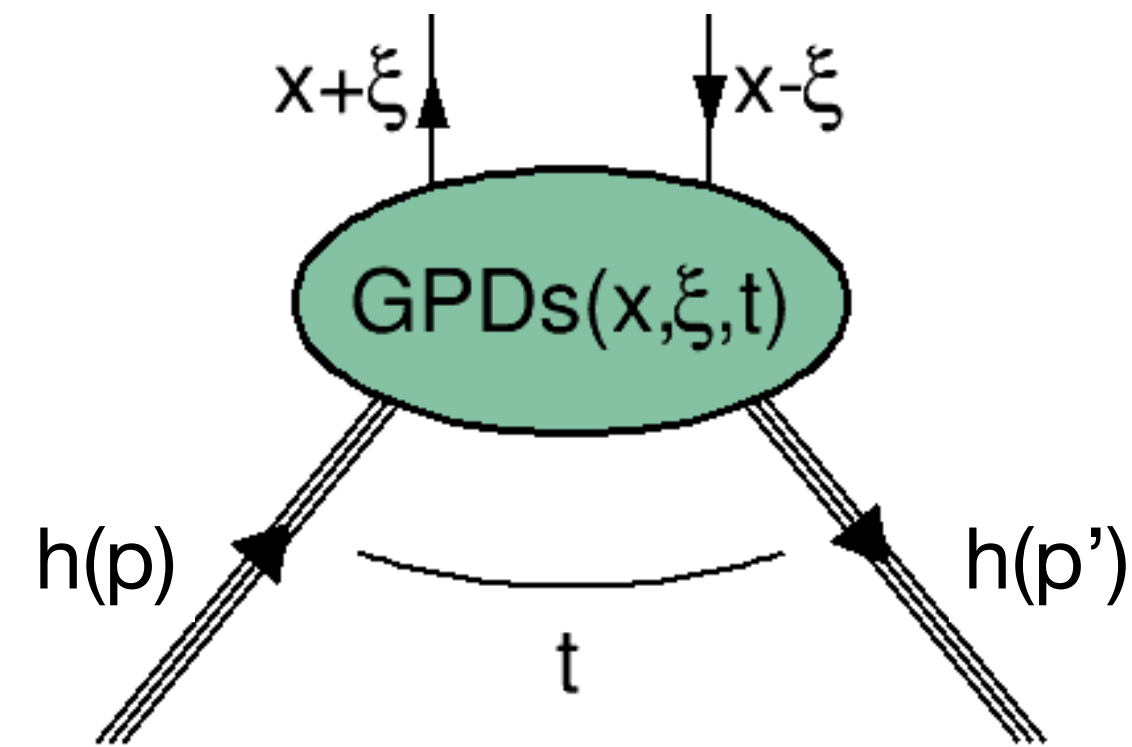


PRD 92 ('00) 071503  
Int. J. Mod Phys. A 18 ('03) 173



# What are generalised parton distributions (GPDs)?

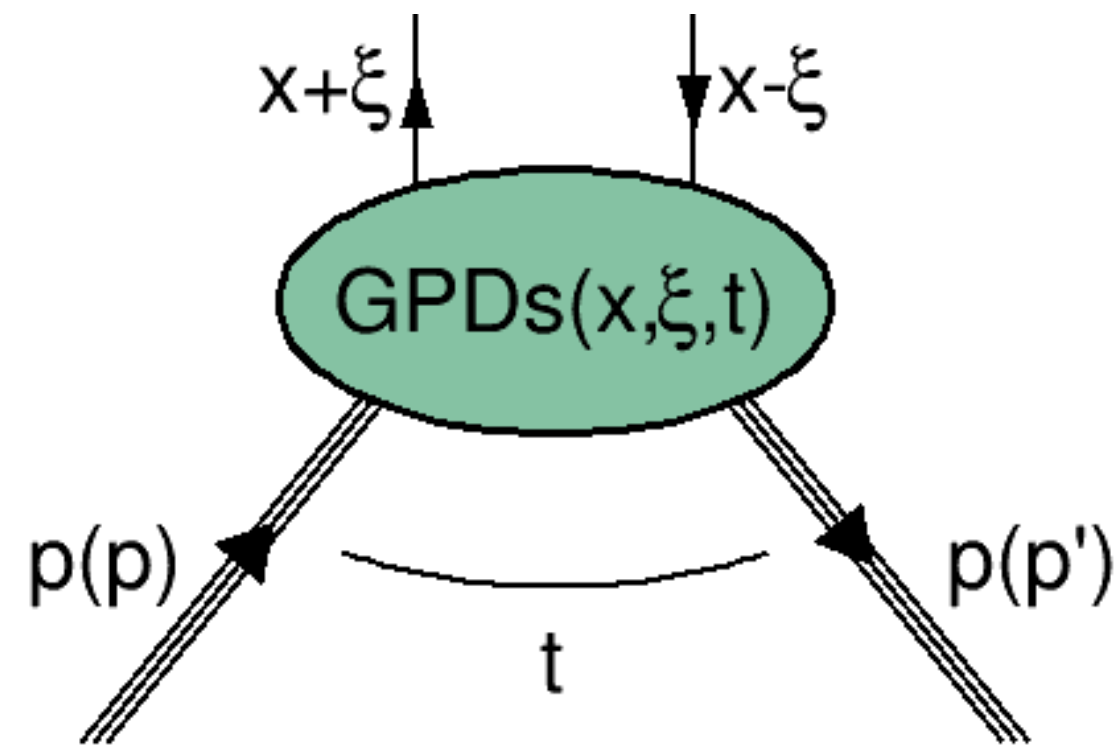
GPDs are probability amplitudes



- $x$ =average longitudinal momentum fraction
- $2\xi$ =longitudinal momentum transfer
- $t$ =squared momentum transfer to hadron
  
- experimental access to  $t$  and  $\xi$
- in general: no experimental access to  $x$

# What are generalised parton distributions (GPDs)?

GPDs are probability amplitudes



- $x$ =average longitudinal momentum fraction
- $2\xi$ =longitudinal momentum transfer
- $t$ =squared momentum transfer to hadron
- experimental access to  $t$  and  $\xi$
- in general: no experimental access to  $x$

- for spin-1/2 hadron:

Four parton helicity-conserving twist-2 GPDs

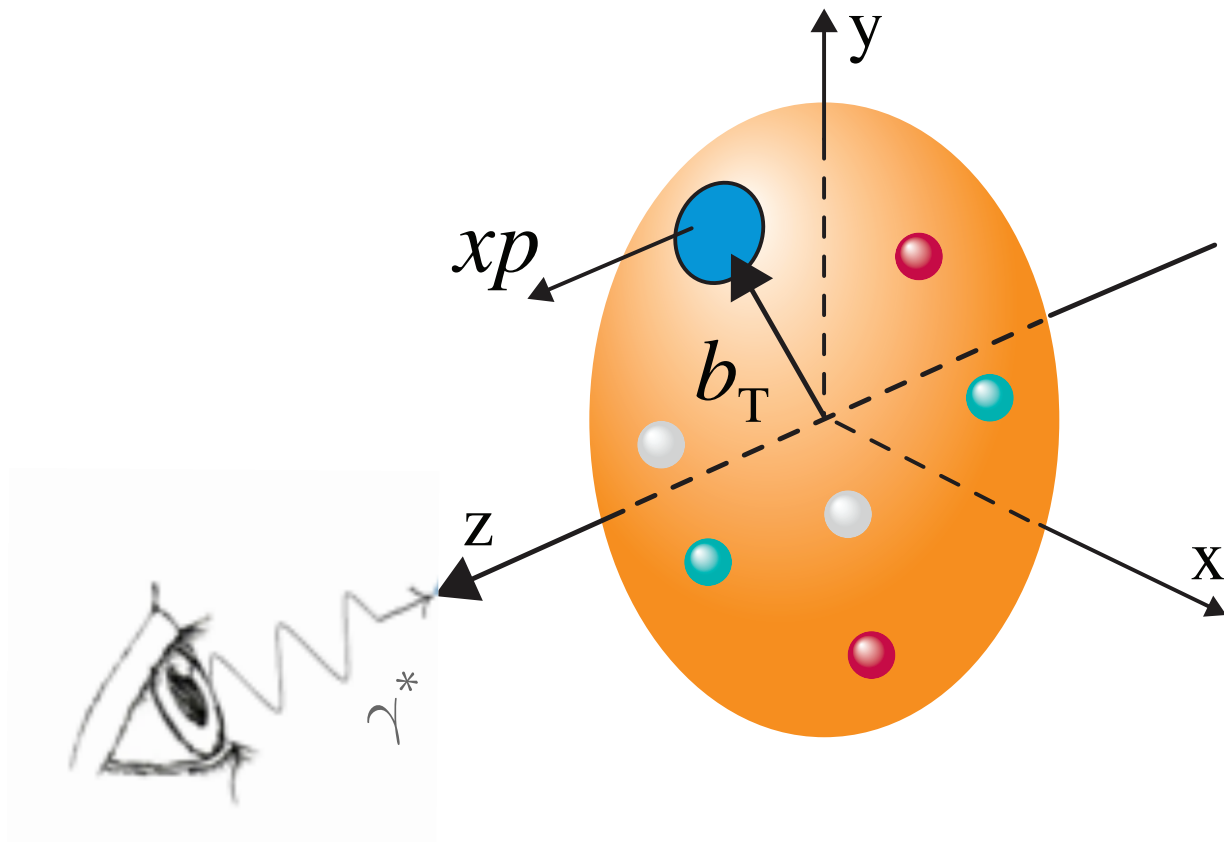
$H(x, \xi, t)$	$E(x, \xi, t)$	parton-spin independent
$\tilde{H}(x, \xi, t)$	$\tilde{E}(x, \xi, t)$	parton-spin dependent
proton helicity non flip	proton helicity flip	

Four parton helicity-flip twist-2 GPDs

$H_T(x, \xi, t)$	$E_T(x, \xi, t)$
$\tilde{H}_T(x, \xi, t)$	$\tilde{E}_T(x, \xi, t)$

# What GPDs tell us about the nucleon

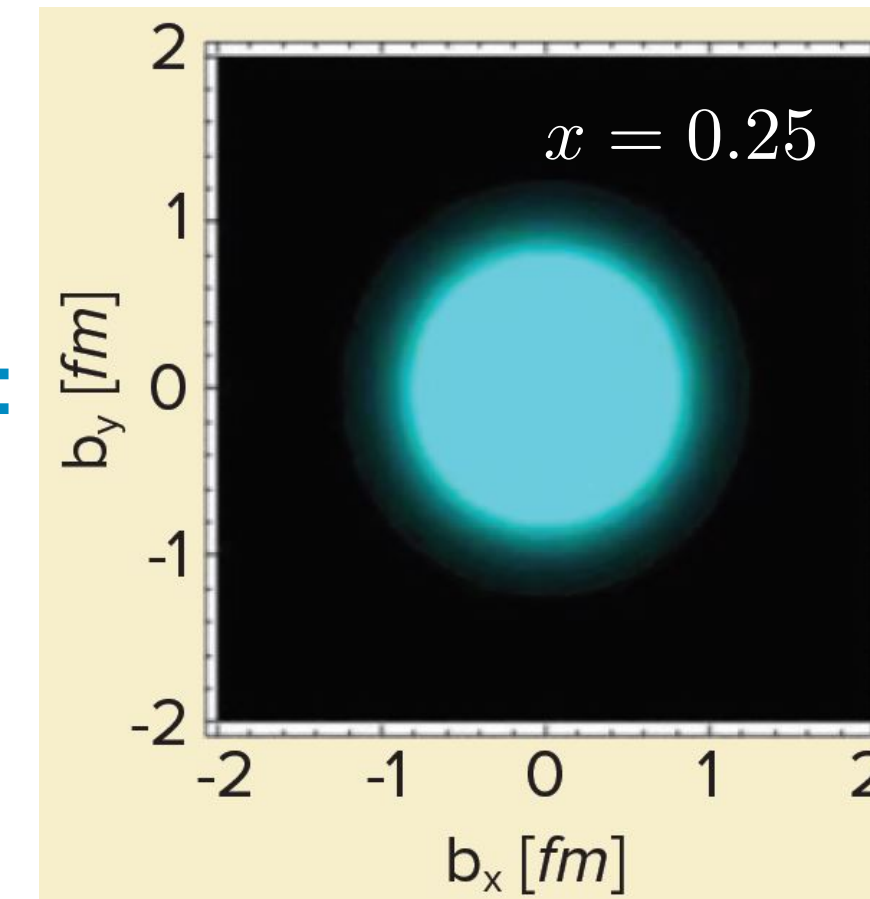
- 3D parton distributions



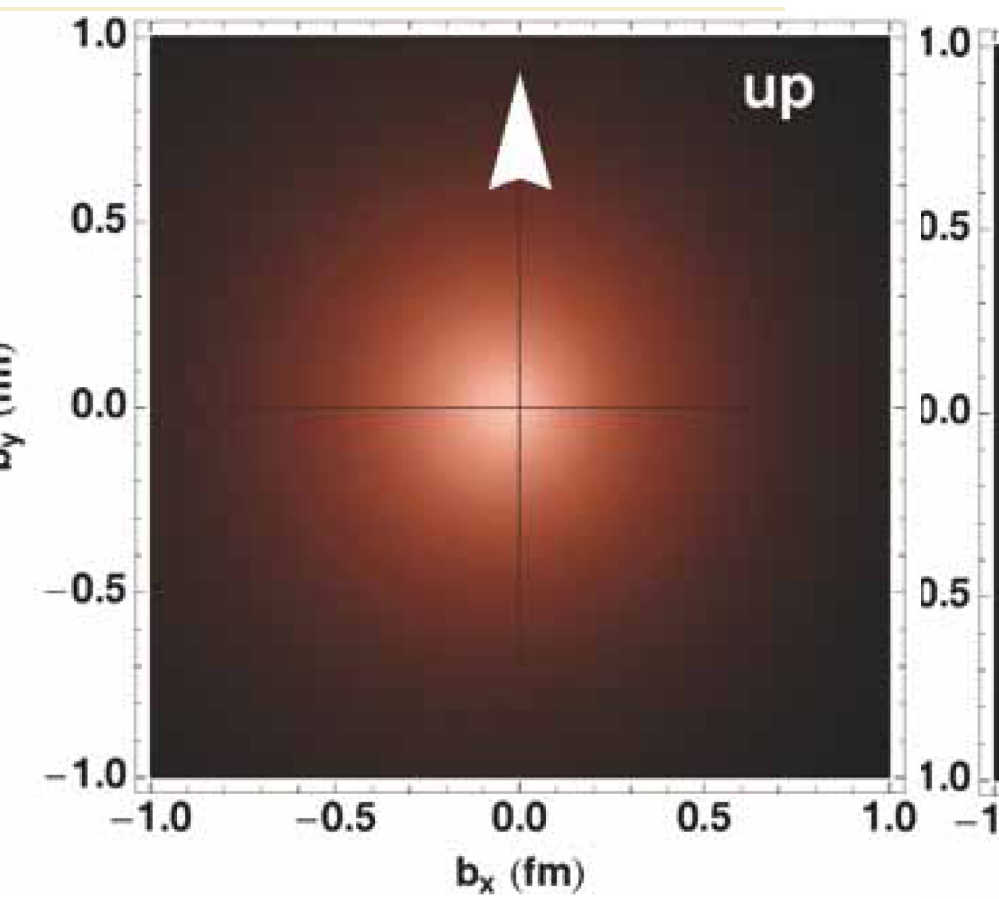
M. Burkardt, PRD **92** ('00) 071503  
Int. J. Mod Phys. A **18** ('03) 173

impact-parameter dependent distributions:  
probability to find parton  $(x, b_T)$

↑ Fourier  
transform for  $\xi=0$   
GPDs



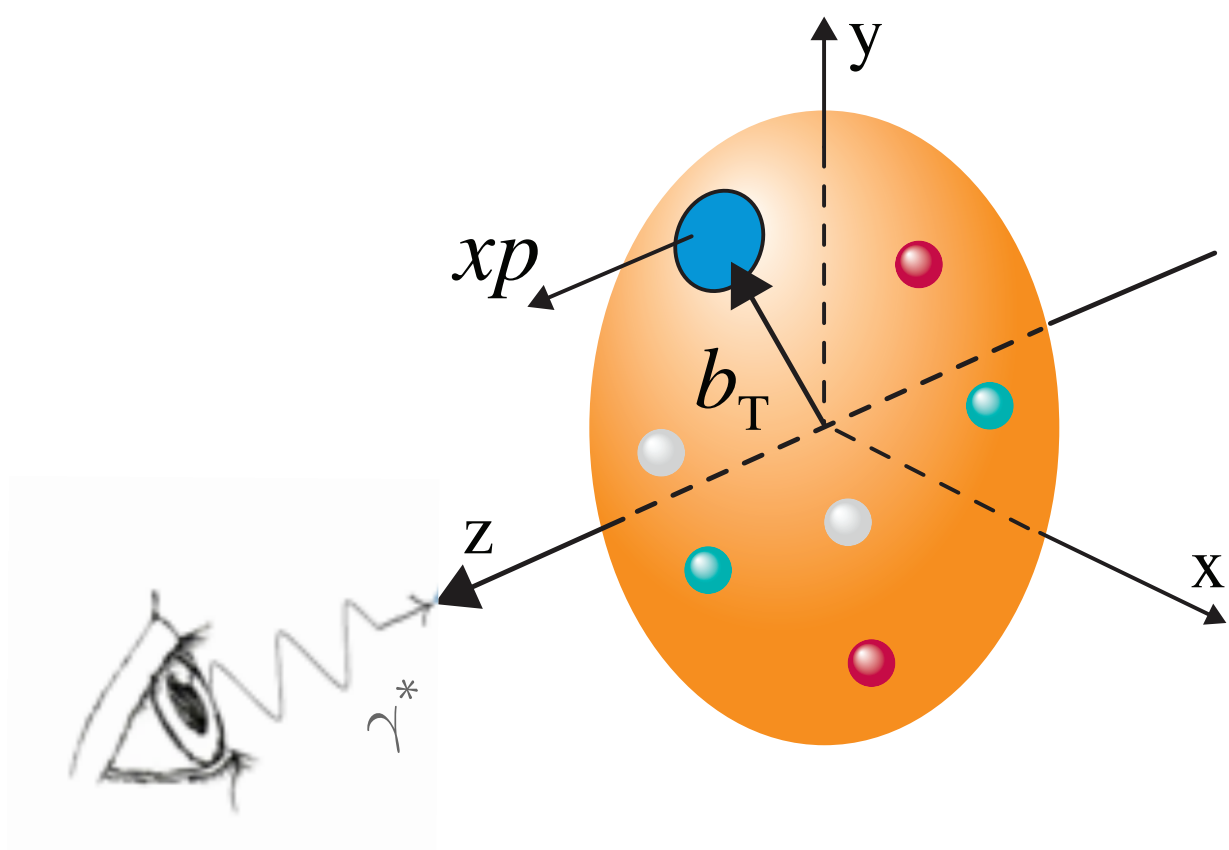
GPD H



GPDs H+E

# What GPDs tell us about the nucleon

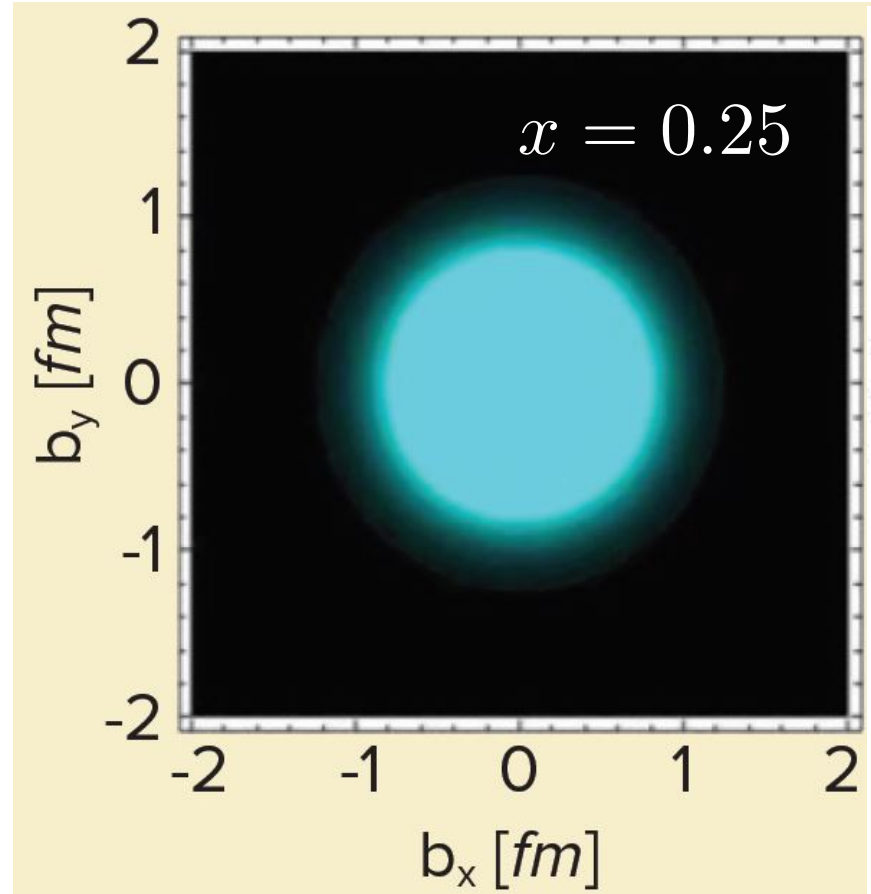
- 3D parton distributions



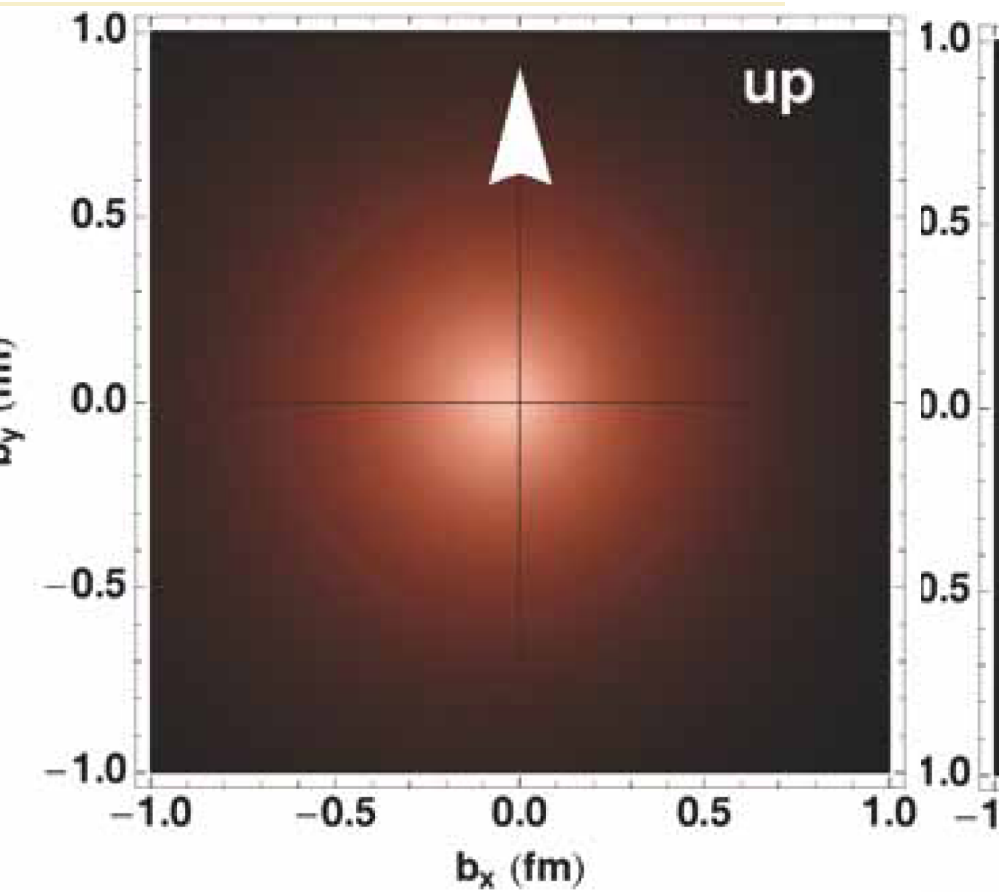
M. Burkardt, PRD **92** ('00) 071503  
 Int. J. Mod Phys. A **18** ('03) 173

impact-parameter dependent distributions:  
 probability to find parton  $(x, b_T)$

Fourier transform for  $\xi=0$   
 ↑  
 GPDs



GPD H



GPDs H+E

- pressure distributions

GPDs

↓  $\int dx x$

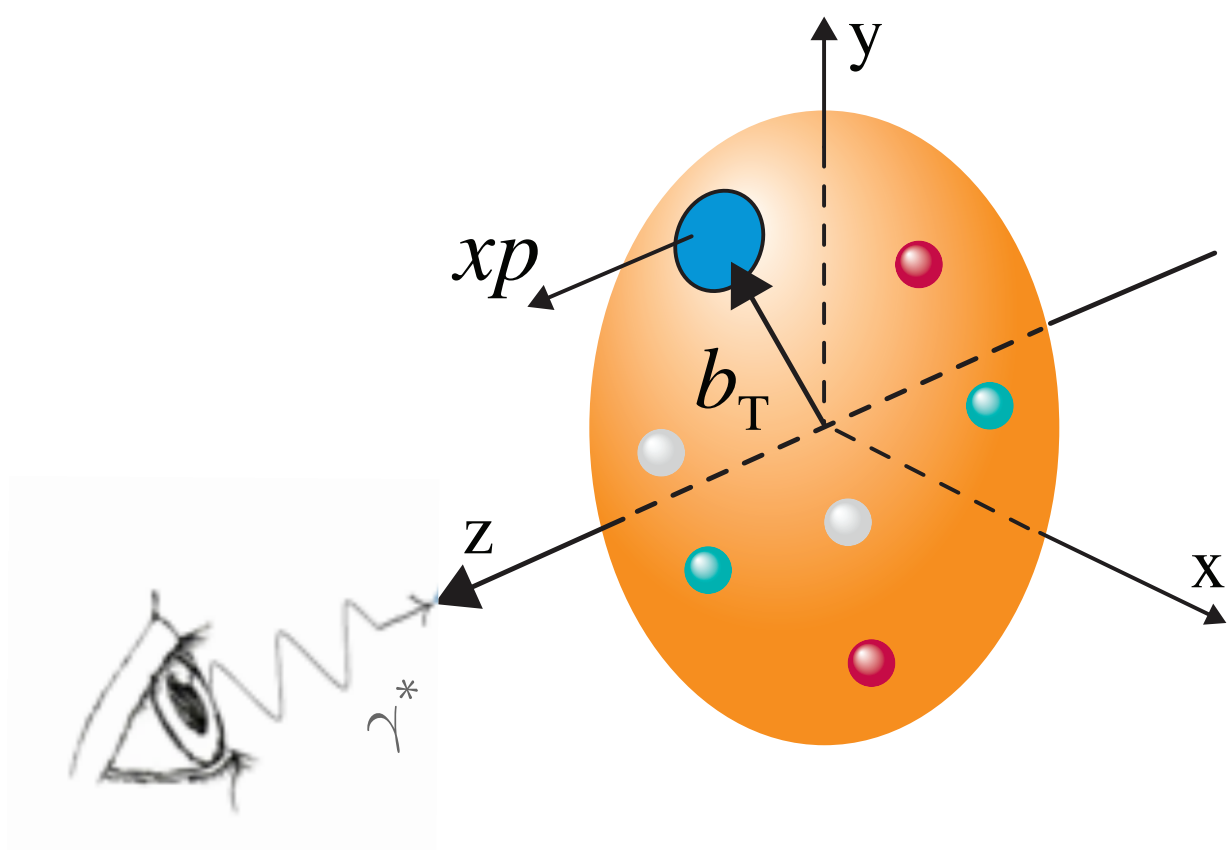
gravitational form factors

↓ Fourier transform

pressure distributions

# What GPDs tell us about the nucleon

- 3D parton distributions

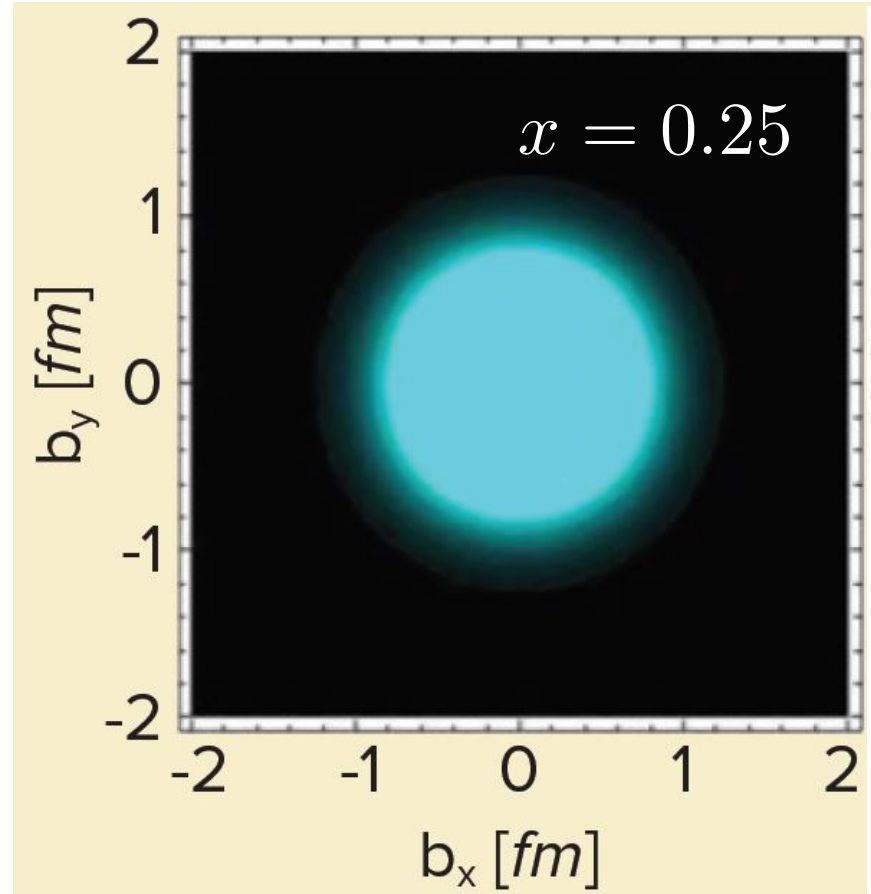


M. Burkardt, PRD **92** ('00) 071503  
 Int. J. Mod Phys. A **18** ('03) 173

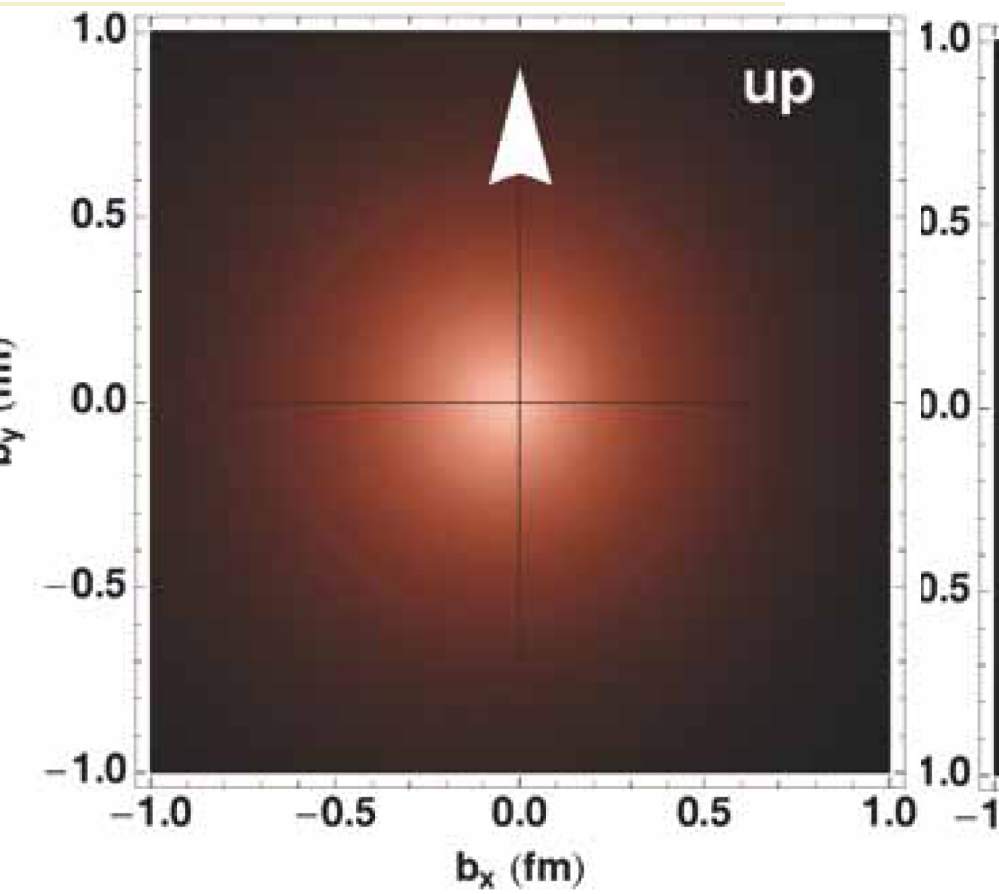
impact-parameter dependent distributions:  
 probability to find parton  $(x, b_T)$

Fourier transform for  $\xi=0$

GPDs



GPD H



GPDs H+E

- pressure distributions

GPDs

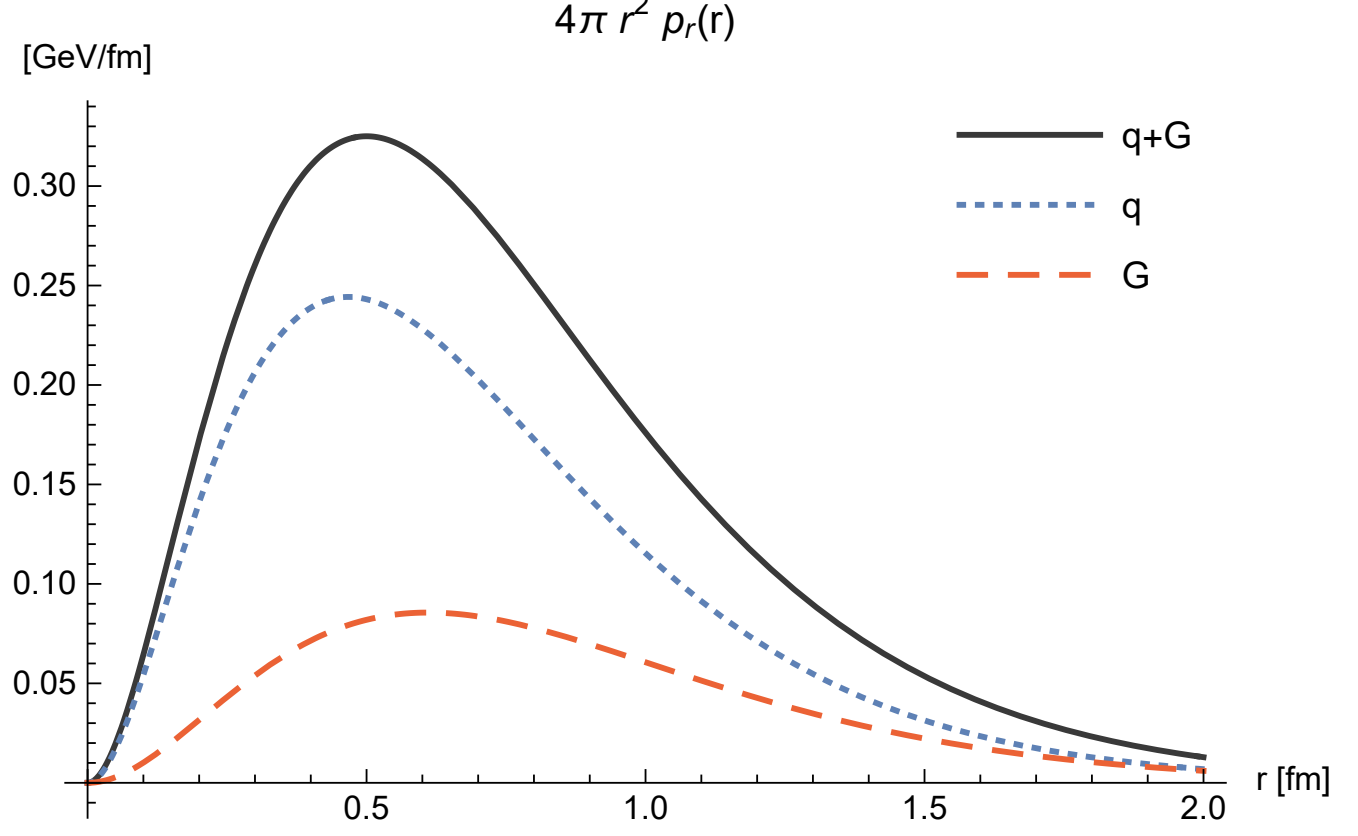
$$\int dx x$$

gravitational form factors

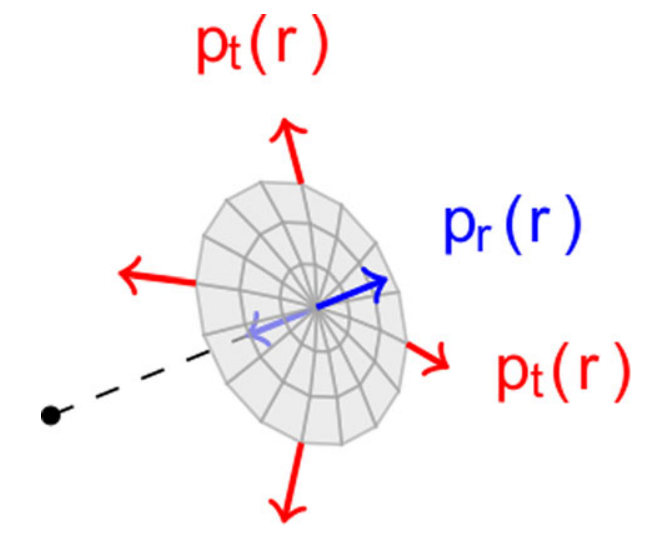
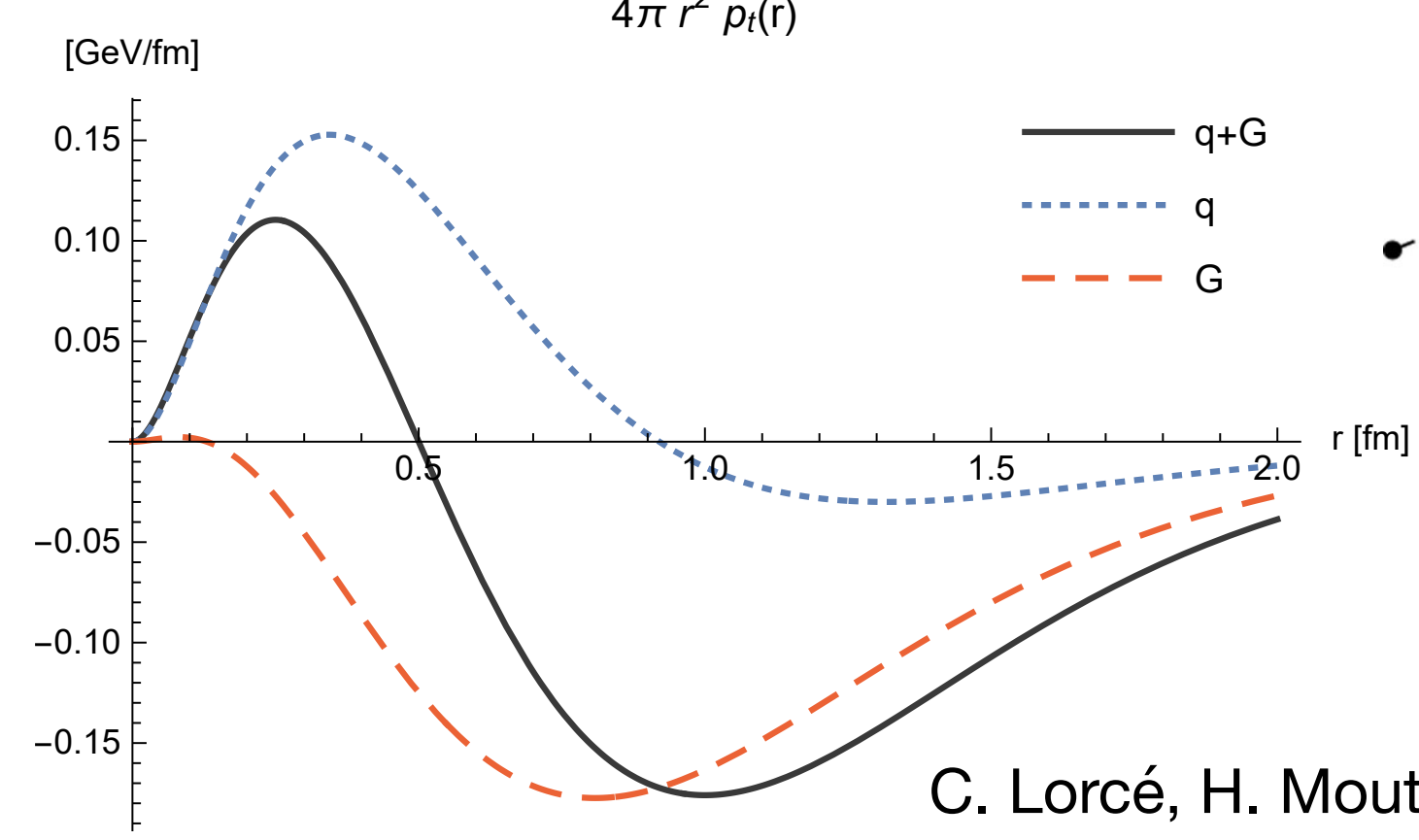
Fourier transform

pressure distributions

radial pressure



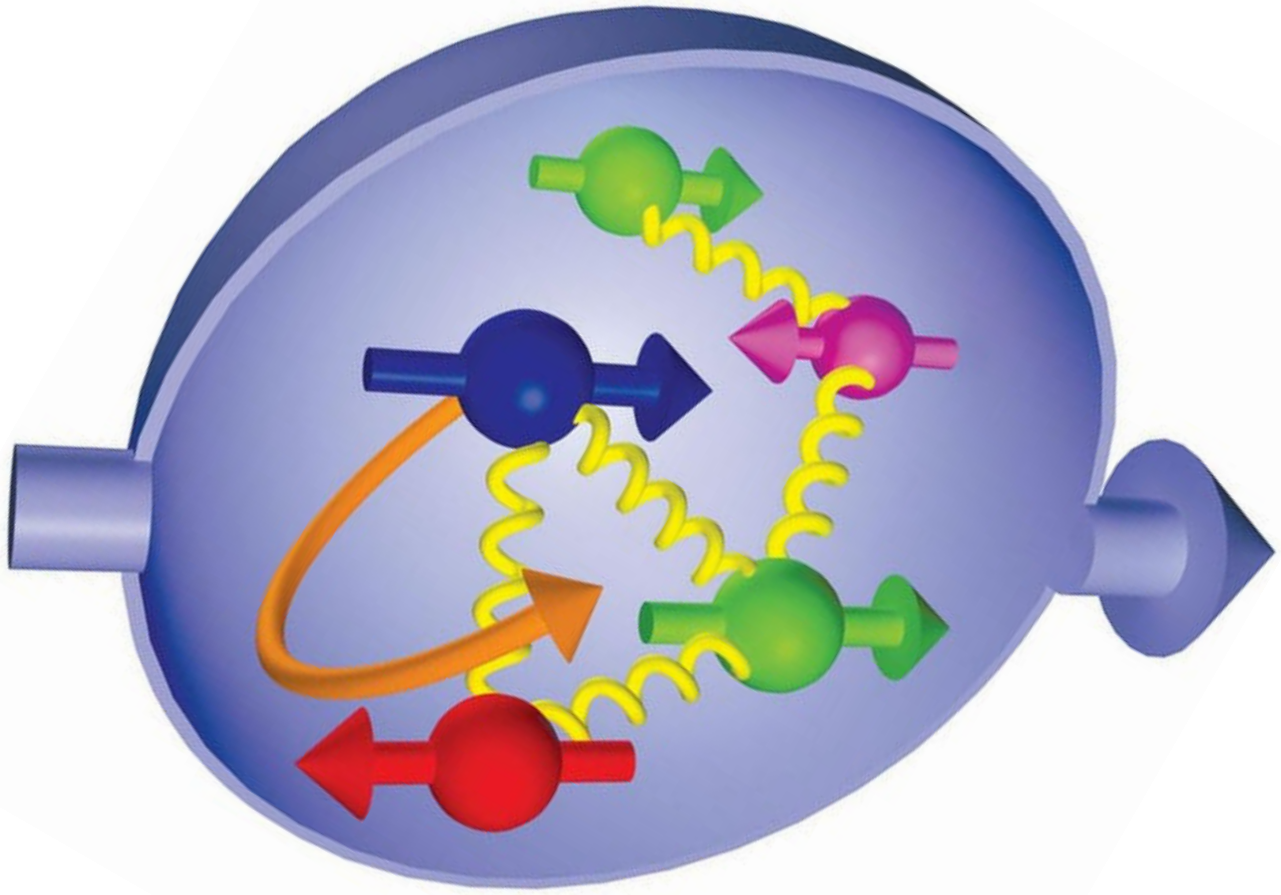
tangential pressure



C. Lorcé, H. Moutarde, A. P. Trawiński  
 Eur. Phys. J. C **79** ('19) 89

# ... and its spin

longitudinally polarised nucleon



proton spin

$$\frac{1}{2} = \frac{1}{2} \sum_q \Delta q + \sum_q L^q + J^G$$

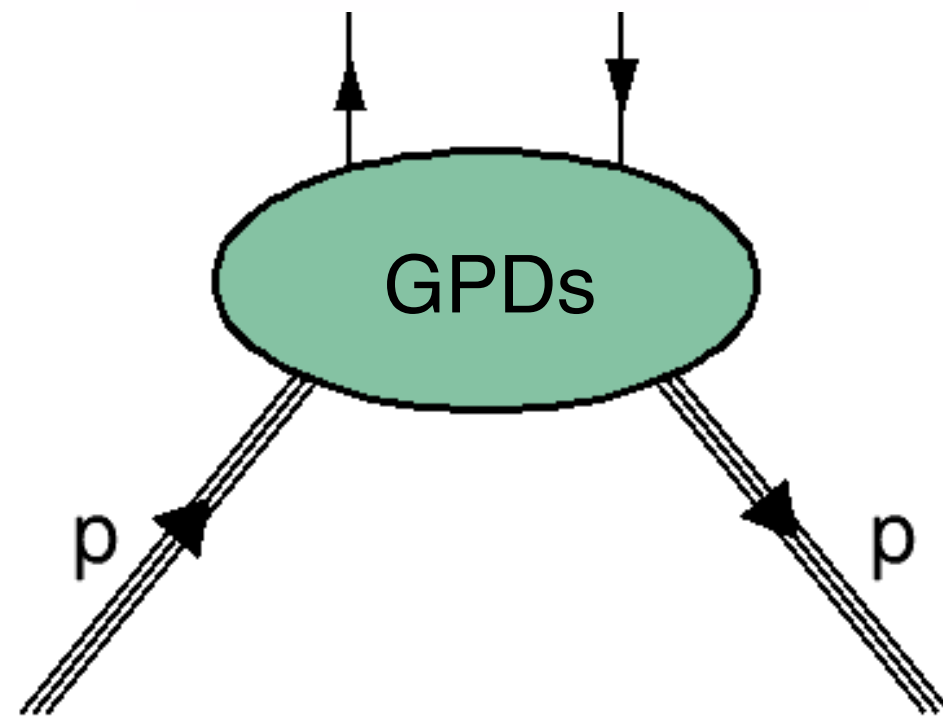
quark spin
quark orbital
gluon  

angular momentum
angular momentum  
30%
?
?

$$J = \lim_{t \rightarrow 0} \frac{1}{2} \int_{-1}^1 dx x [H(x, \xi, t) + E(x, \xi, t)]$$

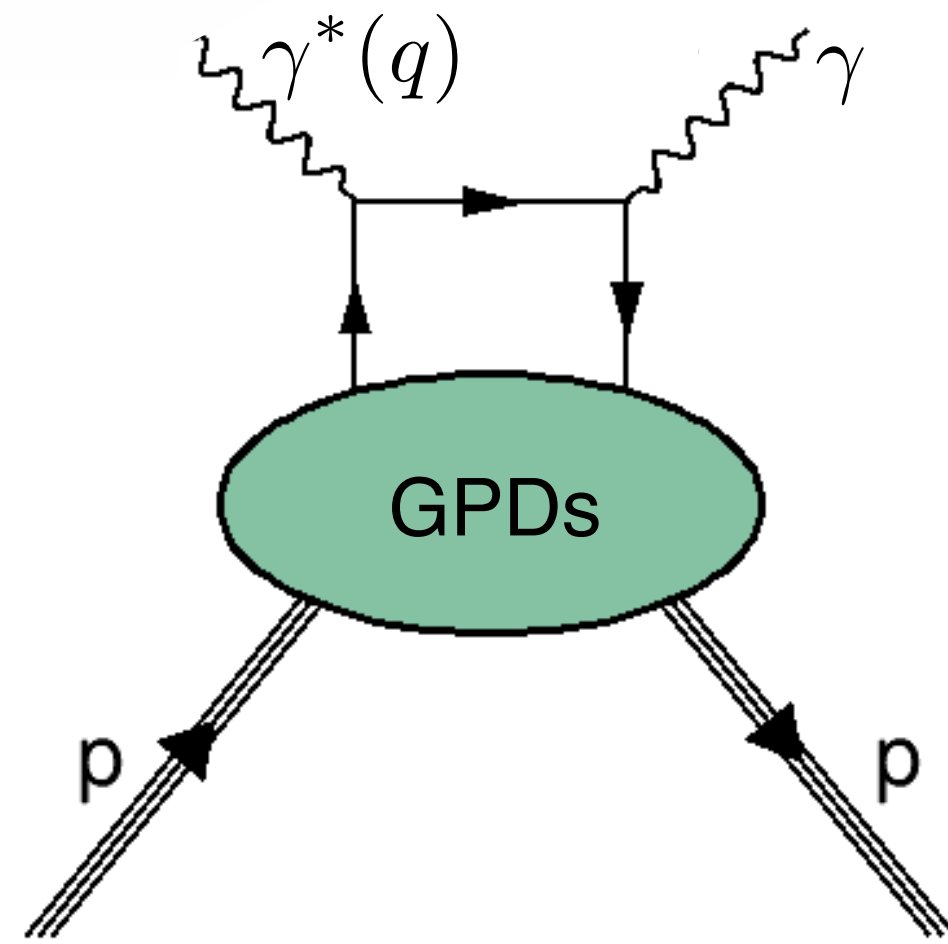
X. Ji, Phys. Rev. Lett. 78 (1997) 610

# Experimental access to GPDs



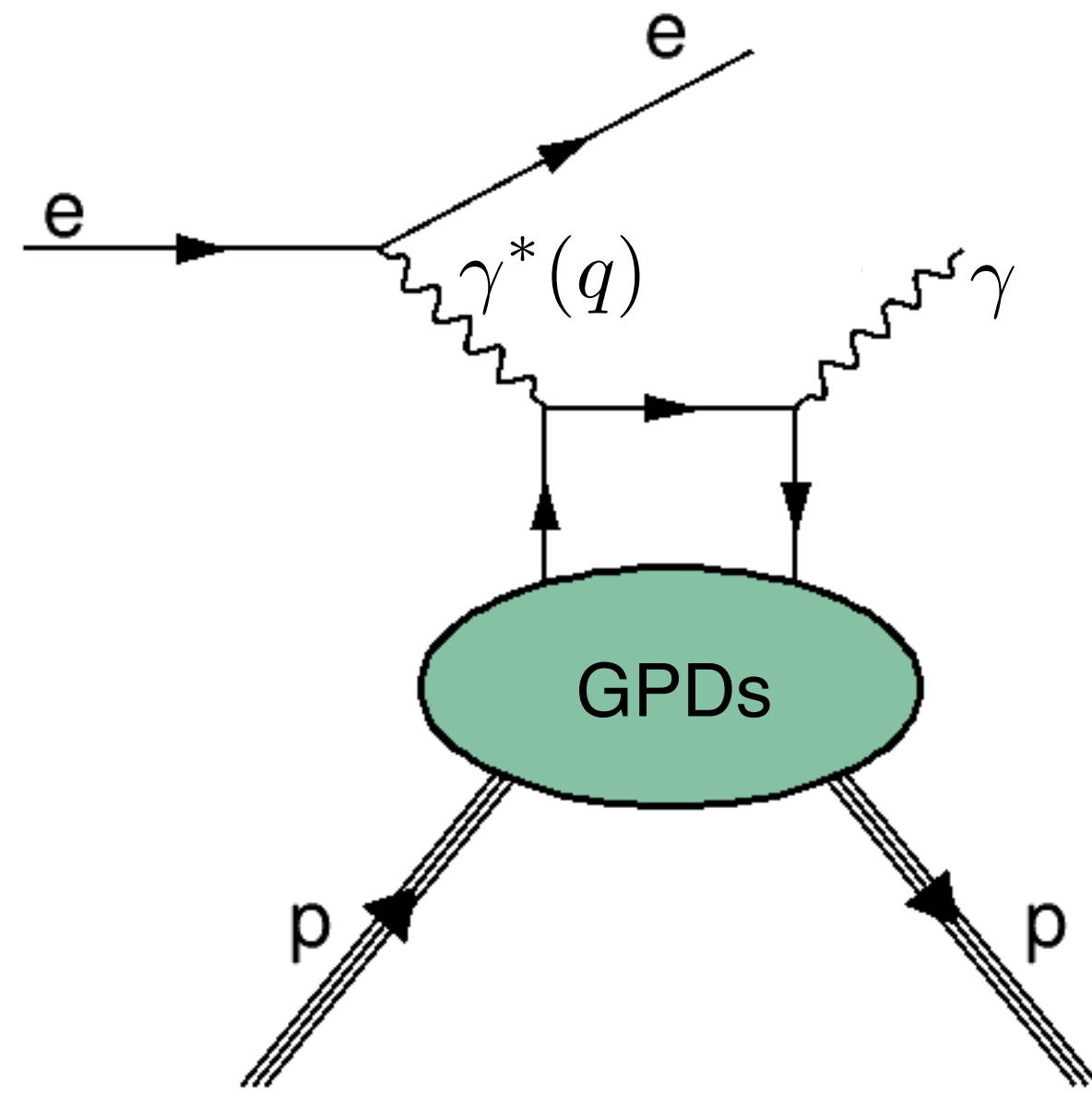


# Experimental access to GPDs



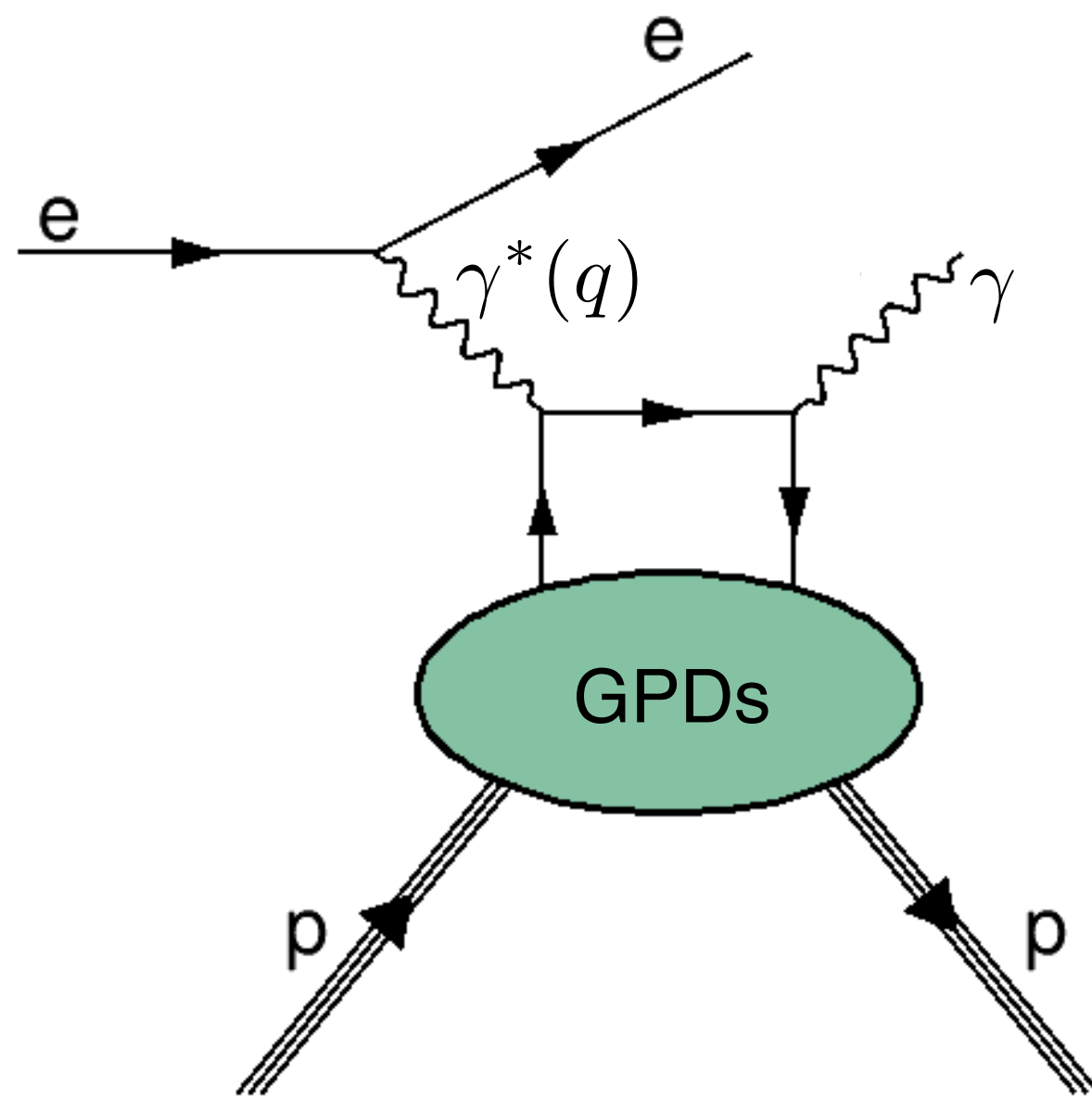
Deeply virtual Compton scattering (DVCS)  
Hard scale=large  $Q^2=-q^2$

# Experimental access to GPDs



Deeply virtual Compton scattering (DVCS)  
Hard scale=large  $Q^2=-q^2$

# Experimental access to GPDs



Deeply virtual Compton scattering (DVCS)  
Hard scale=large  $Q^2=-q^2$

CLAS – PRC 80 ('09) 035206; PRL 87 ('01) 182002; 100 ('08) 162002

COMPASS – arXiv:1702.06315

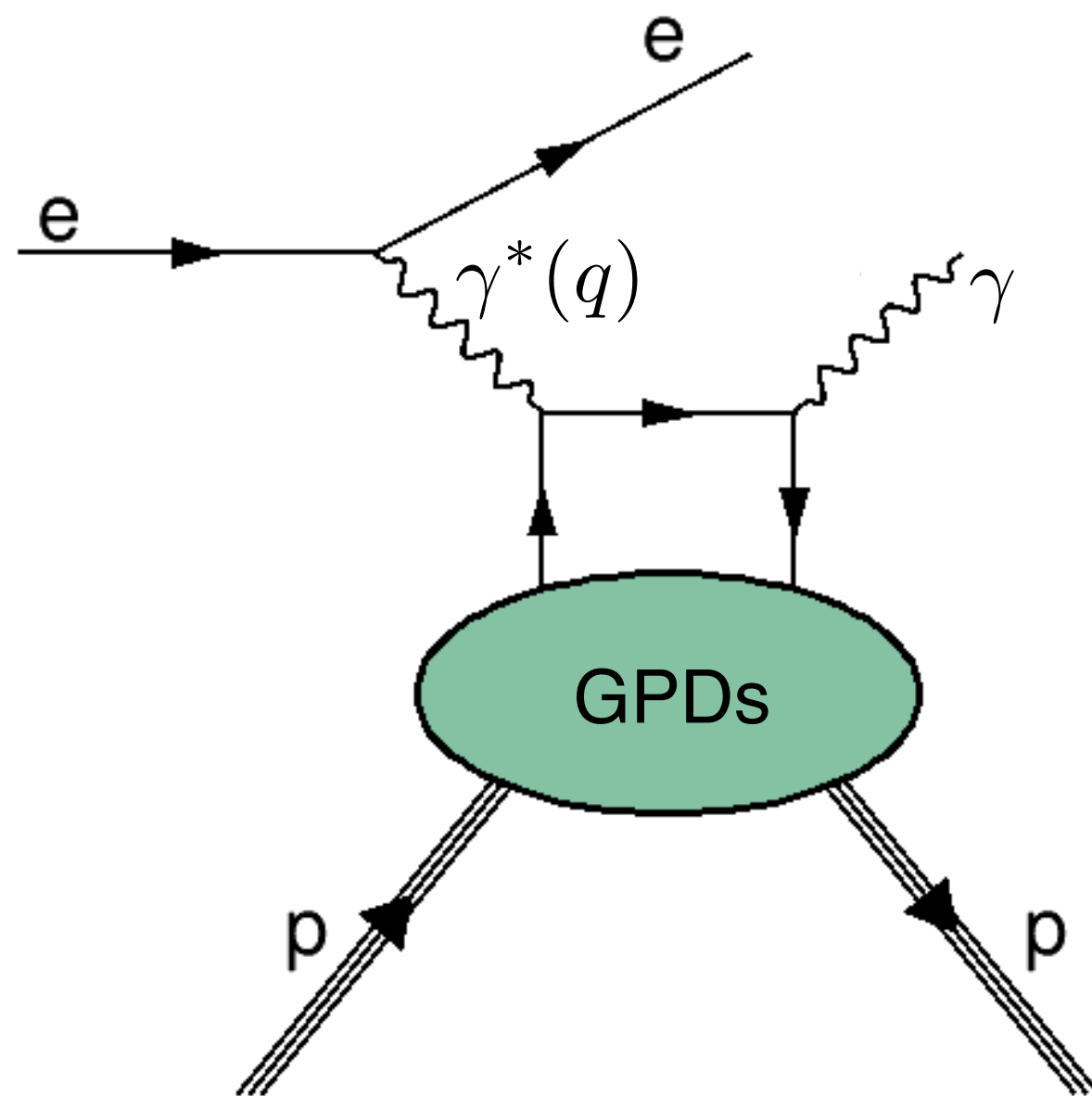
JLab Hall A Collaboration – PRL 99 ('07) 242501; PRC 92 ('15) 055202; Nat. Com. **8** ('17) 1408

HERMES – JHEP 10 ('12) 042; PLB 704 ('11) 15; NPB 842 ('11) 265

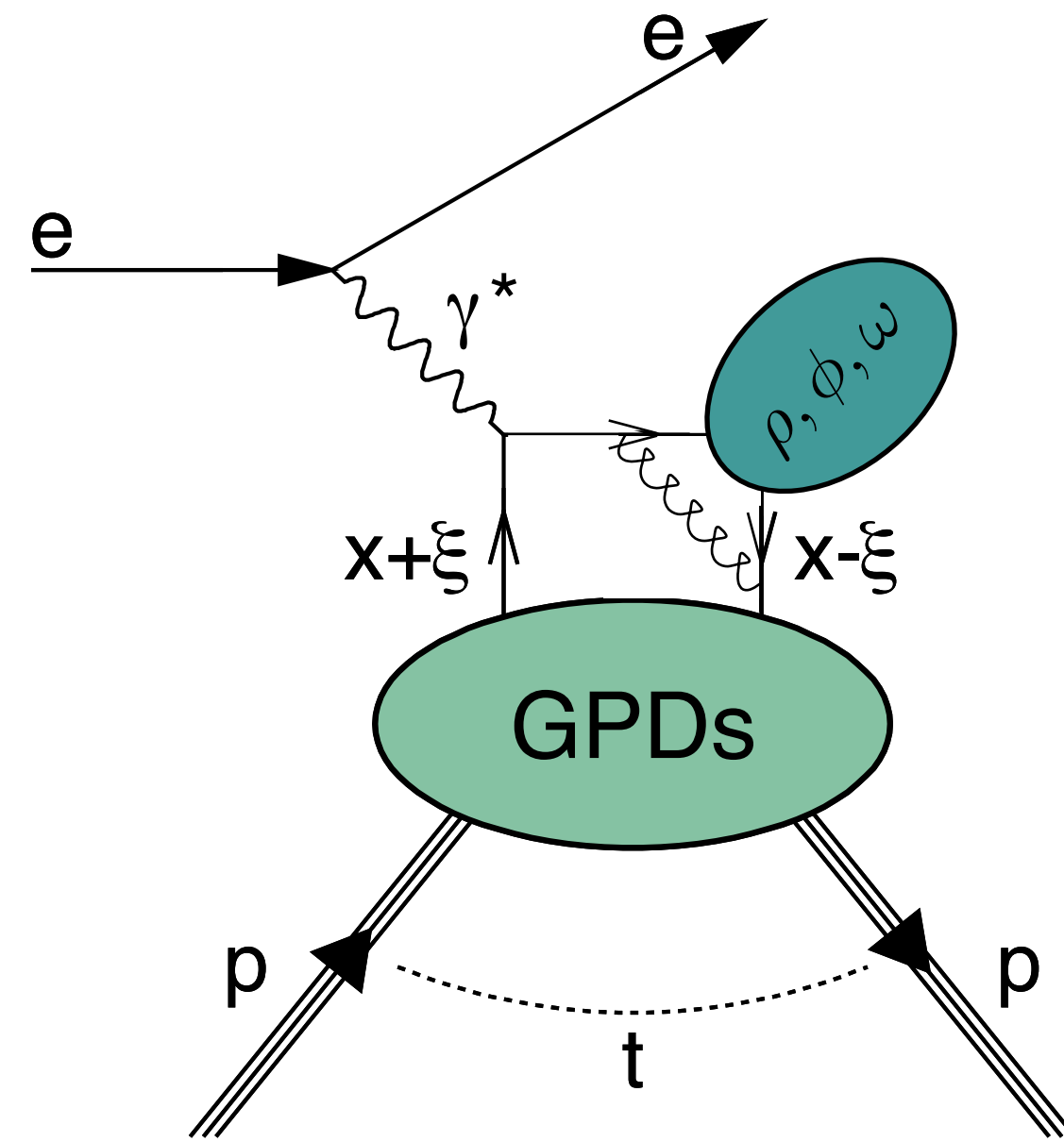
H1 – PLB 681 ('09) 391; 659 ('07) 796; EPJ C 44 ('05) 1

ZEUS – PLB 573 (2003) 46; JHEP 05 ('09) 108

# Experimental access to GPDs



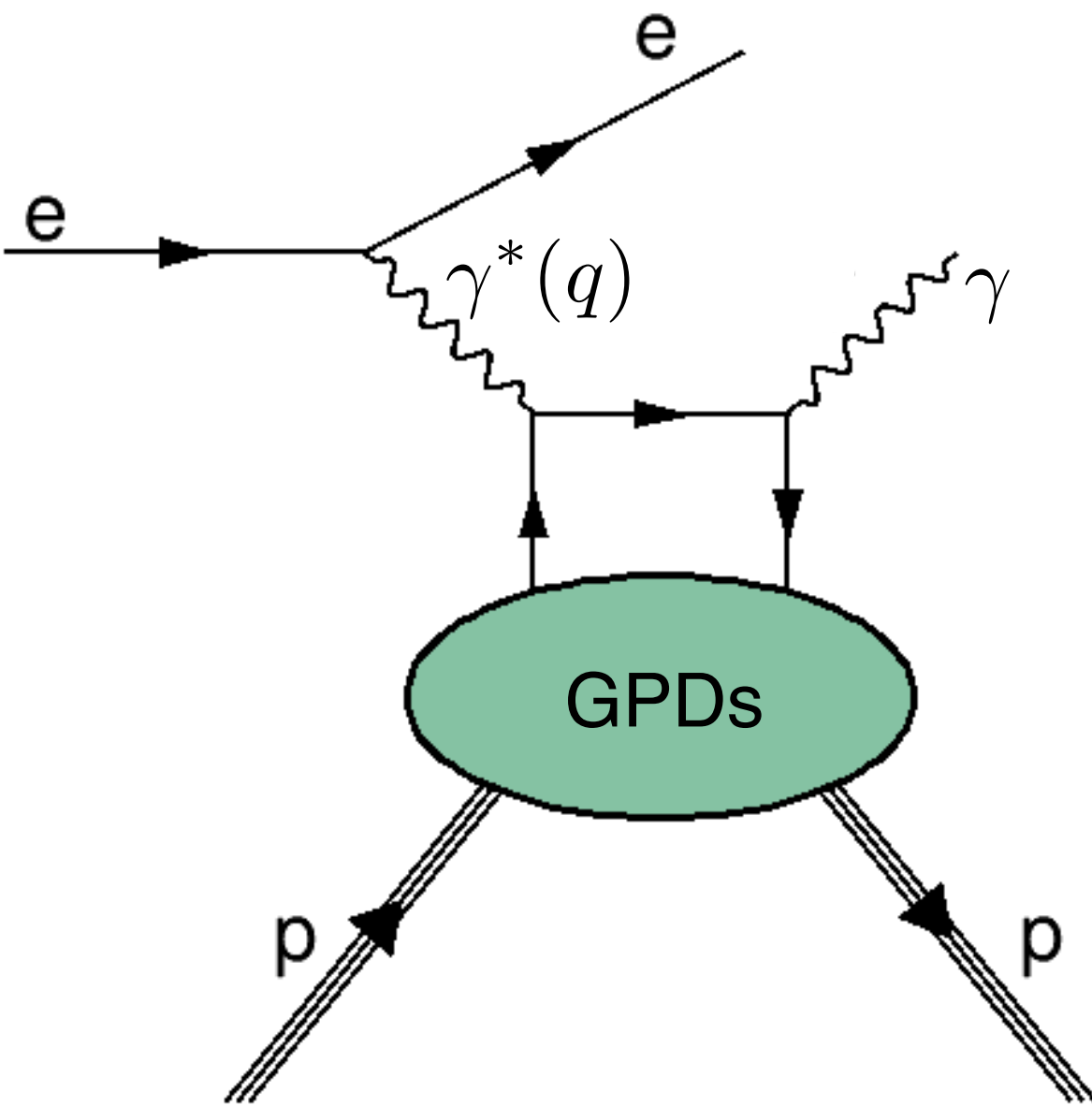
Deeply virtual Compton scattering (DVCS)  
Hard scale=large  $Q^2=-q^2$



Hard exclusive meson production  
Hard scale=large  $Q^2$

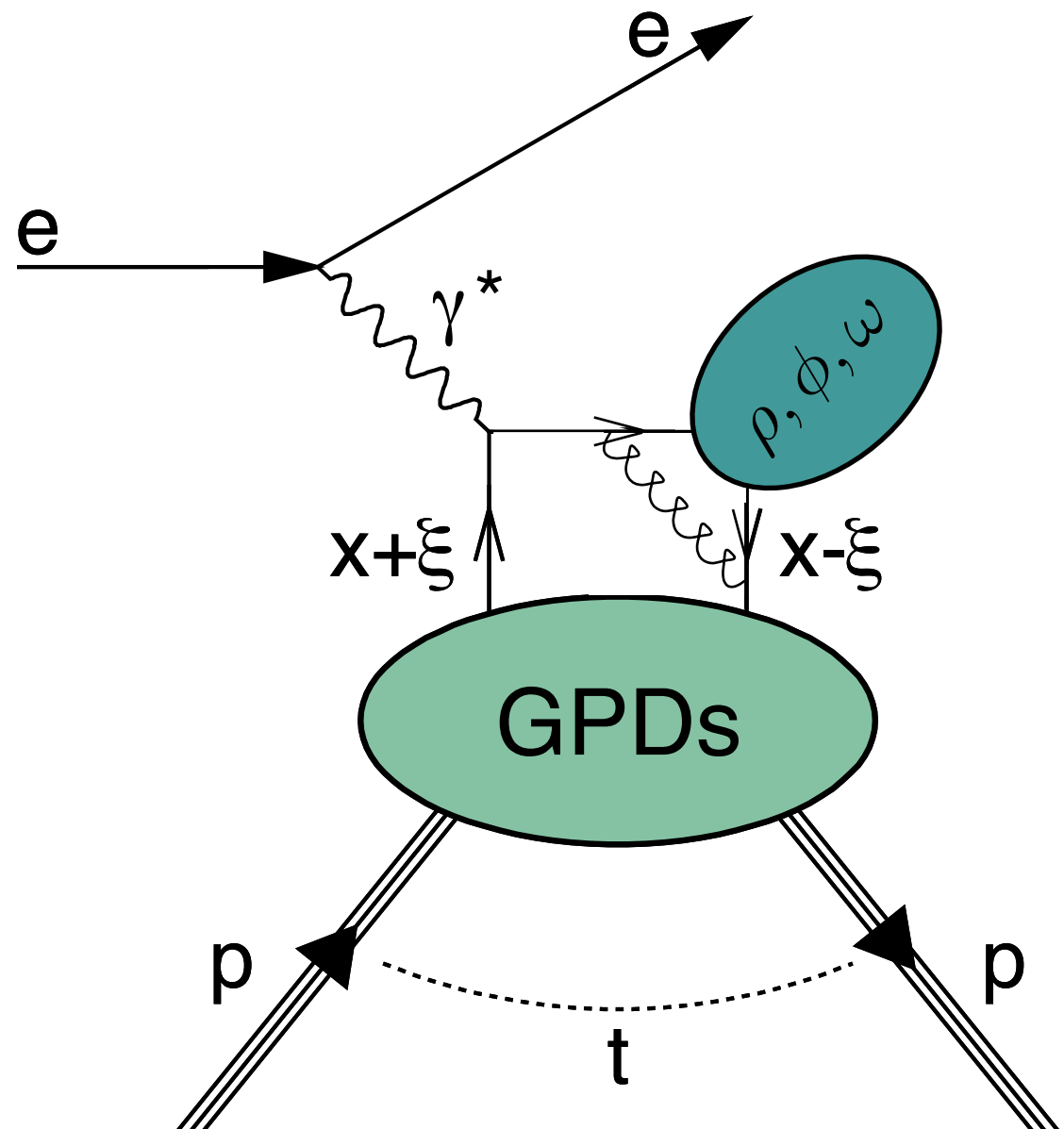
CLAS – PRC 80 ('09) 035206; PRL 87 ('01) 182002; 100 ('08) 162002  
 COMPASS – arXiv:1702.06315  
 JLab Hall A Collaboration – PRL 99 ('07) 242501; PRC 92 ('15) 055202; Nat. Com. 8 ('17) 1408  
 HERMES – JHEP 10 ('12) 042; PLB 704 ('11) 15; NPB 842 ('11) 265  
 H1 – PLB 681 ('09) 391; 659 ('07) 796; EPJ C 44 ('05) 1  
 ZEUS – PLB 573 (2003) 46; JHEP 05 ('09) 108

# Experimental access to GPDs



Deeply virtual Compton scattering (DVCS)  
 Hard scale=large  $Q^2=-q^2$

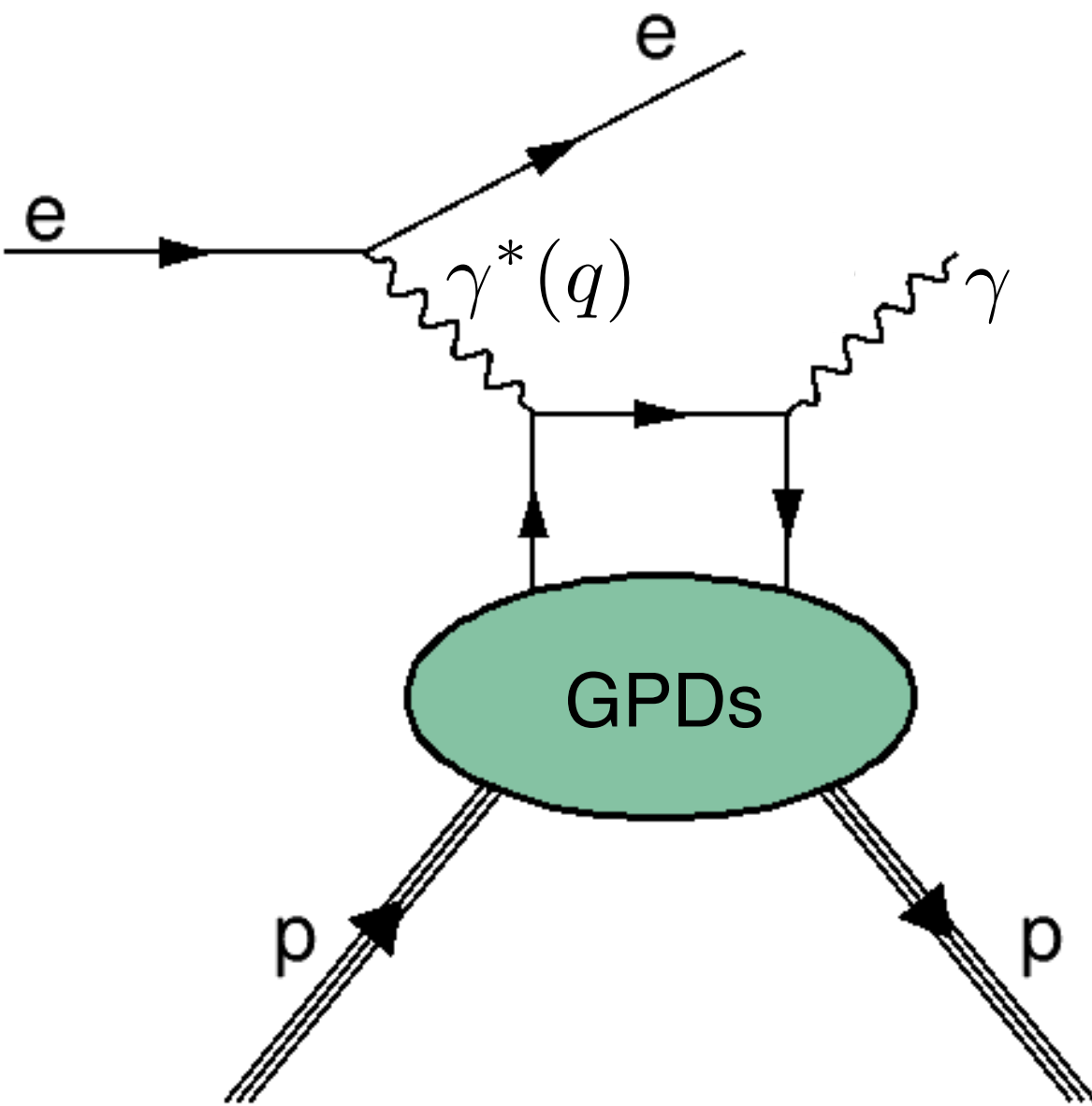
CLAS – PRC 80 ('09) 035206; PRL 87 ('01) 182002; 100 ('08) 162002  
 COMPASS – arXiv:1702.06315  
 JLab Hall A Collaboration – PRL 99 ('07) 242501; PRC 92 ('15) 055202; Nat. Com. 8 ('17) 1408  
 HERMES – JHEP 10 ('12) 042; PLB 704 ('11) 15; NPB 842 ('11) 265  
 H1 – PLB 681 ('09) 391; 659 ('07) 796; EPJ C 44 ('05) 1  
 ZEUS – PLB 573 (2003) 46; JHEP 05 ('09) 108



Hard exclusive meson production  
 Hard scale=large  $Q^2$

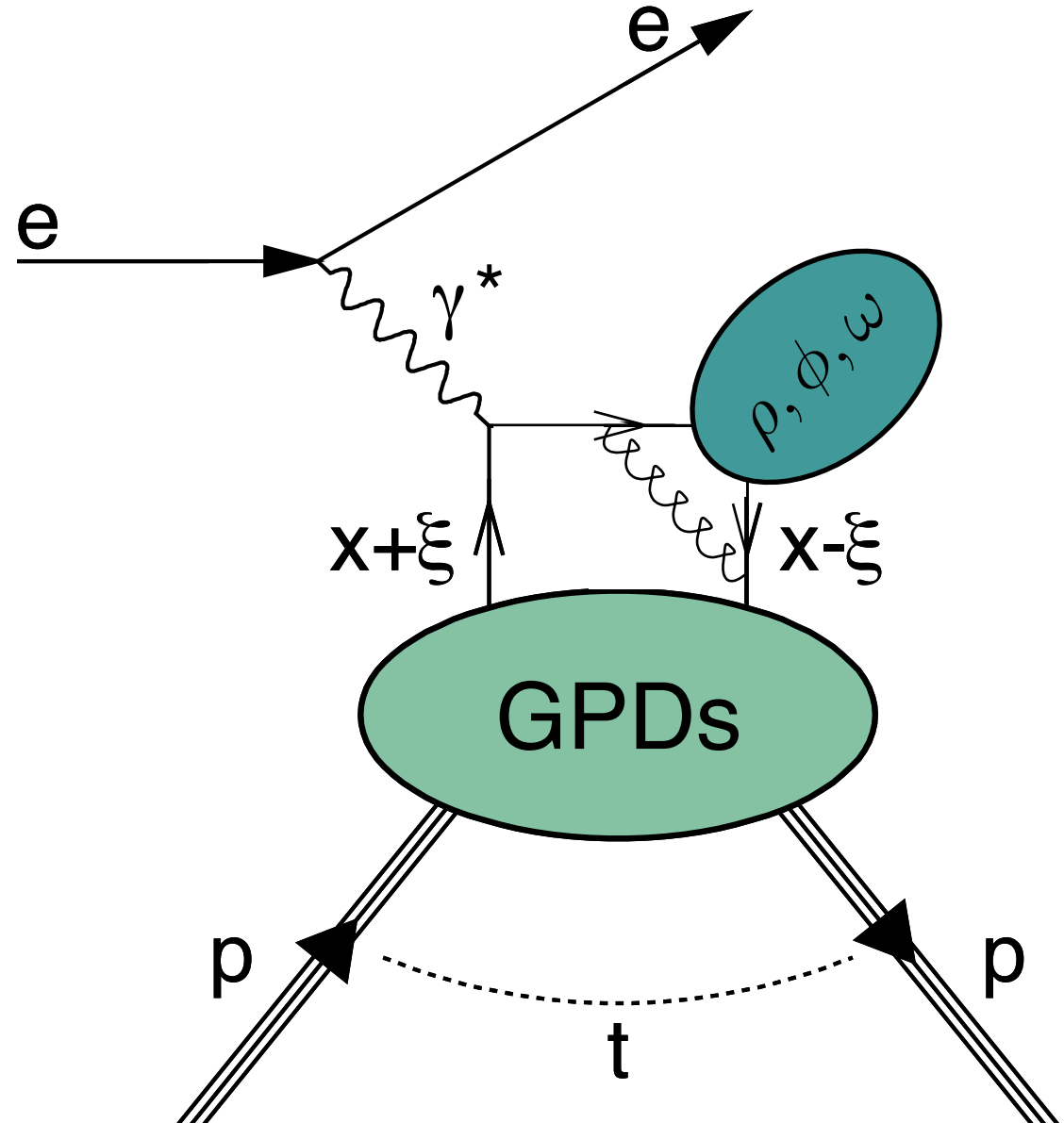
CLAS – PRC 95 ('17) 035207; 95 (2017) 035202  
 COMPASS – PLB 731 ('14) 19; NPB 915 ('17) 454  
 JLab Hall A Collaboration – PRC 83 ('11) 025201  
 HERMES – EPJ C 74 ('14) 3110; 75 ('15) 600; 77 ('17) 378

# Experimental access to GPDs



Deeply virtual Compton scattering (DVCS)  
Hard scale=large  $Q^2=-q^2$

CLAS – PRC 80 ('09) 035206; PRL 87 ('01) 182002; 100 ('08) 162002  
 COMPASS – arXiv:1702.06315  
 JLab Hall A Collaboration – PRL 99 ('07) 242501; PRC 92 ('15) 055202; Nat. Com. 8 ('17) 1408  
 HERMES – JHEP 10 ('12) 042; PLB 704 ('11) 15; NPB 842 ('11) 265  
 H1 – PLB 681 ('09) 391; 659 ('07) 796; EPJ C 44 ('05) 1  
 ZEUS – PLB 573 (2003) 46; JHEP 05 ('09) 108

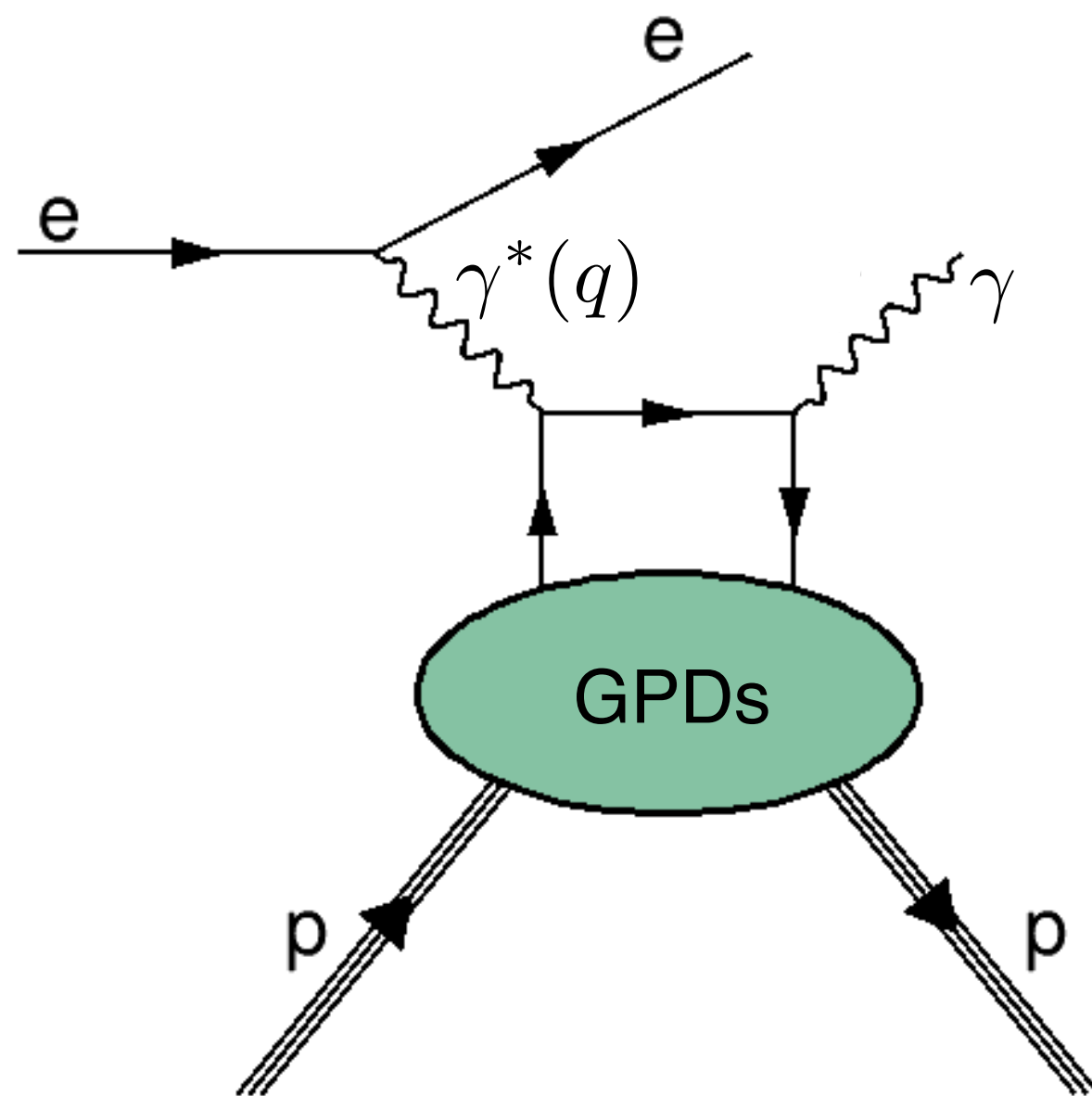


Hard exclusive meson production  
Hard scale=large  $Q^2$

CLAS – PRC 95 ('17) 035207; 95 (2017) 035202  
 COMPASS – PLB 731 ('14) 19; NPB 915 ('17) 454  
 JLab Hall A Collaboration – PRC 83 ('11) 025201  
 HERMES – EPJ C 74 ('14) 3110; 75 ('15) 600; 77 ('17) 378

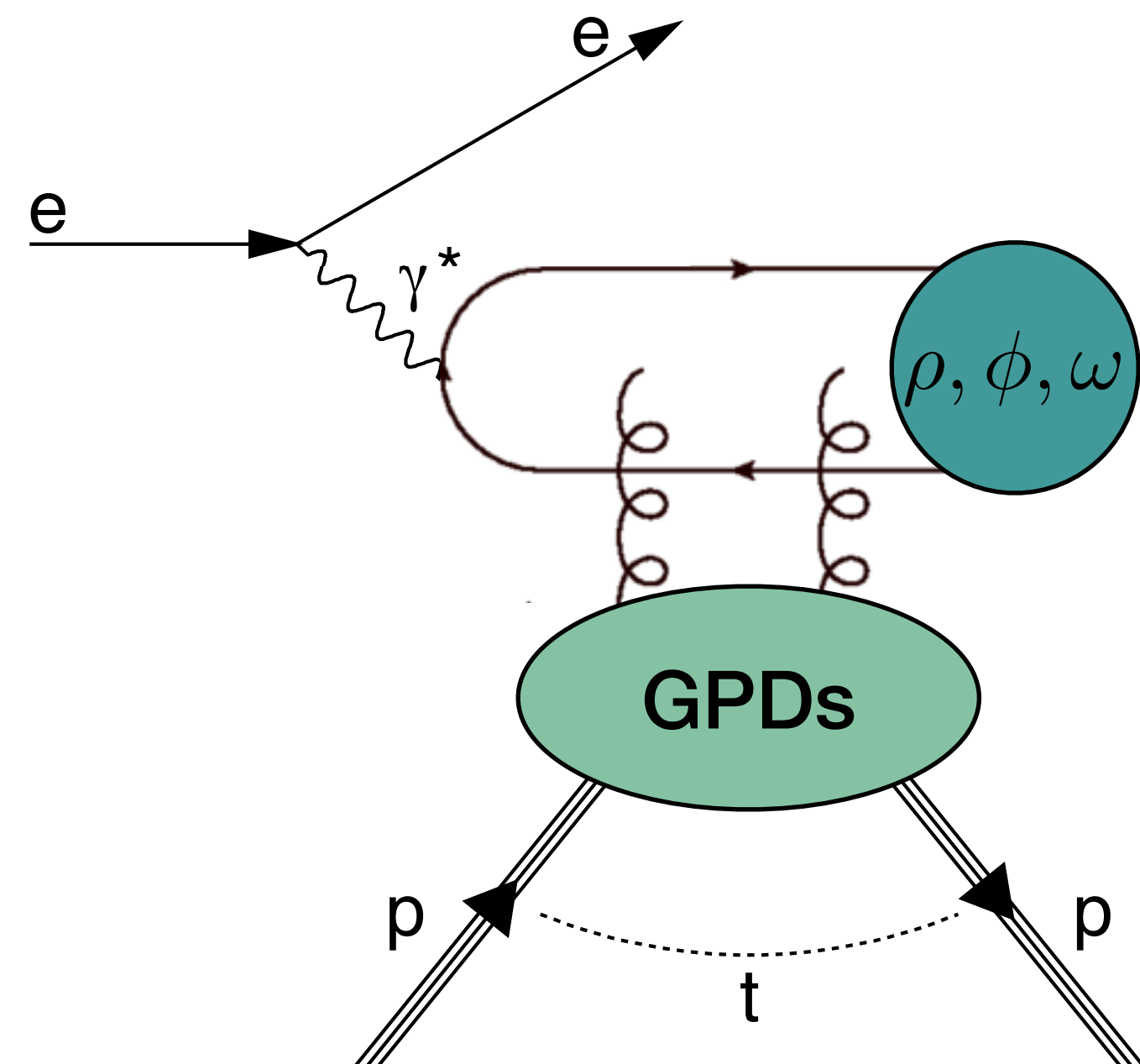
fixed target: medium/large  $x_B$ , quarks

# Experimental access to GPDs



Deeply virtual Compton scattering (DVCS)  
Hard scale=large  $Q^2=-q^2$

CLAS – PRC 80 ('09) 035206; PRL 87 ('01) 182002; 100 ('08) 162002  
 COMPASS – arXiv:1702.06315  
 JLab Hall A Collaboration – PRL 99 ('07) 242501; PRC 92 ('15) 055202; Nat. Com. 8 ('17) 1408  
 HERMES – JHEP 10 ('12) 042; PLB 704 ('11) 15; NPB 842 ('11) 265  
 H1 – PLB 681 ('09) 391; 659 ('07) 796; EPJ C 44 ('05) 1  
 ZEUS – PLB 573 (2003) 46; JHEP 05 ('09) 108

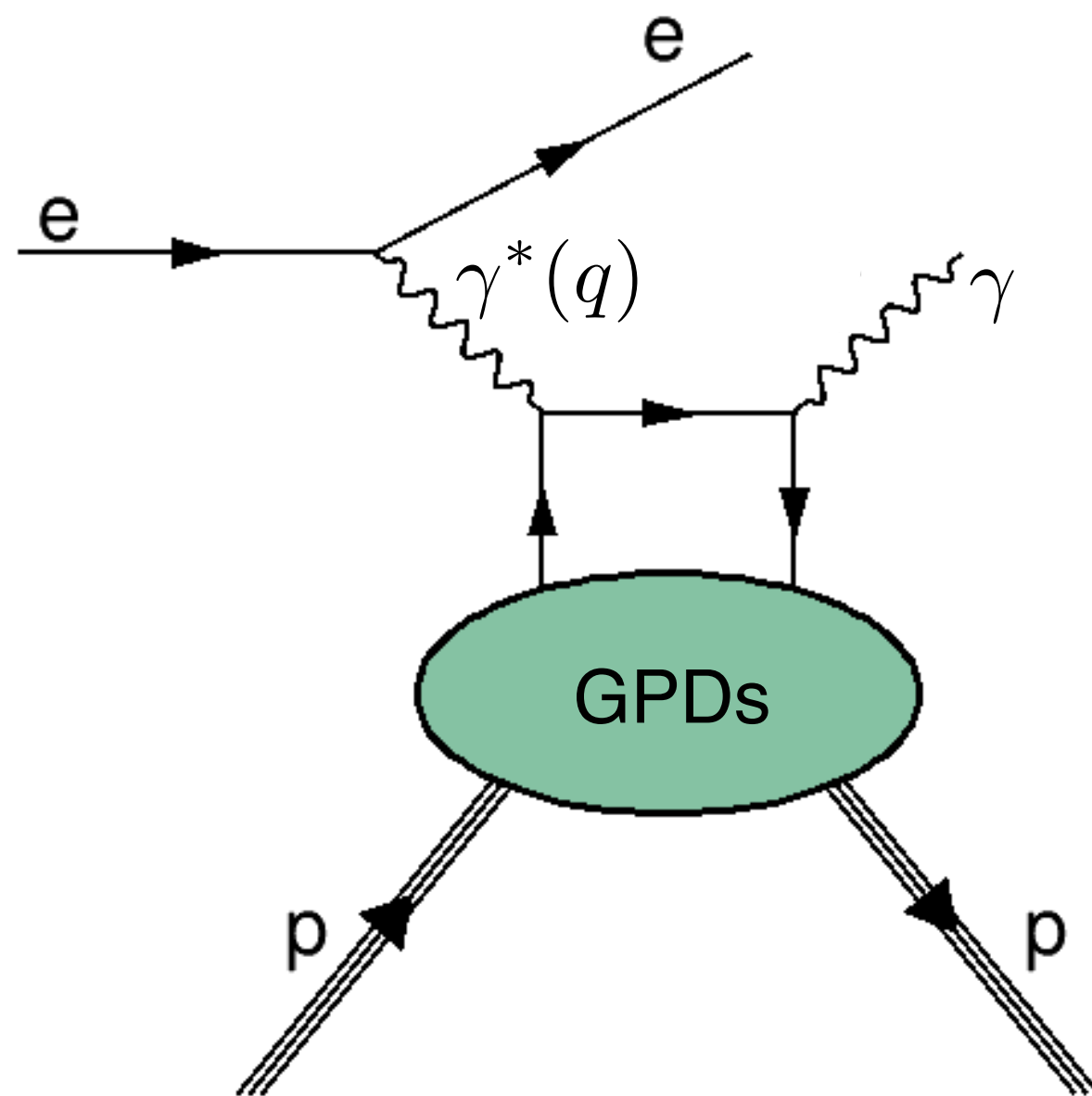


Hard exclusive meson production  
Hard scale=large  $Q^2$

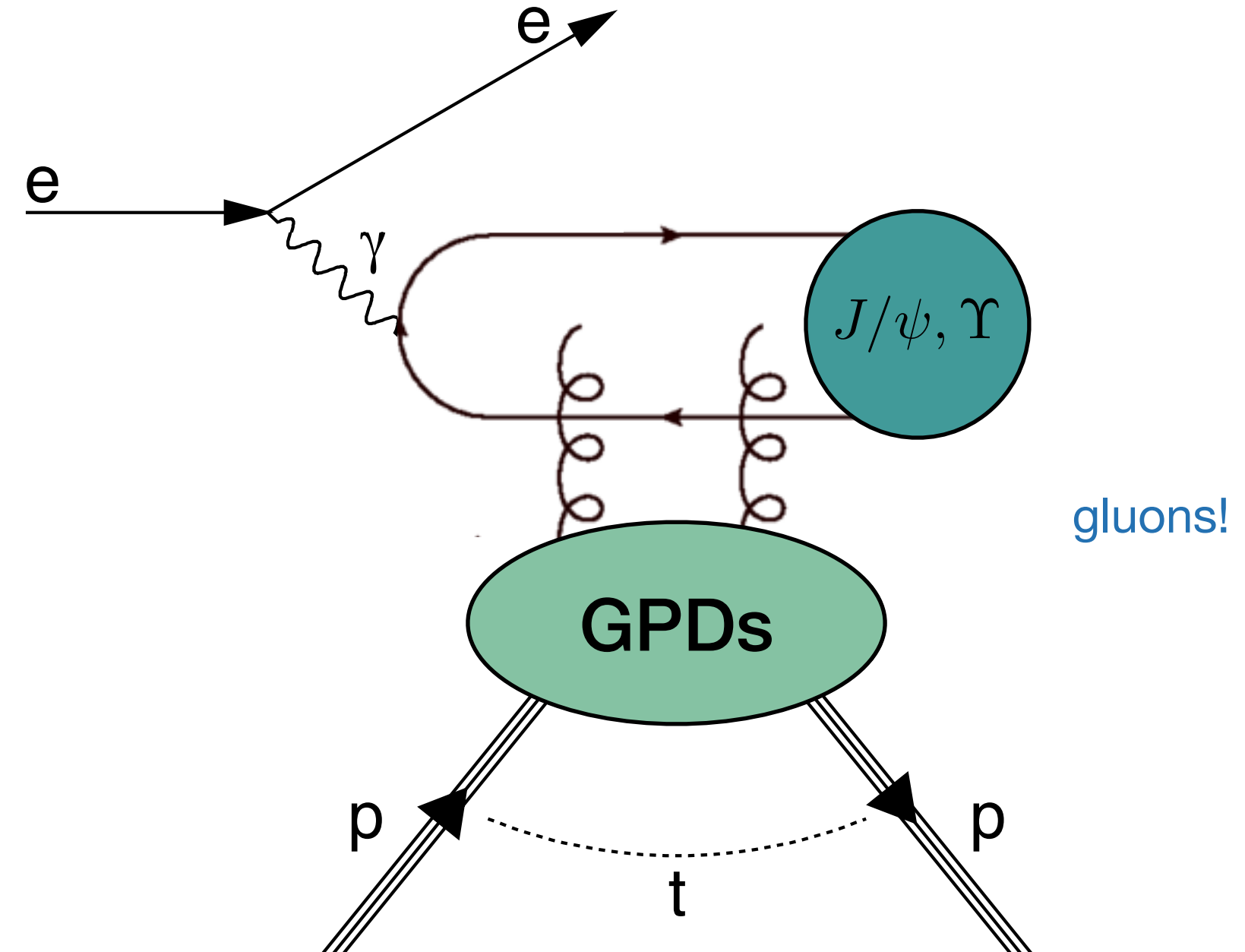
CLAS – PRC 95 ('17) 035207; 95 (2017) 035202  
 COMPASS – PLB 731 ('14) 19; NPB 915 ('17) 454  
 JLab Hall A Collaboration – PRC 83 ('11) 025201  
 HERMES – EPJ C 74 ('14) 3110; 75 ('15) 600; 77 ('17) 378  
 H1 – JHEP 05('10)032; EPJ C 46 ('06) 585  
 ZEUS – PMC Phys. A1 ('07) 6; NPB 695 ('04) 3

colliders, small  $x_B$ , gluons  
 fixed target: medium/large  $x_B$ , quarks

# Experimental access to GPDs



Deeply virtual Compton scattering (DVCS)  
Hard scale=large  $Q^2=-q^2$



Exclusive meson photoproduction  
Hard scale = large charm/bottom-quark mass

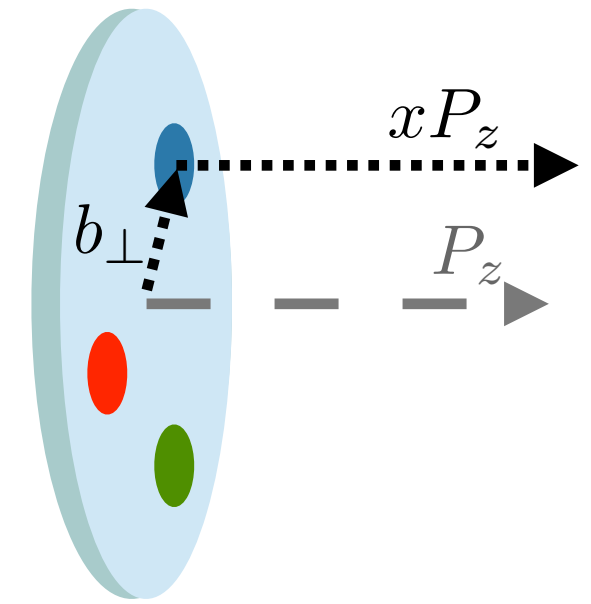
gluons!

CLAS – PRC 80 ('09) 035206; PRL 87 ('01) 182002; 100 ('08) 162002  
 COMPASS – arXiv:1702.06315  
 JLab Hall A Collaboration – PRL 99 ('07) 242501; PRC 92 ('15) 055202; Nat. Com. 8 ('17) 1408  
 HERMES – JHEP 10 ('12) 042; PLB 704 ('11) 15; NPB 842 ('11) 265  
 H1 – PLB 681 ('09) 391; 659 ('07) 796; EPJ C 44 ('05) 1  
 ZEUS – PLB 573 (2003) 46; JHEP 05 ('09) 108

H1 – EPJ C 46 ('06) 585; 73 ('13) 2466; PLB 541 ('02) 251  
 ZEUS – Nucl. Phys. B 695 ('04) 3; PLB 680 ('09) 4

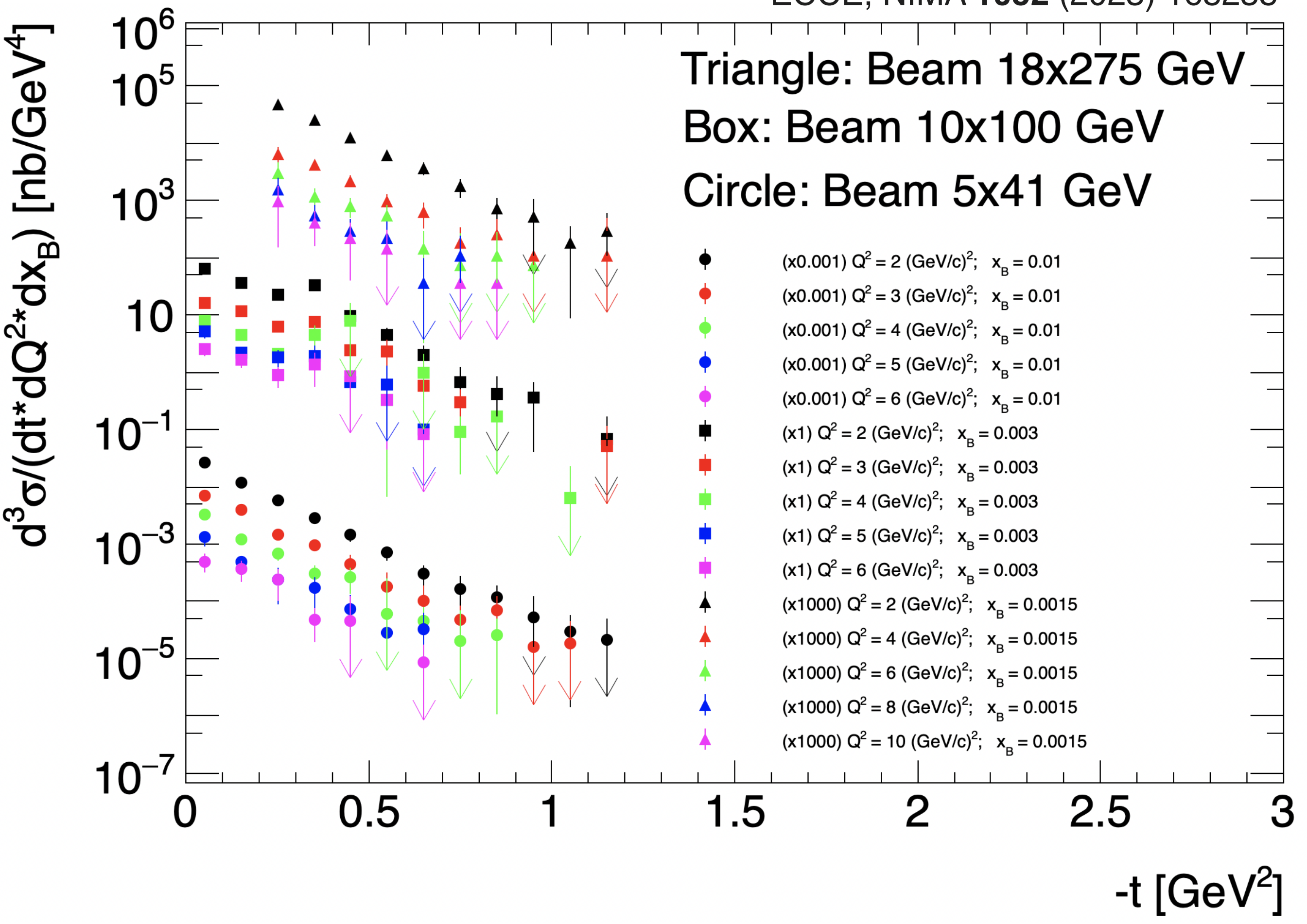


# Exclusive measurements on p with the EIC

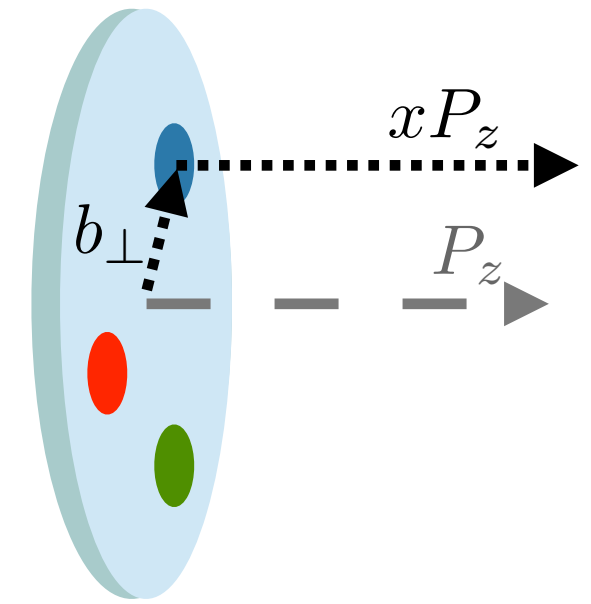


Deeply virtual Compton scattering  
 → sensitive to quarks (and gluons)

ECCE, NIMA 1052 (2023) 168238



# Exclusive measurements on p with the EIC

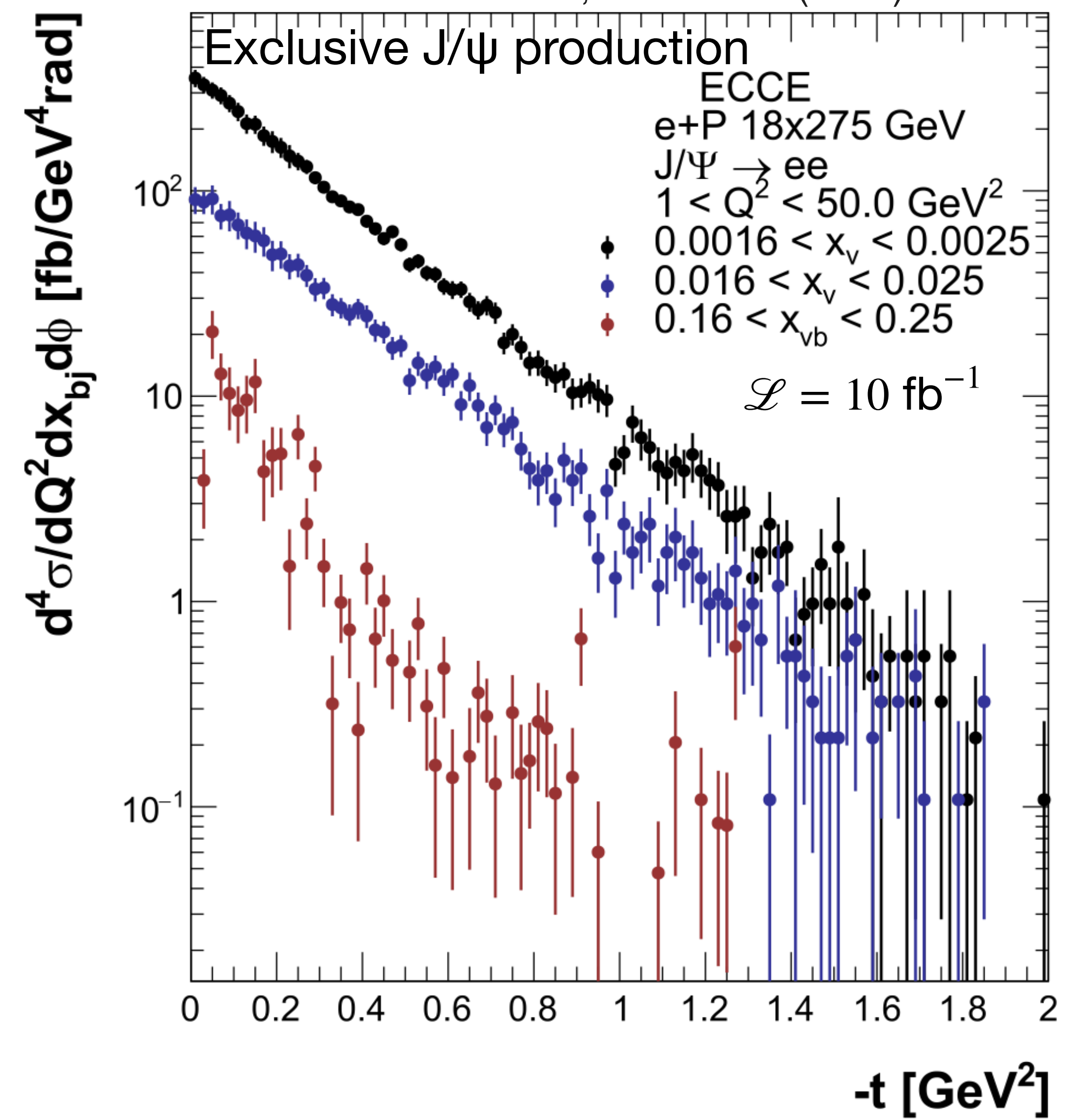
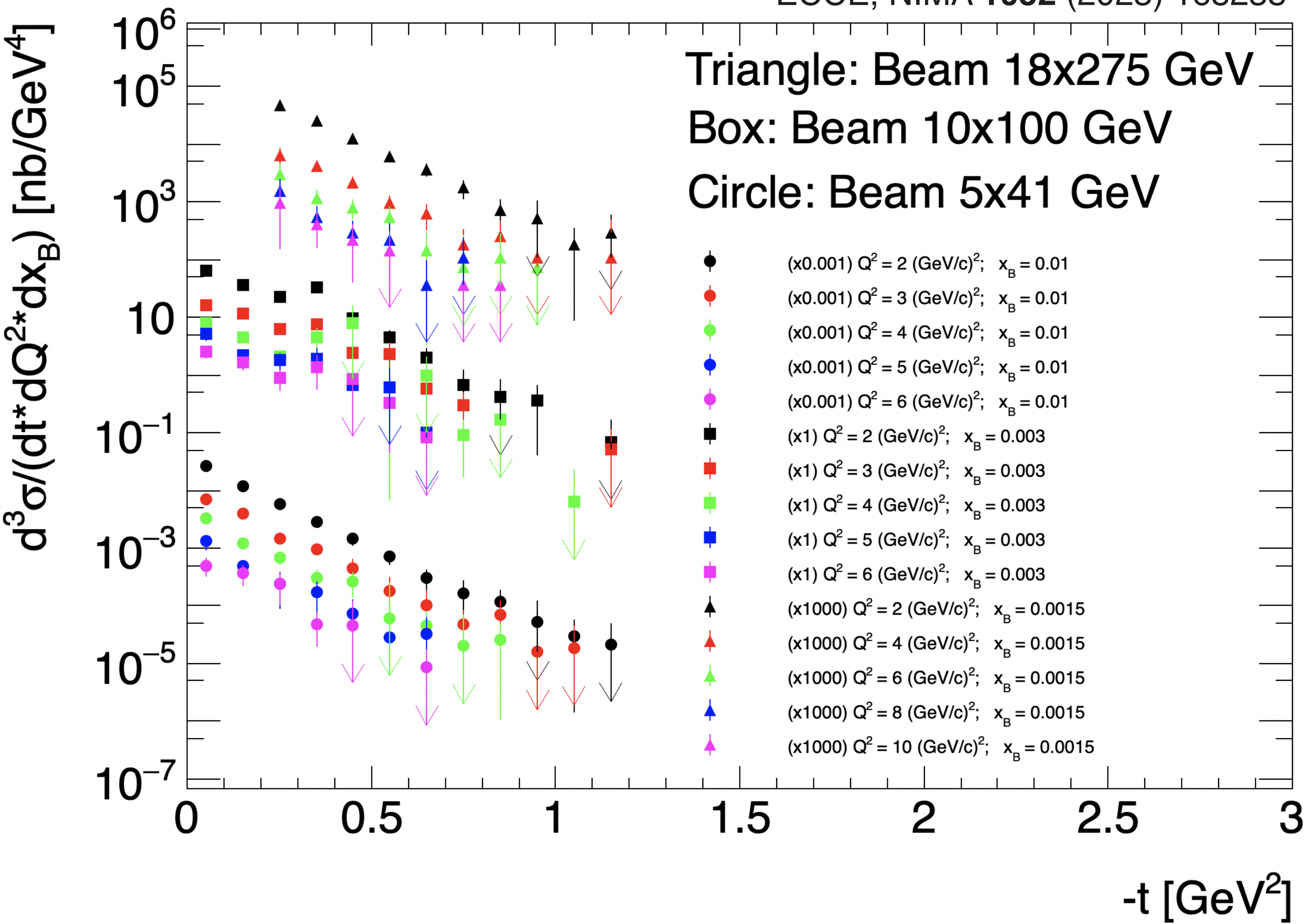


Deeply virtual Compton scattering  
 → sensitive to quarks (and gluons)

Exclusive J/ψ production  
 → excellent to probe gluon GPDs

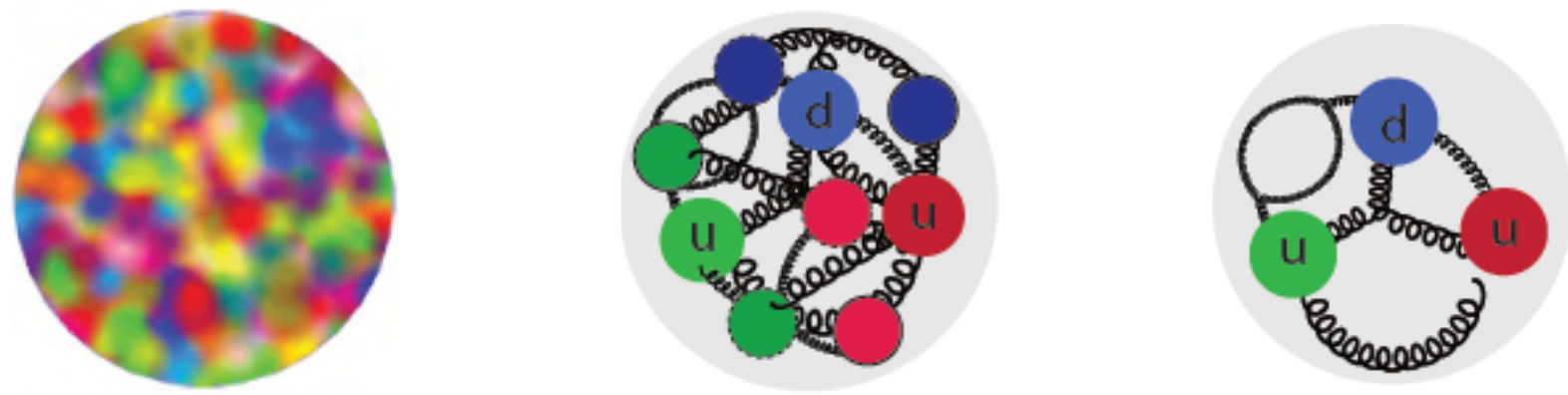
ECCE, NIMA 1052 (2023) 168238

ECCE, NIMA 1052 (2023) 168238

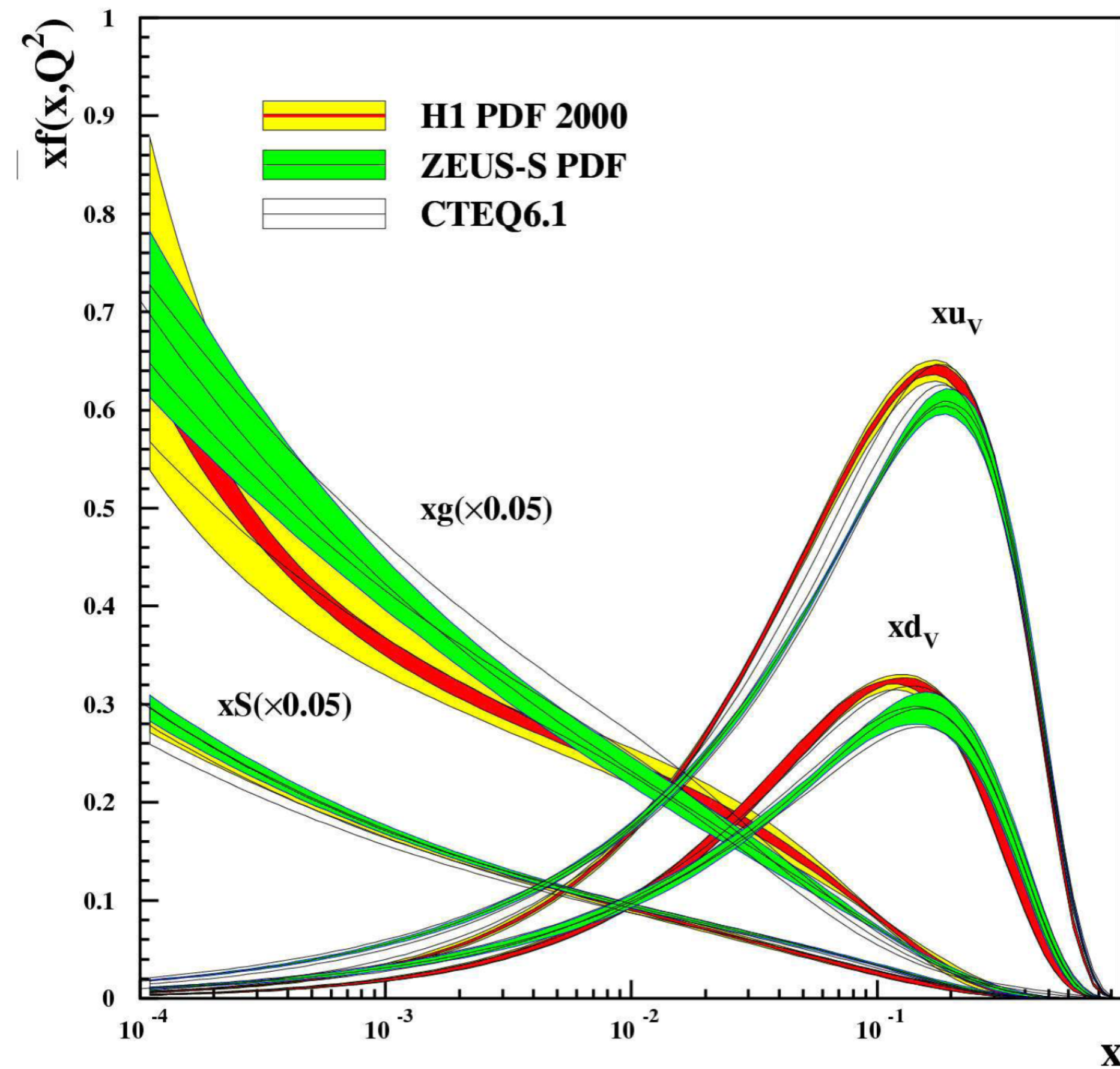


# Why an EIC?

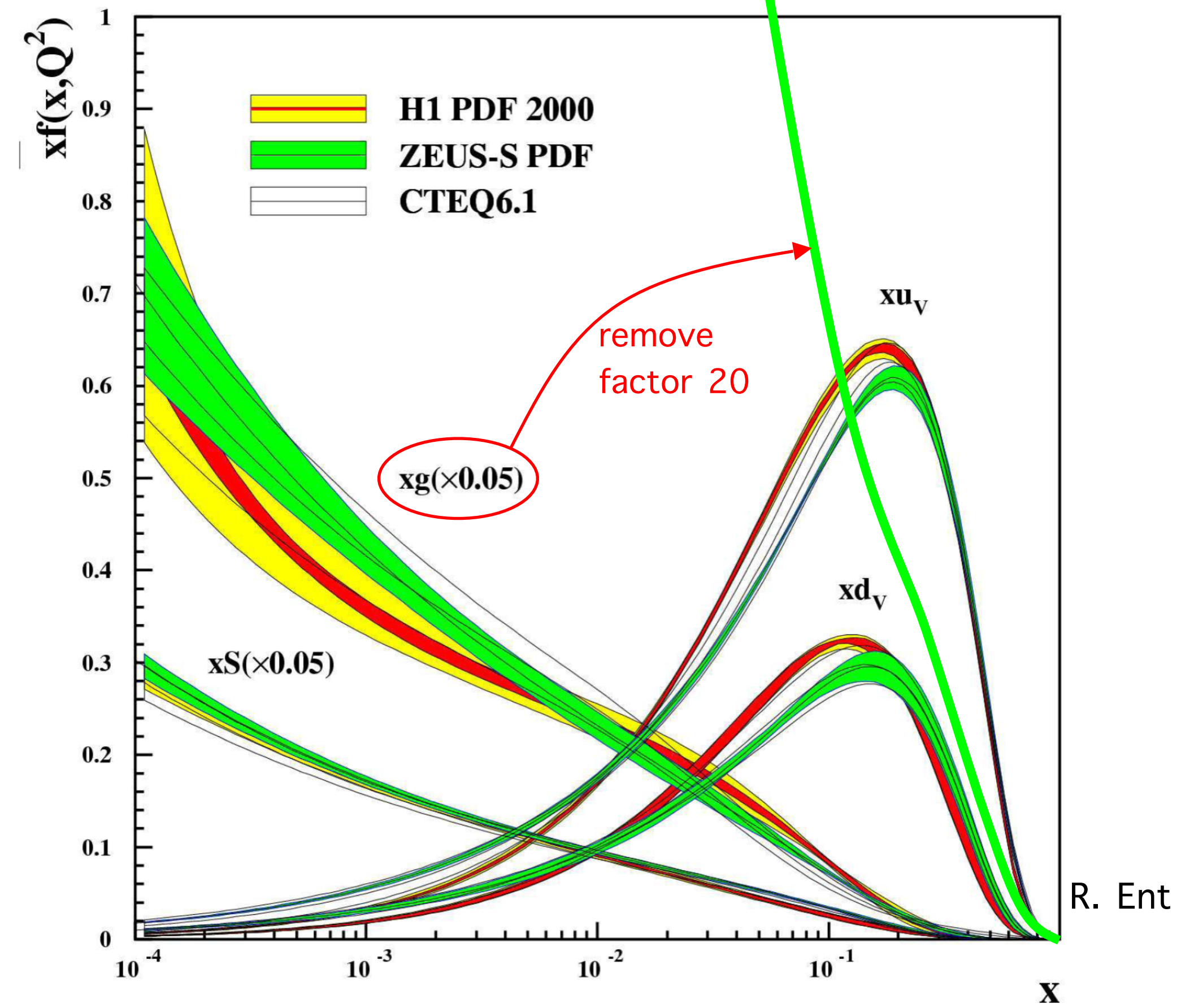
Gluon saturation



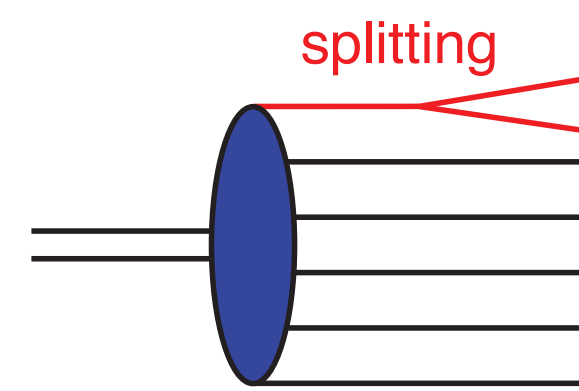
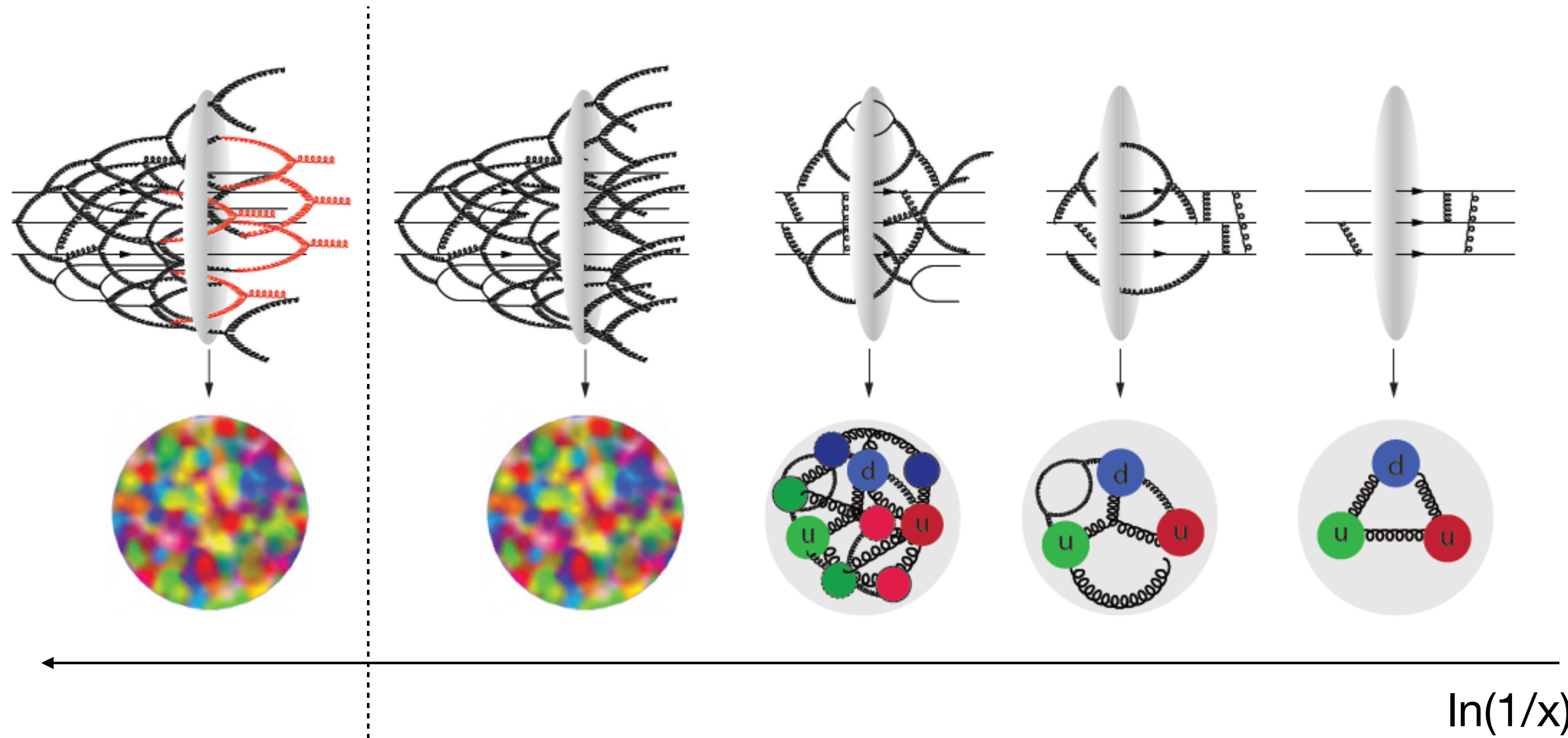
# Spin-independent parton distributions



# Spin-independent parton distributions



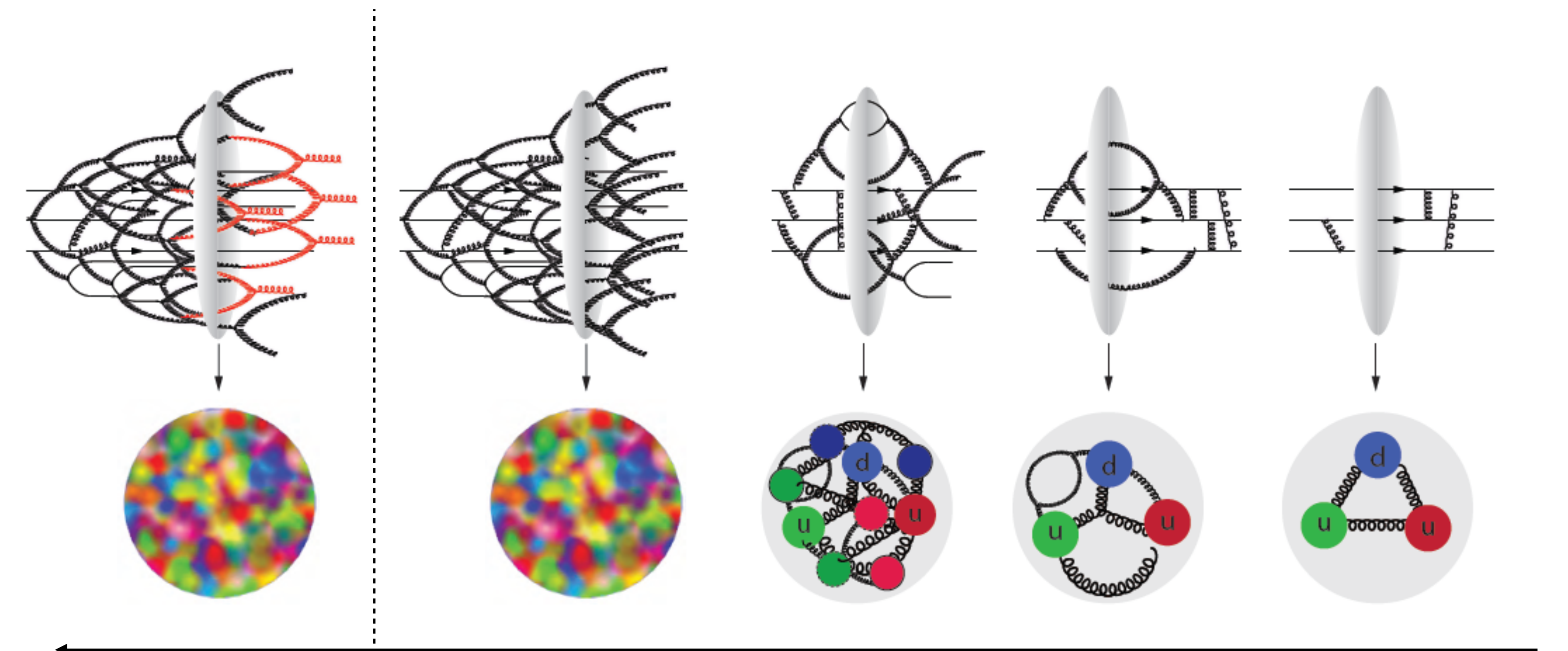
# Gluon splitting and recombination



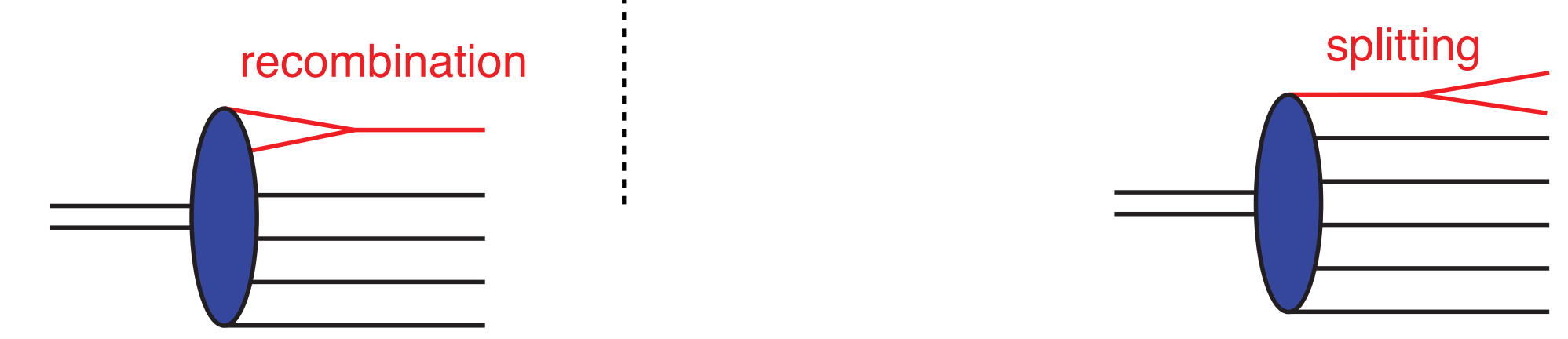
$\ln(1/x)$

$$x \approx Q^2 / W^2$$

# Gluon splitting and recombination



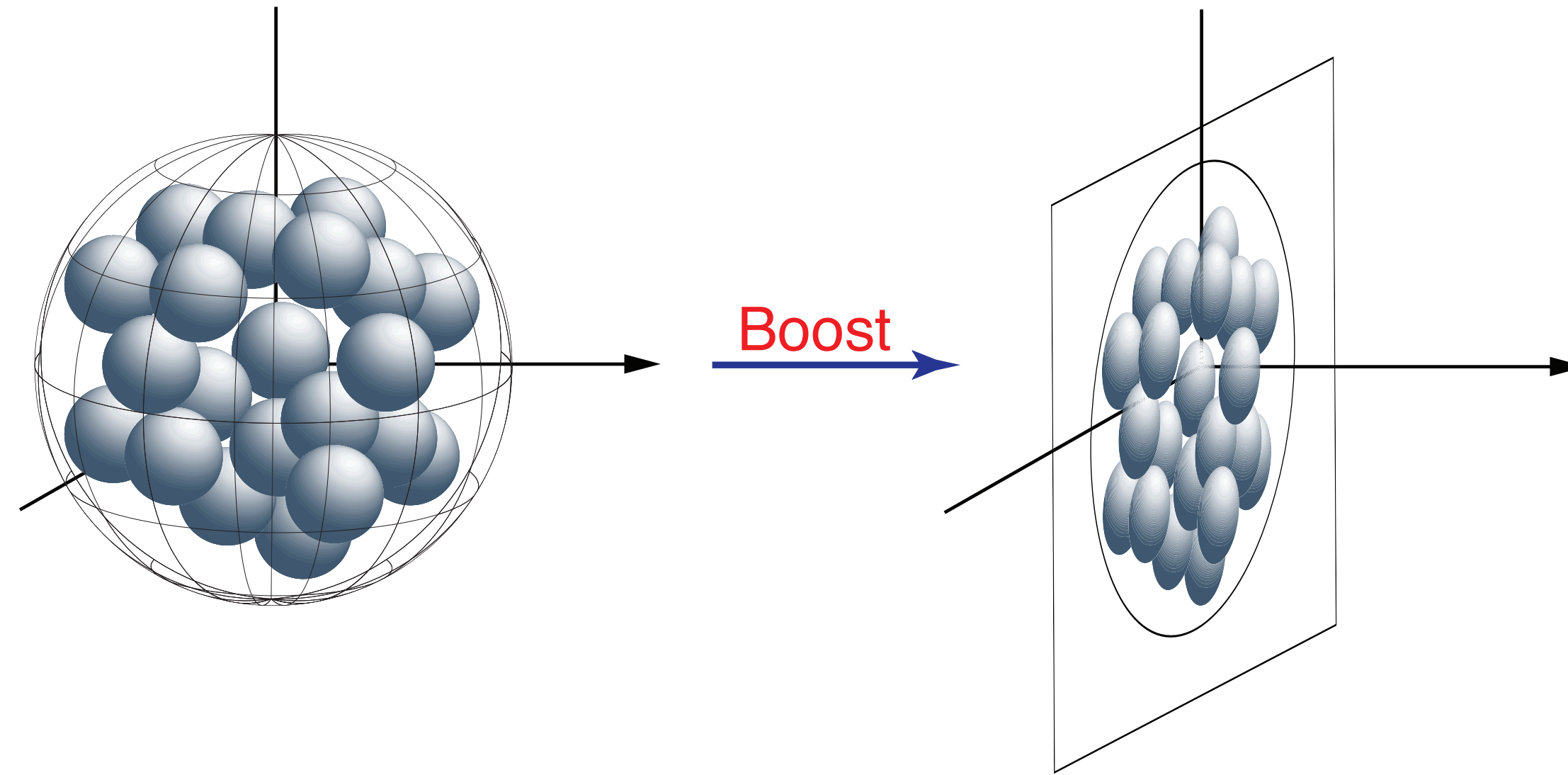
$\ln(1/x)$



saturation

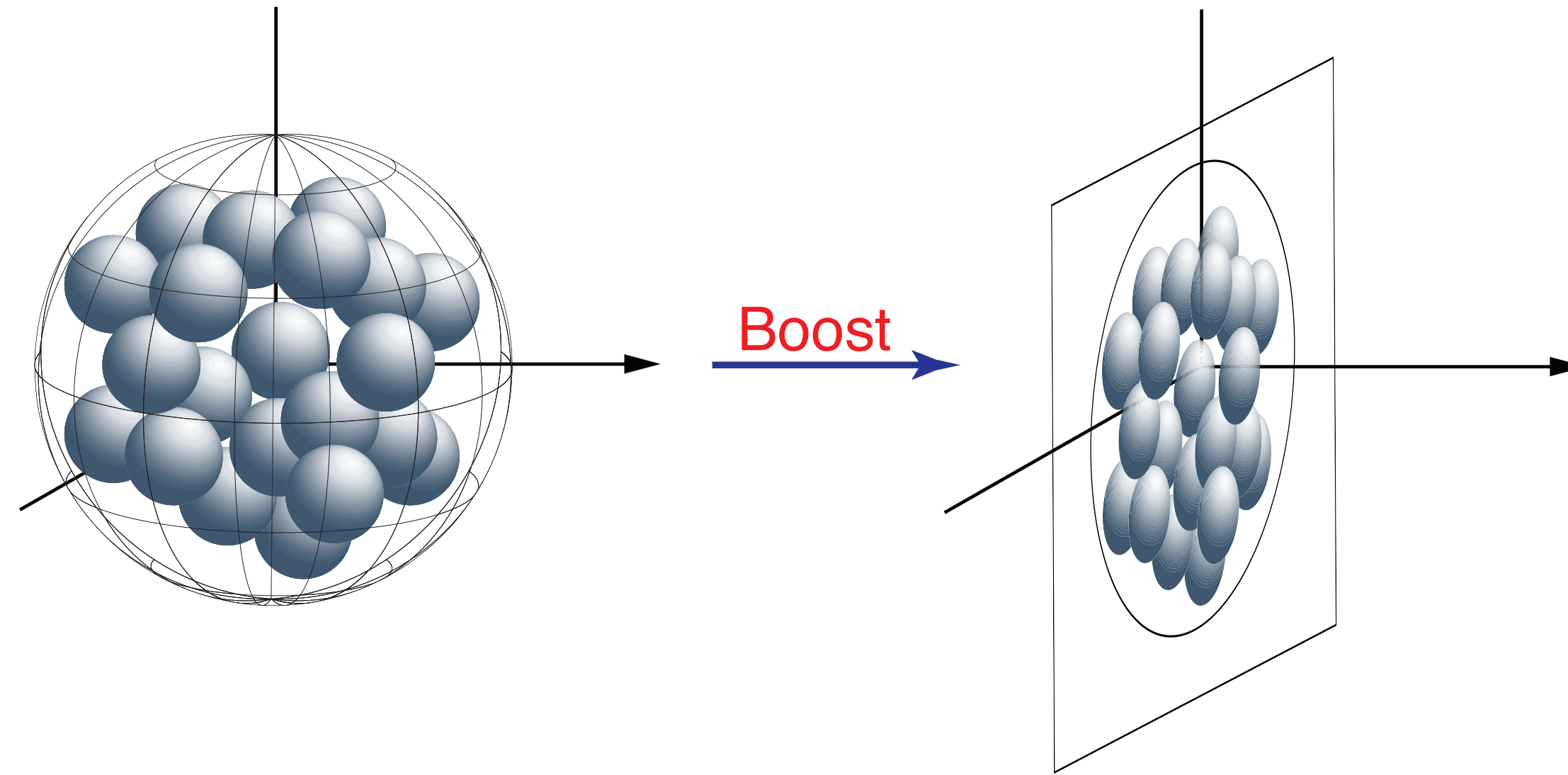
$$x \approx Q^2 / W^2$$

# The Oomph factor





# The Oomph factor



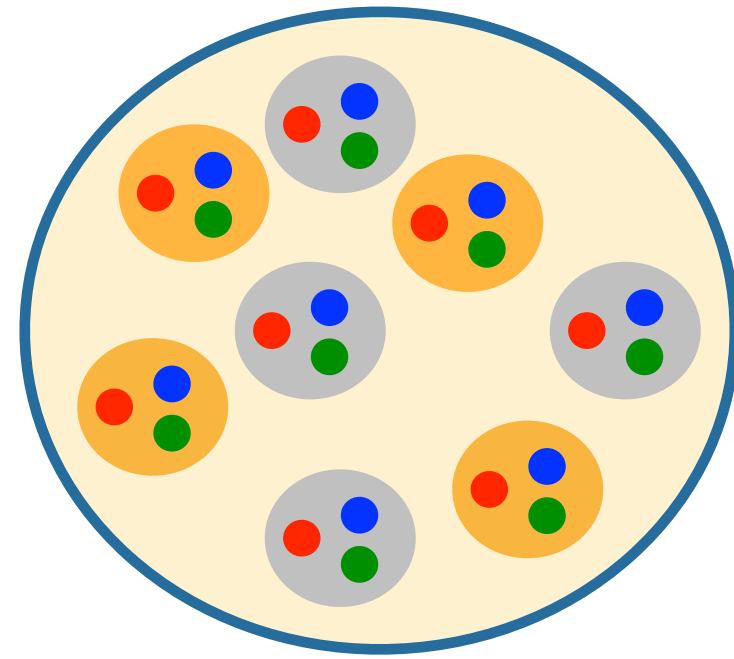
Oomph factor:  $A^{1/3}$  enhancement of saturation effect

# Exclusive/diffractive measurements on nuclei

What object are we probing?

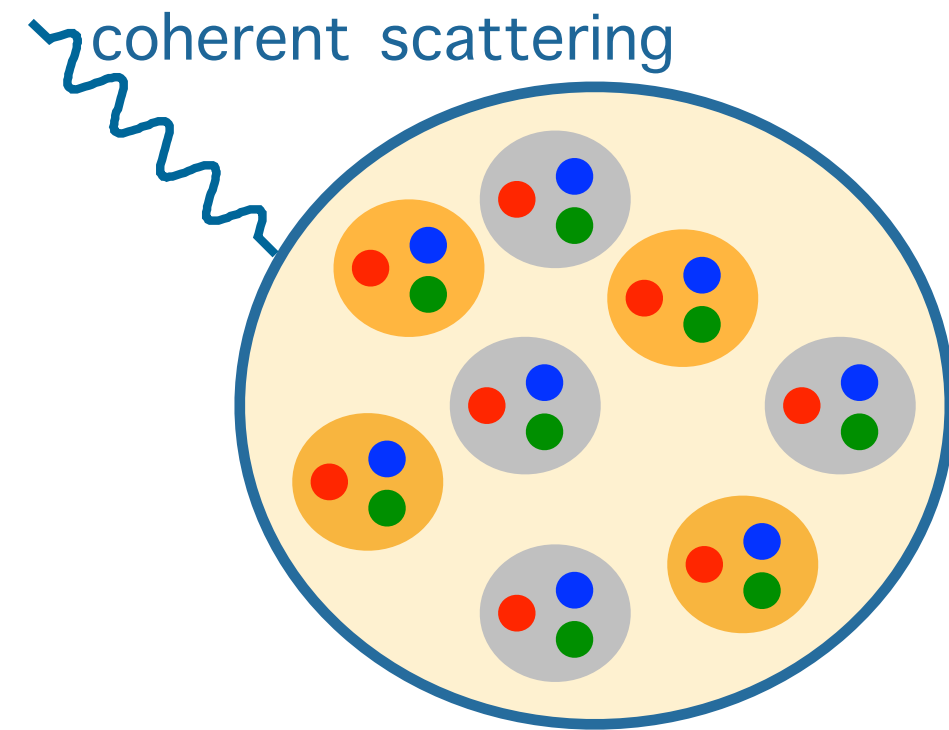
# Exclusive/diffractive measurements on nuclei

What object are we probing?



# Exclusive/diffractive measurements on nuclei

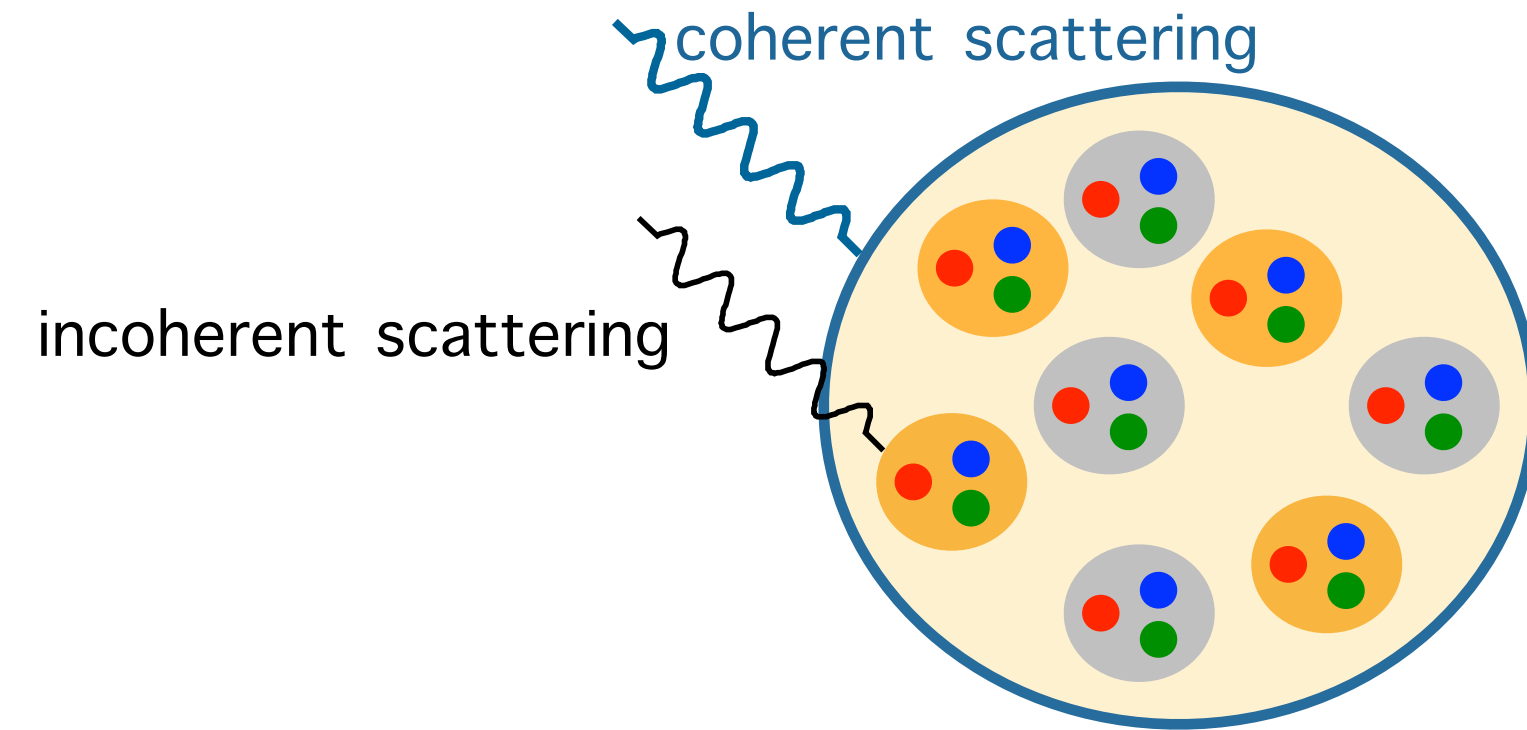
What object are we probing?



Coherent interaction: interaction with target as a whole.  
~ target remains in same quantum state.

# Exclusive/diffractive measurements on nuclei

What object are we probing?

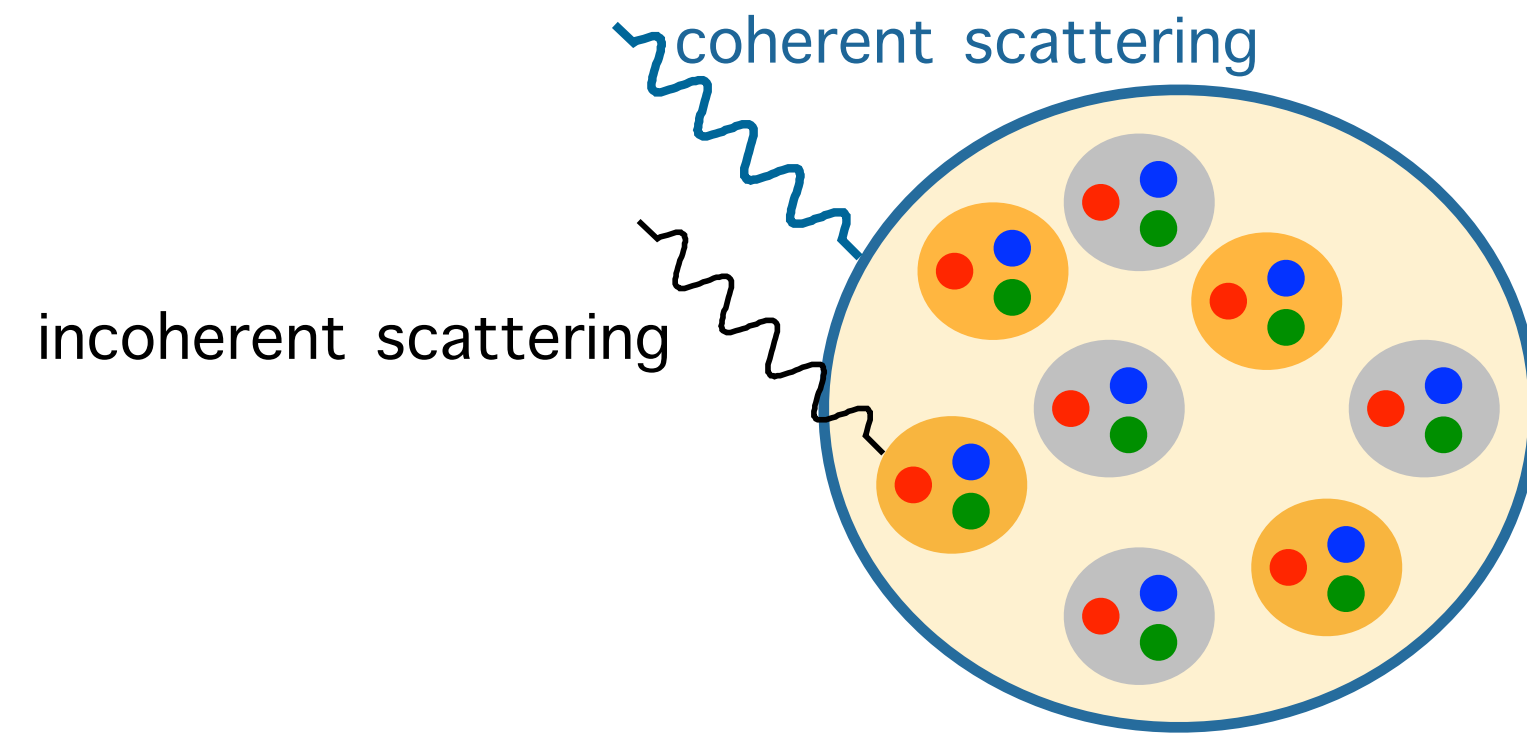


Coherent interaction: interaction with target as a whole.  
~ target remains in same quantum state.

Incoherent interaction: interaction with constituents inside target.  
~ target does not remain in same quantum state.  
Ex.: target dissociation, excitation

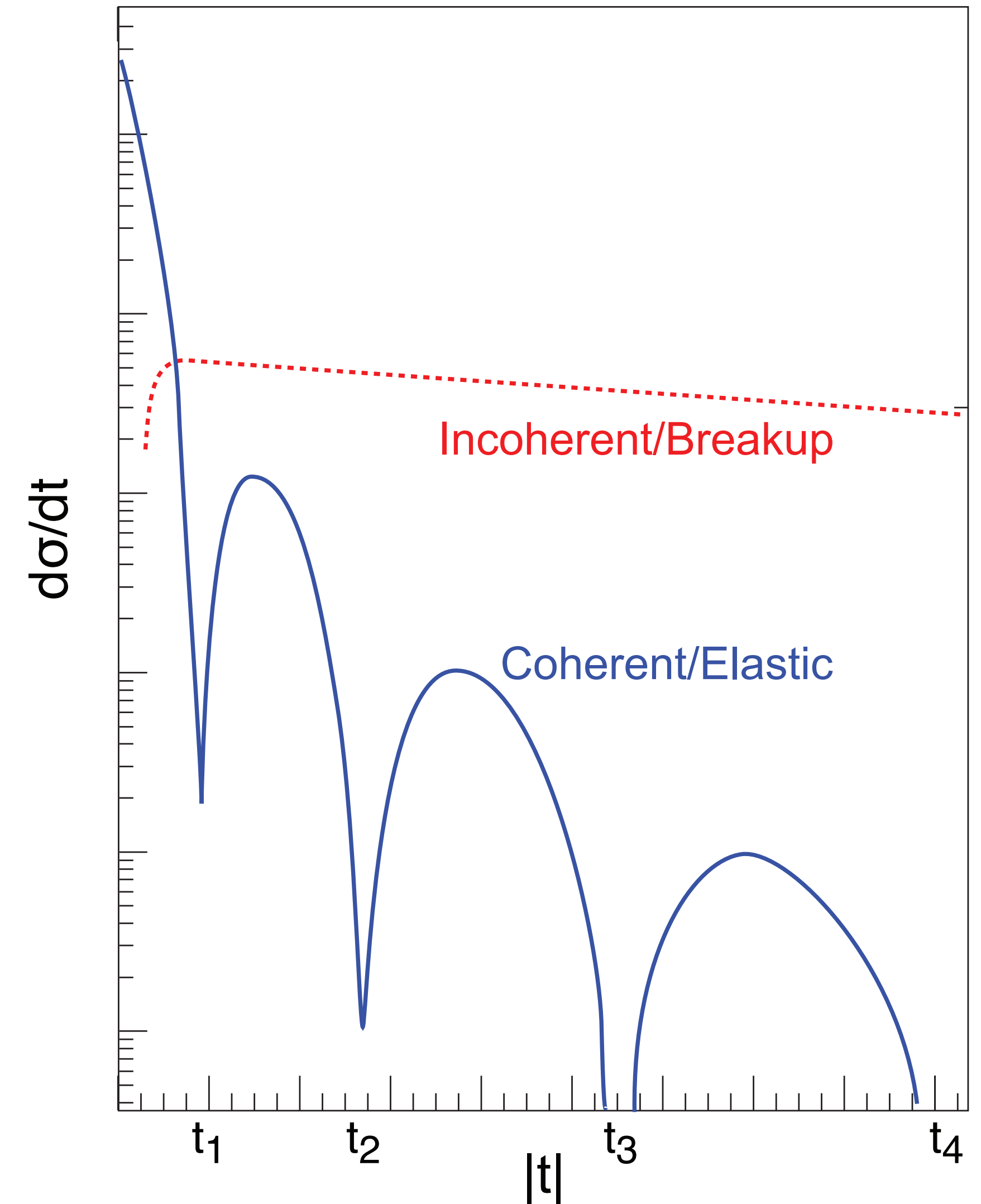
# Exclusive/diffractive measurements on nuclei

What object are we probing?

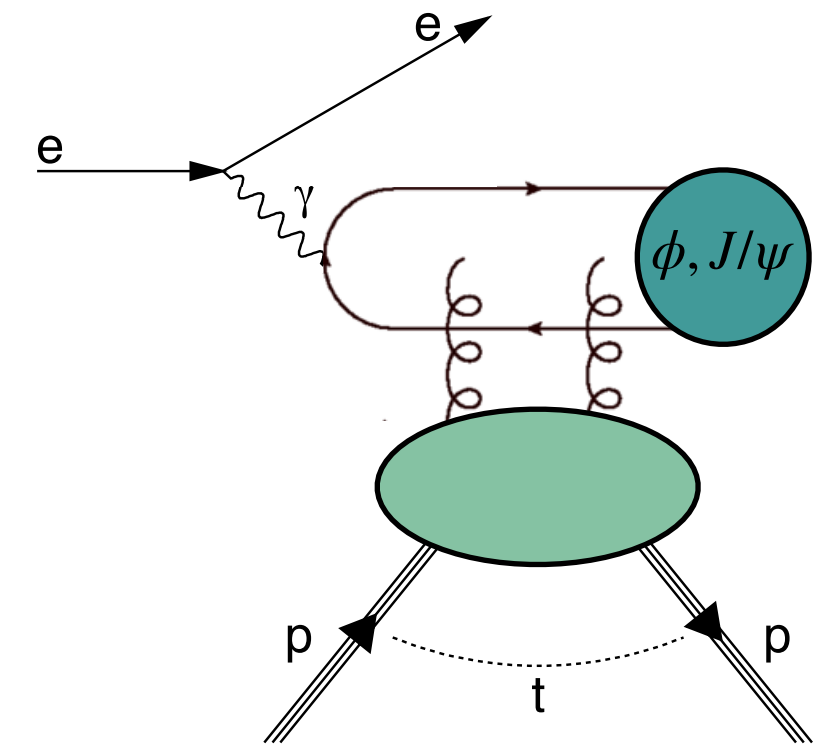


Coherent interaction: interaction with target as a whole.  
~ target remains in same quantum state.

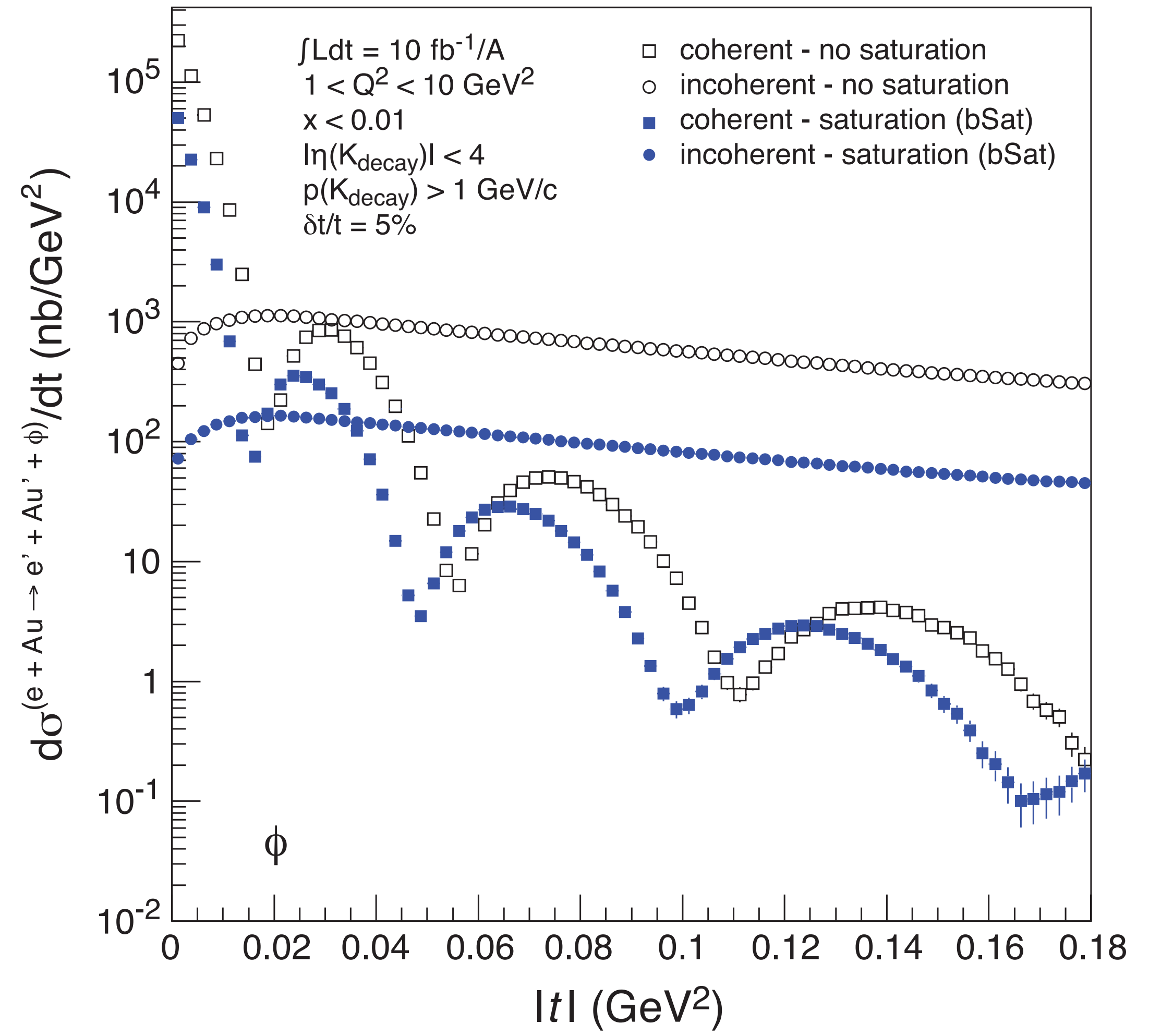
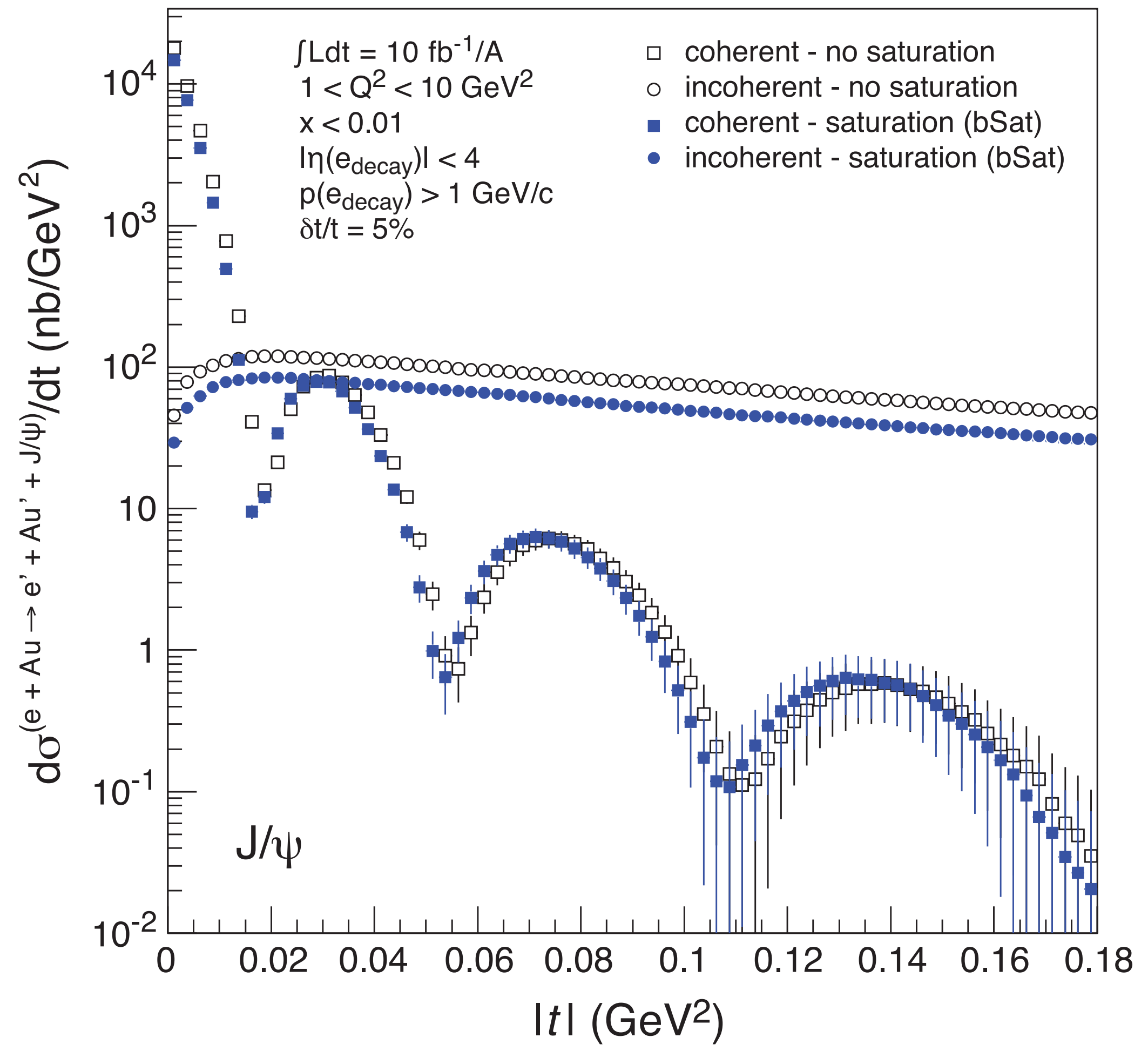
Incoherent interaction: interaction with constituents inside target.  
~ target does not remain in same quantum state.  
Ex.: target dissociation, excitation



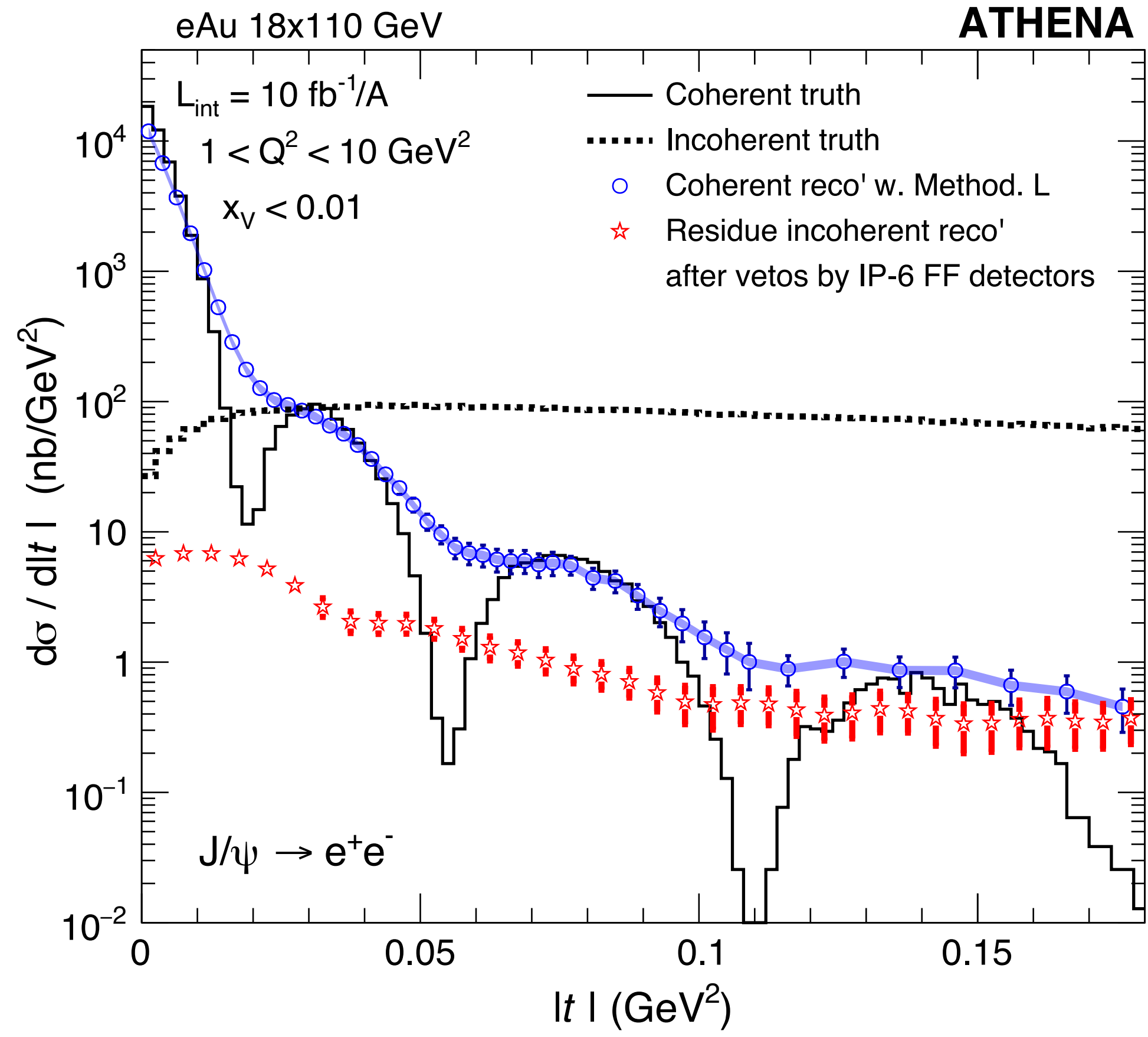
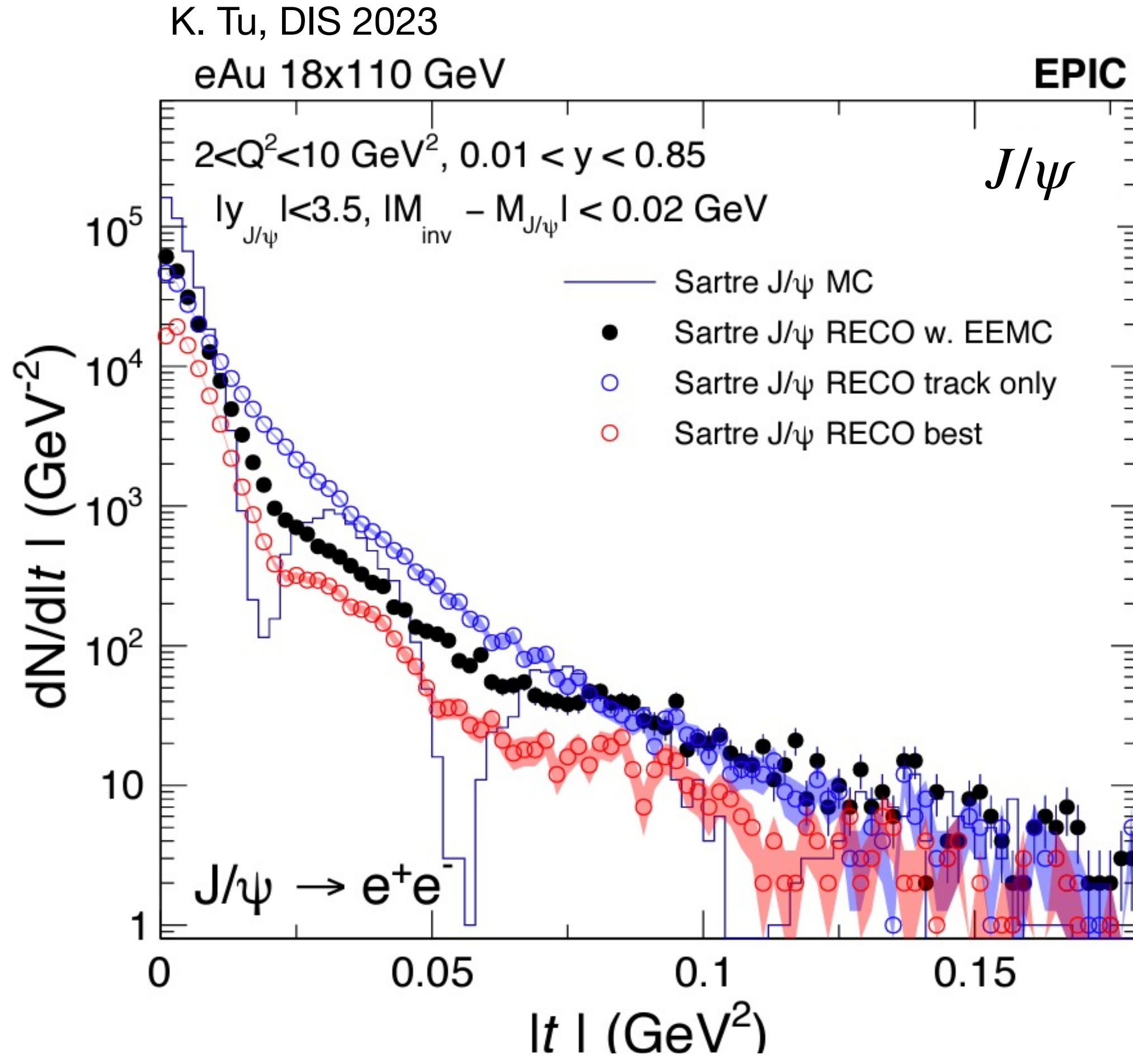
# Diffractive measurements at the EIC



A. Accardi et al., arXiv:1212.1701



# Exclusive measurements on nuclear targets with the EIC

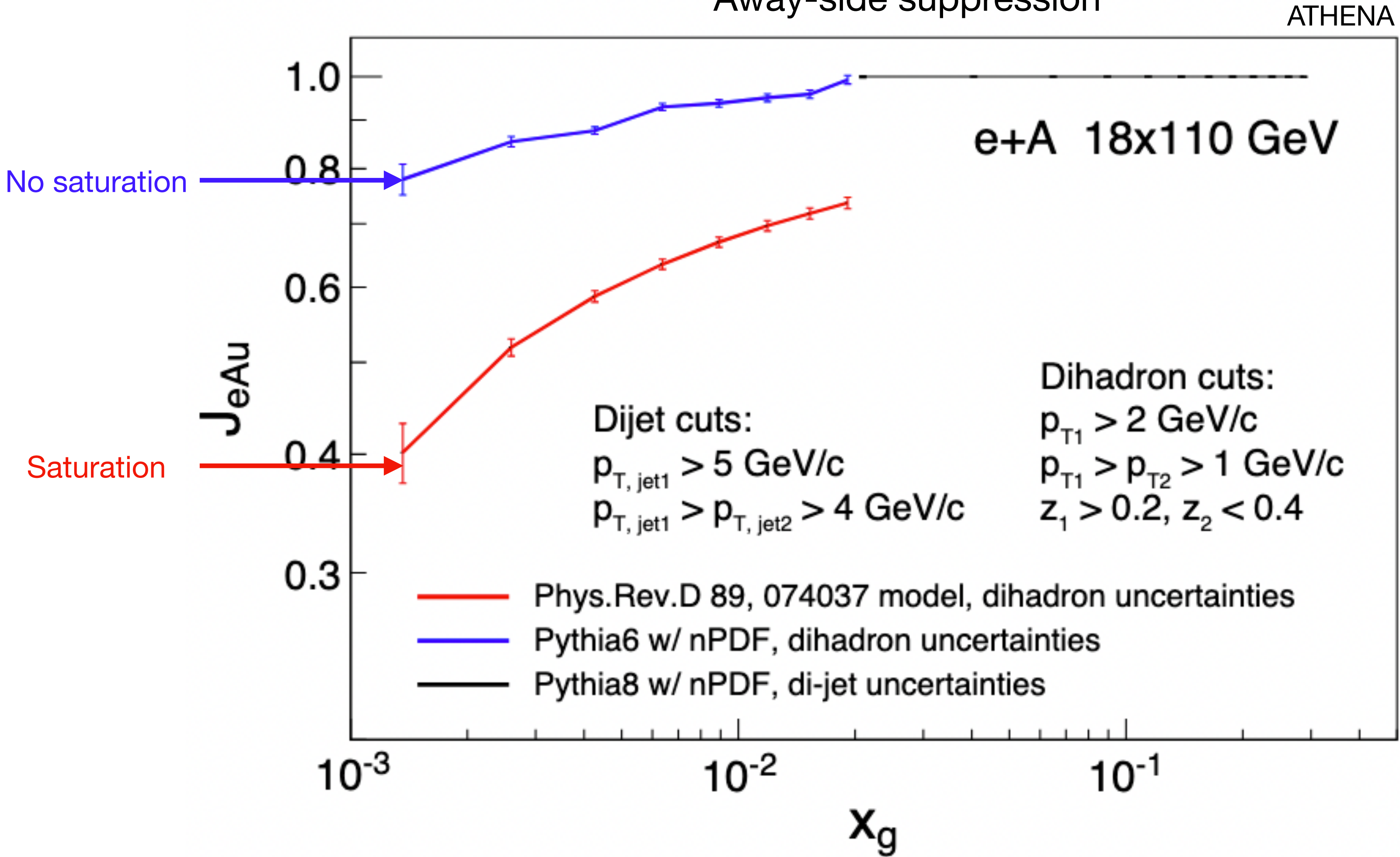
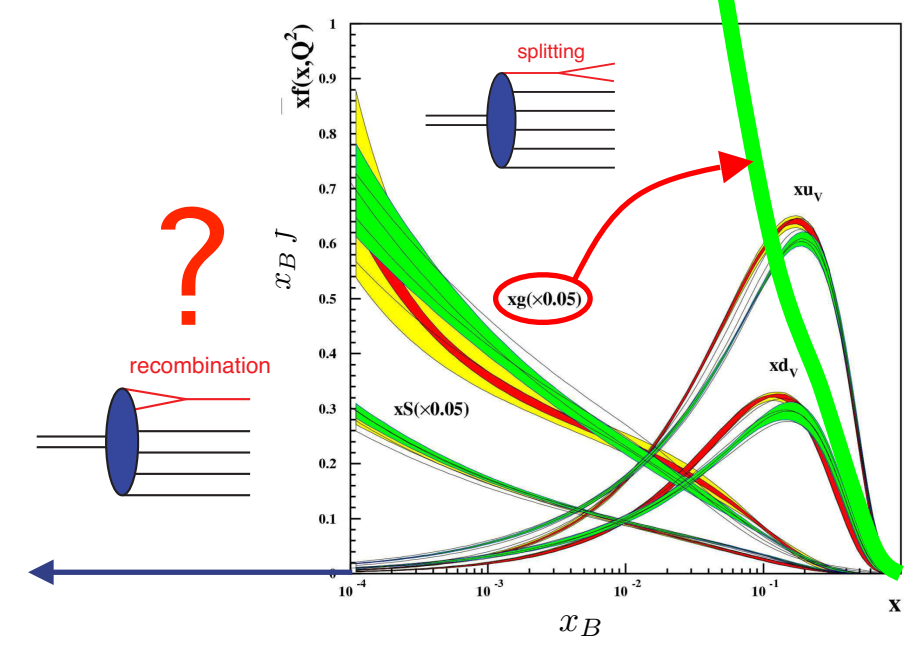




# Di-hadron production and jets in eA

- Complementarity region covered by dihadron and jet production

# correlated back-to-back hadron pairs in e+Au/e+p scaled by  $A^{1/3}$   
 Away-side suppression

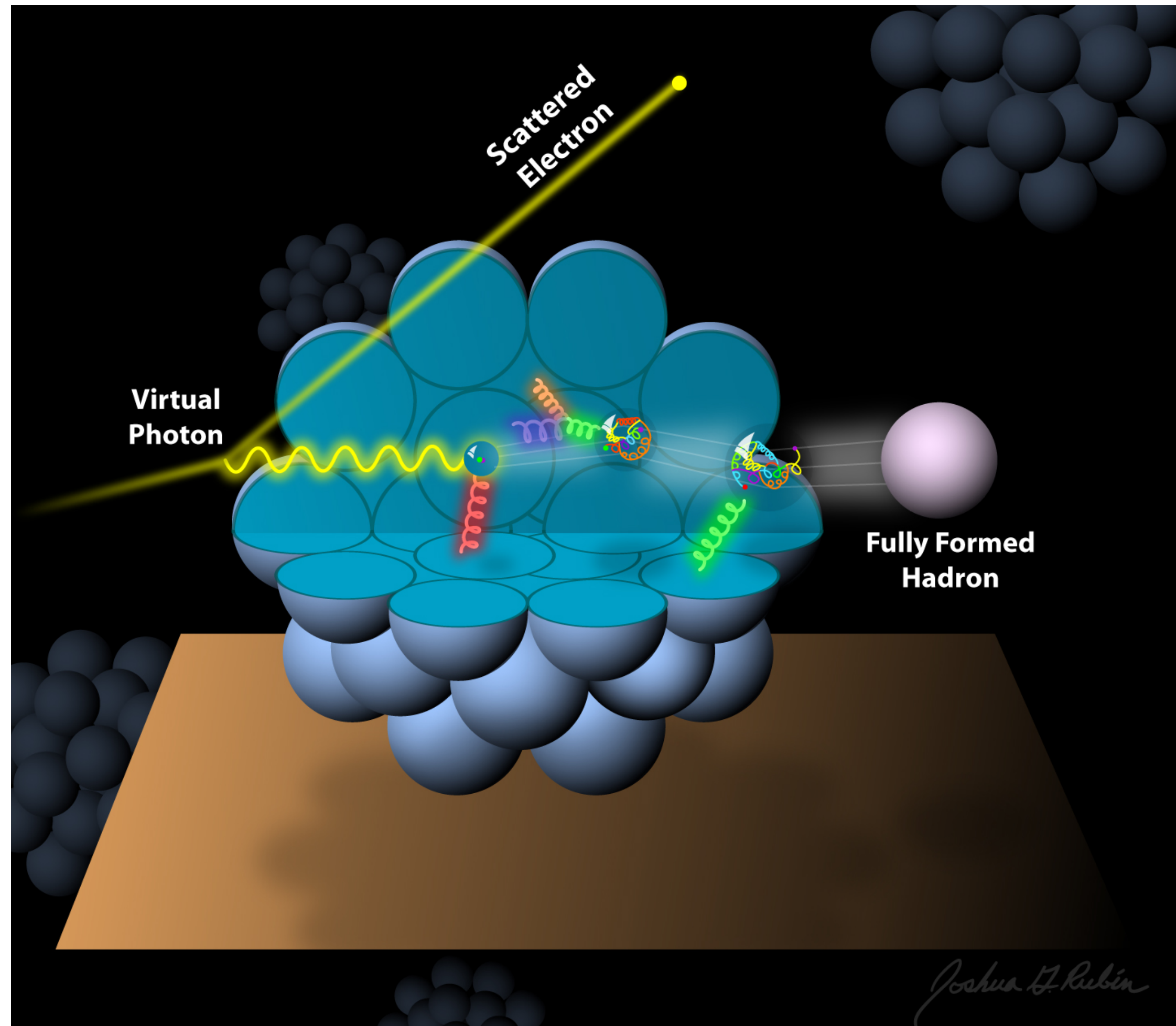


# Why an EIC?

## Hadronisation



# Probing space-time evolution of hadronisation



- Energy loss of parton by medium-induced gluon radiation
  - Energy loss of (pre-)hadrons
    - absorption
    - rescattering (small)
  - Partonic and hadronic processes: different signature
- ➔ probe space-time evolution of hadron formation
- PDFs modified by nuclear medium

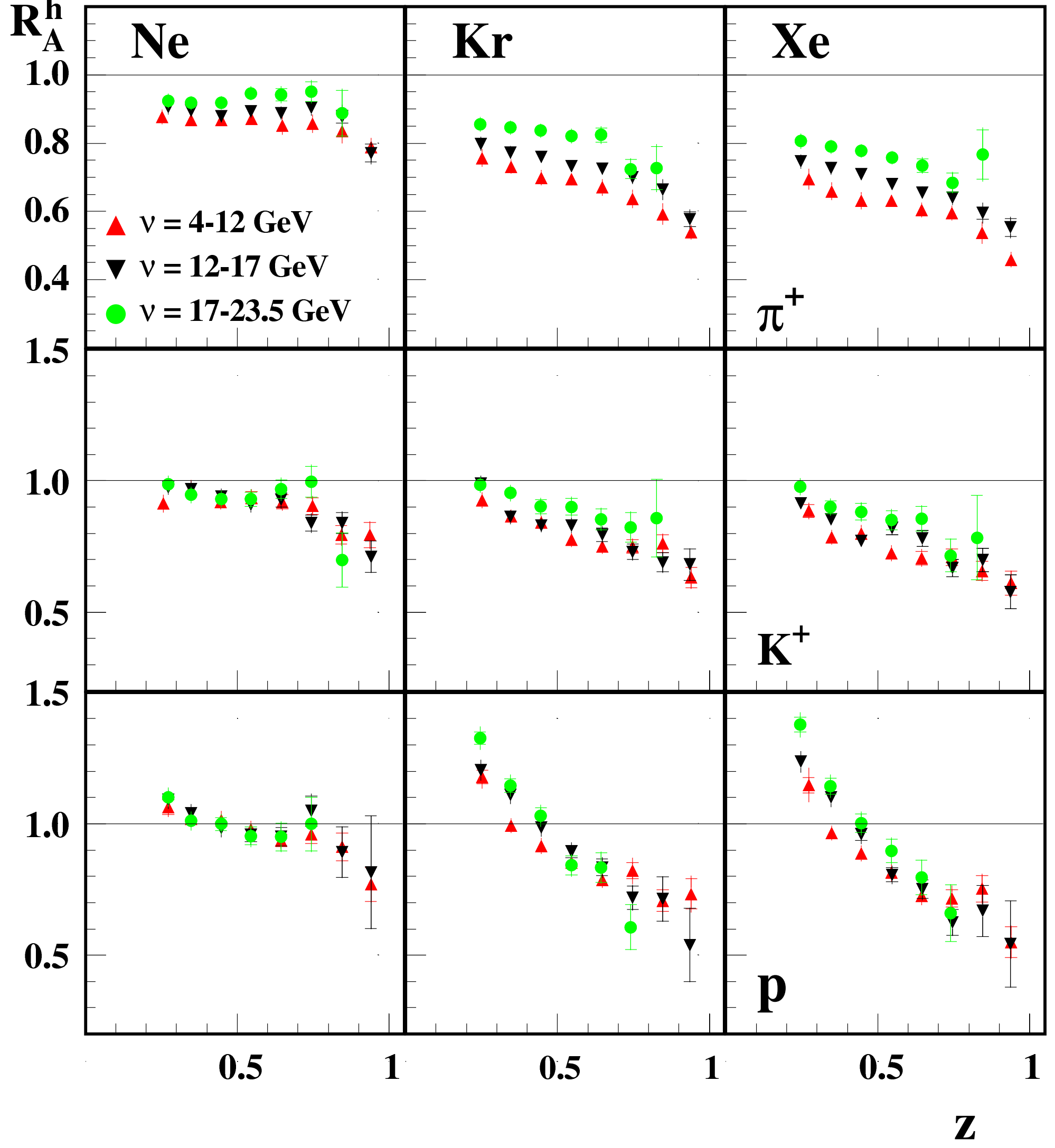
# Multiplicity ratios

Multiplicity ratios:

$$R_A^h = \frac{\left(\frac{N^h}{N_{DIS}}\right)_A}{\left(\frac{N^h}{N_{DIS}}\right)_D}$$

- Ratios → approximate cancelation of
- QED radiative effects
  - limited detector acceptance and resolution

HERMES, Eur. Phys. J. A 47 (2011) 113



At highest z: hadronic absorption

# Summary

EIC with ePIC can address various aspects of the nucleon and nuclear structure through:

- Precise inclusive and semi-inclusive (spin-dependent) DIS measurements via high-resolution EM calorimeters.
- Measurements for 3D (spin-dependent) tomography in momentum space provided by good Cherenkov-based and TOF AC-LGAD hadron PID detectors and tracking.
- Exclusive measurements on protons, using the far-forward detector system.
- Diffractive and exclusive measurements with coherent/incoherent separation via very precise EM calorimeters and far-forward detector system.
- Measurements on a large variety of nuclei: probe gluon saturation and study the space-time evolution of hadron formation.